

FARMACEVTSKI VESTNIK

Special Issue

BOOK OF ABSTRACTS
**10th Central European Symposium on
Pharmaceutical Technology**
September 18 – 20, 2014
Portorož, Slovenia





STROKOVNO GLASILO SLOVENSKE FARMACIJE | PHARMACEUTICAL JOURNAL OF SLOVENIA

FARMACEVTSKI VESTNIK

Special Issue | September 2014 | Vol 65

ODGOVORNI UREDNIK / GUEST EDITOR:
Borut Štrukelj

GOSTUJOČI ODGOVORNI UREDNIKI /
GUEST EDITORS:
Simon Žakelj
Iztok Grabnar
Aleš Mrhar

UREDNIŠKI ODBOR / EDITORIAL BOARD:
Saša Baumgartner
Marija Bogataj
Jelka Dolinar
Rok Dreu
Mirjana Gašperlin
Julijana Kristl
Janez Kerč
Igor Legen
Odon Planinšek
Tomaž Vovk
Franc Vrečer
Jemej Zadnik

NASLOV UREDNIŠTVA /
ADDRESS OF THE EDITORIAL OFFICE:
Slovensko farmacevtsko društvo,
Dunajska 184a, 1000 Ljubljana,
T.: +386 (01) 569 26 01
Transakcijski račun pri Novi LB d.d. Ljubljana:
02010-0016686585.

Izhaja petkrat letno.
Letna naročnina je 70 EUR.
Za tuje naročnike 100 US\$.

Tiska: COLLEGIUM GRAPHICUM
Naklada: 3.400 izvodov

Farmacevtski vestnik (Pharmaceutical Journal of Slovenia) is published 5 times a year by the Slovenian Pharmaceutical Society, Subscription rate in inland 70 EUR other countries US\$ 100.

Farmacevtski vestnik is regularly abstracted in: BIOLOGICAL ABSTRACTS, CHEMICAL ABSTRACTS, PHARMACEUTICAL ABSTRACTS, MEDICAL & AROMATIC PLANTS ABSTRACTS AND INBASE / Excerpta Medica

Farmacevtski vestnik is subsidized by the Slovenian Research Agency.

Guest Editors' Preface

With the main theme "Translation of basic concepts into drug delivery for specific populations" the 10th Central European Symposium on Pharmaceutical Technology (CESPT 2014) brings focus to patients' needs as the ever more important aspect of drug formulation and the entire process of providing the medication »from-lab-to-bed«. The needs of specific patient populations can be better met by employing the latest achievements in pharmaceutical technology, biopharmaceutics and related sciences. A step further, truly personalized medicine requires advanced approaches like in silico modelling to predict the needs of every individual patient. As an integral part of drug development, the increasing importance of novel specialized pharmaceutical dosage forms and complex drug release mechanisms call for advanced physiological-ly relevant in vitro drug testing as many CESPT 2014 participants show by the work presented in this Book of Abstracts.

Presentations at this symposium are divided into four sessions: Advanced drug delivery systems for specific populations, Frontiers of biopharmaceutical evaluation to promote early drug registration, Tuning physicochemical properties of nanomaterials to efficacy and safety and Recent achievements of modelling approach to personalized medicine. The authors of 5 plenary lectures, 5 keynote lectures, 33 oral and 89 poster presentations have met and exceeded the organizers' expectations with the quality and variety of their contributions. Advanced drug delivery systems such as orodispersible drug formulations, minitables, nanosized delivery systems (nanoparticles, nanofibers, nanotubes, nanosuspensions, nanoemulsions, nanocrystals, nanohydrogels), micro-sized delivery systems (microspheres, microemulsions), (magneto) liposomes, thermoresponsive hydrogels, solid self-microemulsifying delivery systems, polymeric micelles, solid dispersions, mucoadhesive delivery systems, chronopharmaceuticals, biopolymers and pellets are investigated, from physicochemical characterization of drugs and excipients to production technologies, in vitro evaluation and translation "from-lab-to-bed". Moreover, in vitro/ex vivo, in vivo and in silico experimental models for the study of mechanisms and kinetics of LADME processes, as well as recent advances in the areas of biorelevant dissolution tests, transdermal transport studies and eye-related bioavailability prediction models are presented.

Over 165 delegates from 20 countries give this symposium a truly international character and represent a strong basis for creative scientific interactions and wide dissemination of new concepts. The organizers are grateful for all the assistance from the supporting societies and associations in promoting the idea of CESPT in the international community.

*Prof. A. Mrhar, President of CESPT
Assist Prof. S. Žakelj, General Secretary of CESPT
Assoc. Prof. I Grabnar, Member of Organizing Committee of CESPT*



CONTENT

4 **PLENARY LECTURES**

11 **KEYNOTE LECTURES**

21 **ORAL PRESENTATIONS**

68 **POSTER PRESENTATIONS**

244 **INDEX OF AUTHORS**



PLENARY LECTURES





THE ROLE OF DRUG DELIVERY TECHNOLOGY IN DRUG THERAPY

A. Goepferich¹

¹ Department of Chemistry and Pharmacy, University of Regensburg, Universitätsstrasse 31 93040 Regensburg, Germany

The development of new medicines depends significantly on the discovery of new disease-specific drug targets and the development of drug molecules with sufficiently high target specificity. 'Classical' small molecular weight drugs are, thereby, either developed via rational design or by testing large compound libraries in cell culture for their interaction with a biological target. Both strategies have led to the discovery of highly affine compounds with outstanding target affinities. In recent years we have concomitantly witnessed the massive development of biologics such as antibodies with superb antigen affinities and high plasma half-lives (1).

This tremendous success in developing more 'efficient' drugs seems to have severe implications for drug delivery technology. Many small molecules suffer from adverse physicochemical properties such as low solubility. Biologics have an unfavorably large size and high charge density. Given the fact that the *in vivo* efficacy of a compound does not only depend on its target affinity but equally important on the sufficient distribution to the target site, these are severe handicaps that may lead to a failure to qualify for the originally intended therapy. This development triggered a change of paradigms making drug delivery science not merely a tool for making good medicines better but an integral part of the therapeutic concept.

A prominent example is the distribution of antibodies. While in recent years a number of highly efficient compounds were developed their distribution is size limited. For this reason age related macular degeneration, a severe retinal disease, needs to be treated by intravitreal rather than i.v. injections. While 'classical' drug delivery technology may help to keep the injection frequencies low by releasing antibodies from a reservoir over a period of a few weeks, it could even worsen side effects that stem from the continuous intraocular VEGF knock down. New concepts deem necessary to overcome this limita-

tion by either implementing discontinuous intraocular drug release patterns or systemic anti VEGF therapies by targeting the retinal endothelium (2).

Another prominent example are nucleic acids such as siRNAs the site of action of which is inside cells and that suffer from a lack of ability to cross cell membranes due to their size and charge density. Drug delivery technology is almost mandatory to overcome these drawbacks.

Besides biologics, small molecules profit tremendously from innovative drug delivery concepts. Over recent years we have witnessed the massive development of a number of technologies that increase the water solubility of lipophilic drugs by using nanotechnological approaches such as the development of drug nanoparticles with increased solubility (3).

Even though the aforementioned examples suggest that drug delivery could easily rescue drug therapy problems related to drug properties, there are shortcomings and even misconceptions. Nanotechnology, for example, offers tremendous opportunities but does not come along without severe intrinsic handicaps. Targeting drugs with the help of nanoparticles via the blood stream can serve a good example. While we may get rid of a number of unfavorable drug properties by using this strategy we may trade them against a number of handicaps that are intrinsic to colloidal particles such as limited drug loading capacity, increased size, immune system activation and a limited ability to leave the blood stream.

The aforementioned examples demonstrate that drug delivery science is a highly active research area with steadily growing significance for the therapeutic success of many drugs.

REFERENCES

1. R.P. Junghans and C.L. Anderson, *The protection receptor for IgG catabolism is the beta2-microglobulin-containing neonatal intestinal transport receptor*, PNAS, 93 (1996) 5512-5516.
2. Pollinger K, Hennig R, Ohlmann A, Fuchshofer R, Wenzel R, Breunig M, Tessmar J, Tamm ER, Goepferich A, *Ligand-functionalized nanoparticles target endothelial cells in retinal capillaries after systemic application*. PNAS 110 (2013) 6115-6120.
3. Luschmann C, Herrmann W, Strauss O, Luschmann K, Goepferich A, *Ocular delivery systems for poorly soluble drugs: An in-vivo evaluation*. Int J Pharm 455 (2013) 331-337.





PREDICTION OF ORAL DRUG DELIVERY SYSTEMS' *IN VIVO* PERFORMANCE: HOW TO SIMULATE PHYSIOLOGICAL VARIABILITY

M. Bogataj

University of Ljubljana, Faculty of Pharmacy,
Aškerčeva 7, 1000 Ljubljana, Slovenia

INTRODUCTION

In vitro dissolution testing is a useful tool to predict dosage form performance after its administration. This prediction has an important role in the development of new dosage forms and represents a basis for a choice of a newly developed formulation for testing in bioavailability / bioequivalence study. To predict well *in vivo* behaviour of the dosage form after administration, we have to know the conditions to which the dosage form is exposed in the human body. Thus, for orally administered dosage forms, the detailed knowledge of the conditions in gastro intestinal (GI) tract is essential. However, the variability of GI tract conditions is huge, so it is frequently very difficult to choose *in vitro* conditions that will reflect well certain *in vivo* situation.

VARIABILITY OF GI TRACT CONDITIONS

The variability of conditions is great already in GI tract of a healthy adult, but the conditions in GI tract of an individual who belongs to one of special populations may vary even more, or deviate from those in healthy adults. Two most important special groups are children and elderly people, but there are other groups like pregnant women, people of different races, and also people with different diseases of GI tract or systemic diseases. GI conditions in individuals from those groups might differ significantly. Thus, some conditions in GI tract of a child differ significantly from the conditions in GI tract of healthy adult, at least in certain life periods. These conditions are very

much dependent on the age of the child. Many researchers divide children on the basis of their age in 5 - 7 groups (1, 2), because of biological differences that appear in different periods in child's body, and thus also in child's GI tract. For example, pH in the stomach of a baby changes strongly already in first hours, days and weeks of life (1, 2, 3). And pH in the stomach is very important for many drugs and can influence their ionization, solubility, stability etc. There are many other variable parameters and basing on the knowledge of different conditions in GI tract of children and drugs' properties, paediatric biopharmaceutical classification system is in preparation (2). Also, the conditions in GI tract of elderly people deviate from those of healthy adults frequently. There are physiological and anatomical conditions that change with increasing age also in healthy older people. Change in acid secretion in stomach appear frequently in elderly (4), also changes in GI tract motility (5), but increasing age represents also an important risk factor for appearance of different diseases which might additionally and strongly influence the conditions in GI tract (5). However, age is not the only factor that produces changes in human body, including GI tract. There exist also groups of people suffering from different diseases independent of their age, which might have great deviations in their GI tract conditions from healthy adults. Thus, Kokubo et al. (6) showed in their meta-analysis study that oro cecal transit time of people with different diseases like celiac disease, cystic fibrosis, etc. differs significantly from healthy adults. They also found out that people with obesity and even pregnant women have prolonged time of transit from mouth to caecum.

IN VITRO SIMULATION OF GI TRACT CONDITIONS VARIABILITY

To predict *in vivo* dosage form performance with high certainty, we have to know well the conditions in GI tract including their variability. In the next phase we have to adapt our dissolution tools in such a way that we will be able to simulate the *in vivo* situation in wide variability of expected physiological / pathological conditions. We have to use suitable apparatuses; in some cases, conventional apparatuses can be used; for example, to simulate only pH or medium composition variability when this is the only or the most critical parameter influencing dosage form performance. However, frequently non-conventional systems have to be applied as certain / extreme values of some physiological parameters cannot be simulated in pharmacopoeial systems.

The influence of variability of GI tract parameters on dissolution profiles has already been shown in many stud-



ies; and different dissolution is frequently reflected in different absorption and plasma profiles. Kambayashi et al (7) demonstrated that variability of plasma profiles could be successfully predicted considering variability of physiological conditions with special emphasis on gastric retention time of tablets, while Nagelj-Kovačič et al. (8) additionally showed that variability of both, gastric pH and tablet gastric emptying time in physiological range might produce substantial contribution to overall variability of plasma profiles through the influence on dissolution. Additionally, Kersten et al (9) showed that variable pH values simulating those in the stomach of newborns in combination with low volume of gastric medium might influence significantly the dissolution of drugs with pH dependent low solubility.

Also variability of transit times of pellets through fasted or fed stomach might contribute significantly to variability of dissolution profiles. Transit times through stomach are especially important for dosage forms which have pH dependent drug release. In the work of Klein et al (10) it was shown that variability of pellet gastric emptying kinetics can contribute substantially to the variability of dissolution / absorption / plasma profiles.

Additionally, different experimental setups were developed to simulate different variable situations in GI tract, different movement patterns (11), exposure to different physical burdens inside different parts of GI tract or in sphincters (12), etc. Also TIM pediatric model was developed mimicking different conditions in GI tract of infants and children to predict bioaccessible amounts of drugs after administration (13).

CONCLUSION

Thus, there is a huge variability of GI conditions in healthy individual and even greater in special groups of people, but their influence on a dosage form performance depends also on the dosage form properties and drug susceptibility to certain parameter. However, we still do not know conditions in GI tract in their specific details well enough; we need more knowledge about the dosage form performance under specific conditions and new tools to simulate and predict it.

REFERENCES

1. Bowles A, Keane J, Ernest T et al. *Int. J. Pharm.* 2010; 395: 37–43.
2. Abdel-Rahman S, Amidon GL, Kaul A. et al. *Clin. Ther.* 2012, 34(11): S11–S24.
3. Kaye JL. *Int. J. Clin. Pharm.* 2011; 33:20–24
4. Britton E, McLaughlin JT. *Proc. Nutr. Soc.* 2013; 72: 173–177.
5. O'Mahony D, O'Leary P, Quigley EMM. *Drugs Aging* 2002, 19 (7): 515-527.
6. Kokubo T, Matsui S, Ishiguro M. *Pharm. Res.* 2013; 30: 402–411.
7. Kambayashi A, Blume H, Dressman J. *Eur. J. Pharm. Biopharm.* 2013; 85: 1337–1347.
8. Nagelj Kovačič N, Pišlar M, Ilić I et al. *Int. J. Pharm.* 2014, in press.
9. Kersten E, Klein S. *9th World Meeting on Pharmaceutics, Biopharmaceutics and Pharmaceutical Technology, Lisbon, 2014.*
10. Klein S, Garbacz G, Pišlar M et al. *J. Control. Rel.* 2013; 166: 286–293.
11. Bogataj M, Cof G, Mrhar A. 2010, *PCT, WO 2010/014046 A1.*
12. Garbacz G, Wedemeyer RS, Nagel S et al. *Eur. J. Pharm. Biopharm.* 2008, 70: 421–428.
13. Havenaar R, Anneveld B, Hanff LM et al. *Int. J. Pharm.* 2013; 457: 327–332.





TAILORING NANOMATERIALS FOR PERSONALIZED DRUG DELIVERY: SAFETY AND EFFICACY

E. Fattal^{1,*}

¹ Université Paris Sud, Institut Galien Paris-Sud, CNRS-UMR 8612, Faculté de Pharmacie, 92296 Châtenay-Malabry, France

INTRODUCTION

Poly(lactide-co-glycolide) (PLGA) nanoparticles has been widely applied to the delivery of several drugs among which anti-infective drugs systemically and by pulmonary administration and anticancer drugs mainly by systemic administration. In this latest case, the potentialities of nanoparticles have mainly been based on the observation that the endothelium surrounding solid tumours are permeable to colloidal carriers which could use this pathway to extravasate from blood to tumour tissues. This so-called enhanced penetration and retention (EPR) mechanism is highly discussed today since there are a lot of inter-individual physiological differences in each patient regarding extravasation and diffusion across the extracellular matrix. To circumvent this problem, we are developing a strategy that combine imaging and drug delivery which should, by ultrasound imaging or MRI, allow following the fate of nanoparticles and helping in the decision of pursuing the treatment or not (1,2). Moreover, before getting into clinics, nanoparticles need to be clearly demonstrated as safe. One tissue very sensitive to nanotoxicity is lungs. We have investigated the impact of biodegradable nanoparticles on this specific organ (3).

Nanoparticles for theranostics

PLGA-PEG nanocapsules containing a liquid core of perfluorooctyl bromide were synthesized by an emulsion-evaporation process and designed as contrast agents for 19F MRI (4, 5, 6). Physico-chemical properties of plain and PEGylated nanocapsules were compared. The encapsulation efficiency of PFOB, estimated by 19F NMR spectroscopy, is enhanced when using PLGA-PEG in-

stead of PLGA. PLGA-PEG nanocapsule diameter, measured by Dynamic Light Scattering is around 120nm, in agreement with Transmission Electron microscopy (TEM) observations. TEM and Scanning Electron Microscopy (SEM) reveal that spherical core-shell morphology is preserved. PEGylation is further confirmed by Zeta potential measurements and X-ray Photoelectron Spectroscopy. *In vitro*, stealthiness of the PEGylated nanocapsules is evidenced by weak complement activation. Accumulation kinetics in the liver and the spleen was performed by 19F MRI in mice, during the first 90 minutes after intravenous injection. In the liver, plain nanocapsules accumulate faster than their PEGylated counterparts. We observe PEGylated nanocapsule accumulation in CT26 xenograft tumor 7 hours after administration to mice, whereas plain nanocapsules remain undetectable, using 19F MRI. Our results validate the use of diblock copolymers for PEGylation to increase the residence time of nanocapsules in the blood stream and to reach tumors by the Enhanced Permeation and Retention (EPR) effect.

The same nanocapsules were loaded with paclitaxel. The loading was high and likely to be limited to the shell of the nanocapsules. Pharmacokinetics and biodistribution show that drug loaded nanocapsules follow the same profile observed in imaging experiments.

Nanoparticle Safety

Modifying nanoparticle surface has large impact on toxicity. Whereas PLA nanoparticles induce the secretion of acute phase protein after *i.v.* administration (7). This is not the case for PLA-PEG nanoparticles. Moreover, we have shown no toxicity on Calu-3 or A549 cells of PLGA nanoparticles (7, 8, 9).

To extend the toxicity studies to other organ such as lungs, we have developed a co-culture model of THP-1/A549 cells (Figure 1)) to evaluate the toxicity of the PLGA NPs.

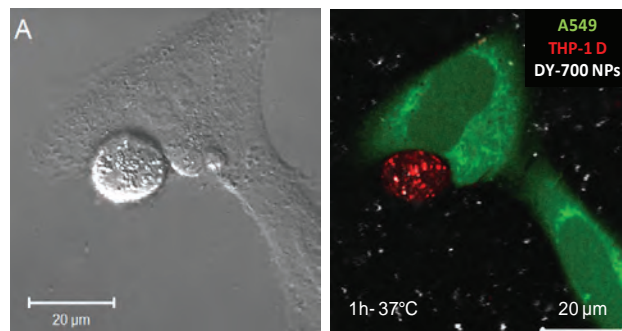


Fig. 1: Nanoparticle uptake by both A549 and THP-1 cells in coculture. Particles are labelled with DY700 (white dots)



This model was shown to be relevant for *in vitro* pulmonary nanotoxicology studies. It was possible to detect a mild inflammatory response to PLGA nanoparticles stabilized by three different hydrophilic polymers PVA, CS and PF68, but very limited compared to well-known inflammatory compounds (Table 1).

In vivo in mice the administration of biodegradable NPs did not induce an inflammation process as opposed to non biodegradable NPs for which all parameters measured clearly evidenced a toxicity after acute administration.

CONCLUSIONS

Our results validate the use of diblock copolymers for PEGylation to increase the residence time of nanocapsules in the blood stream and to reach tumors by the Enhanced Permeation and Retention (EPR) effect. This added to a low toxicity should support the optimisation of PLGA nanoparticles for drug delivery.

Table 1. Neutrophils and macrophage counting and cytokine expression in broncho-alveolar lavage of mice treated with different nanoparticles

	Vehicule	NP PLGA/CS	NP PLGA/PVA	NP PLGA/PF68	NP PS	NP TiO ₂ (a)	NP TiO ₂ (r)
Macrophages	-	-	-	-	-	-	+
Neutrophils	-	-	-	-	-	+	-
IL-6	-	-	-	-	+	+	-
MCP-1	-	-	-	-	+	+	-
TNF- α	-	-	-	-	-	+	-

REFERENCES

1. Diou O., N. Tsapis, E. Fattal Targeted nanotheranostics for personalized cancer therapy. *Exp. Op. Drug Deliv.*, 2012; 9:1475-1487.
2. Diaz-Lopez R., N. Tsapis, E. Fattal Liquid Perfluorocarbons as Contrast Agents for Ultrasonography and 19F-MRI. *Pharm. Res.*, 2010; 27:1-16.
3. Fattal E., Grabowski N., Mura S., Vergnaud J., Tsapis N., Hillaireau H. Lung toxicity of biodegradable nanoparticles. *Journal of Biomedical Nanotechnology* (in press 2014).
4. Pisani E., C. Ringard, V. Nicolas, E. Raphaël, V. Rosilio, L. Moine, E. Fattal, N. Tsapis Tuning microcapsules surface morphology using blends of homo and copolymers of PLGA and PLGA-PEG. *Soft Mat.*, 2009; 5, 3054-3060.
5. Pisani E., N. Tsapis, B.Galaz, M.Santin, R.Berti, N.Taulier, E. Kurtisovski, O. Lucidarme, M. Ourevitch, B. Thuy Doan, J-C. Beloeil, B. Gillet, W. Urbach, L. Bridal, E. Fattal - Perfluorooctyl bromide polymeric capsules as dual contrast agents for ultrasonography and magnetic resonance imaging. *Adv. Funct. Mat.*, 2008; 18: 2963-297.
6. O. Diou, N. Tsapis, C. Giraudeau, J. Valette, C. Gueutin, F. Bourasset, S. Zanna, C.Vauthier, E. Fattal. Long-circulating perfluorooctyl bromide nanocapsules for tumor imaging by 19F-MRI. *Biomaterials*, 2012; 33:5593-602.
7. Fernandez-Urrusuno R., E. Fattal, D. Porquet, J. Feger, P. Couvreur Influence of the surface properties on the inflammatory response to polymeric nanoparticles. *Pharm. Res.*, 1995; 12:1385-1387.
8. Mura S., Hillaireau H., Nicolas J., Kerdine-Römer S., Le Droumaguet B., Deloménie C., Nicolas V., Pallardy M., Tsapis N., Fattal E. Biodegradable nanoparticles meet the bronchial airway barrier: how surface properties affect their interaction with mucus and epithelial cells. *Biomacromolecules*, 12(11), 4136-4143, (2011).
9. Mura S., Hillaireau H., Nicolas J., Le Droumaguet B., Gueutin C., Zanna S. Tsapis N., Fattal E. Influence of surface charge on the potential toxicity of PLGA nanoparticles towards Calu-3 cells. *Int. J. Nanomed.*, 2011; 6:2591-2605.
10. Grabowski N, Hillaireau H, Vergnaud J, Santiago La, Kerdine-Romer S, Pallardy M, Tsapis N, Fattal E. Toxicity of surface-modified PLGA nanoparticles towards lung alveolar epithelial cells. *Int. J. Pharm.* 2013; 454:686-694.





COMPLEX PATIENTS, COMPLEX MODELS: PBPK MADE EASY?

GT Tucker^{1,2}

¹ University of Sheffield UK; ² Simcyp Ltd, Sheffield UK

The application of physiologically-based pharmacokinetic (PBPK) modelling is coming of age in drug development and regulation, reflecting significant advances over the past 10 years in the predictability of key pharmacokinetic parameters from human *in vitro* data and in the availability of dedicated software platforms and associated data bases. With respect to understanding co-variates and variability, focus in applying PBPK has been on anticipating the quantitative impact of drug-drug interactions, age, genetics, racial differences, food effects and pharmaceutical formulation. In principle, it is also possible to incorporate pathological features in PBPK models to predict PK in specific disease states defined by aetiology and/or severity. As a start, some progress has been made in predicting the effects of liver cirrhosis and morbid obesity (including bariatric surgery) based on prior knowledge of physiological and relevant biochemical changes. The consequences of impaired drug metabolism as an accompaniment to progressive deterioration in renal function have also been incorporated into prediction of the impact of renal disease. These extensions of PBPK modelling, along with the incorporation of the PK of biologicals and moves towards linking PBPK to pharmacodynamic (PD) outcome, are clearly of benefit in understanding extremes of risk in different patient populations as part of the process of drug development. Indeed, mechanistic PBPK modelling is the only efficient methodology that can anticipate the combined effects of many patient variables acting simultaneously. Apart from its use in drug development, PBPK also has potential application in the health care arena as an educational tool and for the provision of computerised, 'point of care' advice on personalized drug dosage. Multi-drug treatment of the complex patient is a considerable clinical challenge. One day, when sufficient information is available in the patient, clinicians may be able to link that person to his or her virtual twin within a PBPK-PD model on an iPad to provide safe, effective, individualised dosage, and to avoid undesired drug-drug interactions. If the physician considers this too complex, the friendly clinical pharmacist will be looking over his/her shoulder to provide further guidance.

KEYNOTE LECTURES





SYSTEMS PHARMACOLOGY IN DRUG DEVELOPMENT - TOWARDS PRECISION TREATMENTS

M. Danhof^{1,2}

¹ Leiden University, Leiden Academic Centre for Drug Research, Leiden, the Netherlands

² President European Federation of Pharmaceutical Sciences

INTRODUCTION

Systems pharmacology is an emerging discipline, which connects systems biology to quantitative pharmacology. A specific feature of systems pharmacology is the focus on biological networks as the basis for drug action. This is important as the network concept explains the well-known plasticity of biological systems with regard to i) drug action (i.e. the often observed lack of efficacy) and ii) disease (i.e. the resilience of disease progression to degeneration)

SYSTEMS BIOLOGY - A NOVEL SCIENTIFIC BASIS

Systems biology focuses on the structural and functional integration in biological systems to understand (variation in) function. To this end a combination of “reductionist” and “integrationist” approaches is applied. A unique aspect is the multi-dimensionality of this endeavor. The first dimension is the analysis of biological phenomena as dynamic processes across different time scales, which is often referred to as horizontal integration. Next, systems biology also considers integration at different spatial scales (i.e. at the molecular, the cellular, the organ level), which is referred to as the vertical integration [1,2].

Meanwhile, systems biology approaches (i.e. multivariate statistical analysis of metabolome profiles) are increasingly applied to obtain novel insights in the molecular pathways of disease. So far less attention has been paid to the analysis of the effects of drugs on proteome and metabolome profiles. It is anticipated that the analysis of the effects of “drug challenges” can provide unique insights in the functioning of biological systems [3].

SYSTEMS THERAPEUTICS - TOWARDS PRECISION TREATMENTS

Systems biology constitutes a scientific basis for the development of “systems therapeutics” interventions for serious and chronic progressive disorders. Such therapeutic interventions are personalized treatments, both with regard to the selection of the drug(s) (to account for variation in the characteristics of the disease), and the dosing regimen (to account for variation in the pharmacology between patients). Moreover, these interventions are intended to be disease modifying rather than symptomatic. As a result the emphasis is on pre-emptive and preventive treatments, which may be initiated *prior* to the appearance of the clinical manifestations of the disease. This emphasizes the need for accurate and precise diagnostic tools. Finally, to overcome the plasticity of biological systems, these therapeutic interventions are likely to be complex, including the use of multi-target drugs or rational drug combinations. The successful application of systems therapeutics interventions requires the availability of novel biomarkers not only for diagnostic purposes (the characteristics of the disease, to assess the responsiveness to a given treatment) but, in the absence of clinical signs in the early phases of the disease, in particular also for monitoring of the treatment response. Systems therapeutic interventions are “precision treatments”. The development and the implementation of “precision treatments” in clinical practice will have major implications for both the pharmaceutical sciences and pharmacy practice.

MECHANISM-BASED PKPD MODELING

In recent years important progress has been made in the field of mechanism-based pharmacokinetic-pharmacodynamics (PKPD) modeling. PKPD modeling aims at the characterization and prediction of the time course of drug effects *in vivo*. To this end it considers the cascade of processes on the causal path between drug administration and response. The pertinent processes considered are: a. the target site distribution kinetics, b. the target binding and activation kinetics, and c. the transduction and homeostatic feedback [4,5]. For this purpose, mechanism-based PKPD modeling utilizes concepts from physiology-based pharmacokinetic (PBPK) modeling, receptor theory and dynamical systems analysis. Most recently, to characterize the effect of drug treatment on disease progression, the concept of disease systems analysis has been introduced [6]. Mechanism-based PKPD modeling relies on biomarkers which reflect, in a quantitative manner, the processes on the causal path between drug administration and effect [7].



To date mechanism-based PKPD modeling is widely used in translational research for the prediction of drug effect in man, as the basis of early proof-of-concept studies. Meanwhile mechanism-based PKPD modeling is increasingly used in clinical research, as the basis to understand inter-individual variation in drug response. This is important for optimization of the design of clinical trials in special patient groups and for the individualization of drug treatment in clinical practice [8].

CONCLUSION

Through the interfacing of systems biology and mechanism-based PKPD modeling, systems pharmacology arises as a novel discipline. It constitutes the scientific basis for the design, the development and the use of novel systems therapeutics interventions

REFERENCES

1. Kohl P, Crampin EJ, Quinn TA, Noble D (2010) Systemsbiology – an approach. *Clin. Pharmacol. Ther.* 88: 25-33.
2. Quantitative and Systems Pharmacology in the Post-genomic Era: New Approaches to Discovering Drugs and Understanding Therapeutic Mechanisms (Sorger PK and Allerheiligen SRB eds.), NIH, 2011.
3. Arrell DK, Terzic A. (2010) Network systems biology for drug discovery. *Clin. Pharmacol. Ther.* 88, 120–125.
4. Danhof M, de Jongh J, De Lange EC, Della Pasqua O, Ploeger BA, Voskuyl RA (2007): Mechanism based pharmacokinetic-pharmacodynamic modeling: biophase distribution, receptor theory, and dynamical systems analysis. *Annu Rev PharmacolToxicol.* 47:357-400
5. Westerhout J, Ploeger B, Smeets J, Danhof M, de Lange EC. (2012): Physiologically based pharmacokinetic modeling to investigate regional brain distribution kinetics in rats. *AAPS J.* 14(3):543-553.
6. Post TM, Schmidt S, Peletier LA, de Greef R, Kerbusch T, Danhof M (2013) Application of a mechanism-based disease systems model for osteoporosis to clinical data. *J Pharmacokinet Pharmacodyn.* 40(2):143-156.
7. Danhof M, Alvan G, Dahl SG, Kuhlmann J and Paintaud G (2005). Mechanism-based Pharmacokinetic-Pharmacodynamic Modelling – A new classification of biomarkers. *Pharm. Res.* 22: 1432-1437.
8. Krekels EH, Tibboel D, de Wildt SN, Ceelie I, Dahan A, van Dijk M, Danhof M, Knibbe CA (2014): Evidence-Based Morphine Dosing for Postoperative Neonates and Infants. *Clin Pharmacokinet.* 2014 Feb 5. [Epub ahead of print]

NANOMEDICINES FOR TARGETING THE EPITHELIAL BARRIERS OF GUT, SKIN AND LUNG

Claus-Michael Lehr

Helmholtz-Institute for Pharmaceutical Research Saarland (HIPS)
Saarland University, 66123 Saarbrücken, Germany

INTRODUCTION

The focus of our research over the past few years has been on the epithelial barriers of the gastro-intestinal tract, the skin and the lungs. While these outer biological barriers of the human body are the major routes for non-invasive drug delivery in general, they may also sometimes represent important therapeutic targets by themselves, in particular in the context of inflammatory and infectious diseases. This presentation will highlight some of our recent work in these three areas, either concerning the development of new in-vitro models or of new drug carriers systems, for which the nano-size often has turned out to be advantageous.

PARTICLE TARGETING TO THE INFLAMED INTESTINAL MUCOSA

For the treatment of inflammatory bowel diseases (IBD) we could previously demonstrate that anti-inflammatory drugs show a prolonged alleviation of colitis syndromes in animal models and a reduction of central nervous side effects, when delivered by polymeric nanocarriers compared to the same dose of the drug administered as an aqueous solution. [1, 2]. In order to study the mechanisms of this intriguing phenomenon we established 3D co-culture model of the intestinal mucosa, comprising human epithelial as well as dendritic cells and macrophages grown on a collagen support. In this system, an inflammation can be experimentally induced and its level be quantified by measuring interleukin release [3,4]





TRANSFOLLICULAR DELIVERY OF ANTIGENS

By studying the interaction of nanoparticles with the skin barrier, we found a surprising, size dependent penetration into hair follicles [7]. An excellent correlation was found between follicular penetration in human forearm skin *in vivo* and pig ear skin *in vitro* [8]. Hypothesizing that this route would possibly allow the non-invasive delivery of antigens to dendritic cells of the skin hair follicles, ovalbumin was encapsulated in chitosan-coated PLGS nanoparticles and applied to the back of shaved mice, but verifying that the skin barrier was not impaired, indeed. The results of an adoptive transfer model of TCR transgenic CD4+ cells in mice provided first evidence that such transfollicular immunization through the intact skin is possible, thereby stimulating antigen-specific T cells without the need of using any needles, chemical or physical penetration enhancers [9].

INHALATION NANOPHARMACEUTICALS

Due to their large surface area and excellent blood supply, the lungs represent an attractive alternative for drug delivery, both for local as well as for systemic action. However, alveolar surfactant and bronchiotracheal mucus represent significant non-cellular barriers [10,11]. In this context, we are working on new *in vitro* models as well computational approaches to optimize particle deposition on pulmonary cell culture systems, as well as to modulate their mucociliary clearance, their penetration through mucus, as well as the interaction with lung surfactant proteins [12,13]. In order to engineer safer nanomaterials, there is a need to understand, systematically evaluate, and develop constructs with appropriate cellular uptake and intracellular fates; in this context also NP geometry and surface orientation were found to influence the mode of cellular uptake [14]. Last but not least, inhalation nanopharmaceuticals bear also some interesting opportunities to improve the efficacy of anti-infective drugs: Ultra-small, mucus-penetrating solid lipid nanoparticles were found to significantly enhance the pulmonary delivery and anti-virulence efficacy of novel quorum sensing inhibitors [15].

REFERENCES

1. Lamprecht, A, N Ubrich, H Yamamoto, U Schäfer, H Takeuchi, P Maincent, Y Kawashima, and C-M Lehr. *Biodegradable Nanoparticles for Targeted Drug Delivery in Treatment of Inflammatory Bowel Disease*. *J.Pharmacol.Expt.Therap.* 299 (2001): 775–81.
2. Lamprecht, A, U Schäfer, and CM Lehr, *Size-Dependent Bioadhesion of Micro- and Nanoparticulate Carriers to the Inflamed Colonic Mucosa*. *Pharm. Res.* 18 (2001): 788–93.
3. Leonard F., Collnot EM, and Lehr CM, *Mol. Pharm* 7, (2010) 2103–2119
4. Leonard, F, H. Ali, E.-M. Collnot, B. J. Crieleard, T. Lammers, G. Storm, and C.M. Lehr, *ALTEX* 29 (2012) 275–285
5. Schmidt, C., Lautenschlaeger, C., Collnot, E.-M., Schumann, M., Bojarski, C., Schulzke, J.-D., Lehr, C.-M., and Stallmach, J. *Control Rel.* 165 (2013) 139-145
6. Ali, H, B Weigmann, MF Neurath, EM Collnot, M Windbergs, and CM Lehr. *Budesonide Loaded Nanoparticles with pH-Sensitive Coating for Improved Mucosal Targeting in Mouse Models of Inflammatory Bowel Diseases*. *J.Control.Rel.* 183 (2014) 167–77.
7. Patzelt, A, H Richter, F Knorr, U Schäfer, CM Lehr, L Dähne, W Sterry, and J Lademann. *Selective Follicular Targeting by Modification of the Part. Sizes*. *J.Control.Rel.* 150 (2011) 45-48.
8. Raber, AS, A Mittal, J Schäfer, U Bakowsky, J Reichrath, T Vogt, UF Schaefer, S Hansen, and CM Lehr. *Quantification of Nanoparticle Uptake Into Hair Follicles in Pig Ear and Human Forearm*, *J. Control. Rel.* 179 (2014): 25–32.
9. Mittal, A, AS Raber, UF Schaefer, S Weissmann, T Ebensen, K Schulze, CA Guzmán, S Hansen, CM Lehr, *Vaccine*, 31 (2013) 3442-3451
10. Ruge CA, J. Kirch, and CM Lehr. *Pulmonary Drug Delivery: From Generating Aerosols to Overcoming Biological Barriers- Therapeutic Possibilities and Technological Challenges*. *Lancet. Resp. Med.* 1 (2013) 402–13.
11. Kirch, J, Schneider, A, Abou, B, Hopf, A, Schaefer, U.F., Schneider, M., Schall, C., Wagner, C., Lehr, CM *Optical tweezers reveal relationship between microstructure and nanoparticle penetration of pulmonary mucus*, *PNAS* 109 (2012) 18355-18360
12. Ruge, C.A., Schäfer, U.F., Herrmann, J., Kirch, J., Ca adas, O., Echaide, M., Pérez-Gil, J., Casals, C., Müller, R., Lehr, C.-M., *PLoS ONE*, 7 (2012) e40775.
13. Schäfer, J., Schulze, C., Marxner, E.E.J., Schäfer, U.F., Wohlleben, W., Bakowsky, U., Lehr, C.M., *ACS Nano*, 6 (2012) 4603-4614.
14. Herd, H, N Daum, AT Jones, H Huwer, H Ghandehari, and CM Lehr. *NP Geometry and Surface Orientation Influence Mode of Cellular Uptake*. *ACS Nano* 7 (2013) 1961–73.
15. Nafee, N, A Husari, CK Maurer, C. Lu, C de Rossi, A Steinbach, RW Hartmann, CM Lehr, and M Schneider. *Antibiotic-free nanotherapeutics: Ultra-small, mucus-penetrating solid lipid nanoparticles enhance the pulmonary delivery and anti-virulence efficacy of novel quorum sensing inhibitors*, *J. Control. Rel.* 192 (2014) 131–140



PROTAMINE – OLIGONUCLEOTIDE – NANOPARTICLES: RECENT ADVANCES IN DRUG DELIVERY AND DRUG TARGETING

A. Zimmer ^{1,*}

*¹ University of Graz, Institute of Pharmaceutical Sciences,
Department of Pharmaceutical Technology, Universitätsplatz 1,
8010 Graz – member of: BioTechMed-Graz, Austria*

In the year 2000 for the first time a new method for preparing solid nanoparticles from antisense oligonucleotides together with the cationic peptide protamine was invented by our group. Before, the aggregation into compact structures with short segments of single-stranded DNA was only reported with the polycation poly(L-lysine). We have named this new drug delivery system “proticles” [1]. Within our next study comparing the polycations protamine, spermine and spermidine in terms of their potential to condense different types of oligonucleotides and antisense drugs, protamine was found to be most efficient to form nanoparticles in the size range of 100 - 200 nm [2]. Protamine a peptide well known as pharmaceutical excipient is derived from the sperm of salmon with a molecular mass of approx. 4000 Da and consists of about 70 mol% arginine. In our first evaluations as colloidal nanosuspension these nanoparticles protected oligonucleotides very efficiently against enzymatic digestion caused by nucleases. Also the very early research in this field demonstrated an improved cellular uptake of oligonucleotides combined with significant antisense effects in-vitro [2].

Antisense drugs in general were evaluated as potential anti-viral substances starting from 1990 and in this field of research we could demonstrate for proticles loaded with an AS-PTO drug directed against human immunodeficiency virus type 1 (HIV-1) tat mRNA a very efficient transfection of HIV-1 target cells. Protamine was used to complex AS-ODN and AS-PTO to form nanoparticles with

diameters of about 180 nm and surface charges up to +30 mV. Cellular uptake of these nanoparticles was significantly enhanced compared to naked oligonucleotides and showed the release of the antisense compound leading to a specific inhibition of tat mediated HIV-1 transactivation [3]. Further research in this field characterized the physicochemical properties of these new nanoparticles and a comparison between different transfection reagents showed lowest cytotoxicity in-vitro for proticles but highest efficacy for cationic lipids [4,5]. Therefore next steps in research included further optimization of the protamine nanoparticles. Albumin was found to be a potent stabilizer of proticles and in addition to the basic binary systems, ternary systems showed superior properties in terms of cellular uptake and intracellular ODN distribution [6-8]. A combination of proticles with liposomes was reported in 2005. Junghans et al. showed the possibility to coat the protamine ODN particle with a lipid film. Further innovation came from the application of protamine sulfate to modify the particle diameter in the lower nanometer range more efficiently [9,10]. One year later the first publication which evaluated the immunogenic properties of proticles showed also the possibility to improve the immune-modulation of CpG oligonucleotides which were loaded into proticles [11]. Most successfully proticles with non-immunogenic CpG control oligonucleotides were found to be not immunogenic at all and all basic proticle formulation including pure protamine were tolerated very well and were also found to be highly biocompatible in-vivo.

Therefore the next steps in research addressed the question of active drug targeting by coating the nanoparticle with targeting sequences or to use the proticles as depot system for peptide drugs [12,13]. Consequently in 2010 it was demonstrated for the first time to target proticles loaded with VIP specifically to tumor cells which overexpressed the VPAC receptor. This approach could be also demonstrated in human lung tumor tissue ex-vivo [14]. Further, targeting of proticles was established for diagnostic purposes using adiponectin as targeting sequence for enhanced imaging of atherosclerotic plaques [15]. More recently our research included also methods to simulate the self-assembly process which is responsible for the nanoparticle formation and to establish a microreactor technology to scale-up the manufacturing process [16-17]. Up to now, this improved technology again was applied to study the possibility of proticle to act as adjuvant and immune-modulator in-vivo [18] and in combination with an improved IL-10 mediated targeting differences were investigated between proticles and targeted liposomes ex-vivo in mice [19].





All together, this presentation will provide a comprehensive overview about our research in this field during the last 15 years.

REFERENCES

1. Junghans M., Kreuter J., and Zimmer A., Antisense delivery using protamine - oligonucleotide - particles, *Nucleic Acids Res* 28 (2000) E45.
2. Junghans M., Kreuter J., and Zimmer A., Phosphodiester and phosphorothioate oligonucleotide condensation and preparation of antisense nanoparticles, *BBA [Protein Structure and Molecular Enzymology]* 1544 (2001) 177-188.
3. Dinauer, N., Lochmann, D., Demirhan, I., Bouazzaoui, A., Zimmer A., Chandra, A., Kreuter, J., and von Briesen, H., Intracellular tracking of protamine/antisense oligonucleotide nanoparticles and their inhibitory effect on HIV-1 transactivation, *J Control Release* 96 (2004) 497-507.
4. Lochmann, D., Weyermann, J., Kreuter, J., Vogel, V., Schubert, D., Dinauer, N., Von Briesen, H., and Zimmer A., Physicochemical characterization of protamine-phosphorothioate nanoparticles, *J Microencapsulation* 21 (2004) 625-641.
5. Weyermann, J., Lochmann, D., and Zimmer A., Comparison of antisense oligonucleotide drug delivery systems, *J Control Release* 100 (2004) 411-423.
6. Vogel, V., Lochmann, D., Weyermann, J., Mayer, G., Tziatzios, C., van den Broek, J. A., Haase, W., Wouters, D., Schubert, U. S., Kreuter, J., Zimmer A., and Schubert, D., Oligonucleotide-protamine-albumin nanoparticles: preparation, physical properties, and intracellular distribution *J Control Release* 103 (2005) 99-111.
7. Lochmann, D., Weyermann, J., Georgens, C., Prassl, R., and Zimmer A., Albumin-protamine-oligonucleotide nanoparticles as a new antisense delivery system. Part 1: Physicochemical characterization, *Eur J Pharm Biopharm* 59 (2005) 419-429.
8. Weyermann, J., Lochmann, D., Georgens, C., and Zimmer A., Albumin-protamine-oligonucleotide-nanoparticles as a new antisense delivery system. Part 2: cellular uptake and effect, *Eur J Pharm Biopharm* 59 (2005) 431-438.
9. Junghans M., Loitsch S.M., Steiniger S., Kreuter J., and Zimmer A., Cationic lipid-protamine-DNA (LPD) complexes for delivery of antisense c-myc oligonucleotides, *Eur J Pharm Biopharm* (2005) 287-294.
10. Mayer G., Vogel V., Weyermann J., Lochmann D., van den Broek J. A., Tziatzios C., Haase W., Wouters D., Schubert U. S., Zimmer A., Kreuter J., and Schubert D., Oligonucleotide-protamine-albumin nanoparticles: Protamine sulfate causes drastic size reduction, *J Control Release* 106 (2005) 181-187.
11. Kerkmann M., Lochmann D., Weyermann J., Marschner A., Poock H., Wagner M., Zimmer A., Endres S., Hartmann G. Immunostimulatory properties of CpG-oligonucleotides are enhanced by the use of protamine nanoparticles, *Oligonucleotides* 16 (4) (2006) 313-322.
12. Kratzer I., Wernig K., Panzenboeck U., Bernhart E., Reicher H., Wronski R., Windisch M., Hammer A., Malle E., Zimmer A., Sattler W. Apolipoprotein A-I coating of protamine-oligonucleotide nanoparticles increases particle uptake and transcytosis in an in vitro model of the blood-brain barrier, *J Control Release* 117 (2007) 301-311.
13. Wernig K., Griesbacher M., Andrae F., Hajos F., Wagner J., Mosgoeller W. and Zimmer A., Depot formulation of Vasoactive Intestinal Peptide by protamine-based biodegradable nanoparticles, *J Control Rel* 130 (2008) 192-198.
14. Ortner A., Wernig K., Kaisler R., Edetsberger M., Hajos F., Köhler G., Mosgoeller W., and Zimmer A., VPAC receptor mediated tumour cell targeting by protamine based nanoparticles, *J Drug Target* 18 (6) (2010) 457-467.
15. Almer G., Wernig K., Saba-Lepek M., Haj-Yahya S., Rattenberger J., Wagner J., Gradauer K., Frascione D., Pabst G., Leitinger G., Mangge H., Zimmer A., Prassl R. Adiponectin-coated nanoparticles for enhanced imaging of atherosclerotic plaques, *International Journal of Nanomedicine* 6 (2011) 1279-1290.
16. Eitzlmayr A., Petschacher Ch., Radl S., Suzzi D., Zimmer A., Khinast J.G., Modeling and Simulation of Polyacrylic acid/Protamine Nanoparticle Precipitation, *Soft Matter* 7 (2011) 9484-9497.
17. Petschacher C., Eitzlmayr A., Besenhard M., Wagner J., Barthelmes, J., Bernkop-Schnürch A., Khinast J.G. Zimmer A., Thinking continuously: a microreactor for the production and scale-up of biodegradable, self-assembled nanoparticles. *Polymer Chemistry* (2013) 4 , 2342 – 2352
18. Pali-Schöll I., Szöllösi H., Starkl P., Scheicher B., Stremnitzer C., Hofmeister A., Roth-Walter F., Lukschal A., Diesner S.C., Zimmer A., Jensen-Jarolim E., Protamine nanoparticles with CpG-oligodeoxynucleotide prevent an allergen-induced Th2-response in BALB/c mice, *European Journal of Pharmaceutics and Biopharmaceutics* (2013) 56-64
19. Almer G., Summers K.L., Scheicher B., Kellner J., Stelzer I., Leitinger G., Gries A., Prassl R., Mangge H. and Zimmer A., Interleukin 10-coated nanoparticle systems compared for molecular imaging of atherosclerotic lesions (2014) in press.



RECENT DEVELOPMENTS ON NANOTHERAPEUTICS: NANOTUBES, QUANTUM DOTS, LIPID BASED CARRIERS

İsmail Tuncer Değim

Gazi University Faculty of Pharmacy, Department of Pharmaceutical Technology, 06330, Etiler, Ankara, Turkey
e-mail: tunc@tr.net

Nanotechnology is growing and developing rapidly especially in engineering and medical sciences. In recent years it has been proposed that carbon materials can be used for drug delivery. Latest study results indicate that transdermal route is the safest way for nanosized materials. If carbon nanotubes (CNTs) are able to penetrate through skin layers or if they can be able to provide enough drug molecules on to the skin surface they can be used to deliver active drug substances for therapeutic purposes but exploration of these kind of pharmaceutical delivery systems and their applications are still at a very early stage of development¹. It has been shown that single-walled carbon nanotubes (SWNTs) and multiwalled carbon nanotubes (MWNTs) can be internalized by living cells and they can pass across the biological membranes in cell culture studies². The internalization of carbon nanotubes by corneocytes has been shown³ in the literature but their drug carrying properties through the skin have not been fully evaluated. In our previous study it has been first shown MWNTs can be used to deliver drug molecules through deeper skin layers. The application of iontophoresis using carbon nanotube electrode having adsorb drug molecules on their surface has been shown and molecules transferred successfully to deeper skin layers⁴. CNTs have been also used to increase dermal penetration of drugs^{5,6}. The penetration enhancement was found to be higher with double walled carbon nanotubes (DWCNTs) and MWCNTs, however the mechanism was still unknown. Penetration of indomethacin was

found to be much higher when indomethacin molecules were introduced to the skin surface with CNTs⁵.

Other materials like quantum dots can also be used for diagnosis and monitoring of living cell trafficking⁷. Recently it has been proposed that quantum dots can be used for drug delivery⁸. Similarly, Zhang et al. have synthesized highly uniform quantum dot-doped chitosan nanobeads for traceable siRNA delivery⁹ and most recently Jia et al. have combined PEI-coated carbon nanotubes with quantum dots for antisense oligonucleotide delivery¹⁰. These innovative approaches have opened up exciting opportunities in targeted DNA and RNA delivery. For example, after being treated with quantum dots – oligonucleotides, cells with differential expression levels of the protein of interest, which correlates with quantum dots fluorescence, can be isolated using fluorescence-activated cell sorting; and, if multicolor quantum dots are used, it will allow the screening of siRNA sequences and the monitoring of downstream cell behaviors in a multiplexed manner.

Lipid based drug delivery systems including liposomes, their derivatives, solid lipid nanoparticles and recently developed system called “Cochleates” have been shown to deliver actively drug substance to targeted tissues. Among them cochleates may be the most interesting ones being recently developed system and they have been recently tested for anticancer drug delivery and enhanced effectiveness on tumor tissues^{11,12}.

As a conclusion some literature based information will be discussed with some case studies for carbon materials, quantum dots and lipid based carriers in the talk. Recent developments, important factors for formulations, ingredients will be given and the mechanisms will be evaluated.

REFERENCES

1. C.R. Martin, P. Kohli, *The emerging field of nanotube biotechnology*, *Nat. Rev. Drug Discov.* 2:29 (2003).
2. Lacerda L, Raffa V, Prato M, Bianco A, Kostarelou K, *Cellpenetrating carbon nanotubes in the delivery of therapeutics*, *Nano Today*, 2: 38 (2007).
3. Monteiro-Riviere NA, Inman AO, Wang YY, Nemanich RJ, *Surfactant effects on carbon nanotube interactions with human epidermal keratinocytes*, *Nanomedicine: Nanotechnology, Biology and Medicine*, 1: 293 (2005).
4. Martínez-Pla JJ, Martín-Biosca Y, Sagrado S, Villanueva-Camañas RM, Medina-Hernández MJ, *Evaluation of the pH effect of formulations on the skin permeability of drugs by biopartitioning micellar chromatography*, *J. Chromatogr. A.*, 1047: 255 (2004).
5. I.T. Degim, D.J. Burgess, F. Papadimitrakopoulos, *Carbon nanotubes for transdermal drug delivery*, *J Microencapsul.* 27: 669 (2010).
6. S. Ilbasmiş-Tamer, S. Yilmaz, E. Banoğlu, I.T. Degim, *Carbon nanotubes to deliver drug molecules*, *J Biomed Nanotechnol.*, 6:20 (2010).
7. Sonvico, Fabio, Dubernet, Catherine, Colombo, Paolo, Couvreur, Patrick. *Metallic Colloid Nanotechnology, Applications in*



Diagnosis and Therapeutics, Current Pharmaceutical Design, Volume 8, Number 16, June 2005, pp. 2091-2105(15)

8. Tan WB, Jiang S, Zhang Y. Quantum-dot based nanoparticles for targeted silencing of HER2/neu gene via RNA interference. *Biomaterials*, 28:1565 (2007).
9. Jia N , Lian Q, Shen H, et al. Intracellular delivery of quantum dots tagged antisense oligodeoxynucleotides by functionalized multiwalled carbon nanotubes. *Nano Lett* , 7:2976 (2007).
10. Degim I.T. and Kadioglu D. Cheap, Suitable, Predictable and Manageable Nanoparticles for Drug Delivery: Quantum Dots *Current Drug Delivery*, 10, 32-38 (2013).
11. Yucel, C, Degim Z, Yilmaz, S, Nanoparticle and liposome formulations of doxycycline: Transport properties through Caco-2 cell line and effects on matrix metalloproteinase secretion, *Biomedicine & Pharmacotherapy*, 67, 459 (2013).
12. Mutlu Agardan, B, Degim, Z, An investigation on tamoxifen or raloxifen (SERM - Selective estrogen receptor modulators) containing new drug delivery systems, PHD Thesis, Gazi University, Faculty of Pharmacy, Ankara Turkey 2013





SELF-ASSEMBLED POLYSACCHARIDE NANOHYDROGELS: A TOOL FOR DRUG SOLUBILIZATION AND DELIVERY

P. Matricardi¹, C. Di Meo¹, G. D'Arrigo¹, E. Montanari¹, T. Coviello¹, F. Alhaique^{1*}

¹ Department of Drug Chemistry and Technologies, "Sapienza" University of Rome, Piazzale Aldo Moro 5, 00185, Rome, Italy

INTRODUCTION

Polysaccharide hydrogels can be formulated in the form of macro-, micro- and nano- systems. Macroscopic networks include films, slabs, beads, as well as matrices for tissue engineering. Recently, nanohydrogels (NHs), i.e., nano-sized hydrogel networks, attracted an ever increasing attention because of the relevant variations of their physical (mechanical, electrical, optical, etc.) properties when compared to those of macroscopic systems. Among the different methods suitable for NHs preparation, the self-assembling approach proposed here is based on hydrophobically modified polysaccharides which, by means of an energy supply (ultrasound, heat, etc.), can aggregate in the form of nanosystems. For this purpose, prednisolone (Pred), a poorly water soluble anti-inflammatory drug, which represented the hydrophobic moiety responsible for the self assembling process, was chemically conjugated to the carboxylic groups of Gellan gum (Ge), whose molecular weight was previously reduced (1). The obtained Ge-Pred NHs have a core-shell structure which allows the entrapment of hydrophobic drugs; thus, considering that an inflammatory microenvironment is an essential component of all tumors and that anti-inflammatory therapy is not cytotoxic on its own, paclitaxel (PCT) was physically loaded within the NHs hydrophobic core, leading to an innovative multi-drug delivery system suitable for a combination therapy in cancer. Preparation, characterization, release behaviour and cytotoxicity of the new NHs are reported. Also other

polysaccharides can be used for the preparation of NHs according to this approach (2): we report here some recent results obtained with hyaluronic acid (HA).

MATERIALS AND METHODS

Ge and HA tetrabutylammonium salt were kindly provided by Fidia Advanced Biopolymers, Abano Terme (Italy). Pred, cholesterol (CH) and PCT were Sigma products. Other chemicals were reagent grade and used without further purification. Ge depolymerization was carried out with a probe type sonicator, using a pulsed mode and the obtained polymer was dissolved in N-methyl-2-pyrrolidone. Due to the steric hindrance of the polysaccharide, a short spacer was needed for the synthesis of Ge-Pred and Ge-CH, thus the Br-butyric derivatives of Pred or CH were previously prepared. The starting polymers as well as their derivatives were characterized by ¹H-NMR and FTIR. Self-assembling was obtained by bath sonication and the obtained NHs were analyzed by dynamic light scattering (DLS), ζ-potential and transmission electron microscopy (CRYO-TEM). For the preparation of the PCT-loaded NHs a dry film of this drug was hydrated and vortexed with the Ge-Pred or Ge-CH NHs previously prepared; HPLC determination of the not-incorporated PCT, which was removed by centrifugation, allowed to calculate the entrapment efficiency. Cellular cytotoxicity was assessed on several types of cells. For an alternative energy supply leading to NHs, a JunoLiarre autoclave operating at 121 °C and 1.10 bar was employed.

RESULTS AND DISCUSSION

The sonication treatment reduced the polymer molecular weight without causing any changes in the chemical structure of the macromolecule, as assessed by bidimensional NMR analysis. Pred moiety, chemically linked to the carboxylic groups of the sonicated Ge allowed the self-aggregation. The average size of NHs was about 300 nm, with a unimodal size distribution, and their ζ-potential values were negative. Biological tests showed that the Ge-Pred NHs are able to promote the pro-apoptotic activity as well as the free Pred, thus suggesting a similar bioavailability of the drug. It is therefore possible to conclude that gellan-based NHs can be considered as efficient innovative Pred carriers. Taking into account that the combination of PCT and steroids is already used in cancer therapy and allows to obtain several advantages, PCT was loaded within the Ge-Pred NHs. Compared to reported PCT solubility in aqueous medium (< 0.1 µg/ml), a 1000 fold increase was detected for the PCT-Ge-Pred NHs formulation. PCT release from the new formula-





tion was evaluated *in vitro* and PCT-mediated cytotoxicity, which was tested on different cell lines (Fig 1), was always remarkably higher than that of the free drug. In order to confirm the above depicted approach, cell viability tests were carried out also using reference NHs prepared with CH (i.e. a not anti-inflammatory steroid) instead of Pred. Obtained results indicated that the PCT-loaded Ge-Pred NHs always significantly improved PCT toxicity with respect to the corresponding PCT-loaded Ge-CH NHs, thus confirming, once more, the synergic effect related to the co-administration of the two drugs (3).

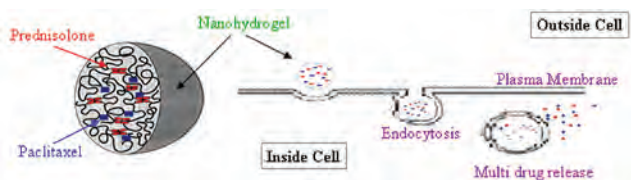


Fig. 1: Scheme of the PCT-Ge-Pred nanohydrogel and of its cellular uptake.

As above mentioned, the self-assembling approach was tested also using other polysaccharides and a different energy supply (4). For this purpose HA-CH was obtained according to the same procedure used for Ge-CH preparation. 20 min autoclaving of water dispersions of each polysaccharide derivative yielded sterile NHs in only one step. Furthermore, within the same step, hydrophilic and lipophilic drugs could be loaded, thus leading to a sterile formulation that can be directly used for administration or for vial filling. The features of NHs obtained according to this procedure were perfectly comparable with those obtained by sonication. In order to increase the stability of the self-assembled systems, the obtained water dispersions can be lyophilized in the presence of a cryoprotectant, leading to the original NHs after re-dispersion in water.

CONCLUSIONS

Collected data suggest that, using hydrophobically modified polysaccharides, self-assembled NHs can be easily prepared by sonication and by autoclaving (in this last case leading directly to a sterile formulation). The obtained NHs are suitable for single or a multi-drug delivery and their structure is stable also after lyophilization. A synergistic effect of the combination of anti-inflammatory and anti-cancer drugs was detected *in vitro* on several types of cells.

REFERENCES

1. D'Arrigo G, Di Meo C, Gaucci E, Chichiarelli S, Coviello T, Capitani D, Alhaique F, Matricardi P, Self-assembled gellan gum nanohydrogel as a tool for prednisolone delivery. *Soft Matter* 2012; 8: 11557-1564.
2. Montanari E, Capece S, Di Meo C, Meringolo M, Coviello T, Agostinelli E, Matricardi P, Hyaluronic acid nanohydrogels as a useful tool for BSAO immobilization in the treatment of melanoma cancer cells. *Macromol. Biosci.* 2013; 13: 1185-1194
3. D'Arrigo G, Navarro G, Di Meo C, Matricardi P, Torchilin V, Gellan gum nanohydrogel containing anti-inflammatory and anti-cancer drugs: a multi-drug delivery system for a combination therapy in cancer treatment. *Eur. J. Pharm. Biopharm.* 2014; 87: 208-216
4. Montanari E, De Rugeris MC, Di Meo C, Coviello T, Alhaique F, Matricardi P, One-step formation and sterilization of gellan and hyaluronan hydrogels using autoclave (submitted).

ORAL PRESENTATIONS





ORODISPERSIBLE FORMULATIONS WITH PREDNISOLONE TASTE-MASKING MICROPARTICLES

E. Maślak^{1*}, W. Brniak¹, R. Jachowicz¹

¹ Department of Pharmaceutical Technology and Biopharmaceutics, Jagiellonian University Medical College, ul. Medyczna 9, 30-688 Krakow, Poland

INTRODUCTION

Orodispersible tablets (ODT) and orodispersible films (ODF) are solid oral dosage forms disintegrating or dissolving rapidly when placed in the mouth. They are intended mainly to be administered to the patients having difficulty in swallowing, particularly in geriatric or paediatric population. The simplest and most popular method of the ODTs manufacturing is direct compression since it requires only conventional tableting equipment and gives the tablets with good mechanical properties. Fast dissolving films (ODF) have the form of a thin strip and are usually produced by solvent casting method. Their main advantage is the low risk of choking, ease of application, and no need of water to wash down the drug.

One of the main issues related to the orodispersible formulation preparation is an efficient taste masking of a bitter drug substance (1). There is a wide spectrum of taste masking technologies (addition of sweeteners and flavors, forming complexes with cyclodextrins, microencapsulation, etc.) (2). The aim of this study was to evaluate the possibility of the formulation of orodispersible dosage forms containing microparticles masking a bitter taste of the prednisolone.

MATERIALS AND METHODS

Materials

Pharmaburst (SPI Polyols, USA), Pruv – sodium stearyl fumarate (JRS Pharma, Germany), prednisolone base (Henan Lihua, China), Eudragit E100 (Degussa, Germany), Aerosil 200 – colloidal silicon dioxide (Evonik, Germany), Pharmacoat 606 (ShinEtsu Chemical Co., Japan), glycerin (Pharma Cosmetics, Poland).

Preparation of microparticles

Prednisolone was dissolved in the acetone-isopropanol-water solution of Eudragit E100. The solution was spray-dried in temperature 40 °C with Büchi Mini Spray Dryer B-191. The drug to polymer ratio was 1:2.

Preparation of tablets

Orodispersible tablets containing 15% of microparticles, i. e. 10 mg of prednisolone were directly compressed with single punch tablet press Korsch EK0. They contained Pharmaburst (82,5%), sodium stearyl fumarate (2,0%) and silicon dioxide (0,5%) as the excipients. Their diameter was 9 mm and mass 200 ± 10 mg.

Preparation of films

The films were prepared by casting method. HPMC (10% Pharmacoat 606) was dissolved in water. The solutions were mixed and glycerol (15% w/w) was added. The microparticles were mixed with the solutions for 30 min. The solutions were poured on the foil using a motorised film applicator (Elcometer 4340 Elcometer, Belgium). The wet films have a thickness of 1 mm. The films were allowed to dry at room temperature for 12 hours and then were cut into rectangular strips (2 x 3 cm).

Tablets parameters

The hardness, friability and disintegration time of prepared tablets were measured with pharmacopoeial methods.

Disintegration time of films

Films with dimensions 3,5 x 4,0 cm were placed in a photo slide frames. The 200 µl of distilled water was dropped on the film, and the time until the film disintegrated was measured (3).

Mechanical properties of films

Mechanical properties were evaluated using the texture analyzer (Shimadzu EZ-SX, Japan). Tensile strength was evaluated according to standard DIN EN ISO 527. Films (2 cm x 15 cm) were placed into the jaws of apparatus and extended with speed 10 mm/min. Percentage of elongation and tensile force was recorded.

Puncture resistance test was performed with the specimens 3,7 x 3,7 cm. They were placed in a holder with a circular hole of 14 mm diameter. The 10 mm diameter spherical probe was moved downward to the film with a constant speed of 10 mm/min. The force needed to puncture the film was recorded (4).



Dissolution test

Dissolution test was performed with a dissolution apparatus type II (SR8 Plus Dissoette II, Hanson Research, USA) in 900 mL of distilled water at 37°C. The rotation speed was 50 rpm. The samples after filtration were assayed with UV-VIS spectrophotometer (V-530, Jasco, Japan).

RESULTS AND DISCUSSION

Prepared ODTs were of excellent mechanical properties. Their hardness was 63N, friability 0,12% while disintegration time was maintained around 27s.

Placebo films prepared with 10% HPMC and 15% glycerol were flexible, elastic, smooth, transparent and without entrapped air bubbles. However, after incorporation of microparticles, films became brittle and their surface was rough. Some air bubbles remained in the matrix. Tensile strength and puncture resistance were higher for placebo films compared with films containing active substance. Disintegration time for placebo films was shorter than 1 min but for those containing microparticles exceeded 2 min.

Dissolution studies showed good taste masking properties of prepared microparticles. The amount of prednisolone released during the first 5 min was below 2%. However, after incorporation to the final orodispersible forms, i. e. ODT and ODF, it increased up to 23% after 2 minutes. The increased release of prednisolone in the orodispersible form could be the result of the faster wetting of the microparticles while dispersed in hydrophilic matrices. In the case of ODT, also the compression force during tableting process could destroy the taste masking layer on the microparticles.

CONCLUSIONS

The research has proved the possibility of effective taste masking of prednisolone by formation of microparticles with Eudragit E100. Nevertheless, the prepared orodispersible formulations need further optimization in order to maintain the desirable release characteristic of the microparticles.

REFERENCES

1. Ayenew Z. et al.: *Trends in Pharmaceutical Taste Masking Technologies: a Patent Review. Recent Pat Drug Deliv Formul.* 2009, 3(1), 26-39.
2. Kawano Y. et al.: *Preparation of Orally Disintegrating Tablets with masking of Unpleasant Taste: Comparison with Corrective-adding Methods. Yakugaku Zasshi.* 2010, 130(1), 75-80.
3. Preis M., Woertz Ch., Schneider K., Kukawka J., Broscheit J., Roewer N., Breitskreutz J.: *Design and evaluation of bilayered buccal film preparations for local administration of lidocaine hydrochloride. European Journal of Pharmaceutics and Biopharmaceutics,* 2014, 86, 552-556.
4. Preis M., Knop K., Breitskreutz J.: *Mechanical strength test for orodispersible and buccal films. International Journal of Pharmaceutics,* 2014, 461, 22-29.





DESIGN AND EVALUATION OF SPECIFIC BI-PHASE EXTENDED RELEASE SYSTEM BASED ON DIFFERENTLY COATED MINI-TABLETS

A. Aleksovski^{1,*}, R. Dreu¹

¹ Department of Pharmaceutical Technology, Faculty of Pharmacy, University of Ljubljana, Aškerčeva cesta 7, 1000 Ljubljana, Slovenia

INTRODUCTION

Mini-tablets - MTs (diameter \leq 3 mm) can be the basis of the multiple unit systems, which offer possibility of combining different drugs and/or combination of different release kinetics with aim to decrease the dosing frequency, improve the intended plasma concentration profile and/or improve the compliance in polypharmacy [1-2]. MTs are produced by using ordinary tablets presses equipped with multiple tip tablet compression tooling and are suitable for subsequent coating [1].

Paliperidon is weakly basic compound belonging to the class of atypical antipsychotics. It is present on the market as 24 hours extended release tablet, produced in form of three layer osmotic pump (OROS[®] push-pull) providing slightly ascending release rate pattern [3]. Pharmaceutical osmotic pumps bring the benefit of the pH independent steady drug release, but also pose disadvantages such as complex and expensive production process of the units and possible bowel blockage in patients with postoperative bowel constriction due to its non-disintegrative nature and size.

The aim of the research was to develop extended release multiple unit oral dosage form of paliperidon based on MTs, containing different matrix-composition and coated with different pH-dependend polymers, a dosage form which would comprise similar *in-vitro* drug release pattern as the osmotic pump system and would be at the same time more patient friendly and more cost-beneficial.

MATERIALS AND METHODS

Materials

Paliperidone - PAL (MSN Laboratoires); Kollidon[®] SR - KSR (polyvinyl acetate/ polyvinyl pyrrolidone) (BASF); milled (mesh 200) - LM and spray dried lactose - LS (DFE Pharma.); magnesium hydroxide - MGH (Fluka); magnesium stearate - MGST (Faci S.p.A.) HPMC 2910, 6 cps (Harke Group); Eudragit[®] L30 D-55 and Eudragit[®] FS 30 D (Evonik). All other reagents were with analytical grade

Mini-Tablet preparation and evaluation

MTs were produced with instrumented single-punch tablet press (Killian SP300, IMA), equipped with flat multi-tip punches and die of 2.5 mm diameter. Formulation F1 was prepared by direct compression, while F2 by wet granulation of the PAL, MGH and LM, subsequent mixing with the rest of the components and compression. The target core mass was 15 mg. MT's coating was performed in a fluid bed coater (BX-CGD1, Brinox). Obtained MTs were investigated for friability, mass uniformity-MU and units uniformity-UU (HPLC) according to pharmacopoeial tests. Drug release studies on 4 MTs (6 mg PAL) and original drug (Invega[®], Janssen) were performed on a USP III apparatus (BioDis, VanKel) in fasted GIT conditions (transit time and pH) through 24 hours (Table 1).

Tab. 1: Dissolution test conditions (pH and cumulative time)

Vessel/GIT part	pH/medium	Cumulative time
1/Stomach	1.2/0.1 M HCl	1h
2/duodenum	5.5/Phosphate buf.	1h 15min
3/jejunum	6.8/ Phosphate buf.	2h 57min
4/ileum	7.4/ Phosphate buf.	4h 15min
5/colon	6.6/ Phosphate buf.	until 24 h

Combined formulation of F1 (1 MT) and F2 (3 MT) was compared to the original one by calculating the similarity factor *f*₂.

RESULTS AND DISCUSSION

After careful evaluation of over thirty formulations we chose two basic formulations for creating combined release system (Tab. 2).





Tab. 2 – Combined product formulation

	F1 (%) / 1MT	F2(%) / 3MT
PAL	10	10
KSR	40	30
LS	49	27
LM	/	27
MGH	/	5
MGST	1	1
HPMC	qs	qs
Eudragit L30 D55	qs	/
Eudragit FS 30 D	/	qs

In both F1 and F2 KSR with dominantly hydrophobic behaviour showed high capability of retarding the drug release and thus its combination with highly soluble diluent such as lactose was required. Due to higher KSR % F1 has shown slower drug release than F2 and with the decay of Eudragite L30 D55 coating at pH 5.5 it was suitable for approx. 23-hours drug release. F2 formulation provided faster drug release compared to F1 and due to that it was coated with the colon-targeting polymer Eudragite FS 30 D (decays in the ileal simulated pH 7.4) and was aimed for PAL release during period of approx. 21 hours. Incorporation of pH modifier MGH into the F2 formulation was done with the intention to decrease the initial release of the active compound and thus increase the similarity factor f_2 between the original formulation Invega® and F2. MGH is pointed as suitable pH modifier since it has high basic strength and low water solubility (possibility to remain longer in the matrix). Combination of 1 MT F1 and 3 MTs F2 provided the required bi-phasic release (similar to the original drug) with slower release pattern ($\approx 10\%$) in the first 4 hours (due to safety reasons) and faster drug release ($\approx 100\%$) up to 24 hours. The combined formulation and the original one showed in-vitro similarity ($f_2=55.31$). Additionally combined MT formulation was compared to a theoretically calculated zero order release kinetics. MT combined formulation showed also high similarity to the linear profile ($f_2=59.11$). The drug release profiles of combined MT formulation and the original drug together with the linear profile are given in Fig. 1.

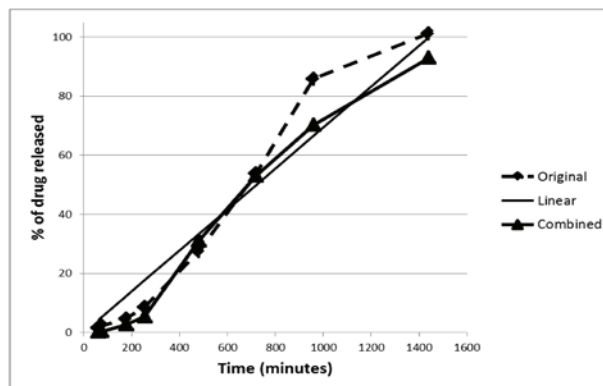


Fig. 1: 24h drug release profiles of dosage forms

Besides providing suitable drug release profile, F1 and F2 individually exhibited acceptable properties regarding pharmacopoeial demands on friability, mass and unit uniformity (Tab. 3)

Tab. 3: Friability, mass and unit uniformity of F1 and F2

	F1	F2
Friability (%)	0.45	0.39
MU (mg)	15.1 ± 0.3	15.08 ± 0.28
CU (AV)	11.80	12.07

CONCLUSIONS

Combining differently coated MTs in one multiple unit formulation proved to be a promising pathway for designing systems with specific extended release patterns (ascending or linear like). Proposed system exhibits low dosage form complexity and low manufacturing costs.

REFERENCES

1. Tissen C, Woertz K, Breitzkreutz J, Kleinbude P Development of mini-tablets with 1mm and 2mm diameter, *Int. J. Pharm.* 2011 ; 416:164-170.
2. Ishida M, Abe K, Hashizume M, Kawamura M. A novel approach to sustained pseudoephedrine release: Differentially coated mini-tablets in HPMC capsules. *Int. J. Pharm.* 2008; 359:46-52.
3. Scientific Discussion – Invega® tablets. EMEA. 2007: 1-58





SIMPLE, BIOCOMPATIBLE AND COST-EFFECTIVE INULIN BASED siRNA DELIVERY SYSTEMS

C. Sardo¹, M. Licciardi¹, C. Scialabba¹, G. Giammona¹, G. Cavallaro¹, F. Tonon², R. Farra², B. Dapas³, M. Grassi², G. Grassi³.

¹ Lab of Biocompatible Polymers, Dipartimento di Scienze e Tecnologie Biologiche, Chimiche, Farmaceutiche (STEBICEF), University of Palermo, Palermo 90123, Italy

² Department of Engineering and Architecture, University of Trieste, Trieste, Italy

³ Department of Life Sciences, Cattinara University Hospital, Trieste University, 34149, Trieste, Italy

INTRODUCTION

Short interfering RNAs (siRNAs) (1), represent an emerging paradigm for the treatment of many human diseases (2-3), however, owing to its hydrophilicity and negative charges, siRNA molecules are not readily taken up by cells and are susceptible to nuclease degradation (4). Thus, much effort has been placed in the development of siRNA delivery systems. Polyplexes, colloidal systems originated from the electrostatic interaction between negative nucleic acids and positive charged polymers, emerged as one of the most versatile systems for nucleic acid delivery (5). In this work, diethylenetriamine (DETA) molecules were grafted onto inulin backbone to generate a novel siRNA delivery system (Inu-DETA).

RESULT AND DISCUSSION

Characterization of Inu-DETA

Among synthetic methods, the use of microwave irradiation in organic synthesis has become increasingly popular within the polymer synthesis and modification area (6). Here, an alternative recent method to perform microwave-assisted organic reactions, termed "Enhanced Microwave Synthesis" (EMS), has been employed (7). By cooling the reaction vessel, under simultaneous microwave irradiation, more energy can be applied to the reaction mixture, ensuring a high, constant level of microwave energy into the reaction, while keeping constant the reaction tem-

perature. The Inu-DETA polymer so generated was able to completely arrest the run of siRNA in an agarose gel, starting from a weight ratio (R) polymer/siRNA of 7; notably, at lower R an interaction between polymer and nucleic acid is still visible. Additionally, DLS results (Figure 1) revealed that although Inu-DETA formed complexes with siRNA at R lower than 7, polyplexes below R10 exhibited a large size, up to 700 nm, with a high polydispersity, suggesting that aggregation occurs. Starting from R10 polyplexes exhibited a decrease of sizes that remain in the range between 300 and 400 nm.

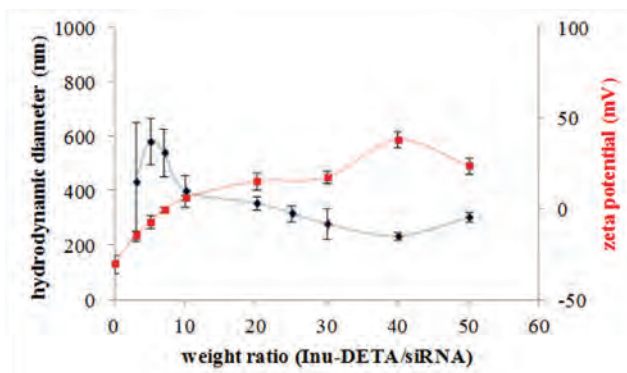


Figure 1. Characterization of Inu-DETA/siRNA polyplexes: hydrodynamic diameter (red square) and ζ -potential measurements (blue circles).

The ζ -potential of Inu-DETA/siRNA polyplexes (Figure 1) increases by increasing the weight amount of copolymer in the polyplex formation: starting from a value of -30 mV for naked siRNA, ζ -potential becomes positive near to R7, and reach the value of ~ 40 mV at R40. These results are in agreements with the data obtained from electrophoresis assay on agarose gel and with size distribution obtained with DLS, in which the higher size and polydispersity values are related to polyplexes with lower ζ -potential. Analysis of Inu-DETA/siRNA polyplexes at R20 by TEM confirmed DLS measurements data.

Impact of Inu-DETA on cell viability

The possible toxic effects were evaluated in 16HBE and JHH6 cell lines. Inu-DETA polymer alone was incubated with cells, in a range of concentrations from 25 to 1000 $\mu\text{g/ml}$ for 4, 24 and 48 hrs. MTT tests on cells treated with Inu-DETA did not show appreciable cytotoxicity, even after 48 hrs of incubation for the entire range of concentrations. Comparable results were obtained incubating the cells with Inu-DETA/siRNA polyplexes.



Efficacy of Inu-DETA in siRNA delivery

Inu-DETA was complexed with a siRNA directed against the mRNA of E2F1 (siE2F1), a protein involved in the promotion of cell cycle (8). As control, Inu-DETA complexed with siGL2, a non-functional siRNA, was used. At R4 and 3 days after administration in JHH6, Inu-DETA/siE2F1 reduced E2F1 mRNA (60% of control) and protein levels compared to controls (Figure 2). This resulted in a reduction of cell growth as evaluated by cell counting (30% reduction) and cell vitality (MTT test, 30% reduction).

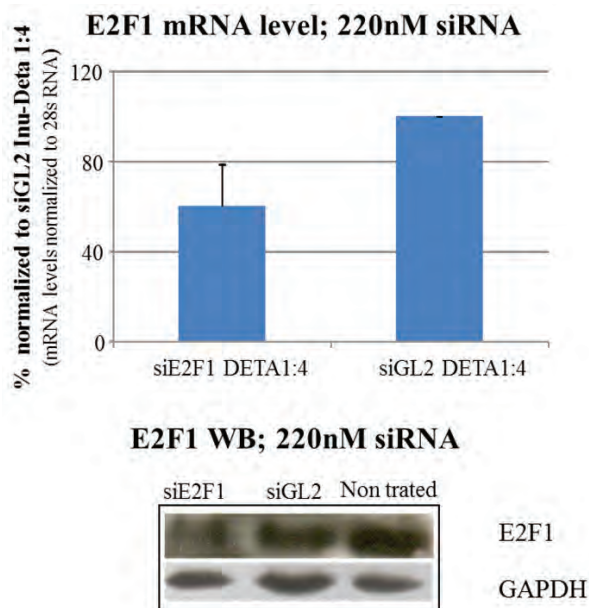


Figure 2. Inu-DETA/siE2F1 specifically reduces E2F1 mRNA and protein levels.

Uptake mechanisms of Inu-DETA

In vitro uptake experiments were performed in 16HBE in the presence of different inhibitors of the cell entry mechanisms; in particular, M β Cy, PAO and WORT were used as lipid mediated endocytosis, clatrin dependent endocytosis and macropinocytosis inhibitors, respectively. Optimal results were obtained using a weight ratio Inu-DETA/siRNA of 40 (R40). As M β Cy but not PAO or WORT inhibited polyplexes uptake (no fluorescence visible in the R40-M β Cy panel compared to R40, Figure 3), it follows that lipid and cholesterol mediated uptake pathways regulate Inu-DETA/siRNA uptake.

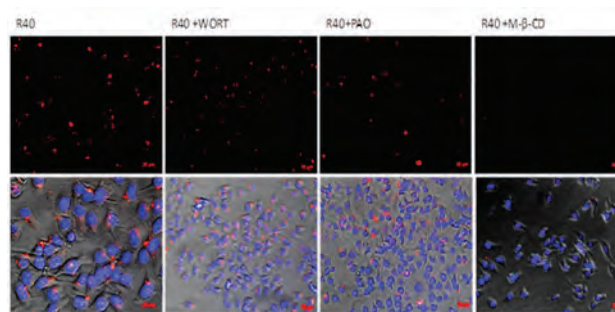


Figure 3. Inhibition of uptake by M β Cy, PAO or WORT. Blue: cell nuclei; red: siRNA

CONCLUSIONS

In this work, DETA molecules were grafted onto inulin backbone to generate a novel siRNA delivery system. The polymer efficiently complexes siRNA and delivers it to model cell lines preserving siRNA functions. Finally, the lipid and cholesterol mediated uptake pathways regulates polymer/siRNA uptake.

REFERENCES

1. Grassi, M., Cavallaro, G., Scirè, S., *Curr Signal Transd T.* 5(2), 92 (2010)
2. Grassi G., Scaggiante B., Dapas B., et al. *Current Medicinal Chemistry.* 20 (28): 3515-38 2013
3. Deng, Y., Wang, C.C., Choy, K.W., Du, Q., Chen, J., Wang, Q., Li, L., Kwok Hung Chung, T., Tang, T., *Gene*, 538, 217 (2014)
4. Li, C.X., Parker A., Menocal, E., Xiang, S., Borodyansky, L. and Fruehauf, J.H., *Cell Cycle*, 5, 2103 (2006)
5. Ballarín-González, B. and Howard, K.A., *Adv Drug Deliv Rev.*, 64, 1717 (2012)
6. Hayes, B.L., *Aldrichimica Acta*, 37(2), 66 (2004)
7. Joubert, J., Sharma, R., Onani, M., Malan, S.F., *Tetrahedron Lett.*, 54, 6923 (2013)
8. B Dapas, R Farra, M Grassi, C Giansante, N Fiotti, Rainaldi, A Mercatanti, A Colombatti, P Spessotto, , G Guarnieri and G Grassi. *Molecular Medicine*, 2009, 15: 296-306



THIOLATED AND S-PROTECTED HYDROPHOBICALLY MODIFIED POLY(ACRYLIC ACID)- A NEW GENERATION OF MULTIFUNCTIONAL POLYMERS

S. Bonengel^{1,*}, S. Hauptstein¹, G. Perera¹,
A. Bernkop Schnürch¹

¹ Center for Chemistry and Biomedicine, Center for Molecular Biosciences, Department of Pharmaceutical Technology Institute of Pharmacy, University of Innsbruck, Innrain 80/82, 6020 Innsbruck, Austria

INTRODUCTION

Alkyl-modified (C10-C30) carbomers (AC1030) with amphiphilic properties are representatives of multifunctional polymers. According to their chemical nature these polymers display additional emulsifying properties compared to non-alkylated carbomers. A further polymer modification, namely thiolated polymers (thiomers), emerged to be valuable multifunctional polymers with noteworthy mucoadhesive properties.

Their ability to form covalent bonds with cysteine-rich subdomains in the mucus gel layer provides excellent mucoadhesive properties (1, 2). As thiol groups are highly susceptible to oxidation, the concept of S-protection was established. Disulphide bonds between the polymeric thiol group and an aromatic thiol bearing ligand are established providing a higher reactivity and stability towards oxidation (3). In order to combine these promising strategies, thiolated AC1030 as well as the preactivated version thereof were synthesized within this study and evaluated as semisolid emulsifying mucoadhesive delivery systems.

MATERIALS AND METHODS

Materials

Carbomers (Carbopol® Ultrez 20/ AC1030 and Carbopol® 981) were kindly supplied by Lubrizol Europe. 2-Mercaptopyridine (2-MNA) was purchased from ABCR GmbH & Co KG, Germany. All other chemicals were purchased from Sigma Aldrich Austria.

METHODS

Synthesis

AC1030-cysteine was synthesized by covalent attachment of L-cysteine via amide bond formation mediated by a water-soluble carbodiimide (EDAC). Purified thiolated AC1030 was obtained after dialysis and lyophilization. Preactivation was achieved by disulphide bond formation between the polymeric thiol groups and 2-MNA according to a previously described method. Dialyses were performed for purification and the preactivated thiomers were lyophilized (Figure 1).

Mucoadhesion

Adhesion to native small intestinal mucosa of the novel conjugates was evaluated by tensile studies as described by our research group (4).

Emulsification capacity

Medium chain triglycerides were incorporated into aqueous polymer solutions. Stability of the resulting formulations (30 % oil, 70 % water and 0.5 % polymer) was determined by centrifugation at 273 g (Table 2).

RESULTS AND DISCUSSION

Synthesis

A schematic description of the synthesized polymers is provided in Figure 1.

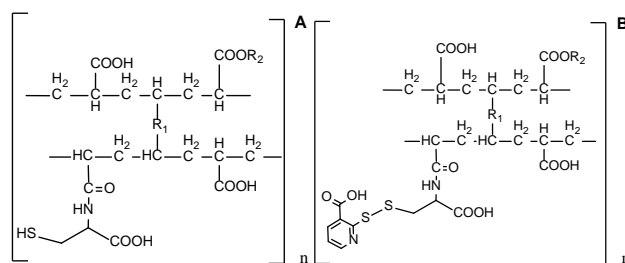


Figure 1: Presumptive structure of thiolated (A) and S-protected (B) AC1030



Mucoadhesion

As illustrated in Figure 2, S-protection provides full reactivity as premature inter-and intramolecular disulphide bond formation within the polymer is prevented, which allows covalent binding to mucus proteins.

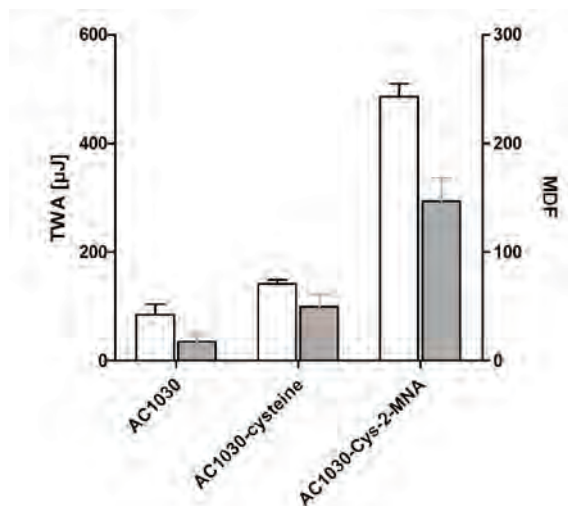


Figure 2: Mucoadhesive properties of AC1030 polymers determined via tensile studies on porcine native small intestinal mucosa

Emulsion stability

Due to their lipophilic residues, all polymers were able to form stable emulsions with oils. Reduced stability of emulsions formed with the preactivated thiomers might be a result of the steric hindrance of the substituent 2-MNA (5).

Tab. 2: Emulsion stability determined via centrifugation at 273 g

	Time stable (min)
NA - carbomer	0
AC1030	> 30
AC1030-cysteine	> 30
Preactivated AC1030	10

CONCLUSIONS

The lipophilic C10-C30 alkyl chains provide the potential for using these polymers with emulsifying properties in semisolid delivery systems. The outstanding mucoadhesive properties, due to thiolation and S-protection make this novel thiomers a valuable excipient for creams exhibiting a prolonged residence time on mucosal tissues, such as vaginal, ocular or nasal mucosa.

REFERENCES

1. Gum JRJ, Hicks JW, Toribara NW, Rothe EM, Lagace RE, Kim YS. The human MUC2 intestinal mucin has cysteine-rich subdomains located both upstream and downstream of its central repetitive region. *The Journal of Biological Chemistry*. 1992;267:21375-83.
2. Bernkop-Schnürch A, Schwarz V, Steininger S. Polymers with Thiol Groups: A New Generation of Mucoadhesive Polymers? *Pharm Res*. 1999;16(6):876-81.
3. Iqbal J, Shahnaz G, Dünnhaupt S, Müller C, Hintzen F, Bernkop-Schnürch A. Preactivated thiomers as mucoadhesive polymers for drug delivery. *Biomaterials*. 2012;33(5):1528-35.
4. Dünnhaupt S, Barthelmes J, Rahmat D, Leithner K, Thurner CC, Friedl H, et al. S-Protected Thiolated Chitosan for Oral Delivery of Hydrophilic Macromolecules: Evaluation of Permeation Enhancing and Efflux Pump Inhibitory Properties. *Molecular Pharmaceutics*. 2012;9(5):1331-41.
5. Boehmer MR, Koopal LK. Association and Adsorption of Nonionic Flexible Chain Surfactants. *Langmuir*. 1990;6:1478-84.





FUNCTIONALITY RELATED CHARACTERISTICS OF HYPROMELLOSE TYPE 2208 USED AS MATRIX FORMER IN PROLONGED-RELEASE TABLETS

T. Stanić Ljubin^{1*}, M. Horvat¹, B. Janković¹, P. Jurkovič¹

¹ Lek Pharmaceuticals, d.d., Sandoz Development Center Slovenia, Verovškova 57, 1526 Ljubljana, Slovenia

INTRODUCTION

Hypromellose is a water-soluble polymer derived from cellulose used as the controlled-release agent in hydrophilic matrix systems.

Polymer hydration and swelling play an important role in controlling the rate of drug diffusion from hydrophilic matrices (1,2).

Ph. Eur 7.0 recognizes following functionality related characteristic (FRC) of hypromellose:

- degree of substitution (hydroxypropyl (HP) and methoxy (MC) content),
- molecular weight distribution,
- viscosity, and
- particle size distribution.

Hypromellose producers suggest following physico-chemical properties to be critical material attributes (CMA) that influence the dissolution rate:

- degree of substitution (hydroxypropyl (HP) content),
- viscosity,
- particle size - pass through sieve 230 mesh (63 microns) (3,4).

The purpose of this work was to evaluate the influence of hypromellose physico-chemical properties (HP content, viscosity, particle size, specific surface area, and moisture content) on dissolution rate.

MATERIALS AND METHODS

Dissolution results for production scale batches of prolonged-release hydrophilic matrix tablets containing low dose of poorly soluble drug substance and hypromellose 2208 (20% w/w) were used to evaluate the influence of hypromellose physico-chemical properties on dissolution rate. Dissolution in 900 mL phosphate buffer pH 6.8, Apparatus 1, Ph. Eur., 100 rpm, performed within batch release testing, was utilized for evaluation (percent of drug substance dissolved at 6th and 10th hour). Hypromellose properties (HP content, viscosity and pass through sieve 230 mesh) were provided by hypromellose producer and also obtained by in-house analyses. Additional parameters, moisture content (determined by loss on drying measurement (LOD), specific surface area (SSA), and particle size distribution (PSD) measured by laser light scattering method ($d_{0,1}$), were obtained by in-house analyses. The influence of hypromellose parameters on dissolution results was assessed by computer software Modde 9.1 and SIMCA-P+ 12.0.

RESULTS AND DISCUSSION

Average dissolution results for 168 production scale batches and physico-chemical properties of seven batches of hypromellose are presented in tab. 1.

Tab. 1: Material attributes of hypromellose batches and dissolution results of tablets batches produced

Viscosity (mPa·s)	HP content (%)	% thru 230 mesh	SSA (m ² /g)	$d_{0,1}$ (μm)	LOD (%)	Average dissolved at 6 th h (%)	Average dissolved at 10 th h (%)
21362	8.2	63	0.78	23	2.1	32.9	51.8
17596	9.6	63	1.09	21	2.0	36.8	57.1
21091	9.4	67	0.76	23	2.3	35.6	55.6
23035	9.7	62	1.08	23	1.4	36.2	56.7
19836	9.2	65	0.9	23	2.2	35.2	56.0
16683	9.2	64	0.65	25	1.6	38.0	59.3
21632	10.0	57	0.54	25	1.5	39.2	59.9

Data presented in tab. 1 were analysed by MLR (multiple linear regression) method by computer software Modde 9.1. Results are presented by fig. 1 and fig. 2.



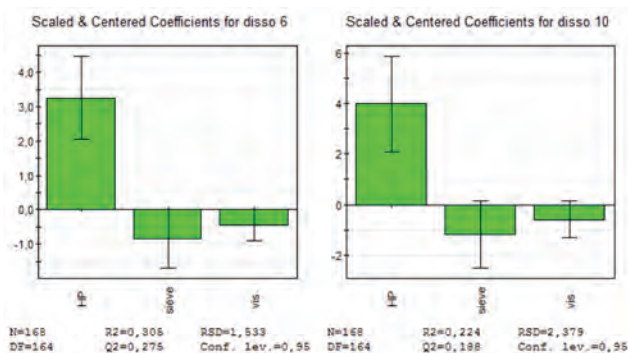


Fig. 1: Coefficient plot – graphical presentation of the influence of viscosity (vis), hydroxypropyl content (HP) and particle size – pass thru sieve 230 mesh (sieve) on dissolution results obtained at 6th and 10th hour

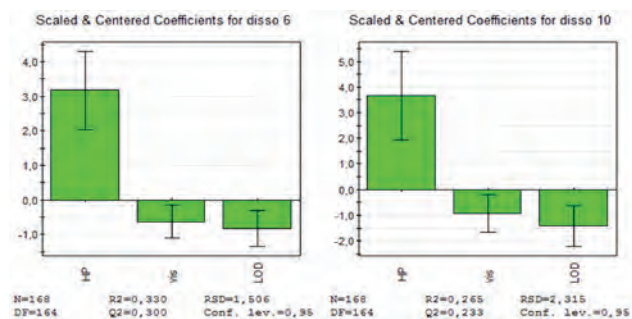


Fig. 2: Coefficient plot – graphical presentation of the influence of viscosity (vis), hydroxypropyl content (HP) and loss on drying (LOD) on dissolution results obtained at 6th and 10th hour

It was observed that hydroxypropyl (HP) content has the most significant influence on dissolution rate. Also, other two physico-chemical properties suggested by hypromellose producers – viscosity and pass through sieve 230 mesh were confirmed to affect the dissolution rate (fig 1.). The influence of $d_{0,1}$ determined by laser light scattering method and SSA was also assessed. $d_{0,1}$ was confirmed to be appropriate parameter for quantifying of PSD, equivalent to pass through sieve 230 mesh, while SSA was demonstrated not to be as good as $d_{0,1}$ and sieve analysis. Therefore, the introduction of other methods than sieve analysis for quality control testing of PSD of hypromellose was not identified as beneficial.

Besides these parameters, also LOD was identified as potential CMA of hypromellose (fig. 2). However, it was observed that LOD is correlated to sieve analysis results and it was not investigated whether moisture content determined by other methods also shows an impact on dissolution rate.

Presented analysis has several limitations. MLR model, obtained from data presented in tab. 1, accounts only

for ~30% of the observed variability of dissolution results. Primarily, the selected material attributes and their analyses are correlated and their impacts on dissolution are aliased. Moreover, additional factors, such as drug substance properties and tablets manufacturing process parameters also impact the dissolution results.

Therefore, we additionally conducted a hierarchical PLS analysis of all available incoming materials and process data. The improved MVDA model was found to explain ~50% of observed dissolution variability. It confirmed quantitatively that all three material attributes suggested by hypromellose producers (HP content, viscosity, and pass through sieve 230 mesh) significantly impact the dissolution rate. Additionally, the moisture content of hypromellose (measured as LOD) was also indicated to be highly important material attribute in this case.

CONCLUSIONS

Following physico-chemical properties of hypromellose were identified as critical material attributes that influence the dissolution rate of poorly soluble drug substance from matrix tablets containing 20% w/w of hypromellose:

- HP content,
- viscosity,
- particle size distribution, and
- loss on drying.

REFERENCES

1. Alderman, D.A., 1984. A review of cellulose ethers in hydrophilic matrices for oral controlled-release dosage forms. *Int. J. Pharm. Tech. Prod. Manuf.* 5, 1–9.
2. Bowstra, J.A., Junginger, H.E., 1993. Hydrogel. In: Swarbrick, J., Boylan, J.C. (Eds.), *Encyclopedia of Pharmaceutical Technology*, vol. 7. Dekker, New York, pp. 441–465.
3. Cabelka, T. et al, *Application of Quality by Design (QbD) principles to the formulation of a hydrophilic matrix tablet of a high dose/high solubility drug*. AAPS annual meeting and exposition, Los Angeles, CA 2009.
4. Deng H. et al, *Application of Quality by Design (QbD) principles to the formulation of extended release, propranolol hydrochloride hydrophilic matrix tablets*. AAPS annual meeting and exposition, New Orleans 2010.





THE PHARMACOLOGICAL ACTIVITY OF COMPOSITES OF BETULIN ESTERS WITH ARABINO GALACTAN

T.P. Shakhtshneider^{1,2}, M.A. Mikhailenko¹, S.A. Kuznetsova^{3,4}, Yu.N. Malyar³, A.S. Zamai³, V.V. Boldyrev^{1,2}, E.V. Boldyreva^{1,2,*}

¹ Institute of Solid State Chemistry and Mechanochemistry SB RAS, Kutateladze 18, Novosibirsk, 630128 Russia

² Novosibirsk State University, Pirogov str., 2, Novosibirsk, 630090 Russia

³ Institute of Chemistry and Chemical Technology SB RAS, Krasnoyarsk, Russia

⁴ Siberian Federal University, Krasnoyarsk, Russia

INTRODUCTION

Betulin and its esters extracted from the birch bark exhibit antioxidant, hypolipidemic, hepatoprotective, and other forms of pharmacological activity. The main drawback for their internal and external application in pharmacology is the poor water-solubility of the preparations. The mechanical activation of drugs with the polymers is a well-known efficient method for preparing powder systems which are characterized by an increased solubility and dissolution rate. Earlier the mechanocomposites of betulin with water-soluble polymers, polyvinylpyrrolidone and polyethylene glycol were prepared, which have showed a higher solubility of betulin and improved gastroprotective properties [1]. The purpose of this paper was to prepare the composites of betulin esters, diacetate and dipropionate, with water-soluble biopolymer arabinogalactan, in order to see, if an even better form can be suggested.

MATERIALS AND METHODS

Materials

Betulin diacetate (BDA) and betulin dipropionate (BDP) (Fig. 1) as well as arabinogalactan (AG) were obtained by the originally developed methods [2-4].

Methods

The mechanocomposites were prepared by mechanochemical treatment of the mixtures of betulin esters with arabinogalactan in the SPEX 8000 ball mill. The composites of betulin diacetate and betulin dipropionate were also obtained by dissolution of the mechanocomposite or the mixtures of the initial components in water and subsequent solvent evaporation.

The physicochemical properties of the composites were studied by gel permeation chromatography, X-ray diffraction, infrared spectroscopy, electron and atomic force microscopy methods. Release of the biologically active substances from the composites was studied using dissolution tester 705 DS (Varian).

Antitumor activity of BDA, BDP, AG and their composites against Ehrlich ascites carcinoma cells and lung cancer cells was determined *in vitro* by estimating the fraction of apoptotic and necrotic cells 24 h after application of the compounds in Hanks solution by fluorescence method.

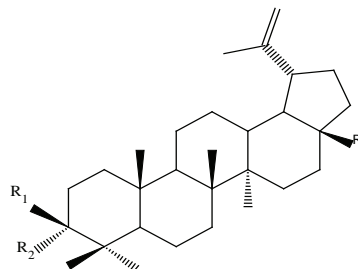


Fig. 1: The molecular structures of betulin ($R_1=OH$, $R_2=H$, $R_3=CH_2OH$), betulin diacetate ($R_1=OAc$, $R_2=H$, $R_3=CH_2OAc$), and betulin dipropionate ($R_1=OPr$, $R_2=H$, $R_3=CH_2OPr$).

RESULTS AND DISCUSSION

Under mechanical treatment of the mixtures of BDA and BDP with AG, the practically amorphous products were obtained. It was found that in the case of the mechanocomposites, the solubility of betulin derivatives increased as compared to the initial substances. It was by IR spectroscopy method detected that there was no hydrogen bonding in the composites of BDA and BDR with AG. Nevertheless, the formation of the complexes of BDA and BDP with AG in the ball-milling mixtures and in the solutions was suggested due to restoration of molecular weight of the mechanically activated polymer and accord-



ing to the fact that the esters were not extracted by hexane from the aqueous solutions.

The obtained composites were non-toxic and exhibited antitumor properties against the Ehrlich ascites carcinoma cells. The data on antitumor activity of BDA-AG mechanocomposite against EAC cells can be found in [5] and for BDP-AG mechanocomposite, they are presented in the Table 1.

Tab. 1: Effect of mechanical composites of BDP with AG and starting components on elimination level of Ehrlich ascites carcinoma cells.

Survival of AEC cells, %	AG	BDP	Mechanical composite of BDP – AG (1:9, w/w)	Control
Necrosis	6.6±0.8	3.9±0.6	5.4±0.7	7.3±0.5
Apoptosis	16.7±1.8	25.0±3.1	41.0±5.4	3.1±2.8

After dissolution of the mechanocomposites or the mixtures of betulin esters with AG in water and subsequent solvent evaporation, the composites were obtained as the thin amorphous films. From the films, the complexes of BDA and BDP with AG were totally water-soluble that made the films very attractive for pharmacological applications. As an example, the data on antitumor activity of the BDA-AG films against lung cancer cells are presented in the Table 2.

Tab. 2: Effect of the composite of BDA with AG as a film and starting components on elimination level of lung cancer cells.

Survival of lung cancer cells, %	BDA	BDA-AG (1:9, w/w) physical mixture	BDA-AG (1:9, w/w) composite as a film	Control
Necrosis	0.4±0.04	0.5±0.04	0.4±0.04	0.3±0.05
Apoptosis	28.3±0.7	27.7±2.1	82.3±3.9	2.1±0.08

CONCLUSIONS

Using mechanochemical methods, the composites of betulin diacetate and betulin dipropionate with water-soluble polysaccharide arabinogalactan were obtained. They showed higher dissolution rate and solubility in comparison with the initial substances. The possible reasons of increasing the solubility are disordering of crystal structures of biologically active substances and formation of molecular complexes with the polymer.

It has been shown in *in vitro* studies that mechanocomposites of betulin esters with arabinogalactan as well as the composites prepared as the thin water-soluble films exhibited higher antitumor activity in comparison with the initial substances.

ACKNOWLEDGMENTS

The work was partly supported by the RFBR grant No. 14-03-31900 and the program of the Russian Academy of Sciences "Fundamental Sciences for Medicine".

REFERENCES

1. Mikhailenko MA, Shakhtshneider TP, Brezgunova ME, Kuznetsova SA, Boldyrev VV, *The composition of betulin with biocompatible polymers and the method of its preparation*, R.F. Patent 2401118, October 10, 2010.
2. Kuznetsova SA, Kuznetsov BN, Red'kina ES, Sokolenko VA, Skvortsova GP, *The method of obtaining betulin diacetate*, R.F. Patent 2324700, May 20, 2008.
3. Kuznetsova SA, Kuznetsov BN, Mikhailov AG, Skvortsova GP, *The method of obtaining arabinogalactan*, R.F. Patent 2273646, April 6, 2006.
4. Kuznetsova SA, Skvortsova GP, Malyar YuN, Vasil'eva NYu, Kuznetsov BN, *The method of obtaining betulin dipropionate*, R.F. Patent 2469043, December 10, 2012.
5. Shakhtshneider TP, Kuznetsova SA, Mikhailenko MA, Zamai AS, Malyar YuN, Zamai TN, Boldyrev VV, *Effect of mechanochemical treatment on physicochemical and antitumor properties of betulin diacetate mixtures with arabinogalactan*. Chem. Nat. Comp. 2013; 49: 470-474.





INVESTIGATION OF DISSOLUTION MECHANISMS BY IMAGING METHODS

K. Punčochová^{1,3*}, J. Beránek³, A. Domicic³,
A. Ewing², S. G. Kazarian², F. Štěpánek¹

¹ Institute of Chemical Technology Prague, Technická 3, Prague, Czech Republic

² Imperial College London, South Kensington Campus, London, Great Britain

³ Zentiva, k.s., U Kabelovny 130, Prague 10, Czech Republic

INTRODUCTION

The dissolution testing of pharmaceutical formulations is basic methodology for determination of drug release. The design of tablets or capsules plays important role to drug delivery. Basic dissolution test provides information about concentration of active pharmaceutical ingredient (API) as a function of time. The result is a rate of drug release but there is limited information about the mechanism of release.¹ Moreover, polymer dissolution significantly influences the release of drug. The understanding of polymer dissolution mechanism and related to drug dissolution process is useful to predict a behavior of poorly soluble drugs during dissolution and choosing of a candidate formulation, polymers or additives.²

Therefore, the purpose of the present work is to investigate the physical and chemical processes of dissolution in a more detailed way, focusing on water penetration, polymer swelling, drug dissolution and precipitation in order to explain the mechanism of drug release from the dosage form, especially the release of poorly soluble drugs from solid dispersions.

A several analytical approaches allow investigating the physical and chemical processes of dissolution, including FT-IR imaging, MRI, UV imaging and Raman spectroscopy.

MATERIALS AND METHODS

The mechanisms of dissolution were observed using imaging methods including ATR-FTIR imaging, Magnetic Resonance Imaging (MRI), and UV imaging in a flow cell using poorly soluble Aprepitant, Valsartan and polymers

PVP and Soluplus. The dissolution mechanism of two types of formulations, solid dispersion prepared by spray drying and physical mixture, were studied.

RESULTS AND DISCUSSION

In spite of the different principles of the imaging methods used, consistent dissolution mechanism of pure API, physical mixtures and solid dispersions was confirmed. PVP had a fast dissolution rate, similar to the rate of water penetration. However, the dissolution of PVP significantly slowed down in combination with a poorly soluble Aprepitant. Moreover, precipitation of API was recognized by ATR-FTIR imaging and can be explained by fast dissolution of PVP, high concentration of water and local supersaturation of API (see in Figure 1). Presence of Aprepitant also decreases the dissolution rate of Soluplus in solid dispersion but Soluplus creates the wide gel layer which helps to keep Aprepitant dissolved and inhibits the precipitation. MRI showed a good wettability of tablet related to high wetting properties of PVP. Different mechanisms of water penetration were confirmed in the case of physical mixture and solid dispersion, which is illustrated in Figure 2. The physical mixture, as the polymer dissolved and tablet has disintegrated. On the other hand, tablet made from a solid dispersion was wetted and a gel layer as well as a dry core were created. UV-Imaging allowed observing of release the API from the dosage form.

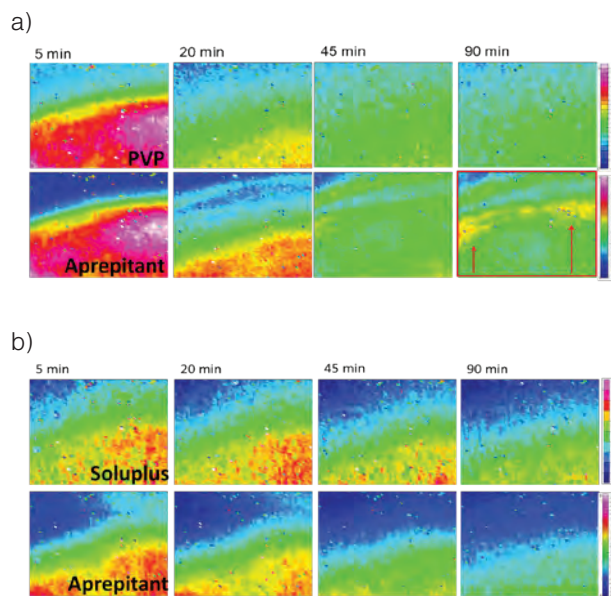


Fig. 1: ATR-FTIR Images of dissolution process of solid dispersions with combination a) Aprepitant and PVP with precipitation and b) Aprepitant and Soluplus.

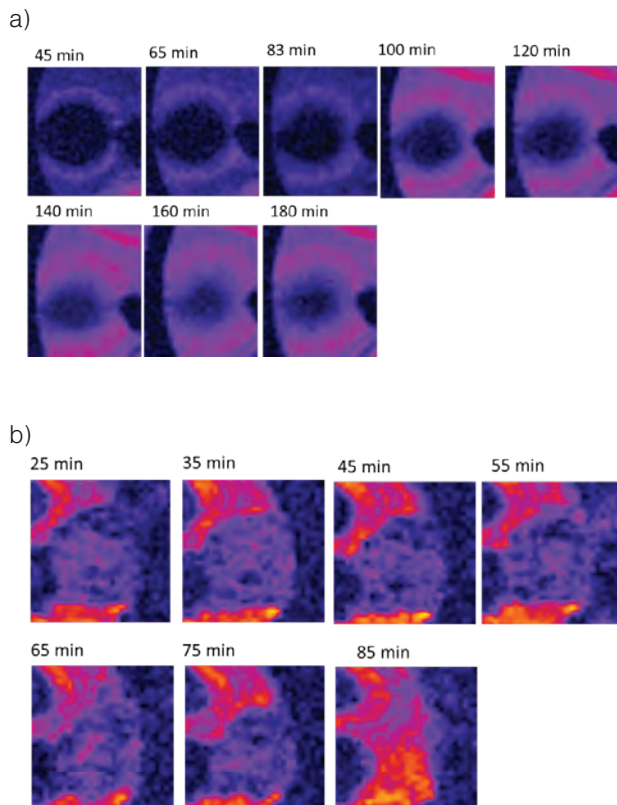


Fig. 2: Penetration of water to the tablet of Aprepitant and Soluplus a) solid dispersion and b) physical mixture.

CONCLUSIONS

The imaging methods were useful to characterize the physical and chemical processes of dissolution. The interactions API-polymer in solid dispersion decreased the dissolution rate of polymer in contrast with enhancing of dissolution rate of Aprepitant. The concentration gradient of polymer which was determined in gel layer caused by water penetration and dissolution of polymer improved the release of poorly soluble drugs by increasing the supersaturated concentration of drug and by inhibiting precipitation.

REFERENCES

1. Dressman, J. F.; Amidon, G. L.; Reppas, Ch.; Shah, V. P. Dissolution testing as a Prognostic Tool for Oral Drug Absorption: Immediate Release Dosage Forms. *Pharmaceutical Research* 1998, 15 (1), 11–21.
2. Miller-Chou, B. A.; Koenig, J. L. A review of polymer dissolution. *Progress in Polymer Science* 2003, 28, 1223–1270.

IMPORTANCE OF ABSORPTIVE ENVIRONMENT SIMULATION IN DETECTION OF EXCIPIENT-MEDIATED PRECIPITATION INHIBITION OF SIROLIMUS

M. Petrusevska^{1,*}, M. Homar², D. Kocjan², L. Peternel²

¹ Institute of pharmacology & toxicology, 50 Divizija 6, Skopje, R. Macedonia

² Sandoz Development Centre Slovenia, Verovskova 57, Ljubljana, Slovenia

INTRODUCTION

The rate limiting step of BCS class II drug absorption is either the drug solubility or the dissolution rate in the lumen of the gastrointestinal tract (GIT). A variety of formulation approaches have been developed to tackle this challenge (1). The goal of these approaches is to assure an adequate fraction of dissolved drug in the GI lumen and consequently a satisfactory flux across the intestinal epithelia. However, when the drug is released in the GIT from these formulations drug precipitation can occur, subsequently leading to a decreased fraction of the dissolved drug and a decreased flux across the intestinal epithelia (1, 2).

Herein, we present the results of the sirolimus excipient mediated precipitation inhibition in presence of hydroxypropyl methyl cellulose (HPMC). Additional spectroscopic and permeability studies implied that HPMC inhibits the precipitation of sirolimus out of supersaturated solutions. Finally, in the proof-of-concept human pharmacokinetic study we developed formulation with HPMC that showed a significantly higher AUC and C_{max} in comparison to the reference Rapamune®.





MATERIALS AND METHODS

Materials

Sirolimus was supplied by Biocon (India) and Rapamune® was supplied by Wyeth Medica (Ireland). The tested excipients as precipitation inhibitors are given in Tab. 1. SIF™ Powder (Phares AG, Switzerland) was used for the preparation of fasted/fed state simulated intestinal fluid (Fa/FeSSIF) buffer.

Tab. 1. Tested precipitation inhibitors

Surfactants: Tween® 80, Tween® 20, Cremophor® RH40, Cremophor® EL, Lutrol® F68, Lutrol® F127 (Poloxamer 407) (BASF, Germany), Gellucire® 44/14, Labrasol® (Gattefosse, Germany), Texapon® K15, (Cognis, The Netherlands).
Polymers: Pharmacoat® 606, Pharmacoat® 603 (HPMC), (Harke, Germany), Klucel EF® (Hercules Inc, Germany), Kollidon® K30, Kollidon® K25, Kollidon® VA 64, Kollidon® K17 (BASF, Germany).
Other: Elvanol® (DuPont™), D-Mannitol, Poly(ethylene glycol) M _n 6000, Propylene glycol, Poly(ethylene glycol) M _n 400, (Sigma-Aldrich, Belgium), Kollicoat® IR (BASF, Germany), α - cyclodextrin, (Merck, Germany).

In vitro high-throughput (HT) precipitation inhibitor screening method

Solutions containing precipitation inhibitors were prepared by a HT Freedom EVO liquid handler, followed by addition of stock DMSO solution of sirolimus in McIlvaine buffer pH 6.8, incubated at 37°C followed by sampling at pre-determined time points. Samples were analyzed for the amount of drug remaining in the solution by UPLC method (3).

Confirmation of precipitation inhibitors in absorptive environment

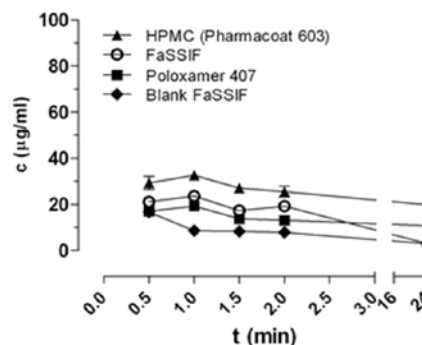
The identified precipitation inhibitors (HPMC and Poloxamer 407) were tested in FaSSIF and FeSSIF. In addition their impact on increased flux across intestinal epithelia was investigated using PAMPA assay. Investigation of developed interactions between HPMC and sirolimus were characterized using solid state characterization techniques (IR and DSC).

A randomized, double blind study under fasting conditions was conducted with 12 healthy adult volunteers. The subjects were given a reference product Rapamune® and the test formulation with a 14 day wash-out period. Samples were taken at predetermined time points and analyzed by a HPLC/MS and automated extraction for the determination of sirolimus in human whole blood (4).

RESULTS AND DISCUSSION

The screening campaign revealed that some excipients effectively inhibited sirolimus precipitation. Among them, HPMC and Poloxamer 407 were identified as 'hit' precipitation inhibitors and were further evaluated in a physiologically more relevant dissolution media, namely Fa/FeSSIF (Fig. 1).

A.



B.

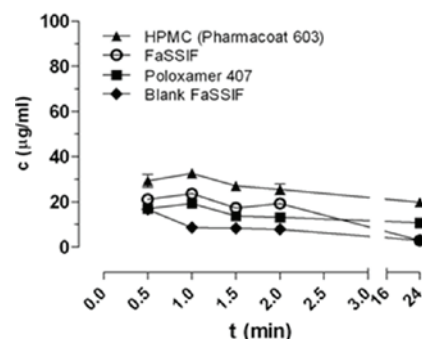


Fig. 1: Impact of "hit" excipients HPMC 603 (0.1%) and Lutrol F127 (Poloxamer 407) (0.1%) on sirolimus precipitation in (A). FaSSIF and (B). FeSSIF incubation media. The results are shown as mean \pm SEM ($n = 4$).

These results demonstrated that sirolimus supersaturation can be created and maintained to a certain degree in the absence of precipitation inhibitors due to the solubilizing components in Fa/FeSSIF. The solubilizing components of Fa/FeSSIF inhibited the sirolimus precipitation to the extent that the addition of Poloxamer 407 did not cause any additional effects of sirolimus precipitation inhibition. In PAMPA experiment, HPMC significantly increased the sirolimus flux across the lipid bilayer (ANOVA, $p < 0.01$), what is most probably related to the HPMC mediated increase of sirolimus concentrations in the donor compartment (Fig. 2).

DSC and IR spectroscopic studies confirmed that certain



interactions between sirolimus and HPMC are indeed developed. These interactions most likely prevent sirolimus to precipitate out of solution resulting in increased absorption of sirolimus across intestinal epithelia.

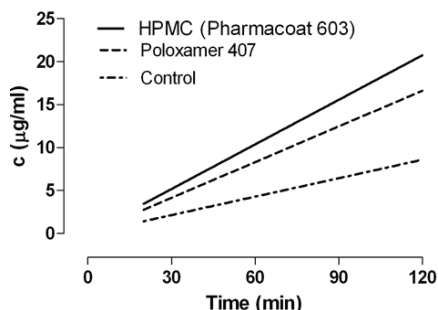


Fig.2 The impact HPMC (0.1%) and Poloxamer 407 (0.1%) on the flux of sirolimus in the parallel artificial membrane permeability assay (PAMPA). The results are shown as linear regression lines ($R^2 > 0.8243$, $p < 0.05$) obtained from the concentration-time profiles ($n=4$).

In vitro sirolimus precipitation data are in line with the outcome of the human PK study (Tab. 2). Test formulation contained HPMC and larger sirolimus particle size in comparison to Rapamune, which in contrast to test formulation did not contain precipitation inhibitor.

Tab.2: Sirolimus PK parameters after oral administration of Rapamune® and test formulation to fasted human volunteers. Results are shown as mean ($n=11$) \pm S.D.

	C_{max} (pg/mL)	AUC (pg x h/ mL)
Rapamune	7655 \pm 1896	51089 \pm 15754
Test formulation	12616 \pm 2867	64793 \pm 12878

CONCLUSION

Precipitation inhibition can play a significant role in determining the amount of dissolved drug available for absorption and consequently in determining the AUC and C_{max} values of investigated drug.

REFERENCES

1. Brouwers J, Brewster ME, Augustijns P. Supersaturating drug delivery systems: the answer to solubility-limited oral bioavailability? *J. Pharm. Sci.* 2009; 98: 2549-2572
2. Bevernage J, Brouwers J, Brewster ME, Augustijns P. Evaluation of gastrointestinal drug supersaturation and precipitation: strategies and issues. *Int. J. Pharm.* 2013; 453: 25-35
3. Petruševska M, Urleb U, Peternel L. Evaluation of a high-throughput screening method for the detection of the excipient-mediated precipitation inhibition of poorly soluble drugs. *Assay Drug Dev. Technol.* 2013; 11: 117-129
4. Petruševska M, Petruševska M, Homar M, Petek B, Resman A, Kocjan D, Urleb U, Peternel L. Hydroxypropyl methylcellulose mediated precipitation inhibition of sirolimus: from a screening campaign to a proof-of-concept human study. *Mol. Pharm.* 2013; 10: 2299-2310.

DEVELOPMENT OF PHYSIOLOGICALLY RELEVANT DISSOLUTION METHODS FOR EVALUATION OF HYDROPHILIC MATRIX TABLETS USING NEW DISSOLUTION APPARATUS

U. Klančar^{1,*}, B. Markun¹, I. Legen¹

¹ Lek Pharmaceuticals d.d., Sandoz Development Center Slovenia, Verovškova 57, SI-1526 Ljubljana, Slovenia

INTRODUCTION

Depending on predominant drug release mechanism, hydrophilic matrix tablets have different drug release and mechanical susceptibility (1, 2). Consequently, the drug release rate may vary after tablet exposure to variable gastrointestinal conditions *in vivo* or dissolution apparatus conditions *in vitro*. Considering *in vivo* gastrointestinal conditions the *in vitro* tests should be designed. However, appropriate models simulating stress conditions *in vivo* are difficult to develop by only using conventional dissolution Apparatus. Some modifications of conventional and novel dissolution methods have been suggested, including the use of the USP dissolution Apparatus 3 (reciprocating cylinder, Bio-dis) (3, 4). In one of our previous studies, USP 3 Apparatus in combination with plastic beads was used to mimic mechanical stress on HPMC matrices. It was concluded that incorporation of beads was crucial in discriminating the tablets *in vitro* and in establishing a good correlation with *in vivo* data (2). The aim of the present study was to verify the applicability of newly developed dissolution model on three different additional cases. Obtained results were compared with *in vivo* results and IVIVC was suggested.





MATERIALS AND METHODS

Materials

Three different matrix tablet formulations for analysing with novel dissolution method were developed in Lek d.d. Basic formulations characteristics are described in Tab. 1. Reference samples were obtained from wholesale supplier.

Methods

Dissolution testing was performed simultaneously for test and reference product. The dissolution testing model consists of USP 3 Apparatus (Varian Vankel Bio-dis III, US) and 8 mm plastic beads of density about 1.1 g/cm³. Testing was performed in 250 ml of water medium at 37°C ± 0.5°C. Plastic beads to fill approximately ¼ of the vessels were placed into reciprocating cylinders. Then, the tablets were added and cylinders were attached to the Bio-dis. The stainless steel mesh on both sides of the cylinders was 2 mm in size. The DPM rate program was set at 20 DPM with short 10 min interval at 1.5 hours set to 40 DPM. The sampling time points were selected depending on the formulation studied. Withdrawn samples were analysed with HPLC.

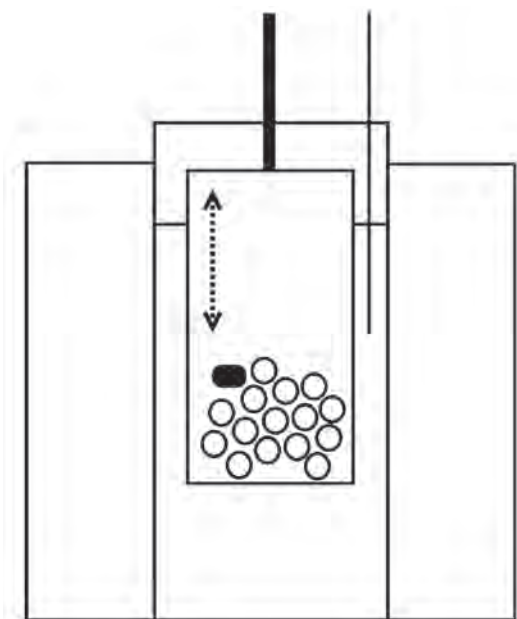


Fig. 1: Novel dissolution testing device incorporating plastic beads into USP3 dissolution Apparatus (Bio-Diss, Varian, US). Tablet moves reciprocally with plastic beads which exert additional mechanical stress on matrices.

RESULTS AND DISCUSSION

Dissolution results for three different test formulations compared to reference products analysed with beads dissolution method are presented in Fig 2.

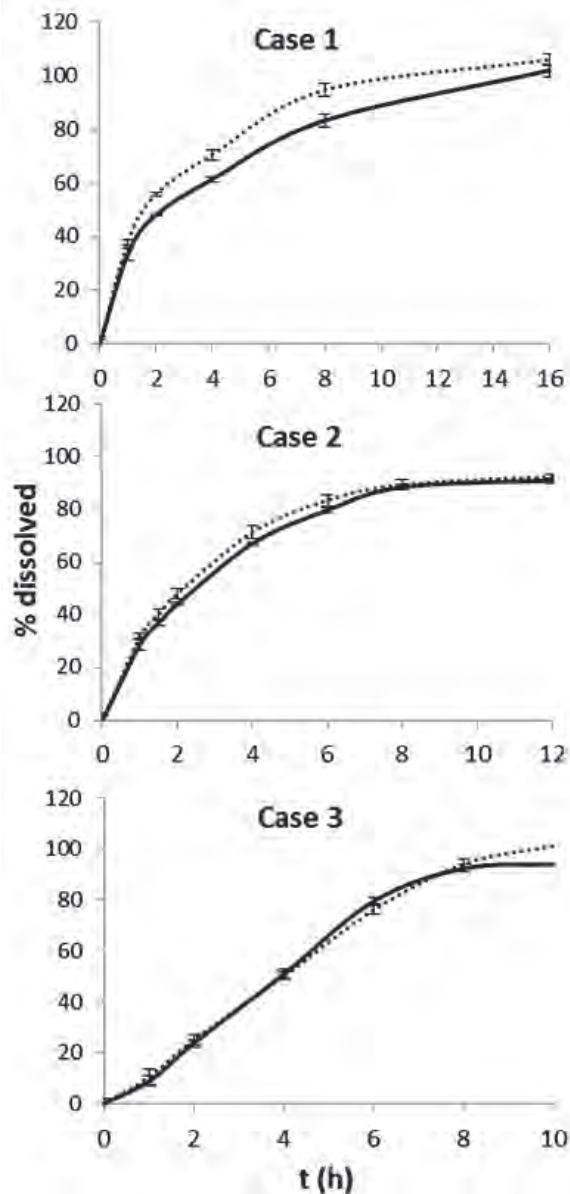


Fig. 2: Dissolution results for three case studies with SD values (N=3). Test product T (dotted lines), reference product R (solid lines).

Results show that in Case 1, test formulation is slightly more susceptible to mechanical stress compared to the reference formulation. Dissolution rate was accelerated after 10 min stress manipulation at 40 DPM initiated at 1.5 h. This acceleration was not evident when the tablets



were analysed using conventional methods. Dissolution profiles for Case 2 and Case 3 show good robustness and overall similarity between test and reference formulations. All studied examples were evaluated in bioequivalence study and results were correlated with *in vitro* data. In first two cases we found IVVC Level C correlation and in Case 3 the correlation was Level A (Tab.1).

Tab. 1: Description of formulations and API with corresponding level of IVVC after comparing dissolution results to *in vivo* results obtained from bioequivalence studies.

Example	Matrix type	API solubility	Correlation
Case 1	Eudragit, HPMC	pH dependant	Level C
Case 2	HPC	good	Level C
Case 3	HPMC	low	Level A

Examination of the profiles also indicates that drug release mechanism differs between cases and that is most linear and erosion controlled in Case 3.

CONCLUSIONS

New, beads dissolution testing method was introduced in the evaluation of three different matrix formulations. Obtained results were in good agreement with *in vivo* data which indicates the methods bio relevance and usefulness for analysing different hydrophilic matrix tablets.

REFERENCES

1. Wang Z, Shmeis RA. Dissolution controlled drug delivery systems. In: Li X, Jasti BR. Design of Controlled Release Drug Delivery Systems. United States: McGraw-Hill; 2006. p. 139-172.
2. Klančar U, Markun B, Legen I, Baumgartner S. A novel beads-based dissolution method for the *in vitro* evaluation of extended release HPMC matrix tablets and the correlation with the *in vivo* data. *AAPS Journal*. 2013; 15(1): 267-277.
3. Kostewicz ES et al. *In vitro* models for the prediction of *in vivo* performance of oral dosage forms. *Eur. J. Pharm. Sci.* 2013; <http://dx.doi.org/10.1016/j.ejps.2013.08.024>.
4. Fotaki N, Aivaliotis A, Butler J, Dressman JB, Fischbach M, Hempenstall J, Klein S, Reppas S. A comparative study of different release apparatus in generating *in Vitro* - *in Vivo* correlations for extended release formulations. *Eur. J. Pharm. Biopharm.* 2009; 73: 115–120.

EVALUATION OF CATIONIC MICROSPHERES WITH MELATONIN USING EYE-RELATED BIOAVAILABILITY PREDICTION MODELS

Marieta Duvnjak Romić^{1,*}, Marina Juretić^{2,#}, Biserka Cetina-Čizmek¹, Ivan Pepić², Anita Hafner², Jasmina Lovrić², Jelena Filipović-Grčić²

¹ Pliva Croatia Ltd., Prilaz B. Filipovića 25, 10000 Zagreb, Croatia

² Department of Pharmaceutics, Faculty of Pharmacy and Biochemistry, University of Zagreb, A. Kovačića 1, 10000 Zagreb, Croatia

* These authors contributed equally to this work

INTRODUCTION

The conventional dosage forms suffer from poor ocular bioavailability due to fast precorneal elimination owing to lachrymation, tear turnover, nasolachrymal drainage, metabolic degradation and nonproductive adsorption/absorption, and the relative impermeability of the corneal epithelial membrane. Therefore, current efforts are directed towards the development of innovative drug delivery systems and concomitant development of *in vitro* models to enable the prediction of eye-related bioavailability (1). The aim of this study was to investigate the potential of chitosan/Poloxamer 407 microspheres as carriers for topical ocular delivery of melatonin by evaluating its eye-related bioavailability using cell-based epithelial cornea model. Melatonin, methoxyindole secreted by the pineal gland, has pleiotropic bioactivities among which is its ability to modulate intraocular pressure.

Chitosan is a biocompatible and biodegradable polycationic polymer. At pH below 6.5 it is positively charged and electrostatically interacts with negatively charged epithelial surface resulting in mucoadhesion. Moreover, it can act as a permeation enhancer increasing paracellular drug permeation.

Poloxamer 407, polyoxyethylated nonionic surfactant, has been proposed to increase drug permeability through corneal epithelial cell membranes.





MATERIALS AND METHODS

Low-viscosity chitosan (C) and melatonin (M) were purchased from Sigma-Aldrich and Poloxamer 407 (P) from BASF. Microspheres were prepared by spray-drying (Buchi 190 mini spray dryer) of formulations prepared by mixing M/P ethanol solution with chitosan acetic acid solution (1 %, w/v). Drying conditions were as follows: compressed air flow rate of 700 Nl h^{-1} , spray flow rate of 2.59 mL/min , inlet air temperature of 145°C. Microspheres were evaluated in terms of size (Olympus BH-2 microscope), zeta-potential (Zetasizer 3000 HS), drug loading and *in vitro* release (Franz diffusion cell).

MTT assay was performed to assess the biocompatibility of microspheres with corneal epithelial cells (HCE-T cell line, Rikken).

The cell-based epithelial cornea model was cultivated on Transwell® polycarbonate filter inserts coated with type I rat tail collagen and fibronectin. The HCE-T cells suspended in the culture medium were seeded onto the filter and cultivated submerged for seven days, after which they were exposed to the air-liquid interface during the following three days (2). The permeability experiment was performed directly in the Transwell® using Hank's Balanced Salt Solution buffer (HBSS pH 6.3). For the determination of tight junction opening and cell viability transepithelial electrical resistance (TEER) was measured during the experiment. The quantitative determination of melatonin was performed by HPLC (Agilent 1100).

RESULTS AND DISCUSSION

Melatonin-loaded C/P microspheres (MCP) are characterized by size and surface charge suitable for ocular delivery (Table 1) offering longer precorneal retention. *In vitro* melatonin release and permeability from MCP are shown in Fig. 1.

Table 1. The composition and the main characteristics of melatonin loaded chitosan/P407 microspheres.

Micro-sphere	CC (g/l)	M/C (w/w)	C/P (w/w)	Size (μm)	ζ (mV)
MCP	8	1:2	5:1	2.23±0.04	29.6±3.0

Strong correlation between melatonin *in vitro* release and permeability was observed as shown in Fig. 2.

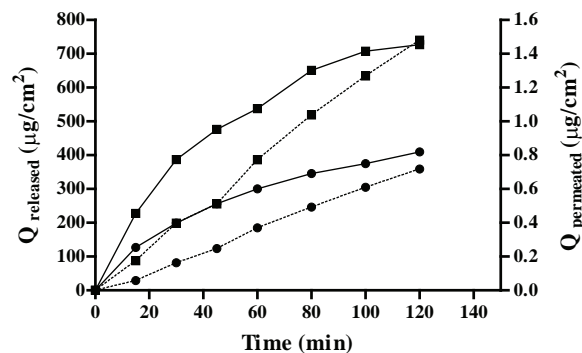


Fig. 1: *In vitro* melatonin release (—) and permeability (-----) from solution (■) and MCP (●).

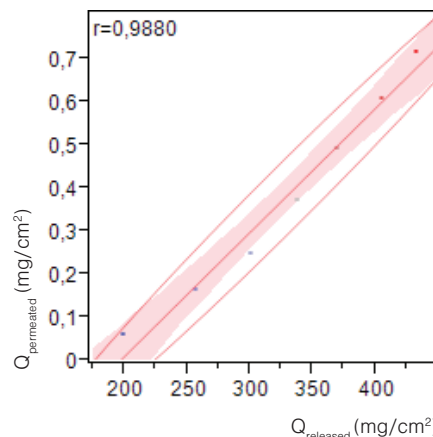


Fig. 2: The correlation of melatonin *in vitro* release and permeability from MCP ($n=5$, JMP® 10.0.2, SAS Inst. Inc).

The effect of MCP on tight junction opening and cell viability was investigated by monitoring TEER values across HCE-T epithelial barrier for 2 days starting from the application of test samples to the cells. MCP induced the decrease in TEER due to chitosan interaction with tight junctions glycoproteins (2). TEER reversibility suggested MCP biocompatibility with epithelial barrier (Fig. 3).

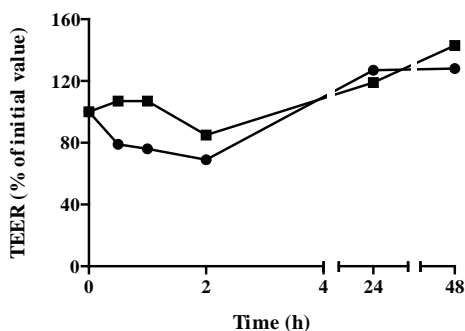


Fig. 3: Influence of melatonin solution (■) and MCP (●) on the TEER of HCE-T cell model. At the end of permeability study (2 h), cell surface was rinsed with HBSS and the receptor compartment was filled with culture medium.

Despite MCP-related TEER decrease, no increase in apparent melatonin permeability coefficient (P_{app}) was observed ($(1.64 \pm 0.11) \cdot 10^{-5}$ cm/s and $(1.92 \pm 0.13) \cdot 10^{-5}$ cm/s for MCP and solution, respectively). Therefore, it can be concluded that melatonin permeated transcellularly across epithelial model barrier. The permeation was controlled by its release profile as confirmed by established correlation.

MTT assay showed no decrease in cell viability of HCE-T cells upon MCP treatment (30 min, 0.05-1.00 mg/ml).

CONCLUSIONS

Developed cell-based epithelial cornea model is suitable for the prediction of eye-related bioavailability of drug delivered by chitosan-based systems. MCP were shown to interact with epithelial cornea barrier in safe and reversible manner. However, in case of melatonin, it resulted in no increase in permeability across cornea model suggesting transcellular melatonin transport.

REFERENCES

1. Pepić I, Lovrić J, Cetina-Čižmek B, Reichl S, Filipović-Grčić J. Toward the practical implementation of eye-related bioavailability prediction models. *Drug Discov. Today*. 2014; 19(1): 31-44.
2. Hafner A, Lovrić J, Voinovich D, Filipović-Grčić J. Melatonin-loaded lecithin/chitosan nanoparticles: Physicochemical characterisation and permeability through Caco-2 cell monolayers. *Int. J. Pharm.* 2009; 381(2): 205-213.

ASSESSMENT OF LIPOSOMES FOR (TRANS)DERMAL DRUG DELIVERY: THE SKIN-PVPA AS A NOVEL *IN VITRO* MODEL FOR THE STRATUM CORNEUM

Z. Palac^{1,*}, A. Engesland², G.E. Flaten², N. Škalko-Basnet², J. Filipović-Grčić¹ and Ž. Vanić¹

¹ University of Zagreb, Faculty of Pharmacy and Biochemistry, Department of Pharmaceutical Technology, A. Kovačića 1, 10000 Zagreb, Croatia

² University of Tromsø, Faculty of Health Sciences, Department of Pharmacy, Drug Transport and Delivery Research Group, Universitetsveien 57, 9037 Tromsø, Norway

INTRODUCTION

Over the last few decades liposomes have received particular attention as a promising nanosystem for improving skin delivery of drugs. While conventional liposomes generally enhance skin deposition of the drug without affecting percutaneous permeation and transdermal delivery, new types of phospholipid vesicles, such as deformable (flexible, elastic) liposomes and propylene glycol-containing liposomes, have been shown to increase the transport of active substances through the *stratum corneum* into the deeper layers of skin or even transdermally (1). In order to optimize their composition and achieve successful (trans)dermal drug delivery, drug permeability studies performed on robust and reliable models are essential. The complex nature of biological tissue, the inter- and intra-individual variability of human skin samples and ethical issues limit the use of human skin in the early stages of formulation assessment. On the other hand, measurements obtained by using Franz diffusion cell and animal skin are only partially standardized, leading to substantial variations in the results of permeability tests. The skin-phospholipid vesicle-based permeation assay (PVPA) is a novel *in vitro* skin barrier model based on the tightly





packed phospholipid vesicles mimicking structure and composition of *stratum corneum* (2). This assay provides a valuable method for the evaluation of skin permeation of different drugs and has the potential to be used to estimate (trans)dermal formulations. Present study evaluated the applicability of *stratum corneum* mimicking PVPa barrier in determining the drug penetration abilities of various types of liposomes: conventional liposomes (CL), deformable liposomes (DL) and propylene glycol liposomes (PGL).

MATERIALS AND METHODS

CL, DL and PGL of two different lipid concentrations (26 or 52 mM) were prepared by the film hydration method keeping the concentration of a model drug diclofenac sodium (DCS) constant (47 mM). All of the liposome preparations were extruded three times through the 400 nm pore size polycarbonate membranes (LiposoFast, Avestin, Canada). The mean diameters, size distributions (polydispersity) and zeta potentials of the liposomes were determined by photon correlation spectroscopy (Zetasizer 3000HS, Malvern Instruments, Malvern, UK). Separation of the untrapped drug from the liposomal fraction was performed using gel chromatography. Thereafter the concentrations of both the untrapped (free) and the liposome-entrapped drug were determined spectrophotometrically (Ultraspect Plus, Pharmacia LKB, Cambridge, UK). The membrane elasticity of the liposomes was assessed with a home-made device, as previously reported (3). The DCS permeability of various liposomes was evaluated on the recently developed skin-PVPa barrier model (2).

RESULTS AND DISCUSSION

The mean diameters of all of the extruded liposomes prepared with both lower lipid concentration (denoted as CL-A, DL-A, PGL-10-A and PGL-30-A) and higher lipid concentration (denoted as CL-B, DL-B, PGL-10-B and PGL-30-B) were in the range from 147 nm (DL) to 166 nm (PGL-30). Increasing the lipid concentration resulted in a larger size of vesicles and a broader size distribution. The highest entrapment of the drug was achieved by PGL-30 (>160 µg/mg lipid) and the lowest by DL (Tab. 1). Regarding the determined degree of liposome membrane elasticity (E), DL and PGL-10 were calculated to have an almost 5-fold higher elasticity than the CL. The assessment of the penetration ability of various liposomes containing DCS was performed using two PVPa barriers: a simple PVPaC consisting of phospholipid vesicles made of egg phosphatidylcholine and cholesterol and more skin-like

PVPAs prepared with phospholipid vesicles composed of lipids normally found in *stratum corneum*. To validate the permeability experiments, the barrier integrity was tested by measuring the electrical resistance across the barriers throughout the study. Fig. 1 shows the slight improvement in the DCS permeation profiles using DL-A and PGL-10-A on PVPaC as compared to the CL-A. However, when experiments were performed on the PVPAs the overall permeation and the difference between formulations were higher. All of the liposomal formulations exhibited significantly higher permeabilities than the DCS aqueous solutions, most probably due to the penetration-enhancing effect of the phospholipids. The highest Papp of DCS was attained with PGL-10-A, followed by DL-A, and the lowest values were obtained by CL-A. These results are consistent with the high elasticity of PGL-10-A and DL-A. Our findings demonstrate the increased permeation of hydrophilic drug by using elastic vesicles.

Tab. 1: The physicochemical properties of different types of liposomes containing DCS.

Formulation code	Mean diameter (nm)	Zeta potential (mv)	Entrapment efficiency DCS/lipid (µg/mg)	Degree of liposome elasticity (E)
CL-A	161±3	-58,8 ± 0,4	130,7 ± 3,5	1,08 ± 0,11
CL-B	147±4	-58,6 ± 0,8	88,7 ± 1,6	-
DL-A	153±1	-57,3 ± 0,3	61,7 ± 2,5	5,59 ± 0,23
DL-B	153±1	-67,8 ± 0,6	49,0 ± 1,8	-
PGL-10-A	156±4	-69,3 ± 1,4	137,9 ± 6,6	5,21 ± 0,31
PGL-10-B	161±4	-70,0 ± 0,8	93,4 ± 3,8	-
PGL-30-A	166±1	-67,9 ± 0,6	160,5 ± 7,9	3,69 ± 0,17
PGL-30-B	157±4	-60,7 ± 0,9	99,3 ± 4,7	-

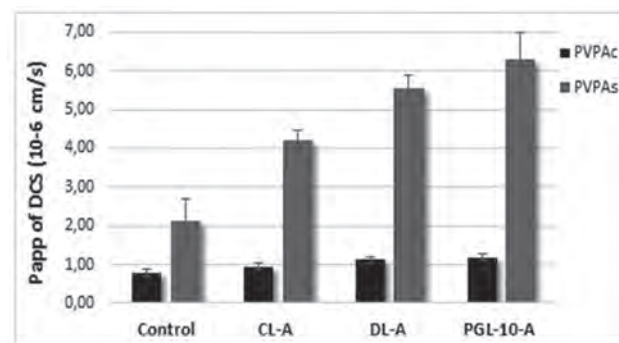


Fig. 1: The permeability of DCS from the liposomal formulations on PVPaC and PVPAs barriers. The values denote the mean ± S.D. (n=3).



CONCLUSIONS

The permeation of the hydrophilic drug from the liposomes was affected by their physicochemical properties, which were influenced by the lipid composition and the presence of the edge activator or penetration enhancer. This study demonstrates the potential of the newly developed skin-PVPA for the screening and optimization of liposomes at the early preformulation stage.

REFERENCES

1. El Maghraby GM, Williams AC, Barry BW. (2006). Can drug-bearing liposomes penetrate intact skin? *J Pharm Pharmacol* 58:415–29.
2. Engesland A, Skar M, Hansen T, et al. (2013). New applications of phospholipid vesicle-based permeation assay: permeation model mimicking skin barrier. *J Pharm Sci* 102:1588–600.
3. Vanič Ž, Hurler J, Ferderber K, et al. (2014). Novel vaginal drug delivery system: deformable propylene glycol liposomes-in-hydrogel. *J Liposome Res* 24:27–36.

A STUDY ON THE APPLICABILITY OF IN-LINE MEASUREMENT IN THE MONITORING OF THE PELLET COATING PROCESS

G. Hudovornik¹, K. Korasa^{1,*}, F. Vrečer¹

¹ Krka, d.d., Novo mesto, Šmarješka cesta 6, 8501 Novo mesto, Slovenia

INTRODUCTION

In recent years, regulatory authorities have demanded a better understanding of products and processes by requesting an “enhanced approach” using Quality by Design (QbD) in new registration applications. One of the ways to achieve this is to implement new technologies, such as the process analytical technology (PAT) (1). A part of PAT are new measurement tools, such as in-line process analysers, which enable collection of data in real time (2).

In our study we tested the applicability of two in-line measurement probes, a probe for the determination of moisture by near infrared (NIR) diffuse reflectance spectroscopy (3) and a spatial filtering technique (SFT) probe for the evaluation of particle size (4).

MATERIALS AND METHODS

The probes were evaluated during the process of applying polymer film coating onto drug layered pellets. We manufactured five pilot scale batches in a fluid bed coater (Aeromatic Fielder™ MP3/2/4, GEA Pharma Systems). Compositions of coating dispersions for the first three batches were the same (Eudragit® RS 30 D (Evonik Industries, Germany), Eudragit® RL 30 D (Evonik Industries, Germany), talc (Imerys Talc, Italy), triethyl citrate (Vertellus Performance Materials, USA), purified water), the composition of the coating dispersion of the fourth batch was changed quantitatively and the composition of the fifth batch was changed qualitatively (Eudragit® L 30 D (Evonik Industries, Germany), talc, triethyl citrate, purified water) compared to the first three batches.

NIR spectra were collected by Lighthouse Probe™ (GEA





Pharma Systems) and afterwards treated by standard normal variate transformation (SNV) and 2nd Savitzky Golay derivative. The partial least square (PLS) regression was used to predict Karl Fischer (KF) (V30, Mettler Toledo) and loss on drying 85°C/20 min (LOD) (Mettler Toledo, HR73 Halogen Moisture Analyzer) values from pre-treated NIR data. Samples for off-line determination were collected every 10 minutes during the coating of the pellets. A multivariate data analysis was performed with Unscrambler® X 10.2 (CAMO Software). We used the results of the first two batches (19 samples) to calibrate and validate (cross-validation) the PLS model. This model was later used to predict KF and LOD values from NIR data of the last two batches.

SFT measurements were made by Parsum IPP70 probe (Malvern Instruments). In-line particle size measurements were compared to the sieve analysis (Air Jet Sieve 200LS-N, Hosokawa Alpine) and static image analysis (Morphologi G3, Malvern Instruments) results. The sieve analysis was made using 250, 500, 710, 1000, and 1250 µm mesh size sieves. Samples for off-line particle size determination were taken every 20-30 min. Samples of the first four batches were used for sieve analysis and static image analysis (26 samples). Samples of the last batch were used to determine the degree of agglomeration (9 samples).

RESULTS AND DISCUSSION

The NIR data of the first two batches showed high correlation with both off-line methods after PLS regression was made (Tab. 1). The third batch was not used for NIR moisture determination due to attrition of the pellets during the process.

Tab. 1: R² values of calibration and validation after PLS regression; we used 2 factors for calculation. Measured off-line values were between 2.5-10.0%.

Method	R ² calibration	R ² validation
Karl Fischer	0.9812	0.9640
Loss on drying	0.9855	0.9756

We used above PLS models to predict off-line values (KF, LOD) from NIR data of the fourth and fifth batch.

The predicted values of the fourth batch (quantitative composition variation) were not comparable to the measured ones. High deviations were noticed for both off-line methods.

At first, the predicted values of the fifth batch (qualitative composition variation) did not correlate well with the measured values. Afterwards, we calibrated both PLS mod-

els in the range of the measured LOD and KF values of the fifth batch (2.0-5.5%). The predicted values with these models matched well with the measured values. The relative errors were 7.0% and 6.2% for LOD and KF predictions, respectively.

The medians of volume distribution (x50) obtained by the SFT probe were lower than x50 values measured by static image analysis. However, a high correlation between the x50 values of both methods was found. The R² and slope values after linear regression were 0.9933 and 1.044, respectively.

When comparing the SFT particle size distribution with the sieve analysis, we could notice that the SFT values were lower and the particle size distribution was wider. However, both methods responded similarly to particle size changes during the process (Fig. 1)

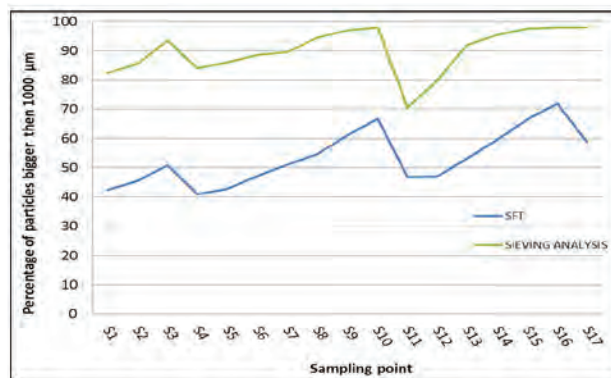


Fig. 1: Percentage of particles bigger than 1000 µm for samples of the first, second and fourth batch (n=17). Due to attrition of pellets during the third batch this parameter is not suitable for the particle size evaluation of this batch, thus it is not present on this chart.

The SFT in-line particle size parameters did not detect agglomeration of particles and were not consistent with the number of the agglomerates determined by off-line counting.

CONCLUSIONS

The NIR probe correlated well with the traditional methods for off-line moisture determination and it showed a potential to predict moisture content in the pellets with slightly different formulation.

The SFT probe proved to be a very useful tool for the in-line pellet size measurements.



ACKNOWLEDGEMENT

Authors would like to thank Krka, d. d., Novo mesto for providing support for the study.

REFERENCES

1. *Pharmaceutical CGMPs for the 21st Century – A Risk-Based Approach, Final report. Department of Health and Human Services, U.S. Food and Drug Administration, September 2004.*
2. *Guidance for Industry, PAT – A Framework for Innovative Pharmaceutical Development, Manufacturing, and Quality Assurance. U.S. Department of Health and Human Services, Food and Drug Administration, September 2004.*
3. Bogomolov A, Engler M, Melichar M, Wigmore, A. *In-line Analysis of a Fluid Bed Pellet Coating Process Using a Combination of Near Infrared and Raman Spectroscopy. J. Chemometrics 2010; 24 (7-8); 544-557.*
4. Roßteuscher-Carl K, Fricke S, Hacker M C, Schulz-Siegmund M. *In-line Monitoring of Particle Size in a Fluid Bed Granulator: Investigations Concerning Positioning and Configuration of the Sensor. Int. J. Pharm 2014; 466; 31-37.*

CRITICAL ATTRIBUTES OF NANOFIBERS: PHYSICAL PROPERTIES, DRUG LOADING AND TISSUE REGENERATION

J. Kristl^{1*}, P. Kocbek¹, S. Baumgartner¹, R. Rošic¹, J. Pelipenko¹, B. Janković¹, Š. Zupančič¹

¹ University of Ljubljana, Faculty of Pharmacy, Aškerčeva 7, 1000 Ljubljana, Slovenia

INTRODUCTION

In regenerative medicine, therapies generally focus on specific tissue (skin, bone, heart, vessels, ligament, tendons) and their cellular behavior due to repair degenerative changes and other damages, occurred by ageing of population (1). Skin tissue engineering strategies focus on epidermal, dermal or composite tissue generation or regeneration. In the case of chronic wound is imbalance between synthesis and degradation of natural extracellular matrix (ECM), which offers support for cell growth. In the field of development of modern wound dressings, which would temporary replace natural ECM and offer support for cell growth, nanofibers have gained a lot of attention (2). To construct *in vivo* like microenvironment with nanofabricated structures that mimic biological entities and cell-specific functions, it is necessary to benefit nano-technological approaches. Among available methods is electrospinning a new method in pharmaceutical technology and the most promising tool for generating nanopatterned scaffolds.

The objective of this study was to identify skin specific nanostructures, followed by development of electrospinning parameters for production of polyvinyl alcohol (PVA) nanofibers, varied in alignment and thickness. Finally, the research was focused on skin cells response grown on nanofibers in order to discover the crucial properties for clinical use.





MATERIALS AND METHODS

PVA (Mowiol® 20-98, Mw = 125.000 g/mol) nanofibers empty or loaded with API (antibiotic, resveratrol, blood-derived growth factors for dermal wound healing) were prepared by electrospinning (Fig.1) with static or rotating collector. Morphological (diameter, roughness) and mechanical properties of nanofibers were determined by SEM and AFM. Cells (keratinocytes and fibroblasts) were seeded on tested support (randomly and aligned nanofibers or glass coverslip as a control). Based on images the average nanofiber diameter, average interfibrillar pore size and cell size were determined by measuring 40 randomly selected objects using ImageJ 1.44p software (NIH, USA). The speed of cell adhesion was determined by counting of unattached cells, proliferation by MTS assay. The effect of nanofibrillar support on cell morphology was studied as cell shape index, which was calculated on the basis of cell images taken with confocal fluorescent microscope.

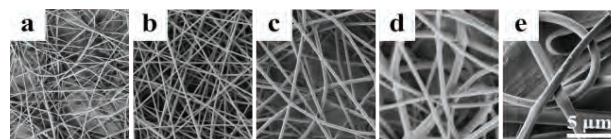
RESULTS AND DISCUSSION

Skin ECM consists collagen rich fibers with diameters 30-130 nm (1), responsible for modulating cell proliferation, migration, differentiation as well as providing mechanical support and a network that enable nutrient transport and diffusion. Scaffolds could emulate native tissue properties, such as ECM architecture, promote cell attachment and clinically assist in the healing and regeneration process.

Electrospinning parameters (Table 1): polymer concentration, relative humidity, applied voltage and collector type and distance to the needle are decisive combination for production of planned nanofibers (more 3-5).

Tab. 1: Electrospinning parameters used for production of PVA nanofibers, corresponding diameters and SEM images

Sample	PVA conc %	Tip to collector distance [cm]	Applied voltage [kV]	Relative humidity [%]	Nanofiber diameter [nm]
a	8	15	15	60	70
b	160				
c	10			33	305
d	4			665	
e	15			2	1115



Drug loading depends on physicochemical similarity of nanofiber polymer and API, from dissolution to dry product, and results in molecularly distribution (Fig 1A, B) or crystallization API (Fig. 1C) (more 6, 7).

Cell responses on nanofibrillar surface

Grown surface influence cell adhesion (Fig. 3A). Random or aligned nanofibers modulated spreading shape and cytoskeletal organization of investigated cells (Fig.2B). The morphology of the same cells differs on various structured scaffolds (Fig.3). Randomly oriented nanofibers limit cell mobility comparing to aligned due interfibrillar penetration of soft part of the cells (more in 8-10).

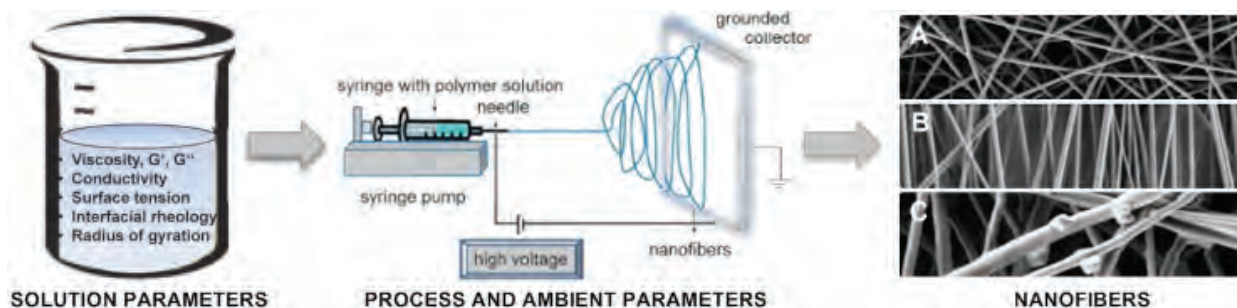


Fig. 1: A scheme illustrating the basic principles of the electrospinning process. An electric field is produced between a needle and a collector. The polymer solution is ejected from the needle towards the collector under the influence of the electric field. SEM images of (A) random, (B) aligned, and (C) loaded nanofibers are also shown.

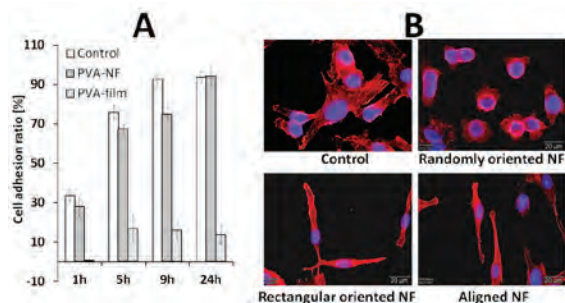


Fig. 2: Effects of PVA nanofibrillar support on cell growth. A – effect of nanofibrillar substrate on the keratinocytes' adhesion rate, B – effect of nanofiber alignment on keratinocytes' morphology.

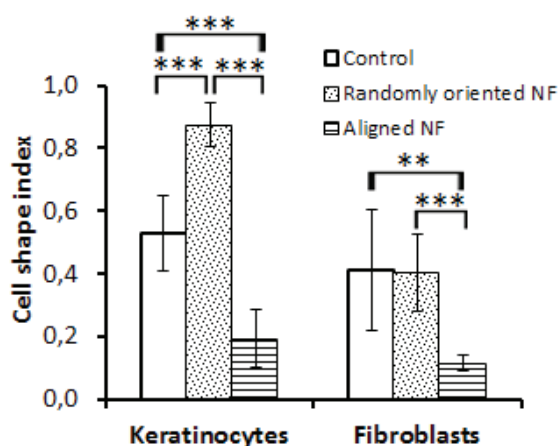


Fig. 3: Cell shape index on different supports (elongated cells have values close to zero, circular cells closer to 1).

CONCLUSIONS

These results especially highlight a) importance of combination of electrospinning parameters for nanofiber production, b) nanofiber alignment are more affected on cells as their size, c) the adhesion and morphology of the skin cells are a consequence of topographical properties of nanofibers, d) cell response is cell line specific. To manage numerous different parameters that affect the production of nanofibres with electrospinning the computer simulation is recommended.

ACKNOWLEDGMENTS

The authors gratefully acknowledge the financial support provided by the Slovenian Research Agency for Programme P1-0189, Projects J1-4236 and J1-6746, and Grant Numbers 1000 – 09 – 310085, 1000 – 11 – 310213.

REFERENCES

1. Kim, H.N., et al. Nanotopography-guided tissue engineering and regenerative medicine. *Adv Drug Del Rev* 65, 2013.536.
2. Engel, E., et al. Nanotechnology in regenerative medicine: the materials side. *Trends in Biotechnology*, 26, 2008. 39–47.
3. Rošic, R., et al., The role of rheology of polymer solutions in predicting nanofiber formation by electrospinning. *Eur Polym J*. 48, 2012, 1374-1384.
4. Rošic, R., et al., Physical characteristics of poly (vinyl alcohol) solutions in relation to electrospun nanofiber formation. *Eur Polym J* 49, 2013, 290-298.
5. Pelipenko, J., et al., The impact of relative humidity during electrospinning on the morphology and mechanical properties of nanofibers. *Int. J. Pharm.* 456, 2013, 125-134.
6. Rošic, R., et al., Nanofibers and their biomedical use. *Acta Pharm.* 63, 2013, 295-304,
7. Bertonecelj, V., et al., Development and bioevaluation of nanofibers with blood-derived growth factors for dermal wound healing. *Eur. J. Pharm. Biopharm.* 2014. doi: 10.1016/j.ejpb.2014.06.001
8. Pelipenko, J. et al., The topography of electrospun nanofibers and its impact on the growth and mobility of keratinocytes. *Eur. J. Pharm. Biopharm.* 84, 2013, 401-411.
9. Janković, B., et al., The design trend in tissue-engineering scaffolds based on nanomechanical properties of individual electrospun nanofibers. *Int. J. Pharm.* 455, 2013, 338-347.
10. Pelipenko, J., et al., Nanofiber diameter as a critical parameter affecting skin cell response. *Eur. J. Pharm. Sci in Press*





IN VITRO STUDY OF PERMEABILITY OF NANONIZED MELOXICAM FROM DIFFERENT NASAL FORMULATIONS BY SIDE-BI-SIDE™ HORIZONTAL CELL MODEL

P. Szabó-Révész^{1*}, T. Horváth¹, Cs. Bartos^{1,2}, R. Ambrus¹

¹ Department of Pharmaceutical Technology, University of Szeged, Eötvös u. 6, H-6720-Szeged, Hungary

² Richter Gedeon Ltd., Gyömrői út 19-21, H-1103 Budapest, Hungary

INTRODUCTION

Nasal dosage forms of drugs have gained importance in recent years because of (i) the rapid onset of action, (ii) circumvention of the first-pass elimination by the liver and GI tract, (iii) non-invasive and simple daily administration (1). In this work, the Side-Bi-Side™ (Crown Glass, USA) horizontal cell model was applied as a novel approach for an *in vitro* study of the permeability of nanonized meloxicam (MEL) from nasal formulations (2-4).

The aim was to optimize the horizontal cell method, and investigate and compare the diffusion of the drug from different nasal formulations (gel, spray and powder).

MATERIALS AND METHODS

Materials

MEL was obtained from EGIS Ltd. (Budapest, Hungary). The grinding additive, polyvinylpyrrolidone (PVP) K25, was purchased from BASF (Ludwigshafen, Germany). Sodium hyaluronate (HA, Mw = 1400 kDa) was obtained from Gedeon Richter Ltd. (Budapest, Hungary).

Preparation of MEL nanoparticles and the nasal formulations

An aqueous suspension of untreated MEL (rawMEL) (D0.5 = 58.4 µm) was used for the preliminary examinations. During the comparative studies, a co-ground product of MEL and PVP (nanoMEL/PVP) and their physical mixture (MEL/PVP mix) were formulated and investigated. MEL and PVP in a ratio of 1:1 were mixed and ground in a planetary monomill (Fritsch GmbH, Idar-Oberstein, Germany), which resulted in amorphous nanoparticles of MEL (D0.5 = 140±69 nm) (4).

To prepare a nasal gel, nanoMEL/PVP and MEL/PVP mix were dispersed in a gel of HA (1:5 mg/ml). Liquid forms containing nanoMEL/PVP and MEL/PVP mix were applied as nasal sprays with HA (1:1 mg/ml). For the dry powders, the co-ground product (nanoMEL/PVP) and the physical mixture (MEL/PVP mix) were used.

Preliminary examinations

The model comprised compartments, membranes and magnetic fixing (Fig.1). Gel and liquid forms were added by pipette. Dry powder was washed directly into the donor compartment. Samples were removed with a syringe needle.

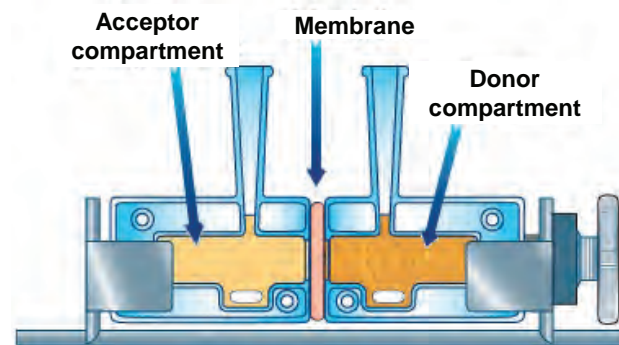


Fig. 1: Side-Bi-Side™ horizontal diffusion system.

Comparative permeability studies

The investigations were carried out at 37 °C. Each compartment had a volume of 3.0 ml. The pH of the donor compartment was 5.6, and that of the acceptor compartment was 7.4. An artificial membrane impregnated with isopropyl myristate was used between the donor and acceptor compartments (pore size: 0.45 µm). The samples in both compartments were stirred with a magnetic stirrer. Sampling was carried out at 5, 10, 15 and 60 minutes. The quantity of diffused MEL was determined spectrophotometrically at 364 nm.



RESULTS AND DISCUSSION

Rheological parameters such as the viscosity of the nasal gel and spray forms may influence the rate of diffusion of the MEL. The gel form containing 0.5% HA exhibited a higher viscosity than that of the spray form containing 0.1% HA (Fig. 2). Under shear stress, the structure of the gel form underwent a smaller change than that of the spray form, where the viscosity was 10 times lower than in the starting state.

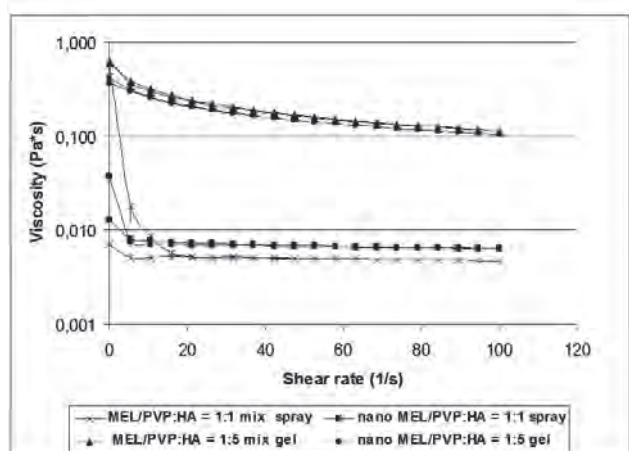


Fig. 2: Viscosity curves of HA-containing nasal gel and nasal spray.

For each formulation, the diffusion of the MEL from nano-sized samples was more significant than that from the physical mixture. As concerns the diffusion from the three formulations in the case of the co-ground product, the greatest amount of drug diffused from the nasal powder formulation, followed by the nasal spray and then the gel form (Fig. 3).

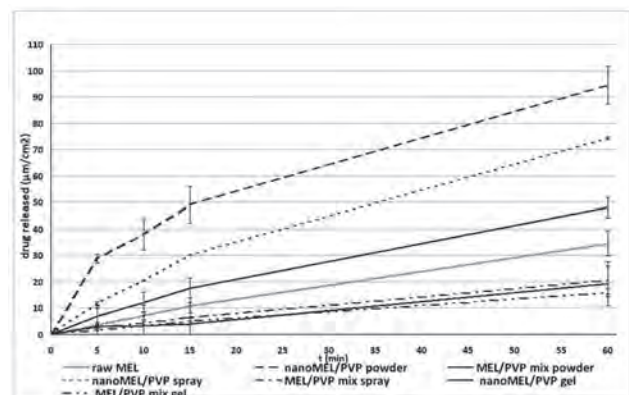


Fig. 3: Measurements of diffusion of MEL from different nasal formulations.

Since the Side-Bi-Side cell model was not suitable for the investigation of the nasal gel, the Franz vertical cell model (Hanson Research Company, USA) was used in the comparative studies. The results showed that the Franz cell method ensures a contact between the gel and the vertical membrane which results in well-controlled diffusion (Fig. 4).

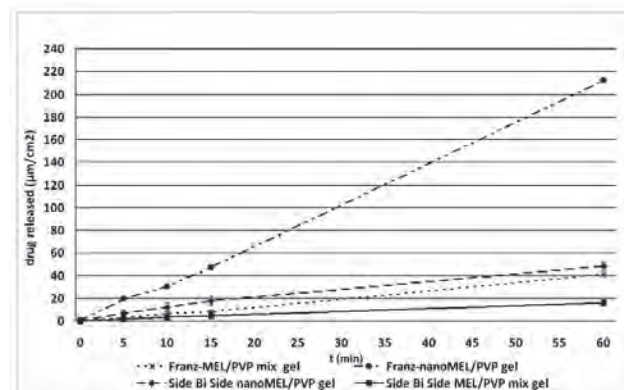


Fig. 4: Comparative diffusion studies with the Franz cell and Side-Bi-Side methods.

CONCLUSIONS

It was concluded that the Side-Bi-Side horizontal diffusion system is suitable for permeability studies of formulations for nasal delivery. The small compartment volume (3 ml) well simulates the nasal conditions. Primarily nasal sprays and powders can be investigated with the discussed method. Validation of the Side-Bi-Side method is in progress. The system may be suitable for ex vivo permeability studies, to investigate diffusion through mucous membranes prepared from humans and animals.

The presentation is supported by the European Union and co-funded by the European Social Fund. Project number: TÁMOP-4.2.2.A-11/1KONV-2012-0047

REFERENCES

1. Illum L, Nasal drug delivery: new developments and strategies. *Drug Discovery Today* 2002; 7: 1184-1189.
2. Arora A, Sharma S, Garg S, Permeability issues in nasal drug delivery. *Drug Discovery Today* 2002; 18: 967-975.
3. Kürti L, Veszelka S, Bocsik A, Khue Dung NT et al. The effect of sucrose esters on a culture model of the nasal barrier. *Toxicol. In vitro* 2012; 26: 445-454.
4. Kürti L, Gáspár R, Márki Á, Kápolna E et al. In vitro and in vivo characterization of meloxicam nanoparticles design for nasal administration. *Eur. J. Pharm. Sci.* 2013; 50: 86-92.





THE DEVELOPMENT AND CHARACTERIZATION OF THIOLATED POLYACRYLIC ACID-POLYALLYL AMINE NANOPARTICLES

J. Grießinger^{1,*}, S. Dünnhaupt¹, I. Nardin¹ and A. Bernkop-Schnürch²

¹ ThioMatrix GmbH, Research Center Innsbruck, Trientlgasse 65, 6020 Innsbruck, Austria

² Department of Pharmaceutical Technology, Institute of Pharmacy, University of Innsbruck, Innrain 80/82, 6020 Innsbruck, Austria

INTRODUCTION

For oral drug administration nanoparticulate delivery systems offer the advantage of providing a prolonged residence time in the small intestine leading to a comparatively higher drug uptake. In order to further improve the intestinal residence time of nanoparticles (NPs) their diffusion into the mucus gel layer followed by their immobilization in the mucus close to the absorption membrane would be advantageous. To render NPs more slippery in the mucus, on the one hand, a high density of positive and negative charges with a neutral net charge on their surface seems beneficial (1), as it is known from viruses exhibiting such surface properties to permeate almost unhindered through mucus (2). On the other hand, a fixation in deeper mucus regions should be feasible by the introduction of thiol groups on the surface of NPs forming comparatively more rapidly disulfide bonds with the mucus close to the absorption membrane where the pH is around 7 then in the more luminal mucus with a pH around 5.5.

In order to design such systems, it was the aim of this study to prepare and characterize NPs with a high charge density and thiolation on their surface by combining anionic and cationic (thiolated) polymers with each other.

MATERIALS AND METHODS

Materials

Polyacrylic acid (1.8 kDa; PAA), poly(allylamine hydrochloride) (58 kDa, PAH), L-cysteine hydrochloride (Cys), thioglycolic acid (TGA) 1-ethyl-3-(3-dimethylaminopropyl) carbodiimide (EDAC), fluorescein isothiocyanate (FITC), minimal essential medium (MEM), TritonTM X-100 and resazurin were obtained from Sigma-Aldrich, Germany. All other chemicals used in this study were of analytical grade.

Methods

PAA-cysteine conjugates (PAA-Cys) were synthesized by the covalent attachment of cysteine to PAA in presence of EDAC at pH 4.5. PAH conjugation with thioglycolic acid (TGA) was arranged at pH 5.0 in presence of EDAC. Eight different NPs were prepared and investigated by ionic gelation via complexation of PAA and PAH (Tab. 1). Resazurin assay was performed on Caco-2 cells to determine the in-vitro cytotoxicity of these NPs. For mucus diffusion studies FITC was coupled to PAH and fluorescence labelled NPs were prepared at pH 7.3. Particle size, polydispersity index and zeta potential of NPs were determined using a particle sizer (Nicom PSS 388, USA). Diffusion studies were performed in natural porcine intestinal mucus at pH 5.5 and pH 6.8 across a transwell system over 240 min (3).

Tab. 1: Combination of the eight different NPs

First polymer solution	Added polymer solution
PAA	PAH
PAA	PAH-TGA
PAA-Cys	PAH
PAA-Cys	PAH-TGA
PAH	PAA
PAH	PAA-Cys
PAH-TGA	PAA
PAH-TGA	PAA-Cys

RESULTS AND DISCUSSION

Unmodified and thiolated nanoparticles were prepared via ionic gelation due to electrostatic interaction between the negatively charged PAA and positively charged PAH. FITC labelled NPs showed a narrow particle size distribution and a slightly negative zeta potential (Tab. 2). Compared with NPs without FITC the particle size increased when more PAH solution was used. FITC was covalently coupled to



PAA and PAA-Cys by an oxidative disulfide coupling. Therefore less free amino groups were available for ionic gelation between the two polymers. The zeta potential of the NPs was found between 0 and -1 mV. This indicated a neutral charged surface.

Tab. 2: Particle size, polydispersity index and zeta potential of unmodified and modified PAA-PAH-FITC NPs (MD ± SD; n = 3)

	particle size [nm]	polydispersity index [P.I.]	Zeta potential [mV]
PAA + PAH-FITC	133.2 ± 55.6	0.17	-0.698 ± 0.32
PAA-Cys + PAH-FITC	214.4 ± 74.4	0.12	-0.446 ± 0.30
PAA-Cys + PAH-TGA-FITC	250.5 ± 85.2	0.12	-0.265 ± 0.23

The resazurin-assay after 3 h of incubation showed that the order of the NP preparation between PAA and PAH had an effect on the cell viability. The cytotoxic character of PAH could be eliminated when the PAH solution was added to a propound PAA solution (Fig. 1).

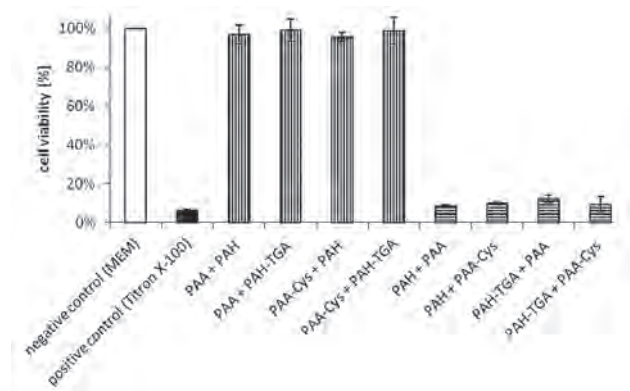


Fig. 1: Cytotoxicity potential of the eight NPs (0.5% m/V) in comparison to MEM solution; (MD ± SD; n = 3)

The diffusion study through mucus (Fig. 2) showed that thiolated NPs still can permeate the mucus but to a lower extend than unthiolated NPs. NPs prepared of thiolated PAA and thiolated PAH (PAA-Cys+PAH-TGA-FITC) showed a 40% decreased diffusion rate compared to unthiolated NPs. This demonstrates that thiolated NPs have higher mucoadhesive properties due to their capability of forming disulphide bonds with the mucus. pH dependent diffusion behaviour of thiolated NPs, however, could not be demonstrated.

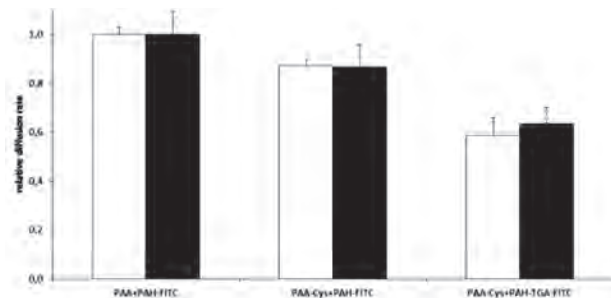


Fig. 2: Diffusion rate of PAA-Cys+PAH-FITC NPs and PAA-Cys+PAH-TGA-FITC NPs after 240 min across mucus (pH 5.5 (white bars) and pH 6.8 (black bars) within transwell system; (MD ± SD; n = 3)

CONCLUSIONS

Within this study a successful preparation of nanoparticles with a high positive and negative charge density and thiolation on their surface was demonstrated. The diffusion rates of thiolated NPs and unmodified NPs indicated an improved mucoadhesion of thiolated NPs due to their ability to form disulfide bonds with the mucus. Furthermore, the cytotoxic character of PAH could be eliminated by the preparation order of the NPs. Both the high charge density and the higher mucoadhesive properties suggest thiolated PAA-PAH NPs as a drug delivery system to target various mucosal surfaces.

ACKNOWLEDGEMENTS

We acknowledge EC for supporting this research through the FP7-2011-NMP-280761 "ALEXANDER" project.

REFERENCES

- Lai SK, Wang YY, Hanes J. Mucus-penetrating nanoparticles for drug and gene delivery to mucosal tissues. *Adv Drug Deliv Rev.* 2009; 61(2): 158-171
- Olmsted SS, Padgett JL, Yudin AI, Whaley KJ, Moench TR, et al. Diffusion of macromolecules and virus-like particles in human cervical mucus. *Biophysical J.* 2001; 81: 1930 - 1937
- Friedl H, Dünnhaut S, Hintzen F, Waldner C, Parikh S et al. Development and evaluation of a novel mucus diffusion test system approved by self-nanoemulsifying drug delivery systems. *J. Pharm. Sci* 2013; 102: 4406-4413





SURFACE PLASMON RESONANCE AND CONTACT ANGLE MEASUREMENTS FOR DRUG-EXCIPIENT INTERACTION STUDIES

L. Peltonen^{1*}, P. Liu¹, T. Viitala², A. Kartal-Hodzic², H. Liang², T. Laaksonen², J. Hirvonen¹

¹ Division of Pharmaceutical Chemistry and Technology, Faculty of Pharmacy, P.O. Box 56, 00014 University of Helsinki, Finland

² Division of Pharmaceutical Biosciences, Faculty of Pharmacy, P.O. Box 56, 00014 University of Helsinki, Finland

INTRODUCTION

Poor solubility is one of the main problems faced in drug delivery and nanocrystallization techniques are widely utilized to improve the solubility properties. Nanocrystals are solid drug particles covered by a stabilizer layer and the size of them is typically from 100 to 500 nm. The most problematic step in production of nanocrystals is the selection of appropriate stabilizer for a certain drug. Some studies are published on that subject but the selection of drug-stabilizer combination is still made on trial and error base (1).

The aim of this study was to reach an insight into the interaction mechanisms involved in nanocrystallization between the drug and stabilizer. Accordingly, the affinity of polymers on solid drug particles was measured by surface plasmon resonance (SPR) and contact angle techniques. Indomethacin was used as a model drug and the affinity of five different, but structurally closely related, poloxamers on indomethacin surface were measured. The corresponding nanocrystals were produced by nanomilling technique.

MATERIALS AND METHODS

Materials

Indomethacin was used as a model drug (Hawkins, USA), and Pluronic® F68 and 17R4, Tetronic® 908 and 1107 (BASF, Germany) and Pluronic® L64 (Aldrich, USA) as stabilizers. The water used was ultrapurified Millipore® water (Millipore, France).

Ball milling

Nanocrystals were produced by wet-ball milling technique (Pulverisette 7 Premium, Fritsch Co., Germany) with 1 mm zirconium oxide pearls. The drug:stabilizer ratio used in this study was 1:0.4.

Contact angle

The contact angle was measured with the sessile drop method (CAM 200, Attension Biolin Scientific Oy, Finland). Indomethacin powder compact was compressed to a disc with a hydraulic press (Specac, UK) and the contact angle of aqueous stabilizer solutions on compressed powder surface was measured.

Surface plasmon resonance, SPR

For SPR measurements indomethacin was deposited on the golden SPR sensor surface. The SPR sensograms were obtained by measuring the change in the SPR angle during the injection of a concentration series of aqueous stabilizer solutions over the indomethacin coated sensor surface.

Particle size

Mean particle size and polydispersity index, PI, of the nanocrystalline suspensions were measured by dynamic light scattering, DLS, technique (Malvern Zetasizer 3000 HS, Malvern Instrument, UK).

RESULTS AND DISCUSSION

Contact angle

When contact angle was measured, the highest contact angle was found with pure water and the contact angle was decreased when any of the stabilizers was added to the solution. Small contact angle between the drug and the stabilizer means higher affinity/wettability. In this study the affinity of the stabilizers was in the following order: L64 > 17R4 > T1107 ≈ F68 ≈ T908.

SPR

Binding efficiency was calculated from the SPR results. Binding efficiency can be used to describe the interaction strength. The molecular weight of the stabilizer is taken into account when calculating the binding efficiency,



which enables the comparison of the interaction strength between the drug and different stabilizers independently of the complexity of the interaction mechanisms. Higher binding efficiency means stronger interaction.

In this study the binding efficiency was lowered in the order L64 > 17R4 > F68 ≈ T908 ≈ T1107. When binding efficiency was compared to the contact angle results, they agreed very well.

Nanocrystallization

In nanocrystallization studies good nanocrystals were formed with all the other stabilizers except for 17R4 (Table 1). With 17R4 formed nanocrystals tend to aggregate into bigger clusters.

Tab. 1: Size information of nanocrystals produced with different stabilizers.

Stabilizer	Size/nm	PI
17R4	➤ 3 μm	1
L64	370	0.30
F68	290	0.24
T1107	310	0.26
T908	290	0.22

Discussion

The strongest binding strength was found with L64 and it formed nanosized nanocrystals though the polydispersity was higher. The shorter hydrophilic PEO chains were less efficient in stabilizing the nanocrystals though the binding efficiency was high.

17R4 had second strongest affinity, but its unfavourable telechelic structure with shorter PEO chains lead to larger nanocrystal clusters. F68, T908 and T1107 had lowest binding strengths due to the steric factors caused by the long PEO blocks, which decreased the adsorption of polymers.

For efficient stabilization with non-ionic polymers the polymer needs to attach firmly to the nanocrystal surface, fully cover the particles and offer polymer chains long enough for steric stabilization (2). The efficiency can not be explained only by the interaction studies.

CONCLUSIONS

SPR and contact angle measurements were successfully utilized in the interaction studies between drug and stabilizer. For efficient nanocrystal stabilizer high attachment forces and full coverage of the particle surfaces as well as suitable hydrophobic/hydrophilic chain length balance are important requirements, and the interaction measurements alone can't explain the stabilizing efficiency.

REFERENCES

1. Peltonen L, Hirvonen J, *Pharmaceutical nanocrystals by nanomilling : critical process parameters, particle fracturing and stabilization methods*. *J. Pharm. Pharmacol.* 2010; 62: 1569-1579.
2. Liu P, Viitala T, Kartal-Hodzic A, Liang H, Laaksonen T, Hirvonen J, Peltonen L, *Interactions studies between indomethacin nanocrystals and PEO/PPO copolymer stabilizers*. Submitted manuscript.





PREPARATION, CHARACTERIZATION AND EVALUATION OF LIPOSOMAL GELS INCORPORATING TERBINAFINE HYDROCHLORIDE.

C. Koutsoulas^{1*}, N. Pippa², C. Demetzos²,
A. Wagner³, E. Suleiman³, M. Zabka¹

¹ Faculty of Pharmacy, Department of Galenic Pharmacy, Comenius University in Bratislava, Odbojárov 10, 832 32 Bratislava, Slovakia

² Faculty of Pharmacy, Department of Pharmaceutical Technology, University of Athens, Panepistimioupolis, Zografou, Athens 15771, Greece

³ Polymun Scientific, Immunbiologische Forschung GmbH Donaustraße 99 3400 Klosterneuburg, Austria

INTRODUCTION

Terbinafine hydrochloride (TBH) is an effective, well tolerated broad spectrum antifungal agent, which belongs to the group of allylamines. TBH inhibits specifically squalene epoxide activity, thus inhibits ergosterol production, a major component of the fungal cell wall (1). From physicochemical point of view, TBH is sparingly soluble in water making it necessary to use solubilization techniques in order to incorporate it in an aqueous dosage form. Liposomes and other vesicles have already been used in order to overcome this water-insolubility problem (2,3). Moreover, liposomes are claimed to achieve improved transdermal permeation compared to conventional dosage forms(4). Their composition is similar to this of the skin, so they are delivering an API in a more physiological way, reducing thus possible hypersensitivity reactions (5). The aim of the present study is to prepare, characterize and evaluate a suitable liposomal dosage form intended for topical application, incorporating TBH.

MATERIALS AND METHODS

Materials

EggPC of $\geq 60\%$ purity was purchased from Sigma Aldrich (Germany), EggPC of 99% purity was purchased from Avanti Polar Lipids Inc. (Albaster, AL, USA), POPC of GMP grade was purchased from Lipoid (Germany) and cholesterol was purchased from Dishman (Netherlands). Chloroform and 2-propanol, were purchased from Centralchem s.r.o. (Slovakia). Dialysis membranes used for purification of liposomes and for *in vitro* drug release study were purchased from Spectrum Laboratories, Inc. (Netherlands). Centrifugal ultrafiltration tubes (centrisart) were purchased from Sartorius (Germany). All reagents used were of analytical grade.

Methods

Liposomes were prepared by thin film hydration method and down-sized in an Avanti MiniExtruder® (Albaster, AL, USA) through 200 nm polycarbonate membrane. Untrapped TBH was removed by dialysis using regenerated cellulose membrane (12000-14000 MWCO) against the same buffer as used for the preparation of liposomes. Size, pdi and physical stability of liposomal populations over time were measured by PCS. TBH retention in liposomes was studied using centrifugal ultrafiltration tubes to separate liposomes from free drug. Hydrogels were prepared by mixing Carbopol 934 or Hydroxyethylcellulose with water at different concentrations and liposomal gels were prepared by simple mixing of gels and liposomes to a final TBH concentration of 0.01%. Viscosity of the gels was measured in an oscillatory rheometer at fixed shear rates and *in vitro* drug release from liposomal gels was studied in vertical Franz diffusion cell system through dialysis membrane (12000-14000 MWCO).

RESULTS AND DISCUSSION

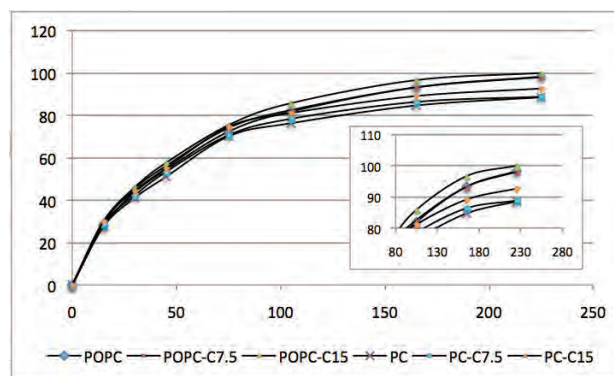


Fig. 1: Release profiles of terbinafine hydrochloride from HEC 3% liposomal gels.

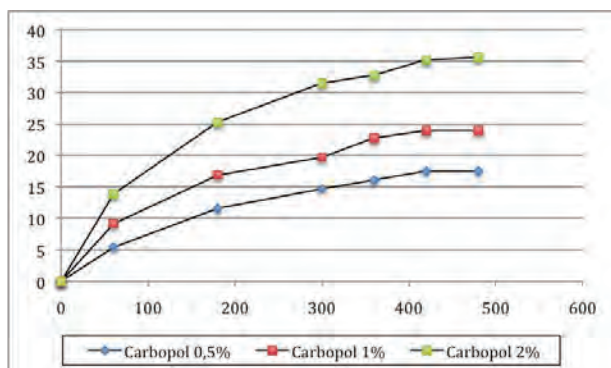


Fig. 2: Release profiles of terbinafine hydrochloride from Carbopol 934 liposomal gels.

Tab. 1: Composition and incorporation efficiency of liposome samples prepared.

Batch name	Lipid composition [mol : mol]*	Incorporation efficiency \pm sd [%]
E1	EggPC (99%)	88.64 \pm 4.41
E2	Egg PC (99%): Chol (92.5 : 7.5)	85.81 \pm 0.95
E3	Egg PC (99%): Chol (85 : 15)	87.55 \pm 3.44
E4	EggPC (\geq 60%)	61.78 \pm 3.65
P1	POPC	82.42 \pm 0.09
P2	POPC:Chol (92.5 : 7.5)	80.85 \pm 2.74
P3	POPC:Chol (85 : 15)	79.77 \pm 0.22

CONCLUSIONS

EggPC of two different purity grades (>60% and 99%) and POPC of synthetic origin (GMP grade) were used to prepare liposomes with or without cholesterol incorporating TBH. Moreover, effect of pH, drug to lipid ratio, lipid concentration, choice of gelling agent and gel viscosity were examined in order to optimize the final formulation. Physical stability and drug retention in liposomes were investigated over time at two different storage temperatures (2-8°C and RT) and drug release from liposomal gels was studied in vertical Franz diffusion cell system. From the obtained results it is concluded that purity of the phospholipid used to formulate a liposomal gel incorporating TBH has a major impact so on *in vitro* drug release profile from liposomal gels as on the physical stability of the liposomal formulation over time. On the other hand, the

origin of the phospholipid used to formulate a liposomal gel (natural/synthetic) seems to have minor importance with regard to drug release, physical stability and integrity of a liposomal formulation. Similarly, storage conditions during the studied period (21 days) do not seem to have a significant effect on the stability of liposomal formulations. Moreover, choice and concentration of the gelling agent used to formulate a liposomal gel seem to affect markedly the release behavior and the release kinetics of the final liposomal formulation.

REFERENCES

1. N. S. Ryder, Br. J. Dermatol. 126, 2 (1992).
2. Koutsoulas C, Pippa N, Demetzos C, Zabka M., J Nanosci Nanotechnol. 2014 Jun;14(6):4529-33.
3. Koutsoulas C, Suleiman E, Wagner A, Zabka M. J Liposome Res. 2014 Apr 28. [Epub ahead of print]
4. Tannverdi S.T., Özer Ö. (2013). Novel topical formulations of Terbinafine-HCl for treatment of onychomycosis. Eur J Pharm Sci, 48:628-636.
5. J.-P. Zhang, Y.-H. Wei, Y. Zhu, Y.-Q. Li, and X.-A. Wu, Arch. Pharm. Res. 35, 109 (2012).





NANOSCALE ANALYSIS OF SUBERIZED CELLULOSIC FILMS INTENDED FOR PHARMACEUTICAL MOISTURE BARRIER APPLICATIONS

J. Heinämäki^{1*}, A. Halenius², M. Paavo¹, U. Paaver¹, S. Alakurtti³, P. Pitkänen³, M. Pirttimaa³, K. Kogermann¹, P. Veski¹, J. Yliruusi²

¹ University of Tartu, Faculty of Medicine, Department of Pharmacy, Nooruse 1, 50411 Tartu, Estonia

² University of Helsinki, Division of Pharmaceutical Chemistry and Technology, P.O. Box 56, FI-00014 University of Helsinki, Helsinki, Finland

³ VTT Technical Research Centre Finland, P.O. Box 1000, FI-02044 VTT, Espoo, Finland

INTRODUCTION

Suberin is a biopolyester found in the cell walls of external tissues of plants where it plays a fundamental role as a protective barrier between the organism and its environment (1). Suberin polymer can be hydrolyzed by base treatment and fractionated to fatty acids (FA), which are potential raw materials in many industries (1,2). It is evident that the application of suberin FA as such, or combined with polymers could lead to new manufacturing opportunities for a wide range of pharmaceutical and biomedical systems intended for human and/or veterinary medicine applications. The objective of the present study was twofold: (a) to investigate film formation and surface morphology of suberin FA loaded aqueous cellulosic film and (b) to evaluate the water vapor barrier properties of the present suberized films.

MATERIALS AND METHODS

Suberin FA (Batch Pilot 1/14.01.2013 VTT, Espoo, Finland) was used as such in free films. Chemical composition of suberin FA mixture was similar as reported in literature (3). Hydroxypropyl methyl-cellulose, HPMC (Methocel E5, Dow Chemicals, USA) was used as a cellulosic film forming polymer. Polyethylene glycol (PEG 400) was used as a plasticizer.

For preparing polymer solution, HPMC was first dispersed in ethanol at a ratio of 5-8 parts of solvent to 1 part of HPMC. Cold water was then added to produce the final weight (0-8% of HPMC w/w). The solution was mixed until HPMC completely dissolved. This solution was gently heated on a water bath up to 40°C. Suberin FA was added by gently mixing into a warm solution. For plasticized films, PEG 400 was added to the polymer solution(s) (20% w/w of the solid polymer mixture weight). Free films were prepared in polytetrafluoroethylene (Teflon®) molds by a pouring method. The thickness of each film sample was measured at least at five different points by a micrometer. The final concentration levels of suberin FA in the HPMC free films were selected as 2.5%, 5%, 10% and 15% (w/w) from the HPMC weight.

Surface topography and morphology of free films were investigated with a high-resolution scanning electron microscope, SEM (Zeiss EVO® 15 MA, Germany) and atomic force microscope, AFM (Autoprobe CP, Thermomicroscopes, USA). The water vapor permeability (WVP) of the films was determined as described by Jia et al. (4) with some modification. The films were cut into a suitable size, fixed onto the mouth of anhydrous calcium chloride containing glass vials and immediately tightly sealed with a thin elastic band and Parafilm® M barrier film. The exposed surface area was 113.1 mm². The glass vials were held at 23 ± 2°C and 85% RH, and the increase in weight was measured at regular intervals after 1,2,3,4,5 and 7 days of storage.

RESULTS AND DISCUSSION

The dry thickness of the films ranged from 140 μm to 260 μm. Film formation was dependent on the presence or absence of an external plasticizer and the concentration of suberin FA (Figure 1).



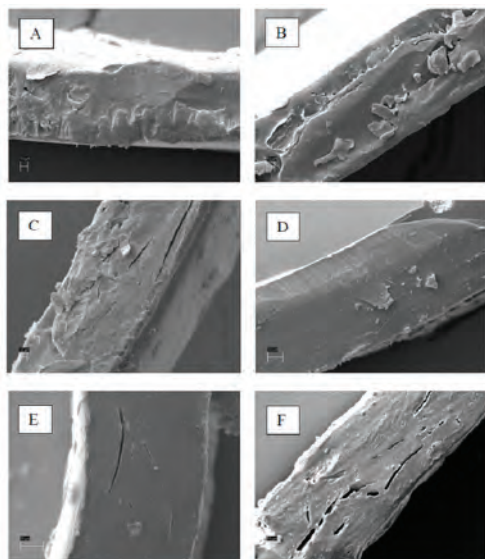


Fig. 1: SEM micrographs of the suberized HPMC free films. Key: Plasticized (A) and non-plasticized (B) reference HPMC film without added suberin FA; Plasticized (C) and non-plasticized (D) HPMC film with suberin FA (2.5% of the polymer weight); Plasticized (E) and non-plasticized (F) HPMC film with suberin FA (5.0% of the polymer weight). Magnification 1000x.

Surface topography and morphology analysis (AFM) showed differences in film structure between the non-suberized and suberized cellulosic films (Figure 2).

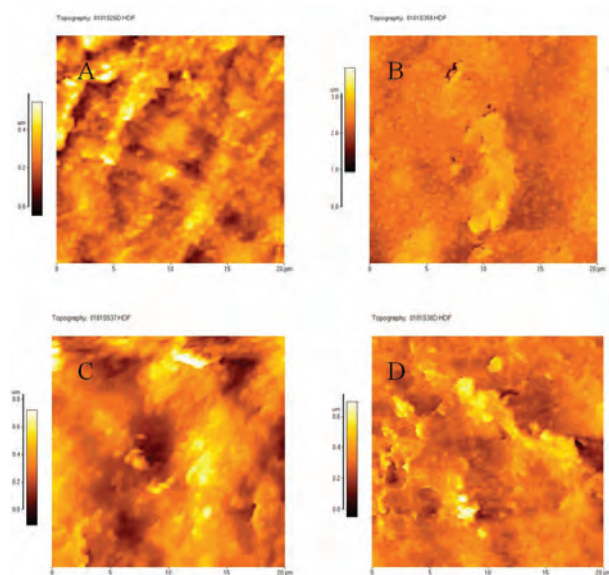


Fig. 2: Surface topography and morphology analysis of the suberized HPMC films with AFM. Key: Plasticized (A) and non-plasticized (B) reference HPMC film without added suberin FA; Plasticized (C) and non-plasticized (D) HPMC film with suberin FA (5.0% of the polymer weight).

The inclusion of suberin FA in the HPMC films resulted in a clear improvement in the moisture barrier of films compared to that obtained with the reference non-suberized HPMC films. The WVP of the films decreased with increasing suberin FA concentration in the films (Table 1).

Tab. 1: Water vapor permeability (WVP) of the plasticized and non-plasticized suberized hydroxypropyl methylcellulose (HPMC) films ($n = 3$).

HPMC film composition*	Water vapor permeability (WVP) [$\times 10^{-6}$ g/(mm ² h) \times mm/Pa]
HPMC	2.00
HPMC + PEG 400	2.13
HPMC + Suberin (2.5%)	2.08
HPMC + Suberin (2.5%) + PEG 400	1.82
HPMC + Suberin (5%)	1.71
HPMC + Suberin (5%) + PEG 400	1.70
HPMC + Suberin (10%)	1.13
HPMC + Suberin (10%) + PEG 400	1.25
HPMC + Suberin (15%)	0.69
HPMC + Suberin (15%) + PEG 400	0.77

*Amount of suberin calculated from the HPMC polymer weight

CONCLUSIONS

Suberin FA is a readily available bio-material and potential new excipient for pharmaceutical coating applications. Clear relationships can be found between the film surface morphology, WVP and the amount of suberin FA added in the HPMC films. Inclusion of suberin FA improves the moisture barrier properties of HPMC films.

ACKNOWLEDGEMENTS

This work is part of the targeted financing project no SF0180042s09 and ETF grant project no ETF7980. The research was also supported by the European Social Fund's Doctoral Studies and Internationalization Program DoRa, and GREASE Woodwisdom-ERANET (Tekes decision 40375/11).

REFERENCES

- Gandini A, Neto CP, Silvestre AJD. Suberin: A promising renewable resource for novel macromolecular materials. *Prog. Polym. Sci.* 2006; 31: 878-892.
- Alakurtti S. Synthesis of betulin derivatives against intracellular pathogens, Doctoral dissertation (article-based), University of Helsinki, Finland, 2013.
- Ekman R. The suberin monomers and triterpenoids from the outer bark of *Betula verrucosa* Ehrh. *Holzforschung* 1983; 37: 205-211.
- Jia D, Fang Y, Yao K. Water vapor barrier and mechanical properties of konjac glucomannan-chitosan-soy-protein isolate edible films. *Food Bioprod. Process.* 2009; 87: 7-10.





THE ROLE OF NEURO-FUZZY MODELS FOR PREDICTION OF BIOEQUIVALENCE STUDIES OUTCOME

J. Opara^{1*}, I. Legen¹,

¹ Lek Pharmaceuticals d.d., Verovškova 57, 1526, Ljubljana, Slovenia.

INTRODUCTION

Bioequivalence (BE) studies play an important part in generic drug development. They are unavoidable while requested by regulatory agencies, but on the other hand expensive and time consuming for sponsors. For this reason it is important to take the right decision before the start of a study while expensive or failed studies can limit the development of a generic product. We were looking for tools that are able to reduce the number of bioequivalence studies and have significant effect on development costs and timeliness. Modeling can be used to facilitate BE outcome predictions and with such enhanced knowledge of IVIVR incorporated in a model, the number of developed formulations and failed BE studies are reduced. Modeling *in vivo* data meet many challenges like limited databases, high variability of data and high complexity. For these reasons it is often difficult or impossible to build mathematical models for *In Vitro / In Vivo* correlations (IVIVC) that are preferred by regulatory agencies and described in Guidance (1,2). *In vitro* dissolution data are not always sufficient to describe *in vivo* behavior and for drugs with complicated pharmacokinetics or for immediate release drugs, we need to develop more complex models than level A, B, C or multiple level C correlation. Neuro-fuzzy (NF) systems were recognized as a reasonable method in comparison to the published approaches for development of IVIVR. The usefulness of NF models as an alternative *in vitro-in vivo* relationship (IVIVR) tool is presented in the continuation.

MATERIALS AND METHODS

NF systems belong to a group of artificial intelligence models and combine features of neural nets and fuzzy systems to provide a hybrid between the two techniques. Although both fuzzy and neural approaches possess remarkable properties when employed individually, there are great advantages to using them synergistically (4,5). The applicability of neuro-fuzzy models is increased with the transparency of included knowledge into the system. NF models were built to predict 144 pharmacokinetic (PK) parameter ratios required for demonstration of bioequivalence (BE) for 88 pivotal BE studies. The modeling process involved building hybrid artificial intelligence systems—NF models with the use of commercial software Neuframe version 4.0 (Neosciences 2000). Input parameters of models included dissolution data and their combinations in different media, presence of food, formulation strength, technology type, particle size, and spray pattern for nasal sprays. Ratios of PK parameters C_{max} or AUC were used as output variables. Database used for modeling consisted of PK parameters obtained in bioequivalence studies intended for regulatory submissions. Internal and external predictability of models were calculated and evaluated based on the currently valid guidelines for IVIVC (1,2).

RESULTS AND DISCUSSION

Statistical evaluation of prediction performance of models was performed. The prediction performance of models resulted in the following values: 79% of models have acceptable external prediction error (PE) below 10%, 13% of models have inconclusive PE between 10 and 20%, and remaining 8% of models show inadequate PE above 20%. Average internal predictability (LE) is 0.3%, and average external predictability of all models results in 7.7%. Basic statistics of external predictability of all models is presented in Table 1 (3).

Tab. 1: Basic statistics of external predictability of all models

PE%	All models	C_{max} models	AUC models
Mean	7.7%	8.9%	5.6%
Median	5.5%	6.6%	4.3%
Min	0.01%	0.20%	0.01%
Max	34.4%	34.4%	28.0%
N of models	144	88	56

With kind permission from Springer Science+Business Media: The AAPS Journal, Neuro-fuzzy Models as an IVIVR Tool and Their Applicability in Generic Drug Development, Mar;16(2), 2014, 324-34, J.Opara, I.Legen, Table III.



Based on results in Table 1 we can conclude that all mean and median values of external prediction errors for C_{max} and AUC models are below requested 10%. Drugs we used for modeling were also members of different BCS classes. Mean external prediction errors for individual BCS class were the following: 6.9, 8.4, 2.9 and 7.6, for BCS 1, 2, 3 and 4, respectively. All BCS 1 class drugs we used for modeling were incorporated in modified release formulations. One-way ANOVA was performed with BCS class as a factor to define statistical differences of PE% among BCS classes. We were not able to reject the H_0 about equality and we can conclude that there are no statistical differences in PE% between different BCS class drugs (3).

CONCLUSIONS

In average, models have acceptable internal and external predictabilities with PE lower than 10% and are therefore useful for IVIVR needs during formulation development. NF models facilitate the determination of impact factors for rate and extent of drug absorption and can be used as a support to QbD and for the prediction of BE studies outcome. With their properties, NF models were recognized as an alternative and reasonable method in comparison to the published approaches for *in vitro in vivo* correlation and preferential for solving of complex IVIVR problems. Prediction of BE studies outcome with NF models can support decisions when they need to be taken based on incomplete data.

ACKNOWLEDGMENTS

Many thanks to our colleagues at Lek Pharmaceuticals d.d. for their hard work in achievement of *in vivo* relevant dissolutions, BE data and other analytical measurements needed as inputs into the models.

REFERENCES

1. *Guidance for Industry, Extended Release Oral Dosage Forms: Development, Evaluation, and Application of In Vitro/In Vivo Correlations*. CDER, September 1997.
2. *Note for Guidance on quality of modified release products: A: oral dosage forms B: transdermal dosage forms*. EMA, CPMP July 1999.
3. J. Opara, I. Legen. *Neuro-fuzzy Models as an IVIVR Tool and Their Applicability in Generic Drug Development*. AAPS J. 2014; Mar;16(2): 324-34. (DOI) 10.1208/s12248-014-9569-8.
4. Tsoukalas LH, Uhrig RE. *Fuzzy and Neural Approaches in Engineering*. John Wiley & Sons, Inc., New York 1997.
5. *Manual Neuframe version 4.0, Neuscience 2000*.

LONGITUDINAL STUDY OF BISOPROLOL PHARMACOKINETICS IN ELDERLY PATIENTS WITH CHRONIC HEART FAILURE

K. Cvan Trobec¹, I. Grabnar², M. Kerec Kos², T. Vovk^{2,*}, J. Trontelj², M. Lainscak¹

¹ *University Clinic of Respiratory and Allergic Diseases, Pharmacy Department, Golnik 36, 4204 Golnik, Slovenia*

² *Faculty of Pharmacy, University of Ljubljana, Askerceva 7, 1000 Ljubljana, Slovenia*

INTRODUCTION

Bisoprolol is one of the most commonly used beta-blockers in the treatment of chronic heart failure (HF). It has a balanced clearance, with half of the dose being excreted via the kidney and another half via liver. It is equally hydrophilic and lipophilic drug, only 30% bound to plasma proteins, and its volume of distribution of more than 200 litres suggests binding to tissue proteins (1). It was also showed that bisoprolol pharmacokinetics is altered in obese subjects and thus suggests the dependence of bisoprolol pharmacokinetics (PKs) on body composition (2). For patients with HF, little is known about bisoprolol PKs. In the extremes of renal or liver function and body composition, the beta-blockers associated side effects or even toxicity may develop. The aim of this study was to investigate the PKs of bisoprolol in chronic HF patients by population pharmacokinetic modelling. We specifically assess changes over time, also in relation with body composition, renal and liver function. Finally, potential differences in pharmacokinetics between cachectic and non-cachectic subjects were evaluated.

MATERIALS AND METHODS

Patients and study design

Patients with chronic HF (class I-III) were screened for inclusion. Patients on regular therapy with bisoprolol were seen at baseline visit and at follow-up visit at least





6 months after inclusion. Patients attended the visit in the morning, fasting and before taking their morning dose of bisoprolol. Blood samples were drawn prior to morning bisoprolol dose (trough sample), followed by 2, 3 and 4 hours post dose sampling.

Assays

On visits, body composition was determined by dual-energy X-ray absorptiometry (DEXA) to assess fat mass, lean mass and body mineral content. Sum of lean mass in both arms and legs was calculated to obtain appendicular skeletal muscle mass (ASM) and skeletal muscle index (SMI) was calculated by dividing ASM with the square of patient height. Patients were screened for cachexia according to Evans et al (3).

Renal function was measured with iohexol clearance and with four variable Modification of Diet in Renal Disease (MDRD4) equation. Liver function was assessed with direct (BLRD) and total bilirubin (BLRT), aspartate transaminase (AST), alanine transaminase (ALT), gamma glutamyl transpeptidase (γ GT), and alkaline phosphatase (AF) concentration.

Bisoprolol plasma concentrations were determined by solid phase extraction of plasma samples and analysis using high performance liquid chromatography with tandem mass spectrometry.

Pharmacokinetic modelling

PK analysis was performed by a population PK modelling approach using NONMEM software. The structural model used was a one-compartment PK model with first-order absorption and elimination. The first-order conditional estimation method with interaction was used for estimation of apparent clearance (CL/F), apparent volume of distribution (V/F) and absorption rate constant (Ka). Effects of continuous and categorical covariates were tested against the base model. Alternative models were compared by the likelihood ratio test ($\alpha = 0.05$). Significant covariates were rank-ordered and introduced into the full model. The final model was determined by backward elimination of covariates one by one from the full model to see if they should remain in the model using the likelihood ratio test. The models were evaluated by standard diagnostic plots, absence of substantial η - and ϵ -shrinkage, convergence of minimization, successful covariance step, and gradients in the final iteration (range 10^{-3} - 10^2).

RESULTS AND DISCUSSION

Mean clearance of bisoprolol was 10.2 L/h, which is about one third lower than in healthy population (1). This result is comparable to the clearance determined in study of Nikolic et al (11.4 L/h) who also studied bisoprolol pharmacokinetics in chronic HF patients (4). With the final model it was demonstrated that CL/F is influenced only by MDRD4 (power model with the exponent of 0.620), while V/F is linearly related with body weight (WT) and SMI (power model). The final models are presented by the following equations:

$$CL/F [L/h] = 10.4 \cdot (MDRD4 [mL/min] / 60)^{0.620}$$
$$V/F [L] = 218 \cdot (1 + 0.00568(WT [kg] - 70)) \cdot (SMI / 7.32)^{0.715}$$

The difference in volume of distribution between the patient with the lowest SMI and the highest SMI in our study was almost 100%. Patients with lower body weight and SMI have lower volumes of distribution, which reflects in wider concentration fluctuations and higher maximal plasma concentrations of bisoprolol.

Bisoprolol clearance did not change significantly between the two visits, although measured renal function declined. Since bisoprolol is eliminated both via kidney and liver, decreasing renal elimination can be partly compensated by increasing hepatic elimination. On the other hand, the absorption rate constant declined during follow-up, which could suggest slower absorption process (Fig. 1). Moreover, apparent volume of distribution significantly increased, but this was not related to changes in the body composition.

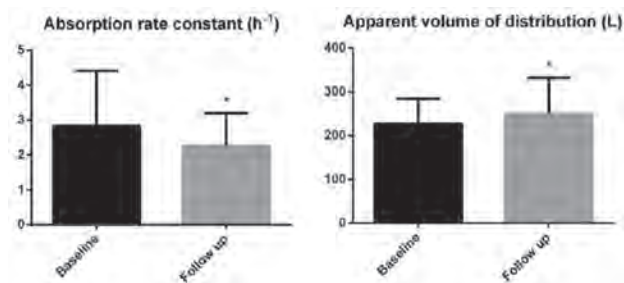


Fig. 1: Changes in pharmacokinetic parameters during follow-up (N=39; paired sample t test, $p < 0.05$).



Cachexia was not found to significantly influence bisoprolol pharmacokinetics. However, study sample was small and only four patients were cachectic at baseline and only three at follow-up.

CONCLUSIONS

Bisoprolol clearance is decreased in patients with chronic HF and is dependent on estimated renal function. Patients with lower body weight and skeletal muscle index have reduced volume of distribution, which results in greater fluctuations and higher peak plasma concentrations of bisoprolol. Bisoprolol pharmacokinetics changes during the course of the disease, but these changes are not related to the changes in body composition.

REFERENCES

1. Leopold G, Pabst J, Ungethüm W, Bühring KU. Basic pharmacokinetics of bisoprolol, a new highly beta 1-selective adrenoceptor antagonist. *J. Clin. Pharmacol.* 1986; 26: 616–21.
2. Le Jeunne C, Poirier JM, Cheymol G, Ertzbischoff O, Engel F et al. Pharmacokinetics of intravenous bisoprolol in obese and non-obese volunteers. *Eur. J. Clin. Pharmacol.* 1991; 41: 171–4.
3. Evans WJ, Morley JE, Argilés J, Bales C, Baracos V et al. Cachexia: a new definition. *Clin. Nutr.* 2008; 27: 793–9.
4. Nikolic VN, Jevtovic-Stoimenov T, Velickovic-Radovanović R, Ilic S, Deljanin-Ilic M et al. Population pharmacokinetics of bisoprolol in patients with chronic heart failure. *Eur. J. Clin. Pharmacol.* 2013; 69: 859–65.

2D DYNAMICAL SIMULATION OF A VIBRATIONAL MILL

M. Abrami¹, D. Hasa², B. Perissutti², D. Voinovich², G. Grassi³, R. Farra¹, M. Grassi^{1,*}

¹ Department of Engineering and Architecture, Trieste University, via A. Valerio 6, I-34127, Trieste, Italy.

² Department of Chemical and Pharmaceutical Sciences, Trieste University, Piazzale Europa 1, Trieste, I-34127, Italy.

³ Department of Life Sciences, Cattinara University Hospital, Strada di Fiume 447, I-34149, Trieste, Italy.

INTRODUCTION

Many delivery systems, especially oral administration ones, consist essentially of a crosslinked polymeric carrier hosting the active agent (drug) inside the three-dimensional network (1). The advantage of using such delivery systems is double. On the one hand, the polymeric network in the swollen state is able to control the drug release kinetics, due to the contact with the external physiological fluid. On the other hand, in the dry, shrunken state, the polymeric network is able to stabilise drug nano-crystals and/or amorphous drug. The interesting aspect of the amorphous drug and drug nanocrystals lies in their improved solubility (2, 3) that reflects in an increased bio-availability, aside from permeability problems (Amidon class II drugs (4)). Among the available techniques (solvent swelling and supercritical fluids, among others) used for drug loading into crosslinked polymers in form of nano-crystals or amorphous state, co-grinding has the considerable advantage of not requiring the use of solvents. Indeed, eliminating solvents from the final formulation is both very difficult and expensive. Albeit not exceptionally energetic (5), the vibrational mill seems a promising tool for drug-polymer co-grinding. Indeed, energy transfer from the grinding media to the drug-polymer system is a continuous (6) rather than an abrupt process that may induce undesired effects such as the occurrence of chemical reactions and/or the formation of polymorphic structures. In order to optimise the milling process, it is desirable, if not mandatory, to grasp the mill dynamics which are strictly connected to the energy transfer among grinding media and the drug-polymer ensemble. Accordingly, the aim of this work was to perform a two dimensional simulation of mill dynamics in order to theoretically select the best mill setup. This was achieved





by means of a home-made FORTRAN software solving the cardinal equations describing mill dynamics.

2D SIMULATION

The vibrational mill under study is a Sweco M18/5 (Florence, USA), equipped with 8 springs, 5 plastic vials (each with an internal volume of 250 cm³) and adopting alumina cylinders (0.5 cm diameter, 0.5 cm height) as grinding media. Co-grinding process optimization was performed focusing on the amount of grinding media (M_{MM}) and on the different angular position occupied by the two mill eccentrics (this angular displacement was indicated as γ) connected to the rotating mill engine shaft and inducing the complex mill dynamics. Accordingly, a two dimensional simulation (in the X, Y plane) of mill dynamics was performed keeping in mind that the 2D model behaves like the real 3D when both share the same total mass (M_T), centre of mass (abscissa X_C , ordinate Y_C) and inertia momentum (I). In order to greatly simplify the dynamic analysis, we chose to neglect the real movement of grinding media inside each vial. Grinding media were thus considered to be a unique body partially filling vials. The cardinal equations describing mill dynamics are:

$$M_T \frac{d^2 X_C}{dt^2} = \sum_{i=1}^n F_{xi}, \quad M_T \frac{d^2 Y_C}{dt^2} = \sum_{i=1}^n F_{yi} \quad (1)$$

$$I \frac{d^2 \alpha}{dt^2} = \sum_{i=1}^{2n} M_i \quad (2)$$

where t is time, n is the number of forces acting on the mill, F_{xi} and F_{yi} are, respectively, the horizontal and vertical components of the i^{th} force acting on mill body, α is the angular rotation around mill mass centre and M_i indicates the i^{th} momentum acting on mill body. In order to turn the 3D problem into a simpler 2D problem, we considered only the XY component of the forces acting on the upper and lower eccentrics due their rotation induced by the rotating mill engine shaft. Eqs.(1) and (2) were numerically solved by a 5th order adaptive step Runge-Kutta method. Mill geometrical and mechanical properties (such as spring elastic properties and materials density) have been experimentally determined or assumed according to mill manufacturer indications. As it is very difficult to establish a unique parameter indicating the grinding process optimal conditions (from the energy transfer point of view), we decided to select vials bottom velocity (V_{CB}) as control parameter. Indeed, grinding media impact energy can be assumed to be proportional to vials kinetic energy.

RESULTS AND DISCUSSION

Figure 1, showing the dependence of grinding chamber bottom velocity (V_{CB}) on grinding media mass (M_{MM}) and eccentrics angular displacement (γ), tells us that whatever M_{MM} , the best choice for γ is always 180°. In addition, although V_{CB} increases with M_{MM} , the choice of $M_{MM} = 2.5$ kg (all 5 vials are completely filled by grinding media) cannot be considered as it would make grinding media movements impossible inside vials.

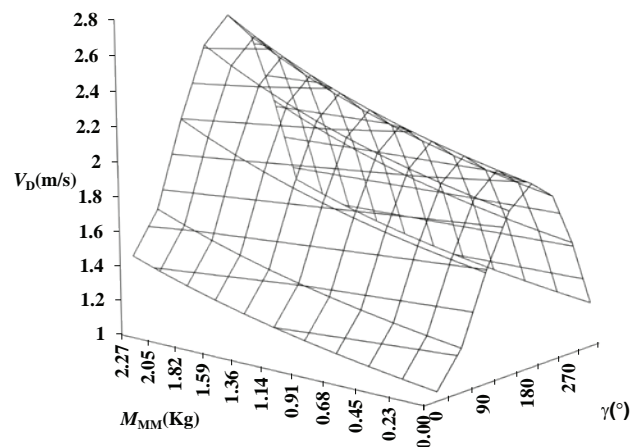


Fig. 1: Dependence of vials bottom velocity (V_{CB}) on grinding media mass (M_{MM}) and eccentrics angular displacement (γ).

CONCLUSIONS

This analysis led to the conclusion that the best mill set up (from the energy input point of view) corresponds to an angular displacement between eccentrics of 180°. In addition, the increase of grinding media mass improves the kinetic energy. Of course, these theoretical results need to be confirmed by experimental tests correlating the different mill set-up with the co-ground drug-polymer characteristics expressed by amorphous drug content and the nano-crystals dimensions.

REFERENCES

1. Lee PI, Diffusion-controlled matrix systems, in *Treatise on Controlled Drug Delivery*; Marcel Dekker: New York, 1992.
2. Hasa D, Perissutti B, Voinovich D, Abrami M, Farra R, S. M. Fiorentino SM, Grassi G, Grassi M. *Drug Nanocrystals: theoretical background of solubility increase and dissolution rate enhancement*. *Chem. Biochem. Eng. Quart.* 2014, in press.
3. Hasa D, Voinovich D, Perissutti B, Grassi G, Fiorentino SM, Farra R, Abrami M, Colombo I, Grassi M. *Eur. J. Pharm. Sci.* 2013; 50: 17-28.
4. Amidon GL, Lennernäs H, Shah VP, Crison JR. *A theoretical basis for a biopharmaceutical drug classification: the correlation of in vitro drug product dissolution and in vivo bioavailability*. *Pharm.*



Res. 1995; 12: 413–420.

5. Colombo I, Grassi G, Grassi M. Drug mechanochemical activation. *J. Pharm. Sci.* 2009; 98: 3961–3986.
6. Castillo J, Coceani N, Grassi M. Theoretical and experimental investigation on the dynamics of a vibrational mill, GRICU 2004 Symposium, "Nuove Frontiere di Applicazione delle Metodologie dell'Ingegneria Chimica", Porto d'Ischia (Na), 12-15 September 2004, Volume I, 165-168

APPLICATION OF MIXTURE EXPERIMENTAL DESIGN AND ARTIFICIAL NEURAL NETWORKS IN THE DEVELOPMENT OF TERNARY CARBAMAZEPINE-SOLUPLUS®-POLOXAMER 188 SOLID DISPERSIONS

Đ. Medarević^{1,*}, P. Kleinebudde², K. Bekčić¹, Z. Đurić¹, S. Ibrić¹

¹ Department of Pharmaceutical Technology and Cosmetology, Faculty of Pharmacy, University of Belgrade, Vojvode Stepe 450, 11221 Belgrade, Serbia, e-mail: djordje.medarevic@pharmacy.bg.ac.rs

² Institute of Pharmaceutics and Biopharmaceutics, Heinrich-Heine-University Duesseldorf, Universitaetsstr.1, 40225 Duesseldorf, Germany, kleinebudde@uni-duesseldorf.de

INTRODUCTION

Since number of currently available solid dispersion (SD) carriers is limited, it is often necessary to combine them to tailor their properties with regards to processability, solubilizing capacity and stabilization of the drug within the dispersion (1). Finding an optimal composition of SD can be difficult, since both proportions of each component of the carrier mixture and proportion of drug can significantly influence on dispersion properties. This study investigates potential of using mixture experimental design (MED) and artificial neural networks (ANNs) for evaluation the influence of the composition of ternary carbamazepine (CBZ)-Soluplus-poloxamer 188 (P188) SDs on CBZ release rate.

MATERIALS AND METHODS

Materials

CBZ, donated by Galenika AD (Belgrade, Serbia), Soluplus®, micronized poloxamer 188 (P188-Kolliphor® P188





micro), both kindly donated by BASF (Ludwigshafen, Germany) and absolute ethanol (Merck, Darmstadt, Germany) were used for SDs preparation.

SDs preparation, *in vitro* drug release testing and data modeling

SD formulations were prepared according to D-optimal mixture experimental design (Table 1.), with the following constraints: $20\% \leq \text{CBZ} \leq 50\%$, $30\% \leq \text{Soluplus} \leq 80\%$, $0\% \leq \text{P188} \leq 20\%$. CBZ, Soluplus and P188 were firstly dissolved in absolute ethanol, followed by ethanol evaporation on glass slides at 60°C. Obtained mass was scraped off and pulverized after storage for 48 h. Dissolution testing was performed on an amount of SDs containing 200 mg of CBZ using rotating paddle apparatus during 2 h (75 rpm, 500 ml water), with spectrophotometric determination of dissolved CBZ at 285 nm. Percentage of CBZ dissolved after 10 min (Q10) was selected as response. MED analysis was performed using Design expert 7.0 software (Stat-Ease, Inc., Minneapolis, MN, USA), while ANN modeling was done in Statistica Neural Networks software (StatSoft, Inc., Tulsa, OK, USA). Formulations F1-F22 were used as test and verification data, while formulations T1-T3 were used as test data. Prediction ability of MED and ANN models was compared by the root mean square error (RMSE) of the test data set:

$$\text{RMSE} = [\sum (y_i^t - y_i^p)^2 / n]^{1/2}$$

where y_i^t and y_i^p are target and predicted response, respectively and n is the number of experiments

RESULTS AND DISCUSSION

CBZ release rate was markedly improved using ternary SDs. While Q10 was about 12% for pure CBZ, for 11 of 22 prepared SDs, Q10 was higher than 80%. Based on statistical parameters (R^2 , adjusted R^2 (Adj R^2), predicted R^2 (Pred R^2) standard deviation (SD) and predicted residual sum of square (PRESS)), cubic model was selected. It gives quantitative relationship between SDs composition and Q10. After excluding terms that were found insignificant using ANOVA, the following model was obtained:

$$\text{Q10} = -4.82A - 0.38B - 43.41C + 0.12AB + 0.84AC + 0.85BC - 0.01ABC - 0.00036BC(B-C)$$

where A, B and C are actual proportions of CBZ, Soluplus and P188, respectively. From the contour plot (Fig. 1) it is evident that the highest Q10 is achieved with SDs containing the lowest proportions of CBZ and the highest proportions of P188. ANN model was obtained using three-layer

feed-forward multi-layer perceptron network with one hidden layer. The following parameters were determined as optimal, giving the lowest test error: two hidden neurons, back propagation training algorithm, hyperbolic activation function, learning rate 0.6 and momentum 0.3. From the 3D surface plot (Fig. 2) obtained by the ANN model it is evident that Q10 increase with decreasing proportion of CBZ and increasing proportions of both Soluplus and P188. Obtained R^2 values of 0.939 and 0.966 for ANN and MED model, respectively, indicated better data fitting to MED model. However, ANN model show better predictability on the test data set, as can be seen from predicted Q10 values and lower values of RMSE (Table 2.).

Table 1. D-optimal experimental design matrix with response values

	Mixture components (%)			Response
	CBZ (%)	Soluplus (%)	P188 (%)	Q10 (%)
F1	50.00	48.92	1.08	44.88
F2	50.00	39.47	10.53	62.94
F3	42.99	57.01	0.00	72.97
F4	50.00	39.47	10.53	64.29
F5	26.15	68.82	5.03	81.72
F6	20.00	80.00	0.00	67.56
F7	34.53	45.53	19.94	85.66
F8	20.00	80.00	0.00	68.17
F9	27.14	54.54	18.32	84.74
F10	20.00	63.59	16.41	93.55
F11	34.72	58.21	7.07	83.52
F12	41.61	48.30	10.09	75.31
F13	47.26	32.74	20.00	77.99
F14	50.00	48.92	1.08	42.86
F15	20.00	63.59	16.41	92.89
F16	47.26	32.74	20.00	80.21
F17	44.33	39.79	15.88	79.88
F18	34.94	51.99	13.07	91.31
F19	22.61	66.19	11.20	86.22
F20	20.00	60.00	20.00	95.54
F21	42.57	52.44	4.99	70.33
F22	33.86	62.73	3.41	74.52
T1	33.57	66.43	0.00	69.20
T2	47.66	46.68	5.66	55.34
T3	28.38	58.49	13.13	93.65

Table 2. Experimental and predicted Q10 values for test data

	Q10 exp	Q10 (ANN)	Q10 (MED)
T1	69.20	71.66	83.91
T2	55.34	55.42	58.97
T3	93.65	91.38	88.48
RMSE		1.93	9.24

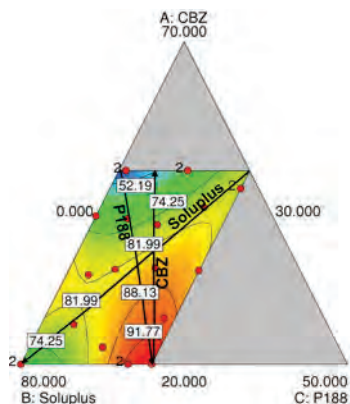


Figure 1. Contour plot of Q10 depending on the SD composition, predicted by MED model (replicated points are marked with 2)

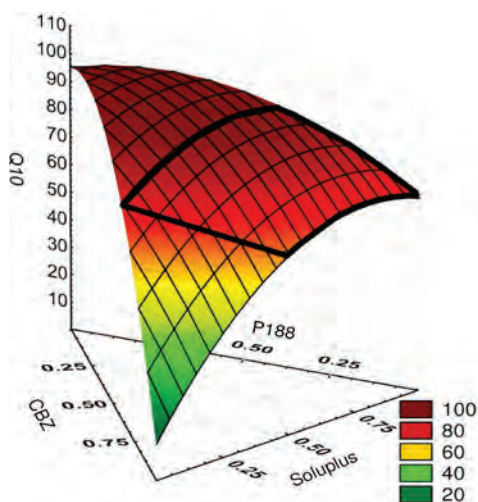


Figure 2. 3D surface plot of Q10 depending on the SD composition, predicted by ANN model (examined experimental space is framed)

CONCLUSIONS

Both MED and ANN model well described relationship between proportions of SD components and CBZ release rate, while ANN exhibit better generalization ability.

ACKNOWLEDGMENT

This work was supported by the project TR34007, funded by the Ministry of Education Science and Technological Development, Republic of Serbia and bilateral Serbia-Germany project: Application of machine learning tools in establishing a design space in solid dosage forms development.

REFERENCES

1. Bley H, Fussnegger B, Bodmeier R. *Int. J. Pharm.* 2010; 390: 165-173.

EFFECT OF THE DESIGN OF EXPERIMENT LAYOUT ON THE ESTIMATION OF PELLET PROPERTIES AND DESIGN SPACE RELIABILITY

T. Sovány^{1*}, Zs. Tislér¹, K. Kristó¹, A. Kelemen¹, G. Regdon jr.¹

¹ University of Szeged, Department of Pharmaceutical Technology, H-6720, Eötvös u. 6., Szeged, Hungary

INTRODUCTION

The use of the Quality by Design approach is a key question of the recent pharmaceutical developments, which has a highly considerable importance in the formulation of biotechnology derived product. Since these APIs have an increasing importance in therapy (1), but their high sensitivity requires careful design of production, and critical evaluation of the collected data, especially during formulation of a solid dosage form.

Present work was focused on the investigation of the effect of the applied experimental design layout on prediction accuracy and design space estimation in the development of a lysozyme containing pellet.

MATERIALS AND METHODS

Materials

Egg-white lysozyme (Lysoch 40000, Handary SA, Brussels, Belgium) was used as model API. The conformation of the enzyme was stabilized with mannitol (Hungaropharma Ltd., Budapest, Hungary) according to the findings of Singh and Singh (2). Microcrystalline cellulose (Avicel pH 101, FMC BioPolymer, Philadelphia, USA) served as the plastic carrier of the formulation.

Methods

The powders (lysozyme, mannitol and cellulose in a ratio of 1:4:5 respectively) was homogenized in a Turbula





mixer (Willy A. Bachofen Maschinenfabrik, Basel, Switzerland) for 10 min.

The homogenized powder mixture was wetted and kneaded in a ProCepT 4M8 high-shear granulator (ProCepT nv., Zelzate, Belgium) with 60 ml of purified water. The critical process parameters were recorded throughout the process.

The wet mass was extruded with a Caleva mini screw extruder and then spheronized with a Caleva MBS spheronizer (Caleva Process Solutions Ltd., Sturminster Newton, UK). The spheronized samples were dried for 48 h at room temperature.

The activity of pellets was determined via the degradation of *Micrococcus lysodeieticus* (VWR International, Budapest, Hungary) and was expressed as a percentage of the activity of the native lysozyme.

A Zeiss stereomicroscope (Carl Zeiss, Oberkochen, Germany) and Leica Quantimet 500 C image analysis software (Leica Microsystems, Wetzlar, Germany) were used for the determination of the size and shape of the particles.

The hardness of the pellets was tested with a special hardness testing apparatus developed at the Department of Pharmaceutical Technology, University of Szeged. The breaking mechanism and the force required to break the pellets was followed and analysed with computer.

RESULTS AND DISCUSSION

The results showed that key issue of the estimation of the design space is the determination of the enzymatic activity of the product. Since this parameter shows considerable variability the effect of determination uncertainties have significant influence on the modelling accuracy.

Fig. 1: Activity of pellets estimated with 2 level (a), Central Composite (b) and 3 level (c) full factorial design

According to our findings the activity determination based on the classical unit definition was insufficient to involve into the statistical evaluation, and the exact determination of the main kinetic parameters were essential to the appropriate modelling of this parameter. Nevertheless, since this parameter is highly sensitive to many environmental conditions the validity of the estimations based on mathematical modelling is still problematic.

Fig 1 shows how the model capability changes with the experimental layout. The increment of the data points used for the calculation of the model significantly improves the estimation accuracy, but the strong nonlinearity necessitates the use of artificial intelligence based applications for the determination of design space and for the certification of the effect estimation of factor interactions.

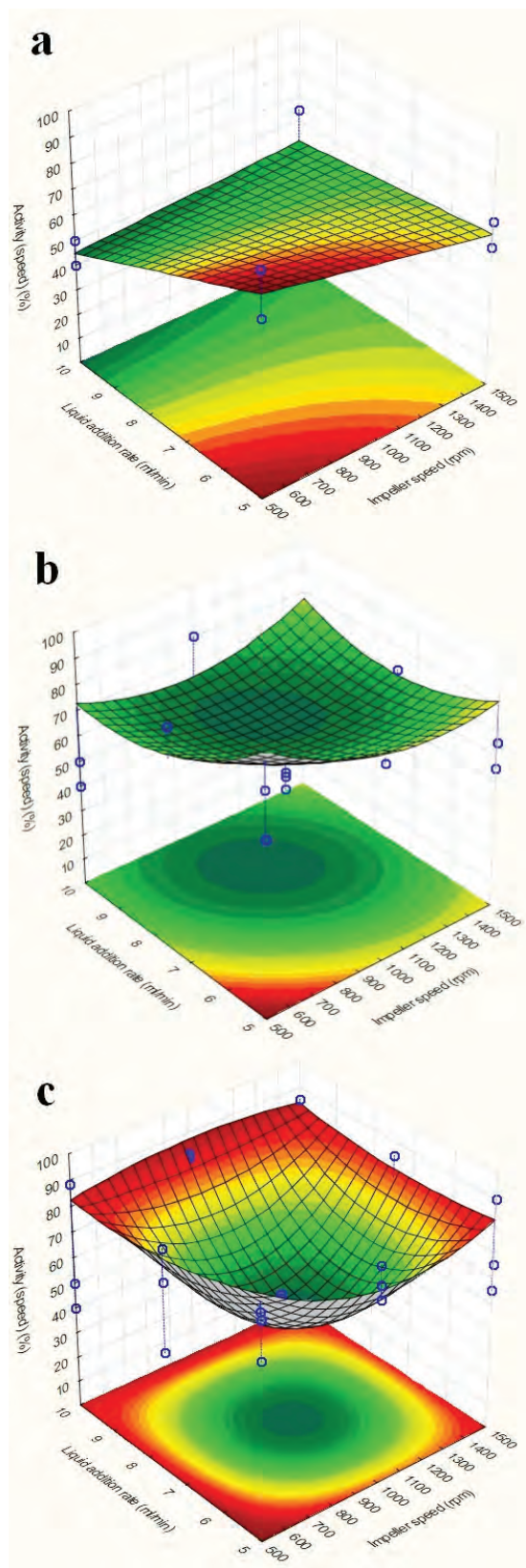


Fig. 1: Activity of pellets estimated with 2 level (a), Central Composite (b) and 3 level (c) full factorial design



CONCLUSIONS

Estimation of enzymatic activity with statistical methods requires more precise statistical data evaluation as other quality parameters, since the methods of determination provides smaller robustness for the evaluated data, which necessitates critical evaluation and the use of advanced predictive models for handling of variability.

ACKNOWLEDGEMENT

This research was supported by the European Union and the State of Hungary, co-financed by the European Social Fund in the framework of TÁMOP 4.2.4. A/2-11-1-2012-0001 'National Excellence Program'.

REFERENCES

1. M. Morishita, N.A. Peppas *Is the oral route possible for peptid and protein drug delivery Drug Discov. Today* 2006; 11: 905-910
2. S. Singh, J. Singh *Controlled release of a model protein lysozyme from phase sensitive smart polymer systems Int. J. Pharm.* 2004; 271: 189-196.



POSTER PRESENTATIONS





NOVEL APPROACH FOR PROLONGED SUBCUTANEOUS RELEASE OF UFH AND LMWH: THERMORESPONSIVE POLOXAMER-BASED HYDROGELS WITH CHITOSAN NANOCOMPLEXES (P01)

M. Radivojša¹, I. Grabnar¹, P. Ahlin Grabnar^{1*}

¹ University of Ljubljana, Faculty of Pharmacy, Aškerčeva 7, 1000 Ljubljana, Slovenia

INTRODUCTION

Heparins are the standards of anticoagulants used in the prophylaxis and treatment of deep vein thrombosis and pulmonary embolism. Unfractionated heparin (UFH) and low-molecular-weight heparin (LMWH) are polyanionic mucopolysaccharides with a mean molecular weight of 15 kDa and 5 kDa, respectively. Due to usual long-term prophylaxis and treatment, the development of prolonged heparin delivery systems has been of continuous interest. Thermally induced gelling systems, such as poloxamer-based hydrogels, seem to be the most promising ones for the development of injectable drug delivery systems. They are viscous liquids at room temperature, but form a rigid semisolid gel at body temperature (1).

The purpose of the present study was to develop thermoresponsive poloxamer-based hydrogels with polyelectrolyte nanocomplexes (PEC) composed of heparin (UFH/LMWH) and chitosan for prolonged subcutaneous release and to evaluate how various factors influence their *in vitro* behaviour.

MATERIALS AND METHODS

Materials

Heparin® Braun 5000 i.e./1ml sodium salt (Braun Melsungen AG), Fragmin® 10000 anti-Factor Xa IU/1ml (Pfizer Inc.), chitosan hydrochloride (CH; Kraeber&Co GmbH), Lutrol® F127 (P407) and Lutrol® F68 (P188) (BASF), Methocel K4M Premium (HPMC; Colorcon), Azure A chloride (Sigma-Aldrich).

Preparation of PECs

PECs were prepared from Stock solutions of CH, UFH and LMWH by polyelectrolyte complexation method using magnetic stirrer.

Characterization of PECs

The mean diameter (d) and polydispersity index (PDI) of PECs were determined by photon correlation spectroscopy and (ZP) by laser Doppler electrophoresis at 25°C with a zeta potential Nano ZS (Malvern Instr., UK).

Preparation of thermoresponsive hydrogels

Various hydrogel formulations (F1-F8) containing P407, P188 and HPMC were prepared by "cold method" (2) (Table 2).

Rheological studies

Oscillatory tests were carried out with a Modular rheometer Physica MCR 301 (Anton Paar, Graz, Austria), using a cone and plate geometry. Storage modulus (G') and loss modulus (G'') values were measured at varied temperatures (10-40 °C) with a constant shear strain of 0.2 %. The crossing point $G' = G''$ is taken to define the sol-gel transition point.

In vitro release study

In vitro heparin release study was conducted using a membraneless model. 1 ml of F1, F2 and F3 cold solutions (UFH and LMWH concentrations of 1 mg/ml and 1.125 mg/ml, respectively) was transferred into graduated test tubes and placed in a 37 °C water bath. After gelation, 2 ml of the release medium (PBS pH 7.4) were layered over the surface of the hydrogel. The amount of UFH/LMWH in the samples was determined according to Azure A colorimetric method (3).





RESULTS AND DISCUSSION

Characterization of PECs

From results in Table 1, it can be concluded that 1:1 for UFH/CH and 1:1.375 for LMWH/CH are the optimal mass ratios to obtain small, homogenous and stable PECs.

Tab. 1: Characteristics of nanocomplexes with different UFH/chitosan and LMWH/chitosan mass ratio.

UFH:CH	pH	Size (nm)	PDI	ZP (mV)
1:0.5	7.32	4233	0.48	-50.7
1:1	5.20	122.6	0.22	+35.5
1:2	4.63	134.6	0.23	+42.5
1:4	4.36	152.1	0.25	+42.9
LMWH:CH	pH	Size (nm)	PDI	ZP (mV)
1:1	6.84	310.0	0.40	-43.5
1:1.375	5.00	121.3	0.13	+32.2
1:1.5	4.64	151.8	0.16	+37.8
1:2	4.35	156.5	0.17	+42.0

Rheological studies

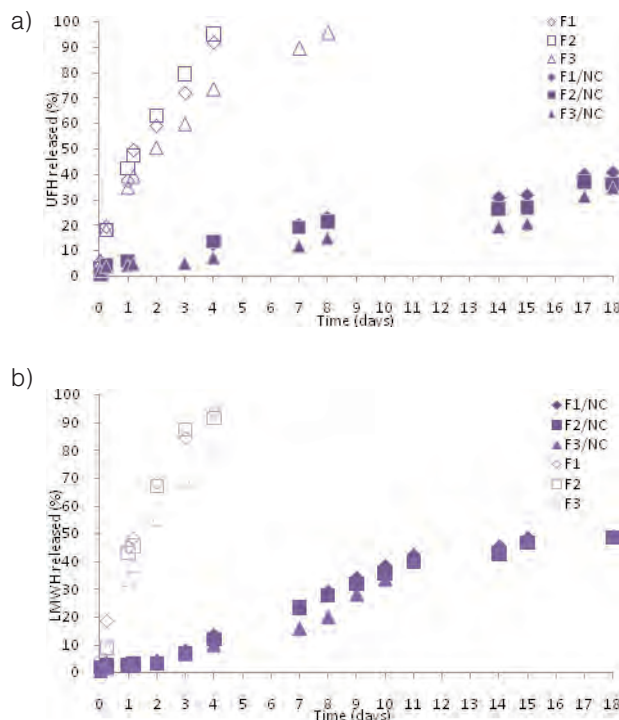
As presented in Table 2, the addition of P188 to P407 gels increased sol-gel transition temperature, while the opposite effect was observed with the addition of HPMC.

Tab. 2: Various hydrogel formulations and sol-gel transition temperatures according to G' and G'' .

Formulation	P407/P188/HPMC (wt %)	T(sol-gel) (°C)
F1	18/0/0	26.5
F2	18/1/0	30.0
F3	18/1/1	25.6
F4	18/0/1	24.1
F5	21/0/0	22.1
F6	21/5/0	27.5
F7	21/0/1	21.3
F8	21/5/1	26.2

In vitro release

In vitro release studies were performed on formulations obtained with UFH and LMWH solutions, as well as with UFH/CH and LMWH/CH nanocomplexes (NC) dispersions. As presented in Fig. 1, hydrogels obtained in PECs dispersions demonstrated more prolonged heparin release. This is attributed to the dually-controlled drug release, by hydrogel dissolution and PECs decomposition. Among various formulations, F3 presented the most



prolonged release due to HPMC swelling and forming of tightly orientated gel structures. In general, hydrogels with UFH and LMWH solutions demonstrated similar release profiles, while release rate of those with LMWH/CH PECs was higher than of hydrogels with UFH/CH PECs.

Fig. 1: *In vitro* release profiles of heparin from hydrogels (F1-F3 with heparin solution, F1/NC-F3/NC with heparin/chitosan PECs). a) UFH and b) LMWH.

CONCLUSIONS

Based on the results obtained it can be concluded that thermoreversible poloxamer-based systems with heparin/hitosan nanocomplexes seem as an attractive approach for subcutaneous prolonged delivery of heparin, requiring less frequent administration during long-term treatment.

REFERENCES

1. Ruel-Gariépy E and Leroux JC, *In situ-forming hydrogels-review of temperature-sensitive systems*. Eur. J. Pharm. Biopharm. 2004; 58: 409-426.
2. Schmolka IR, *Artificial skin I. Preparation and properties of pluronic F-127 gels for treatment of burns*. J. Biomed. Mater. Res. 1972; 6: 571-582.
3. Karewicz A, Zasada K, Szczubialka K, Zapotoczny S, Lach R and Nowakowska M, "Smart" alginate-hydroxypropylcellulose microbeads for controlled release of heparin. Int. J. Pharm. 2010; 385: 163-169.



INFLUENCE OF HUMIDITY AND TEMPERATURE ON STRUCTURAL AND AERODYNAMIC PROPERTIES OF MELOXICAM MICROCOMPOSITES (P02)

R. Ambrus^{1*}, A. Pomazi¹, P. Szabó-Révész¹

¹ Department of Pharmaceutical Technology, University of Szeged, Eötvös u. 6, H-6720, Szeged, Hungary

INTRODUCTION

Among pulmonary preparations, dry powder inhalers (DPIs) can ensure stability, a high payload and patient convenience. A new tendency in the development of DPIs is the design of carrier-based microcomposites with a particle size of 3-5 µm as pulmonary drug delivery systems involving different carriers and adjuvants. In our earlier work a carrier (β-D mannitol: M)-based, crystalline co-spray-dried DPI product containing the low-solubility meloxicam (MX) was developed (1). The pulmonary application of MX is a novelty for local anti-inflammatory treatment because it does not exhibit aspirin-like hypersensitivity reactivity and may therefore be safely applied in therapy for specific populations also. The carriers and the adjuvants significantly influence the physicochemical properties of DPIs during storage and application. There is currently considerable interest in studies of the influence of temperature and RH conditions during storage on the aerodynamic parameters of formulations (2). We therefore additionally investigated the effects of additives (polyvinyl alcohol: PVA, polyvinylpyrrolidone: PVP and L-leucine: L-LEU) in terms of particle size, shape, physicochemical stability and aerosolization of the DPI form by using the Andersen Cascade Impactor Model.

MATERIALS AND METHODS

Materials

MX [4-hydroxy-2-methyl-N-(5-methyl-2-thiazolyl)-2H-benzothiazine-3-carbox-amide-1,1-dioxide] was purchased from EGIS Ltd., Budapest, Hungary, PVP-K25 and PVA 3-88 from ISP Customer Service GmbH, Cologne, Germany, and M and L-LEU from Hungaropharma, Budapest, Hungary.

Methods

The components of the microcomposites are presented in Tab. 1. The microsuspension of MX was spray-dried from a solution of M, LEU and PVP or PVA. The particle size of the MX in the pre-suspension was decreased by cavitation with a high-pressure homogenizer. Such microsuspensions were spray-dried with a Büchi Mini Dryer B-191.

Tab. 1: Compositions of co-spray-dried samples

Products	Materials	Mass (g)
MX-M-PVP-LEU	Meloxicam	5.00
	Mannitol	5.00
	Polyvinylpyrrolidone	0.025
	L-Leucine	0.2
MX-M-PVA-LEU	Meloxicam	5.00
	Mannitol	5.00
	Polyvinyl alcohol	0.1
	L-Leucine	0.2

The stability testing (ICH Q1A (R2)) was performed in a constant-climate (Binder KBF 240) chamber at 40/25 ± 2 °C with 60/75 ± 5% RH. Residual water content was analysed by TG-DTA. The particle size distribution of the microcomposites from the dry dispersion unit was estimated by laser diffraction. For morphology analysis, SEM with ImageJ software was used. The structural characterization was achieved with XRPD and FT-IR. The *in vitro* dissolution was determined by the paddle method in phosphate buffer (pH 7.4) with kinetic evaluation. The fine particle dose (FPD), fine particle fraction (FPF) and mass median aerodynamic diameter (MMAD) were employed to characterize the deposition profile of MX.

RESULTS AND DISCUSSION

The most important parameter of the stored samples the *residual water* content. The microcomposite formulations before storage exhibited water contents ranging between 0.35% and 0.37%. For MX-M-PVP-LEU, the change in water content was higher than that for MX-M-PVA-LEU. The particle size distribution indicated that the content of monodisperse particles was nearly the same before and



after storage. The stored products maintained the *spherical form*; no changes in surface area or aggregation were detected (Fig. 1) and also the dissolution rate was the same.

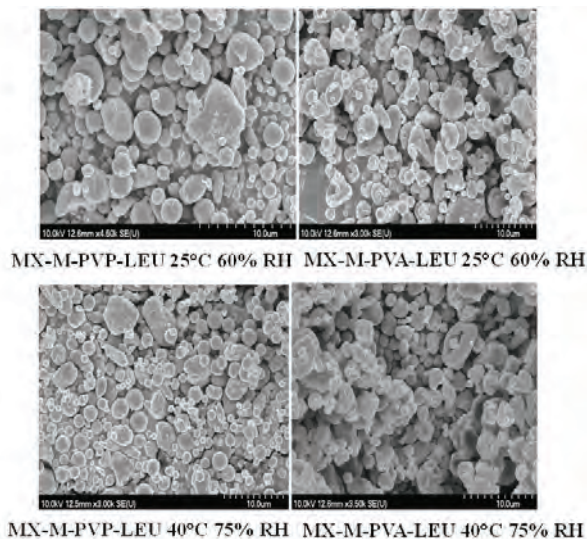


Fig. 1: Scanning electron microscopy of microcomposites before and after storage.

The *in vitro* aerosolization properties of the samples displayed a slight change during storage, but met the requirements for the formulation of a DPI (Tab. 2).

Tab. 2: Deposition of co-spray-dried microcomposites in the cascade impactor at 60 L min⁻¹

Products	FPD (mg)	FPF (%)	MMAD (μm)
MX-M-PVP-LEU Day 0	0.60 ± 0.07	53.05 ± 1.13	3.52 ± 0.13
MX-M-PVP-LEU 25 °C, 60% RH	0.67 ± 0.01	45.76 ± 2.58	3.67 ± 0.83
MX-M-PVA-LEU Day 0	0.29 ± 0.05	57.50 ± 1.0	3.04 ± 0.17
MX-M-PVA-LEU 25 °C 60% RH	0.64 ± 0.06	54.10 ± 0.60	3.19 ± 0.31

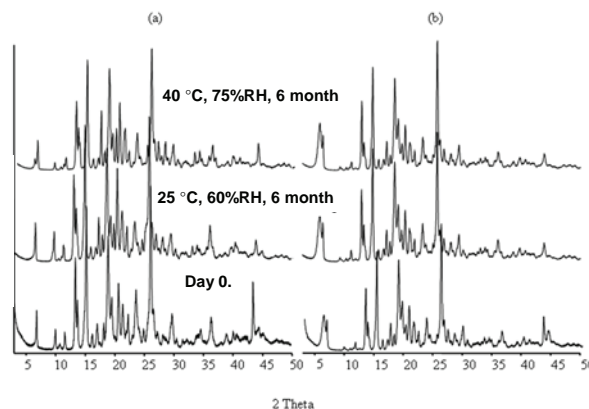


Fig. 2: XRPD patterns of co-spray-dried samples of MX-M-PVP-LEU (a) and MX-M-PVA-LEU (b) before and after storage. During the stability testing, the crystalline phases did not change.

CONCLUSIONS

The stability testing of M-based co-spray-dried MX-containing DPI systems was performed in order to determine the influence of humidity and temperature on the physicochemical properties and aerosolization parameters. The effects of different polymers (PVP and PVA) were additionally analysed during stability testing so as to optimize the final composition. It was found that the nature of the polymer determines the water uptake. PVP has slightly hygroscopic properties; its residual water content was therefore higher. MX-M-PVA-LEU was stable; only minor changes were observed in the physicochemical properties and aerodynamic performance. The sample containing PVA is an innovative product which may be considered suitable for scaled-up processes and pulmonary application.

ACKNOWLEDGEMENTS

This research was supported by the European Union and the State of Hungary, co-financed by the European Social Fund in the framework of TÁMOP 4.2.4. A/2-11-1-2012-0001 'National Excellence Program.

REFERENCES

- Pomázi A, Buttini F, Ambrus R, Colombo P, Szabó-Révész P. Optimization of a meloxicam-mannitol microcomposites for dry powder inhalation systems. *Eur. Polym. J.* 2013; 49: 2518–2527.
- Commission of the European Communities, Committee for Proprietary Medicinal Products Note for Guidance. - Stability testing of new drug substances and products. - III, 3335-92, 1993.



CHARACTERISATION OF ORALLY DISINTEGRATING TABLETS WITH LORATADINE OBTAINED WITH CO-PROCESSED MIXTURE LUDIFLASH® (P03)

A. Amelian^{1,*}, K. Winnicka¹, M. Szekalska¹,
A. Z. Wilczewska², A. Basa³

¹ Department of Pharmaceutical Technology, Medical University of Białystok, Mickiewicza 2C, 15-222 Białystok, Poland

² Department of Natural Products Chemistry, University of Białystok, Hurtowa 1, 15-399 Białystok, Poland

³ Department of Physicochemical Analysis, University of Białystok, Hurtowa 1, 15-399 Białystok, Poland

INTRODUCTION

Orodispersible tablets (ODT) are relatively new solid dosage form, which disintegrates and/or dissolves in contact with the saliva without the necessity of drinking water. In designing of this dosage form, extremely important is to select appropriate excipients – sweeteners, disintegrants, fillers, diluents and lubricants. In the ODT production, mannitol as a diluent is mainly used because of its sweet taste and cooling sensation in the oral cavity (1, 2). Hence, various ready-to-use, co-processed mixtures with mannitol and other excipients were designed and commercialized. One of them is Ludiflash®, which consists of mannitol, crospovidone, polyvinyl acetate and small amounts of povidone (3). The aim of this study was evaluation of the suitability of using Ludiflash® for manufacturing by direct compression method ODT with loratadine.

MATERIALS AND METHODS

Materials

Ludiflash® and crospovidones (Kollidon® CL-SF, Kollidon® CL-F) were obtained from BASF, Germany. Magnesium stearate was a product of Polish Chemical Reagents. Croscarmellose sodium (Ac-Di-Sol®) and loratadine were purchased from FMC Biopolymer, Belgium.

Methods

Tablets were obtained by direct compression method (single punch tablet press type EP1, Erweka, Germany). ODT formulae, based on the preliminary performed tests (4), are given in Table 1.

Hardness of the tablets was measured using hardness tester (5Y, Dr Schleuniger®, Pharmaton, Switzerland). Friability of the tablets was measured using friabilator tester (EF – 1W, Electrolab, India).

Specific surface area measurements were made by nitrogen adsorption porosimeter (Gemini VII, Micromeritics, USA). The adsorbed amount of nitrogen was calculated using the equation according to Brunauer, Emmet and Teller to determine the specific surface – $S_{(BET)}$. Additionally, pore size and pore distribution were evaluated.

Disintegration time (DT) was measured by the *in vivo* and *in vitro* method. DT of the tablets in the oral cavity was evaluated by six healthy volunteers (Research Ethics Committee at Medical University in Białystok approval number R-J-002/460/2013). The end point for DT was the time when the tablet placed on the tongue disintegrated until no lumps remained. DT *in vitro* was estimated using the pharmacopoeial tablet disintegration test apparatus (ED – 2L, Erweka, Germany).

To determine wetting time and water absorption ratio, tablets were put on twice folded filter paper (12 x 10.75 cm) placed in the Petri dish (7 cm) containing 7 ml of 0.05% red dye solution. The time required for complete wetting was measured. The water absorption ratio (AR) was calculated using equation: $AR = 100 \times (W_a - W_b) / W_b$, where W_b – tablet weight before wetting, W_a – tablet weight after wetting.

Loratadine contents and the *in vitro* loratadine release profiles were analyzed by the HPLC method using HPLC system Agilent Technologies 1200 (Agilent, Germany). Mobile phase was 0.025 M phosphate buffer pH 3.7:acetonitrile (1:4 v/v), the flow rate was 1 ml/min, and UV detection was performed at 274 nm. Isocratic separation was achieved on a Zorbax Eclipse XDB-C18, 4.6x150 mm, 5 µm column.

Sensory evaluation (roughness and taste of tablets) was performed *in vivo* by six healthy volunteers.





RESULTS AND DISCUSSION

All obtained formulations were characterised by appropriate mechanical properties (friability < 1%) and hardness (Table 2). Manufactured ODT (L1 – L3) were characterised by the uniform content of the drug substance (10 mg ± 0.6). 100 % of loratadine was released after 2 min. DT of tablets was influenced mainly by the type of the disintegrant used. The shortest DT was observed in formulation L1 (with Kollidon® CL-SF). L1 was also characterised by the shortest wetting time (16 s). The wetting time of formulation L2 was 26 s and of L3 - 36 s. There was no significant correlation between $S_{(BET)}$, pore size and DT. In case of tablets L1, $S_{(BET)}$ value was 0.25 m²/g and it was two times lower than in L3 formulation (0.51 m²/g) (Table 2).

Tab. 1: Composition of manufactured ODT formulations.

Ingredient (mg)	Formulation		
	L1	L2	L3
Ludiflash®	182	182	182
Kollidon® CL-SF	6	-	-
Kollidon® CL-F	-	6	-
Ac-Di-Sol®	-	-	6
Loratadine	10	10	10
Magnesium stearate	2	2	2

Tab. 2: Physicochemical parameters of prepared ODT.

Parameter	L1	L2	L3
Friability (%)	0.38	0.19	0.31
Hardness (N)	53.5	56.9	67.0
Wetting time (s)	16	26	36
AR (%)	53.2	49.4	70.81
DT <i>in vitro</i> (s)	13	33	36
DT <i>in vivo</i> (s)	14	17	37
Pore size (Å)	34	32	48
$S_{(BET)}$ m ² /g	0.25	0.38	0.51

CONCLUSIONS

The obtained results showed that a co-processed mixture Ludiflash® is suitable for preparing by direct compression method ODT with loratadine. Obtained ODT were characterised by suitable physical strength, short disintegration and wetting time, good texture and pleasant taste. Designed ODT are supposed to be a promising alternative oral solid dosage form with loratadine. However, further investigations, with regard to stability of obtained ODT are needed.

REFERENCES

1. Sastry SV, Nyshadham JR, Fix JA, Recent technological advances in oral drug delivery – a review. *Pharm. Sci. Technol. Today.* 2000; 3: 138–145.
2. Porter SC, Novel drug delivery: Review of recent trends with oral solid dosage forms. *Am. Pharm. Rev.* 2001; 4: 28–35.
3. Ludiflash® Technical Information (2011), available on: <http://www.basf.com/group/corporate/en/brand/LUDIFLASH>. (12.05.2014)
4. Amelian A, Winnicka K, Effect of the type of disintegrant on the characteristics of orally disintegrating tablets manufactured using new ready-to-use excipients (Ludiflash® or Parteck®) by direct compression method. *Afr. J. Pharm. Pharmacol.* 2012; 6: 2359–2367.



APPLICATION OF ACOUSTIC CAVITATION IN ORDER TO PREPARE NASAL FORMULATION (P04)

Cs. Bartos^{1,2,*}, P. Szabó-Révész¹, T. Horváth¹, R. Ambrus¹

¹ Department of Pharmaceutical Technology, University of Szeged, Eötvös u. 6, H-6720 Szeged, Hungary

² Richter Gedeon Nyrt., Budapest Gyömrői út 19-21 H-Hungary

INTRODUCTION

Particle design techniques have been developed for modification of the physico-chemical and biopharmaceutical properties of drugs (1). Changes of crystal size, distribution and morphology can open up new, alternative administration routes, e.g. intranasally and the pulmonary route, where the particle size is a determining factor (2). Acoustic cavitation (the collapse of vacuum bubbles or voids formed by sound waves) is a novel possibility for modification of the properties of particles (3-4).

The development of nasal formulations permits new areas of indication and many delivery problems can be solved (5). The large surface area of the nasal mucosa allows the rapid onset of the therapeutic effect, with a potential for direct-to-central nervous system delivery, no first-pass metabolism, and the non-invasiveness does not require a sterile preparation, all of which factors maximize patient comfort and compliance (6).

Our aims were to prepare a nasal formulation with appropriate stabilizer content and to investigate its *in vitro* permeability by using the Side-Bi-Side horizontal cell model.

MATERIALS AND METHODS

Materials

Meloxicam (MEL) [4-hydroxy-2-methyl-N-(5-methyl-2-thiazolyl)-2H-benzothiazine-3-carboxamide-1,1-dioxide] was obtained from EGIS Ltd. (Budapest, Hungary). The grinding additive, PVP K-25 (polyvinylpyrrolidone), was purchased from BASF (Ludwigshafen, Germany).

Preparation of sonicated formulations

A power ultrasound device (a Hielscher UP 200S Ultrasonic processor operating at 200 W; Germany) was applied for energy input. The ultrasonic amplitude was 90% and the sonication time was 60 min. The sonotrode was immersed to 75% of the total depth of the liquid. The concentration of MEL was 20 mg/10 ml in each sample. 0.1%, 0.5% and 2% of PVP K-25 as a stabilizer was dissolved in 25 ml water. Before sonication, the suspensions were stirred with a magnetic stirrer for 5 min. The temperature (50 °C) was set with a thermostat (Julabo, Germany). Physical mixtures of MEL-PVP were prepared as a reference.

Permeability studies of sonicated samples

The investigation was made with a Side-Bi-Side model at 37 °C. An artificial membrane was used between the donor and acceptor compartments. Sampling was performed after 5, 10, 15 and 60 minutes of stirring with a magnetic stirrer in both compartments. The quantity of active substance that diffused into the acceptor compartment was determined spectrophotometrically at 364 nm.

Investigation methods

The MEL particle size distribution was measured by laser diffraction. For morphology analysis of the dried product SEM was used. The structural characterization was carried out by DSC and XRPD.

RESULTS AND DISCUSSION

The MEL particle size was determined directly in the sonicated suspensions. Sample with 0.5% PVP showed the smallest particle size of MEL (Table 1): D0.5 was 2.79 µm. However, the difference between the D0.5 values was not significant in the three cases; all of them were suitable for nasal administration.

Tab. 1: Particle size distribution of sonicated products

	PVP (%)	D0.1 (µm)	D0.5 (µm)	D0.9 (µm)
rawMEL	-	10.82	34.03	75.81
Sample1	0.1	0.16	3.08	16.80
Sample2	0.5	0.14	2.79	19.09
Sample3	2	0.28	3.93	12.91



Characterization of dried product

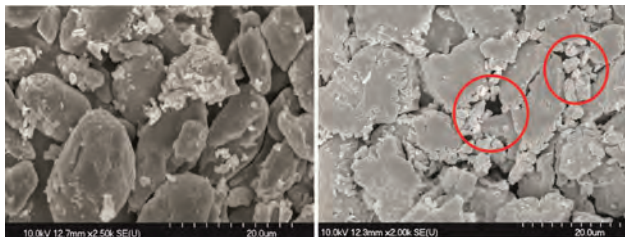


Fig. 1: SEM pictures of raw MEL (A) and sonicated dried product (B)

Scanning electron microscopy (SEM) images showed that the sonication resulted in irregular shape of particles (Figure 1). MEL crystals could be detected between the amorphous PVP particles.

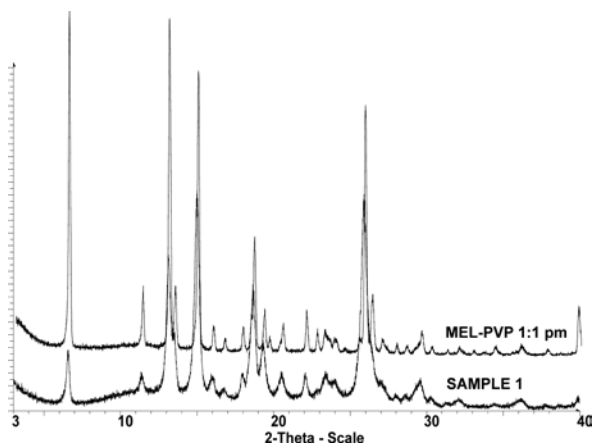


Fig. 2: XRPD examinations of MEL-PVP physical mixture and sonicated, dried product

Thermoanalytical (DSC) and X-ray powder diffraction (XRPD) examinations revealed the crystalline structure of the MEL (Figure 2).

Results of permeability studies

Micronization and the presence of PVP resulted in greater diffusion of MEL compared with the raw material. The largest amount of drug diffused from the formulation was obtained with Sample 1, which contained 0.1% of PVP, followed by Samples 3 and 2 containing 2% and the 0.5% PVP respectively.

CONCLUSIONS

This study applied acoustic cavitation to achieve a reduction of the MEL particle size and at same time to form a nasal suspension with appropriate stabilizer content. Sonification resulting in a change of crystal habit may decrease the particle size of MEL significantly. 0.5% PVP resulted in the smallest particle size, but the greatest amount of drug diffused from the formulation which contained 0.1% PVP. The low excipient concentration is advantageous in terms of cytotoxicity studies.

ACKNOWLEDGEMENTS

The financial support of the projects: TÁMOP-4.2.2.A-11/1/KONV-2012-0047.

REFERENCES

1. Maghsoodi M, Taghizadeh O, Martin G. P, Nokhodchi A, Particle design of naproxen-disintegrant agglomerates for direct compression by a crystallo-co-agglomeration technique. *Int. J. Pharm.* 2008; 351: 45-54.
2. Pomázi A, Ambrus R, Sipos P, Szabó-Révész P, Analysis of co-spray-dried Meloxicam-mannitol systems containing crystalline microcomposites. *J. Pharm. Biomed. Anal.* 2011; 56: 183-190.
3. Bartos Cs, Szabó-Révész P, Ambrus R, Optimization of technological parameters by acoustic cavitation to achieve particle size reduction. *Farmacia.* 2014; 62: 34-47.
4. Raman V, Abbas A, Experimental investigations on ultrasound mediated particle breakage, *Ultrason. Sonochem.* 2008; 15: 55-64.
5. Kúrti L, Gáspár R, Márki Á, Kápolna E, Bocsik A, Veszelka Sz, Bartos Cs, Ambrus R, Vastag M, Deli M. A, Szabó-Révész P, In vitro and in vivo characterization of meloxicam nanoparticles designed for nasal administration, *Eur. J. Pharm. Sci.* 2013; 50: 86-92.
6. Costantino H. R, Illum L, Brandt G, Johnson P. H, Quaya S. C, Intranasal delivery: Physicochemical and therapeutic aspects, *Int. J. Pharm.* 2007; 337: 1-24.



RHEOLOGICAL AND NMR CHARACTERIZATION OF XANTHAN GELS AND CORRELATION WITH DRUG RELEASE

(P05)

S. Baumgartner^{1,*}, U. Mikac², A. Sepe², J. Kristl¹

¹ University of Ljubljana, Faculty of Pharmacy, Aškerčeva 7, 1000 Ljubljana, Slovenia

² Jožef Stefan Institute, Jamova 39, 1000 Ljubljana, Slovenia

INTRODUCTION

The demographic changes in Europe are showing great increase in elderly population, meaning increasing problems with age related chronic diseases (cardiovascular, neurodegenerative, etc.). The therapy of these diseases usually demands prolonged time of therapeutic concentration of drug in systemic circulation. Therefore, the development of prolonged release dosage forms like hydrophilic matrix tablets is necessary (1).

Xanthan (XAN) is well known anionic biopolymer with relatively complex structure, therefore its behaviour is media dependent (2). The swelling properties of XAN matrix tablets were intensively investigated and it was proven that at acidic pH or high ionic strength gel layer is thinner compared to neutral pH (3).

The aim of the present study was rheological and NMR characterization of XAN gel structure in different media and its correlation with drug release and mechanical resistance of swollen tablets during *in vitro* studies.

MATERIALS AND METHODS

Materials

Xanthan; MW=2x10⁶; pentoxifylline (PF); MW = 278.3; Media used: purified water and HCl pH 1.2 with NaCl to μ = 0.28M.

Methods

Preparation of XAN gels and tablets

XAN was homogeneously dispersed in the medium in different w/w concentrations. For tablets XAN and PF were

mixed in ratio 1:1 and the tablets were compressed (SP 300, Kilian, G): m = 0.40g, 2r = 12mm, crushing strength 100 N.

Oscillatory measurements of XAN gels

Frequency sweep test were performed using cone-plate measuring system at deformation of γ = 0.1 % and in frequency region ω = 0.1 – 100 rad/s, T = 25 °C (Rheolab MC 100, Anton Paar, Austria).

NMR relaxation times of XAN gel

The NMR spin-spin (T₂) relaxation times were measured at ν_H = 100MHz using Apollo (TecMag, USA) MRI spectrometer with a superconducting 2.35 T horizontal bore magnet (Oxford Instruments, UK) equipped with gradients and RF coils for MR microscopy (Bruker, G). The T₂ times of gels were measured using the CPMG pulse sequence (90° - τ - [180° - τ - AQ - τ]_N) with τ = 1 ms and N = 3000. The T₂ value was determined from measurements by fitting the signal intensity (S) obtained at different t values to

$$S(\tau) = a + b e^{-\tau/T_2}$$

where *a* and *b* are constants.

Dissolution studies

The release from XAN tablets was studied using paddle method (USP Apparatus II, VanKel, model VK 7000, USA) and Bio Dis (VanKel Bio-Dis Testing Station, 25-1100, USA). Paddle conditions: V = 900 mL, 50 rpm, T = 37°C. Bio-Dis conditions: V = 250 mL, 10 dpm, T = 37°C, used stainless steel screens were 40 mesh or of 20 mesh. At predetermined time intervals 10 ml samples were withdrawn and analyzed at the λ=274 nm (HP diode array spectrophotometer UV-VIS, 8453, Germany).

RESULTS AND DISCUSSION

The results of rheological measurements of XAN dispersions in range from 1% to 10% show that elastic modulus G' was always above plastic G'' in water as well as in acidic conditions over the whole frequency range and both moduli were only weakly frequency dependent, what is typical gel-like behavior. Further, it is clearly seen that XAN gels at low pH were stiffer, since both moduli were above those in water media. It was also observed that the same gel stiffness can be achieved, when XAN concentration in water is twice as large as in acid medium. This is valid above 2.5% XAN concentration (Fig.1).



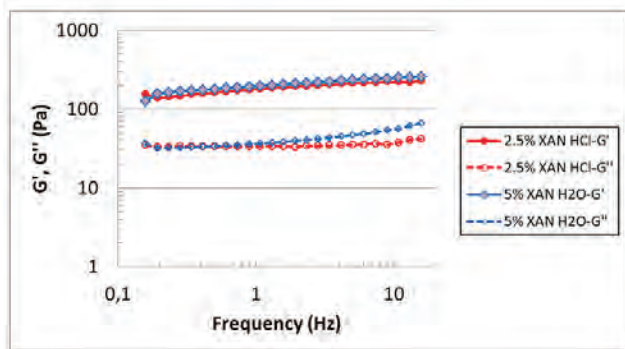


Fig. 1: Frequency sweep results of 2.5% XAN gel in HCl and 5% XAN gel in water.

Measured spin-spin relaxation time T_2 depends on the proportion and on the T_2 value of bound water, which depends on the correlation time due to hindered rotation of bound water as well as on the tumbling of polymer molecules to which the water molecules are bound (4). Our results show that spin-spin relaxation rate T_2^{-1} increases with higher XAN concentration in both media, what is the result of decreasing polymer mobility and proportion of free/bound water with decreasing amount of water in gels. It was also observed that T_2^{-1} is significantly shorter in pure water than in acid medium. Longer T_2^{-1} in acid medium is attributed to more restricted mobility of XAN chains and thus to the formation of more rigid gel in acid medium compared with the gel formed in water. This is in accordance with the results of oscillatory rheometry.

According to the gel stiffness, which was obviously higher at acidic pH than in water, it was expected, that drug release from tablets at pH 1.2 would be slower. However, our results did not prove it. On the other hand it was proven that tablets in water media are more susceptible to hydrodynamic conditions during release studies (Fig.2). When tablets were exposed to more rigorous hydrodynamic conditions using cylinders equipped with more opened mesh 20, the erosion of XAN tablets in water increased and the release was fast, while tablets in acid medium were more resistant resulting in constant release. This is the consequence of different release control from matrix tablets, namely in water the release was erosion controlled while at acidic conditions it was diffusion controlled

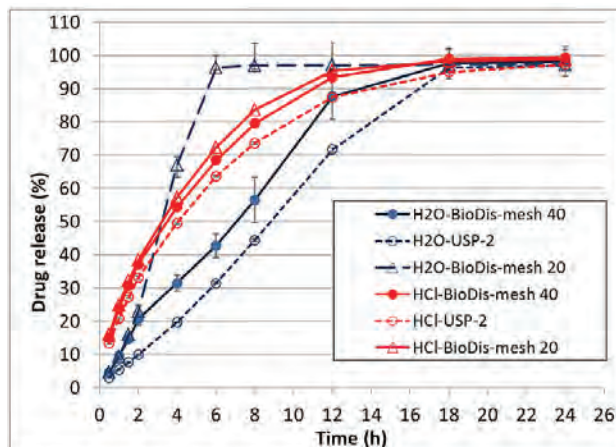


Fig. 2: Drug release profiles from XAN tablets using different media and dissolution methods.

CONCLUSIONS

Stiffer gel structure does not lead into slower drug release, if release is diffusion controlled. But on the other hand, weaker gel structure enables faster drug release under more rigorous hydrodynamic conditions, if release is erosion controlled.

REFERENCES

1. <http://ec.europa.eu/social/main.jsp?catId=502&>
2. Janković B, Sovány T, Pintyé-Hodi K, Škarabot M et al. Addressing potent single molecule AFM study in prediction of swelling and dissolution rate in polymer matrix tablets. *Eur J Pharm Biopharm.* 2012; 80: 217-225.
3. Mikac U, Sepe A, Kristl J, Baumgartner S. A new approach combining different MRI methods to provide detailed view on swelling dynamics of xanthan tablets influencing drug release at different pH and ionic strength. *J Control. Release.* 2010; 145: 247-256.
4. Blinc A, Lahajnar G, Blinc R, Zidanšek A et al. Proton NMR study of the state of water in fibrin gels, plasma, and blood clots. *Magn. Reson. Med.* 1990; 14: 105-122.



ASYMMETRICAL FLOW FIELD-FLOW FRACTIONATION WITH ON-LINE DETECTION FOR DRUG TRANSFER STUDIES: INVESTIGATING TRANSFER KINETICS OF A LIPOPHILIC MODEL DRUG BETWEEN LIPOSOMAL BILAYERS (P06)

A. Hinna¹, S. Hupfeld², J. Kuntsche¹, M. Brandl^{1*}

¹ Department of Physics, Chemistry and Pharmacy, University of Southern Denmark, Campusvej 55, 5230 Odense, Denmark

² Aker BioPharma AS, Fjordallèen 16, N-0115 Oslo, Norway

INTRODUCTION

To develop an *in vitro* method for prediction of premature loss of lipophilic/amphiphilic drug compounds from liposomal drug carriers via transfer to biological sinks upon intravenous administration. Here we report further refinement of a drug transfer assay, where liposomes are employed as a sink (Hinna et al., 2014) and its application to determine transfer kinetics of a lipophilic model drug, 5,10,15,20-tetrakis (4-hydroxyphenyl) 21H, 23h-porphine (*p*-THPP).

MATERIALS AND METHODS

Small (*mean diameter* ~70 nm) *p*-THPP-loaded donor liposomes (DL) were incubated with large (*mean diameter* ~270 nm) drug-free acceptor liposomes (AL) at a total lipid concentration of 45 mg/mL with lipid mass ratio 1: 0.8 (DL: AL) at 37°C. Samples were taken at intervals for up to 48 h. Asymmetrical flow field-flow fractionation (AF4) was employed to separate donor- from acceptor-liposomes, and fractions were collect-

ed. *p*-THPP in both liposome types was quantified by on-line UV/VIS extinction measurements at 519 nm, under correction for turbidity using drug-free liposomes (blank). Methanolic solutions (1:10 v/v) of the collected fractions were analyzed offline by HPLC to validate on-line quantification.

RESULTS AND DISCUSSION

The amount of *p*-THPP in both donor- and acceptor liposomes could be determined by on-line UV/VIS extinction measurements at all time-points up to 48 h with unprecedented precision. The contribution of turbidity to the overall measured UV/VIS extinction of DL and AL were as small as ≤ 6% and 53% respectively at equilibrium. In consequence, on-line quantification of model drug was found reproducible (rel SD ≤ 5%), and in general in good agreement with off-line analysis by HPLC (no significant difference in DL fraction, ≤ 10% difference in AL fraction). The relative amount of *p*-THPP was plotted, and the transfer kinetics analyzed. Rate constants were ~0.0023 min⁻¹ with half-lives of ~300 min.

CONCLUSIONS

Our refined method was found suited to determine transfer kinetics of the model drug *p*-THPP between liposomal bilayers.

REFERENCES

Hinna, A., Steiniger, F., Hupfeld, S., Brandl, M., Kuntsche, J. *Asymmetrical flow field-flow fractionation with on-line detection for drug transfer studies: a feasibility study.* (2014) *Analytical and Bioanalytical Chemistry*, pp. 1-13.





INVESTIGATING THE UNDERLYING REASON OF THE SOLUBILITY ENHANCEMENT OF CARBAMAZEPINE IN THE PRESENCE OF SOLUPLUS® (P07)

M. Windorf^{1,3}, Th. Cech^{1,*}, P. Hebestreit², K. Mäder³

¹ European Pharma Application Lab, BASF SE, Carl-Bosch-Straße 38, 67056 Ludwigshafen, Germany

² Pharma Ingredients & Services Europe, BASF SE, Chemiestraße 22, 68623 Lampertheim, Germany

³ Department of Pharmacy, Martin-Luther-University Halle-Wittenberg, Wolfgang-Langenbeck-Straße 4, 06120 Halle/Saale, Germany

INTRODUCTION

When formulating a poorly soluble active pharmaceutical ingredient (API), the phenomena of polymorphism and pseudo polymorphism must be considered. This is essential for the selection of the best solubiliser, since some are described to improve solubility of APIs and others to prevent the formation of less soluble hydrates in the presence of water (1). Studies showed that the solubility of carbamazepine (CBZ) in an aqueous environment can be improved by the presence of Soluplus® (2). The aim of this study was to examine the underlying reason of this solubility enhancement.

MATERIALS AND METHODS

CBZ was selected as poorly soluble API and Soluplus® as solubility enhancer (both products BASF SE).

Solubility testing

Some amount (1 g/l) of CBZ and CBZ dihydrate were added to either 0.08 N HCl or phosphate buffer pH 6.8 containing various amounts of Soluplus® (37°C, ±0.5 K). After stirring for 24 hours (USP Dissolution Apparatus 2, 50 rpm) samples (n=3) were passed through a filter (0.22 µm, PVDF), and absorption was measured (285 nm, HP 8458, Agilent).

Particle morphology

Size and shape of CBZ were differentiated by using light microscopy (Axio Lab.A1, Carl Zeiss).

Thermal analysis

Differential Scanning Calorimetry (DSC) was used to distinguish between different modifications and pseudo polymorphic compounds (DSC 200/1/F, Netzsch). Scans were conducted in aluminium pans with a pierced lid at a heating rate of 10 K/min up to 210°C.

RESULTS AND DISCUSSION

CBZ is known to convert rapidly into the less soluble CBZ dihydrate when exposed to water. Using the two polymorphic forms and comparing the solubility as a function of pH-value and Soluplus® concentration, a distinct difference could be seen (Fig. 1).

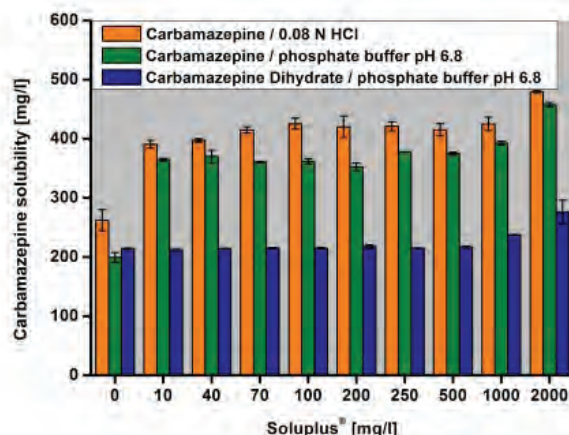


Fig. 1: Dependence of drug solubility on Soluplus® concentration.

In general, solubility of CBZ is slightly dependent on pH-value, with more dissolved API in the acidic medium. However, adding merely 10 mg/l Soluplus® to the medium, increased the solubility of CBZ in phosphate buffer pH 6.8 by some 83% whereas hardly any enhancement of solubility could be achieved with an increasing amount of Soluplus®. Only at a solubiliser concentration of 1000 mg/l, a higher solubility was achieved in both media.

A similar solubility of CBZ dihydrate and CBZ could be found for formulations in phosphate buffer pH 6.8 without Soluplus® (Fig. 1). This effect can be explained by the formation of CBZ dihydrate deriving from anhydrous CBZ, resulting in an equivalent amount of dissolved API for both cases.

The different appearances of CBZ suggested different polymorphic modifications. Interestingly, the diverse polymorphic forms even affected the macroscopic appear-



ance of the aqueous formulations. Suspensions without Soluplus® for instance showed some grainy sediment in addition to some floating needle-like particles. In contrast, suspensions containing Soluplus® had very fine floating particles, but similar sediment. Hence, in a further experiment, sediment and floating particles of both samples were separated by centrifugation and examined by DSC (Fig. 2).

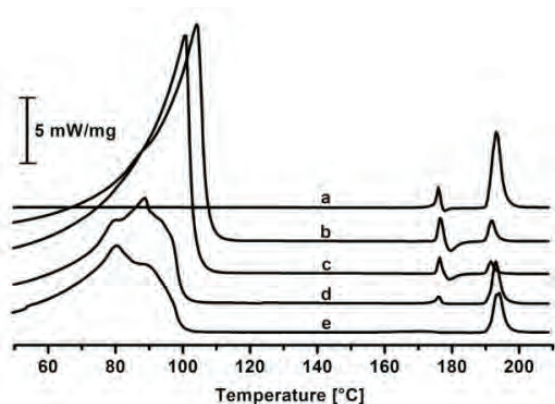


Fig. 2: DSC curves of anhydrous CBZ powder (a), the floating particles of suspensions with (b) and without Soluplus® (c) and the sediment of suspensions with (d) and without Soluplus® (e).

The DSC profile of anhydrous CBZ powder indicates two endothermic peaks (a). The first peak at 175.9°C is the melting of the CBZ modification III followed by a small exothermic recrystallization peak of the CBZ modification I at 177.9°C. The distinct peak at 193.9°C specifies the melting of recrystallized modification I (3). Curves gained from the floating particles (b, c) are almost equal to (a). The large peak in the range of 110°C indicates the evaporation of water. The melting peaks however, are identical to the thermal characteristics of anhydrous CBZ powder (a), suggesting that under DSC conditions, CBZ dihydrate III transforms to anhydrous CBZ III and then undergoes a phase change to anhydrous CBZ I.

The curves of the sediment (d, e) show a broad peak of water below 100°C as well. After the removal of water, particles of suspensions containing Soluplus® (d) revealed melting peaks of anhydrous CBZ III at 176.1°C and anhydrous CBZ I at 193.0°C. On the other hand, the sediment particles of the Soluplus®-free suspension (e) shows no melting peak of anhydrous CBZ III at all. This observation is due to the presence of only CBZ dihydrate I, which is consistent with previously published data (4).

CONCLUSIONS

It can be assumed that the solubility enhancement of CBZ with respect to Soluplus® is based on the fact that the polymer either prevents or delays the transformation from dissolved CBZ into the less soluble CBZ dihydrate I, compared to the CBZ dihydrate III which occurs in Soluplus® containing media.

REFERENCES

1. Tian F, et al., Visualizing the conversion of carbamazepine in aqueous suspension with and without the presence of excipients: A single crystal study using SEM and Raman microscopy, *Eur. J. Pharm. Biopharm.*, 64, 326-335 (2006).
2. Windorf M, et al., Preparing oral formulations of carbamazepine using the multifunctional solubilizer Soluplus®. 9th World Meeting on Pharmaceutics, Biopharmaceutics and Pharmaceutical Technology (2014).
3. Adam L, et al., Comparison of the Four Anhydrous Polymorphs of Carbamazepine and the Crystal Structure of Form I, *J. Pharm. Sci.*, 92, 2260-2271 (2003).
4. McMahon LE, et al., Characterization of Dihydrates Prepared from Carbamazepine Polymorphs, *J. Pharm. Sci.*, 85, 1064-1069 (1996).





THE EFFECT OF ELECTROLYTES ON N-TRIMETHYLCHITOSAN NANOPARTICLES

(P08)

M. Cegnar^{1,*}, A. Miklavžin², J. Kristl¹, E. Žagar³
and J. Kerč^{1,2}

¹ Lek Pharmaceuticals, d.d., Sandoz Development Center Slovenia, Verovškova 57, SI-1526 Ljubljana, Slovenia

² Faculty of Pharmacy, University of Ljubljana, Aškerčeva 7, SI-1000 Ljubljana, Slovenia

³ National Institute of Chemistry, Hajdrihova 19, SI-1000 Ljubljana, Slovenia

INTRODUCTION

Recently, nanoparticles (NPs) have increasingly been investigated as carriers for hydrophilic macromolecular drugs (e.g. proteins, peptides, vaccines) to improve stability and permit administration through nonparenteral routes. In recent years self-assembly of protein with natural or synthetic polyelectrolytes to form polyelectrolyte complexes with drug candidates has drawn increasing attention. The specificity of polyelectrolyte complexation method is in association in NPs. The method is influenced by a variety of parameters such as strength and location of ionic site on the polymer, polymer chemistry and chain rigidity and conditions such as system pH, ionic strength, temperature, mixing intensity, polymer/protein ratio, etc.(1)

N-trimethylchitosan (TMC), a quaternized chitosan derivative, shows good water solubility over a wide pH range, which is crucial for NPs delivery through different delivery routes. Compared to chitosan, TMC has better mucoadhesive properties even at neutral pH. TMC represents an attractive alternative to chitosan for designing of protein loaded NPs. (2)

The aim of this study was to evaluate the effect of electrolytes on NPs preparation.

MATERIALS AND METHODS

Materials

Erythropoietin (2.3 mg/ml, phosphate buffer, pH 7) (Lek Pharmaceuticals d.d.) was used as a model protein. Chondroitin sulphate was obtained from Sigma-Aldrich, USA. Trimethylchitosan (degree of trimethylation is 83 %) was synthesized in collaboration with National Institute of

Chemistry, Laboratory for Polymer Chemistry and Technology, Slovenia. All other chemicals used in this study were of analytical grade.

Methods

Continuous titrations of one polymer with another were performed to evaluate the effect of electrolytes in the buffer solution and optimize the NPs composition of trimethylchitosan (TMC), erythropoietin (EPO) and chondroitin sulphate (ChS), monitoring the particle size, zeta potential and average count rate throughout the experiments using Zetasizer Nano ZS ZEN 3600 (Malvern Instruments, UK). For NPs evaluation, association efficiency (AE) of EPO, entrapped in NPs, was determined indirectly after separation of NPs from the supernatant containing non-associated protein.

RESULTS AND DISCUSSION

Polyelectrolyte complexation method was used for NPs preparation. Polymers, TMC and ChS, were dissolved in buffer pH7 or water to evaluate the impact of electrolytes on NP-formation. Zeta potential of TMC dissolved in water and buffer was +41 mV and +20 mV. We assume that the difference in zeta potential was due to the presence of electrolytes in buffer and negligible difference in pH (pH of TMC in water and buffer was 6.8 and 7.0, respectively). The addition of EPO solution to TMC solution was found to have no influence on NPs formation and both dispersions, with or without electrolytes, began to show the turbidity only when ChS was added.

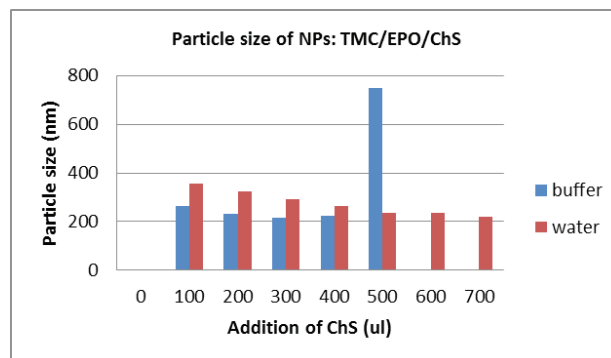


Figure 1. Particle size of NPs during titration of TMC/EPO complexes with ChS in buffer pH7 and water.

By the addition of ChS up to 700 ml (dissolved in water) and 400 μ l (dissolved in buffer), particle size decreased from 360 nm in water and 260 nm in buffer to 220 nm. Further addition of ChS led to particle growth and precipitation (Fig. 1).

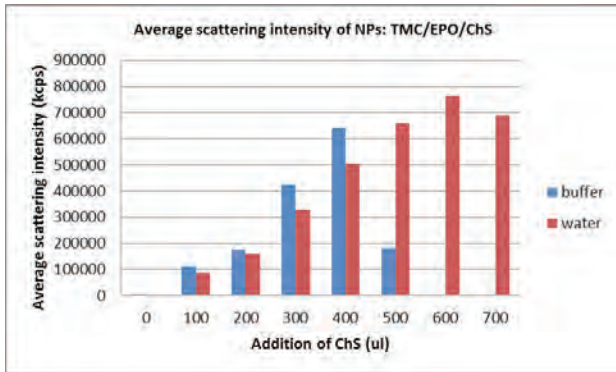


Figure 2. Average scattering intensity of NPs during titration of TMC/EPO complexes with ChS in buffer pH7 and water.

The scattering intensity increased during titration with ChS (up to 600 μ l in water and 400 μ l in buffer) reflecting the formation on NPs, and then started to decline when particles aggregated (Fig.2). Scattering intensity increased more substantially in water than in buffer, revealing more efficient NP-formation in water. This indicated higher capacity of TMC to associate with ChS in water in comparison to buffer, which is probably because of higher zeta potential of TMC in water. In addition, charge shielding effect of salt in buffer solutions likely weakened the association of polyelectrolytes in NPs. Zeta potential of particles decrease by the addition of ChS, reaching the value of +24 mV and +13 mV in water and in buffer, respectively.

Formulations with minimum and maximum addition of ChS dissolved in water and buffer were prepared to evaluate the association efficiency of EPO in NPs.

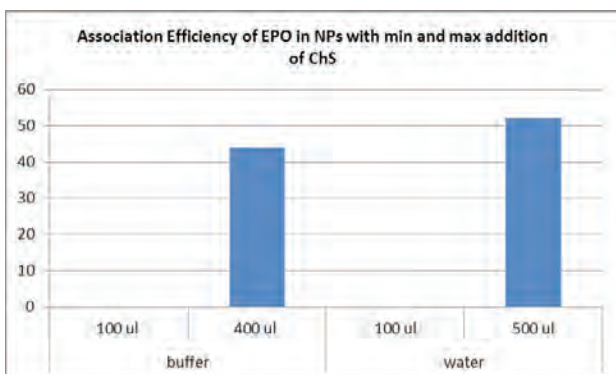


Figure 3. Association efficiency of EPO in nanoparticles prepared with min and max addition of ChS dissolved in buffer pH 7 and water.

The association efficiency of protein entrapped into NPs depends on the amount of ChS added. No EPO was associated when min amount of ChS was added. When max amount of ChS was added, the association efficiency of EPO in NPs reached 52% or 44% in water or buffer, respectively (Fig. 3). This indicated that electrolytes negatively influenced on protein association.

CONCLUSIONS

N-trimethylchitosan NPs were successfully prepared using polyelectrolyte complexation method. Although electrolytes in buffer solution allowed the complexation between EPO and polymers to form NPs they were found to have significant influence on NPs characteristics, which resulted in lower zeta potential of prepared TMC NPs, lower scattering intensity and lower association efficiency of EPO in TMC/EPO/ChS nanoparticles.

ACKNOWLEDGEMENTS

We acknowledge EC for supporting this research through the FP7-2011-NMP-280761 "ALEXANDER" project.

REFERENCES

1. Mao S et al. Self-assembled polyelectrolyte nanocomplexes between chitosan derivatives and insulin. *J Pharm Sci.* 2006; 95: 1035–1048.
2. Amidi M. et al. Preparation and characterization of protein-loaded N-trimethyl chitosan nanoparticles as nasal delivery system. *J Control. Release.* 2006; 111: 107-116.





MATHEMATICAL MODELLING OF DOSAGE FORM DISINTEGRATION AND DRUG DISSOLUTION IN VISCOUS MEDIA (P09)

S. Cvijić^{1*}, M. Radonjić¹, D. Rafailović¹, Lj. Đekić¹, J. Parojčić¹, P. Langguth²

¹ Department of Pharmaceutical Technology and Cosmetology, University of Belgrade - Faculty of Pharmacy, Vojvode Stepe 450, Belgrade, Serbia

² Department of Biopharmaceutics and Pharmaceutical Technology, Institute of Pharmacy and Biochemistry, Johannes Gutenberg University, Staudingerweg 5, Mainz, Germany

INTRODUCTION

With the right choice of experimental conditions, tablet disintegration and drug dissolution tests can be used to *in vitro* assess drug biopharmaceutical properties, and to identify potential food effects on drug bioavailability. Several studies emphasized that media viscosity is an important factor affecting dosage form disintegration and drug dissolution in the postprandial state, and therefore, should be considered in biorelevant disintegration and dissolution tests design (1-3). The objective of this study was to estimate the influence of increased medium viscosity on tablet disintegration time and drug release rate by using different products of drugs with various biopharmaceutical properties. In addition, mathematical modelling of the experimental results aimed to identify possible relationship between viscosity-mediated tablet disintegration and drug dissolution rate.

MATERIALS AND METHODS

The investigated products included commercially available IR tablets (Tab.1). Disintegration tests were performed according to the USP method without disks, and dissolution tests were carried out in a rotating paddle apparatus (50 rpm; 900 ml of media). The studies were performed at 37±0.5 °C, using aqueous media without/with the addition of 0.5% or 1.4% hydroxypropyl methyl-

cellulose (HPMC). Rheological measurements were performed on the rotational rheometer with the rotating cylinder measuring device Z3 DIN within the shear rate range 0-100 s⁻¹. Dissolution data were described by dissolution efficiency values, DE(%):

$$DE(\%) = \frac{\int_{t_1}^{t_2} y \times dt}{y_{100} \times (t_2 - t_1)} \times 100$$

(y-% of drug dissolved at time t, y₁₀₀-100% of drug dissolved). Regression analysis was used to assess the relationship between disintegration and dissolution data.

Tab. 1: The investigated products.

Drug	Products (symbol)
Paracetamol	film tbl. (PAR1); uncoated tbl. (PAR2)
Atenolol	uncoated tbl. (ATN1); (ATN2)
Metoprolol tartrate	uncoated tbl. (MTP1); film tbl. (MTP2)
Amlodipine besylate	uncoated tbl. (AML1); (AML2)

RESULTS AND DISCUSSION

The average disintegration times of the investigated products are shown in Fig.1, and dissolution data in various media are presented in Fig.2. The obtained results indicate that medium viscosity can have a pronounced effect on tablet disintegration time, and drug dissolution rate. However, the magnitude of this effect largely depended upon drug product characteristics. Mathematical modelling of the obtained results revealed that the effect of media viscosity on tablet disintegration time can be described by the power function. Still, the shape of the generated function differed between products (Tab.2). The influence of increased medium viscosity on drug dissolution rate followed the pattern observed in the disintegration study, but DE(%) decreased in a manner that was best defined by a linear function (Tab.2). Furthermore, decreased dissolution in viscous media was observed in the case of MTP1 tablets, where the addition of HPMC had only minor effect on tablet disintegration time under USP standard conditions.

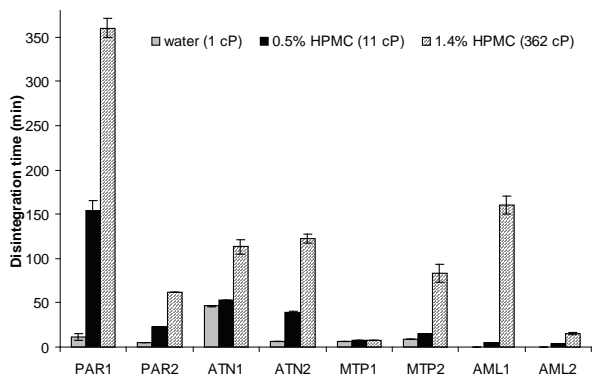


Fig. 1: Disintegration times (mean ± SD) of the investigated products in different media. Values in parentheses refer to the apparent viscosity at the shear rate 100 s⁻¹.

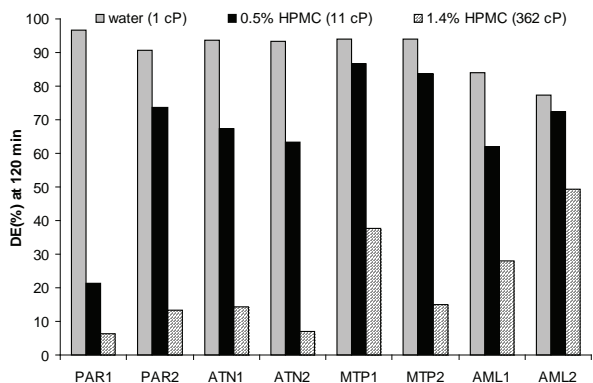


Fig. 2: Dissolution efficiency of the investigated products in different media. Values in parentheses refer to the apparent viscosity at the shear rate 100 s⁻¹.

Tab. 2: Relationship between tablet disintegration times, or dissolution efficiency values in water, 0.5% HPMC, and 1.4% HPMC.

Product	Disintegration Function (R ² value)	Dissolution Function (R ² value)
PAR1	y=12.379x ^{3.231} (0.981)	y=-45.116x+131.74 (0.871)
PAR2	y=5.291x ^{2.194} (0.996)	y=-38.547x+136.30 (0.904)
ATN1	y=41.582x ^{0.751} (0.742)	y=-39.535x+137.54 (0.963)
ATN2	y=5.969x ^{2.738} (0.999)	y=-43.063x+140.65 (0.970)
MTP1	y=6.059x ^{0.217} (0.917)	y=-28.088x+128.89 (0.845)
MTP2	y=7.392x ^{1.871} (0.805)	y=-39.402x+143.05 (0.845)
AML1	y=0.105x ^{6.336} (0.979)	y=-28.068x+114.19 (0.984)
AML2	y=0.159x ^{4.204} (0.998)	y=-13.972x+94.233 (0.872)

The relationship between tablet disintegration times and drug dissolution rates at the beginning of dissolution process could be described by the power function (R² values for individual products ranged between 0.80 and 0.99,

except for MTP1 and AML2). However, the correlation for the pooled data set was poor (Fig.3). Similar results were obtained for the relationship between tablet disintegration times and DE(%) values, with the correlation described by the linear function (R² between 0.79 and 0.99 for individual products (except for MTP1), and R² = 0.51 for the pooled data set).

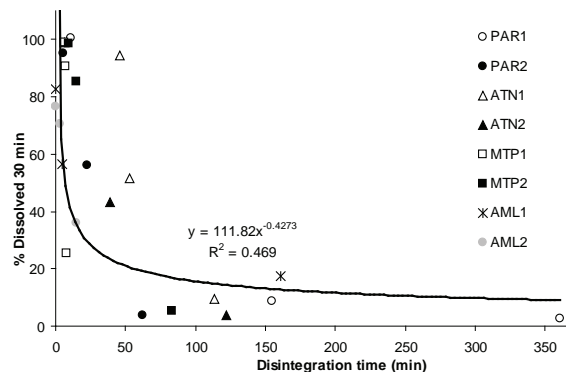


Fig. 3: Relationship between tablet disintegration times and drug dissolution rates (30 min time point) for the investigated products.

CONCLUSIONS

Increased medium viscosity was recognized as an important factor that governs dosage form disintegration and drug dissolution, with drug product characteristics being an interfering factor in relation to the impact of medium viscosity. In addition, it might be speculated that tablet disintegration time could serve as an indicator of drug dissolution rate in viscous media, but disintegration study should be performed under more discriminatory conditions (e.g. less intensive agitation) in order to correlate better with drug dissolution data.

ACKNOWLEDGMENTS

This work was done under the project TR34007 (Ministry of Education, Science and Technological Development, RS).

REFERENCES

1. Parojic J, Vasiljevic D, Ibrić S, Djuric Z. Tablet disintegration and drug dissolution in viscous media: paracetamol IR tablets. *Int. J. Pharm.* 2008; 355: 93–99.
2. Radwan A, Amidon GL, Langguth P. Mechanistic investigation of food effect on disintegration and dissolution of BCS class III compound solid formulations: the importance of viscosity. *Biopharm. Drug. Dispos.* 2012; 33: 403-416.
3. Cvijić S, Parojčić J, Langguth P. Viscosity-mediated negative food effect on oral absorption of poorly-permeable drugs with an absorption window in the proximal intestine: In vitro experimental simulation and computational verification. *Eur. J. Pharm. Sci.* April 18, 2014 [Epub ahead of print]





PREPARATION OF A SOLID SMEDDS FOR ENHANCED NAPROXEN SOLUBILITY (P10)

K. Čerpnjak^{1*}, A. Zvonar², F. Vrečer^{1,2}, M. Gašperlin²

¹ Krka, d.d., Novo mesto, Šmarješka cesta 6, 8501 Novo mesto, Slovenia

² Faculty of Pharmacy, University of Ljubljana, Aškerčeva 7, 1000 Ljubljana, Slovenia

INTRODUCTION

One of the most promising approaches for enhancing drug solubility and consequently oral bioavailability is the utilization of lipid based formulations, containing self-microemulsifying drug delivery systems (SMEDDS) (1). SMEDDS are isotropic mixtures of lipids and surfactants that form o/w microemulsions (ME) under dilution with intestinal fluids *in vivo* after oral application (2). Self-emulsification of formulation enables drug to remain entrapped in the oily droplets of ME and is advantageously delivered in its dissolved form during its transition through gastrointestinal tract, which results in enhanced release and absorption (2-4). In order to combine the above mentioned advantages of lipid based formulations with those of solid dosage forms (e.g. low production costs, convenience of process control, high stability and reproducibility, improved patient compliance) liquid SMEDDS are transformed into solid state (5).

In this study we prepared and evaluated solid SMEDDS which was obtained via spray-drying technique, with the aim of preserving self-microemulsifying characteristics and improving the dissolution of model drug naproxen.

MATERIALS AND METHODS

Materials

Naproxen (NPX) and maltodextrin (MD) (DU (dextrose units) 13.0-17.0) were donated by Krka, d.d., Slovenia. Peceol™ (glycerol monooleates (type 40)) and Gelucire® 44/14 (lauroyl macrogol-32 glycerides) were obtained from Gattefossé, France. Miglyol® 812 (caprylic/capric triglyceride) was obtained from Sasol, Germany and Solutol® HS 15 (polyethylene glycol (15)-hydroxystearate) was obtained from BASF, ChemTrade GmbH, Germany.

Methods

The solid SMEDDS were prepared by spray-drying technique, using the Büchi Mini Spray Dryer B-290 (Büchi, Switzerland). The aqueous dispersion of MD as carrier and liquid SMEDDS consisted of Miglyol 812® (30% w/w), Peceol™ (30% w/w), Gelucire® 44/14 (20% w/w) and Solutol® HS 15 (20% w/w) capable of NPX loading up to 6 % w/w, were prepared and water was evaporated by spray drying. Self-microemulsifying ability of solid SMEDDS was evaluated with average droplet size and polydispersity index (PDI) of formed ME by photon correlation spectroscopy (PCS) using a Zetasizer Nano series instrument (Malvern Instruments Inc, Southborough, MA). The macroscopic structure of the solid SMEDDS was investigated by scanning electron microscopy (SEM; Ultra Plus, Carl Zeiss, Germany). The DSC curves were recorded using a differential scanning calorimeter (DSC1 STAR® System Mettler Toledo). *In vitro* dissolution test was carried out by USP Apparatus 2 (VK7000, VanKel, Cary, NC), in dissolution media of pH 1.2.

RESULTS AND DISCUSSION

Self-microemulsifying ability of the system was preserved during liquid to solid transformation. As presented in Tab. 1 monodisperse ME with droplet size below 50 nm were formed upon dilution of all systems tested. Prepared solid SMEDDS were composed of smooth particles with size up to 10 µm that were spherical in shape and partially aggregated (Fig. 1).

Tab. 1: Droplet size with corresponding PDI of ME formed upon dilution (mean±SD, n=2).

Formulation	Size (nm)	PDI
Liquid SMEDDS (unloaded)	39.9±0.1	0.221±0.001
Liquid SMEDDS (NPX loaded)	31.9±0.5	0.185±0.028
Solid SMEDDS (NPX loaded)	36.5±0.2	0.147±0.006

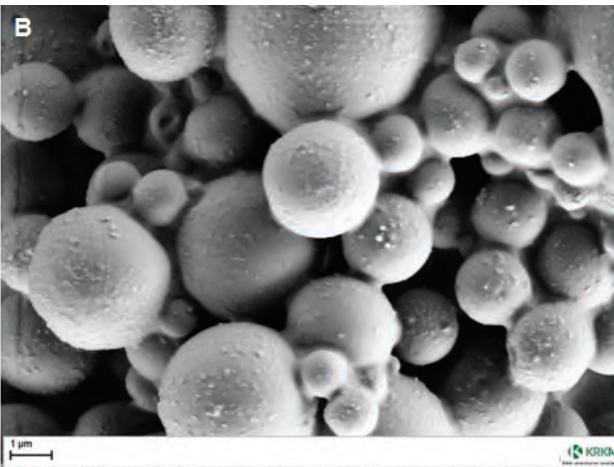
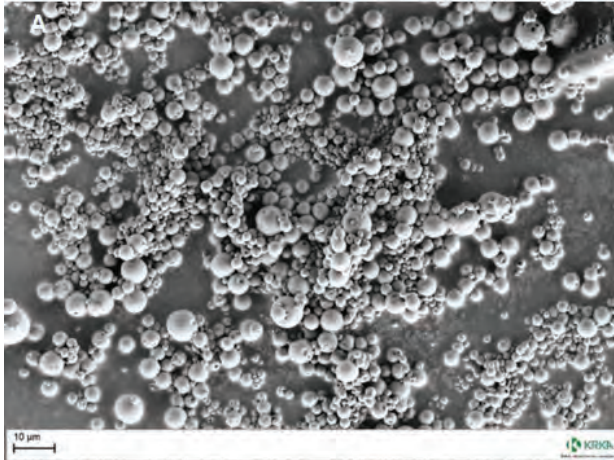


Fig. 1: SEM micrograph of solid SMEDDS at different magnification: A-magnification 2000 ×, B-magnification 20.000 ×.

DSC analysis (Fig. 2) confirmed that NPX remains in solid SMEDDS in a non-crystalline form.

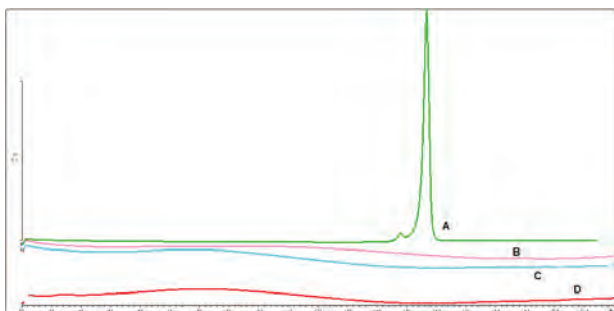


Fig. 2: DSC thermograms of A: NPX, B: MD, C: placebo solid SMEDDS, D: solid NPX-loaded SMEDDS.

The liquid and solid SMEDDS formulations significantly improved the amount of NPX released (~99%) compared to pure NPX and its physical mixture (~64%). In addition, dissolution rate was also significantly improved (Fig. 3).

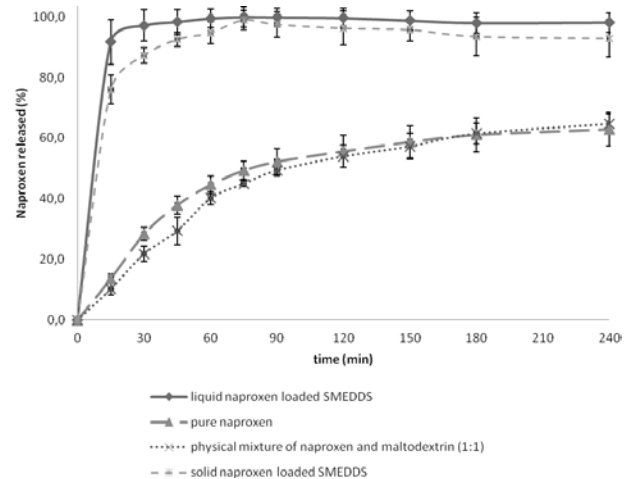


Fig. 3: In vitro dissolution profile of liquid and solid SMEDDS compared with pure NPX and physical mixture of NPX and MD (1:1).

CONCLUSIONS

Liquid SMEDDS was encapsulated into the MD carrier via spray drying. Produced solid SMEDDS preserved self-emulsifying of liquid SMEDDS, as NPX remains entrapped in a non-crystalline form. Furthermore, both SMEDDS formulations significantly improved solubility and dissolution rate compared to pure naproxen.

ACKNOWLEDGEMENTS

The authors would like to thank Krka, d.d., Novo mesto, Slovenia for supporting this study.

REFERENCES

- Čerpnjak K, Zvonar A, Gašperlin M, Vrečer F. Lipid-based systems as a promising approach for enhancing the bioavailability of poorly water-soluble drugs. *Acta Pharmaceut.* 2013; 63: 427-445.
- Constantinides P. Lipid microemulsions for improving drug dissolution and oral absorption: physical and biopharmaceutical aspects. *Pharm. Res.* 1995;12:1561-1572.
- Parul J, Geeta A, Amanpreet K. Bioavailability enhancement of poorly soluble drugs by SMEDDS: A review. *J. Drug Deliv. Ther* 2013;3:98-109.
- Pouton CW. Lipid formulations for oral administration of drugs: non-emulsifying, self-emulsifying and self-microemulsifying drug delivery systems. *Eur. J. Pharm. Sci.* 2000;11: 93-98.
- Sudheer P, Kumar MN, Puttachari S, Shankar UMS, Thakur RS. Approaches to development of solid- self micron emulsifying drug delivery system: formulation techniques and dosage forms – a review. *Asian J. Pharm. Life Sci.* 2012; 2:214-225.



THE INFLUENCE OF O/W MICROEMULSION AND CARBOPOLS ON THE RELEASE OF TERBINAFINE HYDROCHLORIDE (P11)

M. Čuchorová^{1*}, L. Starýchová¹, M. Špaglová¹,
M. Vitková¹, K. Bartoníková¹, M. Čierna¹,
K. Gardavská¹, I. Zajacová¹

¹ Department of Galenic Pharmacy, Faculty of Pharmacy,
Comenius University, Odbojárov 10, 832 32 Bratislava, Slovakia

INTRODUCTION

Terbinafine belongs to a group of synthetic allylamine antifungal drugs with a broad spectrum of activity on fungal infections including those with dermatophytes and yeast. Due to its higher lipophilicity, it accumulates in hair, nails and in the skin. It is administered orally – 250mg or 500mg per day or topically. Topical application can reduce adverse effects of Terbinafine compared to oral application due to lower concentration. But its solubility, limited in water and in lipids, can cause quite low bioavailability, considering topical application (1). Therefore the formulation of Terbinafine into the topical dosage form is limited by the solvent and vehicles, which can affect drug permeation through the skin (2).

One of the problems with topical application is the permeability of the drug through the skin. It forms a natural protective barrier between the external and internal environment of the organism. The upper layer of epidermis – stratum corneum - is impermeable for hydrophilic substances, other layers are resistant to lipophilic ones. Therefore, the physical and the chemical properties of a drug, such as liposolubility, molecular weight, dissociation constant and vehicles, are important for the permeation of drugs (3).

Microemulsions have gained a great attention as a novel delivery strategy in the past two decades to improve the therapeutic performance of an array of drugs because of their attractive features (4). The small droplet size pro-

vides a large interfacial area for rapid release. On the other hand, they can lower the release, prolong the effect and be used as a reservoir (5).

Due to their unique structure, microemulsions provide enhanced solubilization for poorly soluble drugs, which can make them superior drug delivery systems (6). Use of microemulsions, for topical applications, is limited by low viscosity. Therefore gelling agent, as viscosity imparting agents, are required to increase the viscosity of a formulation.

MATERIALS AND METHODS

Materials

Following materials were used: Terbinafine hydrochloride (THCl) (acquired from Zentiva, a.s., Slovakia) as active substance, Carbopol 940 (from Sigma Aldrich Chemie GmbH, Germany), Carbopol 934, 974P and 980 (from Ashland, USA) and O/W microemulsion.

Preparation of samples

Carbopol gels were prepared in concentrations 1% w/w by neutralization with triethanolamine. THCl (1% w/w) was dissolved in ethanol (96% w/w) or microemulsion and added to gel, while stirring. The ratio of microemulsion and gel was 1:4.

In vitro permeation studies

The release of THCl from formulations was evaluated by using Franz cells through the regenerated cellulose membrane SpectraPor® in phosphate buffered saline. The released amount of THCl was determined spectrophotometrically (Spectrophotometer Phillips PV 9652 UV/VIS) at 224nm.

RESULTS AND DISCUSSION

This work evaluates the influence of microemulsion and different types of carbopols on the release of Terbinafine hydrochloride.

Gel based formulations prepared by using different polymers, are employed to optimize the topical formulation of drugs (2). Carbopol 934, 940, 947P and 980 was used as gelling agent, in concentration 1% w/w. The structural differences are induced by the degree of cross-linking and manufacturing conditions. The release of THCl was changed depending on types of carbopol. Carbopol 940 proved a higher release compared to other formulations. O/W microemulsion consisted from distilled water, oleic acid and Tween 80 as surfactant. This system improves the drug release significantly ($p < 0,05$). *In vitro* release profiles indicate a 3,38% - 35,1% increase in a liberation due the presence of microemulsion.



Combination of O/W microemulsion and Carbopol 974P as gelling agent, in ratio 1:4, showed the highest output of terbinafine hydrochloride (Fig.1).

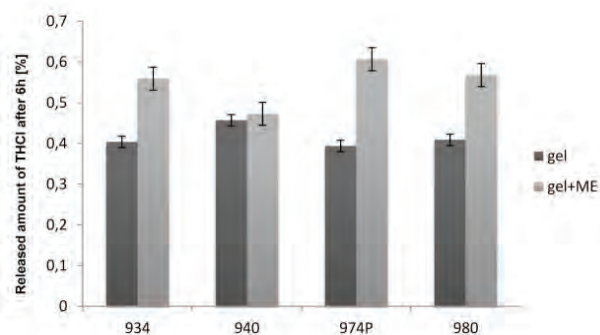


Fig. 1: The released amount of THCl after 6h from carbopol gels (934, 940,974P, 980) with and without microemulsion.

CONCLUSIONS

Ease of manufacturing, improved solubility, favourable cutaneous drug delivery and good physical stability makes a microemulsion an attractive drug delivery system (6). In this study, different types of carbopols with and without microemulsion were designed according to the liberation of a poorly soluble drug. Microemulsion had a positive influence on the drug release. Prepared formulation of THCl, O/W microemulsion and Carbopol 974P was found to be the most optimal and may be progressed for further development.

ACKNOWLEDGEMENTS

The research was supported by Grant of Comenius University UK 356/2014, UK 432/2014 and Grant of Faculty of Pharmacy FaF UK 55/2014.

REFERENCES

1. Zhang J.P. et al. *Ethosomes, Binary Ethosomes and Transferosomes of Terbinafine Hydrochloride: A Comparative Study*. *Arch Pharm Res*. 2012; 35: 109-117.
2. Alberti I. et al. *Effect of ethanol and isopropyl myristate on the availability of topical terbinafine in human stratum corneum, in vivo*. *Int J Pharm*. 2001; 219: 11-19.
3. Özcan I. et al. *Enhanced topical delivery of terbinafine hydrochloride with chitosan hydrogels*. *AAPS*. 2009; 10: 1024-1031.
4. Stubenrauch C. et al. *Microemulsions- Background, New applications perspective*. Blackwell Publishing Ltd., West Sussex, 2009.
5. Lawrence M.J., Rees G.D. *Microemulsion-based media as novel drug delivery systems*. *Adv Drug Deliv Rev*. 2012; 45: 89-121
6. Shalviri A. et al. *Low-surfactant microemulsions for enhanced topical delivery of poorly soluble drugs*. *J Pharm Pharm Sci*. 2011; 14: 315-324.

ENCAPSULATION OF CHOKEBERRY (*Aronia melanocarpa L.*) EXTRACT IN ALGINATE AND ALGINATE/INULIN SYSTEM BY ELECTROSTATIC EXTRUSION (P12)

N. Čujić^{1*}, K. Šavikin¹, K. Trifković², B. Bugarski², S. Ibrić³, D. Pljevljakušić¹

¹ Institute for Medicinal Plants Research, T. Košćuška 1, 11000 Belgrade, Serbia

² University of Belgrade, Faculty of Tehnology and Metalurgy, Department of Chemical Engineering, Kargenijeva 4, 11000 Belgrade, Serbia

³ University of Belgrade, Faculty of Pharmacy, Vojvode Stepe 450, 11000 Belgrade, Serbia

INTRODUCTION

Chokeberry are recognized as excellent sources of bioactive components with beneficial effect on human health such as anthocyanins, flavonols, procyanidins, and phenolic acids. One way to preserve the health beneficial properties of plant extracts is to encapsulate them within a matrix or a membrane in the particulate form to achieve the desirable effects. The purpose of encapsulation is to improve the stability of extracted compounds during storage and processing, to achieve controlled delivery, separate incompatible compounds, or mask unpleasant taste of bioactives (bitter taste of polyphenolic compounds). Electrostatic extrusion is one of the most convenient method for controlled production of small particles of uniform and desirable size. Encapsulation of 50% chokeberry ethanolic extract of with calcium alginate gel as the matrix was employed. Encapsulation systems were examined and compared in order to choose the optimal one with respect to entrapment efficiency.





MATERIALS AND METHODS

Electrostatic extrusion was applied for encapsulation of chokeberry extract (4.11mg GAE/g DW) in alginate gel beads. Sodium alginate powder was dissolved in the 50% ethanolic chokeberry extract (the ethanol was evaporated). Different type of 1.5% alginate, low viscosity and medium viscosity, and combination alginate/inulin were used to obtain various microbeads. Alginate/extract solution (1.5% alginate or 1.5% alginate/0.5% inulin) was extruded through a positively charged blunt stainless steel needle (18, 20 and 22 gauges), at a constant flow rate by a syringe pump. The potential difference was controlled by a high voltage unit, and kept at a constant voltage 6 kV. The collecting solution was chokeberry extract containing calcium-chloride as a crosslinking agent. The release profiles for the polyphenols from microbeads in water were investigated determining the total polyphenol content (TPC) using Folin-Ciocalteu method. Statistical analysis was done by one-way ANOVA using Statistica 7.0 software, $P < 0.05$ was considered as significant.

RESULTS AND DISCUSSION

The effects of certain candidate factors on chokeberry phenolics microencapsulation process and their controlled release were evaluated. Statistical significance of time, needle size and type of carrier was monitored. Polyphenolic compounds were released relatively rapidly from native hydrogel beads. Time had statistically significant influence ($P=0.000001$) on the release of polyphenols from microbeads and best release was achieved after 15 min (1.97 ± 0.21 mg GAE/l/g beads), when polyphenolic compounds reached a plateau. In the case of beads containing inulin as a filler, the release was extended to 20-30 minutes. The release of polyphenols was consistent with diffusion controlled release through the alginate gel matrix. Needle size did not reach statistical significance ($P=0.07971$) in the release of polyphenols and the best result was achieved with a needle of 20 gauges (1.86 ± 0.26 mg GAE/l/g beads). Type of carriers showed statistical significance between pure alginate as carrier and the combination of alginate/inulin, and the best result was achieved with alginate/inulin medium solution (1.97 ± 0.22 mg GAE/l/g beads).

CONCLUSIONS

This study demonstrates the potential of using hydrogel material for encapsulation of chokeberry polyphenols to improve their functionality and stability. Our result showed that stability of chokeberry polyphenols might be

improved using microencapsulation technologies. Chokeberry polyphenol microcapsules, due to their antioxidant potential, represent a promising food additive for incorporation into dietary supplements, functional food or pharmaceutical and cosmetic preparations.

Acknowledgments: Ministry of Education, Science and Technology of Serbia for financial support, project number 46013.

REFERENCES

1. Cvitanović-Belscak A, Stojanović R, Manojlović V, Komes D, Cindrić JI, Nedović V, Bugarski B, Encapsulation of polyphenolic antioxidants from medicinal plant extracts in alginate-chitosan system enhanced with ascorbic acid by electrostatic extrusion, *Food Research International*, 2011, 44: 1094-1101
2. Bakowska-Barczak AM, Kolodziejczyk PP, Black currant polyphenols: Their storage stability and microencapsulation, *Industrial Crops and Products*, 2011, 34: 1301-1309
3. Flores FP, Singh KR, Kerr WL, Pegg BP, Kong F, Total phenolic content and antioxidant capacities of microencapsulated blueberry anthocyanins during in vitro digestion, *Food Chemistry*, 2014, 153: 272-278
4. Betz M, Kulozik U, Microencapsulation of bioactive bilberry anthocyanins by means of whey protein gels, *Procedia Food Science*, 2011, 1: 2047-2056
5. Stojanović R, Cvitanović-Belscak A, Manojlović V, Komes D, Nedović V, Bugarski B, Encapsulation of thyme *Thymus serpyllum* L. aqueous extract in calcium alginate beads, *Journal of Science of Food and Agriculture*, 2012, 92: 685-696





CLINICALLY RELEVANT DISSOLUTION TESTING: EXPLORING ALBUMIN CONCENTRATIONS IN TESTING OF PARENTERAL FORMULATIONS ^(P13)

D.M. D'Arcy¹*, Y. Connell¹, M.J. Santos-Martinez¹

¹ School of Pharmacy and Pharmaceutical Sciences, Trinity College Dublin, Dublin 2, Ireland

INTRODUCTION

It has been recognised that there is a need for development of biorelevant dissolution media and test conditions for parenteral dosage forms (1). Furthermore, for many parenteral preparations, the target patient population can have significant illness and comorbidity, such as oncology or critically ill patients. Thus clinical patient factors can alter the environment into which the drug product is being delivered. Hypoalbuminaemia, for example, is common in critically ill patients, and has been known to significantly affect the pharmacokinetics of highly protein bound drugs (2). Furthermore, although albumin has also been thought to act as a dysopsonin, it has been shown to correlate with clearance of liposomes in mice (3). Clinically relevant albumin concentrations should therefore also be considered when designing dissolution media for assessment of lipid based parenteral products for specific target populations. The aim of this work is to explore use of the dissolution test as an in-vitro method to assess factors clinically relevant to parenteral drug administration in a target patient population. The objective of the current study was to investigate the use of albumin solutions at clinically relevant concentrations, as biorelevant dissolution media, to examine the dissolution of Amphotericin B (AmB), a poorly soluble highly protein bound drug.

MATERIALS AND METHODS

The CE1 flow-through dissolution apparatus (Sotax AG, Basel, Switzerland) was used in a closed cell configuration with the 22.6 mm cell at 16 ml/min flow rate (low velocity), or the 12 mm powder cell at 50 ml/min flow rate (high velocity).

Dissolution media consisted of 0%, 2% (hypoalbuminaemic) or 4% (healthy patient) bovine serum albumin in 5% dextrose (both Sigma life sciences, M.O., USA) at 37°C. Approximately 5 mg of AmB (EDQM, Strasbourg, France) was placed on a glass fibre filter (Whatman, GE Healthcare, UK) on top of a bed of glass beads which filled the conical part of the dissolution cell. The medium was sampled at 10, 15, 20, 30, 45 and 60 minutes by withdrawing 3 ml of liquid from the reservoir and replacing with 3 ml of fresh dissolution medium. Analysis of AmB was by UV spectrophotometry at 389 nm (UV-1700 Pharmaspec UV visible spectrophotometer, Shimadzu, Japan). For pH measurement an Orion 420A+ pH meter (Thermo Scientific, UK) was used, and for osmolality a Vapro 5520 vapour pressure osmometer (Wescor, USA).

RESULTS AND DISCUSSION

The dissolution results are presented in figure 1.

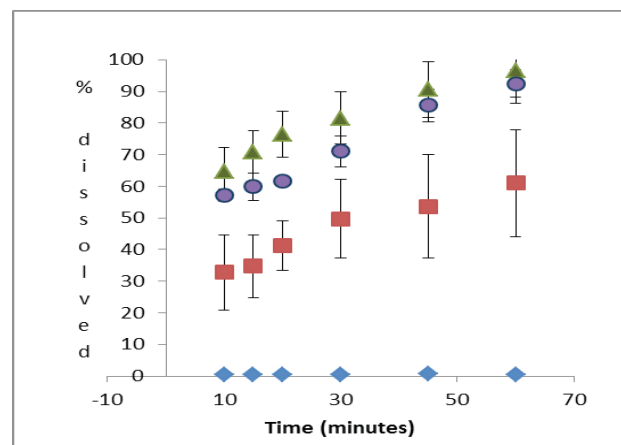


Figure 1: % AmB dissolved vs time (minutes) in ♦ 5% dextrose, low velocity ■ 2% albumin in 5% dextrose, low velocity ▲ 4% albumin in 5% dextrose, low velocity; and ● 2% albumin in 5% dextrose, high velocity.

It is clear from figure 1 that the presence of albumin in the dissolution medium has a notable effect on the dissolution of AmB. Furthermore, the dissolution of AmB in the 4% albumin solution is faster than that at the 2% concentration. The major effect of the albumin appears to take place within the first 10 minutes, implying that the





solubilising effect of albumin assists in drug dispersion and initial dissolution. After this time point, the dissolution profiles from the 2% and 4% albumin increase in a similar manner.

Interestingly, the dissolution profile from the 2% albumin solution in the high velocity conditions shows an increased dissolution over the same medium in low velocity conditions, with a profile closer to that from the 4% albumin medium in low velocity conditions. These results suggest that either increasing the concentration of albumin or increasing the flow rate can result in increased accessibility of AmB to albumin binding sites.

In terms of biorelevance of the media composition, osmolality of the dissolution media ranged from 260-365 mOsm L⁻¹, which is physiologically relevant. The pH ranged from 5.19 (5% dextrose) to 5.49 (4% albumin in 5% dextrose). Although lower than physiological pH, as 5% dextrose is commonly used as an intravenous infusion fluid, these pH values would not be considered bioincompatible.

In the current study the effect of albumin concentration on AmB solubilisation was being explored. *In vivo*, an increase in unbound drug allows an increase in drug clearance from the bloodstream, and thus a lower concentration of drug circulating in the bloodstream. The analogy in the *in vitro* case is that the unbound drug is not circulating in the dissolution medium. Therefore a well-designed biorelevant dissolution medium could assist in predicting pharmacokinetic performance of a parenterally administered highly protein bound drug in the target patient population.

Furthermore, the observed increase in dissolution with the increased albumin concentration in the current study is consistent with the effect of albumin concentration on volumes of distribution of AmB (reflecting clearance from bloodstream), following administration of AmB lipid complex, observed in critically ill patients (4).

Consideration of use of other plasma proteins such as alpha-1-acid glycoprotein and relevant buffer salts would further develop the biorelevance of this medium composition, depending on the formulation type and clinical situation being explored.

CONCLUSION

Clinically relevant albumin concentrations, representing healthy and hypo-albuminaemic patients, had a notable effect on the dissolution of AmB. Fluid velocity in addition to albumin concentration could be tailored to mimic the *in vivo* availability to albumin binding sites. The dissolution media was approaching biorelevance in terms of osmolality and pH. Dissolution media reflecting the physiological environment of a parenterally administered dosage

form should reflect clinically relevant factors present in the target patient population. There is scope to further develop the biorelevance of the *in vitro* test to incorporate factors relevant to drug release from different parenteral formulations.

REFERENCES

1. Seidlitz A, Weitschies, W. *In vitro* dissolution methods for controlled release parenterals and their applicability to drug-eluting stent testing. *J Pharm Pharmacol.* 2012; 64: 969-985.
2. Ulldemolins M, Roberts JA, Rello J, Paterson DL, Lipman J. The effects of hypoalbuminaemia on optimizing antibacterial dosing in critically ill patients. *Clin Pharmacokinet* 2011; 50: (2) 99-110.
3. Crielaard BJ, Yousefi A, Schillemans JP, Vermehren C, Buyens K, Braeckmans K, Lammers T, Storm G. An *in vitro* assay based on surface plasmon resonance to predict the *in vivo* circulation kinetics of liposomes. *Journal of Controlled Release* 2011; 156 307-314.
4. Malone ME, Gowing CG, Barry M, Deasy E, Kavanagh P, Corrigan OI, D'Arcy DM, Donnelly M. Can routine clinical chemistry results be related to the volume of distribution of amphotericin B lipid complex in critically ill patients? *Intensive Care Medicine* 2012; 38 (1) S154





PREPARATION AND CHARACTERIZATION OF PROTEIN-LOADED LIPID-POLYMER HYBRID NANOPARTICLES WITH POLYCAPROLACTONE AS POLYMERIC CORE MATERIAL (P14)

B. Devrim^{1*}, A. Bozkır¹

¹ Ankara University, Faculty of Pharmacy, Department of Pharmaceutical Technology, 06100, Tandoğan, Ankara-Turkey

INTRODUCTION

Use of nanoparticle has shown great potential as novel drug delivery systems. Nanoparticulate delivery systems such as liposomes and polymeric nanoparticles (NPs) have been extensively developed for delivering hydrophilic macromolecules such as nucleic acids and proteins (1). Liposomes are biocompatible, biodegradable, nontoxic, flexible, and nonimmunogenic for systemic and local administration. However, liposomes have several limitations from the viewpoint of physical and chemical stability, batch-to-batch reproducibility, sterilization and manufacturing scale-up (2). On the other hand, polymeric nanoparticles possess high structural integrity afforded by the rigidity of the polymer matrix, and are thus inherently more stable than liposomes (3).

The limitations of polymeric NPs include use of toxic organic solvents in the production process, poor drug encapsulation for hydrophilic drugs, polymer cytotoxicity and polymer degradation.

Lipid-polymer hybrid NPs (LPNs) combining the positive attributes of both liposomes and polymeric NPs are increasingly being considered as promising candidates to carry therapeutic agents safely and efficiently into targeted sites. LPNs exhibit high structural integrity, stability during storage, and controlled release capability attrib-

uted to the polymer core, and high biocompatibility and bioavailability owed to the lipid layer (4).

In this study, poly(ϵ -caprolactone) (PCL) was chosen as the polymeric core material due to its great biodegradability; phosphatidylcholine (PC) and glyceryl tripalmitate were selected as lipids. The modified emulsion method was developed and optimized to prepare the LPNs. Lysozyme was used as a model protein.

MATERIALS AND METHODS

Materials

Lysozyme, egg white was obtained from Vivantis (USA). Poly(ϵ -caprolactone) (PCL) (Mw = 14 kDa) was purchased from Aldrich (USA). L- α -phosphatidylcholine (PC), glyceryl tripalmitate and Pluronic F-127 were purchased from Sigma (USA). Dichloromethane (DCM) (99.9%, HPLC grade) and *Micrococcus lysodeikticus* (ATCC No. 4698) were obtained from Sigma-Aldrich (Germany). All other chemicals used were analytical grade.

Lipid-polymer hybrid nanoparticle (LPNs) preparation and characterization

The LPNs are prepared by a $w_1/o/w_2$ double-emulsification-solvent-evaporation method. Briefly, 200 mg PCL and 45 mg PC:glyceryl tripalmitate mixture are dissolved in 8 mL DCM:acetone mixture to form the oil phase, while 10 mg of lysozyme is dissolved in 1 ml aqueous SDS solution to form the internal aqueous phase (w_1). Next, the aqueous protein solution is emulsified in the organic solution by sonication for 2 min. The resultant nano-emulsion is poured into 10 ml %1 (w/v) Pluronic F-127 solution (w_2) and is sonicated again for 5 min. Afterwards, the nano-emulsion is stirred overnight at room temperature to evaporate off organic solvents, and the resultant NPs are collected by centrifugation using Vivaspin 20 centrifugal concentrator (Sigma-Aldrich, USA). Compositions used for LPNs are shown in Table 1.

Tab. 1: Composition of lipid-polymer hybrid NPs.

Formulation code	Amount of PCL (mg)	Amount of PC (mg)	Amount of glyceryl tripalmitate (mg)
PN1	200	-	-
LPN1	200	9	36
LPN2	200	15	30
LPN3	200	22.5	22.5
LPN4	200	30	15
LPN5	200	36	9

PCL: Polycaprolactone; PC: Phosphatidylcholine





The size, polydispersity index and zeta potential of the LPNs are measured by dynamic light scattering (DLS) (Zetasizer Nano-ZS instrument, Malvern, UK). The drug encapsulation efficiency is determined from the ratio of the encapsulated lysozyme to the lysozyme initially added. The amount of lysozyme was determined by using microBCA protein assay reagent kit. The protein loading is determined from the ratio of the encapsulated protein amount to the whole LPNs mass (i.e. protein + polymer + lipid).

Estimation of bioactivity of lysozyme

Lysozyme activity was determined using the decrease in optical dispersion at 450 nm of a *M. lysodeikticus* suspension. Briefly, 0.2 mg/ml dispersion of *M. lysodeikticus* (Sigma-Aldrich, USA) was prepared in a 66 mM phosphate buffer pH 6.6. To 2.9 ml of this suspension, 0.1 ml of the lysozyme-containing solution from the encapsulation efficiency was added, and the decrease in time of the $OD_{450\text{ nm}}$ monitored. Enzyme activity was deduced from the slope of the curve.

RESULTS AND DISCUSSION

The size of the LPNs were not significantly changed with increasing the ratio of PC:glyceryl tripalmitate ($p < 0.05$). However, the zeta potentials of LPNs were tended to decrease (more negative) with increasing the ratio of PC:glyceryl tripalmitate.

Tab. 2: Physicochemical characterization of LPNs.

Formulation code	Particle size (nm)	Zeta Potential (mV)	Yield (%)
PN1	107.9±0.404	-3.28±0.19	68.60
LPN1	116.57±1.84	-5.82±0.31	85.00
LPN2	112.32±0.30	-10.9±0.40	71.82
LPN3	117.1±2.63	-10.5±0.058	64.09
LPN4	110.43±1.68	-21.77±0.93	55.25
LPN5	124.53±2.26	-17.33±1.27	57.46

As shown in Fig. 1, increasing the ratio of PC:glyceryl tripalmitate caused an increase in encapsulation efficiencies of NPs significantly ($p < 0.05$).

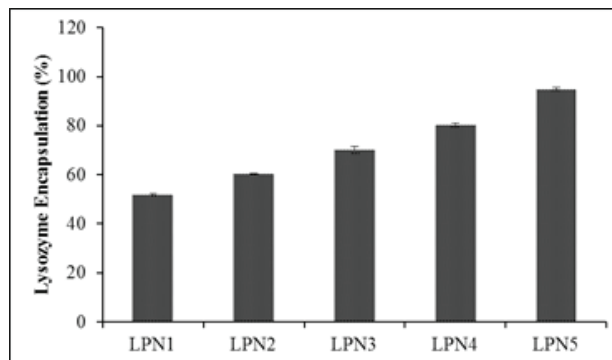


Fig. 1: Drug carrying capacity of LPNs.

According to the results of bioactivity assay results, 63.86% bioactive lysozyme was recovered from the LPNs.

CONCLUSIONS

The lysozyme-loaded LPNs were successfully formulated by using PCL as hydrophobic polymeric core material. Physicochemical properties of LPNs were affected from ratio of PC:glyceryl tripalmitate.

REFERENCES

1. Desai PR, Srujan M, Patel AR, Voshavar C, Chaudhuri A, Singh M. Topical delivery of anti-TNF α siRNA and capsaicin via novel lipid-polymer hybrid nanoparticles efficiently inhibits skin inflammation in vivo. *J. Control. Release* 2013; 170:51–63.
2. Mandal B, Bhattacharjee H, Mittal N, Sah H et al. Core-shell-type lipid-polymer hybrid nanoparticles as a drug delivery platform. *Nanomedicine*. 2013; 9:474–491.
3. Cheow WS, Hadinoto K. Factors affecting drug encapsulation and stability of lipid-polymer hybrid nanoparticles. *Colloids Surf B Biointerfaces*. 2011; 85:214–220.
4. Hadinoto K, Sundaresan A, Cheow WS. Lipid-polymer hybrid nanoparticles as a new generation therapeutic delivery platform: A review. *Eur J Pharm Biopharm*. 2013; 85:427–443.



CORE-SHELL CROSSLINKED POLYMERIC MICELLES AS CARRIERS FOR CANCER CHEMOTERAPY (P15)

B. Djurdjic^{1*}, S. Dimchevska¹, N. Geskovski¹,
V. Gancheva², G. Georgiev², P. Petrov²,
K. Goracinova¹

¹ Institute of Pharmaceutical Technology, Faculty of Pharmacy,
Ss Cyril and Methodius, Vodnjanska 17, 1000 Skopje, Macedonia
² Department for polymerization processes, Institute of Polymers,
Bulgarian Academy of Sciences, Akad. G. Bonchev Street 103A,
1113 Sofia, Bulgaria

INTRODUCTION

Amphiphilic self-assembled polymeric micelles have generated great interests as carriers for targeted anticancer drug delivery as they possess improved ability for solubilization of poorly water soluble drugs as well as long circulation time due to their hydrophilic corona (1, 2). Also, stable or “frozen” polymeric micelles in a kinetic sense can be arranged from copolymers composed of blocks with high enough hydrophobicity and large enough glass transition temperature due to the large activation energy required for molecular exchange. Therefore, in this study, amphiphilic A-B-A self-assembling triblock copolymer composed of poly(ϵ -caprolactone) (PCL) and poly(acrylic acid) (PAA) was synthesized. Further, PAA₁₃-PCL₃₅-PAA₁₃ was used for preparation of kinetically stable micelles by nanoprecipitation procedure. These stimuli-responsive drug delivery system composed of PCL hydrophobic core and PAA hydrophilic corona, with slightly negative zeta potential and prolonged circulation time are appealing carriers for pulmonary, peritoneal, parenteral as well as gastrointestinal delivery. GIT delivery is additionally supported by the PAA shell mucoadhesive properties and pH sensitivity. Having this in mind and in order to customize the properties of PAA-PCL-PAA micelles for GIT delivery (increase stability against aggregation in strong

acidic environment and improve controlled release at higher pH values) chemical crosslinking of the PAA shell was performed via EDC chemistry (Fig. 1a) and by loading of the PAA shell with PETA (pentaerythritol tetraacrylate, Fig 1 b). PETA was further cross-linked “in situ” with UV assistance.

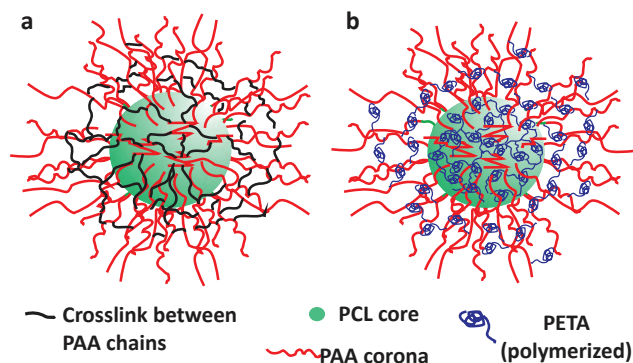


Figure 1. a) PAA chains crosslinked by EDC chemistry b) PETA cross-linked in the micelle shell

MATERIALS AND METHODS

Materials

Poly(acrylic acid)-poly(ϵ -caprolactone)-poly(acrylic acid) block copolymer (PAA₁₃-PCL₃₅-PAA₁₃) was synthesized and characterized at the Institute of Polymers, BAS, Bulgaria. SN-38 (7-ethyl-10-hydroxycamptothecin) was obtained from Biotech Co., China. All other chemicals were of analytical grade.

Preparation and evaluation of SN-38 loaded stabilized micelles

Nanoprecipitation method: SN-38 and PAA-PCL-PAA copolymer were dissolved in THF under continuous stirring. The polymer drug solution (25 ml) was added drop-wise into 25 ml of 0.01 M NaOH under continuous mixing by Ultra-turrax T-25 (IKA, Germany) and the water phase was neutralized to pH 5.5 using 0.01M HCl. Afterwards, THF was removed from the samples using Rotovapor (25°C, 70mbar, 65rpm, R200, Buchi, Swiss). Separation of non-encapsulated drug from micelles was performed by filtration of crystallized SN-38 from the dispersion immediately after evaporation of the organic solvent using 0.45 μ m filter, followed by centrifugal ultrafiltration with Vivaspin 20 ultrafiltration spin columns, 1000 KDa used for nanoparticle concentration (Sartorius Stedim Biotech GmbH, Germany). Self assembled micelles (NP1) were crosslinked using PETA and carbodiimide chemistry. PETA was added as acetone solution (10% of polymer content) to the micelle dispersion under continuous stir-





ring and elevated temperature (30 min, 30-40°C), followed by UV irradiation for 45 min (NP2). The PAA shell chains of the micelles were also crosslinked simply by reacting with a desired amount of 2,2-(ethylenedioxy)bis(ethylamine) in the presence of EDAC in the micelle dispersion as carboxyl activating agent (sample NP3). Stabilized micelles were purified by washing with deionized water and centrifugal ultra-filtration. Drug loading (HPLC method), particle size, zeta potential (Zetasizer Nano ZS, Malvern Instruments) and drug dissolution rate (pH 7.4, sink conditions, horizontal shaker, 75 rpm, 37° C) of the prepared micelles were evaluated and compared.

RESULTS AND DISCUSSION

Prepared polymeric micelles showed low polydispersity index and mean diameter of 122 ± 3 nm, 107 ± 1 nm and 136 ± 2 nm for sample NP1, NP2 and NP3, respectively. Zeta potential was shifted to lower values due to the crosslinking (-40 mV, -20 mV and -15mv for NP1, NP2 and NP3 respectively). Drug release profiles of noncrosslinked micelles showed high burst release which was substantially decreased by the process of crosslinking. Moreover, PETA stabilized micelles showed significantly lower drug release rate compared to micelles crosslinked via EDC chemistry. The interpenetrating network of poly(PETA) chains in which the polyether blocks were physically entrapped was additional barrier to drug dissolution. On the other hand EDAC reacts with carboxyls to promote peptide bond formation with the bifunctional crosslinker leading to formation of network with lower density compared to PETA crosslinked chains.

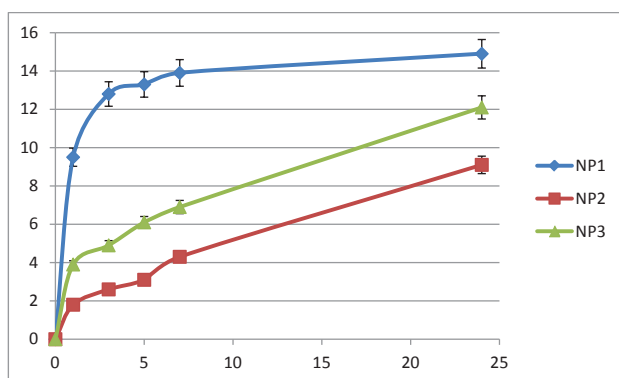


Figure 2: In vitro release profiles of SN-38 from micelles

CONCLUSIONS

PAA shell crosslinking of PAA-PCL-PAA self assembled micelles successfully inhibited premature drug release at higher pH values. Interpenetrating PETA network resulted with slower drug release rate compared to EDC crosslinking. Our future work will further explore the suitability and application of these carriers as drug delivery systems for anticancer therapy.

REFERENCES

1. Deng C, Jiang Y, Cheng R, Meng F, Zhong Z, Biodegradable polymeric micelles for targeted and controlled anticancer drug delivery: Promises, progress and prospects. *Nano Today* 2012; 7: 467-480.
2. Danhier F, Feron O, Préat V, To exploit the tumor microenvironment: Passive and active tumor targeting of nanocarriers for anti-cancer drug delivery. *J. Control. Release* 2010; 148:135-146.
3. Petrov P, Tsvetanov CB, Jerome R, Stabilized mixed micelles with a temperature-responsive core and functional shell. *J.Phys. Chem.B* 2009; 113: 7527-7533.



PREPARATION AND CHARACTERIZATION OF CARVEDILOL SOLID DISPERSIONS IN NEUSILIN[®] USING SPRAY DRYING METHOD (P16)

I. Dovnik^{1,*}, O. Planinšek¹, I. Ilič¹

¹ Department of Pharmaceutical Technology, Faculty of Pharmacy, University of Ljubljana, Aškerčeva 7, SI-1000, Ljubljana, Slovenia

INTRODUCTION

Newer active substances are often poorly soluble. As a result, their dissolution in the gastrointestinal track is slow, resulting in poor bioavailability. Carvedilol is a typical example of such a poorly soluble drug which belongs to class II (low solubility, high permeability) according to the BCS.

The aim of our study was to improve the dissolution profile of carvedilol by preparing solid dispersions (SD) using Neusilin[®] with the spray drying method. We also investigated the impact of different drug-carrier ratio for preparation of sprayed suspension (1, 2).

MATERIALS AND METHODS

Carvedilol was obtained from Krka (Novo Mesto, Slovenia), *Neusilin[®] US2* mesoporous Mg-aluminometasilicate, was obtained from Fuji Chemical Industry CO., LTD., Japan, *Acetone* was obtained from Merck, Germany.

Preparation of solid dispersions

SD were prepared with the spray drying method (3) using BÜCHI Mini Spray Dryer B-290, Switzerland. We used different drug-carrier ratios (1:3, 1:1, 3:1) for preparation of sprayed suspensions. Appropriate amount of Neusilin[®] US2 according to drug-carrier ratio was suspended in 100 ml of acetone into which 2.0 g of carvedilol had been dissolved. The process of spraying was carried out in a nitrogen atmosphere.

Drug content

15 mg of sample was dissolved in 200 ml of methanol, stirred on magnetic stirrer for 2 h and put in ultrasound bath for 15 min.

Drug content in SD was determined spectrophotometrically at 332 nm using UV-VIS spectrophotometer Hewlett Packard 8453, Germany.

Determination of crystallinity

Differential scanning calorimetry: DSC curves were recorded with a calorimeter DSC 1, Mettler Toledo, Switzerland. Samples were heated from 273 to 404 K at rate 5 K/min under nitrogen flow 40 ml/min. The calorimeter was calibrated with indium.

Dissolution studies

Dissolution experiments were carried out in 900 ml phosphate buffer with pH 6.8 using USP II dissolution test apparatus Vankel 7000, USA. Samples containing 25 mg of carvedilol were put into the dissolution vessel at 37 ± 0.5 °C and stirred at 50 rpm. The concentration of carvedilol was determined spectrophotometrically at 332 nm.

Specific surface area

Specific surface area and total pore volume of SD and pure Neusilin[®] US2 were recorded with nitrogen gas adsorption technique at 77.35 K using a Micromeritics TriStar 3000, USA (BET equation, t-plot method of Lippens and De Boer) (4).

Helium pycnometric density

The true density of SD, Neusilin[®] US2 and drug were measured with a helium pycnometer AccuPyc 1330, Micromeritics, USA. Around 1 g of the sample was accurately weighted for determination.

RESULTS AND DISCUSSION

The product recoveries decreased with the increase of the proportion of drug in in solid dispersions (1:3 – 81.9 %, 1:1 – 81.3 %, 3:1 – 55.6 %). At high drug-carrier ratios the product was more sticky and deposited on the wall of the process chamber and cyclone.





Tab. 1: Specific surface area and total pore volume of SDs and pure Neusilin® US2

SD and Neusilin® US2	Specific surface area (m ² /g)	Total pore volume (cm ³ /g)
Neusilin® US2	317,4	1,16
1:3	192,1	0,74
1:1	109,7	0,41
3:1	78,6	0,31

Glass transition at 38 °C and the absence of a melting peak of crystalline carvedilol at 110 °C was observed on DSC thermograms of SD. DSC results confirmed that carvedilol was transformed into an amorphous form. The decreasing specific surface area and total pore volume from BET analysis (Tab. 1) suggested that carvedilol was incorporated into the pores of the carrier.

Two unwanted processes were identified during the preparation of SDs: loading of drug particles on the surface of the carrier material and agglomeration of particles. In this case, carvedilol in an amorphous form does not have any spatial limitations (like in pores); thus, it can transform into the crystal form more easily during storage. The processes were more noticeable at SDs with drug-carrier ratio 3:1, which showed a poorer dissolution profile (Fig. 1). Dissolution profile of all SDs was faster compared to pure carvedilol or the physical mixture of drug with Neusilin® US2. This was attributed to adsorption of the drug in amorphous form in pores of a hydrophilic carrier, which improves wetting and dissolution rate of the drug. Helium pycnometric densities were compared to drug-carrier ratios. Measured values of the true densities deviate from linearity and are lower than expected.

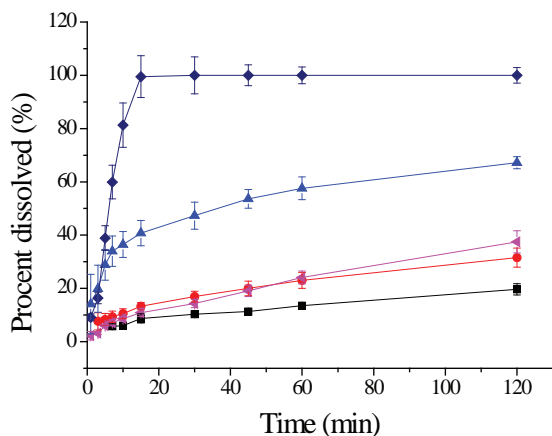


Fig. 1: Dissolution profiles of SDs: ● 1:3, ▲ 1:1, ▼ 3:1; ▼ physical mix., ■ crystalline carvedilol.

This suggests partial loading of drug on the surface of Neusilin® US2, which leads to the closure of the pores. As helium cannot penetrate into these closed pores, the measured volume was falsely overestimated and thus true density of SDs was underestimated (Fig. 2).

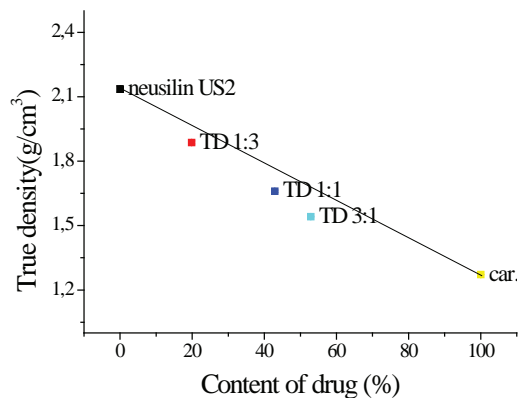


Fig. 2: True density of SD, Neusilin® US2 and carvedilol compared to drug content

CONCLUSIONS

The study showed that the most suitable ratio between the drug and the mesoporous carrier was 1:1 or less.

REFERENCES

1. Planinšek O. Contemporary approaches to solid dispersions production with improved drug bioavailability. *Farm Vestn*, 2009; 60: 169-176
2. Tiwari R., Tiwari G., Srivastava B., Rai A.K. Solid Dispersions: An Overview To Modify Bioavailability Of Poorly Water Soluble Drugs. *Int. J. PharmTech Research*. 2009; 1 (4): 1338-1349
3. Paudel A., et. al. Manufacturing of solid dispersions of poorly water soluble drugs by spray drying: Formulation and process considerations Review Article *Int. J. Pharm.* 2013; 453: 253-284
4. Planinšek O., Kovačič B., Vrečer F. Carvedilol dissolution improvement by preparation of solid dispersions with porous silica. *Int. J. Pharm.* 2011; 406: 41-48



INFLUENCE OF DIE DIAMETER ON POWDER COMPRESSION BEHAVIOUR AND TABLET MECHANICAL PROPERTIES (P17)

R. Dreu^{1*}, B. Janković¹, R. Šibanc¹, I. Ilić¹, S. Srčič¹

¹ Department of Pharmaceutical Technology, Faculty of Pharmacy, University of Ljubljana, Aškerčeva 7, SI-1000, Ljubljana, Slovenia

INTRODUCTION

Tablets are a common and widely used dosage form, due to many advantages for patients and manufacturers. Tablets quality depends on properties of substances and the process of compression itself.

It has been already reported (1) that die diameter influences the properties of the tablets, although findings are limited to one composition and reasons for this behavior were not further elucidated experimentally. Mini-tablets are gaining wide interest due to their suitability for pediatric population or as a basis for modified release multiple unit dosage form. Therefore it is of interest to know what to expect from mechanical point of view, when compressing materials with different mechanical properties in a small diameter dies, especially if mini-tablets are intended for coating after compression in a pan or fluid-bed coater. The aim of this study was to investigate how the diameter of the die impacts the process of compression and consequently tablets properties, in respect to selected lubricated excipients, which differentiate by mechanical properties (2).

MATERIALS AND METHODS

Materials

Avicel PH200 (microcrystalline cellulose, FMC) - **Avicel**, Supertab 14SD (spray dried lactose, DFE pharma) - **LacSD**, Starch 1500 (pregelatinized starch, Colorcon) - **Starch** and Bekapress D (di-calcium phosphate 2-hydrate, BK) - **Beka** were lubricated by addition of 0,5 % (w/w) Mg stearate (Faci) and pressed into tablets.

Methods

Tablets were pressed using instrumented column press (Kilian SP300, IMA) and flat round punches with diameters of 12, 10, 7, 5.5 mm and where applicable with 2.5 mm punches at 35 tablets/min. Mass of tablets was modified for different die diameters in order to maintain tablet thickness to diameter ratio at zero porosity. In case of mini-tablets ratio of thickness to diameter was increased in order to overcome limitations of the tablet press.

Out-die Heckel analysis (n=25-30) was performed in this study in order to compare Heckel coefficients within the same material, pressed with tableting tooling of different diameters. Tensile strength of tablets was calculated (3) after determination of tablet crushing strength, either via tablet hardness tester (VK 200, Varian) or rheometer (Physica MCR 301, Anton Paar). Compactibility plot was constructed (n=25-30) and the slope C_p determined. Transmitted to applied pressure ratio and normalized displacement (current punch displacement divided by its maximum) were determined by sampling pressure (for upper and lower punch) and displacement (upper punch) data of the instrumented press. Displacement data were compensated for the deformation of punches and tablet press.

Local tablet indentation hardness was evaluated via nanoindentation technique (G200, Agilent) in a continuous stiffness measurement mode. Tablets were analyzed at upper and lower tablet surface center as well as near the edge. Additionally, side surface of the tablet was probed for hardness at three different heights.

RESULTS AND DISCUSSION

From Fig. 1 one can observe more or less steady decrease of Heckel coefficients, determined for investigated materials, pressed in dies of reducing diameters (d). This increase in tablet bed stiffness is in accordance with increase of die wall friction relative to tablet volume, as die surface to tablet volume increases with ratio of $4/d$, while die diameter decreases.



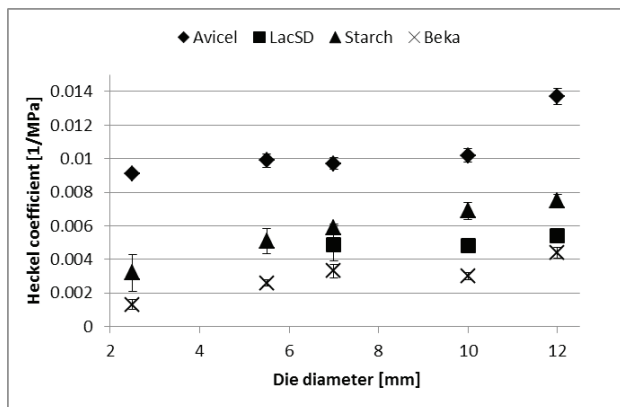


Fig. 1: Heckel coefficients as a function of die diameter

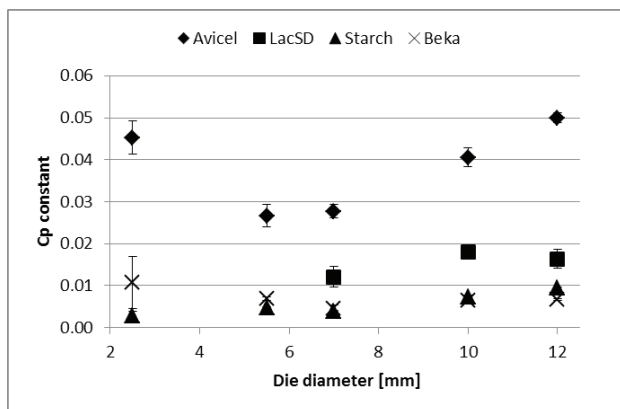


Fig. 2: Material compactibility as a function of die diameter

Surprisingly, Fig. 2 in case of Avicel (plastic material) and Beka (brittle material) demonstrates an increase in Cp values after initial drop in a series of experiments with reducing die diameter. For Starch (elastic-plastic material) this was not the case and we can see a steady decrease of material compactibility, when smaller and smaller dies are used. Results of LacSD are inconclusive. The results of pressure transmission reduction at maximum upper punch pressure (i.e. near normalized displacement of one) for Avicel and Beka (Tab.1) were expected due to anticipated increase of die wall friction, although the decrease in pressure transmission occurred only after 5.5 mm to 2.5 mm die change.

Tab. 1: Selected pressure transmissions for Avicel and Beka

Material	Die diameter [mm]	Pressure transmission coefficient
Avicel	12	0.95
	5.5	0.97
	2.5	0.89
Beka	12	0.94
	5.5	0.95
	2.5	0.58

Results of Heckel coefficient change and especially those of pressure transmission coefficient can only be interpreted in a light of compactibility increase (Avicel and Beka, d=2.5 mm) in such a way that increased die wall friction and corresponding shear forces improved mechanical properties, but only in case of small die tablets. It can be postulated that shear forces can act, due to limited number of particles, almost across the die diameter, which leads to uniform densification of larger portion of the mini-tablet volume. Nanoindentation experiments have for Avicel tablets indeed shown much more uniform results of indentation hardness in case of 2.5 mm tablets than in case of 5.5 and 12 mm tablets.

CONCLUSIONS

Study has shown that die diameter significantly influences the compression of powder and that one can expect favourable mechanical properties of mini-tablets, but only when pressing brittle or plastic materials.

REFERENCES

1. Lennartz P, Mielck JB, Minitabletting: improving the compactability of paracetamol powder mixtures. *Int. J. Pharm.* 1998; 173: 75–85.
2. Janković B, Ilić I, Šibanc R, Dreu R, Srčić S, The use of single particle mechanical properties for predicting the compressibility of pharmaceutical materials. *Powd. Tech.* 2012; 225:43-51.
3. Fell JT, Newton JM, Determination of tablet strength by the diametral-compression test. *J. Pharm. Sci.* 1970; 59:688–691.



DISSOLUTION STUDY OF A MODEL DRUG CRYSTAL USING ATOMIC FORCE MICROSCOPY (P18)

A. Dular^{1,*}, P. Bukovec¹, F. Vrečer^{1,2}

¹ Krka, d.d., Novo mesto, Šmarješka cesta 6, 8501 Novo mesto, Slovenia

² University of Ljubljana, Faculty of Pharmacy, Aškerčeva, 1000 Ljubljana, Slovenia

INTRODUCTION

Atomic force microscopy (AFM) is a widely used technique for characterization of particles and crystal surfaces on a nanometer to sub-angstrom scale (1). Since the instrument can be easily operated not only in air but also in fluid environment, AFM has been successfully utilized to study the dynamics of the dissolution process of crystal surfaces (2, 3). The understanding of the dissolution process of crystals on the level of individual crystal planes is important in pharmaceutical research, since it provides an insight into the dissolution mechanism, which has to be considered especially in the development of poorly soluble drug formulations (4).

The purpose of the present study was to examine the usage of AFM for the monitoring of drug dissolution from crystal planes on the nanoscale level.

MATERIALS AND METHODS

All materials used in the study were donated by Krka, d.d., Novo mesto, Slovenia.

Sample preparation

Large single crystals were obtained by dissolving the model drug in a mixture of polar solvents (acetone as solvent and water as antisolvent) and in the non-polar solvent heptane with the co-solvent ethanol. The prepared samples were left in an open flask at room conditions, allowing the solvents to evaporate slowly and crystals to grow in approximately 5 days.

Tab. 1: Crystallization conditions used for sample preparation

SAMPLE	SOLVENT	CONDITIONS
PB1	acetone + water (volume ratio 2:3)	no stirring, slow addition of water, slow evaporation of solvents
NB1	ethanol + heptane (volume ratio 1:20)	no stirring, slow evaporation of solvents

Sample characterization

SEM: Crystal morphology and nanostructure of the dominant crystal plane were studied before and after the dissolution analysis by scanning electron microscope (Carl ZEISS ULTRA plus, Germany).

AFM: The Innova atomic force microscope, Veeco, USA, with CP-II MicroCell, was used for the *in situ* dissolution study of samples. At first, the surface of the crystal (50 x 50 μm) was imaged in air using contact mode scanning. Then, approximately 1 ml of the dissolution medium phosphate buffer pH 7.0 with addition of 0.2% SDS was added into the cell and images of the same surface were recorded by contact mode scanning in fluid at preselected timepoints until the tip of the cantilever could no longer move across the sample due to pronounced surface roughness of the crystal. The 3D AFM image analysis was done with the NanoScope Analysis software.

RESULTS AND DISCUSSION

The *in situ* dissolution study of the dominant crystal planes of the samples crystallized from polar and less polar solvents was performed using AFM. As can be seen from microphotographs on Figures 1–5, dissolution of drug molecules from the crystal plane took place in a way that nanoscale trenches were formed on the surface of the crystal plane. These trenches continued to increase in their depth and width. The results suggested that the sample that crystallized from a more polar solvent dissolved faster than the sample that crystallized from a less polar solvent.



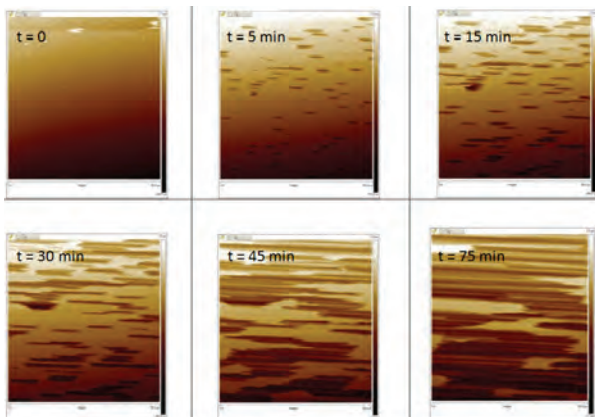


Fig. 1: Dissolution of dominant crystal face of sample PB1 – in situ AFM images at different time points

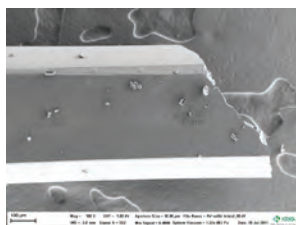


Fig. 2: SEM image of sample PB1 before the dissolution analysis (t=0)

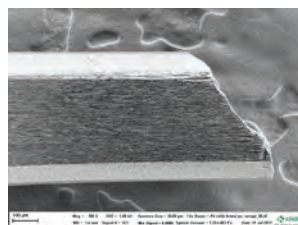


Fig. 3: SEM image of sample PB1 after the dissolution analysis (t=3 h)

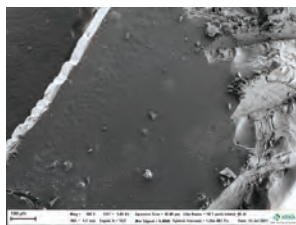


Fig. 4: SEM image of sample NB1 before the dissolution analysis (t=0)



Fig. 5: SEM image of sample NB1 after the dissolution analysis (t=5 h)

Based on the 3D AFM images, the volume of dissolved parts of the crystal at different time points was calculated. Much faster dissolution was observed in crystals obtained by crystallization from the acetone/water crystallization system.

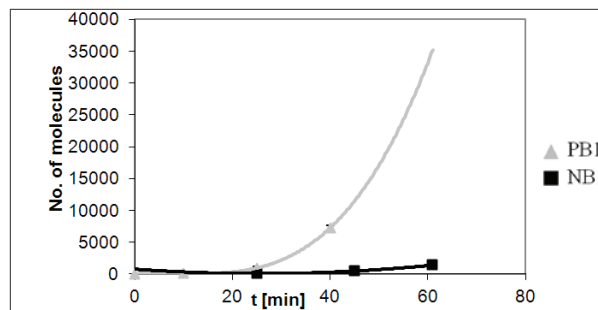


Fig. 8: Estimated number of dissolved molecules from the dominant crystal plane of samples PB1 and NB1 in time

CONCLUSION

AFM proved to be a useful method for dissolution studies of crystals on the nanoscale level, as it allows three-dimensional monitoring of dissolution behavior and provides an insight into the dissolution rate of single crystal planes.

The results of the experiments show that the dominant crystal faces of crystals obtained by crystallization with high-polarity index crystallization solvent show higher dissolution rates than those of crystals where a crystallization solvent with lower polarity is used. From this we can propose that there is a difference in polarity of dominant crystal planes between crystals crystallized from polar and less polar solvents.

ACKNOWLEDGEMENT

The authors would like to acknowledge Krka, d.d., Novo mesto for the support of the study.

REFERENCES

1. Johnson D, Hilal N, Richard Bowen W, *Basic principles of Atomic Force Microscopy*, Atomic Force Microscopy in Process Engineering, Chapter 1, Elsevier, New York, 2009, pp. 1–25.
2. Danesh A, Connell SD, et al. An In Situ Dissolution Study of Aspirin Crystal Planes (100) and (001) by Atomic Force Microscopy. *Pharmaceutical Research* 2001; 18: 299–303.
3. Mao G, Lobo L, et al. Nanoscale Visualisation of Crystal Habit Modification by Atomic Force Microscopy. *Chem. Mater.* 1997; 9: 773–783.
4. Rodriguez HN, Kelly RC et al. *Crystallization: General Principles and Significance on Product Development in Encyclopedia of Pharmaceutical Technology*, Vol. 2, Informa Healthcare, London, 2007, pp. 834–857.



CRYSTALLINE DRUG COMPRESSIBILITY PREDICTED WITH YOUNG'S MODULUS AND INDENTATION HARDNESS (P19)

M. Egart^{1,*}, B. Jankovič¹, I. Ilič¹, N. Lah², S. Srčič¹

¹ Faculty of Pharmacy, University of Ljubljana, Aškerčeva 7, Ljubljana, Slovenia

² Faculty of Chemistry and Chemical Technology, University of Ljubljana, Aškerčeva 5, Ljubljana, Slovenia

INTRODUCTION

Generally, all solid dosage forms are manufactured from powders which consist of solid particles, predominantly in crystalline state. One of the specific characteristic of crystals is polymorphism. Different polymorphic forms of the same substance might have different physicochemical and mechanical properties. Determination and understanding of these might be of crucial importance for successful production of solid dosage forms. Adequate mechanical properties (elastic/plastic and/or fracture behaviours) are crucial in all processes where material is exposed to stress, i.e. milling, mixing, tableting. Preferably, combination of plastic and brittle properties is desirable for the production of compacts. Plasticity in pharmaceutical crystals is typically associated with the presence of slip planes. These planes have the weakest intermolecular interactions and can be easily broken upon stress resulting in plane slide and irreversible plastic deformation (1, 2). The aim of our study was to establish whether deformational parameters of single pharmaceutical crystals determined with instrumented nanoindentation can be used to predict the powder bulk compaction properties, i.e. compressibility and compactibility. For that purpose, several active pharmaceutical ingredients - APIs (famotidine, nifedipine, olanzapine, piroxicam) were mechanically tested.

MATERIALS AND METHODS

Single crystals of investigated APIs' polymorphic forms were prepared according to the procedures described in

the literature, however, certain modifications have been used as well. For bulk studies, the commercially available and thermodynamically stable forms were used as received. To confirm the presence of specific polymorphic form, DSC and FTIR were used. Single crystals identification and characterization were performed with single crystal x-ray diffractometry. The face indexing of individual crystal was conducted using CrysAlis PRO software (Agilent Technologies). Oriented crystals of investigated APIs were analyzed at different crystal faces using instrumented nanoindentation (continuous stiffness measurement, CSM, mode) (4). Bulk deformational properties were assessed by modified Walker and Heckel models. For evaluation of elastic deformation, elastic relaxation index (ER) was calculated. Compactibility was determined by measuring the crushing strength of the tablets made from selected APIs powders (3, 5).

RESULTS AND DISCUSSION

Single crystals of investigated APIs' were evaluated according to their deformational properties with instrumented nanoindentation. Interlocked structures were characteristic for most polymorphic forms what is resulting in isotropic mechanical properties. The presence of slip planes was detected for famotidine B only, indicating its higher plasticity. This was confirmed with its lower indentation hardness in comparison to famotidine A. According to the ratio between indentation hardness and yield stress, preferentially brittle behaviour of the used APIs was determined. The mechanical elastic component was more expressed in the case of piroxicam I, nifedipine α , olanzapine I and famotidine B what was additionally confirmed on bulk level with higher elastic relaxation index.

The predictive values of nanoindentation parameters for investigated APIs was further confirmed by correlating plastic (Fig. 1) and elastic (Fig. 2) deformational parameters.

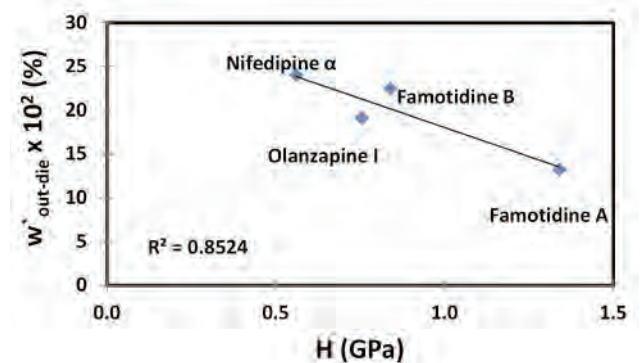


Fig. 1: Out-die Walker coefficient ($w'_{out-die}$) versus indentation hardness (H).



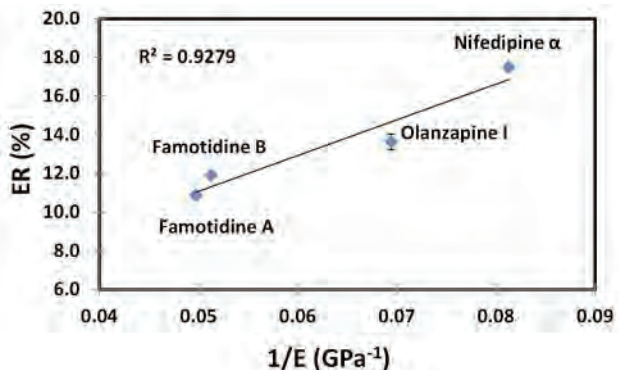


Fig. 2: Elastic relaxation index (ER) versus compliance (1/E).

The study also showed that bulk compactability (ability of the powder to form coherent compacts) is largely dependent from plasticity parameters. Good correlations were obtained between indentation hardness on single crystal level and compactability coefficient for investigated APIs (Fig. 3).

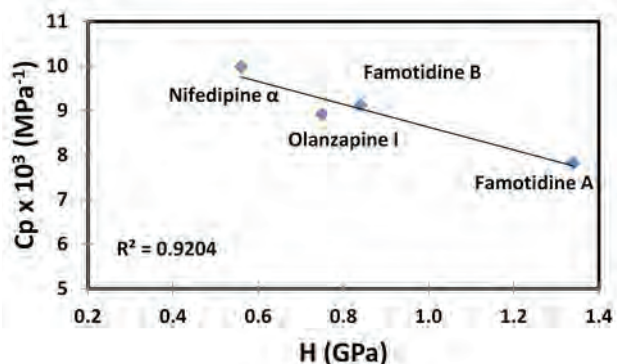


Fig. 3: Compactibility coefficient (C_p) versus indentation hardness (H).

It seems that the increased surface area accomplished by plastic deformation contributes essentially to the increased mechanical strength of the compacts (more interactions among particles can be established).

CONCLUSIONS

It was confirmed that the bulk deformational properties could be estimated on the single crystal deformational parameters. Therefore, Young's modulus (E) and indentation hardness (H) as the main nanomechanical attributes, present a valuable quantitative data during the preformulation studies of pharmaceutical materials.

The results also demonstrated that the strength of the API compacts is largely influenced by the extent of plastic deformation.

REFERENCES

1. Shariare MH, Leusen FJJ, De Matas M, York P, Anwar J. Prediction of the Mechanical Behaviour of Crystalline Solids. *Pharm. Res.* 2012; 29: 319–331.
2. Datta S, Grant DJW. Crystal structures of drugs: Advances and determination, prediction and engineering. *Nature Reviews. Drug discovery.* 2004; 3: 42–57.
3. Janković B, Škarabot M, Lavrič Z, Ilić I, Srčić S, Planinšek O. Consolidation trend design based on Young's modulus of clarithromycin single crystals. *Int. J. Pharm.* 2013; 454: 324–332.
4. Oliver WC, Pharr GM. Measurement of hardness and elastic modulus by instrumented indentation: Advances in understanding and refinements to methodology. *J. Mater. Res.* 2004; 19: 3–20.
5. Ilić I, Govedarica B, Šibanc R, Dreu R, Srčić S. Deformation properties of pharmaceutical excipients determined using an indie and out-die method. *Int. J. Pharm.* 2013; 446: 6–15.



COMPARISON BETWEEN MECHANICAL CHARACTERIZATION AND SENSORIAL EVALUATION OF NANOLIPIDGEL FORMULATIONS (P20)

M. Estanqueiro^{1,*}, J. Conceição¹, M.H. Amaral¹, J. M. Sousa Lobo¹

¹ Laboratory of Pharmaceutical Technology, Department of Drug Sciences, Faculty of Pharmacy, University of Porto, Rua de Jorge Viterbo Ferreira, n.º 228, 4050-313 Porto, Portugal

INTRODUCTION

In the last decades, lipid nanoparticles, such as solid lipid nanoparticles (SLN) and nanostructured lipid carriers (NLC), have been studied intensively for dermal application (1). The inclusion of aqueous dispersions of lipid nanoparticles in semisolid dermal carriers, like creams or gels, is required for topical application. Nanolipidgel, a term assigned by Wavikar and Vaviato, is a system comprising lipid nanoparticles incorporated into a gel base (2). Concerning the application and performance on skin, the consistency, spreadability, sensorial properties and adherence to the skin are important parameters to take into account (3). The sensation produced by application in the skin is one of the most important properties of dermatological and cosmetic formulations. A challenging prospect can be to relate the rheological measurements (instrumental analysis) with the consumer perception (4). The main objective of this study was the development of semisolid formulations based on NLC containing argan oil or jojoba oil as liquid lipids, by addition of Carbopol®934 or Carbopol®980 as gelling agents, followed by the comparison between instrumental analysis and sensorial evaluation.

MATERIALS AND METHODS

Materials

Table 1 presents the composition of nanolipidgels.

Tab. 1: Composition of nanolipidgels (% w/w).

	ARGC934	JOJC934	ARGC980	JOJC980
Compritol E ATO®	6	6	6	6
Argan oil	4	-	4	-
Jojoba oil	-	4	-	4
Tween® 80	0.5	0.5	0.5	0.5
Cetrimide®	0.5	0.5	0.5	0.5
Purified water	q.s.100	q.s.100	q.s.100	q.s.100
Carbopol®934	0.5	0.5	-	-
Carbopol®980	-	-	0.5	0.5
Triethanolamine	q.s.	q.s.	q.s.	q.s.

Methods

Nanolipidgels presented in Table 1 were prepared as previously described (5). Additionally, GC934 and GC980 hydrogels without lipid nanoparticles were also prepared by dispersion of 0.5% (w/w) of each carbomer in water followed by neutralization with triethanolamine.

Particle size (PS) and polydispersity index (PI) analysis were performed by dynamic light scattering (DLS) (Brookhaven Instruments, Holtsville, NY, USA). All the formulations presented nanosized particles.

Textural analysis were performed using a texturometer (Stable Micro Systems, TA-XT2i, UK) by carrying out a penetration test, using a cylindrical probe with 13mm diameter, a penetration depth of 5mm, and a test speed of 3mm/s. The maximum force (firmness) and the negative area (adhesiveness) were calculated. All the measurements were performed in triplicate.

Rheological analysis were performed using a rotational viscometer (HAAKE Viscotester 550, Germany), with a coaxial cylinder sensor SV-DIN. The study was started with a shear rate of 1 s⁻¹ up to a maximum of 500 s⁻¹ and back to 1 s⁻¹, and the resulting shear stress was measured. The experiments were performed at 20°C.

To evaluate the acceptability of formulations, a questionnaire was answered by each volunteer (n = 17), who was asked to evaluate sensorial attributes such as firmness, adhesiveness, consistency and spreadability. Before the test each volunteer was instructed about each attribute definition and procedure. Each parameter was evaluated using a scale from 1 to 5.



RESULTS AND DISCUSSION

Table 2 shows the results of textural parameters, namely firmness and adhesiveness of semisolid formulations.

Tab. 2: Results of firmness and adhesiveness determined for each semisolid formulation.

	Firmness (N)	Adhesiveness (N*mm)
GC934	0.103±0.002	-0.391±0.017
GC980	0.121±0.001	-0.417±0.013
ARGC934	0.134±0.004	-0.386±0.023
JOJC934	0.097±0.003	-0.320±0.015
ARGC980	0.285±0.006	-0.486±0.024
JOJC980	0.234±0.002	-0.418±0.012

With respect to nanolipidgels, it can be seen that the formulations with Carbopol®980 showed the greatest values of firmness and adhesiveness. Figure 1 represents the rheological behavior of semisolid formulations. All formulations presented a shear-thinning (or pseudoplastic) behavior. Only the nanolipidgels with Carbopol®980 showed thixotropy. Figure 2 delineate the obtained results from sensorial evaluation. Regarding the spreadability, the volunteers attributed greater scores, around 4, implying good spreadability. JOJC980 received greater scores in the remaining parameters.

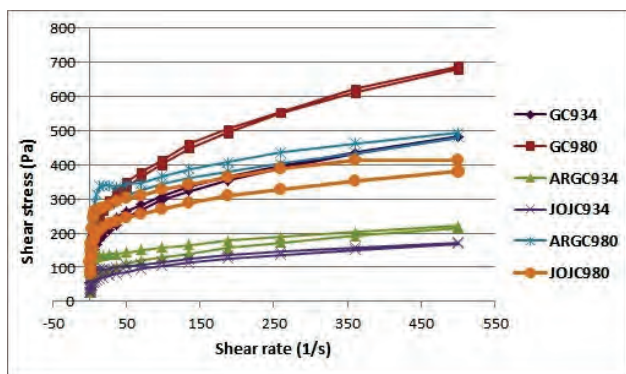


Fig. 1: Rheograms (shear stress as a function of shear rate) of semi-solid formulations.

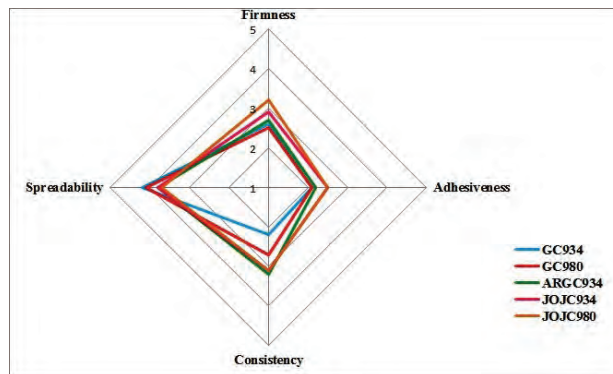


Fig. 2: Results of sensorial evaluation, expressed as mean values.

CONCLUSIONS

Despite the subjectivity of sensorial analysis, reasonable correlations between instrumental determinations and sensorial evaluation were obtained. Nanolipidgels obtained with Carbopol®980 showed better characteristics for application in the skin.

REFERENCES

1. Pardeike J, Hommoss A, Müller RH. Lipid nanoparticles (SLN, NLC) in cosmetic and pharmaceutical dermal products. *Int J Pharm.* 2009;366(1-2):170-84.
2. Wavikar P, Vavia P. Nanolipidgel for Enhanced Skin Deposition and Improved Antifungal Activity. *AAPS PharmSciTech.* 2013;14(1):222-33.
3. Lippacher A, Müller RH, Mäder K. Liquid and semisolid SLN dispersions for topical application: rheological characterization. *Eur J Pharm Biopharm.* 2004;58(3):561-7.
4. Tadros T. Application of rheology for assessment and prediction of the long-term physical stability of emulsions. *Adv Colloid Interface Sci.* 2004;108-109:227-58.
5. Estanqueiro M, Conceição J, Amaral MH, Sousa Lobo JM. Characterization, sensorial evaluation and moisturizing efficacy of nanolipidgel formulations. *Int J Cosmet Sci.* 2014;36(2):159-66.



INFLUENCE OF VEHICLE TYPE ON THE TEXTURE AND RELEASE PROPERTIES OF LIPOSOMES-IN-VEHICLE FORMULATIONS (P21)

Z. Palac¹, J. Hurler², N. Škalko-Basnet², J. Filipović-Grčić¹ and Ž. Vanić^{1*}

¹ University of Zagreb, Faculty of Pharmacy and Biochemistry, Department of Pharmaceutical Technology, A. Kovačića 1, 10000 Zagreb, Croatia

² University of Tromsø, Faculty of Health Sciences, Department of Pharmacy, Drug Transport and Delivery Research Group, Universitetsveien 57, 9037 Tromsø, Norway

INTRODUCTION

Effective (trans)dermal drug delivery depends on both the selection of drug and the properties of the delivery system. Due to their physiological suitability, phospholipid nature, non-toxicity and ability to encapsulate different compounds (hydrophilic, lipophilic and amphiphilic), phospholipid vesicles (liposomes) have shown great potential for improving the topical delivery of drugs. Despite these advantages, topical application of liposomal suspensions can be limited by their liquid nature. Therefore, to achieve the proper viscosity and stability of the formulation they are usually incorporated into a suitable vehicle. Moreover, dermatological vehicles could affect drug bioavailability and play an important role in the skin care. Vehicle composition has been proven to influence the release properties of the incorporated drug and the penetration ability across/into the skin. Therefore, the selection of the appropriate vehicle is an important factor in increasing the efficacy of a topically applied drug or drug delivery system (1).

Texture analysis has been proven to be a valuable method for the evaluation of mechanical properties of different liposomes-in-vehicle, such as hardness, adhesiveness and cohesiveness. These properties have been directly

correlated with the administration parameters *in vivo*, such as spreadability (hardness), retention of the formulation on the skin (adhesiveness) or its removal from the container (cohesiveness) (2).

MATERIALS AND METHODS

Deformable (DL), propylene glycol (PGL) and conventional liposomes (CL) were prepared by the film hydration method, followed by extrusion (3x400 nm). Each of the liposome suspension, containing only liposomally-entrapped hydrophilic model drug diclofenac sodium (DCS), was mixed into the following vehicles: hydrogel, cream base or derma membrane structure base cream classic (DMS base) (10% w/w, liposome suspension/vehicle). The release of the drug from the liposomes incorporated into different vehicles was determined by the method originally introduced by Peschka et al. (3) and adapted for liposomal hydrogels (4). A Texture Analyzer TA.XT Plus (Stable Micro Systems Ltd., Surrey, UK) was used to examine the texture properties of the liposomes-in-vehicle formulations.

RESULTS AND DISCUSSION

The results of the release study (Tab. 1) confirm slower release of the drug from all of the liposomes-in-vehicle formulations as compared to the control (solution of the drug in vehicles). Differences in the drug release profiles were observed between all of the liposomes and vehicles examined. The slowest release of DCS was observed for the cream base, followed by the hydrogel and DMS base. A comparison of the drug release profiles from different types of liposomes incorporated in hydrogel or cream base confirmed the slowest drug release from CL, whereas the drug release from PGL and DL was significantly faster ($p < 0.05$). The assessed texture characteristics were significantly different between all of the examined vehicles. The cream base showed the highest values of all of the parameters assessed, followed by the hydrogel and DMS base. Mixing liposomes into the cream base lowered the initial hardness by approximately 30% for the CL and PGL and slightly more for the DL (35%) (Fig. 1). Results based on texture analysis indicate a possible physical instability of liposomes in DMS base. Namely, nearly 2-fold decrease of the initial hardness was observed after incorporation of the liposomes into DMS base. This assumption was additionally supported with the release study in which the ratio of intact liposomes released was lower than 1%, even after 24 hours. The smallest decrease in the original hardness was observed with liposomes in the hydrogel (Fig. 1). Thus, all types of lipo-





somes were compatible with the hydrogel. The other two texture parameters (cohesiveness and adhesiveness) followed similar patterns for the examined liposomes-in-vehicle formulations.

Tab. 1: The cumulative amount (%) of the released diclofenac sodium from various liposomes-in-vehicle after 24 hours (DL – deformable liposomes; PGL – propylene glycol liposomes; CL – conventional liposomes). The values denote the mean \pm S.D. (n = 3).

Liposome formulation \ Vehicle type	Vehicle type		
	Hydrogel	Cream base	DMS base
CL	32,3 \pm 1,7	24,1 \pm 1,1	80,5 \pm 4,1
DL	49,1 \pm 1,0	35,8 \pm 2,1	76,1 \pm 2,9
PGL	45,8 \pm 0,9	32,8 \pm 1,4	80,9 \pm 3,8
Control	89,3 \pm 2,2	64,3 \pm 2,4	76,9 \pm 7,1

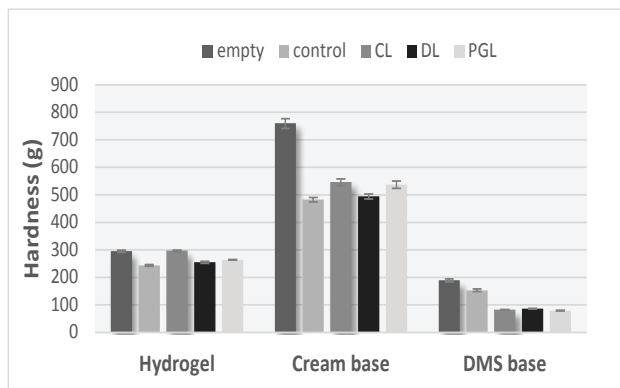


Fig. 1: Influence of the liposome types on the hardness of vehicles (DL – deformable liposomes; PGL – propylene glycol liposomes; CL – conventional liposomes). The values indicate the mean \pm S.D (n=5).

CONCLUSIONS

Based on these studies, propylene glycol liposomes-in-hydrogel seems to be the most suitable formulation for improving skin delivery of hydrophilic drug. Further investigations involving *in vivo* animal studies are necessary to confirm its applicability in skin therapy.

REFERENCES

1. Daniels R, Knie U. Galenics of dermal product - vehicles, properties and drug release. *J Dtsch Dermatol Ges* 2007; 5:369-383.
2. Hurler J, Engesland A, Kermay BP, Škalko-Basnet N. Improved texture analysis for hydrogel characterization: Gel cohesiveness, adhesiveness and hardness. *J Appl Polym Sci* 2012;125:180-188.
3. Peschka R, Dennehy C, Szoka FC. A simple *in vitro* model to study the release kinetics of liposome encapsulated material. *J Control Release* 1998; 56:41-51.
4. Pavelić Ž, Škalko-Basnet, N, Filipović-Grčić, J, Martinac A, Jalšenjak I. Development and *in vitro* evaluation of a liposomal vaginal delivery system for acyclovir. *J Control Release* 2005; 106: 34-43.



INFLUENCE OF PROCESS VARIABLES ON THE PROPERTIES OF SELF-EMULSIFYING GRANULES PRODUCED BY HIGH SHEAR WET GRANULATION (P22)

E. Franceschinis¹, A.C.Santomaso², L.Benda¹, B.Perissutti³, D. Voinovich³, N.Realdon¹, A. Trotter^{1*}

¹ PharmaTeG - Pharmaceutical Technology Group, Dept. of Pharmaceutical and Pharmacological Science, University of Padova, Via Marzolo 5, 35131 Padova, Italy

² APTLab - Advanced Particle Technology Laboratory, Dept. of Industrial Engineering, University of Padova, via Marzolo 9, 35131 Padova, Italy

³ Dept. of Chemical and Pharmaceutical Sciences, University of Trieste, P.le Europa 1, 34127 Trieste, Italy

INTRODUCTION

The absorption of class II molecules can be greatly improved by formulating them in self-emulsifying drug delivery systems (SEDDS) in fact their clinical usefulness is evident from the commercially available formulations (1, 2). SEDDS are mixtures of drug, oils, surfactants and/or co-solvents which form fine oil-in-water emulsions upon dilution with aqueous medium or *in vivo* administration and they are usually found in liquid form (3, 4, 5). The drawbacks of these formulations can be avoided producing solid-SEDDS by their adsorption into powder/nanoparticles to create solid dosage forms. Although Franceschinis and co-workers (6, 7) have already demonstrated that it is possible to produce solid-SEDDS by high shear granulation (HSWG) using a microemulsion as granulating liquid, few information is present about the effect of this type of granulating liquid and operating variables on the final granule properties. Consequently, the purpose of this investigation was to compare the effects

of impeller speed and massing time on the granule properties when water or an oil-in-water microemulsion were used as granulating liquids. In order to evaluate also their effect on the drug release, simvastatin (SV) was selected as a model drug and included in the granulating liquid.

MATERIALS AND METHODS

Materials

Simvastatin (SV), Microcrystalline cellulose (MCC), Polyvinylpyrrolidone K 90 (PVP) and Monohydrate Lactose (Lac) were obtained from Acef (Fiorenzuola D'Arda, Italy), Propylene glycol-monolaurate (Lauroglycol 90) and Diethylene glycol-monoethyl-ether (Transcutol®HP) were obtained from Gattefossé (Saint-Priest, France). Polyoxyl-35-castor oil (Cremophor EL) was supplied by BASF (Ludwigshafen, Germany).

Granulation procedure

The granules were obtained using a one-step high shear mixer Rotolab (IMA SpA, Italy). The granulation procedure were standardized on the basis of preliminary trials: 200 g of powder mixture comprising 70% of MCC, 27% of Lac and 3% of PVP was dry-mixed, successively, 160 g of granulating liquid (water or microemulsion) containing 2% of SV was dripped on dry powders. To evaluate the effect of the impeller speed and massing time on granule properties the experiments were planned using an factorial design ($3^1 \times 2^2$) consisting of 12 experiments. The granules were dried and characterized by sieve and size analysis and *in vitro* dissolution tests.

RESULTS AND DISCUSSION

The excipients were selected on the basis of SV solubility studies while the microemulsion formulation was identified by pseudo-ternary phase diagrams. Formulation named C14 containing 20% of Lauroglycol 90 as oil phase, 15% of Transcutol HP as co-solvent and 5 % of Cremophore EL as surfactant was selected to prepare solid-SEDDS in consideration of its low viscosity (0.019 Pa s) and its small modal droplet size (0.111 μm). The interaction between the powders and the granulating liquid (water and microemulsion) was evaluated by measuring the liquid-solid contact angle using sessile drop method (8). Data shows that even though the microemulsion surface tension was half than that of water, the resulting penetration time was two orders of magnitude larger than that of water. This can be justified by the contact angle value which was larger than 90° for microemulsion, indicating a poorer wetting ability.





As expected from the penetration time values, the PSDs of the granules obtained with microemulsion were broader than that with water. Indeed for water-based granules the d_{10} and the d_{90} are roughly 500 and 3000 μm , while for microemulsion-based granules the d_{10} was always smaller than 500 μm and the d_{90} always larger than 3500 μm , meaning larger PSDs.

The granules underwent a morphological analysis from which the roundness Φ_R is obtained. Data show that while an increase in massing time produced an increase in Φ_R , the impeller speed did not affect the shape. Moreover the microemulsion-based granules resulted in larger values of Φ_R . In order to verify the effect of the process variables on drug dissolution rate, granules also underwent a dissolution test. In the absence of a surfactant SV is unable to dissolve in simulated intestinal dissolution medium, as a consequence, granules produced using water are not able to release SV. Self-emulsifying granules instead show that the amount of SV released depends on massing time and in particular, the lower the massing time, the greater the amount of released SV.

CONCLUSIONS

The results showed that the granulation processes are greatly influenced by the type of binder. In particular, when water is used as a binder the final characteristics of the granules are influenced by all the experimental variables studied, instead when microemulsion is used as a granulating liquid the system was relatively insensitive to impeller speed and could only be moderately modified through the massing time. On the whole the wet granulation process in a high shear mixer has proved to be a useful technique to produce solid-SEDDS and increase drug dissolution rates of poorly water-soluble drugs.

REFERENCES

1. Strickley R.G., 2007. Currently Marketed Oral Lipid-based dosage forms: drug products and excipients. In: *Oral lipid-based formulations enhancing the bioavailability of poorly water-soluble drugs*, Ed. Hauss D.J.
2. Talegaonkar S., Azeem A., Ahmad F.J., Khar R.K., Pathan A., Khan Z.I., 2008. Microemulsions: A novel approach to enhanced drug delivery, *Recent Pat Drug Deliv Formul.* 2, 238-257.
3. Hauss D.J., 2007. Oral lipid-based formulation: bringing the gap between knowledge and Know-how-Strategies for exploiting the full potential of oral-lipid based drug delivery systems, *Bull. Tech. Gattefossè* 100, 8-11.
4. Gursoy R.N., Benita S., 2004. Self-emulsifying drug delivery systems (SEDDS) for improved oral delivery of lipophilic drugs, *Biomed. Pharmacother.* 58, 173- 182.
5. Porter C.J.H., Pouton C.W., Cuine J.F., Charman W.N., 2008. Enhancing intestinal drug solubilization using liquid-based delivery systems, *Adv. Drug Deliver. Rev.* 60, 673-691.
6. Franceschinis E., Voinovich D., Grassi M., Perissutti B., Filipovic-Grcic J., Martinac A., Meriani-Merlo F., 2005. Self-emulsifying granules prepared by wet granulation in high-shear mixer: influence of formulation variables and preliminary study on the in vitro absorption, *Int. J. Pharm.* 291, 87-97.
7. Franceschinis E., Bortoletto C., Perissutti B., Dal Zotto M., Voinovich D., Realdon N., 2011. Self-emulsifying pellets in a lab-scale high shear mixer: Formulation and production design. *Powder Technol.* 207, 113-118.
8. Susana L., Campaci F., Santomaso A.C., 2012. Wettability of mineral and metallic powders: Applicability and limitations of sessile drop method and Washburn's technique. *Powder Technol.* 226, 68-77.



THE USE OF HYDROPHOBIC SUGAR ESTERS IN PREPARATION OF SUSTAINED RELEASE MATRIX TABLETS BY THERMOPLASTIC AGGLOMERATION (P23)

T. German¹, J. Böhm¹, O. Planinšek², F. Vrečer^{1,2}

¹ KRKA d.d., Novo mesto, Šmarješka cesta 6, 8501 Novo mesto, Slovenia

² University of Ljubljana, Faculty of Pharmacy, Aškerčeva cesta 7, 1000 Ljubljana, Slovenia

INTRODUCTION

Thermoplastic agglomeration is an alternative to classical technological processes for preparation of both immediate-release and sustained-release solid dosage forms. It offers a number of advantages. Since it does not require the use of solvents, the drying phase is eliminated and consequently the dosage form production process is shortened and more economical. A wide range of melt-able binders with different chemical and physical characteristics, which can be used to prepare controlled release granules or to enhance the dissolution rate of poorly water soluble drugs are available. Hydrophilic binders such as macrogols (PEGs), Gelucire and poloxamers have been shown to successfully enhance the dissolution of poorly soluble drugs using hot melt technology, while hydrophobic binders including waxes, fatty acids and fatty alcohols have been used for sustained release dosage forms. (1,2)

Sugar esters (SE) are non-ionic surface-active agents consisting of sucrose as hydrophilic moiety and fatty acids as lipophilic groups. They have been applied in hot melt technology, but their use in this field has been less widely investigated. Depending on the nature of esterified fatty acid and the degree of esterification a wide range of hydrophilic-lipophilic balance (HLB) values can be obtained. Lipophilic SEs have been used as controlled-

release agents in various drug delivery systems including matrix tablets. (3)

The aim of present study was to investigate the effect of different binders on dissolution of a water soluble model drug from solid dosage form prepared via thermoplastic agglomeration process.

MATERIALS AND METHODS

Materials

A highly water soluble drug (Krka, d.d., Novo mesto, Slovenia) was used as a model drug. The following hydrophobic melt-able excipients were used: sugar esters D-1803, D-1805, D-1807 and D-1809 with HLB values 3, 5, 7 and 9 respectively (SE, Surfhope® SE Pharma, Japan), glyceryl behenate (Speziol® GDB Pharma, Cognis GmbH, Germany). Lactose monohydrate was used as a diluent (DMV, The Netherlands) and magnesium stearate as a lubricant (Faci SPA, Italy).

Preparation of granules and tablets

Granules were prepared by hot melt granulation in a Pro-cept Mi-Pro high-shear mixer equipped with a double jacket for heating/cooling and a six-bladed impeller. Produced granules were then mixed with magnesium stearate and compressed into tablets using a single punch tableting machine (Fette, Germany). Five different granulates and tablets were prepared, each with different binder but the same quantitative composition with binder:drug ratio 1:1.

Drug release studies

The drug release studies were performed in purified water, basket method (Apparatus I, Erweka DT 800), 900 mL, 100 rpm, 37°C±0.5 °C. Samples were analysed at 274 nm using UV spectrophotometer (Agilent 8453).

Inverse gas chromatography (IGC)

IGC of produced granules was carried out on Agilent Technologies 6890N chromatograph with flame ionization detector at 30°C.

Scanning electron microscopy (SEM)

Scanning electron microscope (Ultra Plus 4051, Carl Zeiss, Germany) was used for determination of particle morphology.

RESULTS AND DISCUSSION

The results showed that prolonged release of model drug could be achieved by the use of different binders with melt granulation technology (Fig 1).





The slowest dissolution was achieved with the use of SE with the lowest HLB value, while the fastest dissolution was observed with the use of glyceryl behenate. With increasing HLB value faster dissolution rate was expected, however tablets with sugar esters of different HLB values exhibit similar dissolution profiles. Only slightly faster dissolution rate was observed for samples with higher HLB value which can be attributed to an additional ability of sugar esters with higher HLB values to form gels in an aqueous environment and consequently prolong the drug release from tablets.

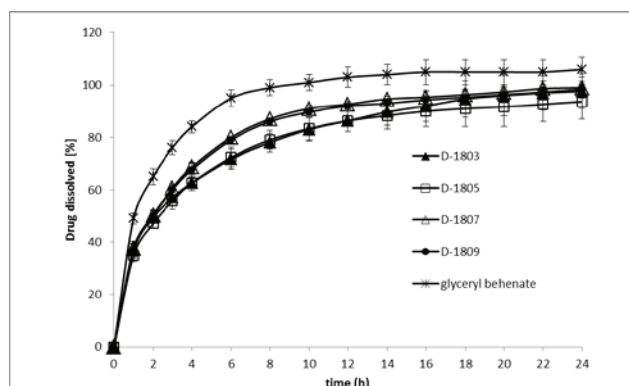


Fig. 1: Release profiles of a model drug from granules containing different binders.

IGC measurements of the dispersive component of the total surface free energy (γ_s^d) showed insignificant differences in the nonpolar parameters of the granules while glyceryl behenate shows different polar characteristic than the samples with SEs (Tab.1). Values for polar properties (K_a and K_d) for glyceryl behenate are higher indicating stronger interaction with water and thus faster release of the model drug.

Tab. 1: Surface energy parameters of granules containing different binders.

Sample	γ_s^d	K_a	K_d
Model drug	34,04	0,0258	0,3288
Glyceryl Behenate	37,27	0,1633	0,1523
D-1803	34,56	0,0380	0,2178
D-1805	31,11	0,0354	0,2060
D-1809	32,36	0,0371	0,1921

Scanning electron images (Fig.2) show smooth and even surfaces of granules produced with sugar ester, while granules with glyceryl behenate show porous and rough surfaces with higher specific surface which further explains differences in drug release.

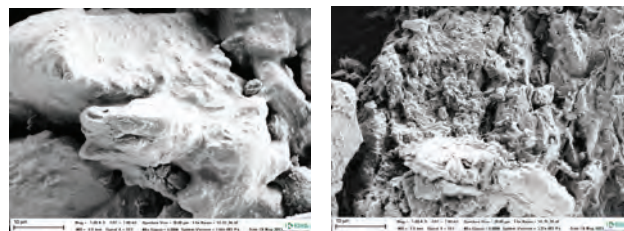


Fig. 2: Scanning electron images of granules containing sugar ester (left) and glyceryl behenate (right).

CONCLUSIONS

The results of this study show that thermoplastic agglomeration is an effective technology for achieving sustained release of a highly water soluble drug. All tested binders prolonged the drug release from the tablet. Slower dissolution rate was achieved when sugar esters were used as binders compared to glyceryl behenate.

ACKNOWLEDGEMENT

The authors would like to thank Harke Pharma GmbH for donation of samples of sugar esters and KRKA, d.d., Novo mesto for the support in performing the study.

REFERENCES

- Royce A, Suryawanshi J, Shah U, Vishnupad K. Alternative Granulation Technique: Melt Granulation. *Drug. Dev. Ind. Pharm.* 1996; 22(9&10): 917-924.
- Passerini N, Calogera G, Albertini B, Rodriguez L. Melt granulation of pharmaceutical powders: A comparison of high-shear mixer and fluidised bed processes. *Int. J. Pharm.* 2010; 391: 177-186.
- Szuts A, Szabó-Révész P. Sucrose esters as natural surfactants in drug delivery systems – A mini-review. *Int. J. Pharm.* 2012; 433: 1-9.



SPRAY-DRIED MELATONIN LOADED CHITOSAN/ POLOXAMER 407 MICROSPHERES: PHYSICO-CHEMICAL CHARACTERISATION AND ANTIMICROBIAL ACTIVITY (P24)

M. Duvnjak Romić¹, M. Šegvić-Klarić², J. Filipović-Grčić³, B. Cetina-Čižmek¹, A. Hafner³

¹ Pliva Croatia Ltd., Prilaz B. Filipovića 25, 10000 Zagreb, Croatia

² Department of Microbiology, Faculty of Pharmacy and Biochemistry, University of Zagreb, Schrottova 39, 10000 Zagreb, Croatia

³ Department of Pharmaceutics, Faculty of Pharmacy and Biochemistry, University of Zagreb, A. Kovačića 1, 10000 Zagreb, Croatia

INTRODUCTION

Melatonin, methoxyindole secreted by the pineal gland, has pleiotropic bioactivities as a neurotransmitter, hormone, cytokine and biological-response modifier. It has been reported that melatonin may have antibacterial effects (1). Naturally-occurring bioadhesive polysaccharide chitosan has been known for its antimicrobial and anti-biofilm properties (2). Due to its positive charge at pH below 6.5 chitosan interacts with anionic components of biofilm and bacterial surface. Spray-drying is recognised as a suitable method for the preparation of microspheres with desired properties (3). Chitosan microspheres allow controlled release and improved drug delivery across epithelial barriers (4). The aim of this study was to characterise spray-dried melatonin loaded chitosan/poloxamer 407 (P407) microspheres and to investigate their potential antibacterial and anti-biofilm properties.

MATERIALS AND METHODS

Low-viscosity chitosan (C) and melatonin (M) were purchased from Sigma-Aldrich and P407 from BASF. Microspheres were prepared by spray-drying (Buchi 190 mini spray dryer, Switzerland) of formulations prepared by mixing M/P407 ethanol solution with chitosan acetic acid solution (1 %, w/v). The influence of five factors (chitosan concentration, inlet temperature, M/C ratio, feed rate and C/P407 ratio) at two levels was studied with a 2⁵⁻¹ fractional factorial design. Based on production yield, particle size (Olympus BH-2 microscope), moisture content (TGA Q5000) and zeta-potential (Zetasizer 3000 HS) two samples have been selected for further study (MCP407 and MC; Table 1). Drying conditions were as follows: compressed air flow rate of 700 Nl h⁻¹, spray flow rate of 2.59 mL/min, inlet air temperature of 145°C. Selected dried products were further evaluated in terms of morphology, bulk and tap density, swelling properties and *in vitro* release.

Crystalline nature of the drug was examined by XRPD and DSC analysis.

The antimicrobial activity of MCP407 and MC microspheres was investigated with respect to M, C and P407 alone. Spray-dried microspheres, M and P407 suspensions were diluted with Mueller-Hinton broth-MHB with respect to concentration of melatonin. Antimicrobial activity of prepared samples was tested on *Staphylococcus aureus* (ATCC 29213) and five clinical isolates *S. aureus* MRSA strains (No. 101, 124, 164, 176, 177). Minimal inhibitory concentrations (MICs) were assessed by two-fold microdilution assay following NCCLS method (5). Inhibition of *S. aureus* biofilm formation and biofilm eradication were tested according to Walencka et al. (6) with some modifications. Viability of biofilm was assessed by MTT test (6).

RESULTS AND DISCUSSION

Study based on 2⁵⁻¹ fractional factorial design revealed optimal conditions for the preparation of melatonin loaded chitosan microspheres (MCP407 and MC; Table 1) resulting with high process yield (65-70%) and satisfactory powder flow and swelling characteristics.





Table 1. Melatonin loaded chitosan microspheres selected on the basis of 2^{5-1} fractional factorial design: microsphere composition and process parameters

Micro-sphere sample	CC (g/l)	T (°C)	M/C (w/w)	F(ml/min)	C/P407 (w/w)
MCP407	8	145	1:2	2,59	-
MC	8	145	1:2	2,59	5:1

Selected microspheres were characterised by high process yield (65-70%), satisfactory powder flow and swelling characteristics, positive surface charge (29-33 mV) and low moisture content (3.5-4%). Microspheres prepared were spherical in shape and of smooth surface (Figure 2).

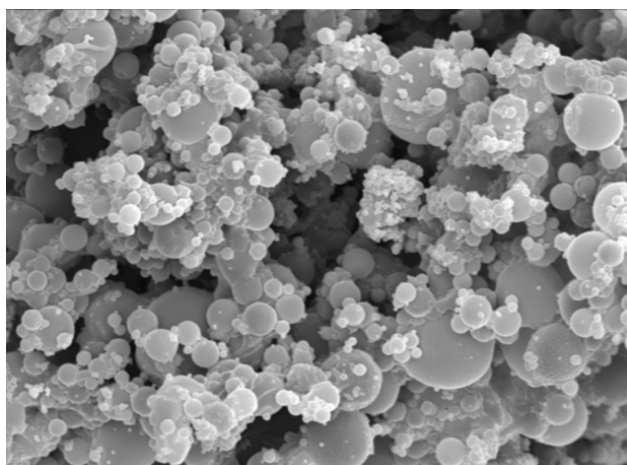


Fig. 2: SEM image of spray dried MCP407 microspheres.

MCP407 microspheres were characterised by faster melatonin *in vitro* release than MC microspheres. MCP407 showed the strongest antimicrobial activity (Table 2) against planktonic *S. aureus* ATCC 29213 (MIC=0.125 mg/mL). The MICs of MC microspheres and melatonin-free C and CP407 microspheres were twice as higher for *S. aureus* MRSA strains. M and P407 used alone did not exert antibacterial activity, but it seems that potentiated activity of MCP407. This formulation inhibited *S. aureus* ATCC 29213 biofilm formation at concentration 0.67 mg/mL, while BIC for *S. aureus* MRSA strains was twice as higher. As it was expected, nor M or P407 applied alone did not show any antibiofilm activity. The BIC value of MCP407 microspheres necessary for biofilm eradication was 2.7 mg/mL in all test-strains of *S. aureus*.

Table 2. Antibacterial activity of chitosan microsphere formulations against planktonic and biofilm *S. aureus*

Microsphere sample	MIC (mg/mL)		BIC (mg/mL)	
	ATCC	MRSA	ATCC	MRSA
MCP407	0.125	0.250	0.67	1.35
MC; CP407; C	0.250	0.250	1.35	1.35

MIC- minimal inhibitory concentration; BIC- biofilm inhibitory concentration

CONCLUSIONS

Spray-drying technique is suitable for the preparation of melatonin loaded chitosan/P407 microspheres with low moisture content and positive surface charge. Entrapment of melatonin in chitosan/P407 seemed to potentiate chitosan antimicrobial and anti-biofilm activity.

REFERENCES

1. Tekbas, O.F., et al., Melatonin as an antibiotic: new insights into the actions of this ubiquitous molecule. *Journal of Pineal Research*, 2008. 44(2): p. 222-226.
2. Carlson, R.P., et al., Anti-biofilm properties of chitosan-coated surfaces. *Journal of Biomaterials Science, Polymer Edition*, 2008. 19(8): p. 1035-1046.
3. Cal, K. and Sollohuv, K. Spray drying technique. I: Hardware and process parameters. *J Pharm Sci* 2009; 99: 575-586.
4. Martinac, A. et al. Spray-dried chitosan/ethylcellulose microspheres for nasal drug delivery: swelling study and evaluation of *in vitro* drug release properties. *J Microencapsul* 2005; 22: 549-561.
5. NCCLS. *Methods for dilution antimicrobial susceptibility tests for bacteria that grow aerobically: approved standard (5th edn)*. M7-A5. Wayne, PA: NCCLS, 2001.
6. Walencka, E., et al., Lysostaphin as a potential therapeutic agent for staphylococcal biofilm eradication. *Pol J Microbiol* 2005;54:191-200.



PREPARATION AND EVALUATION OF SIROLIMUS SOLID DISPERSION FOR PERORAL APPLICATION (P25)

M. Homar^{1,*}, P. Petelin¹, B. Petek¹, J. Kerč¹

¹ *Lek Pharmaceuticals, d.d., Sandoz Development Center Slovenia, Verovškova 57, 1526 Ljubljana, Slovenia*

INTRODUCTION

Sirolimus (also known as Rapamycin) is a macrolide antibiotic used for inhibiting rejection in transplantation in man. Poor water solubility (2.6 µg/ml) of sirolimus poses a challenge in formulating the drug into suitable dosage form. Currently, sirolimus is available in two dosage forms, namely tablet and oral solution. Sirolimus solubility issue has been solved by decreased particle size (between 400-600 nm) in the tablet preparation and inclusion of solubilizers in the solution formulation (1).

Many approaches can be used to improve the solubility and dissolution properties including salt formation, particle size reduction, formation of nanoparticles, pH adjustment, use of surfactants, inclusion complexes, lipid formulations, self-emulsifying drug delivery systems, and others.

Solid dispersion technique was used in this study to prepare stable oral formulation of sirolimus which exhibited higher or comparable dissolution rate to the marketed nanoparticles based product.

MATERIALS AND METHODS

Materials

Sirolimus was obtained from Biocon (India). Other excipients were hydroxypropyl cellulose (HPC) (Hercules, USA), low substituted hydroxypropyl cellulose (L-HPC) (JRS Pharma, Germany), polyvinylpyrrolidone (PVP) (BASF, Germany), pregelatinized starch (Colorcon, USA), sodium stearyl fumarate (Faci, Italy), magnesium stearate (Faci, Italy), stearic acid (Merck, Germany), glyceryl behenate (Gattefosse, France), silicified microcrystalline cellulose (SMCC) (JRS Pharma, Germany), Colloidal Silicon Dioxide (FMC, USA) and Ethanol 96% (Sasol, Germany).

All other chemicals used were of laboratory grade. Rapamune® 2 mg tablets produced by Pfizer (formerly by Wyeth) were used as the reference for stability and dissolution studies.

Methods

Solid dispersions were prepared in fluid bed apparatus (Glatt GPCG 3, Glatt, Germany). The apparatus was assembled in top spray setup with the 1.2 mm nozzle in the upper position. The drug and tested excipients were dissolved in ethanol and sprayed onto fluidized pregelatinized starch in the fluid bed apparatus. Tablets were compressed from the dried granulate.

Lubricants were tested either as powders in binary mixture with the drug or (in the case of glyceryl behenate) compressed into tablets with drug in solid dispersion.

Final dosage form was compressed from sirolimus solid dispersion mixed with selected lubricant and additional excipients on a rotary tablet press.

Stability of the powders and tablet was evaluated on different stability conditions (14 days at 60°C and 1 month at 40°C/75% RH). Pure crystalline drug and pure amorphous drug were also tested on these stability conditions. Dissolution rate of selected formulations was assessed in comparison to the reference formulation in USP apparatus 2 (paddle) in 0.2% sodium lauryl sulphate solution.

RESULTS AND DISCUSSION

Composition of tested solid dispersion tablets is given in Table 1. Tested lubricants and their ratios are given in Table 2.

Tab. 1: Composition of different solid dispersion tablets.

Sample	Drug substance and excipients in the tablets compressed directly from granulates (% w/w)
SD1	Sirolimus 1.3% PVP 3.9% Pregelatinized starch 94.8%
SD2	Sirolimus 1.3% HPC 3.9% Pregelatinized starch 94.8%
SD3	Sirolimus 1.3% L-HPC 6.5% Pregelatinized starch 92.2%





Tab. 2: Composition of samples for lubricant screening.

Sample	Drug substance and excipients in the powder samples used for lubricant screening (% w/w)
Lub1	Sirolimus 40% Sodium stearyl fumarate 60%
Lub2	Sirolimus 40% Magnesium stearate 60%
Lub3	Sirolimus 0.7% HPC 1.9% Pregelatinized starch 47.4% Glyceryl behenate 50%
Lub4	Sirolimus 25% Stearic acid 75%

Results from stability studies are shown in Figure 1. As expected, crystal drug exhibits greater stability than amorphous drug. A decrease in stability can also be observed when the drug particle size is reduced (comparison between crystalline drug and Rapamune®). Stability of amorphous drug in the solid dispersions (confirmed by XRPD) is increased and varies with the polymer used – PVP has less influence on improvement in sirolimus stability compared to HPC or L-HPC.

From previous compatibility studies (data not shown) of all tested excipients lubricants have had the strongest influence on stability. From the evaluated lubricants glyceryl behenate was chosen as the most suitable one. Data for stearic acid is not shown, since the sample was almost completely degraded.

Based on solid dispersion and lubricant stability screening the composition of the final dosage form (Test1) was selected as: sirolimus 1.2%, colloidal silicon dioxide 0.8%, HPC 5.5%, pregelatinized starch 77.0 %, glyceryl behenate 4.0%, SMCC 11.5% (all % w/w).

As evident from Figure 1 the stability of the final dosage form (Test1) was improved compared to the Rapamune®. Furthermore, the dissolution rate and solubility of the final dosage form was also improved compared to the marketed reference (Fig. 2).

Impurities increase on stability

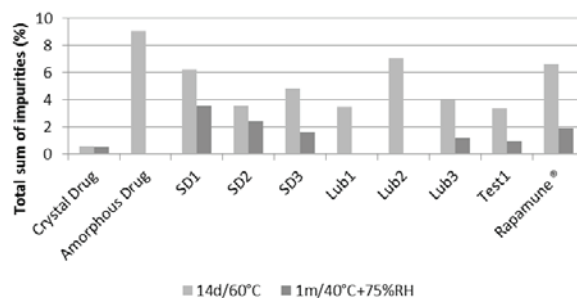


Fig. 1: Impurities increase on different stability conditions. Data for sample Lub4 is not shown, since almost complete degradation of sample occurred.

Apparatus 2, 100 rpm, 0.2% NaLS

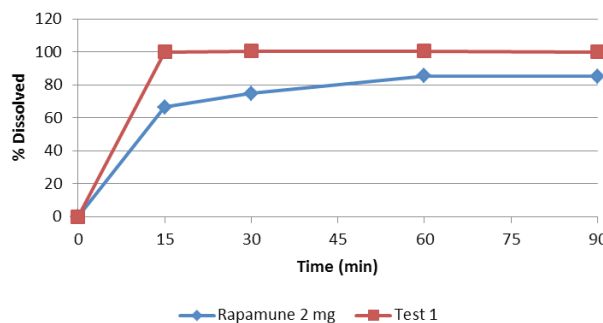


Fig. 2: Dissolution profiles for solid dispersion containing final dosage form (Test1) and marketed product.

CONCLUSIONS

A solid dosage form containing sirolimus in solid dispersion was developed which exhibited better stability and improved dissolution rate and solubility compared to the marketed product.

REFERENCES

- Nagi AS, Rapamycin formulations for oral administration, U.S. Patent 5989591, November 23, 1999.



DESIGN OF EXPERIMENTS: TOWARDS HARDNESS INSENSITIVE DISSOLUTION OF EXTENDED RELEASE FORMULATION WITH THREE RELEASE MODIFYING EXCIPIENTS (P26)

M. Ilič^{1*}, A. Lebar¹, U. Klančar¹, Z. Abramović¹

¹ Lek Pharmaceuticals d.d., Verovškova 57, 1000 Ljubljana, Slovenia
* Corresponding author: *E-mail: milos.ilic@sandoz.com

INTRODUCTION

The proposed drug product is a tablet containing combination of hydrophilic and enteric rate-controlling polymers in order to produce a similar performance (*in-vitro* and *in-vivo*) to the extended release reference tablets. We investigated the impact and interaction of composition parameters (content of HPMC, Eudragit, Glycerol Behenate and Ludipress) and compression force on tablet dissolution. Contents of other excipients were not varied. Design of experiments (DoE) approach was employed in planning the experiments (1). Multiple Linear Regression was employed for the analysis of experimental results.

MATERIALS AND METHODS

We determined tablet hardness and measured percent of API released from tablets in six time points (1h, 2h, 4h, 8h, 15h and 20h,) with a pH simulation dissolution method: (pH 1,2 (2 h) → pH 6,8; Apparatus 1, 100 rpm).

Two Multiple Linear Regression models fitting experimental data have been built using Modde 9.1 software package. In both models there were six responses, corresponding to percents of API dissolved in the six time-points. Both models had four parameters, three of them

being content of HPMC, content of Glycerol Behenate and tableting pressure. In first model (Model 1) the fourth parameter was content of Eudragit. In second model (Model 2) the fourth parameter was content of Ludipress. Interaction terms were added. The model was optimised by manual removing of parameters in order to minimize the overall number of parameters and maximize model R2 and Q2.

Both models give very similar conclusions with regard to common parameters.

RESULTS AND DISCUSSION

Dissolution prediction

4D sweet spot plot is shown on Figure 1 for Model 1 and on Figure 3 for Model 2. Different colours demonstrate design space for which predicted dissolution matches 80%-125% dissolution value of reference product. Predictions for different time points (1, 8 and 20h) are denoted with different color.

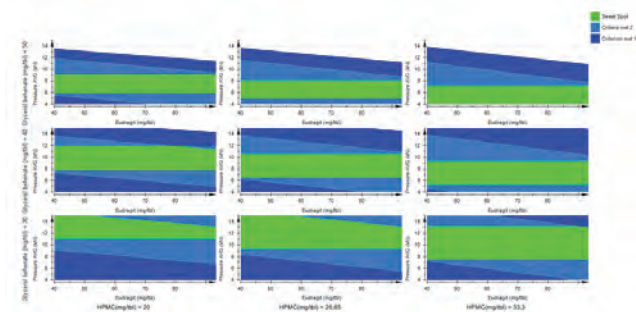


Fig. 1: 4D sweet spot plot for Model 1.

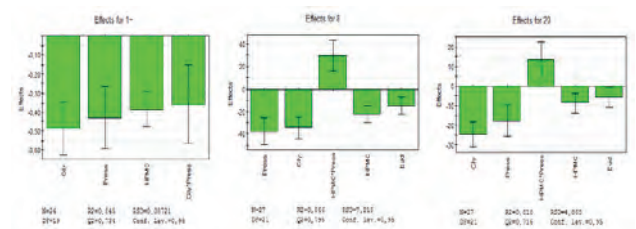


Fig. 2: Main effects plot for Model 1.



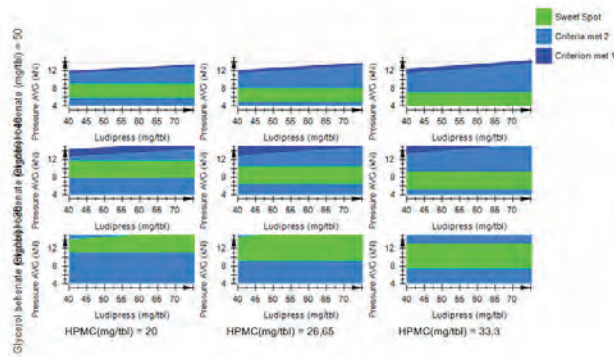


Fig. 3: 4D sweet spot plot for Model 2.

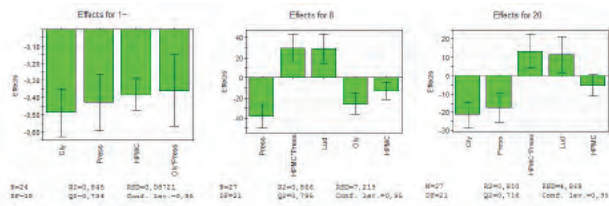


Fig. 4: Main effects plot for Model 2.

From the above diagrams it can be derived that:

- Compression pressure at which dissolution optimally matches that of reference product increases on decreasing polymer content.
- Dissolution comparable to reference in first timepoint (1h) is only met in restricted range of compression pressure which largely depends on content of Glycerol Behenate and HPMC in formulation and only slightly on content of Eudragit in formulation. Generally, with less Glycerol Behenate and more HPMC broader range of compression pressure gives comparable results to reference product.
- Dissolution comparable to reference in fourth and sixth timepoint (8h and 20h) is met for a much broader range of compression pressure. The dependence on Glycerol Behenate and HPMC content is similar as for timepoint 1.
- Higher content of polymers leads to slower dissolution. The effect of Eudragit content is inferior to the effects of Glycerol Behenate and HPMC content. The influence of Eudragit content is only present for dissolution times equal or larger than 4 hours.
- There is practically no interaction between contents of individual excipients. The only observed interactions are those between polymer content and tableting pressure.
- Formulations with less Glycerol Behenate and more

HPMC result in dissolution being less dependent on tableting pressure.

- Increased content of HPMC and/or Glycerol Behenate results in slower dissolution. Comparatively, variation of Glycerol Behenate results in slightly larger variation of dissolution than equal variation of HPMC.
- Tableting pressure and content of Glycerol Behenate have interaction effect on dissolution: increased tableting pressure and increased content of Glycerol Behenate result in slower dissolution.
- Tableting pressure and content of HPMC have opposite interaction effect on dissolution: increased tableting pressure and increased content of HPMC result in faster dissolution. To one extent this interaction may be regarded complementary to before mentioned interaction between tableting pressure and content of Glycerol Behenate, as more HPMC in formulation may automatically mean less Glycerol Behenate in formulation.

CONCLUSIONS

Dissolution comparable to that of reference product can be met in a reasonably broad range of investigated formulation and process parameters (8 h and 20 h). This range is narrowest for meeting comparable dissolution of first dissolution point (1h).

REFERENCES

1. Shivhare M, McCreath G, *Practical Considerations for DoE Implementation in Quality By Design*, 2010, Vol. 8, No. 6, 22–30



SUCROSE ESTERS-BASED NANOEMULSIONS FOR IMPROVED PENETRATION OF ACECLOFENAC: PORCINE EAR SKIN VS. HUMAN SKIN (P27)

T. Isailović^{1,*}, S. Đorđević¹, I. Pantelić¹, B. Marković¹, N. Cekić^{2,3}, R. Daniels⁴, S. Savić¹

¹ Department of Pharmaceutical Technology and Cosmetology, Faculty of Pharmacy, University of Belgrade, Belgrade 11221, Serbia

² Faculty of Technology, University of Niš, Leskovac, 16000, Serbia

³ DCP Hemigal, Leskovac, 16000, Serbia

⁴ Institut für Pharmazeutische Technologie, Eberhard-Karls Universität, Tübingen, Germany

INTRODUCTION

During the last decades, different strategies have been employed for increasing drug penetration through the skin – penetration enhancers, colloidal formulations, and physical enhancement methods (1).

Considering this, the aim of present study was to develop physically stable lecithin based nanoemulsions (NEs) with skin-friendly sucrose esters as co-emulsifiers and aceclofenac (ACF) as model drug by means of experimental design. ACF penetration profiles from optimal NEs and recently developed alkyl polyglucoside (APG)-stabilized semisolid emulsion system with/without isopropyl alcohol (IPA, as potential penetration enhancer) (2) through porcine ear skin and human skin were compared using tape stripping technique.

MATERIALS AND METHODS

Materials

For the preparation of investigated samples the following ingredients were used: ACF (Jinan Jiaquan Chemical Co. Ltd, China), medium chain triglycerides (MCT), castor oil, butylhydroxytoluene, cetostearyl alcohol, isopropyl alcohol (all Ph. Eur. quality), egg lecithin (Lipoid® E80, Lipoid

GmbH, Germany), sucrose stearate S-970 (SS), sucrose palmitate P-1670 (SP) (Ryoto Sugar Ester®, Mitsubishi-Kagaku Food Corporation, Japan), cetearyl glucoside and cetearyl alcohol (Sepineo SE® 68, Seppic, France), and ultrapure water.

Preparation and characterization

NEs were prepared by hot high pressure homogenization (EmulsiFlex-C3, Avestin, CA) at 50°C (20 cycles). Mean droplet size (Z-Ave), polydispersity index (PDI) and zeta potential (ZP) were determined with Zetasizer Nano ZS90 (Malvern, UK). To exclude presence of larger droplets, laser diffractometry was used (Malvern Mastersizer 2000).

Experimental design

D-optimal combined experimental design (Design-Expert, Stat-Ease, MN) was used to study the effects of three mixture components (lecithin, 1-2%; SS, 0-2%; SP, 0-2%) and two non-mixture variables (homogenization pressure, 500/800 bar; presence of ACF) on NE characteristics, called response variables (Z-Ave and PDI). By this methodology, it was possible to find emulsifier mixture composition and processing conditions leading to NEs with optimal properties.

Tape stripping method

Fresh porcine ears, immediately after slaughter, were washed carefully under cold running water, dried with soft tissue and stored at -20°C. After defrosting, ears were fixed on styrofoam plates and when transepidermal water loss (TEWL) reached 15 gm⁻²h⁻¹, investigated formulations (5 mg/cm²) were applied on assigned sites. After 2 h, tape stripping, according to previously described procedure (2), was started. The same protocol was repeated on human forearm skin (n≥4).

RESULTS AND DISCUSSION

Based on previously conducted solubility study, mixture of MCT and castor oil at the ratio 1:1 was chosen as oil phase. Concordant with applied combined design, a total of 23 NEs were prepared. Experimental design results showed that generated models for Z-Ave and PDI were significant, highlighting the importance of interactions between mixture and process variables to develop NEs with optimal properties (Fig. 1).



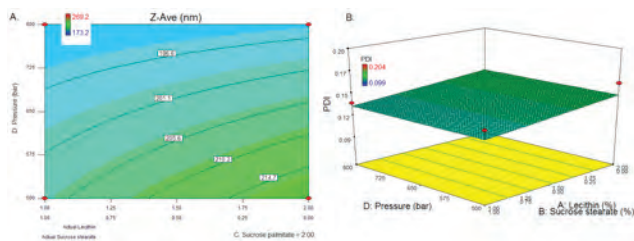


Fig. 1: Contour and 3D surface mix-process plots showing the effects of emulsifier mixture components and homogenization pressure on Z-Ave (A) and PDI (B) of NEs

The goal was Z-Ave in range 170–190 nm and PDI 0.09–0.13. Numerical optimization method showed many solutions; the most desirable NE formulations containing 1% of ACF (F1: 1.5% lecithin, 0.5% SS, and 2% SP; F2: 1% lecithin, 1% SS, and 2% SP) were obtained at 800 bar (Tab. 1).

Tab. 1: Characteristics of optimal NE formulations

	Z-ave (nm)±SD	PDI±SD	ZP (mV)±SD	d (0.9) (µm)
After preparation				
F1	186.1±2.9	0.10±0.01	-37.6±-2.9	0.283
F2	179.1±2.3	0.13±0.01	-35.4±0.9	0.273
After 6 month storage				
F1	177.2±3.8	0.11±0.02	-34.6±0.5	—*
F2	188.7±3.2	0.13±0.03	-39.9±1.3	—*

*not determined

Results of the *in vivo* tape stripping experiments (Fig. 2) showed that the amount of penetrated ACF from F1 NE was significantly higher than from F2 NE as well as from APG base without (S1) and with (S2) 10% IPA. Penetration depth was comparable for all investigated samples, irrespective of formulation type. Addition of IPA, as potential penetration enhancer, did not significantly affect the ACF penetration from S1.

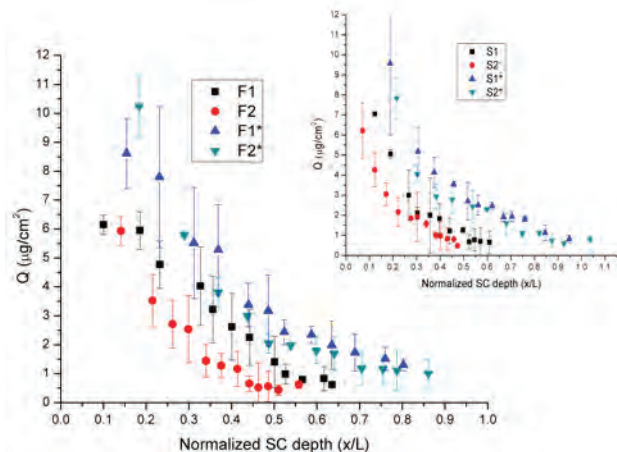


Fig. 2: Comparative ACF penetration profiles through porcine ear skin and human skin (labelled with *) from optimal nanoemulsions (F1, F2) and APG emulsion systems (S1, S2)

The extent of ACF delivery into porcine ear *stratum corneum* was significantly lower than into human skin. Despite this difference, comparable tendencies between *ex vivo* and *in vivo* penetration profiles for all tested formulations were observed (Fig. 2).

CONCLUSIONS

D-optimal combined design could be useful tool for development of physically stable NEs with improved skin penetration profile. Porcine ear skin may be useful model for selecting novel drug vehicles capable to provide satisfactory drug absorption through human skin.

ACKNOWLEDGEMENT

The authors are grateful to the Ministry of Education, Science and Technological Development, Republic of Serbia, for financial support within the project TR34031.

REFERENCES

1. Tuan-Mahmood T, McCrudden M et al. Microneedles for intradermal and transdermal drug delivery. *Eur. J. Pharm. Sci.* 2013; 50: 623-637.
2. Jaksic I, Lukic M et al. Compounding of a topical drug with prospective natural surfactant-stabilized pharmaceutical bases: Physicochemical and *in vitro/in vivo* characterization – A ketoprofen case study. *Eur. J. Pharm. Biopharm.* 2012; 80: 164-175.



ACECLOFENAC LOADED SUCROSE ESTERS-BASED MICROEMULSIONS: PHYSICO-CHEMICAL AND BIOPHARMACEUTICAL CHARACTERIZATION

(P28)

M. Todosijević¹, N. Cekić^{2,3}, M. Gašperlin⁴, T. Isailović^{1*}, S. Savić¹

¹ Department of Pharmaceutical Technology and Cosmetology, Faculty of Pharmacy, University of Belgrade, Belgrade 11221, Serbia

² Faculty of Technology, University of Niš, Leskovac 16000, Serbia

³ DCP Hemigal, Leskovac 16000, Serbia

⁴ Department of Pharmaceutical Technology, Faculty of Pharmacy, University of Ljubljana, Ljubljana 1000, Slovenia

INTRODUCTION

As thermodynamically stable, optically isotropic dispersions, microemulsions (MEs) have a combination of features that make them highly effective in (trans)dermal drug delivery, such are large surface area of the internal phase, improved drug solubility and long-term stability (1). In addition, the proposed low skin sensitization potential and established skin penetration enhancement have led to the increased research interest in the Sucrose Esters' (SEs) (trans)dermal application (2). Thus, in order to improve the transport of aceclofenac (AC) across the skin, SEs-based MEs may be taken into consideration. Prospective (trans)dermal delivery of AC loaded in MEs has several potential benefits such as improved drug solubility, increased patient compliance, as well as improvement of targeting in the therapy of osteoarthritis, rheumatic arthritis and ankylosing spondylitis (3).

MATERIALS AND METHODS

Materials

SEs (Sucrose Laurate (SL) D-1216 and Sucrose Myristate (SM) C-1416) and Isopropyl Alcohol (IPA) were used as surfactants and cosurfactant, respectively. Isopropyl My-

ristate (IPM) was used as an oil phase and ultrapure water as a water phase. Carbomer 934 and 980 were used as thickening agents.

Methods

The pH, electrical conductivity and rheological behavior of blank and AC-loaded MEs were evaluated using HI9321 pH meter (Hanna Instruments Inc., Michigan), CDM23 Conductivity Meter (Radiometer, Denmark) and DV-III ULTRA Programmable Rheometer & Rheocalc software v.4.3 (Brookfield Engineering Laboratories, Middleboro USA), respectively.

DSC thermograms (25 to -60°C, cooling rate of 10°C/min) of non-thickened and gel-like MEs were obtained using Mettler Toledo DSC 1, STARe System (Mettler Toledo GmbH Analytical, Germany).

In vitro release profiles of the non-thickened and gel-like MEs were obtained using a rotating paddle apparatus (Erweka DT70, Hausenstamm, Germany), modified by addition of enhancer cell (VanKel Industries Inc., Edison, USA) as well as using Franz diffusion cells and hydrophilic cellulose membrane. The acceptor medium was phosphate buffer pH 7.4.

RESULTS AND DISCUSSION

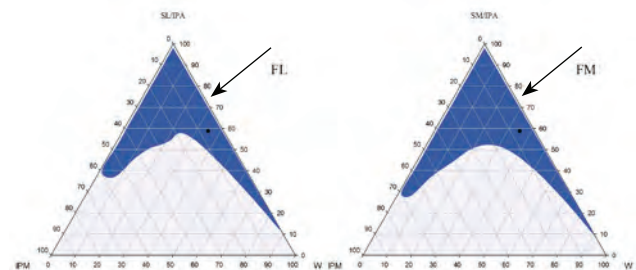


Fig. 1: Pseudo-ternary phase diagrams for the system Isopropyl Myristate/Surfactant-Isopropyl Alcohol/Ultrapur Water using as a surfactant: Sucrose Laurate and Sucrose Myristate, respectively.

The conductivity values (Table 1) suggested bicontinuous structure of selected MEs with 35% (w/w) of water (Fig. 1), which showed maximum solubilization capacity for AC.

Tab. 1: pH, conductivity and viscosity values of blank and AC-loaded MEs.

	FLPI	FL	FMPI	FM
pH	6.48 ± 0.01	3.38 ± 0.01	6.31 ± 0.01	3.22 ± 0.01
Conductivity [µS/cm]	58.13 ± 0.21	63.9 ± 0.10	50.5 ± 0.82	56.83 ± 0.21
Viscosity [mPa s]	16.87	18.31	19.88	19.62



MEs possess a very low viscosity (Table 1) and therefore their application may be restricted due to inconvenient use. Thus, several different thickening agents were used in order to modify rheological properties of MEs. Transparent viscous gels were obtained only when Carbomer 934 and Carbomer 980 (2.5% (w/w)) were used as thickeners.

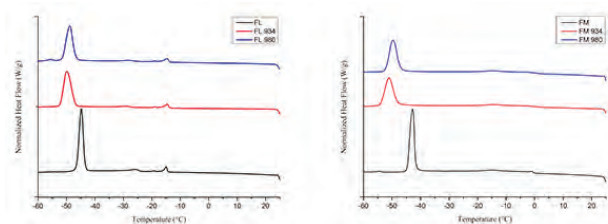


Fig. 2: DSC cooling curves of the non-thickened and gel-like AC loaded SL and SM-based MEs.

As expected, a shift of freezing point of water in gel-like MEs toward lower temperatures was observed, meaning that in these systems water was bound stronger than in non-thickened MEs (Fig. 2).

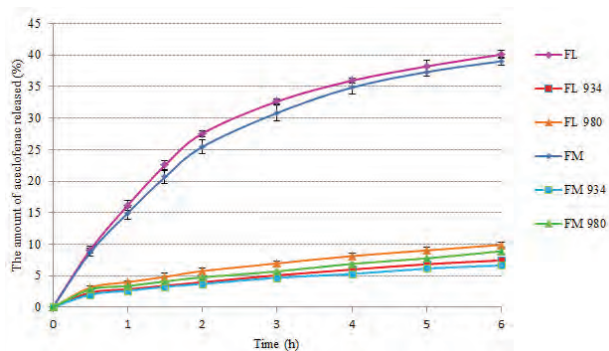


Fig. 3: Liberation profiles of AC from the investigated ME vehicles obtained using a rotating paddle apparatus modified by addition of enhancer cell.

AC released amounts from gel-like MEs were significantly lower than from corresponding MEs. SL-based ME showed higher quantity of AC released after 6h in comparison with SM-based ME. The same pattern was obtained in case of Carbomer 934 and Carbomer 980 thickened MEs (Figs. 3 and 4).

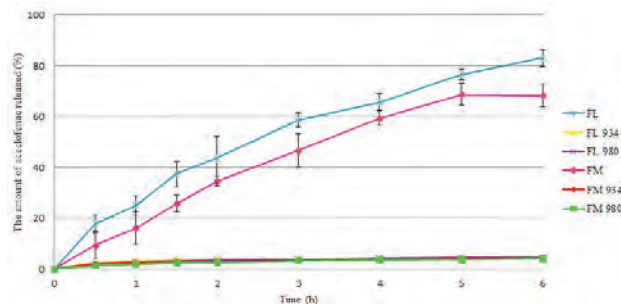


Fig. 4: Liberation profiles of AC from the investigated ME vehicles obtained using Franz diffusion cells.

AC release profiles were in accordance with the Higuchi model for all investigated systems, indicated carrier controlled release.

Interestingly, comparable *in vitro* release profiles were obtained using a rotating paddle apparatus modified by addition of enhancer cell as well as using Franz diffusion cells.

CONCLUSIONS

Due to the expected benefits of its bicontinuous structure after topical application, thickened and non-thickened AC-loaded MEs with SL and SM as surfactants should be further investigate *ex vivo* and *in vivo*.

ACKNOWLEDGMENTS

The authors would like to acknowledge the financial support from the Ministry of Education, Science and Technological Development, Republic of Serbia, through Project TR34031. The authors are grateful to Mitsubishi-Kagaku Foods Corporation for supplying Sucrose Esters.

REFERENCES

- Sahle FF, Metz H, Wohlrab J, Neubert RH. Lecithin-based microemulsions for targeted delivery of ceramide AP into the stratum corneum: formulation, characterizations, and *in vitro* release and penetration studies. *Pharm. Res.* 2013; 30: 538-551.
- Bolzinger-Thevenin MA, Grossiord JL, Poelman MC. Characterization of a Sucrose Ester Microemulsion by Freeze Fracture Electron Micrograph and Small Angle Neutron Scattering Experiments. *Langmuir* 1999; 15: 2307-2315.
- Gaur PK, Mishra S, Aeri V. Formulation and evaluation of Guggul lipid Nanovesicles for transdermal delivery of Aceclofenac. *Sci. World J.* 2014: 534210.



THE PREPARATION OF LYOPHILISED ORODISPERSIBLE TABLETS USING FENUGREEK SEED MUCILAGE AS MATRIX FORMER AGENT (P29)

S.Iurian^{1*}, R.Păltinean², E.Dinte¹, C.Bogdan³, I.Tomuța¹, M.Moldovan³, S.E.Leucuța¹

¹ Department of Pharmaceutical Technology and Biopharmacy, University of Medicine and Pharmacy "Iuliu Hatieganu", V.Babes 41, 400012, Cluj-Napoca, Romania;

² Department of Pharmaceutical Botany, University of Medicine and Pharmacy "Iuliu Hatieganu", Ion Creangă 12/3, 400010, Cluj-Napoca, Romania;

³ Department of Dermopharmacy and Cosmetics, University of Medicine and Pharmacy "Iuliu Hatieganu", V.Babes 41 400012, Cluj-Napoca, Romania.

INTRODUCTION

Natural materials are valuable resources, being cost effective, easily available and non toxic. This study aimed the formulation and *in vitro* characterisation of lyophilised orodispersible tablets, based on colloidal dispersions of *Trigonella foenum graecum* seed mucilage (FSM).

MATERIALS AND METHODS

Materials

The materials used were *Trigonella foenum graecum* (fenugreek) seeds, Meloxicam (Uquifa, Spain) and mannitol (Parateck M200, MERCK).

Methods

1. FSM isolation. FSM was obtained by a previously reported method. Briefly, the seeds were soaked in distilled water and boiled until the formation of slurry. The upper clear solution was decanted, concentrated and poured into acetone. The precipitate was dried and kept in desiccators (1).

2. Preparation of colloidal dispersions. Seven dispersions with concentrations ranging from 0.25% to 2% FSM were obtained by hydrating the dry product with distilled water for 30 min, at room temperature, maintaining in water bath at 50°C, for 2h, and then keeping under stirring at 1000 rpm, for 30 min.

3.Evaluation of rheological characteristics. The viscosity of each mucilage sample was determined with a Brookfield DV III Ultra viscometer, by gradually increasing and then decreasing the spindle's rotation speed, from 0.2 to 100 rpm and backwards.

4. Preparation and freeze drying of the meloxicam suspensions. 1.5% (w/v) meloxicam was added to the 5 chosen dispersions containing 0.5%, 0.75% 1%, 1.25% and 1.5% (w/v) FSM and 5%(w/v) dissolved mannitol. 0.5ml suspension were poured in blister sockets and progressively cooled to -55°C, for 2h, annealed at -8°C for 3h, dried at -20°C for 20h and at 5°C, for another 10h.

5. Physical characterization of tablets. Disintegration tests were performed according to the European Pharmacopoeia method (2). Wetting time and water absorption ratio were evaluated according to literature reported techniques (3). The tablet's hardness was evaluated using TexturePro CTV1.5 texture analyzer (Brookfield Engineering Laboratories, USA). Compression test was applied, using an acrylic cylindrical probe, with a trigger load of 10g and a test speed of 0.1mm/s. The pore sizes were evaluated using Motic Microscop K-500L, equipped with MoticamPro 205A camera. The analyzed images were magnified 300x.

RESULTS AND DISCUSSION

The rheological data showed good fitting to the Hershel-Burkley model. Based on viscosity data and literature reported behaviour of FSM as suspending agent (4), 5 dispersions were chosen for further studies. They had to be fluid enough to be poured into blister sockets and viscous enough to prevent meloxicam sedimentation. The lyophilisation process produced light orodispersible tablets with characteristics as listed in Table 1.





Tab. 1: Disintegration and water absorption properties for FSM containing orodispersible tablets

FSM content (%)	Disintegration time (s)	Wetting time (s)	Water absorption ratio (%)
0.5	4.00	1.00	158.32
0.75	5.33	1.00	249.59
1	10.67	89.33	326.46
1.25	14.67	151.00	341.47
1.5	46.50	201.67	369.78

The tablets had fast disintegration times, much lower than the limit imposed by Eur.Ph.8.0 - 180 s. The disintegration process was slowed down by the increase in FSM content, because of the high viscosity it creates in the dispersion media.

The tablet's texture was highly correlated with the percentage of FSM (Figure 1).

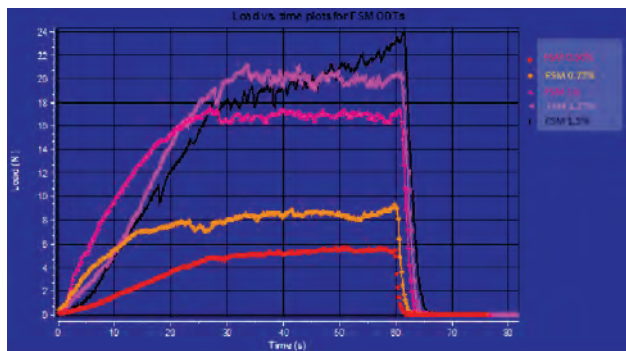


Fig. 1: Load-time curves of anhydrous orodispersible tablets containing increasing FSM percentages

The hardness values were calculated using TexturePro software, as the maximum load value of the compression cycle. They ranged between 5.9N for 0.5% FSM tablets and 24.13N for 1.5% FSM tablets. The porous structures of tablets are highlighted by the fracture results, which mathematically represent sharp drops in load. The number of fractures increases from 16, for tablets containing 0.5% FSM to 19, for those with 1.25% FSM, pointing to an enhancement in number of pores. Fracturability values indicate the brittleness of the products and are calculated as the load values at the first fracture. The results showed that the lowest fracturability was met by tablets with 1% FSM. A low FSM concentration in tablets yielded a small number of pores, with high surfaces, determining a quick hydration and further disintegration (Figure 2).

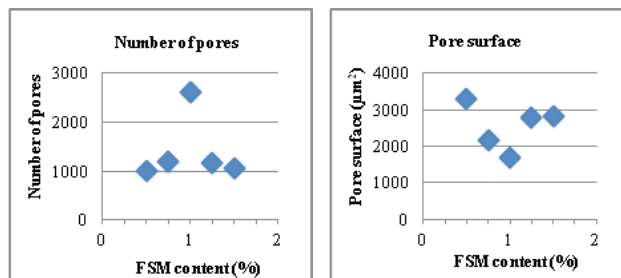


Fig. 2: a. Number of pores vs. content of FSM in tablets; b. Pore surface vs. content of FSM in tablets

Tablets containing 1% FSM had the most and the smallest pores, while increasing the FSM percentage led to less pores, with higher diameters, but with lower hydration capacity, due to the larger polymer concentration.

CONCLUSIONS

The fenugreek seed mucilage is a suitable polymer for the preparation of porous lyophilized matrices with quick disintegration times. Further research will concentrate on improving tablets' hardness.

REFERENCES

1. Nayak A.K., Pal D., Pradhan J., Hasnain M.S. Fenugreek seed mucilage-alginate mucoadhesive beads of metformin HCl: design, optimization and evaluation. *Int. J. Biol. Macromol.* 2013; 54: 144-154.
2. European Pharmacopoeia 8.0. consulted at <http://online6.edqm.eu/ep802/>.
3. Chandrasekhar R., Hassan Z., AlHusban F., Smith A.A.M., Mohammed A.R., *Eur.J.Pharm.Biopharm.* 2009;72: 119-129.
4. Nayak A.K., Pal D., Pradhan J., Ghorai T. The potential of *Trigonella foenum-graecum* L seed mucilage as suspending agent. *Ind J Pharm Edu Res.* 2012: 46:312-317.



EUDRAGIT S100 MICROSPHERES AS A NOVEL CHRONOPHARMACEUTICAL FOR ZALEPLON DELIVERY (P30)

J. Jablan^{1,*}, N. Kujundžić¹, M. Jug¹

¹ Faculty of Pharmacy and Biochemistry, University of Zagreb, A. Kovačića 1, 10 000 Zagreb, Croatia

INTRODUCTION

Insomnia is one of most common sleep disorders affecting about 30% of adult population, while its prevalence is even higher among elderly and psychiatric patients. Therefore, the aim of this work was to develop pH-responsive microspheres of zaleplon (ZAL) with delayed drug release, as a novel chronopharmaceutical drug delivery system, suitable for treatment of a specific type of insomnia characterised by premature awaking and inability to fall asleep again (1). ZAL is rapidly cleared from the body ($t_{1/2} = 1\text{h}$), therefore it would be suitable for development of such formulation (2). Eudragit® S100 (ES₁₀₀), a 1:2 methacrylic acid and methylmethacrylate copolymer, with pH dependent solubility (pH>7) was used as the base of this formulation (3).

MATERIALS AND METHODS

Materials

Zaleplon (ZAL) was donated by Belupo (Croatia), Eudragit® L100 (ES100) was obtained by Evonik Industries (Germany), glycerol monostearate (GMS) and NH₄HCO₃ were obtained by Sigma (Germany), while randomly methylated β-cyclodextrin was obtained from Wacher Chemie GmbH (Germany). All other chemicals used were of reagent grade.

Preparation of the microspheres

Different microspheres were prepared by spray-drying the feed solution prepared in 0.96% aqueous NH₄HCO₃ medium as shown in Table 1., using Buchi mini spray drier at air flow of 400 NL/h, feed flow of 5 mL/min, inlet and outlet air temperature of 100 and 60°C, respectively.

Prepared microspheres were further thermally treated at 85°C for 3.5 h to regenerate the ES₁₀₀ insoluble form.

Table 1: Composition of the spray-drying feed.

Sample	ZAL (g)	ES ₁₀₀ (g)	GMS (g)	RAMEB (g)
MS ₁	0,2	2	-	-
MS ₂			-	-
MS ₃			0,2	0,21
MS ₄			0,42	
MS ₅			0,84	

Characterization of the microspheres

Drug loading was assessed after extraction of ZAL with hydro-methanolic medium followed by spectrophotometrically drug determination at 335 nm. SEM micrographs were obtained by sputtering the samples with a thin layer of gold/palladium. FTIR spectra were obtained by the KBr method, while XRPD spectra were recorded using CuKα radiation and a graphite monochromator in the 5-40 2θ°. The *in vitro* dissolution studies were performed by introducing the sample containing 10 mg of ZAL in 250 mL of simulated gastric (pH 1.2) or intestinal (pH 6.8) medium thermostated at 37°C and stirred at 50 rpm. The withdrawn aliquots at predetermined time intervals were analyzed spectrophotometrically at 335 nm for the drug content.

RESULTS AND DISCUSSION

Microparticles were prepared by spray-drying of ZAL/ES₁₀₀ dispersion from aqueous NH₄HCO₃ solution (MS₁), transforming ES₁₀₀ into soluble, thermolabile ammonium salt. After spray-drying procedure, ES₁₀₀ was regenerated by thermal treatment at 85° for 3.5h, eliminating completely soluble ammonium salt from the microparticles, as confirmed by FTIR analysis (data not shown). In all preparations, high ZAL encapsulation efficiency (95.5-99.6%) into microspheres with mean particle diameter of 1.62-1.76 μm was achieved (Fig. 1).



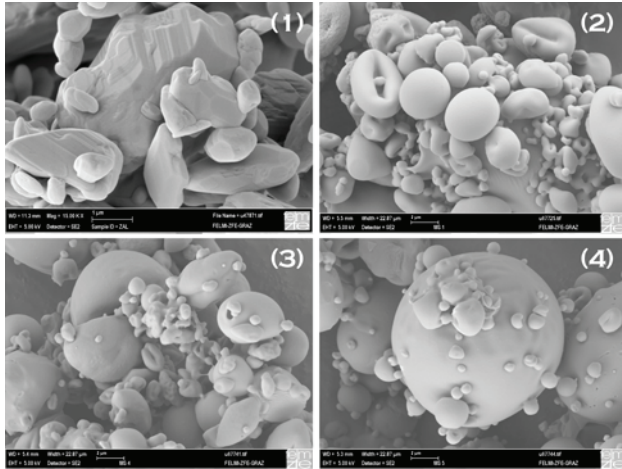


Fig. 1: SEM micrographs of ZAL (1) and some selected microspheres prepared (MS₁ (2), MS₂ (3) and MS₄ (4)).

However, *in vitro* dissolution profile of MS₁ showed rather high drug leaking in the simulated gastric medium 24.7±0.5% of ZAL in 2h (Fig. 2). XRPD analysis showed that this behaviour could be attributed to a thermally induced amorphization of ZAL into ES100 matrix (Fig. 3).

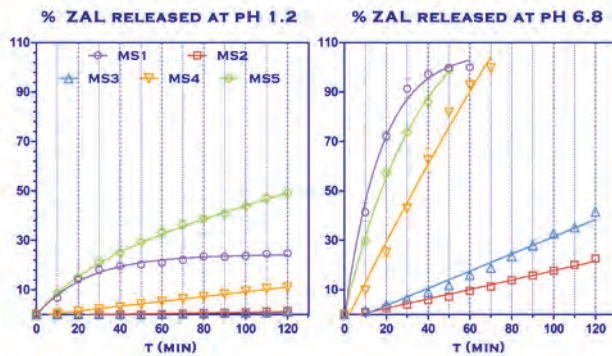


Fig. 2: *In vitro* ZAL release from microspheres prepared in simulated gastric (pH 1.2) and intestinal medium (pH 6.8).

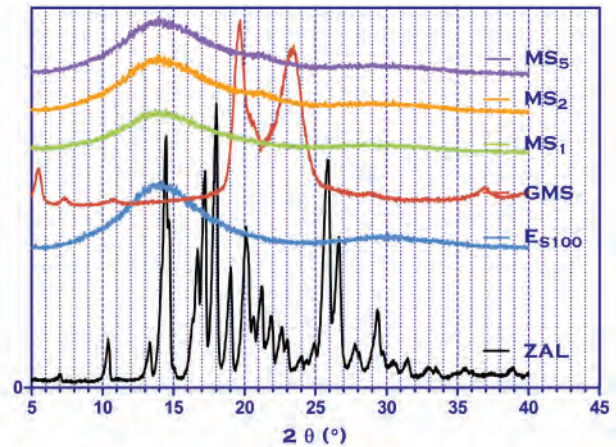


Fig. 3: XRPD diffractograms of pure components (ZAL, ES100 and GMS) and some selected microspheres prepared (MS₁, MS₂ and MS₄).

Therefore MS₁ formulation was further optimised through addition of 10% of GMS (MS₂), which sufficiently reduced unwanted drug release in simulated gastric medium to only 1.1±0.3% of encapsulated drug dose, but in the same time, reduced significantly the drug release rate in simulated intestinal medium (pH 6.8) to only 19.1 µg/min (Fig. 1). To overcome this obstacle, randomly methylated β-cyclodextrin (RAMEB) was added to the feed solution in quantities which would result in complexation of 25, 50 and 100% of the drug dose (MS₃, MS₄ and MS₅, respectively).

CONCLUSIONS

The optimal MS formulation contained 50% of the drug dose in form of an inclusion complex with RAMEB, resulting in an acceptable drug release level in the simulated gastric medium (pH 1.2) of about 10% of the ZAL doze after 2h and a zero-order release ($r^2 > 0.98$, $k = 155.0$ µg/min) in simulated intestinal medium (pH 6.8).

REFERENCES

- Minkel J, Krystal AD, Optimizing the Pharmacologic Treatment of Insomnia: Current Status and Future Horizons. *Sleep Med. Rev.* 2013; 8: 333-350.
- Heydorn WE, Zaleplon-a review of a novel sedative hypnotic used in the treatment of insomnia. *Expt. Opin. Invest. Drugs* 2000, 4: 841-858.
- Alhnan AA, Kidia E, Basit AW, Spray-drying enteric polymers from aqueous solutions: a novel, economic, and environmentally friendly approach to produce pH-responsive microparticles *Eur. J. Pharm. Biopharm.* 2011; 79: 432-439.



SEGREGATION IN VERTICAL CHUTE WITH CLOSED OUTLET: EVALUATION OF SEGREGATION ON MODEL POWDER MIXTURE (P31)

M. Jaklič^{1,*}, U. Krajnc¹

¹ Lek Pharmaceuticals, Verovškova 57, SI-1526 Ljubljana, Slovenia

INTRODUCTION

Gravitational transport of granular material through vertical pipes (chutes) is commonly employed in pharmaceutical industry (1). Granular material discharge and flow into vertical chute is a short, but very intensive process, where powders are readily fluidized and segregated by escaping air. Segregation is based on powder's particle size, density and shape: this phenomenon is also known as elutriation process.

Powder mixtures are prone to such segregation process, since properties of each individual component are rarely matched. In cases where vertical chutes are used for delivery of powder mixtures to machines for formation of final dosage forms (tableting, capsule filling, sachet filling) such segregation is especially troublesome, since it may lead to content uniformity variations beyond the acceptable limits as set by Pharmacopoeias (2).

Vertical chute segregation of simple powder mixture was studied on laboratory scale model of vertical chute: testing apparatus was constructed from glass with dimensions set in accordance with previously published research (3).

MATERIALS AND METHODS

Materials

Low molecular weight, well crystallized substance was used as model API. Two types of cellulose base fillers with different particle size distribution were used (labelled B and C). Mineral oil was used as liquid binder. Particle size distribution comparison of API and the fillers is presented in Tab.1.

Tab. 1: Comparison of API, B and C particle size distribution as determined by sieve analysis.

	API	B	C
Mesh size (mm)	Retained (%)	Retained (%)	Retained (%)
Bottom	0.20	0.70	0
0.045	20.30	1.94	0.1
0.100	45.06	9.58	0.4
0.200	29.42	22.52	34.2
0.315	4.58	20.36	65.4
0.400	0.38	21.38	/
0.500	0.06	17.64	0.2
0.630	/	6.32	0.1

Methods

Powder mixtures were prepared in planetary mixer as follows: to one half of the filler mineral oil was added while mixing, which was followed by slow addition of API and finally the rest of the filler. Samples contain either 2 or 10% of API, Type B or C filler and 3, 6 or 10% of mineral oil as binding liquid (samples were labelled accordingly: e.g. 2/C/6).

Vertical chute model consists of two glass tubes with inner diameter of 70 mm aligned in vertical position one above the other with knife valve separating the both. The upper glass tube is the powder container, whereas the bottom tube represents the vertical chute with 1200 mm fall. Bottom of the chute is closed with "sampling valve" which enables equivolumetric, vertically stratified sampling of powders from chute during sampling phase. Both valves are air-tight.

Segregation test was performed by placing the test material into the powder container (height approx. 20 cm). Material was discharged from the powder container by opening the knife valve. Powder samples were collected with sampling valve: from each experiment 5 samples equally distributed throughout the whole powder bed height were collected. Each segregation experiment was done in triplicate. API content was determined by qualified HPLC method.

RESULTS AND DISCUSSION

Results on API content are presented on Fig.1 and 2 in form of 5 consecutive bars corresponding to average API content in layers (bottom to top) with respective standard deviation (SD) values for each layer. Fig. 1 shows API content variation on 2% API formulations: in general API concentration variation is high. No specific trend of API content increase or decrease was detected, however





results show that mixture has high tendency for segregation. It was, however, observed that batches with higher amount of mineral oil (6%) have lower API content variation. Type of filler does not seem to influence segregation amount, however B type of filler seems to be more appropriate. 2/B/6 experiment shows lowest variation between and within locations, slight segregation trend with increasing API content is indicated.

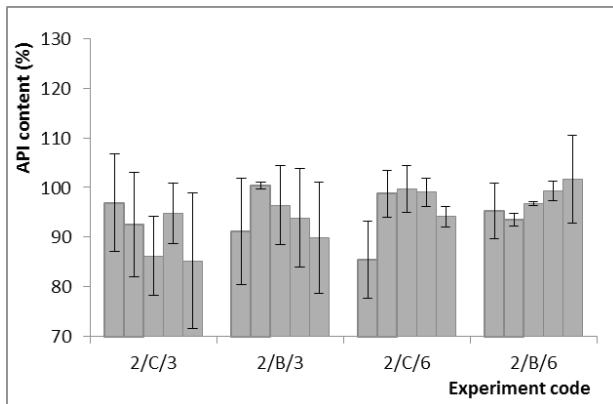


Fig. 1: API content variation on formulations containing 2% API.

Formulations with 10% API containing 3% and 6% mineral oil shows API content variations comparable to those observed in 2% API formulations with high variations between locations indicating erratically occurring segregation. Again, a trend of decreasing content variation between experiments with increasing amount of mineral oil present in formulation is observed. Lowest segregation is observed on experiments with 10% mineral oil showing lowest content variation regardless of filler type.

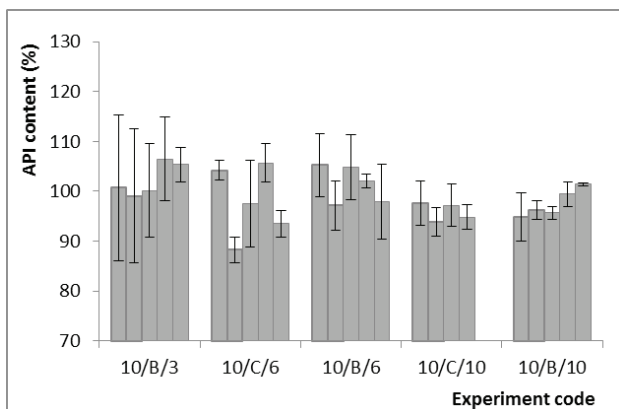


Fig. 2: API content variation on formulations containing 10% API.

High tendency for mixture segregation could be anticipated from PSD of components: all components have large non-cohesive particles, which are different in size. Addition of liquid binder increases binding of API to filler particles which is observed as reduction of API content variation within and between locations.

CONCLUSIONS

Segregation testing in vertical chute shows high tendency for segregation of model mixture. It was shown that immobilization of the API onto filler particles by addition of liquid binder is an effective approach for reduction of segregation.

REFERENCES

1. Peck GE, Anderson NR, Banker GS. Principles of Improved Tablet Production System Design. In: *Pharmaceutical dosage forms Volume 3*. New York, Basel: Marcel Dekker Inc. 1990: 6-16.
2. Prescott JK, Barnum RA. On Powder flowability. *Pharmaceutical Technology*. October 2000: 60-84.
3. Liss ED, Conway SL, Zega JA, Glasser BJ. Segregation of powders during gravity flow through vertical pipes. *Pharmaceutical Technology*. 2004; 28(2): 78-97.



INORGANIC MODIFICATION OF DIATOMITE AS AN APPROACH FOR FUNCTIONALITY IMPROVEMENT OF A POTENTIAL PHARMACEUTICAL EXCIPIENT (P32)

J. Janičijević^{1*}, D. Krajišnik¹, B. Čalija¹, V. Dobričić², J. Milić¹

¹ Department of Pharmaceutical Technology and Cosmetology, Faculty of Pharmacy University of Belgrade, V. Stepe 450, 11221 Belgrade, Serbia

² Department of Pharmaceutical Chemistry, Faculty of Pharmacy University of Belgrade, V. Stepe 450, 11221 Belgrade, Serbia

INTRODUCTION

Diatomite, a siliceous sedimentary rock usually used as filter aid for pharmaceutical purposes, is being investigated from recently as a potential drug carrier (1, 2). Promising results for untreated diatomite were obtained, but drug loading and release characteristics of drug loaded diatomite can be further tailored by surface modification method (3, 4). In this study pharmaceutical technological characteristics, adsorption of model drug - diclofenac sodium and the release of the drug adsorbed were investigated for an inorganically modified diatomite - a potential pharmaceutical excipient.

MATERIALS AND METHODS

Materials

Diatomite (D) from Serbian mine "Kolubara" was used after refinement by thermal treatment (550 °C) and sieving (125 µm). Diclofenac sodium (DS) was donated from pharmaceutical industry (Galenika a.d., Serbia). All other chemicals and reagents used were of analytical grade.

Diatomite modification

Specified amount of diatomite (500 mg) was homogeneously suspended in aqueous aluminum sulfate solution (50 ml 0.02 g/ml $Al_2(SO_4)_3 \cdot 16H_2O$) under magnetic stirring and to the obtained stirred dispersion a base (60 ml 0.1 M NaOH) was added in a thin jet from a rotating reservoir. Precipitate formed (inorganically modified diatomite - MD) was separated by filtration, dried and pulverized before further investigations.

Pharmaceutical technological characterization

Measurement of bulk density, tapped density and flowability for starting (D) and modified (MD) diatomite was performed using apparatus and methods which meet the requirements of the pharmacopoeial tests for apparent volume and flowability.

Zeta potential measurements

The zeta potential of D and MD samples was measured using a Zetasizer NanoZS90 instrument (Malvern Instruments, UK) in aqueous suspensions (0.1 mg/ml).

Drug adsorption and isotherm study

Accurately weighted samples of D or MD (0.6 g) were transferred into flasks containing 80 ml of appropriate DS solutions (1 - 4 mg/ml) and shaken on a laboratory shaker for 2 or 6 h respectively. After equilibrium DS concentration in aqueous phase was assayed spectrophotometrically for the drug uptake calculation. Samples with the highest drug loading were filtered, dried, compressed and used for *in vitro* drug release studies.

In vitro drug release studies

Drug release from comprimates containing DS adsorbed onto D (DD) or MD (DMD) was studied using a flow-through cell dissolution tester DFZ 60 (Erweka GmbH, Germany) in 900 ml of phosphate buffer pH 7.5 under a constant medium flow rate of 8 ml/min at 37 °C. Drug loadings in the tested comprimates were determined by HPLC analysis prior the experiments. The amount of DS released was assayed spectrophotometrically. All experiments were done in triplicate.

RESULTS AND DISCUSSION

The modification of diatomite resulted in increase of bulk and tapped density for 73% and 46% respectively and improvement of flowability for 45% (Tab. 1). Change in zeta potential of diatomite (-29 mV) after modification (+8.5 mV) implied alteration in surface characteristics. Adsorbent loading of diatomite for DS (~73 mg/g) was





significantly improved after modification (~368 mg/g) (Fig. 1). Adsorption isotherm of DS onto MD fitted well to Langmuir model indicating monolayer coverage of DS over homogenous surface of MD.

Tab. 1: Values of bulk, tapped density and flowability for D and MD samples

Sample	Bulk density (g/ml)	Tapped density (g/ml)	Flowability (g/s)
D	0.15	0.25	0.67
MD	0.26	0.36	0.97

High adsorbent loading of MD enabled the preparation of DMD comprimates containing therapeutic daily dose of DS (approximately ~80 mg per comprimete), which is very important feature for potential application of this drug carrier in various pharmaceutical dosage forms. DD comprimates released 82% of DS in 60 min indicating weak interaction between DS and diatomite. Conversely, DMD comprimates released 37% of DS in 8 h (Fig. 2). Permanent drug release in a sustained manner over the entire testing period from DMD comprimates is indicative of strong interactions between DS and modified diatomite.

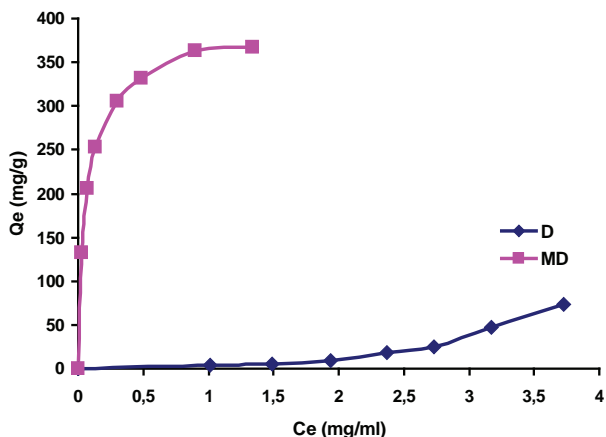


Fig. 1: Adsorption isotherms of DS onto D and MD samples

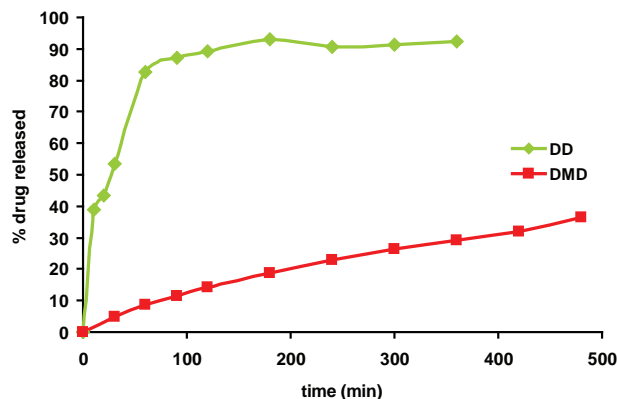


Fig. 2: DS release from DD and DMD comprimates

CONCLUSIONS

In this study diatomite, low-cost, biocompatible and non-toxic material was successfully modified with partially neutralized aluminum sulfate. The obtained results regarding improved functional characteristics of modified diatomite, significant adsorption of drug molecules followed by modified drug release encourage further investigations of this material as a potential pharmaceutical excipient.

REFERENCES

1. Aw MS, Simovic S, Yu Y, Addai-Mensah J, Losic D. Porous silica microshells from diatoms as biocarrier for drug delivery applications. *Powder Technol.* 223 (2012) 52-58.
2. Aw MS, Simovic S, Addai-Mensah J, Losic D. Silica microcapsules from diatoms as new carrier for delivery of therapeutics. *Nanomedicine* 6 (2011) 1159-1173.
3. Aw MS, Bariana M, Yu Y, Addai-Mensah J, Losic D. Surface-functionalized diatom microcapsules for drug delivery of water-insoluble drugs. *J. Biomater. Appl.* 28 (2013) 163-174.
4. Bariana M, Aw MS, Kurkuri M, Losic D. Tuning drug loading and release properties of diatom silica microparticles by surface modifications. *Int. J. Pharm.* 443 (2013) 230-241.



pH-SENSITIVE CHITOSAN-EUDRAGIT® L100-55 SUBMICRON POLYELECTROLYTE COMPLEXES – PREPARATION AND PHYSICO-CHEMICAL CHARACTERIZATION

(P33)

B. Čalija¹, I. Denčić¹, N. Stanković¹, J. Janičijević^{1*}, B. Marković², J. Milić¹

¹ Department of Pharmaceutical Technology and Cosmetology, Faculty of Pharmacy University of Belgrade, V. Stepe 450, 11221 Belgrade, Serbia

² Department of Pharmaceutical Chemistry, Faculty of Pharmacy University of Belgrade, V. Stepe 450, 11221 Belgrade, Serbia

INTRODUCTION

Mixing of oppositely charged polymers solutions leads to the spontaneous formation of polyelectrolyte complexes (PECs) (1). The reversible nature of interaction between comprising polymers and stimuli-responsive nature, particularly the pH-sensitivity, make PECs suitable for drug delivery applications (2).

The aim of presented study was to investigate pH-sensitivity and short-term stability of chitosan/Eudragit®L100-55 (CH/EL) submicron PECs prepared from CHs of different molecular weight.

MATERIALS AND METHODS

Materials

Oligochitosan (OCH) with a deacetylation degree (DD) >85% and a MW around 3 kDa was procured from the Fu Zhou Corona Science (China). Low (LCH; 50–190 kDa, DD 75%–85%) and medium (MCH; 190–300 kDa, DD 75%–85%) MW CHs were purchased from Sigma-Aldrich (USA). EL was generously donated by Evonik Industries AG (Germany). All other chemicals and reagents were of the highest grade and commercially available.

Preparation of submicron CH/EL PEC dispersions

PEC dispersions were prepared by dripping 0.1 % (m/m) EL solution (pH 5.6) in the 0.1 % (m/m) CS solution (pH 5.6) under vigorous stirring. The volume ratio of these stock solutions was varied from 9:1 to 1:1 (CH/EL), while the volume of resulting PEC dispersion was kept constant at 100 ml. To investigate the structure of PECs, dispersions were ultracentrifuged at 15000 rpm for 30 min, resulting precipitate was washed with deionized water, dried at 50 °C and subjected to the thermal and FT-IR analysis as described below.

Particle size and ζ-potential measurements

Measurements of PECs size and ζ-potential were performed by using a Zetasizer NanoZS90 instrument (Malvern Instruments, UK). Each measurement was repeated three times at 25 °C and the average values were calculated.

Fourier transform infrared (FT-IR) spectroscopy

The FT-IR spectra were recorded using a Nicolet iS10 FT-IR Spectrometer (Thermo Fisher Scientific, UK) in the wavelength range between 3500 and 650 cm⁻¹ with a resolution of 4 cm⁻¹.

Differential scanning calorimetry (DSC)

The DSC measurement was carried out using a DSC Q1000 instrument (TA Instruments, USA). The samples were crimped in a standard aluminum pan and heated from 25 to 320 °C at a heating rate of 10 °C/min under a constant N₂ flow rate of 20 ml/min.

RESULTS AND DISCUSSION

The unimodal size distribution was confirmed for all investigated CH/EL PECs. The Z-average was in the range between 201 and 1088 nm immediate upon preparation and increased with increasing EL/CH mass ratio. Still, the initial size reduction was observed when amount of added EL was increased due to the more intensive CH/EL interaction and consequently tighter packing of the polymers. The larger PECs were formed when CH of higher MW was used. This could be ascribed to the chain length of the CH, since the shorter polymer chains could form denser and hence smaller PECs.

Z-potential for all prepared formulations had positive value and was in range between 20 and 37 mV. The positive values of ζ-potential and can be ascribed to excess of protonated -NH₂ groups of CH in comparison to deprotonated -COOH groups of EL. Surprisingly, ζ-potential was not significantly influenced by CH/EL ratio. This was reported earlier for PEC nanoparticles consisted of CH and could be ascribed to the more significant influence of





polycation positive charge density in comparison to that of polyanion (3).

Most of the formulations did not show significant increase in size nor coalescence after one month storage at 4 °C. Size of the PECs was strongly affected by pH value and the lowest size and narrowest size distribution was observed in pH range between 5.0 and 6.0.

As can be seen in Fig. 1a, absorption bands characteristic for the individual polymers could be observed in the spectrum of CH/EL PEC, confirming presence of the both polymers in the PECs structure. However, a new absorption band was observed on the spectrum of PEC suggesting the formation of PEC between CH and EL. These findings are consistent with previously published experiments on films comprised of CH and different carboxylate polyanions (4) and also with the results of thermal analysis. Namely, instead of degradation exotherms of CH and EL, a new exotherm was evident on thermogram of the PEC (Fig 1b), which could be ascribed to a strong ionic interaction between the two polymers.

for preparation of submicron PECs with acceptable short-term stability and pH-sensitivity, which is relevant to their potential use as drug carriers. Furthermore, significant influence of CHs MW on CH/EL PECs size and stability was confirmed.

REFERENCES

1. Moustafine RI., Margulis EB, Sibgatullina LF, Kemenova VA, Mooter GVD. Comparative evaluation of interpolyelectrolyte complexes of chitosan with Eudragit® L100 and Eudragit® L100-55 as potential carriers for oral controlled drug delivery. *Eur. J. Pharm. Biopharm.* 2008; 70: 215–225.
2. Hamman JH Chitosan based polyelectrolyte complexes as potential carrier materials in drug delivery systems. *Mar. Drugs.* 2010; 8: 1305–1322.
3. Alonso-Sande M, Cuña M, Remuñán-López C, Teijeiro-Osorio D et al. Formation of new glucomannan-chitosan nanoparticles and study of their ability to associate and deliver proteins. *Macromolecules.* 2006; 39: 4152–4158.
4. Silva CL, Pereira JC, Ramalho A, Pais AA, Sousa JJ. Films based on chitosan polyelectrolyte complexes for skin drug delivery: Development and characterization. *J. Membrane Sci.* 2008; 320, 2682–279.

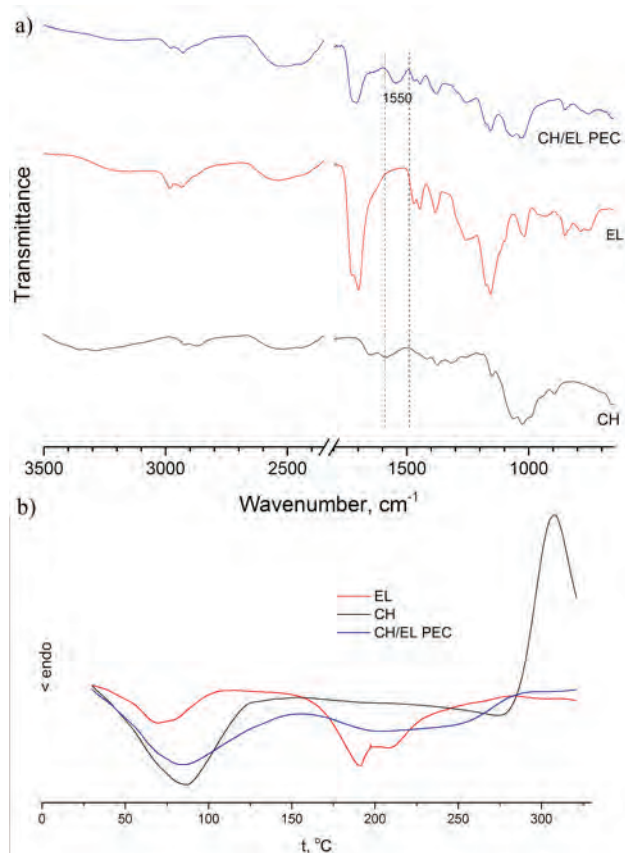


Fig. 1: a) FT-IR and b) DSC spectra of CH/EL PEC and consisting polymers.

CONCLUSIONS

Obtained results revealed that CH and EL can be used



THE INFLUENCE OF VARIOUS TESTING CONDITIONS ON RHEOLOGICAL PROPERTIES OF SWOP EMULSION (P34)

R. Korać¹, D. Krajišnik¹, J. Janićijević, J. Milić¹

¹ Department of Pharmaceutical Technology and Cosmetology, Faculty of Pharmacy, University of Belgrade, Vojvode Stepe 450, 11221 Belgrade, Serbia

INTRODUCTION

Emulsions are widely used as cosmetic and pharmaceutical formulations. Each type of emulsion has specific characteristics that determine its application. The best properties of both oil in water (o/w) and water in oil (w/o) emulsions are merged in SWOP (Switch Oil Phase) emulsions. SWOP emulsions are based on formulation of o/w emulsions which invert into w/o emulsions during application on the skin. The aim of this study was to investigate and compare rheological behaviour of the SWOP emulsion and the referent o/w emulsion under various testing conditions: in the presence of ions and at different temperatures and to reveal the influence of these external factors on behaviour of the SWOP emulsion on the skin.

MATERIALS AND METHODS

The compositions of prepared emulsions are listed in Table 1. The SWOP emulsion (test emulsion, labelled as T) was prepared using the combination of a w/o polymeric emulsifier with a mild surfactant in ratio 4:1.5 with addition of stabilizing polymer (1). The samples were prepared using hot/hot emulsification procedure by slowly adding oil phase (Phase I, Table 1) preheated at 70 °C to the water phase (Phase II, Table 1) also preheated at 70 °C. The stirring was performed by mechanical stirrer (Heidolph RZR 2020, Germany) at 500 – 2000 rpm until cooling to approximately 25 °C. The o/w emulsion (referent emulsion, labelled as R) stabilized with o/w nonionic emulsifier was prepared in the same manner. The emulsions (T and R) were characterized by conductometric (CDM 230, Radiometer, Denmark) and rheological (Rheometer Rheolab MC 120, Paar Physica, Germany) testing.

Tab. 1: Composition of the test (T) and referent (R) emulsions

Sample labels		T	R
Composition (INCI)	Phase I		
	Polyglyceryl-2-Dipolyhydroxystearate	4.0	/
	Polyglyceryl-2-Dipolyhydroxystearate, Lauryl Glucoside, Glycerin	/	3.0
	Cetearyl Alcohol	2.0	2.0
	Paraffinum liquidum	8.0	8.0
	Caprylic/Capric Triglyceride	8.0	8.0
	Helianthus Annuus Seed Oil	8.0	8.0
Phase II	Glycerin	3.0	3.0
	Sodium Lauryl Glucoside Carboxylate, Lauryl Glucoside	1.5	/
	Phenoxyethanol, Methylparaben, Propylparaben, Ethylparaben, Butylparaben, Isobutylparaben	0.5	0.5
	Sodium Polyacrylate	0.8	0.7
	Distilled Water	62.7	64.4

Artificial sweat (AS) solution (Table 2) (2) was used as a source of ions. It is known that the normal sweat rate for humans is approximately 0.38 ± 0.14 mg/cm²/min (3) and the amount of applied emulsion on the skin is approximately 0.5 – 2 mg/cm² (4). Based on these data, the mixtures of the emulsions (Table 1) and AS in ratio 5.3:1 were used in this study.

Tab. 2: Composition of artificial sweat solution

Ingredients (INCI)	Quantity (% w/w)	Adjust pH to 6.5 by adding ammonia.
Sodium Chloride	0.5	
Lactic Acid	0.1	
Urea	0.1	
Distilled Water	99.3	

To investigate the influence of dilution effect on viscosity of the emulsions, the mixtures with distilled water, in the same ratio, were also prepared. Conductivity measurements (at 20 °C) and rheological characterization (at 20 °C and 32 °C) were performed for the tested samples with and without presence of ions.

RESULTS AND DISCUSSION

The T emulsion showed higher conductivity than the R emulsion, probably due to the presence of ions from the anionic surfactant and polymeric stabilizer. With the addition of AS, conductivity of the tested samples increased and the conductivity increment was higher for the R emulsion (up to 170 %) in comparison with the T emulsion (up to 67 %) (Table 3).





Tab. 3: Conductivity of test (T) and referent (R) emulsions with and without AS addition

Sample	Conductivity (mS/cm)
Artificial sweat	9.380
T	1.370
R	0.479
T with AS	2.280
R with AS	1.291

Both emulsions (T and R) revealed shear-thinning plastic flow behaviour (Fig. 1).

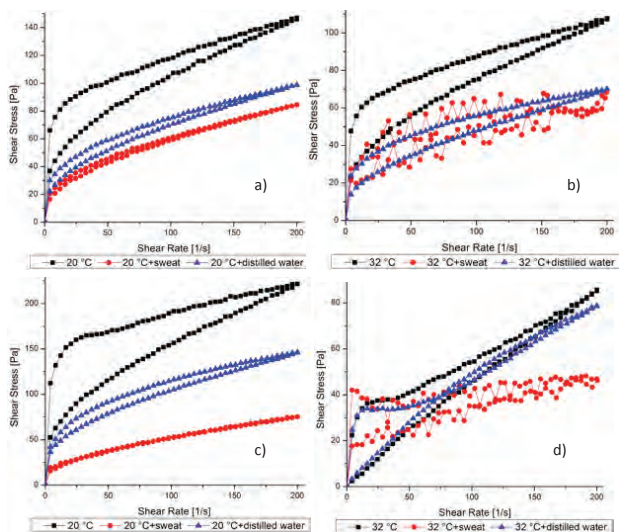


Fig. 1. Flow curves for: a) T emulsion at 20 °C; b) T emulsion at 32 °C; c) R emulsion at 20 °C; d) R emulsion at 32 °C.

Addition of distilled water (at 20 °C), due to the dilution effect, changed flow behaviour lowering thixotropy (Fig.1) and values of apparent viscosity (Table 3) for both T and R emulsions. It should be noted that addition of distilled water had stronger influence on the R emulsion than on the T emulsion. Addition of AS (at 20 °C), due to the presence of ions, changed the structure of the emulsions leading to Bingham plastic behaviour at higher shear rate (above 50 s⁻¹) (5), but decrement of apparent viscosity (η_1) was more pronounced for the R emulsion (Table 4).

Tab. 4: Apparent viscosities η_1 and η_2 (at 8.2 s⁻¹ and at 200 s⁻¹, respectively) for the test (T) and referent (R) emulsions

Samples	T		R	
	η_1 (Pas)	η_2 (Pas)	η_1 (Pas)	η_2 (Pas)
Conditions				
20 °C	9.20	0.74	16.19	1.11
20 °C + AS	3.03	0.42	2.50	0.38
20 °C + distilled water	4.24	0.49	6.22	0.73
32 °C	6.80	0.53	3.70	0.43
32 °C + AS	3.47	0.33	5.08	0.23
32 °C + distilled water	3.40	0.35	3.80	0.39

At the higher temperature (32 °C), changes of the same parameter (Table 4) were lower for the SWOP emulsion (in range from 26% to 63%) compared to the o/w emulsion (in range from 68% to 77%), for all the testing conditions.

CONCLUSIONS

Obtained results indicated that rheological properties i.e. stability of the tested emulsions were changed under the influence of the investigated external factors. It seems that the action of both factors simultaneously has a stronger influence on SWOP emulsion providing faster inversion during application on the skin.

REFERENCES

1. Beuché M, Amela CC, Domingo M, Aqueous meta-stable oil-in-water emulsions U.S. Patent 20100215596 A1, August 26, 2010.
2. Midander K, Wallinder IO, Heim K, Leygrafa C, Nickel release from nickel particles in artificial sweat, *Cont. Derm.* 2007; 56: 325-330.
3. De Berker D, Rees JL, Normal sweat secretion rate in patients with alopecia areata, *Br. J. Dermatol.* 1995; 132: 402-404.
4. K.A. Walters, *Dermatological and Transdermal Formulations*, Taylor & Francis, 2002.
5. Barnes HA, The yield stress- a review or panta rei everything flows? *J Non-Newt Fluid Mech* 1999; 81: 133-178.



MUCOADHESIVE WAFERS LOADED WITH ECONAZOLE-CYCLODEXTRIN COMPLEXES FOR TREATMENT OF ORAL CANDIDIADIS (P35)

M. Jug^{1,*}, I. Kosalec¹, N. Mennini¹, S. Orlandini², S. Furlanetto², P. Mura²

¹ Faculty of Pharmacy and Biochemistry, A. Kovačića 1, Zagreb, Croatia

² School of Human Health Sciences, Via Schiff 6, Sesto Fiorentino I-50019, Florence, Italy

INTRODUCTION

Candidosis is one of the most common fungal infections of the oral cavity in humans, caused by yeasts of the genus *Candida*. Its clinical aspects run from relatively trivial conditions, such as oral thrush, up to systemic super-infections in immuno-compromised patients, with mortality of 30-50% (1). Despite the availability of several effective antimycotics for the treatment of oral candidosis, failure of the therapy is not uncommon, due to the unique properties of the oral cavity, where both the saliva flushing and the oral musculature cleansing action tend to reduce the local drug concentration to sub-therapeutic levels (2). Therefore, the aim of this work was to develop a lyophilized wafer formulation based on mixtures of low methylester amidated pectin (LMAP) and carboxymethylcellulose (CMC), which applied to the oral mucosal surface, should allow a prolonged residence time and a controlled release of econazole nitrate (ECN). To overcome the problems of low ECN solubility, the drug was loaded as a ternary complex with sulphobutyl- β -cyclodextrin (SBE β CD) and citric acid (CA).

MATERIALS AND METHODS

Materials

Econazole nitrate (ECN) was kindly donated by Italfarmaco (Italy); sodium salt of sulfobutylether- β -cyclodextrin with a substitution degree of 0.9 (SBE β CD) kindly provided by CyDex, Inc. (USA). Mucoadhesive polymers used were carboxymethylcellulose sodium salt (CMC; Sigma, Italy), and low methylester amidated citrus pectin (LMAP Amid CF02), kindly gifted by Herbert and Fox KG Pektin-Fabriken, Germany). All other chemicals used were of reagent grade.

Wafer preparation and characterization

Wafers were prepared by freeze-drying of different hydrogels based on LMAP and CMC mixtures, loaded with ECN at 0.1% w/w, added as co-ground product with SBE β CD and CA. Experimental design methodology was applied to optimize the wafer composition, maximizing its mucoadhesive properties, evaluated "ex vivo" in terms of residence time and mucoadhesive strength to excised porcine mucosa. Drug release studies in simulated saliva were performed on the optimized formulation by using an open-compartment dissolution apparatus to maintain sink conditions (3).

Time-kill assay

To evaluate the therapeutic potential of the optimised formulation, the time-kill assay was performed with *C. albicans* ATTC 90028 and *C. krusei* ATTC 6258 as model fungal strains. The optimized wafer formulation was added to the inoculum suspension in the liquid nutrient medium, and the viability of *Candida* strains was monitored as a function of time using mitochondrial dehydrogenase activity assay.

RESULTS AND DISCUSSION

A product with the desired and predicted quality was developed using the experimental design. The examined formulation variables were amidation degree of LMAP and concentrations of LMAP and CMC. Their influence on mucoadhesive strength, *in situ* residence time and % of drug released at a given time, chosen as the responses indicative of the system performance, were examined by an initial screening design. This enabled identification of the variables influencing on the considered responses, and determination of their best levels for the response optimization. A response surface study was then performed, to investigate in depth the values of the responses for all possible combinations of the factors selected in the previous screening phase (Fig.1).



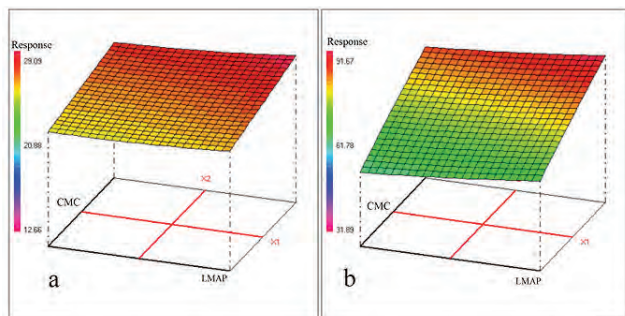


Fig. 1: Response surface plots of the effect of % LMAP and % CMC on the mucoadhesion strength (a) and in situ residence time (b) of the wafer formulations.

The desirability function allowed finding the optimal wafer composition: LMAP 7.2 % (w/w) and CMC 5.2% (w/w). The experimental values of adhesive strength ($28.4 \pm 0.04 \text{ g/cm}^2$) and residence time ($88.1 \pm 0.1 \text{ min}$) given by the optimized formulation were very close to the predicted values, demonstrating the validity of the applied model. The optimized wafer formulation showed an appropriate and controlled drug release (Fig.2), of about 5 mg/h, during the observed residence time on the mucosa surface, thus enabling the maintenance of therapeutic ECN levels during the whole wafer application time.

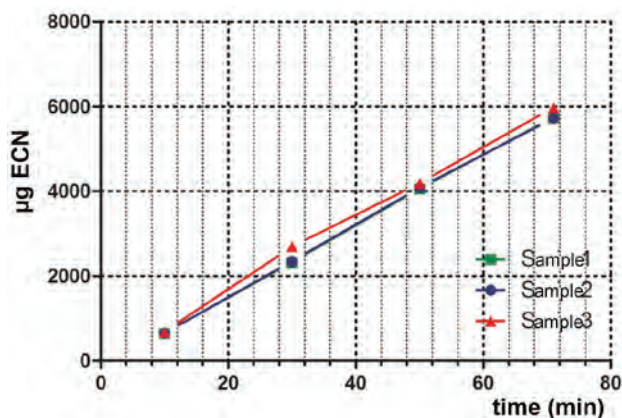


Fig. 2: Release profile of ECN (as coground ternary system with SBEB CD and CA) from the optimized wafer formulation.

Finally, the analysis of the antimycotic activity of the optimized ECN wafer formulation (Fig. 3) demonstrated its good potential as a novel effective topical delivery system able to improve the existing therapy of oral candidosis.

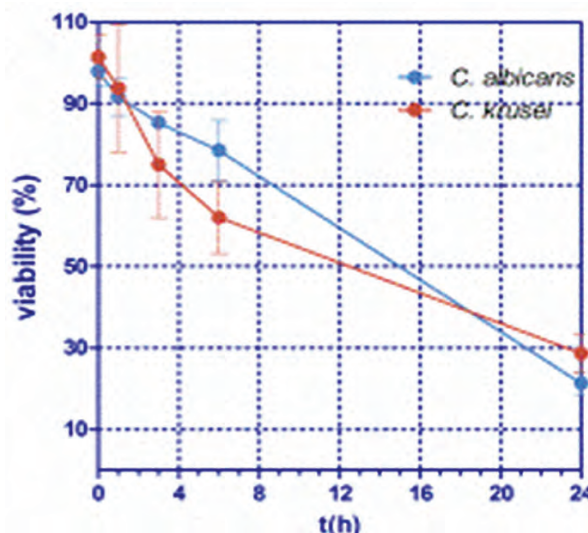


Fig. 3: Antimycotic activity of the optimized formulation against *C. albicans* and *C. krusei*

CONCLUSIONS

Combination of LMAP and CMC, in suitable proportions, allowed preparation of lyophilized wafers able to form mucoadhesive hydrogels on contact with saliva and to ensure a prolonged residence time and controlled release of the drug.

REFERENCES

1. Williams D.W., Kuriyama T., Silva S., Malic S., Lewis M.A.O. *Candida* biofilms and oral candidosis: treatment and prevention. *Periodontol.* 2011; 55: 250-265.
2. Ellepola A.N.B., Samaranyake L.P. Oral Candidal infections and antimycotics, *Crit. Rev. Oral Biol. Med.* 2000; 11: 172-198.
3. Patel, V.F. Liu, F. Brown M.B. Modelling the oral cavity: In vitro and in vivo evaluations of buccal drug delivery systems, *J Control Release*, 2012; 161: 746-756.



DEVELOPMENT OF COUPLED *IN VITRO*/ *EX VIVO* MODELS TO PREDICT EYE-RELATED BIOAVAILABILITY (P36)

M. Juretić^{1,*}, J. Lovrić¹, I. Krtalić², B. Cetina-Čižmek², I. Pepić¹, J. Filipović-Grčić¹

¹ University of Zagreb, Faculty of Pharmacy and Biochemistry, Department of Pharmaceutical Technology, A. Kovačića 1, 10000 Zagreb, Croatia

² Pliva Croatia Ltd., Prilaz baruna Filipovića 25, Zagreb, Croatia

INTRODUCTION

Aging of population worldwide and consequent higher occurrence of eye diseases have intensified innovative or generic ophthalmic product (OP) development. One of the major obstacles in the development process is the ability to model eye barriers in a timely, reproducible, predictable and cost-effective manner.

Coupled *in vitro/ex vivo* models have the potential for routine use in research laboratories and/or the pharmaceutical industry to overcome various obstacles in OP development and registration. Such an approach of using high-throughput, but less predictive *in vitro* models in conjunction with low-throughput, but more predictive *ex vivo* models would exponentially improve the efficacy of permeability screening and would help to decrease both the costs of, and development time for, OPs (1).

The aim of this study was therefore to establish a correlation between *in vitro* and *ex vivo* cornea models considering key biorelevant conditions using permeability markers differing in the mechanism of transport across corneal barrier. Further simulation of the *in vivo* eye environment would then be stepwise conducted approaching more closely toward an *in vitro/ex vivo* model for the prediction of eye-related bioavailability.

MATERIALS AND METHODS

The permeability experiments on excised porcine corneas, freshly obtained from the local slaughterhouse, were performed in horizontal diffusion chambers (Harvard Apparatus). The experiment was conducted in Krebs Ringer buffer (KRB pH 7.4), oxygenated and mixed with oxygen gas. After the addition of the test compound dissolved in KRB to the donor compartment samples were taken from the receptor compartment at regular time intervals to determine the permeation coefficient (P_{app}). For the determination of tissue viability transepithelial electrical resistance (TEER) was measured during the experiment.

The cell-based epithelial cornea model was cultivated on Transwell® polycarbonate filter inserts coated with collagen type I from rat tail and fibronectin. The HCE-T cells suspended in the culture medium were seeded onto the filter and cultivated submerged for seven days, after which they were exposed to the air-liquid interface during the following three days (2). The permeability experiment was performed directly in the Transwell® in an analogous manner to the tissue-based experiment.

The concentration of fluorescein and rhodamine B in the samples was quantified using fluorescence plate reader (1420 Multilabel counter Victor³, Perkin Elmer). The analysis of metoprolol and propranolol samples was performed by ultra-performance liquid chromatography (UPLC Infinity 1290, Agilent).

RESULTS AND DISCUSSION

The coupled *in vitro* and *ex vivo* models with optimal viability and barrier characteristics in the biorelevant conditions were established. The comparable barrier properties of the *in vitro* and *ex vivo* corneal models were achieved and their viability during the testing was preserved (Fig. 1).

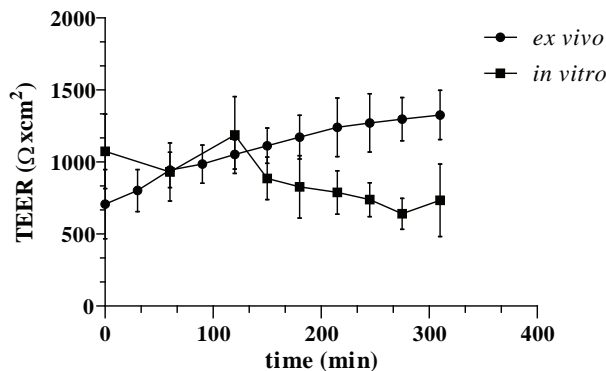


Fig. 1: The transepithelial electrical resistance (TEER) (mean ± SD) of *in vitro* HCE-T cell model and *ex vivo* porcine corneas (n = 12) during permeability experiments.



The permeability of four markers as a function of their physicochemical properties was evaluated using coupled models. Permeability studies showed a correlation ($r^2=0.92$) between *in vitro* HCE-T cell model and *ex vivo* porcine cornea in a horizontal diffusion chamber (Fig. 2).

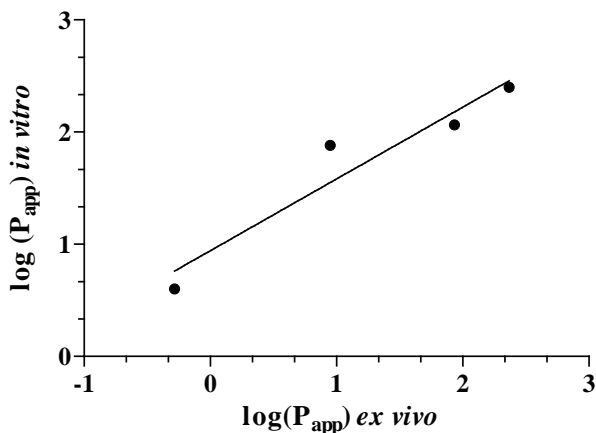


Fig. 2: The comparison of permeation coefficients P_{app} (mean) of fluorescein, rhodamine B, metoprolol and propranolol in *in vitro* HCE-T cell model and *ex vivo* porcine cornea ($n = 12$). The equation and correlation coefficient are $y = 0.64x + 0.94$, $r^2 = 0.92$.

The accomplished equivalence of barrier properties and the resultant correlation of permeability coefficients of the compounds tested indicate the potential of these models for the implementation in the preclinical OP development. However, although the equivalence to native barrier represents a prerequisite in the development of a model for the prediction of *in vivo* permeability, further optimization of the models, such as the simulation of the eye fluid dynamics, as well as the addition of eye fluid proteins with possible influence on drug permeability, is an indispensable step toward obtaining a tool for the accurate prediction of eye-related bioavailability (Fig. 3).

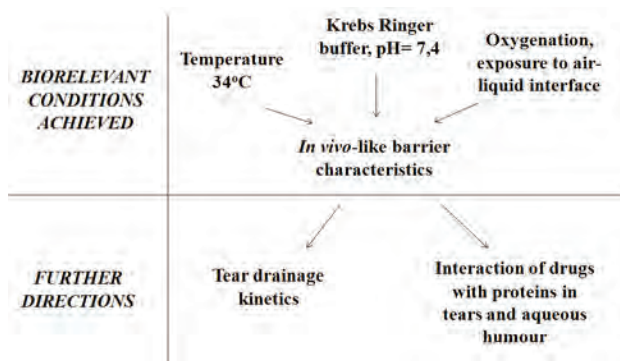


Fig. 2: Toward biorelevant conditions in coupled *in vitro/ex vivo* models for the prediction of eye-related bioavailability

CONCLUSIONS

The *in vitro/ex vivo* coupled model approach moves towards the preclinical assessment of eye-related bioavailability. A good *in vitro/ex vivo* correlation ($r^2=0.92$) was obtained suggesting that these coupled models have good predictive power, indicating their usefulness for OP development.

ACKNOWLEDGEMENTS

This work was supported by a Partnership in Research project 04.01/56 funded by the Croatian Science Foundation and PLIVA Croatia LTD.

REFERENCES

1. Pepić I, Lovrić J, Cetina-Čižmek B, Reichl S, Filipović-Grčić J. Toward the practical implementation of eye-related bioavailability prediction models. *Drug Discov. Today*. 2014; 19(1): 31-44.
2. Hahne M, Reichl S. Development of a serum-free human cornea construct for *in vitro* drug absorption studies: The influence of varying cultivation parameters on barrier characteristics. *Int. J. Pharm.* 2011; 416(1): 268-279.



OPTIMIZATION OF TABLET FORMULATION WITH PULSATILE RELEASE OF CARVEDILOL USING EXPERIMENTAL DESIGN (P37)

O. Kaljevic^{1,*}, Dj. Medarevic¹, J. Djuris¹, S. Ibric¹

¹ Department of Pharmaceutical Technology, Faculty of Pharmacy, University of Belgrade, Vojvode Stepe 450, 11221 Belgrade, Serbia

INTRODUCTION

Chronotherapeutic systems with pulsatile drug release after predetermined *lag time* are first choice in the treatment of disease where application of drug during night or early in the morning is necessary (hypertension, asthma, rheumatoid arthritis) (1, 2). Compression coating is one of the approaches in the formulation of chronotherapeutic systems. It is simple and economic way to obtain therapeutic systems with pulsatile drug release. The press-coating manufacturing processes employ several steps shown in Fig. 1. The inner core tablet is formulated, and then compressed under appropriate conditions. The tableting machine die is pre-filled with shell-coating materials to form a powder bed, the compressed inner core tablet is placed at the center of the bed, and any remaining outer coating shell materials added. Finally, the outer coating shell is compressed around the inner core tablet (2). Polyethylene oxides (PEO) with different molecular weight are used as components of tablet coating to delay drug release. Factors important for delayed drug release are: type, proportion and molecular weight of polymer, coating thickness and compression force. Composition of tablet core is important for drug release profile after *lag time* (2). The aim of this study was formulation of pulsatile release compression coated tablets. Carvedilol was used as a model drug. Compositions of tablet cores were varied according to 3² factorial design, in order to obtain optimal *lag time* and complete drug release afterwards.

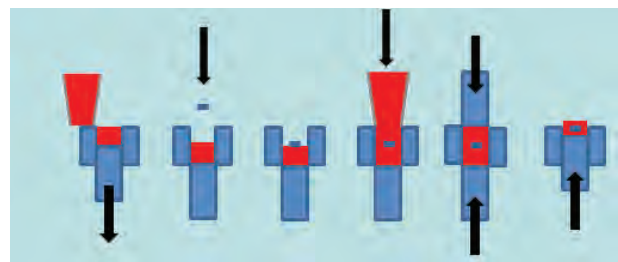


Fig. 1: Manufacturing process of press-coating

MATERIALS AND METHODS

Tablet cores contained carvedilol, magnesium stearate and anhydrous lactose. Using 3² full factorial design, two factors (concentration of sodium starch glycolate (SSG) and sodium chloride (NaCl)) were varied on three levels (0%, 5%, 10%) giving 9 formulations in total (F1-F9) shown in Tab. 1. Tablet coat of all formulations contained Polyox WSR N60K (35%) and lactose monohydrate (65%).

Tab. 1: Composition of tablet cores

Formulations	F1	F2	F3	F4	F5	F6	F7	F8	F9
Carvedilol (mg)	12.5	12.5	12.5	12.5	12.5	12.5	12.5	12.5	12.5
NaCl (%)	0	0	0	5	5	5	10	10	10
SSG(%)	0	5	10	0	5	10	0	5	10
Magnesium stearate (%)	0.5	0.5	0.5	0.5	0.5	0.5	0.5	0.5	0.5
Lactose, anhydrous (mg)	ad 150								

Drug release rate was determined during 8,5h using rotating paddle apparatus (0,1 M HCl, 900 ml, 50 rpm, 37°C). The time required for the release of 50% of carvedilol after *lag time* (t_{50}) was selected as response variable.

RESULTS AND DISCUSSION

Carvedilol released profiles are shown in Fig. 2. The highest percent of released carvedilol is noticed from tablet formulations F7, F2 and F4, respectively. F4 and F7 formulations containing higher concentration of NaCl, without SSG, show higher amount of released carvedilol than formulations containing both of these two excipients. Formulation F2 released high amount of carvedilol, but showed very short *lag time*.



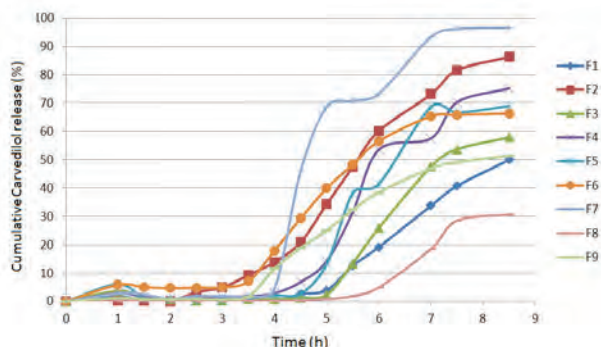


Fig. 2: Carvedilol release profiles

The longest *lag time* is achieved with the formulations F8 and F3 (Tab. 2). Formulation F8 containing 10% of NaCl and 5% of SSG showed delaying of starting release for 6h, but just 30% of carvedilol is released.

Also, 5h *lag time* is achieved with the tablet formulation F3 containing 10% of SSG, without NaCl, but it has incomplete release of carvedilol.

Tab. 2: Formulations with belonging *lag time*

Formulations	F1	F2	F3	F4	F5	F6	F7	F8	F9
<i>Lag time (h)</i>	5	3	5	4	4,5	3	4	6	3,5

t_{50} values are given in Fig. 3. Formulations F4 and F7, containing 5 and 10% of NaCl, respectively, without SSG exhibit the shortest t_{50} . It is observed that formulations F8 and F9 containing higher percent of SSG and NaCl have longer t_{50} . F8 released less than 50% of carvedilol during the examination time, which is shown as the longest t_{50} in the Fig. 3.

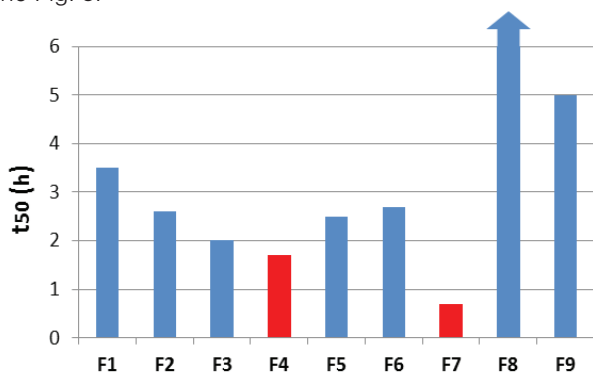


Fig. 3: t_{50} for the formulations

CONCLUSIONS

The fastest carvedilol release after *lag time* was achieved with formulations F4 and F7.

The most convenient carvedilol release profile considering *lag time* and t_{50} for chronotherapy have formulations F4 and F7 with NaCl in core composition.

The influence of NaCl on carvedilol release was more pronounced compared to SSG.

ACKNOWLEDGMENT

This work was supported by the project TR34007, funded by the Ministry of Education Science and Technological Development.

REFERENCES

1. Maroni A., Zema L., Del Curto M.D., Loreti G., Gazzaniga A., Oral pulsatile delivery: Rationale and chronopharmaceutical formulations, *International Journal of Pharmaceutics* 398 (2010) 1–8.
2. Lin S-Y., Kawashima Y., Current status and approaches to developing press-coated chronodelivery drug systems, *Journal of Controlled Release* 17 (3) (2012) 331-53.



SIMULTANEOUS DETERMINATION OF EMERGING PHARMACEUTICAL POLLUTANTS IN WASTE WATER BY SOLID PHASE EXTRACTION AND LC-MS/MS (P38)

Anita Klančar^{1*}, Jurij Trontelj¹, Robert Roškar¹

¹ University of Ljubljana, Faculty of Pharmacy, Aškerčeva 7, 1000 Ljubljana, Slovenia

INTRODUCTION

The occurrence of pharmaceuticals in the environment may have adverse effects in living organisms. Pharmaceuticals can be introduced into water sources through sewage, which carries the excreta of patients, from uncontrolled drug disposal (discarding into toilets) and from agricultural runoff comprising livestock manure (1, 2). The concentration range of pharmaceuticals is very broad, ranging from mg/L to low ng/L. The aim of our work was to develop a new simple and sensitive analytical method for the simultaneous determination of different compounds in water samples using LC-MS/MS method. The pharmaceuticals were selected based on environmental occurrences that belong to different pharmacological groups; also two agricultural pollutants were included.

MATERIALS AND METHODS

Materials

All selected standards: atrazine (ATR), bisoprolol (BIS), carbamazepine (CAR), ciprofloxacin (CIP), clofibrac acid (CLO), diclofenac (DIC), fluoxetine (FLU), imatinib (IMA), metoprolol (MET), simazine (SIM) were purchased from Sigma-Aldrich (Germany) and ¹³C haloperidol (IS) (Alsa Chim, France). Real wastewater samples were obtained from wastewater-treatment-plant Polhov Gradec, Slovenia.

Sample preparation

To 100 mL of water sample was added 10 mL of 250 mM KH₂PO₄ buffer adjusted to pH 7, and mixed by shaking for a few seconds. The sample was subjected to a solid phase extraction using Strata-X 60mg/3mL (Phenomenex, USA) on Visiprep™ SPE Extraction Vacuum Manifold (Supelco, USA). Before the transfer of prepared water sample to the SPE cartridge, the cartridge was activated and conditioned with 3 mL of methanol followed by 3 mL of 25 mM KH₂PO₄ buffer adjusted to pH 7, at a flow-rate of 1 mL/min. Sample was then introduced to the cartridge at a flow rate of 8 mL/min by negative pressure. Cartridge was vacuum-dried for 10 min and eluted sequentially with 2 mL MeOH: ACN 1:1 (v/v) and 2 mL 2% acetic acid in MeOH:ACN 1:1 (v/v), respectively. The eluted sample was dried in a stream of nitrogen at 60°C in a Caliper TurboVap apparatus (Zymark, USA) and reconstituted with 250 µL of 0.1% formic acid in methanol. The reconstituted sample was transferred to autosampler vial with insert and subjected to LC-MS/MS analysis.

Preparation of calibration and quality control samples

Water mixture solution of the standards was prepared at a concentration of 1 mg/L for each analyte. Nine calibration standards were prepared at concentrations corresponding to 2.5-2500 ng/L in water. Quality control samples were prepared the same way as calibration samples, at following concentrations: 25, 250 and 1500 ng/L. Evaluation of SPE procedure was accomplished by addition of appropriate amounts of the water mixture solution to 100 mL of MilliQ water. To all samples ¹³C haloperidol as IS was added (250 ng/L final concentration).

Liquid chromatography-tandem mass spectrometry conditions

The Agilent 1290 Infinity LC coupled to Agilent 6460 triple quadrupole mass spectrometer (Agilent Technologies, USA) was used. 1 µL of sample was injected onto a 50 x 2.1 mm, 2.6 µm Kinetex C₁₈ column (Phenomenex, USA) at 50°C and eluted with mobile phase A (0.1% formic acid in water) and B (acetonitrile) using the following linear gradient (time [min]; %B; flow rate [mL/min]): (0;5;0.35), (0.5;5;0.35), (1.1;9;0.35), (1.2;40;0.65), (1.3;50;0.65), (2.0;60;0.65), (2.5;60; 0.65), Total run time was 3.2 min. For MS, a JetStream® electrospray source was used. The dynamic MRM transitions and other quantification settings for analytes are presented in Table 1.

Tab. 1: Quantification settings for analytes





Analyte	MRM (m/z)	CE (eV)	Fr (V)	P
ATR	216.1 > 174.0	13	80	+
BIS	326.2 > 116.1	9	144	+
CAR	237.1 > 194.1	13	100	+
CIP	332.1 > 314.1	16	134	+
CLO	213.0 > 127.0	10	80	-
DIC	296.0 > 214.0	15	55	+
FLU	310.1 > 148.1	1	100	+
IMA	494.0 > 394.0	32	170	+
MET	268.2 > 116.0	12	96	+
SIM	202.1 > 68.1	33	110	+
IS	382.0 > 165.0	21	135	+

RESULTS AND DISCUSSION

In order to achieve a better extraction efficiency on SPE several factors were taken into account, as follows: various types of cartridges (C18 from different suppliers, Oasis HLB, StrataX), pH of water media (3-7), elution and reconstitution solvent mixtures. To improve the sensitivity and selectivity, chromatographic and MS conditions were also optimized. Isotope labelled haloperidol was selected as internal standard.

The developed analytical method was validated and the results are presented in Table 2. The method was precise, accurate and linear for all analytes with limits of quantification in ng/L range. Recoveries at concentration 1.5 µg/L ranged from 60.6 to 94.2 % and were reproducible (n = 6).

Tab. 2: Validation parameters for selected compounds

Analyte	Lin. range (ng/L)*	Precision (%RSD)	Recov. (%)	Inst. prec.† (%RSD)
ATR	2.5-2500	4.51	56.5	2.85
BIS	12.5-2500	4.15	83.6	1.02
CAR	2.5-500	4.42	84.2	1.46
CIP	12.5-2500	4.66	60.6	3.77
CLO	2.5-2500	6.81	92.2	2.66
DIC	12.5-2500	7.11	94.2	2.81
FLU	12.5-2500	3.22	76.6	3.85
IMA	12.5-2500	3.13	80.4	7.62
MET	12.5-2500	3.40	82.5	1.65
SIM	2.5-2500	4.32	81.3	5.22

† Instrument precision (repeat injection of samples; n = 5)

* Determination coefficients were larger than 0.999

In the assayed samples from wastewater treatment plants (n=3), the mean concentration levels of ATR, BIS, CAR, DIC, FLU, and MET found were 1.0, 7.9, 69.0, 282.5, 27.3, and 56.0 ng/L, respectively. ATR and BIS concentrations

were only estimated due to being below the calibrated range. Other monitored pharmaceuticals were not detected.

CONCLUSIONS

The presented analytical method was successfully validated and applied to the determination of the target pharmaceuticals in wastewater samples demonstrating its applicability for routine monitoring of pharmaceutical pollutants being discharged into the environment.

REFERENCES

1. Daughton CG, Ternes TA, *Pharmaceuticals and Personal Care Products in the Environment: Agents of Subtle Change?* Environ. Health Persp. 1999; 107: 907-937.
2. Bendz D, Paxeus NA, Ginn TR, Loge FJ, *Occurrence and fate of pharmaceutically active compounds in the environment, a case study: Hoje River in Sweden.* J. Hazard. Mater. 2005; 122: 195-204
3. Loos R, Carvalho R, Comero S, et al. *EU Wide Monitoring Survey on Waste Water Treatment Plant Effluents, Treatment Plant Effluents European Commission, Joint Research Centre, Institute for Environment and Sustainability, Luxembourg, 2012.*
4. Segura PA, François M, Gagnon C, Sauvé S, *Review of the Occurrence of Anti-infectives in Contaminated Wastewaters and Natural and Drinking Waters.* Environ. Health Persp. 2009; 117: 675-68.



FORMULATION OF MAGNETOLIPOSOMES WITH SUPERPARAMAGNETIC IRON OXIDE NANOPARTICLE CLUSTERS (P39)

P. Kocbek^{1*}, M. Jurič¹, S. Kralj^{2,3}

¹ Faculty of Pharmacy, University of Ljubljana, Aškerčeva cesta 7, 1000 Ljubljana, Slovenia

² Jožef Stefan Institute, Materials Synthesis Department, Jamova 39, 1000 Ljubljana, Slovenia

³Nanos Scientifica d.o.o., Teslova ulica 30, 1000 Ljubljana, Slovenia

INTRODUCTION

The research on nanotheranostics, which enable simultaneous diagnostics and therapy, is very intensive in the recent years (1). Such systems demonstrate the potential to change the current medical paradigm of “see and treat” to “detect and inhibit” (2). They are often based on superparamagnetic iron oxide nanoparticles (SPIONs), showing a great promise for a wide spectrum of bioapplications, due to their characteristic magnetic properties exhibited only in the presence of magnetic field (3). They enable visualisation of the system by magnetic resonance imaging and treatment based on magnetic hyperthermia. SPION clustering is a novel approach, which increases the particle size up to the optimal value, making such clusters magnetically guidable, while maintaining their superparamagnetic properties (2). Contrary, the individual SPIONs are too small to be magnetically guided and can also leak from the capillaries of healthy tissues, resulting in limited accumulation on the target site. Therefore, their clustering is favourable in all applications, which depend on magnetic guidance. Such SPION clusters can be incorporated in nanodelivery systems making them magneto-responsive.

The aim of the current research was formulation of magneto-responsive liposomes based on SPION clusters and characterization of their physical properties.

MATERIALS AND METHODS

Materials

A dispersion of superparamagnetic amino functionalized silica-coated iron oxide nanoparticle clusters (Fig. 1) was provided by Nanos Scientifica d.o.o. (Ljubljana, Slovenia) as a custom-made product. Lipoid S 100 and Lipoid S PC-3 were purchased from Lipoid GmbH (Germany) and cholesterol from Lex d.o.o. (Slovenia).

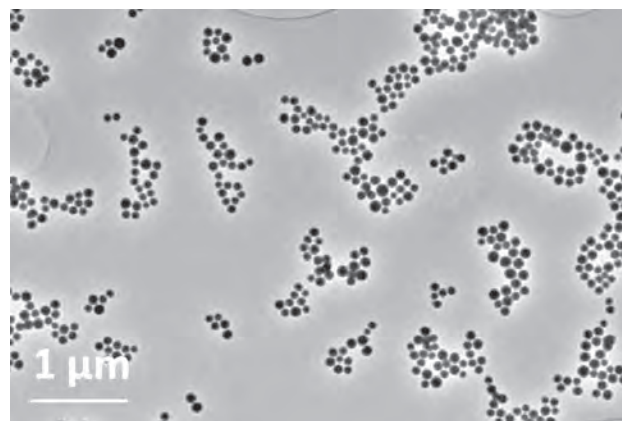


Fig. 1: TEM image of silica-coated SPION clusters.

Preparation of magnetoliposomes

Liposomes were prepared by thin film method. Briefly, phosphatidylcholine and hydrogenated phosphatidylcholine from soybean in weight ratio 9:1 were dissolved in 5 ml of ethanol together with various amounts of cholesterol (15-40%, w/w). Total concentration of lipids in solution was 25 mg/ml. Then solvent was removed at 40°C by a rotary vacuum evaporator (Büchi R-114 Rotavapor) to form a thin film. Hydration of the lipid film at room temperature with 5 ml of aqueous suspension of amino functionalized silica-coated SPION clusters (62.8 μg/ml) resulted in polydisperse dispersion of liposomes. The obtained dispersion was pulsed sonicated (30 s on/ 60 s off up to 10 pulses) to reduce the size of vesicles and their polydispersity.

Characterization of magnetoliposomes

The average hydrodynamic diameter and polydispersity index (PI) of liposomes were determined by photon correlation spectroscopy (Zetasizer Nano-ZS, Malvern Instrument, UK). The structures of SPION clusters and magnetoliposomes were visualised by transmission electron microscopy (TEM) (Jeol JEM 2100).





RESULTS AND DISCUSSION

The preparation method used in this study enabled preparation of liposomes with minimal average size ~115-160 nm obtained after sonication (Fig. 2). The amount of cholesterol in phospholipid bilayer influenced the size of the vesicles, which were generally smaller, if the amount of cholesterol was lower.

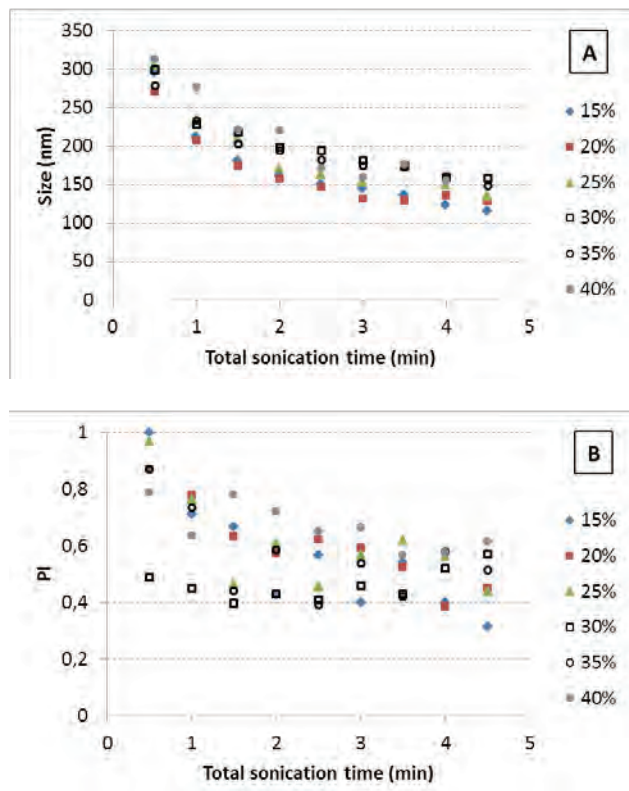


Fig. 2: Effect of sonication on average size (A) and PI (B) of magnetoliposomes prepared with different amounts of cholesterol (15-40%, w/w). The dispersions were prepared in water.

Comparison of the particle size of SPION clusters in dispersion and clusters incorporated in liposomes revealed smaller average size of the latter (Tab. 1), indicating aggregation of SPION clusters in aqueous medium, which can be omitted by their incorporation in phospholipid vesicles. Furthermore, the separation of liposomes from dispersion in an external magnetic field gradient generated by a permanent magnet confirmed their magneto-responsive characteristics. TEM imaging of liposomes revealed association of SPION clusters with organic material, thus, indicating their association with phospholipid vesicles.

Tab. 1: The size and polydispersity of amino functionalized silica-coated SPION clusters and magnetoliposomes with 15% (w/w) cholesterol in water and PBS (pH 7.4).

Time	Medium	SPION clusters	Liposomes
Freshly prepared	PBS	324 nm (PI 0.254)	136 nm (PI 0.363)
	H ₂ O	462 nm (PI 0.265)	106 nm (PI 0.403)
After 7 days	PBS	395 nm (PI 0.390)	131 nm (PI 0.357)
	H ₂ O	377 nm (PI 0.175)	167 nm (PI 0.705)

CONCLUSIONS

In the present study, we prepared magnetoliposomes based on SPION clusters. The smallest size of the vesicles was achieved with 15% (w/w) cholesterol in phospholipid bilayer. These liposomes showed good physical stability in water and PBS (pH 7.4), therefore, showing potential for further development of nanocarriers for targeted drug delivery or theranostic applications.

REFERENCES

1. Kocbek P, Kralj S, Erdani Kreft M, Kristl J. Targeting intracellular compartments by magnetic polymeric nanoparticles. *Eur. J. Pharm. Sci.* 2013; 50: 130-138.
2. Hayashi K, Nakamura M, Sakamoto W, Yogo T, Miki H et al. Superparamagnetic nanoparticle clusters for cancer theranostics combining magnetic resonance imaging and hyperthermia treatment. *Theranostics* 2013; 3: 366-376.
3. Bonini M, Berti D, Baglioni P. Nanostructures for magnetically triggered release of drugs and biomolecules. *Curr. Opin. Coll. Interface Sci.* 2013; 18: 459-467.



DETERMINATION OF CRITICAL FUNCTIONALITY-RELATED CHARACTERISTICS OF HPMC FOR SUSTAINED RELEASE TABLETS (P40)

D. Košir^{1,*}, F. Vrečer^{1,2}, S. Baumgartner²

¹ Krka, d.d., Novo mesto, Šmarješka cesta 6, 8501 Novo mesto, Slovenia
² University of Ljubljana, Faculty of Pharmacy, Aškerčeva 7, 1000 Ljubljana, Slovenia

INTRODUCTION

Hydroxypropyl methylcellulose (HPMC) is one of the most widely used polymers for controlling drug release from hydrophilic matrix systems (1). According to European Pharmacopeia and other literature sources the following functionality-related characteristics (FRC) may be important for HPMC used in hydrophilic matrices: viscosity, degree of substitution, molecular mass distribution, particle size distribution and powder flow (2, 3). The aim of present study was to determine the influence of HPMC with selected properties/functionality related parameters on release rate of carvedilol as a model drug by multiparametric approach.

MATERIALS AND METHODS

Materials

Eight different samples of HPMC K4M (type 2208, Colorcon, Dow Chemical Co., USA) with nominal viscosity 4000 mPas were used as matrix forming agent. Six of these were supplied as QBD samples covering a wide range of design space regarding HPMC characteristics. Carvedilol as poorly water soluble model drug was supplied by Krka, d.d., Novo mesto, Slovenia. Lactose monohydrate as a filler was supplied by Molkerei Meggle Waserburg GmbH & Co., Germany. Colloidal silicon dioxide as a glidant was supplied by Evonik Degussa GmbH, Germany. Magnesium stearat as a lubricant was supplied by Faci Spa, Carasco GE, Italy.

Determination of particle size distribution, viscosity and degree of substitution for each HPMC batch

Particle size distribution was determined by laser diffraction method using Malvern Mastersizer 2000. The results was given based upon volume-weight diameter (D_{10} , D_{50} , D_{90} , mean – $D_{(4,3)}$). The viscosity and degree of substitution: methoxy and hydroxypropoxy were analysed according to methods described in Ph. Eur. 8th Ed. using Brookfield RVDV-III ULTRA Rheometer and Agilent 6890, GC 5 apparatus respectively.

Preparation of tablets

Tablets were prepared with direct compression. All ingredients in selected amounts were homogenized and then compressed with rotary tablet press Killian Pressima using biconvex, oval punches. The composition of tablet was: carvedilol 25 mg, HPMC K4M 40 mg, lactose monohydrate 92.5 mg, colloidal silicon dioxide 0.5 mg, magnesium stearate 2 mg.

Drug release testing

Drug release profiles were obtained using dissolution apparatus with paddle method (apparatus 2, Van Kel 7025 dissolution test station, Varian, USA) in acetate buffer solution (pH = 4.5) at 37 °C ± 0.5 °C. The amount of released drug was determined spectrophotometrically.

Multivariate data analysis

The Multiple linear regression (MLR) models were computed using The Uncsrambler software version 10.3 (Camo).





RESULTS AND DISCUSSION

The release profiles of carvedilol were made with each investigated HPMC batch. Two dissolution profiles presenting the slowest and the fastest release rate of carvedilol are shown in Figure 1. The similarity factor (f_2) is 47.8 meaning that the examined two dissolution profiles are not similar.

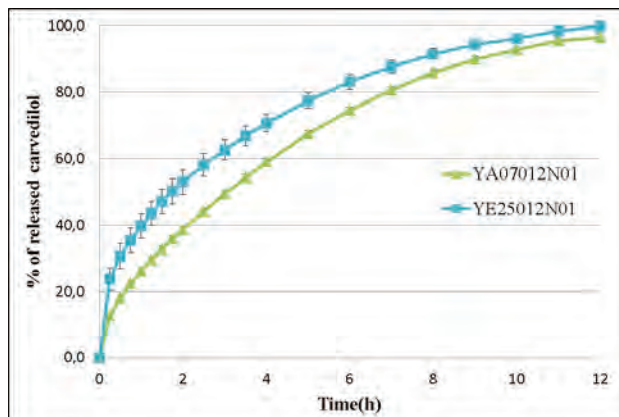


Fig. 1: Dissolution profiles for the slowest (batch HPMC K4M: YA07012N01) and the fastest (batch HPMC K4M: YE25012N01) release rate of carvedilol

To evaluate the influence of different HPMC characteristics onto release profiles of carvedilol many MLR models were generated. The independent variables used in models were: viscosity, methoxy content, hydroxypropoxy content (HP), D_{10} , D_{50} , D_{90} , $D_{(4,3)}$. The dependent variable was the fraction of released carvedilol at each investigated time point. The best MLR models that explain our case include following three HPMC characteristics: HP, Viscosity and D_{10} . Table 1 shows the significance (P value) for each parameter and R square for model at three different time points. The parameter is considered to be significant if $p < 0.05$.

Tab. 1: P value for HP, viscosity, D_{10} and R^2 for MLR models at three time points representing the beginning (2h), middle (6h) and end (10h) of dissolution phase.

Time point	2 h	6 h	10 h
P value HP	0.521	0.034	0.003
P value Viscosity	0.167	0.074	0.005
P value D_{10}	0.012	0.008	0.004
R^2 value	0.910	0.945	0.986

Our results show that D_{10} is the only significant parameter at 2 h meaning that at the beginning of the drug release small particle size of HPMC is important to prevent burst release of carvedilol. Small HPMC particles have larger surface area and therefore more possible contact points with water molecules. The consequence is that small particles swell faster and easier than large particles and form more coherent gel layer. D_{10} is significant also in the middle and at the end phase of drug release profile. In the middle and at the end of dissolution phase HP value is significant. HPMC with higher HP value is more hydrophilic and has more space between polymer chains. This contributes to higher degree of water uptake and more swellable matrix which leads to lower drug release rate. At the end of dissolution phase viscosity becomes also significant parameter. Higher viscosity leads to stronger gel layer and more resistant system to erosion, which results in lower drug release rate.

CONCLUSIONS

In our study particle size distribution (D_{10}), viscosity and hydroxypropoxy content proved to be important FRC parameters for HPMC that can lead to different release profiles. Therefore it is important to use multiparametric approach in development phase to build up robust formulation, identify critical FRC parameters and set up their specifications.

ACKNOWLEDGMENTS

We would like to acknowledge to Krka, d.d., Novo mesto for the support in the experimental work.

REFERENCES

1. Siepmann J, Peppas NA. Modelling of drug release from delivery system based on hydroxypropyl methylcellulose (HPMC). *Adv. Drug Deliv. Rev.* 2011; 48: 139-157.
2. *The European Pharmacopeia, 8th Edition, EDQM Council of Europe, Strasbourg, 2014.*
3. Novak SD, Kuhelj V, Vrečer F, Baumgartner S. The influence of HPMC viscosity as FRC parameter on the release of low soluble drug from hydrophilic matrix tablets. *Pharm. Dev. Technol.* 2013; 18(2): 343-347.



COMPRESSIBILITY OF PLACEBO AND DRUG-CONTAINING GRANULES INTO MINITABLETS (P41)

H. Kotłowska^{1,*}, W. Cybula¹, A. Kluk¹, A. Madanecka², K. Owcarz¹, M. Sznitowska¹

¹ Department of Pharmaceutical Technology, Medical University of Gdansk, Al. Gen. J. Hallera 107, 80-416 Gdansk, Poland

² Pharmaceutical Works Polpharma SA, Pelplinska 19, 83-200 Starogard Gdanski, Poland

INTRODUCTION

Wet granulation is a size enlargement process widely used in pharmaceutical industry for preparation of tableting material (1). Minitablets (MT) are tablets with diameter of 1 mm to 3 mm. They can be successfully manufactured using processes and equipment dedicated for conventional tablets (2).

In the study MT was compressed from placebo and drug-containing granules. Several cardiovascular drugs were chosen as model APIs. MT can be proposed as drug formulation for paediatric patients. They could be the first age-appropriate ready-to-administer solid dosage forms (3). The dosage can be adjust by multiplication of units in relation to the child body weight.

MATERIALS AND METHODS

Two placebo and four drug-containing formulations were prepared. As model drugs candesartan cilexetil (CAN), valsartan (VAL), metoprolol succinate (MET) and enalapril maleate (ENA) were chosen. Composition of prepared formulations is shown in Tab. 1 and 2. Granules were prepared using 5% PVP or 2% HPMC solutions as binders. Tableting mass containing ENA was collected from a production line of the pharmaceutical plant Polpharma. MT 2.5mm/12.5mg and 3mm/17mg were produced using a laboratory rotary tablet press equipped with deep concave single or multiple punches. Compression pressure of 250 or 300 MPa was used. The stability of compression force during tableting process of P1-MT and MET-MT was measured by computer program.

Tab. 1 Composition [%] of placebo formulations

P1	[%]	P2	[%]
Sorbolac 400	37.6	Tabletosse 80	96.2
Vivapur 101	56.3	Ad-di sol	2.0
Ad-di-sol	2.0	PVP K30	0.8
Pharmacoat 606	1.1	MgSt	1.0
PRUV	3.0		

Tab. 2 Composition of drug-containing formulations

CAN 7%	VAL 40%	MET 40%	ENA 7.7%
Lac	Lac	Lac	Lac
	MC	MC	M-Starch
cCMC Na	cCMC Na	cCMC Na	cCMC Na
PVP	PVP	HPMC	NaHCO ₃
MgSt	MgSt	PRUV	MgSt

MC – microcrystalline cellulose, Lac- lactose, M-Starch – modified corn starch, PVP – povidone, cCMC Na – croscarmellose sodium, HPMC – hypromellose, PRUV – sodium stearyl fumarate, MgSt – magnesium stearate, NaHCO₃ – sodium hydrogen carbonate

Flowability of tablet mass was evaluated according to Ph. Eur. monograph. Compressed MT were examined for weight uniformity and friability using pharmacopoeial apparatus. Measurements of disintegration time were performed with a modified Ph. Eur. procedure: 1 mm mesh plate was attached to the bottom of the apparatus tubes.

RESULTS AND DISCUSSION

Placebo formulations

Mass P1 was characterised by a good flow considering Hausner ratio and angle of repose. In contrast flow of P2 mass was classified as passable with tendency to bridging. Nevertheless, from both mixtures it was possible to obtain MT with satisfactory weight uniformity – RSD was in the range of 1-4%. Mass uniformity was confirmed by good stability of the compression force (3% deviation was observed during compression of P1-MT). Compressed MT exhibited good mechanical strength which was assessed by friability measurement (about 0.3% loss in weight was noted). Regardless of the formulation all MT disintegrated in less than 2 min.

Drug-containing formulations

The flow of tableting mixtures with the active substances was classified as fair or passable. Despite relatively low flowability, satisfying mass uniformity of MT was confirmed. However, percentage deviation from the average masses was greater than for placebo MT (about 5-8%),





but still in the range of the requirements. Deviations may result from less stable compression force. For example during tableting of MET-MT 30% deviation from average compression was observed. Parameters obtained for drug-containing MT are shown in Fig.1.

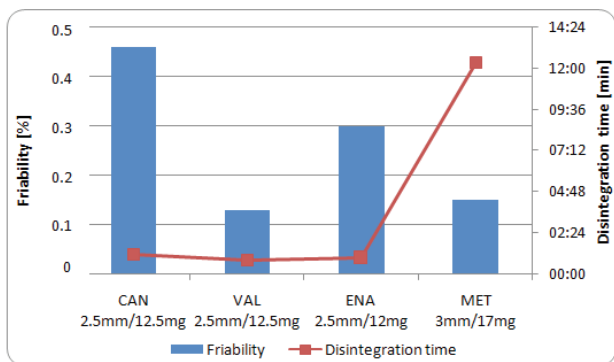


Fig. 1 Quality of drug-containing MT

The friability results indicated good mechanical strength of MT. The greatest loss of mass after drum tumbling (0.45%) was determined for CAN-MT. Disintegration time for most of MT was very short - about 1 min. Much longer disintegration time was observed for MET-MT (12 min). It can be due to high crushing strength (about 40 N) measured with texture analyser.

CONCLUSIONS

On the laboratory scale it is possible to produce MT from fair flowing or passable granule mixtures.

MT with different content of active substances comply with requirements of the basic pharmacopoeial quality tests, which confirms validity of further development of MT dosage form.

There is no need to undertake any composition changes in tableting masses to produce MT. It was confirmed by use of enalapril formulation dedicated for producing conventional commercial tablets.

ACKNOWLEDGEMENTS

The research is financially supported by The National Centre of Research and Development, Poland

REFERENCES

1. Faure A, York P, Rowe R. Process control and scale-up of pharmaceutical wet granulation processes: a review. *Eur. J. Pharm. Biopharm.* 2001; 52(3): 269-277.
2. Lennartz P, Mielck JB. Minitableting: improving the compactability of paracetamol powder mixtures. *Int. J. Pharm.* 1998, 173: 75-85.
3. Ali A, Charoo N, Abdallah D. Pediatric drug development: formulation considerations. *Drug Dev. Ind. Pharm.* January 31, 2014.





STUDY OF TASTE MASKING MECHANISM OF CETIRIZINE USING β -CYCLODEXTRIN IN ORALLY DISPERSIBLE TABLETS (P42)

E. Krejzová^{1,2*}, P. Stasiak¹, A. Dumicic¹, Z. Bělohav^{1,2}

¹ Zentiva, k.s., U Kabelovny 130, 102 37, Prague, Czech Republic

² Department of Chemical Technology, Institute of Chemical Technology, Technická 5, Prague 6, Czech Republic

INTRODUCTION

β -cyclodextrins (β -CDs) are cyclic oligosaccharides known for their ability to form the inclusion complexes with drug molecules. The complex formation between cyclodextrins and bitter compounds can have a taste masking effect. In orally dispersible tablets (ODTs) where the tablet disintegrates rapidly on tongue the complexes can be formed in saliva solution (1). There are also few methods recommended for complex formation in solid state and formulation of ODTs (freeze-drying, spray drying, ball milling etc.) (2).

Cetirizine dihydrochloride (CTZ) is a second generation antihistaminic drug with a very bitter taste. Its molecule consists from two aromatic rings (phenyl and chlorophenyl) which could be complexed with cyclodextrin cavity. The complex formation between CTZ and β -CD has been reported in literature by nuclear magnetic resonance (NMR), isothermal titration calorimetry (ITC) and UV-spectroscopic studies (1) (see Fig. 1). However, no detailed study of the inclusion complexes formed between CTZ and β -CD in solid state has been published. In addition, it has been speculated that interaction and blockage of the gatekeeper proteins of the taste buds by the CDs also adds to the taste masking effect (3).

In the present research the study of taste masking mechanism using β -CDs is based on determination of complex formation in liquid and solid state by thermodynamic and spectroscopic methods and by *in vivo* taste evaluation performed with six healthy volunteers.

The significance of ODT production methodology, namely freeze-drying, spray drying, liquid-assisted grinding, wet granulation and direct compression techniques on taste masking of bitter CTZ will be also discussed.

MATERIALS AND METHODS

The physical mixtures of CTZ and β -CD and their binary mixtures of individually processed precursors were prepared by following techniques: spray drying (BÜCHI Mini Spray Dryer B-290, Germany), freeze-drying (Christ, ALPHA 2-4 LSC, Germany), liquid-assisted grinding (Retsch MM200, Germany) and wet granulation (Eurovent, UK).

The physicochemical properties (complex formation) of all mixtures were investigated in solid state by differential scanning calorimetry (DSC) - DSC Pyris 1, (Perkin Elmer, CT, US), X-Ray diffractometry (XRD), Raman spectroscopy - In Via Reflex (Renishaw, GB) and in liquid state by isothermal titration calorimetry - VP-ITC microcalorimeter (MicroCal Inc., Northampton, Massachusetts) and Raman spectroscopy. The kinetics of complex formation in liquid state was measured by Raman spectroscopy as well.

The cetirizine dihydrochloride was donated by Sigma-Aldrich (Steinheim, North Rhine-Westphalia, Germany) and β -cyclodextrin was obtained from Roquette (Lestrem, France).

RESULTS AND DISCUSSION

The XRD and DSC analysis showed higher conversion of crystalline to amorphous substances in binary mixtures using freeze-drying and liquid-assisted grinding methods, which could further indicate presence of inclusion complexes (4). However, mentioned solid state techniques could not strongly confirm complex-forming interactions in amorphous mixtures. In direct compression and wet granulation method no changes of crystalline substances have been observed.

Data from ITC confirm strong interaction between CTZ and β -CD, further suggesting formation of inclusion complex in water (see Fig. 2). The method demonstrated high binding constant (up to 7216 M⁻¹) of CTZ/ β -CD complex in neutral pH which is similar to oral cavity.

An immediate Raman shift (> 1cm⁻¹) of CTZ bands corresponding to aromatic vibrations was observed after addition of β -CD into CTZ solution. According to Mohan et al., changes of the band intensity and position prove the complex formation (5).

The taste masking effect was evaluated *in vivo* in CTZ/ β -CD solutions at molar ratios of 1:1 and 1:5 (CTZ: β -CD) and in samples of ODTs that contained the CTZ and β -CD at molar ratios of 1:1 and 1:2, processed by studied tech-



niques (see Tab. 1). In both cases, in liquid and solid samples, acceptable taste masking was achieved even at the highest molar ratios, which for liquid and solid samples were 1:5 and 1:2, respectively.

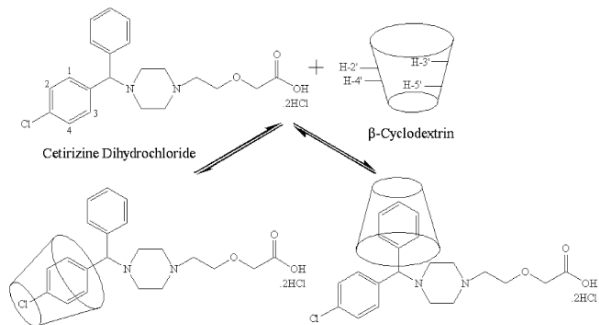


Fig. 1: Proposed structures of two 1:1 β -CD/CTZ inclusion complexes.

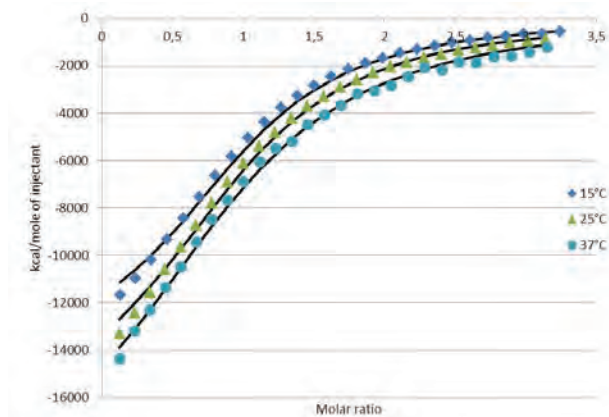


Fig. 2: The experimental data presented as a sigmoid plot from ITC measurement at different temperatures.

Tab. 1: In vivo taste evaluation of ODT samples.

Formulations	6 of volunteers rating the bitterness intensity as						Total score*
	0	1	2	3	4	5	
Wet granulation CTZ:lactosum m. (1:2)					4	2	4,3
Wet granulation CTZ: β -CD (1:1)				5	1		3,2
Wet granulation CTZ: β -CD (1:2)		2	4				1,7
Direct compression CTZ: β -CD (1:2)		4	1	1			1,5
Liquid-assisted grinding CTZ: β -CD (1:2)		3	2	1			1,7
Spray drying CTZ: β -CD (1:2)		2	4				1,7

* total palatability is in range 1-5; 1 = the most palatable and acceptable taste

CONCLUSIONS

Although it was not possible to sufficiently prove the presence of complex in solid state, the results demonstrated dependence of taste masking effect on β -CD amount in formulation rather than dependence on the method of production. The further suggested complex formation possibly ongoing in oral cavity, however, additional research needs to be done to confirm this hypothesis.

REFERENCES

1. Stojanov M, Wimmer R, Larsen KL: *Journal of Pharmaceutical Sciences*, 359, 63-69, 2008.
2. Kurozumi M, Nambu N, Naga T: *Chemical and Pharmaceutical Bulletin*, 23, 12, 3063, 1975.
3. Szejtli J, Szenté L, *Elimination of bitter, disgusting tastes of drugs and foods by cyclodextrins*, *European Journal of Pharmaceutics and Biopharmaceutics*. 61(3):115–125, 2005.
4. Williams RO, Mahaguna V, Sriwongjanya M, *Characterization of an inclusion complex of cholesterol and hydroxypropyl-beta-cyclodextrin*, *European Journal of Pharmaceutics and Biopharmaceutics*, 46:355–360, 1998.
5. Mohan PRK, et al., *Water soluble complexes of curcumin with cyclodextrins: Characterization by FT-Raman spectroscopy*, *Vibrational Spectroscopy*, 62, 77-84, 2012.



EVALUATING POTENTIAL FOR ENHANCED ORAL BIOAVAILABILITY OF CARBAMAZEPINE SMEDDS FORMULATIONS USING PBPK MODELLING (P43)

Marko Krstić¹, Sofija Stanković¹, Jelena Parojčić¹, Zorica Đurić¹, Svetlana Ibrić¹

¹ University of Belgrade, Faculty of Pharmacy, Department of Pharmaceutical Technology and Cosmetology, Vojvode Stepe 450, 11221 Belgrade, Serbia, e-mail: ibrice@pharmacy.bg.ac.rs, mkrstic109@gmail.com

INTRODUCTION

Lipid-based formulations were developed as a method to deliver poorly water-soluble drugs with a particular emphasis on self-microemulsifying drug delivery systems (SMEDDS) [1]. SMEDDS are defined as isotropic mixtures of natural or synthetic oils, surfactants or, alternatively, one or more hydrophilic solvents and cosolvents/surfactants [2].

Carbamazepine (CBZ) was used in this study as a model drug due to its poor solubility in water, leading to incomplete bioavailability [3]. Prediction of *in vivo* drug performance from dissolution test results can be difficult considering that variable physiological factors can also play a role in drug absorption. With the evolution of *in silico* physiologically based pharmacokinetic (PBPK) models, it became possible to estimate the extent and rate of drug absorption based on the relevant physicochemical, physiological and formulation parameters.

The aim of this work was the formulation of solid SMEDDS with CBZ (choosing the appropriate meth-

od and composition) as well as simulation of hypothetical drug absorption from these formulations by combining the *in vitro* dissolution behaviour of formulations with PBPK modelling.

MATERIALS AND METHODS

In the first phase of the study, the surfactant-co-surfactant ratio and the appropriate surfactant type were selected by construction of pseudo-ternary diagrams after titration of a mixture of caprylic-capric triglycerides and the surfactant phase with water. Polysorbate 80 and Cremophore EL were evaluated as surfactants and Macrogol 400 as cosurfactant. The surfactant-cosurfactant ratio 3:1, 2:1 and 1:1 was tested as well. By analysis of pseudo-ternary diagrams, six samples were selected, and after water dilution in a 10:90 ratio, droplet size was determined, applying photon correlation spectroscopy (Zetasizer Nano-ZS90, Malvern Instruments, Malvern, UK), based on which an appropriate SMEDDS was selected. The selected SMEDDS was incorporated onto four different carriers (Neusilin UFL2, Neusilin FL2, Sylysia 320 and diatomites) using two methods: (i) direct adsorption and (ii) evaporation with absolute ethanol (E). The CBZ content was constant (20%), and the carrier - SMEDDS ratio was varied (1:1 and 3:1). The obtained formulations are labeled as given in Table 1. Dissolution testing was performed in the rotating paddle apparatus (Erweka DT70, Germany), medium: water, 900ml, 50rpm, 37°C. Dissolution profiles were compared with that of CBZ powder and CBZ immediate release tablets based on the similarity factor (f1) and difference factor (f2) values.

Tab 1. Solid SMEDDS with CBZ

Method	Carrier: SMEDDS	Neusilin UFL2	Sylysia 320	Diatomites	Neusilin FL2
Direct adsorption	1:1	F1	F3	F5	F7
	3:1	F2	F4	F6	F8
Evaporation	1:1	E1	E3	E5	E7
	3:1	E2	E4	E6	E8



PBPK simulations

Simcyp Population-Based Simulator (version 13.1, Simcyp Ltd., Sheffield, UK) was used to simulate the time course of carbamazepin concentration in plasma. The required input parameters related to carbamazepin physicochemical and pharmacokinetic properties were taken from literature and/or *in silico* estimated. A summary of the input parameters used is given in Table 2.

Tab 2. Summary of the CBZ input parameters employed for *in silico* model development

Parameter	Value
Dose (mg)	400
Molecular weight	236.3
Log P_{ow}	2.45 ^a
Compound type	monoprotic base ^a
pKa	11.83 ^a
Fraction unbound in plasma	0.2 ^b
Solubility (mg/ml)	0.24 ^c
Human jejunal permeability, P_{eff} (cm/s)	$4.3 \cdot 10^{-4}$ ^d
Volume of distribution at steady state (L/kg)	1.043 ^e
Renal clearance (L/h)	1.5 ^f

^aRef [4]; ^b Ref [5]; ^c Ref [6]; ^dRef [7]; ^e Simcyp predicted value; ^f Ref [8]

Characteristics of the virtual subjects in the *in silico* study were set to match those of the subjects participating in the *in vivo* study of reference carbamazepin IR formulation. Model validation was performed based on the percent prediction error (%PE) between the simulated and *in vivo* observed values of the primary pharmacokinetic parameters [9]. Experimentally obtained dissolution profiles were used as input parameters in the *in silico* study.

RESULTS AND DISCUSSION

Based on the constructed pseudo-ternary diagrams (data not shown), it was noticed that the widest microemulsifying area is obtained at a surfactant/cosurfactant ratio 3:1, regardless of the surfactant type. For that ratio, systems with a surfactant phase/lipid ratio 9:1, 8:2 and 7:3 were selected and droplet size was determined. The system in which Polysorbate 80 was used as the surfactant and the surfactant phase/lipid ratio 9:1 have shown as the only

one that was a stable microemulsion with an inner phase droplet size of 17.66 nm and polydispersity index (PDI) of 0.104. This system was used for of solid SMEDDS. Based on the dissolution test results, higher drug release rate was accomplished with direct adsorption systems (Fig. 1). As for the use of carriers, CBZ release rate order is Neusilin UFL2, Sylysia 320, Neusilin FL2 and diatomites, starting from the fastest. From all formulations (except for formulation F5E) a statistically significant increase of CBZ dissolution rate compared to pure CBZ and commercial tablets with instant dissolution was noticed by calculation of the similarity factor and the difference factor. Influence of SMEDDS: adsorbent carrier ratio was not clearly noticed.

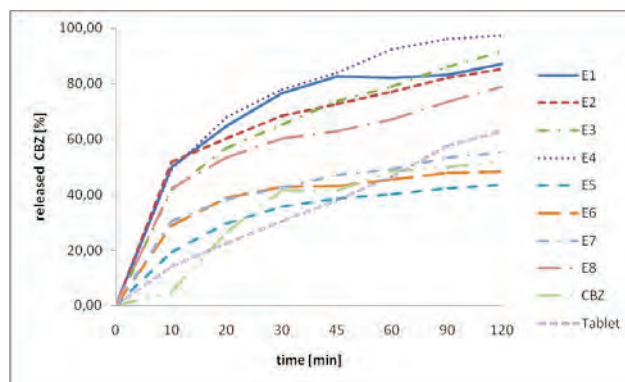
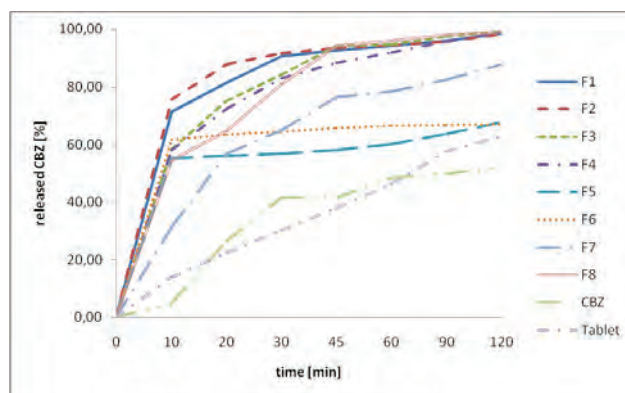


Fig 1. Dissolution profiles of the investigated CBZ formulations.

Drug-specific absorption model for CBZ was developed using Simcyp Simulator characterised with the %PE values of 9.21 for C_{max} and 3.81 for AUC, when compared to the literature data [9].



The *in silico* model developed was used to investigate the potential influence of *in vitro* dissolution kinetics on drug bioavailability. The predicted C_p - t profiles are presented in Fig. 2, together with the actual *in vivo* data. It can be noticed that both the rate and extent of drug absorption for the majority of solid SMEDDS formulations (except formulations F6, E5, E6 and E7 are higher when compared to the *in vivo* data for CBZ IR tablets). The *in silico* predictions indicate potentially enhanced CBZ bioavailability from solid SMEDDS created by direct adsorption method. As for the use of different carriers, the highest plasma concentrations would be expected when Neusilin UFL2, Sylysia 320 were used and the lowest ones with the use of diatomites. This trend is in accordance with the *in vitro* dissolution data.

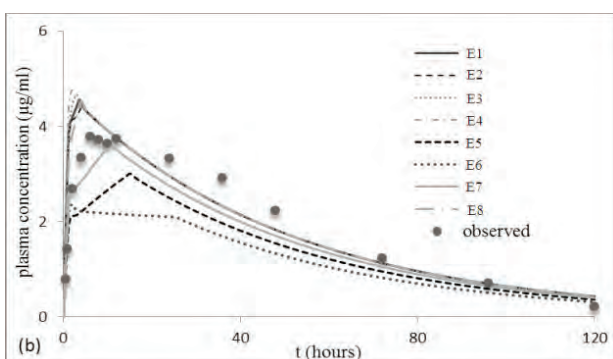
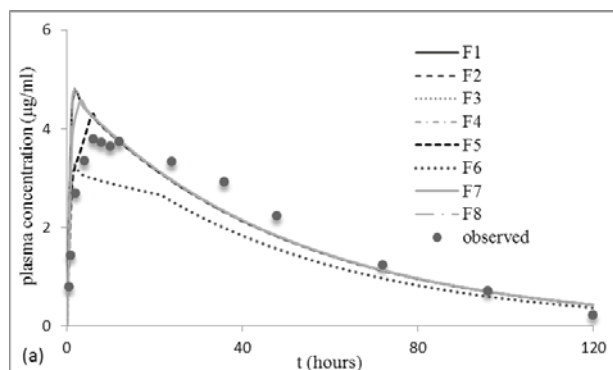


Figure 2. Predicted and *in vivo* observed CBZ plasma profiles

CONCLUSION

Successful development of solid SMEDDS was performed in this work in order to increase CBZ dissolution rate. It was also noted that *in silico* modeling and absorption simulation can be used as a tool in early drug product development of solid SMEDDS formulations with poorly soluble drugs. However, the *in vivo* study of the selected formulations is necessary in order to justify the *in silico* model developed and bioperformance of the selected dissolution test.

ACKNOWLEDGEMENTS

This work was done under the project No. TR 34007, supported by the Ministry of Education and Science, Republic of Serbia.

REFERENCES

1. Gursoy RN and Benita S. *Biomed. Pharmacother.* 2004; 58: 173-182.
2. Pouton C. *Eur. J. Pharm. Sci.* 2006; 29: 278-287.
3. Kobayashi Y et al. *Int. J. Pharm.* 2000; 193: 137-146.
4. [Clarke's Analysis of Drugs and Poisons, 3rd ed.; Pharmaceutical Press: London and Chicago, 2004.
5. Chiou WL, Buehler PW. *Pharm Res.* 2002; 19(6): 868-874.
6. Martindale, *The Extra Pharmacopoeia*, 35th edition, The pharmaceutical Press, London, 2007; 426-432.
7. Lennernäs H, et al. *Eur J Pharm Sci, Suppl.* 1996; 4: 69-71.
8. Webster LK, et al. *Eur J Clin Pharmacol.* 1984; 27: 341-343.
9. Homsek I, et al. *Arzneimittelforschung.* 2007; 57: 511-516.





INFLUENCE OF SURFACTANTS AND ADSORPTION CARRIERS ON DRUG RELEASE RATE FROM SOLID DRUG DELIVERY SYSTEMS

(P44)

Marko Krstić, Djurdjija Spasojević, Slavica Ražić, Dragana Vasiljević, Svetlana Ibrić

University of Belgrade, Faculty of Pharmacy, Department of Pharmaceutical Technology and Cosmetology, Vojvode Stepe 450, 11221 Belgrade, Serbia, e-mail: ibric@pharmacy.bg.ac.rs, mkrstic109@gmail.com

INTRODUCTION

Since absorption and bioavailability of poorly soluble drugs are limited by their dissolution rate, significant efforts are applied to improve solubility and dissolution rate of such drugs. There are several techniques for increasing the dissolution rate, some of which are an application of surfactants, as well as adsorbent carriers of natural and synthetic origin [1,2]. This paper presents the development of solid surfactant drug delivery systems constituted of different types and ratio of surfactants and adsorption carriers in order to increase drug release rate. The model substance was a poorly water soluble drug, carbamazepine (CBZ)[3].

MATERIALS AND METHODS

The experimental part can be divided into three phases. In the first set of experiments the individual effects of the surfactant and cosurfactant were tested, with and without the addition of the adsorbent carrier on the CBZ dissolution rate. The following formulations were created: Poloxamer 338/CBZ (80%/20%); Poloxamer 338/CBZ/Neusiline® UFL2 (40%/10%/50%); Brij®35/CBZ (80%/20%); Brij®35/CBZ/ Neusiline® UFL2 (40%/10%/50%).

In the second set of experiments fractional factorial experimental design was applied (2^{5-2}) for testing the influence of the formulation factors on the CBZ dissolution

rate from solid surfactant systems. The input parameters and the levels at which they were varied are given in Table 1. The experimental plan was given in Table 2. Percentages of released CBZ were followed as output parameters after 10, 20, 30, 45, 60 and 120 minutes (Y1-Y6). The result of each experiment is a linear combination of varied effects:

$$\psi = \beta_0 + \beta_1 \Xi_1 + \beta_2 \Xi_2 + \beta_3 \Xi_3 + \beta_4 \Xi_4 + \beta_5 \Xi_5 + \epsilon$$

With the application of Design Expert® (version 8.0.7.1, Stat-Ease, Inc, Minneapolis, MN, USA), an analysis of factor effects and the influence of input factors onto output factors were performed. Based upon the results obtained in the second set of experiments, output parameters for the third set were determined.

In the third set of experiments the ratio of CBZ was varied at three levels - 10%, 15% and 20%. The optimal formulation was selected based upon the results obtained in the third set of experiments.

Tab. 1: Varied parameters in the second set of experiments

Parameter	Low level (-1)	High level (+1)
Type of Poloxamer (X1)*	P237	P338
Brij® 35 (X2)	10%	20%
CBZ (X3)	10%	20%
Type of adsorption carrier (X4)	Neusilin® UFL2	Diatomites
Adsorption carrier ratio (X5)	33,33%	66,67%

*X1+X2+X3= const=100%

Preparation of solid surfactant systems

All formulations are prepared by melting of surfactants and the cosurfactant at 60°C. CBZ was then added to the molten mass, with vigorous stirring, until a homogenous dispersion was obtained. Mixture was pulverized with mortar and pestle, before being sieved through a 300 µm sieve. The sieved mixtures were mixed with an adsorbent carrier (Neusiline® UFL2 or Diatomites) and final formulations were thus obtained.



Tab. 2: Experimental plan in the second set of experiments

Formulation	Input parameters				
	X1	X2	X3	X4	X5
1	+1	-1	-1	-1	-1
2	-1	+1	+1	-1	-1
3	-1	+1	-1	-1	+1
4	+1	+1	+1	+1	+1
5	-1	-1	-1	+1	+1
6	+1	+1	-1	+1	-1
7	-1	-1	+1	+1	-1
8	+1	-1	+1	-1	+1

In vitro drug release studies

Dissolution testing was performed in the rotating paddle apparatus (Erweka DT70, Germany), medium: water, 900ml, 50rpm, 37°C. Dissolution profiles were compared with that of CBZ powder and CBZ immediate release tablets based on the similarity factor (f1) and difference factor (f2) values.

RESULTS AND DISCUSSION

Addition of Brij[®]35 and P338 increases the dissolution rate compared to pure CBZ (f1=18.31, f1=56.22, respectively). Addition of adsorption carrier increases the dissolution rate even more (f1=27.95, f1=62.84, respectively).

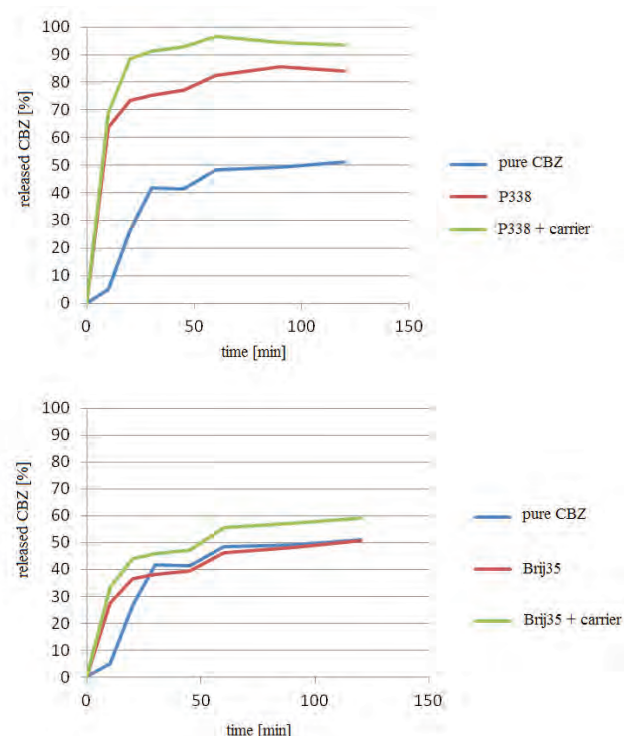


Fig. 1. Release profiles of pure CBZ and formulation from the first set of experiments.

CBZ dissolution rate profiles from formulations in the second set of experiments are given in Fig. 1. Factor analysis in the second set of experiments showed that the ratio of CBZ (X3) and type of carrier (X4) have the largest influence on the release rate profile (Tab.3.).

Tab.3. Analysis of influence formulation factors on CBZ dissolution rate (second set of experiments)

	Y1	Y2	Y3	Y4	Y5	Y6
(X1)	+1.09	+0.31	+1	+1.01	+1.15	0.9
(X2)	-1.8	-2.02	-1.31	-1.47	-1.23	0.037
(X3)	-6.45	-5.8	-5.12	-4.6	-3.86	-3.02
(X4)	-3.17	-5.13	-6.26	-6.15	-5.77	-5.72
(X5)	-5.87	-4.16	-3.53	-3.15	-3.55	-2.33
X2*X3	-3.23	-2.57	-1.99	-1.81	-1.62	-1.26
X2*X5	+3.31	+1.55	+0.8	+0.24	+0.16	-0.14

The input parameters for the second set of experiments were selected as follows: P338, 10% Brij[®]35, Neusilin[®] UFL2 (33.33%). The third set showed that the optimal CBZ ratio is 15%. The optimal formulation was compared with pure CBZ (Fig. 2) and with commercial tablets, showing a higher release rate (f1=56.37, f1=59.41, respectively).

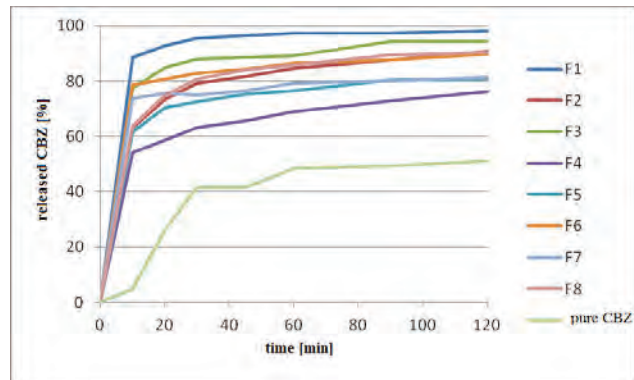


Fig. 2: Release profiles of pure CBZ and formulation from the second set of experiments.



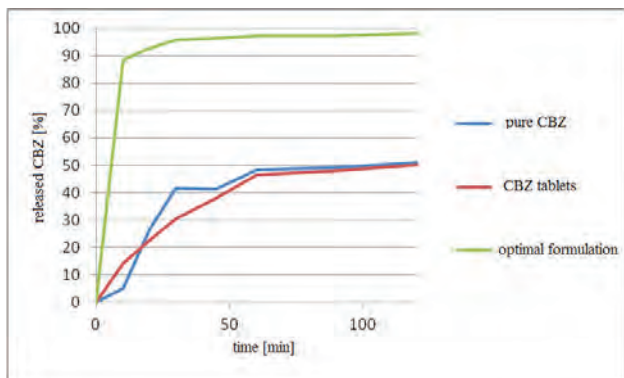


Fig. 3: Release profiles of pure CBZ, commercial CBZ tablets and the optimal formulation.

CONCLUSION

The release rate of CBZ can be increased by proper selection of the type and ratio of excipients. The optimal formulation (P338, 10% Brij®35, 33.33% Neusilin® UFL2, 15% CBZ) showed an increase in drug release rate, compared to pure CBZ and commercial CBZ tablets.

ACKNOWLEDGEMENTS

This work was done under the project No. TR 34007, supported by the Ministry of Education and Science, Republic of Serbia.

REFERENCES

1. Pouton C. *Eur. J. Pharm. Sci.* 2006; 29: 278–287.
2. Milovic, et al. *Hemijska industrija.* 2012; 66: 667-676.
3. Kobayashi Y, et al. *Int. J. Pharm.* 2000; 193: 137–146.
4. Grzesiak AL, et al. *J Pharm Sci.* 2003; 92:2260–71.

DETERMINATION OF ^{14}N NUCLEAR QUADRUPOLE RESONANCE FREQUENCY SETS (QFS) OF FAMOTIDINE POLYMORPHS A AND B (P45)

J. Lužnik²⁺, J. Pirnat², V. Jazbinšek², Z. Lavrič^{1*}, V. Žagar³, S. Srčić¹, J. Seliger³, Z. Trontelj²

¹ University of Ljubljana, Faculty of Pharmacy, Aškerčeva 7, 1000 Ljubljana, Slovenia

² Institute of Mathematis, Physics and Mechanics, Jadranska 19, 1000 Ljubljana, Slovenia

³ Jožef Stefan Institute, Jamova cesta 39, 1000 Ljubljana, Slovenia

INTRODUCTION

Famotidine has two known polymorphic forms (Figure 1) (1, 2). The molecule is a potent H₂ antagonist used in the treatment of gastric and duodenal ulcers. The two polymorphs (famotidine A and B) were studied in detail with ^{14}N NQR method (3, 4). In addition, thermal analysis and infrared spectroscopy were used.

It is important to be able to detect and characterize the occurrence of polymorphism because different crystal structures have different physical properties. This can have a profound influence on the properties that are vital to API's *in vivo* performance. On the other hand, it can cause differences in processability which can lead to manufacturing problems, higher number of out of specification batches and so on. Therefore it is vital to be able to track changes in crystal structure of API's. NQR is a radiofrequency spectroscopic method suitable for the task that in addition has the advantage of being non-destructive and contactless.

NQR can also provide additional information about crystal structure by careful consideration of quadrupole frequency sets (QFS), quadrupole coupling constants (QCC) and electric field gradient (EFG) asymmetry parameters (η). Numerous experiments are usually needed to determine QFS, but once found, they can be used for the purpose of future polymorph characterization and quantification. The



ability of ^{14}N NQR method to differentiate (and see quantitatively the difference) between famotidine polymorphs was shown.

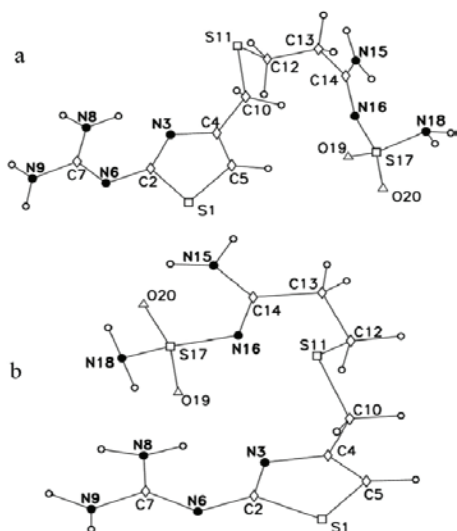


Figure 1. Famotidine molecule (2D projection): enumeration and folding of the atoms in polymorph A (panel a) and the same for polymorph B (panel b).

MATERIALS AND METHODS

Materials

Famotidine was donated by Krka (Novo mesto, Slovenia). It was found to be in form B. Subsequently form A was prepared by recrystallization from aqueous solution of the raw material. Both polymorphs were then analysed by different methods described below.

Solid mixture of famotidine A and B was also analysed. Additionally compacts of famotidine B at different compression forces (5, 10 and 30kN) were prepared on a Killian SP300 eccentric single punch equipped with flat-faced punches (2r=12,0 mm) in order to study the influence of compaction process on ^{14}N NQR spectra.

Differential scanning calorimetry

DSC 1 calorimeter from Mettler Toledo was used. Temperature program with a heating rate of 5 K/min in the temperature interval from 25-180°C was used.

Attenuated Total Reflectance – FTIR

Nicolet Nexus FTIR spectrometer equipped with a diamond ATR DuraSamplIR attachment was used for IR analysis of the samples

^{14}N Nuclear Quadrupole Resonance

Standard pulsed NQR spectrometer consisted of a tank circuit with the sample and a preamplifier, a programmable rf pulse unit (Spin Core Technologies, Gainesville, FL), an rf power amplifier (Tomco Technologies, BT500 AlphaS), and a homebuilt receiver.

RESULTS AND DISCUSSION

The commercially available form of famotidine was found to be pure polymorph B. Though thermodynamically unstable, its transformation to more stable form A is extremely slow.

Prepared polymorph A was confirmed to be pure polymorph A by DSC (T_{melt} at 173°C) and ATR-FTIR (absence of characteristic peaks of form B previously used for its quantification).

Table 1. ^{14}N NQR transition frequencies at room temperature for polymorphic forms A and B of famotidine, belonging to all seven different nitrogen positions in each of the two crystal unit cells

Form A*	v+ [kHz]	v- [kHz]	v0 [kHz]	QCC[kHz]	η
Na	3455	2443	1012	3932	0,51
Nb	2862	2065	797	3285	0,49
Nc	2819	2080	739	3266	0,45
Nd	2738	2274	464	3341	0,28
Ne	2735	2030	705	3177	0,44
Nf	2603	1971	632	3049	0,41
Ng	1979	1457	522	2291	0,46

Form B*	v+ [kHz]	v- [kHz]	v0 [kHz]	QCC [kHz]	η
Nh	3462	2472	990	3956	0,5
Ni	2887	2364	523	3501	0,3
Nj	2848	2234	614	3388	0,36
Nk	2787	2043	744	3220	0,46
Nl	2649	2133	516	3188	0,32
Nm	2587	1765	822	2901	0,57
Nn	1982	1339	643	2214	0,58

The nuclear quadrupole double resonance (NQDR) was initially used to approximately locate frequencies of some of the resonance lines in famotidine A and B. Then numerous trials of pure ^{14}N NQR were used to accurately determine ^{14}N NQR frequencies (Table 1). To analyse samples with famotidine for polymorphic composition of famotidine it suffices to select from the Table 1 one ^{14}N NQR frequency for each polymorph and then measure signal intensity at that frequency. It is most practical to choose two closely positioned frequencies with maximal intensity as this is beneficial for faster determination of polymorphic composition. ^{14}N NQR spectrum of a solid mixture of fa-





motidine A and B polymorphs is shown in Figure 1.

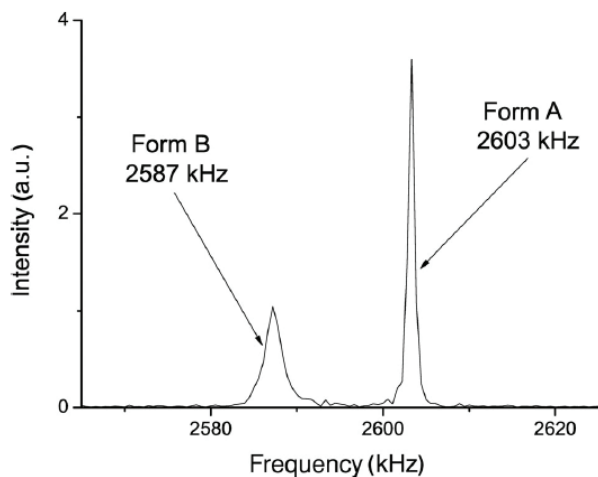


Figure 2. Typical characteristic part of the ^{14}N NQR spectrum for a mixed sample of forms A and B of famotidine (approximately 75% form A and 25% form B).

^{14}N NQR study of prepared compacts displayed spectral line width broadening, that was dependent on compaction force.

CONCLUSIONS

The complete set of ^{14}N NQR frequencies was found for both polymorphic forms of famotidine (A and B). The capability of ^{14}N NQR to non-destructively determine quantitative composition of a mixture of famotidine polymorphs was demonstrated. Additionally ^{14}N NQR spectral line width broadening of famotidine compacts was demonstrated.

REFERENCES

1. Ferenczy GG, Parkanyi L, Angyan JG, Kalman A, Hegedus B. Crystal and electronic structure of two polymorphic modifications of famotidine. An experimental and theoretical study. *Journal of Molecular Structure*. 2000;503:73–79.
2. Overgaard J, Hibbs DE. The experimental electron density in polymorphs A and B of the anti-ulcer drug famotidine. *Acta Crystallogr., Sect. A*. 2004;60:480-487.
3. Das TP, Hahn EL. *Nuclear Quadrupole Resonance Spectroscopy. Solid state Physics, Suppl. 1*, Academic Press, 1958.
4. Lužnik J, Pirnat J, Jazbinšek V, Lavrič Z, Žagar V, Srčič S, Seliger J, Trontelj Z. ^{14}N Nuclear Quadrupole Resonance Study of Polymorphism in Famotidine. *J Ph Sci*. 2014: DOI 10.1002/jps.23956

EVALUATION OF THE NOVEL DISINTEGRATION APPARATUS OD-MATE (P46)

A. Lazzari^{1,*}, D. Sieber², P. Kleinebudde², J. Quodbach², M. Pein²

¹ Department of Chemical and Pharmaceutical Sciences, University of Trieste, Trieste, Italy

² Institute of Pharmaceutics and Biopharmaceutics, Heinrich-Heine-University, Duesseldorf, Germany

* Corresponding author: lazzari.units@gmail.com

INTRODUCTION

Rapidly disintegrating tablets (RDTs) are solid dosage forms that disperse/dissolve in the saliva and are swallowed without additional intake of water. The disintegration time is a fundamental characteristic for the evaluation and development of this new dosage form. Due to limitations of the Ph. Eur. disintegration test (1) an alternative and more suitable method is required.

The aim of this work is evaluating different measurement procedures of the novel disintegration apparatus OD-mate with different types of commercially available tablets and comparing the assessed results with those of the pharmacopoeial apparatus.

MATERIALS AND METHODS

Different types of tablets were evaluated: two types of uncoated tablets (Paracetamol 500 mg, Ratiopharm and Prednisolon 5 mg, Acis Arzneimittel), one coated type (Simvabeta 20 mg, Betapharm Arzneimittel GmbH) and two types of rapidly/orally disintegrating tablets (Imodium Lingual 2 mg, Janssen-Cilag GmbH, as lyophilisate and Xilopar 1.25 mg, Cephalon GmbH, as orally disintegrating tablets)

Disintegration times were determined with the OD-mate (Higuchi Inc., Tokyo, Japan) as well as according to the European Pharmacopoeia.

OD-mate disintegration tester

The OD-mate mimics the force applied by the human tongue on tablets by a piston, consisting of an outer (100 g) and an inner (30 g) weight (Fig.1). The tablets are



placed on a mesh under the inner and outer weight and the complete measurement unit is lowered into a beaker filled with disintegration medium (demineralized water, 37 °C) and a stirrer. Once the mesh has reached a previously set position the measurement starts by interrupting an optical contact.

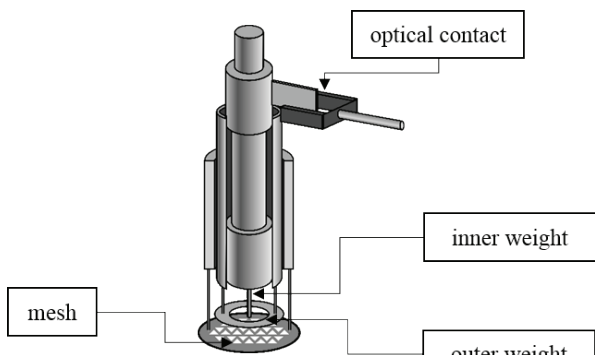


Fig. 1: Sketch of the measurement unit of the OD-mate

The inner weight moves down during disintegration until a defined height is reached (in this study half of the tablet height) and the measurement automatically stops. Three methods are specified by the manufacturer: general, accelerated and filter paper methods, in which differently shaped outer weight, meshes and different volumes of liquid are used (Table 1).

Table 1: Measurement methods according to the manufacturer.

Method	General	Accelerated	Filter Paper
Outer Weight	Round	Blade	Blade
Volume disintegration medium	10 ml	10 ml	1 ml
Temp. disintegration medium	37°C	37°C	37°C
Type of mesh	Triangular	Trapezoid	Trapezoid
Position mesh (distance from the beaker bottom)	7 mm	7 mm	On the bottom
Stirrer	Yes 1000 rpm	Yes 1000 rpm	No
Filter Paper	No	No	Yes

RESULTS AND DISCUSSION

The disintegration times of all different tablets were measured with the three methods (Fig. 2). The uncoated tablets (Paracetamol and Prednisolon)

showed similar disintegration times using the general and accelerated methods (mean of 34.8 s and 27.8 s for Paracetamol, 21.1 s and 23.8 s for Prednisolon). When the filter paper method was used the disintegration time increased to mean values of 278 s and 46.1 s, respectively. The smaller volume of the disintegration medium and the filter paper cause an increase of the tablet wetting time and thereby delay the disintegration. A different influence has the accelerated method on the coated tablets (Simvabeta), which showed a quicker disintegration time (mean of 208 s) compared to the general method (mean of 290 s). The shape of the blade outer weight exerts more pressure on the tablet compared to the round one, causing the lower disintegration time. The filter paper method, on the other hand, showed a considerable increase of the disintegration time for the same reasons mentioned above (> 30 min).

The results of the rapidly disintegrating tablets (Imodium Lingual and Xilopar) are particularly interesting: they disintegrate instantly by using the general and accelerated methods (< 0.5 s). Therefore, the results were discarded. The measurement with the filter paper method was possible but the disintegration times were in any case very short (1.7 s and 3.1 s).

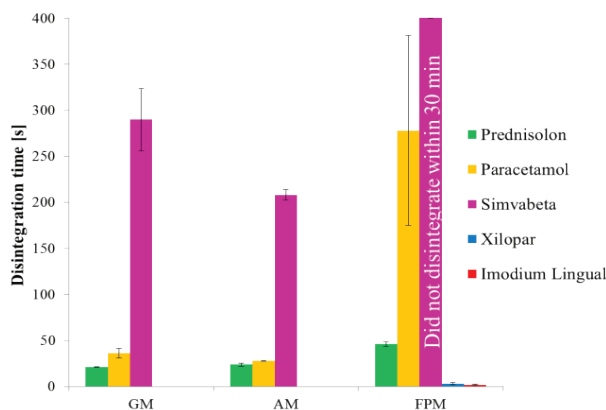


Fig. 2 : Disintegration times of the tablets measured with General (GM), Accelerated (AM) and Filter Paper Method (FPM). n = 3; mean ± s

Since the pressure exerted by the round outer weight is more homogeneous distributed than by the blade outer weight, the results obtained with the general method were chosen for the comparison to the Ph. Eur. disintegration test. In this case, similar results are obtained (Fig. 3). Disintegration time of lyophilisate and orodispersible tablets could not be measured with the Ph. Eur. standard apparatus.

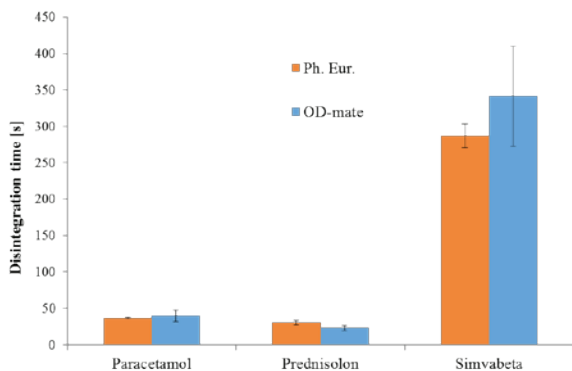


Fig. 3.: Disintegration time of Paracetamol, Prednisolon and Simvabeta using General Method (GM) in comparison to the Ph. Eur. disintegration test results. $n = 6, 5$; mean $\pm s$

CONCLUSIONS

According to the obtained results, the OD-mate has to be modified to be capable of measuring RDTs, since the assessed disintegration times are too short and cannot be used for the characterization of these tablets.

Otherwise similar results to those measured according to the European Pharmacopoeia were assessed for uncoated and coated tablets.

Only small deviations of results were obtained due to automatic endpoint detection. Further studies will be conducted to investigate the applicability of the OD-mate with orodispersible minitables.

REFERENCES

1. Bi, Y. Hisakadzu, S., 1996. Preparation and evaluation of a compressed tablet rapidly disintegrating in the oral cavity. *Chem. Pharm. Bull.* 44, 2121-2127

EYE-RELATED BIOAVAILABILITY PREDICTION MODEL TO DEFINE PATHWAY OF ABSORPTION ENHANCEMENT (P47)

M. Juretić¹, I. Čaklec¹, B. Cetina-Čižmek², J. Filipović-Gričić¹, I. Pepić¹, A. Hafner¹, J. Lovrić^{1*}

¹ University of Zagreb, Faculty of Pharmacy and Biochemistry, Department of Pharmaceutical Technology, A. Kovačića 1, 10000 Zagreb, Croatia

² Pliva Croatia Ltd., Prilaz B. Filipovića 25, 10000 Zagreb, Croatia

INTRODUCTION

Ocular drug delivery is one of the most challenging issues faced by pharmaceutical researchers because of the specific anatomy, physiology and biochemistry of the eye that makes it practically inaccessible to drugs (1). Current research is focused on the development of innovative delivery nanosystems able to improve eye-related bioavailability and therapeutic outcomes. However, to design such systems, reliable and convenient *in vitro* models are necessary to study mechanisms and/or interactions of interest.

There are two possible routes by which a drug/nanosystem can pass across ocular epithelial barriers, paracellularly - between epithelial cells, and transcellularly - across the cell. The drug transport pathway and mechanism depend on the physicochemical properties such as molecular weight and lipophilicity/hydrophilicity of a drug. The possible transport of nanosystem is defined by its size, surface characteristics and flexibility.

To enable the prediction of eye-related bioavailability of drugs delivered by nanosystems, the cell-based epithelial corneal model has been implemented in our laboratory (2). The aim of this study was to establish a tool for the analysis and prediction of nanosystems transport pathway and mode of their interaction with epithelial barriers by determining the interdependence between temperature, transepithelial electrical resistance (TEER) and appar-



ent permeability coefficient. The final goal is to direct the development of nanosystems toward solutions with improved therapeutic performance.

MATERIALS AND METHODS

HCE-T cells were obtained from Rikken, and were cultivated using DMEM/F12 (Lonza) supplemented with fetal bovine serum (5%, Gibco), insulin (5 µg/ml, AppliChem), dimethyl sulfoxide (0.5%, AppliChem), epidermal growth factor (10 ng/ml, AppliChem), penicillin G sodium salt (100 U/ml, Lonza), streptomycin sulphate (100 µg/ml, Lonza), amphotericin B (0.25 µg/ml, Lonza). The cell-based epithelial corneal model was cultivated on Transwell® polycarbonate filter inserts (Corning) coated with type I rat-tail collagen (Sigma) and fibronectin (Sigma). HCE-T cells suspended in the culture medium were seeded onto the filter and cultivated submerged for seven days, after which they were exposed to the air-liquid interface during the following three days (2). The permeability experiments were performed directly in the Transwell® using Krebs Ringer buffer (KRB pH 7.4; 20 or 37°C; 50 rpm). For the determination of tight junction opening, transepithelial electrical resistance (TEER) was measured during the experiments (EVOM, WPI Inc.).

The quantitative determination of fluorescein and rhodamine B was performed by fluorescence spectroscopy (1420 Multilabel counter VICTOR3, Perkin Elmer).

RESULTS AND DISCUSSION

Permeability of fluorescein, as a paracellular marker, and rhodamine B, as a transcellular marker, was investigated at 20 and 37°C using cell-based epithelial corneal model characterised by different initial TEER. To investigate the effect of temperature on TEER, epithelial corneal models with initial TEER values of 800-1000 Ωcm² measured in culture medium at 37°C were selected. After 30 minutes of incubation in KRB at 37°C TEER was reduced to 50.0±4.7% of initial value (n=24). When the incubation in KRB was performed at 20°C slight reduction in TEER compared to initial values was observed (93.0±11.0%). These results confirmed the influence of temperature on TEER during the incubation in KRB.

The correlation of apparent fluorescein permeability coefficients (P_{app}) across cell-based epithelial corneal model with TEER is presented in Fig. 1.

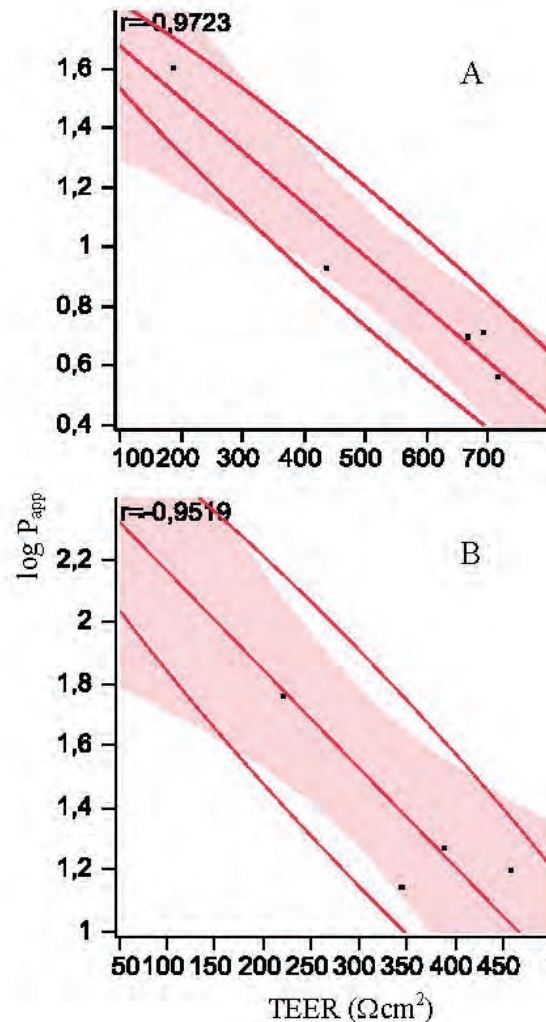


Fig. 1: The correlation of fluorescein $\log P_{app}$ and TEER at 20°C (A) and 37°C (B) (JMP® 10.0.2, SAS Inst. Inc).

The increase in P_{app} of fluorescein with the reduction of TEER is expected since fluorescein is a marker of paracellular pathway.

The relationship of rhodamine B P_{app} across the cell-based epithelial corneal model and TEER is presented in Fig. 2. No influence of TEER on P_{app} of rhodamine B was observed indicating transcellular pathway of rhodamine B transport across cell-based epithelial corneal model. However, P_{app} values at 37°C were higher than at 20°C for similar TEER owing to faster diffusion due to increase in temperature.

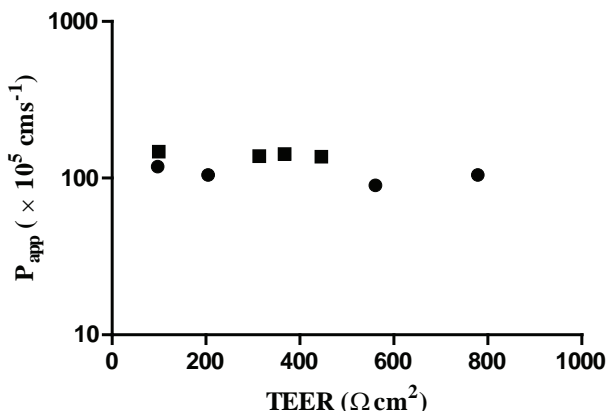


Fig. 2: The relationship of rhodamine B P_{app} and TEER at 20°C (●) and 37°C (■).

CONCLUSIONS

The relationship between fluorescein and rhodamine B P_{app} and TEER established here, confirms the reliability and convenience of the cell-based epithelial corneal model for *in vitro* permeability studies and bioavailability prediction. Moreover, it can serve as a basis for the prediction of nanosystems transport pathway and mode of their interaction with epithelial barriers.

ACKNOWLEDGEMENTS

This work was supported by a Partnership in Research project 04.01/56 funded by the Croatian Science Foundation and PLIVA Croatia LTD.

REFERENCES

1. Pepić I, Lovrić J, Filipović-Grčić J., How do polymeric micelles cross epithelial barriers? *Eur. J Pharm. Sci.* 2013; 50(1):42-55
2. Pepić I, Lovrić J, Cetina-Čizmek B, Reichl S, Filipović-Grčić J. Toward the practical implementation of eye-related bioavailability prediction models. *Drug Discov. Today.* 2014; 19(1): 31-44.

DEVELOPMENT OF ANTIMICROBIAL WOUND DRESSINGS: SPRAY DRIED MUPIROCIN MICROPARTICLES (P48)

M. Lusina Kregar^{1,*}, M. Dürriegl², A. Rožman¹, Ž. Jelčić¹, B. Cetina-Čizmek¹, J. Filipović-Grčić³

¹ Pliva Croatia Ltd., Prilaz baruna Filipovića 25, 10000 Zagreb, Croatia

² PharmaS, Radnička cesta 47, 10000 Zagreb, Croatia

³ Department of Pharmaceutics, Faculty of Pharmacy and Biochemistry, University of Zagreb, A. Kovačića 1, 10000 Zagreb, Croatia

INTRODUCTION

Mupirocin calcium is an antimicrobial agent used for treatment of topical bacterial infections (including wounds and burns) as well as intranasally against methicillin-resistant *S. aureus* (MRSA)(1).

Chitosan is a cationic polysaccharide with antimicrobial properties. Furthermore, chitosan products exhibit biocompatibility, bioadhesion, ability to absorb exudates, wound healing and film forming properties, which makes them good candidates for burn and wound treatment as well as for mucosal administration (2,3).

Eudragit RS is a copolymer of acrylic and methacrylic acid esters used in a variety of pharmaceutical applications, such as film coating of oral formulations or preparation of controlled release matrix systems (e.g. tablets, microparticles). Eudragit RS is a water insoluble, inert and biocompatible polymer (4).

The aim of this study was to prepare mupirocin microparticles using chitosan and Eudragit RS as carriers and to investigate the influence of polymer used on the properties of the obtained microparticle systems.



MATERIALS AND METHODS

Mupirocin calcium dihydrate was kindly donated by PLI-VA Croatia Ltd. Eudragit® RS 100 (ammonio methacrylate copolymer type B) was obtained from Evonik, Germany. Low molecular weight chitosan was obtained from Sigma-Aldrich, USA.

Other chemicals used were of analytical or chromatographic grade.

Spray drying was performed using a Mini Spray Dryer B-290 with Inert Loop B-295 (Büchi, Switzerland).

The spraying solution for chitosan-based microparticles was prepared by mixing chitosan solution (chitosan dissolved in 0.5% acetic acid) and mupirocin calcium dihydrate solution (drug dissolved in methanol). The spraying solution for methacrylate-based microparticles was prepared by dissolving Eudragit® RS 100 and mupirocin calcium dihydrate in methanol.

The microparticles were tested for assay and encapsulation efficiency (HPLC), residual solvent and moisture content (GC, TGA), particle size (image analysis), morphology (SEM), drug-polymer interactions (IR), surface charge (PCS) and swelling properties.

RESULTS AND DISCUSSION

Chitosan-based and methacrylate-based mupirocin microparticles were prepared by spray drying with high process yields (65-81%).

Encapsulation efficiency (percent ratio of actual drug content and theoretical drug content in microparticles) was 85-89% for chitosan-based microparticles and 95-97% for methacrylate-based microparticles.

The water content was around 6% in chitosan-based microparticles and around 1% in methacrylate-based microparticles. The water content depended on the sample composition (and hysteresis of the components).

Low content of moisture is beneficial for the stability of mupirocin products as mupirocin is susceptible to hydrolysis. Analyses of samples stored at ambient conditions have shown that mupirocin degradation rate was higher for chitosan-based microparticles than for methacrylate-based microparticles.

The content of residual methanol in spray dried samples was below the ICH limit of 3000 ppm.

The mean diameter of the produced microparticles was within the range 2 µm – 4 µm.

The morphologies (examined by SEM) of the individually spray dried polymers (blank microparticles) and the respective drug-loaded polymeric microparticles were different. In case of methacrylate-based microparticles the shape changed from "raisin"-like to sub-spherical after incorporation of drug into microparticles. For chitosan-

based microparticles the shape changed from a mixture of smooth spherical and "golf ball"-like to smooth spherical after incorporation of drug into microparticles.

The surface charge of the spray dried drug was negative. However, positive surface charge was obtained after incorporation of mupirocin into polymeric microparticles, indicating that the surface of the particles was mostly covered with polymer. This was confirmed also by elemental mapping (EDS/SEM). Positive charge of chitosan is generally believed to be responsible for its antimicrobial and bioadhesive properties (2).

The swelling properties and fluid uptake ability of the microparticles were evaluated by placing the samples in contact with aqueous medium. The fluid uptake was higher for chitosan-based microparticles which swell and form a gel than for methacrylate-based microparticles.

Hydrogels can promote wound repair by providing a moisturized wound healing environment and are therefore often used as modern wound dressings. Fluid uptake ability is also a desired property of a wound dressing as it prevents the accumulation of exudates in the wound (5). In addition antimicrobial activity of methacrylate-based mupirocin-loaded microparticles was previously tested by our group (1,6). A time-kill assay was performed using *S. aureus* (ATCC 29213) and methicillin-resistant *S. aureus* (MRSA). The results confirmed that encapsulation of mupirocin did not compromise its antibacterial activity.

CONCLUSIONS

Both chitosan-based and methacrylate-based mupirocin microparticles were successfully prepared by spray drying with high process yields.

Both types of microparticles produced seem to be appropriate candidates for further development of topical delivery systems of mupirocin.

The microparticle shape, size, surface charge, moisture content and swelling properties were found to be dependent on the type of polymer used – therefore the choice of polymer would depend on the desired characteristics of the final product.





REFERENCES

1. Dürriegl M, Kwokal A, Hafner A, Šegvić Klarić M, Dumičić A, Cetina-Čižmek B, Filipović-Grčić J. Spray dried microparticles for controlled delivery of mupirocin calcium: Process-tailored modulation of drug release. *J. Microenc.* 2011; 28: 108-121.
2. Dai T, Tanaka M, Huang YY, Hamblin MR. Chitosan preparations for wounds and burns: antimicrobial and wound-healing effects. *Expert. Rev. Anti. Infect. Ther.* 2011; 9: 857-879.
3. Agnihotri SA, Mallikarjun NN, Aminabhavi TM. Recent advances on chitosan-based micro- and nanoparticles in drug delivery. *J. Contr. Rel.* 2004; 100: 5-28.
4. Dittgen M, Durrani M, Lekmann K. Acrylic polymers: A review of pharmaceutical applications. *S.T.P. Pharma Sciences* 1997; 7: 403-437.
5. Wittaya-areekul S, Prahsarn C. Development and in vitro evaluation of chitosan-polysaccharides composite wound dressings. *Int. J. Pharm.* 2006; 313: 123-128.
6. Dürriegl M, Lusina Kregar M, Hafner A, Šegvić Klarić M, Filipović-Grčić J. Mupirocin calcium microencapsulation via spray drying: feed solvent influence on microparticle properties, stability and antimicrobial activity. *Drug. Dev. Ind. Pharm.* 2011; 27:1402-1414.

EXPERIMENTAL DESIGN OF ONDANSETRON FILM-COATED TABLETS 8 MG (P49)

R. Markovska^{*1}, L. Makraduli¹

¹ReplekFarm Ltd., 1000 Skopje, Republic of Macedonia

INTRODUCTION

Ondansetron Hydrochloride Dihydrate is Serotonin 5HT₃ antagonist and it is used for treatment of nausea and vomiting. The chemical name of this drug entity is (3RS)-9-Methyl-3-[(2-methyl-1H-imidazol-1-yl) methyl]-1, 2, 3, 9-tetrahydro-4H-carbazol-4-one hydrochloride dihydrate. It is present as white or almost white powder, sparingly soluble in water and in alcohol, soluble in methanol, slightly soluble in methylene chloride.¹

Ondansetron is especially effective for preventing nausea after protocol treatment with antineoplastic drugs, for example, cisplatin and cyclophosphamide.²

Using D-Optimal design in this experiment, the design space for the pharmaceutical dosage form Ondansetron film-coated tablets 8 mg was predicted. All the significant factors that influenced the disintegration time of Ondansetron film-coated tablets were predicted and analyzed using the computer software Design Expert v. 8.0. The optimal formulation according to the obtained results from analysis of the desirability factor was chosen³

MATERIALS AND METHODS

- Ondansetron HCl dihydrate [E.P], Shodhana Laboratories Ltd
- Calcium hydrogen phosphate, anhydrous Anhydrous Emcompress[®] JRS Rettenmaier & Soehne GmbH+Co KG
- Partially Pregelatinized Maize Starch, Starch 1500[®], Colorcon, Member of the Berwind Pharmaceutical Group, West Point, PA
- Lactose monohydrate, Tablettose[®] 80, Meggle GmbH, Germany
- Crospovidone, Polyplasdone XL-10[®], ISP Fine Chemicals, USA
- Silica, colloidal, anhydrous, Aerosil 200, Degussa, Germany
- Magnesium stearate, Mosselman, Belgium





D-optimal design with 17 model points and 5 replications was used. The total number of predicted experiments was 27. The dependence between chosen variables (dependent and independent variables) was described using Response surface method - Quadratic model.⁴ For the independent variables (responses) in our study were chosen: (A) Concentration of the disintegrant Polyplasdone XL-10 (min. 4%, max. 10%); (B) Concentration of the filler/ disintegrant Starch 1500 (min. 7%, max. 15%) and (C) Concentration of the lubricant Magnesium stearate (min. 1%, max. 2.5%).

As dependent variables (responses) were analyzed:

- (Y1) Disintegration time (sec.),
- (Y2) Dissolution time (>80%, for 45 min.),
- (Y3) Hardness (N),
- (Y4) Friability (%) and
- (Y5) Mass variation (%)

RESULTS AND DISCUSSION

The obtained results from the Design Matrix Evaluation for Response Surface Quadratic Model are presented in the following table:

Tab. 1: Design Matrix Evaluation

No aliases found for Quadratic Model	Aliases are calculated based on your response selection, taking into account missing datapoints, if necessary
Degrees of Freedom for Evaluation	
Model	9
Residuals	17
Lack Of Fit	10
Pure Error	7
Corr Total	26
A recommendation is a minimum of 3 lack of fit df and 4 df for pure error.	
This ensures a valid lack of fit test.	
Fewer df will lead to a test that may not detect lack of fit.	

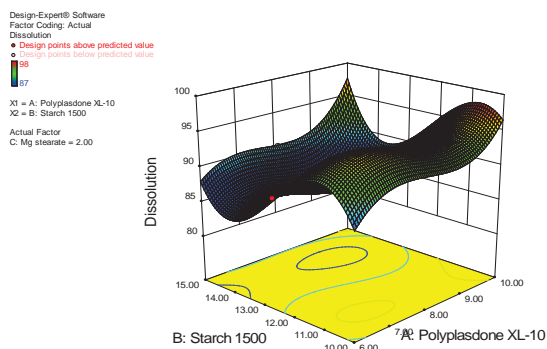


Fig. 1 3D Model graph of parameter dissolution

Tab. 2: Numerical optimization of formulation of Ondansetron film-coated tablets 8 mg

Number	1
Polyplasdone XL-10	10.00
Starch 1500	9.01
Mg stearate	1.75
Predicted Parameters	
Disintegration time	20.000
Dissolution	87.3408
Hardness	50.0826
Friability	0.318623
Mass variation	0.951224
Desirability	0.817
Selected optimal formulation	

CONCLUSIONS

According to the obtained recommendations from the Design Matrix Evaluation for the chosen model of the D-optimal design, it was decided to perform practically all the 27 experimental runs. The obtained results from the physicochemical analysis of the film-coated tablets were evaluated. Two of the experimental trials that have shown the best results from the physicochemical analysis at the beginning, were selected and set for the regular stability studies, according to the prescribed stability protocol. During the experimental work, it was confirmed that the optimised formulation which was selected and recommended by Design Expert v 8.0, with desirability factor of 0.817, was also the formulation which have shown best analysis results and best technological performance during manufacturing process. In addition, the quality control results were within the limits during the stability testing of the formulation and it is a good candidate for market launch.

REFERENCES

1. *British Pharmacopoeia 2012, Volume II, Ondansetron Hydrochloride Dihydrate (Ph Eur Monograph 2016)*, p. 1604;
2. *Sean C. Sweetman et al., MartinDale: The Complete Drug Reference, 36 edition, 2009; p.700-703, p.1692, p.1756-1758;*
3. *Huairui guo, Ph.D. & Adamantios Mettas, Design of Experiments and Data Analysis, 2010 Annual Reliability and Maintainability Symposium*
4. *Design-Expert® software Version 8, Stat-Ease, Inc.*



PHYSICO-CHEMICAL CHARACTERIZATION OF TERNARY CARBAMAZEPIN-SOLUPLUS®-POLOXAMER 188 SOLID DISPERSIONS

(P50)

Đ. Medarević^{1,*}, P. Kleinebudde², J. Đuriš¹, Z. Đurić¹, S. Ibrić¹

¹ Department of Pharmaceutical Technology and Cosmetology, Faculty of Pharmacy, University of Belgrade, Vojvode Stepe 450, 11221 Belgrade, Serbia, e-mail: djordje.medarevic@pharmacy.bg.ac.rs

² Institute of Pharmaceutics and Biopharmaceutics, Heinrich-Heine-University Duesseldorf, Universitaetsstr.1, 40225 Duesseldorf, Germany, kleinebudde@uni-duesseldorf.de

INTRODUCTION

Formulation of solid dispersions (SDs) where the drug is dispersed or dissolved within the polymeric matrix is a powerful method to improve solubility of poorly soluble

drugs. Using of polymeric mixtures, instead of single polymers, can facilitate SDs preparation process and further improve drug dissolution rate and dispersion stability (1,2). The aim of this study was to perform physicochemical characterization of carbamazepine (CBZ)-Soluplus-poloxamer 188 (P188) ternary SDs in order to get insight into CBZ physical state within the dispersion and to determine the influence of the type of solvent used for SDs preparation on the drug physical state in the dispersion.

MATERIALS AND METHODS

Materials

CBZ, donated by Galenika AD (Belgrade, Serbia), Soluplus®, micronized poloxamer 188 (P188-Kolliphor® P188 micro), both kindly donated by BASF (Ludwigshafen, Germany), absolute ethanol (Merck, Darmstadt, Germany) and methanol (Merck, Darmstadt, Germany) were used for SDs preparation.

SDs preparation and characterization

SD formulations were prepared according to 22-run D-optimal mixture experimental design, with the following constraints: $20\% \leq \text{CBZ} \leq 50\%$, $30\% \leq \text{Soluplus} \leq 80\%$, $0\% \leq \text{P188} \leq 20\%$. CBZ, Soluplus and P188 were firstly dissolved in absolute ethanol, followed by ethanol evaporation on glass slides at 60°C. Obtained mass was scraped off and pulverized after 48 h. Nine formulations (Table 1.) were identified as representative and chosen for physicochemical characterization. Additionally, formulations F5 and F6 were also prepared using methanol as a solvent (F5 methanol and F6 methanol).

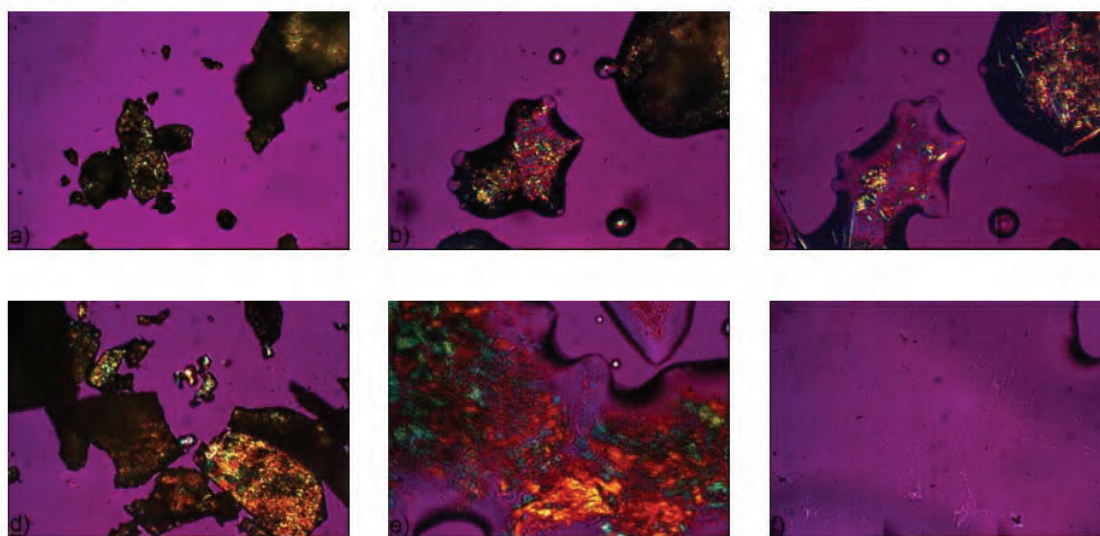


Fig. 1. HSM photomicrographs of formulation F1 at 120°C (a), 170°C (b) and 180°C (c) and formulation F7 at 120°C (d), 170°C (e) and 180°C (f)



Table 1. SD formulations selected for physicochemical characterization

	CBZ (%)	Soluplus (%)	P188 (%)
F1	50.00	48.92	1.08
F2	50.00	39.47	10.53
F5	26.15	68.82	5.03
F6	20.00	80.00	0.00
F7	34.53	45.53	19.94
F12	41.61	48.30	10.09
F13	47.26	32.74	20.00
F22	33.86	62.73	3.41
F23 ¹	15.00	85.00	0.00

¹additional formulation, not included in the D-optimal experimental design matrix

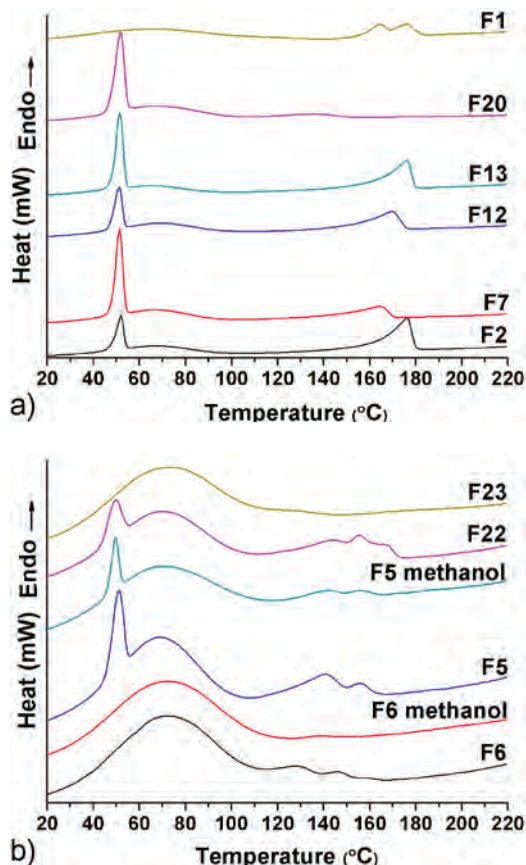


Fig. 2. DSC thermograms of the prepared SDs

Physicochemical characterization of SD samples was performed by differential scanning calorimetry (DSC), powder X-ray diffraction (PXRD) and hot-stage polarized light microscopy (HSM).

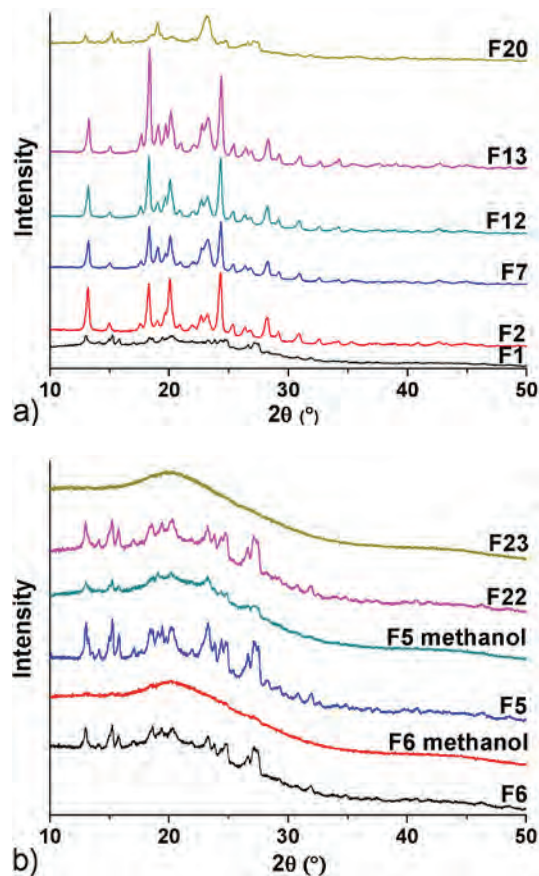


Fig. 3. PXRD pattern of the prepared SDs

RESULTS AND DISCUSSION

Characteristic peaks, arising from the melting of CBZ polymorph III, are evident on the DSC thermograms of all SDs prepared with ethanol (Fig. 2a and 2b). Formulations containing P188 showed peaks of this component, except formulation F1 that contain about 1% of P188. Since both CBZ and P188 were present in the same crystal forms as the starting materials within amorphous Soluplus matrix, these systems should be considered as immiscible in the investigated concentration range. PXRD analysis confirmed crystalline nature of CBZ in the SDs. Both DSC and PXRD showed the presence of amorphous CBZ in the formulation F6 (20% CBZ, 80% Soluplus), prepared with methanol (F6 methanol), while in the SD of the same composition, prepared with ethanol, CBZ was in the crystalline state. Since in the formulation F23 (15% CBZ, 85% Soluplus) CBZ was in the amorphous state, it can be concluded that up to 15% of CBZ can be dispersed in the amorphous state within the Soluplus matrix, if ethanol is used as a solvent. Using of methanol, instead of ethanol,



enables that higher amount of CBZ can be dispersed in the amorphous state. As methanol evaporates faster, due to its higher vapour pressure, less time is available for CBZ crystallization from the solution, which results in the dispersions with lower drug crystalline content. Addition of P188 further facilitates CBZ crystallization by lowering Tg of the mixture. Crystals of P188 can also act as nuclei for CBZ crystallization. Dispersion of CBZ crystals within polymeric matrix is observable on the HSM micrographs of formulations F1 and F7 (Fig. 1a-1f). Change from prismatic (polymorph III) to needle shape (polymorph I) CBZ crystals upon heating is observed on the micrographs of formulation F1, containing higher proportion of CBZ.

CONCLUSIONS

CBZ was present in the crystal form in the ternary CBZ-Soluplus-P188 SDs, prepared with ethanol. Choice of solvent for SD preparation significantly influenced the drug physical state within the dispersion, whereas using methanol enabled preparation of amorphous SDs with higher CBZ content.

ACKNOWLEDGMENT

This work was supported by the project TR34007, funded by the Ministry of Education, Science and Technological Development, Republic of Serbia and bilateral Serbia-Germany project: Application of machine learning tools in establishing a design space in solid dosage forms development.

REFERENCES

1. Bley H, et al. *Int. J. Pharm.* 2010; 390: 165-173.
2. Janssens S, et al. *Int J Pharm.* 2008; 355:100-107.

AN INVESTIGATION INTO THE EFFECT OF DRUG LOAD AND TABLET DIAMETER ON THE CHARACTERISTICS OF ORODISPERSIBLE TABLETS PREPARED WITH DISINTEQUIK™ ODT (P51)

M. Momčilović^{1,*}, N. Cvetković², Dj. Medarević¹, S. Cvijić¹, J. Parojčić¹

¹ Department of Pharmaceutical Technology and Cosmetology, Faculty of Pharmacy, Vojvode Stepe 450, Belgrade 11221, Serbia

² Galenika a.d., Institute for Research and Development, Batajnički drum b.b, Belgrade, Serbia

INTRODUCTION

Although being most commonly used dosage forms, conventional solid oral dosage forms have certain disadvantages (e.g. difficulties in swallowing in some patients) (1). In order to overcome this drawback, a new category of tablets, called orodispersible tablets (ODTs) emerged over the last two decades as a convenient alternative to conventional solid oral dosage forms (2). ODTs are intended to disintegrate rapidly in the oral cavity and be swallowed without the need for water (3). A variety of excipients could be used to formulate ODTs by direct compression. Recently, a new generation of co-processed excipients was developed to facilitate manufacturing and improve characteristics of ODTs (4). One of them is Disintequik ODT, which consists of lactose monohydrate, spray dried mannitol, crospovidone and dextrose monohydrate. Data on its application in ODT formulations are still lacking. The purpose of this study was to assess the effect of drug load and tablet diameter on the characteristics of ODTs prepared with Disintequik™ ODT and caffeine as a model substance.



MATERIALS AND METHODS

The materials used were: Disintequik™ ODT (Kerry, USA), Pruv® (Penwest Pharmaceuticals Co) and caffeine (Ph.Eur). ODT formulations with different drug load (0, 25 and 50% caffeine) were prepared by mixing appropriate amounts of Disintequik™ ODT, caffeine and 0,5% Pruv® and compressed on a single-punch tablet press, using dies with different diameters (6, 9 and 12 mm). Filling volume for each sample was adjusted to yield tablets of uniform thickness. Tablets were analyzed regarding hardness, friability, disintegration time (DT), wetting time (WT) and water absorption ratio (WAR). Tablets hardness, friability and disintegration time (DT) were tested according to European Pharmacopoeia. WT and WAR were determined using slightly modified method described by Bi et al (2). Simulated saliva (5) was used as a medium. In addition, tensile strength was calculated based on tablet's hardness, diameter and thickness.

The influence of formulation parameters (caffeine load- X_1 and tablet diameter - X_2) on tensile strength- Y_1 , friability- Y_2 , DT- Y_3 , WT- Y_4 , and WAR- Y_5 was investigated using 3-level factorial design of experiments (DoE). Statistical significance of parameters effect was estimated based on the p-values ($p < 0,05$).

RESULTS AND DISCUSSION

The experimental design summary is shown in Tab.1. According to the obtained results, tablet diameter showed significant influence on the mechanical characteristics (tensile strength and friability) of the ODTs. Smaller tablets had better mechanical properties, as increase in tablet diameter led to a decrease in their tensile strength and increase in their friability. Relationships between tablet diameter and tensile strength and friability, respectively, are shown in Fig.1.

Tab.1. Experimental design

Formulation parameters (input)		Tablet characteristics (output)				
X_1 (%)	X_2 (mm)	Y_1 (N/mm ²)	Y_2 (%)	Y_3 (s)	Y_4 (s)	Y_5 (%)
0	6	2,12	0,37	29,83	24,45	55,12
25	6	1,71	0,69	23,76	18,69	45,47
50	6	1,61	0,92	16,67	10,50	52,29
0	9	0,54	4,20	42,85	32,71	54,39
25	9	1,22	2,70	27,28	27,35	44,93
50	9	1,03	3,89	18,78	19,90	47,24
0	12	0,63	5,16	49,02	41,65	50,01
25	12	0,80	*	33,00	27,46	42,14
50	12	0,82	*	19,17	18,64	45,33

* tablets broken

Statistical analysis of factor effects revealed that caffeine load and tablet diameter, as well as their combined effect, significantly affect tablet disintegration time. Namely, increase in caffeine load, as well as decrease in tablet diameter, decreased disintegration time of the investigated tablets. Representative response surface depicting the influence of drug load and tablet diameter on tablet disintegration time is shown in Fig.2. Still, all the recorded DT values complied with European Pharmacopoeia requirements for ODT.

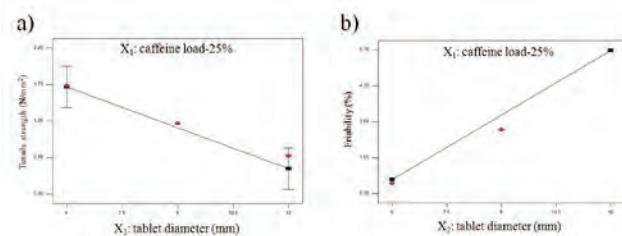
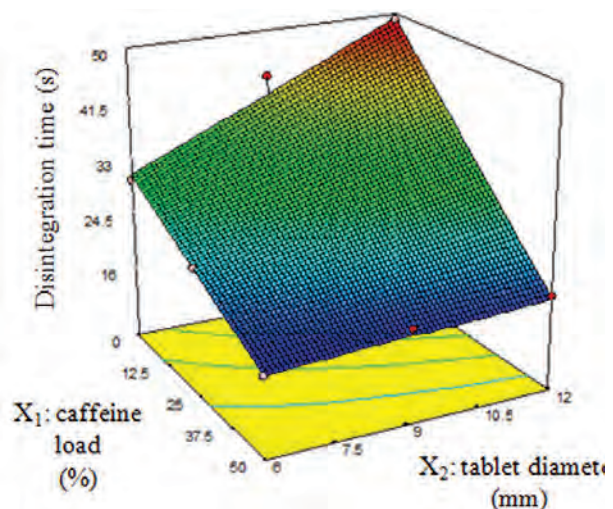


Fig.1. The effect of tablet diameter on: a) tablet tensile strength and b) tablet friability

Wetting time of the investigated ODTs was also influenced by both caffeine load and tablet diameter. Increase in the amount of caffeine and decrease in tablet diameter resulted in the reduced tablets wetting time.

Increase in tablet diameter, irrespective of caffeine load led to decrease in WAR. Changes in WAR values were not in direct correlation with caffeine load. Water absorption ratio was the greatest for tablet samples without caffeine.



$$Y_3 = 29,83 - 11,18X_1 + 5,15X_2 - 4,17X_1X_2$$

Fig.2. The effect of drug load and tablet diameter on tablet disintegration time





CONCLUSIONS

The results obtained demonstrate that drug load and tablet diameter had statistically significant influence on tablet characteristics. Disintequik™ ODT can be used for direct compression of tablets with high drug load. DoE is useful tool for the evaluation of the individual and interactive effect of formulation factors and identification of critical quality attributes in the early stages of drug product development.

ACKNOWLEDGEMENTS

This work was done under the project TR 34007, supported by the Ministry of Education, Science and Technological Development of the Republic of Serbia. The authors would like to thank Kerry (Beloit, Wisconsin, USA) for providing Disintequik™ ODT sample.

REFERENCES

1. Llorca PM. Discussion of prevalence and management of discomfort when swallowing pills: orodispersible tablets expand treatment options in patients with depression. *Ther Deliv.* 2011; 2(5): 611-22.
2. Bi Y, Sunada H, Yonezawa Y, Danjo K, Otsuka A, Iida K. Preparation and evaluation of a compressed tablet rapidly disintegrating in the oral cavity. *Chem. Pharm. Bull.* 1996; 44: 2121-2127.
3. Parkash V, Maan S, Deepika, SKY, Hemlata VJ. Fast Disintegrating tablets: Opportunity in drug delivery system. *J. Adv. Pharm. Tech. Res.* 2011; 2(4): 223-235.
4. Chaudhary SA, Chaudhary AB, Mehta TA. Excipients updates for orally disintegrating dosage forms. *Int. J. Res. Pharm. Sci.* 2010; 1(2): 103-107.
5. Peh KK, Wong, CF. Polymeric films as vehicle for buccal delivery: swelling, mechanical, and bioadhesive properties. *J. Pharm. Pharm. Sci.* 1999; 2(2): 53-61.

CONDUCTIVITY AND PH VALUES OF NANOSPHERES FOR TARGETED DRUG DELIVERY ASSESSED IN THE COURSE OF THE FORCED EQUILIBRIUM DIALYSIS (P52)

W. Musiał^{1*}, J. Pluta², J. Volmajer Valh³

¹ Wrocław Medical University, Faculty of Pharmacy, Department of Physical Chemistry, Borowska 211, 50-556 Wrocław, Poland

² Wrocław Medical University, Faculty of Pharmacy, Department of Pharmaceutical Technology, Borowska 211, 50-556 Wrocław, Poland

³ University of Maribor, Faculty of Mechanical Engineering, Laboratory for Chemistry, Dyes and Polymers, Smetanova 17, 2000 Maribor, Slovenia

INTRODUCTION

Nanospheres have numerous potential applications for medical and pharmaceutical purposes [1-3]. They are proposed as drug delivery carriers, due to small diameters in the range below the size of the blood capillaries. One of the main problems is the impurity of the resulting nanospheres which are usually synthesized in various sorts of emulsion or precipitation polymerization. The purity of produced nanospheres is of high importance in the case of peroral or parenteral applications.

The aim of the study was evaluation of the conductivity and pH of the dispersions of nanospheres - synthesized by surfactant free precipitation polymerization (SFPP) with the use of main monomer: NIPA (N-isopropylacrylamide), crosslinker: MBA (methylene-bis-acrylamide), and anionic co-monomer: AcA (acrylic acid) - in the course of purification of the dispersions via FED (forced equilibrium dialysis).





MATERIALS

In the course of SFPP the following reagents were used: N-isopropylacrylamide (NIPAM, Aldrich, USA, 97%), N, N'-methylenebisacrylamide, (BMA, Aldrich, USA, 99%), ammonium persulfate (APS, Aldrich, Germany, 98%), acrylic acid (AcA, Aldrich, Germany, 99%), purified water of conductivity not exceeding 5 mS cm⁻¹ (osmotic column ODOS-20 Preksim, Poland, with Excelon PES filter, Germany).

METHODS

Glass, round-bottom, four-necked reactor with a volume of 2l, was used to perform the synthesis in the conditions of SFPP, performed in our laboratories earlier. The four-necked cover enabled the control of the environment, and the introduction of the reactants. The temperature was controlled by a contact thermometer, and a magnetic stirrer with a "feed-back" heating element. The reactor was placed in a 5l water bath which was set on a magnetic stirrer.

After completion of the SFPP in inert nitrogen atmosphere the nanospheres have been subjected to the purification via equilibrium dialysis in the system visualized on the Figure 2. 30 mL of every dispersion of nanospheres (A-I to A-VI) was closed in containers prepared from semi-permeable membrane of MWCO ca. 14.000 Da (donor compartment), and placed in glass cuvettes filled by 300 mL of deionized water (acceptor compartment). The water was replaced in regular time periods through 10 days. After 10 days the conductivity in acceptor compartment decreased to stable low values in the range between 2,01 – 2,78 μS×cm⁻¹, and the process was considered as finished. The conductivity and pH was measured before and after purification of nanospheres via forced equilibrium dialysis, in the donor compartment. Membrane with MWCO of 14.000 Da was applied in the process. The measurements evaluated in this study include the initial and final values, from the dialysis which was performed through 10 days, to the stable values of conductivity and pH. We used the Multifunction Computermeter CX-741 (Elmetron, Poland), with glass electrode KSAgP-301 W 887 (Eurosens, Poland) for pH measurements, and with conductivity sensor EPS-2ZN (Eurosens, Poland) with cell constant of 0,85 cm⁻¹ for the conductivity assessments. The measurements were taken in the solution.

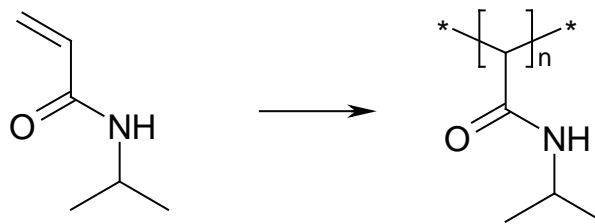


Figure 1. NIPA and polyNIPA

RESULTS AND DISCUSSION

Nanospheres conductivity evaluated in the donor compartment directly after the reaction was in the range between 736,85 ± 8,13 μS×cm⁻¹ and 1048,90 ± 67,53 μS×cm⁻¹. The conductivity of dispersions of nanospheres A-I to A-III, obtained by stirring with the speed of 500 rpm was slightly lower, comparing to that of dispersions of nanospheres A-IV to A-VI synthesized in the same conditions but with higher stirring speed of 1000 rpm. The pH of the post-reaction mixtures was in the range between 3,42 ± 0,23 and 4,30 ± 0,22. The pH values were higher in the case of post-reaction mixtures prepared via stirring at 500 rpm, namely 3,91 ± 0,16 - 4,30 ± 0,22. When stirred with higher speed of 1000 rpm, the reacting mixtures gained the values 3,42 ± 0,23 - 3,62 ± 0,15. The visualisation of the obtained batches of the polyNIPA derivatives is presented in the Fig. 2.

A-I and A-IV are transparent, whereas the A-II and A-V are non-transparent, due to the presence of dense dispersion of cross-linked macromolecules. In A-III and A-VI the high conductivity is connected to the excess of ions released from the carboxyl groups implemented during the polymerization. Some other factors, like the polarization patterns within the macromolecule may also enhance the ionization of the particle, however the evaluation of the phenomena oversteps the field of this study.

CONCLUSIONS

Conductivity and pH measurements performed during the purification via the forced equilibrium dialysis give important information on the composition of resulting nanospheres. If there is a possibility of comparison of nanospheres prepared in controlled conditions, sound information may be evoked. The presence of crosslinker, and acidic co-monomer implemented into polyNIPA macromolecule may be confirmed both by the pH, and by the conductivity measurements. The stirring speed has impact on the resulting conductivity and pH of obtained dispersions of nanospheres.



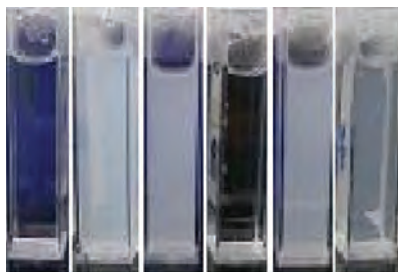


Figure 2. Macro photographs of the dispersions of synthesized nanospheres A-I to A-VI, from left (transparent A-I), to right (semi-transparent A-VI).

REFERENCES

1. J.N. Oh, D.I. Lee and J.M. Park, *Biopolymer-based microgels/nanogels for drug delivery applications*, *Progress in Polymer Science* 34, 1261-1282 (2009).
2. J.N. Oh, R. Drumright, D.J. Siegart et al., *The development of microgels/nanogels for drug delivery applications*, *Progress in Polymer Science* 33, 448-477 (2009).
3. J. Zhou, G. Wang, L. Zou et al., *Viscoelastic Behavior and In Vivo Release Study of Microgel Dispersions with Inverse Thermoreversible Gelation*, *Biomacromolecules* 9, 142-148, (2008).

CO-SPRAY DRYING OF A COCRYSTAL WITH INULIN BOTH IMPROVES PROCESS EFFICIENCIES AND ENHANCES DISSOLUTION (P53)

B.A. Norris^{1*}, D.R. Serrano¹, A.M. Healy¹

¹ School of Pharmacy and Pharmaceutical Sciences, Trinity College Dublin, College Green, Dublin 2, Ireland

INTRODUCTION

Sulfadimidine (SDM) is a poorly soluble anti-infective active pharmaceutical ingredient included in Class 2 of the Biopharmaceutics Classification System. Pharmaceutical cocrystals can improve the solubility, dissolution and bio-availability of poorly water soluble drugs (1). In order to improve the dissolution profile, cocrystals of SDM, using 4-amino salicylic acid (4ASA) as coformer, were formed by the spray drying method, a well-established and effective scale-up technique in the production of cocrystals (2). In addition, a carrier excipient, inulin, (a hydrophilic, biochemically inert and non-toxic excipient for humans (3)) was introduced into the process with the aim of further improving the dissolution characteristics, while minimising the number of unit operations required to obtain a final pharmaceutical form. Cocrystal formation by spray drying in the presence of the third component, i.e. the carrier, was investigated. Dissolution profiles were also assessed.

MATERIALS AND METHODS

Three solution concentrations of 1% (w/v) of SDM:4ASA (Sigma Aldrich, Ireland) in a 1:1 molar ratio were prepared using ethanol. Inulin with a degree of polymerisation of 10 (Fruitafit[®] HD, Sensus, Netherlands) was dissolved in deionised water and then added in increasing amounts to the solutions containing the cocrystal components, so that the final concentration of inulin in solution was 0, 0.1 and 0.5% w/v. The solutions were spray dried using a Büchi B-290 Mini Spray Dryer operating in the open mode





(pump speed 30%, aspirator 100%, nitrogen flow rate 473 NI/h). A physical mixture of spray dried cocrystal and inulin (50/50, w/w) was also prepared by gentle mixing in an agate mortar and pestle. Solid products were analysed by Powder X-ray Diffraction (PXRD), Differential Scanning Calorimetry (DSC) and Attenuated Total Reflectance Fourier Transform Infra Red Spectroscopy (FTIR). Flow-through cell dissolution and intrinsic dissolution testing (using the paddle apparatus) were carried out according to USP specifications using deionised water as the dissolution medium (4-5). Results were analysed by HPLC. Dissolution studies were performed in triplicate.

RESULTS AND DISCUSSION

PXRD analysis (Fig. 1) showed that the characteristic peaks for the cocrystal form prepared by spray drying differ to those of the individual components, SDM and 4ASA. Cocrystal formation occurred in the presence of inulin: the same diffraction peaks were exhibited, but the intensity of the diffraction peaks was decreased compared to the physical mixture of cocrystal and inulin, probably due to some cocrystal amorphising during the spray drying process.

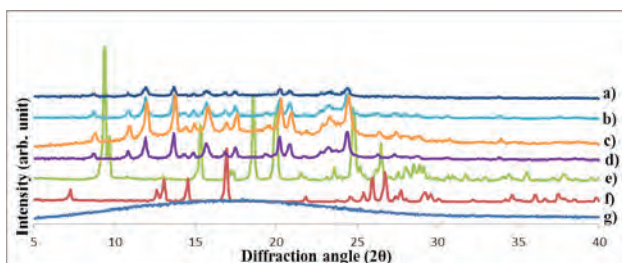


Fig. 1: PXRD patterns of a) cocrystal-in-50% inulin system, b) cocrystal-in-10% inulin system, c) physical mixture of cocrystal and inulin (50/50, w/w), d) spray dried cocrystal, e) SDM, f) 4ASA, g) inulin.

DSC results (Fig. 2) showed that the melting point of the cocrystal was between those of SDM and 4ASA. The melting points of the cocrystal-in-inulin systems were similar to that of the spray dried cocrystal, showing that cocrystal formation still occurred in the presence of the carrier excipient, inulin.

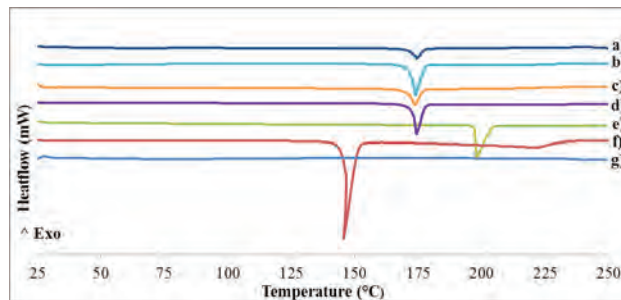


Fig. 2: DSC thermograms of a) cocrystal-in-50% inulin system, b) cocrystal-in-10% inulin system, c) physical mixture of cocrystal and inulin (50/50, w/w), d) spray dried cocrystal, e) SDM, f) 4ASA, g) inulin.

FTIR results demonstrated shifts to different wavelengths for the spray dried cocrystal and cocrystal-in-inulin systems with respect to the pure components. Shifts were attributable to intermolecular interactions, such as hydrogen bonding (shifts in bands at 3482 and 3372 cm^{-1} attributable to the NH_2 stretching of the amine groups, and SO_2 stretching vibrations in SDM and OH bending of the carboxyl group in 4ASA at 1315 and 1275 cm^{-1} respectively). Flow-through cell dissolution testing (Fig. 3) revealed that the presence and increasing concentration of inulin in the system resulted in increased dissolution of the cocrystal. For example, at 30 minutes, there was a 4.6 fold increase in dissolution when it was co-spray dried with 50% inulin.

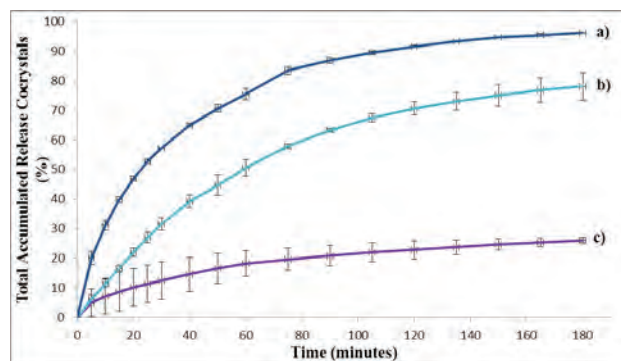


Fig. 3: Dissolution profiles from flow-through cell dissolution testing of a) cocrystal-in-50% inulin system, b) cocrystal-in-10% inulin system, c) spray dried cocrystal

Intrinsic dissolution testing (Fig. 4) revealed that dissolution of the cocrystal-in-inulin systems and the spray dried cocrystal was linear for the first 30 minutes. During this time, the cocrystal-in-50% inulin system showed a 3.8 fold increase in dissolution rate compared to both the cocrystal-in-10% inulin system and the spray dried cocrystal.



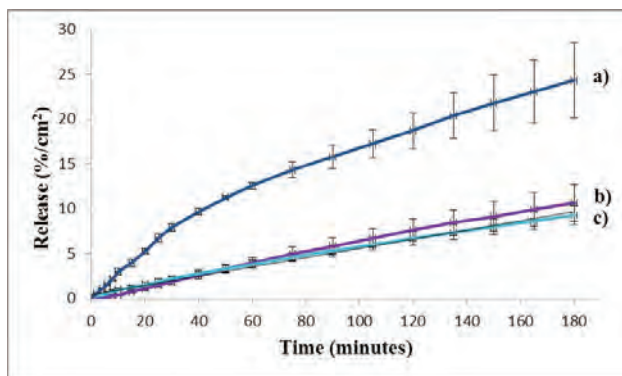


Fig. 4: Dissolution profiles from intrinsic dissolution rate studies of a) cocrystal-in-50% inulin system, b) spray dried cocrystal, c) cocrystal-in-10% inulin system

CONCLUSIONS

Inclusion of inulin as a third component in a solution containing SDM and 4ASA still leads to the formation of the SDM-4ASA cocrystal on spray drying. The inclusion of inulin enhances the dissolution properties of the cocrystal. The spray drying also improves process efficiencies, facilitating cocrystal formation and incorporation into a carrier excipient in a one-step process, effectively consolidating unit operations.

ACKNOWLEDGEMENT

This publication has emanated from research conducted with the financial support of Science Foundation Ireland (SFI) under Grant Number SFI/12/RC/2275.

REFERENCES

1. Good DJ, Rodríguez-Hornedo N, Solubility advantage of pharmaceutical cocrystals, *Cryst. Growth Des.*, 2009, 9 (5), 2252–2264
2. Alhalaweh A, Velaga SP, Formation of cocrystals from stoichiometric solutions of incongruently saturating systems by spray drying, *Cryst. Growth Des.*, 2010, 10, 3302–3305
3. Barclay T, Ginic-Markovic M, Cooper P, Petrovsky N, Inulin – a versatile polysaccharide with multiple pharmaceutical and food chemical uses, *J. Excipients and Food Chem*, 2010, 1 (3), 27–50
4. Grossjohann C, Eccles KS, Maguire AR, Lawrence SE, Tajber L, Corrigan OI, Healy AM, Characterisation, solubility and intrinsic dissolution behaviour of benzamide: dibenzyl sulfoxide cocrystal, Vol. 422, Issues 1-2, *International Journal of Pharmaceutics* 2012, 24–32.
5. USP, General Chapter Dissolution 711

EFFECTS OF A NEW GLIDANT SYLOID ON THE TABLET COMPACTION PROCESS (P54)

P. Ondřejček^{1,*}, P. Svačinová¹, J. Stoniš¹, M. Řehula¹, M. Rabišková¹

¹ Department of Pharmaceutical Technology, Charles University in Prague, Faculty of Pharmacy in Hradec Králové, Heyrovského 1203, 500 05 Hradec Králové, Czech Republic

INTRODUCTION

Glidants play very important role in the production of tablets. They are used to increase the flow rate of powdered tableting mixtures, to prevent sticking of the tablets to the punches and the die, or to provide easier ejection of tablet (1).

Magnesium stearate is classical hydrophobic glidant, that has many negative properties. It reduces tablet hardness, prolongs tablet disintegration and dissolution time, and thus slows the drug release. Sodium stearyl fumarate is newer glidant and compared with the magnesium stearate it has a less significant negative effects (2). Micronized synthetic amorphous silica gel, produced under the brand name Syloid, belongs to new hydrophilic glidants. It can be used as glidant, tableting aid, carrier of active ingredients, disintegrant, desiccant, etc (3). In this experiment, this new glidant Syloid was compared to magnesium stearate and sodium stearyl fumarate.

MATERIALS AND METHODS

Microcrystalline cellulose Avicel PH 200 manufactured by FMC Corporation was used as model pharmaceutical filler for direct compression. Magnesium stearate and sodium stearyl fumarate PRUV manufactured by JRS Pharma GmbH and Co. KG, and micronized synthetic amorphous silica gel Syloid 244 FP EU manufactured by Grace GmbH and Co KG were used as model pharmaceutical glidants were. All used material complied with actual European Pharmacopoeia.



First tablets from microcrystalline cellulose only were prepared as a standard. Then mixtures of microcrystalline cellulose with magnesium stearate, sodium stearyl fumarate and micronized synthetic amorphous silica gel, respectively, were used for tablet preparation.

The three-exponential Řehula equation (4) was used to compare the compaction processes of these mixtures. The influence of the particular glidant on compression equation in the stages of precompression, elastic and plastic deformation was studied. The effect of glidants on tablet hardness was evaluated as well.

RESULTS AND DISCUSSION

Obtained results show that magnesium stearate acted as the most active glidant. It influenced most of the parameters, i.e. the volume reduction caused by particle rearrangement A_1 , the volume reduction caused by plastic deformations A_3 , the rate of volume reduction caused by plastic deformations $1/t_3$, the energy used for particle rearrangement E_1 and the energy used for plastic deformations E_3 , most significantly when compared to other two glidants. The use of magnesium stearate lowered tablet hardness significantly; the difference was 2.41 MPa.

Sodium stearyl fumarate and micronized synthetic amorphous silica gel were less active, but their use less negatively influenced tablet hardness. Influence on the compaction process of these two glidants was similar.

Results also showed that micronized synthetic amorphous silica gel is better to use in higher concentration than other two glidants used. The values of some parameters (A_1 , A_3 , E_1) of a mixture containing 2 % of micronized synthetic amorphous silica gel were similar to the parameters of mixture containing 1 % magnesium stearate. Micronized synthetic amorphous silica gel decreased tablet hardness insignificantly; the difference was 0.44 MPa. It also ensures the highest rate of volume reduction at all stages of the compaction process of the glidants used.

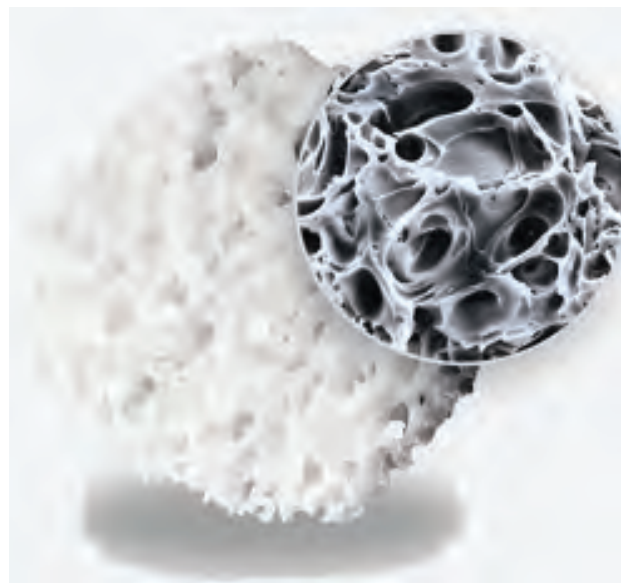


Fig. 1: Porous structure of Syloid 244 FP EU (3)

CONCLUSIONS

These experimental results confirmed that micronized synthetic amorphous silica gel has many advantages compared to the other two glidants that were studied, and therefore it can be used very well in the industrial tablet production.

REFERENCES

1. Armstrong NA, Lubricants, Glidants and Antiadherents, in: Augsburg LL, Hoag SW (Eds.), *Pharmaceutical dosage forms: Tablets*, 3rd edition, Vol. 2: *Rational Design and Formulation*, Informa Healthcare, New York, 2008, pp. 251-267.
2. Bolhuis GK, Holzer AW, *Lubrication Issues in Direct Compaction*, in: Celik M (Ed.), *Pharmaceutical Powder Compaction Technology*, 2nd edition, Informa Healthcare, London, 2011, pp. 205-234.
3. W. R. Grace & Co.-Conn.: *Datasheet – SYLOID® 244 FP EU*. W. R. Grace & Co.-Conn., Columbia, MD, 2011.
4. Rysl T, Řehula M, Adámek A, Klemra P, *Effect of Chemical Structure of Filler on Drug Pellet Pressing*. *Chem. Listy* 2011; 105: 634-639.





APPLICATION OF BIOPOLYMERS IN AN INNOVATIVE PROCEDURE OF ANIMAL CORNEA CRYOSTORAGE (P55)

Ante Orbančić¹, Marina Juretić¹, Jasmina Lovrić¹, Anita Hafner¹, Jelena Filipović-Grčić¹, Ivan Pepić¹

¹ University of Zagreb, Faculty of Pharmacy and Biochemistry, Department of Pharmaceutical Technology, A. Kovačića 1, 10000 Zagreb, Croatia

INTRODUCTION

The development of an ex vivo test system to replace animal testing for eye-related preclinical testing/biomedical research is a great challenge (1). The standard techniques of corneal preservation cannot be applied for eye-related preclinical testing and/or biomedical research.

The cornea is a multi-cellular tissue that contains multiple layers of epithelial and monolayer endothelial cells and keratocytes, which are the corneal stromal fibroblasts. This tissue complexity is reflected in the requirements for corneal cryopreservation. Ice formation in structured tissues during cryopreservation is the single most critical factor restricting the extent to which tissues can survive cryopreservation procedures involving freezing and thawing (2).

The maintenance of the structural and functional integrity of corneal tissue during cryostorage is the main objective of this work. To reduce freezing injury during cryopreservation, animal corneas have been equilibrated with cryoprotectant media consisting of a vehicle solution containing extracellular cryoprotective agents (CPAs).

MATERIALS AND METHODS

Corneal collection and excision

Porcine eyeballs from adult pigs weighing 80-100 kg were obtained from a local abattoir. Corneal-scleral rims, with approximately 4 mm of the limbal conjunctiva present, are dissected using microsurgical instruments and rinsed in sterilized phosphate-buffered saline (PBS). The excised corneas are processed within no more than 2 h of animal circulation cessation.

Corneal Prefreezing Incubation

The dextran 500 (500,000 Da, Alfa Aesar GmbH, Germany) or hydroxypropylmethyl cellulose (HPMC) (Shin-Etsu Chemical Ltd., Japan) used as CPAs were dissolved in Krebs-Ringer isotonic buffer pH 7.4. Each freshly excised cornea was stored in the cryopreservation medium at 4°C for 0.5 h.

Corneal Freezing Procedures

Freezing was performed according to the following protocols: (i) -20°C for 24 h (Protocol 1); (ii) -20°C for 2 h / -70°C for 22 h (Protocol 2); (iii) -70°C for 24 h (Protocol 3).

Corneal Thawing Procedures

Thawing was performed according to the following protocols: (i) spontaneously, by allowing frozen corneas to defrost in Krebs-Ringer isotonic buffer pH 7.4 at 20°C for 2 h (Protocol A); (ii) rapidly, by agitating the frozen corneas in pre-warmed (37°C) Krebs-Ringer isotonic buffer pH 7.4 for 0.5 h (Protocol B).

Corneal Barrier Integrity

The influence of freezing/thawing procedures on the corneal barrier integrity was evaluated by method based on electrophysiological conductance measurements (i.e., the calculation of the Transepithelial Electrical Resistance; TEER) (3).

Statistical analysis

The results of TEER measurement of cryoprotected ($n = 12$) or freshly excised ($n = 30$) corneas were compared with Student's t-test with a significance level $p < 0.05$.

RESULTS AND DISCUSSION

The freshly excised cornea showed TEER of $926 \pm 321 \Omega \times \text{cm}^2$. The effective cryoprotection of animal cornea is complex interplay between the process of corneal freezing/thawing and the composition of complex cryopreservation medium.

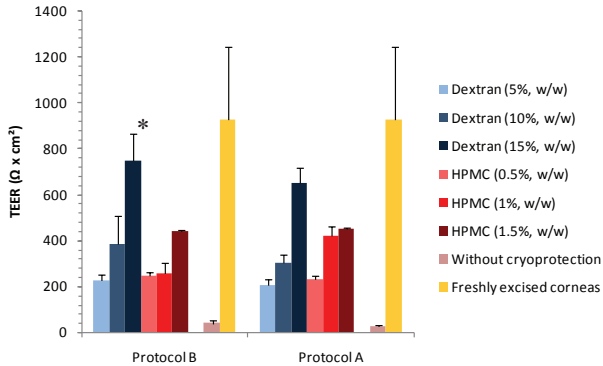


Fig. 1: Comparison of corneal barrier properties with or without CPAs after corneas freezing in accordance with Protocol 1 and corneas thawing in accordance with Protocol A and Protocol B. *Statistical significance of TEER values of cryoprotected cornea ($n = 12$) compared to the TEER values of freshly excised cornea ($n = 30$) ($p > 0.05$).

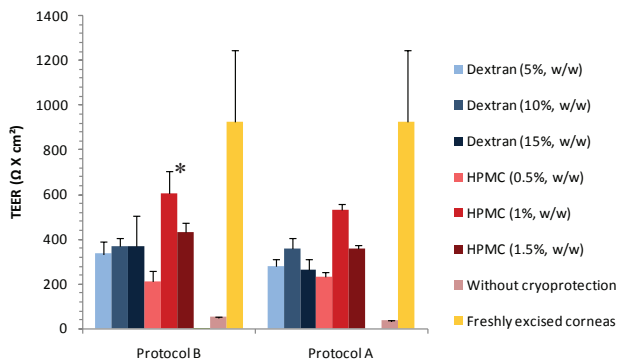


Fig. 2: Comparison of corneal barrier properties with or without CPAs after corneas freezing in accordance with Protocol 2 and corneas thawing in accordance with Protocol A and Protocol B. *Statistical significance of TEER values of cryoprotected cornea ($n = 12$) compared to the TEER values of freshly excised cornea ($n = 30$) ($p > 0.05$).

Optimal cryoprotective effect of dextran 500 on preservation of corneal barrier integrity was observed at a concentration of 15% (w/w) in isotonic Krebs-Ringer's buffer pH 7.4 and in accordance with freezing Protocol 2 (2 hours at -20°C , and then 22 hours at -70°C) (Figure 1). Following this procedure, 80.7% of corneal barrier integrity has been preserved. At the same time, optimal cryoprotective effect of HPMC on preservation of corneal barrier integrity is observed at a concentration of 1% (w/w) in isotonic Krebs-Ringer's buffer pH 7.4 and in accordance with freezing Protocol 3 (24 hours at -70°C) (Figure 2). Following this procedure, 65.4% of corneal barrier integrity has been preserved. Regardless of the freezing methods,

frozen animal cornea optimally thaws by immersion in a thermostated isotonic Krebs-Ringer buffer pH 7.4 in accordance with thawing Protocol B (0.5 hours at 37°C).

CONCLUSIONS

The best preservation of corneal barrier properties following freezing/thawing procedures was obtained by following protocol: vehicle solution: isotonic Krebs-Ringer buffer pH 7.4; prefreezing incubation conditions: $4^{\circ}\text{C}/0.5\text{ h}$; type and concentration of cryoprotective agent: dextran 500 (15%, w/w; freezing protocol: $-20^{\circ}\text{C}/2\text{ h}/-70^{\circ}\text{C}/22\text{ h}$) or HPMC (1%, w/w; freezing protocol: $-70^{\circ}\text{C}/24\text{ h}$); thawing protocol: $37^{\circ}\text{C}/0.5\text{ h}$.

REFERENCES

1. Pepić I, Lovrić J, Cetina-Čizmek B, Reichl S, Filipović-Grčić J. Toward the practical implementation of eye-related bioavailability prediction models. *Drug Discovery Today* 2014; 19: 31-44.
2. Oh JY, Lee HJ, Khwarg SI, Wee WR. Corneal cell viability and structure after transcorneal freezing-thawing in the human cornea. *Clinical Ophthalmology* 2010; 4: 477-480.
3. Miklavčič D, Pavšelj N. Electric properties of tissue. *Wiley Encyclopedia of Biomedical Engineering*, John Wiley & Sons, Inc. 2006.





QUASI-DYNAMIC DISSOLUTION OF ELECTROSPUN POLYMERIC NANOFIBERS LOADED WITH POORLY WATER-SOLUBLE DRUG (P56)

U. Paaver^{1*}, J. Heinämäki¹, I. Kassamakov², T. Ylitalo³, E. Hæggström³, H. A. Santos⁴, J. Yliruusi⁴, I. Laidmäe¹, P. Veski¹, K. Kogermann¹

¹ University of Tartu, Faculty of Medicine, Department of Pharmacy, Tartu, Estonia

² University of Helsinki, Helsinki Institute of Physics, Helsinki, Finland

³ University of Helsinki, Electronics Research Laboratory, Department of Physics, Helsinki, Finland

⁴ University of Helsinki, Division of Pharmaceutical Chemistry and Technology, Helsinki, Finland

INTRODUCTION

Polymeric nanofibrous mats charged with active substance(s) have found use in pharmaceutical and biomedical applications, e.g. as wound dressings and implanted drug delivery systems (1,2). This study investigates and monitors *in situ* wetting and dissolution (drug release) of nanofibers charged with a poorly water-soluble drug and determines the potential solid-state changes in the drug during dissolution.

MATERIALS AND METHODS

Nanofibers of poorly water-soluble piroxicam, PRX (Letco Medical, Inc. USA) and hydroxypropyl methylcellulose, HPMC (*Methocel™ K4M premium CR, The Dow Chemical Company, USA*) were electrospun (ES). A carrier polymer HPMC was combined with PRX at ratios of 1:1, 1:2 or 1:4 in ES. The high voltage power supply Gamma High Voltage Research (*Model No. ES3OP-10W/DAM, USA*) was used for electrospinning. The voltage applied was 7 kV. The distance between the spinneret and the fiber collector was 8 cm. The automatic syringe pump KdScientific (*Model No: KDS-250-CE, Geneq Inc, USA*) was used with a pumping speed of 1 ml/h (3).

Wetting and dissolution of the nanofibers were monitored *in situ* by 3D scanning white light microscopic interferometry (SWLI) (3) and high-resolution optical microscopy (*Leica DMLB, Germany*). Purified water, hydrochloric acid buffer (pH 1.2), and phosphate buffer solutions (pH 7.2) were used as dissolution media.

RESULTS AND DISCUSSION

Poorly water-soluble PRX was homogeneously dispersed in the nanofibers after ES. According to our earlier findings, PRX exists in amorphous state in the ES cellulosic (HPMC) nanofibers (3). The polymeric HPMC-PRX nanofibers dissolved quickly (1-5 sec) in the dissolution media. The amorphous state of PRX hastened the onset of wetting and premature drug release.

In-situ dissolution monitoring indicated that PRX recrystallizes in a micro-crystalline form immediately after wetting and is released from the polymeric nanofibers. Tiny PRX crystals were observed after addition of purified water or phosphate buffer solutions (standardized drop) onto nanofibrous mats (Figs. 1 and 2). Figure 1 shows a SWLI image of a tablet surface, where individual fibers are visible: (I A) initial state of tablet (magnification 30×). The tablet surface is flat and there is no crystal formation visible. This indicates that PRX is located in nanofibers and most-likely is still in the amorphous state (3). The point I B indicates the first wetting point after adding 2 µl of water and evaporating for 1 minute.

Figure 1 (II) describes the surface of the same tablet after wetting with another 2 µl of water and evaporating for 10 minutes. Initiation of crystal formation is visible indicating that PRX is partially released from the nanofibers (visible below the crystals) and that its form is changed from amorphous to crystalline.

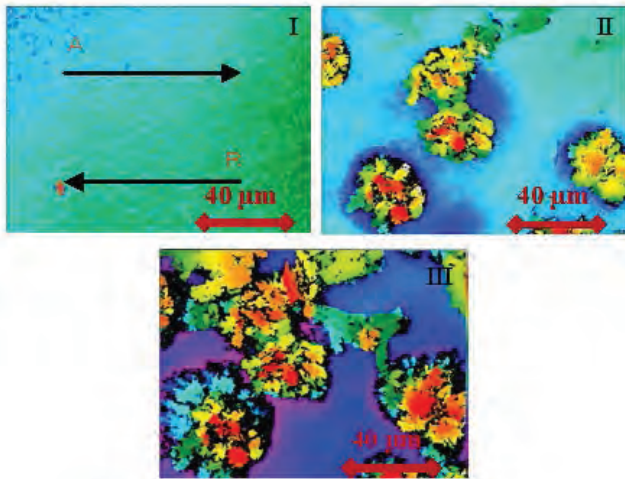


Fig. 1. Time-lapse of wetting induced PRX crystallization and release using SWLI. I: A. Initial state of the tablet. B. After wetting with 2 µl of water and evaporating for 1 minute. II: After wetting a second time with 2 µl of water and evaporating for 10 minutes. III: After wetting a third time with 2 µl water and evaporating for 10 minutes. Magnification 30x.

Figure 1 (III) shows that surface of the same tablet after the identical wetting procedure applied to the same spot for a third time. The release of PRX and crystallization has proceeded rapidly, pointing to poor solubility.

Figure 2 shows a time-lapse-like snapshot of what happens to the nanofibers during dissolution. These nanofibers were never pressed into tablets. The same three phases were observed: I. PRX is inside the nanofibers in an amorphous state. All nanofibers were intact prior to the water front moving into them. II. Crystallization of PRX started inside the nanofibers. III. Recrystallization of PRX was finalized after drug release from nanofibers. Rapid changes in PRX solubility observed. These changes correspond to the three subfigures in Fig. 1 (I-III). However, they cannot be directly compared since the first case shows a pressed tablet and in the other case there is no compaction.

The amount, shape, and size of the PRX crystals depended on the pH of the dissolution media, on the concentration of PRX in the nanofibers, and on the thickness of the nanofibrous mat.

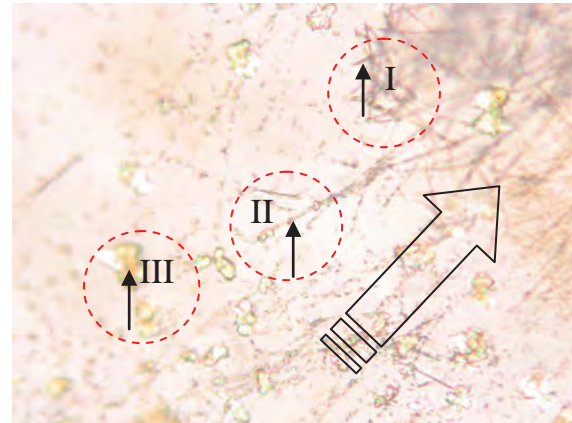


Fig. 2. Three phases of PRX release and crystallization. Light microscope image (magnification 50x) validating the results in Fig. 1. I. PRX inside the nanofibers is in amorphous state. II. Crystallization inside fibers. III. Recrystallization of PRX. The large arrow indicates the propagation direction of the water front.

CONCLUSIONS

PRX recrystallizes in a microcrystalline form after wetting of HPMC nanofibers which could lead to enhanced dissolution of drug. SWLI provides rapid non-contacting and non-destructive *in-situ* monitoring method of early-stage dissolution of nanofibers and regional mapping of crystalline changes (re-crystallization) during wetting.

ACKNOWLEDGEMENTS

This work is part of the targeted financing project no SF0180042s09 and ETF grant project no ETF7980. The research was also supported by the European Social Fund's Doctoral Studies and Internationalization Program DoRa.

REFERENCES

1. Agarwal S, Wendorff JH, Greiner A. Use of electrospinning technique for biomedical applications. *Polymer* 2008; 49: 5603-5621.
2. Paaver U, Tamm I, Laidmäe I, Lust A, Kirsimäe K, Veski P, Kogermann K, Heinämäki J. Soluplus® graft copolymer - Potential novel carrier polymer in electrospinning of nanofibrous drug delivery systems for wound therapy. *BioMed Res. Int.* 2014; Article ID 789765: 1-7.
3. Paaver U, Heinämäki J, Kassamakov I, Hggström E, Ylitalo T, Nolvi A, Kozlova J, Laidmäe I, Kogermann K, Veski P. Nanometer depth resolution in 3D topographic analysis of drug-loaded nanofibrous mats without sample preparation. *Int. J. Pharm.* 2014; 462: 29-37.





MODIFICATION OF CHEMICAL STABILITY, SOLUBILITY, DISSOLUTION, MICROBIOLOGICAL ACTIVITY AND PERMEABILITY OF RUTIN IN THE EFFECT OF COMPLEXION WITH β -CYCLODEXTRINS. STUDIES SUPPORTED BY THEORETICAL APPROACH (P57)

M. Paczkowska^{1*}, M. Mizera¹, H. Piotrowska², K. Lewandowska³, R. Pietrzak⁴, J. Gościańska⁴, D. Szymanowska-Powalowska⁵, J. Cielecka-Piontek¹

1 Department of Pharmaceutical Chemistry, Faculty of Pharmacy, Poznan University of Medical Sciences, Grunwaldzka 6, 60-780 Poznań, Poland

2 Department of Toxicology, Faculty of Pharmacy, Poznan University of Medical Sciences, Grunwaldzka 6, 60-780 Poznań, Poland

3 Department of Molecular Crystals, Institute of Molecular Physics, Polish Academy Sciences, ul. Smoluchowskiego 17, 60-179 Poznań, Poland

4 Faculty of Chemistry, Adam Mickiewicz University in Poznań, Umultowska 89b, 61-614 Poznań, Poland

5 Department of Biotechnology and Food Microbiology, Poznan University of Life Sciences, Wojska Polskiego 48, 60-627 Poznań, Poland

INTRODUCTION

Rutin (quercetin-3-rhamnosyl glycoside) is known for its anti-inflammatory and vasoactive properties as well as the potential to reduce the risk of arteriosclerosis. Rutin shows dose-dependent inhibition of low-density lipoprotein peroxidation and antioxidant activity (1, 2).

The aim of this work were studies of modification of rutin properties, which are important for the its biological activity, as the effect of complexion with β -cyclodextrins (β CD).

MATERIALS AND METHODS

Materials

Rutin and its related substances (isoquercetin, quercetin), beta-cyclodextrin (purity > 98%) were supplied by Sigma-Aldrich (Poland).

Methods

The vibrational infrared spectra were recorded between 400 and 7000 cm^{-1} , with an FT-IR Bruker Equinox 55 spectrometer equipped with a Bruker Hyperion 1000 microscope.

The Raman scattering spectra were obtained with a LabRAM HR800 spectrometer (Horiba Jobin Yvon) with laser excitation $\lambda_{\text{exc}} = 633 \text{ nm}$ (He-Ne laser).

Changes in the concentration of rutin were measured by using UHPLC-DAD (3).

Dissolution studies of rutin from rutin- β CD complex performed by using Vankel diffusion apparatus 7010 connected to the UV-Vis spectrophotometer Cary 50 Bio (Varian).

RESULTS AND DISCUSSION

Equimolar rutin- β -cyclodextrine (rutin- β CD) mixtures were co-grinded in order to achieve host-guest complex. The formation of rutin- β CD complex was confirmed by using spectroscopic (FT-IR, Raman) and thermal (DSC) methods. The theoretical approach based on DFT was used in identification studies of spectra of rutin- β CD complex. Geometry of β CD and rutin supramolecular assembly was also elucidated theoretically. AutoDock Vina software was used to roughly predict most possible conformations. Three best conformations were optimized using MM2 molecular mechanics modeling method. Molecular modeling revealed that the lowest steric energy belongs to complex with dihydroxyphenyl group included in β CD molecule. Further examination with semi-empirical calculations confirmed results obtained with molecular mechanics modeling.

The properties of rutin- β CD complex was studied in regards to: its stability, solubility, dissolution, microbiological as well as permeability studies. As comparator was considered rutin.

Stability and solubility studies

In evaluation of chemical stability and solubility UHPLC-DAD method was used. The rutin- β CD complex was slightly soluble than rutin while the complexed rutin was more significant stable in aqueous solutions and in the solid state when it was susceptible to activity of hydrolytic, oxidizing, photolytic and thermolytic factors.

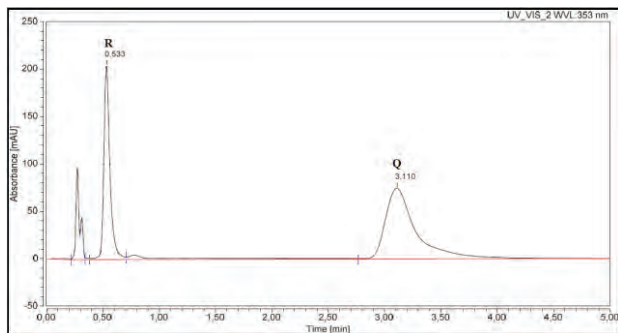


Fig. 1: The chromatogram of mixture of rutin ($c = 0.2 \text{ mg/mL}$) and its relative substances: isoquercetin ($c = 0.2 \text{ mg/mL}$) and quercetin ($c = 0.2 \text{ mg/mL}$).

Dissolution studies

The dissolution behaviors of the rutin- β CD complex was compared with those of rutin in bulk substance. The dissolution studies was conducted by measurement of the concentration of released rutin from rutin- β CD complex by using UV spectroscopy. After 48h 66% of rutin was released from rutin- β CD complex.

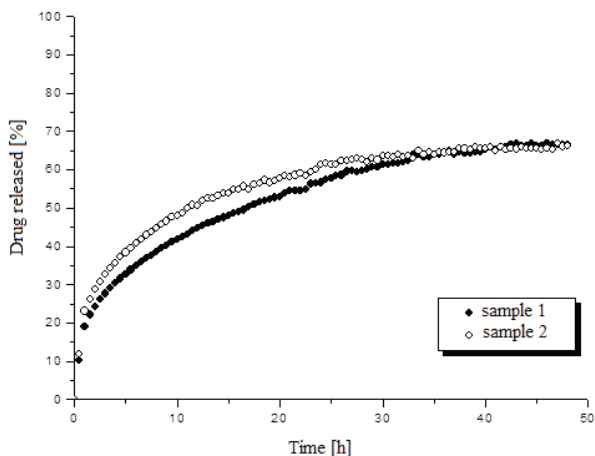


Fig. 2: Dissolution profiles for rutin- β CD complex.

Microbiological studies

The antibacterial activity of rutin- β CD complex was tested *in vitro* against a selection of indicator bacteria strains by determining the minimum inhibitory concentration (MIC) as well as analyzing the kinetics of changes in the concentrations of *P. aeruginosa*, *S. aureus* and *L. monocytogenes* caused by the action of rutin- β CD complex. In compared to rutin, its complex demonstrated slightly lower microbiological activity.

Permeability studies

The effect of rutin- β CD complex on the permeability of rutin in epithelial cells was evaluated in comparison to the effect of free rutin by using SIRC cells – epithelial cells derived from rabbit cornea. The permeability of rutin- β CD inclusion complex increased significantly as a function of time compared to the permeability of free rutin.

CONCLUSIONS

Rutin- β CD inclusion complex was prepared successfully by the co-grinded method. The solubility and the dissolution rate of rutin- β CD were much better than rutin alone as a consequence of the enhanced solubility. It was also demonstrated that the bioavailability of rutin was improved significantly by its inclusion with β CD.

The whole results of this study suggest the potential use of β CD for improving the bioavailability and absorption of rutin.

ACKNOWLEDGEMENTS

This study was supported by grant from the Ministry of Science and Higher Education (Diamontowy Grant DI2012 024342). This research was supported in part by PL-Grid Infrastrucutre.

REFERENCES

1. Cook NC, Samman D. *J. Nutr. Biochem.* 1996; 7:66–76.
2. Yang J, Guo J, Yuan J. *Food. Sci. Technol.* 2008; 41(6): 1060-1066
3. Paczkowska M, Zalewski P, Krause A, Cielecka-Piontek J. *Chromatografia.* Under review.





DEPOSITION OF NANOSUSPENSIONS BY FLEXOGRAPHIC PRINTING (P58)

M. Palo^{1,2,*}, R. Kolakovic¹, T. Laaksonen³,
A. Määttänen¹, N. Genina¹, J. Peltonen¹, N. Sandler¹

¹ Åbo Akademi University, Tykistökatu 6A, FI-20520 Turku, Finland

² University of Tartu, Nooruse 1, EE-50411 Tartu, Estonia

³ University of Helsinki, Viikinkaari 5E, FI-00014 Helsinki, Finland

INTRODUCTION

Production of nanosuspensions is a common method to enhance the solubility and dissolution rate of poorly water-soluble active pharmaceutical ingredients (APIs) (1). Well-known methods, such as freeze-drying and spray-drying, have been used to convert nanosuspensions into stable solid dosage forms (2). However, there is still a need for more cost-effective and feasible methods for preserving nano-size range of particles during re-dispersion of solid dosage forms to provide desired dissolution rate.

Flexographic printing has been investigated as a robust and flexible technology in the manufacturing of personalized medicine (3,4,5).

The aim of this study was to investigate the use flexographic printing as a deposition technique of nanosuspensions.

MATERIALS AND METHODS

Materials

Indomethacin (IND) and itraconazole (ITR) were used as poorly water-soluble model APIs. A non-ionic surfactant Poloxamer 407 (Pluronic® F-127) was used as a stabilizer in the preparation of aqueous nanosuspensions.

The nanosuspensions were printed on 3 different substrates – polyethylene terephthalate (PET) film, Easybake® rice sheet and Blue Dragon® rice paper.

Preparation of nanosuspensions

Aqueous nanosuspensions with IND and ITR were prepared by ball-milling (Pulverisette 7 Premium, Fritsch GmbH, Germany). The concentration of the stabilizer Poloxamer 407 was 60 wt% of the drug amount. The grinding was performed at 1100 rpm with 10 cycles, each cycle consisting of 3 min of grinding and 10 min pause.

Particle size

The mean particle sizes of the nanosuspensions were analyzed by photon correlation spectroscopy (Malvern Zetasizer 3000HS, Malvern, UK).

Flexographic printing

A laboratory scale printability tester (IGT Global Standard Tester 2, IGT Testing system, The Netherlands) was used to prepare formulations with the printed area of 0.5 cm². In case of all the samples 10 layers of ink was applied to the substrates.

X-ray diffraction

X-ray diffractometry (XRD) (Philips, X'Pert PRO MPD, The Netherlands) was used to characterize the solid state of the printed samples. During the measurement Cu K α radiation ($\lambda = 1.54\text{\AA}$) was applied using a voltage of 40 kV and a current of 50 mA. The measuring range was 3-40° with the rate of 0.04°/2 s.

Scanning electron microscopy (SEM)

SEM (LEO Gemini 1530, Oberkochen, Germany) that was equipped with a thermo scientific ultra-dry silicon drift detector was used for the evaluation of deposition quality. Before scanning samples were coated with carbon, using a vacuum evaporator.

Content analysis and dissolution studies

Content analysis and dissolution studies for IND were done in phosphate buffer (pH 5.0) using UV/Vis spectrophotometer at 265 nm. Content analysis and dissolution studies for ITR were done in 0.1N HCl solution using a high performance liquid chromatography (HPLC) for drug amount detection.

RESULTS AND DISCUSSION

Nanosuspensions with IND (145.1 mg/ml) and ITR (112.2 mg/ml) were successfully produced by wet ball-milling.

Particle size

The mean particle sizes of the prepared IND and ITR nanosuspensions were 422.0 nm and 698.1 nm, respectively.

X-Ray diffraction

Crystallinity of APIs was detected in printed formulations with XRD. The interpretation of the diffractograms of printed samples was complicated due to the interference from the substrate (PET) and low amount of the printed API.



SEM

The nanosuspensions were evenly distributed on the substrates after the printing. The SEM images of the flexographically fabricated samples (Fig. 1) did not reveal any agglomeration of the nano-sized particles.

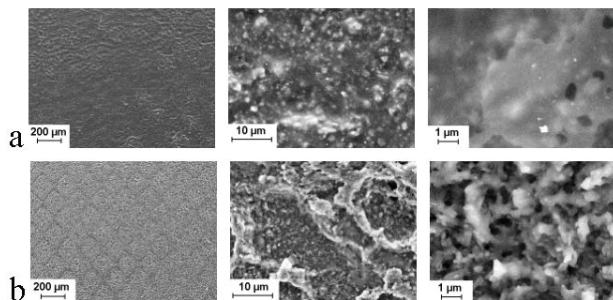


Fig. 1: SEM images of indomethacin (a) and itraconazole (b) printed on PET with 30x, 1000x and 5000x magnification (left to right).

Content analysis and dissolution studies

The API content of the printed samples is shown in Table 1. The dissolution rate of the APIs from nanosuspensions and the printed samples was increased compared to the raw drug substance. Printed formulations of IND and ITR on edible substrates (Easybake[®] rice sheet and Blue Dragon[®] rice paper) showed slower dissolution profiles compared to the samples printed on PET film.

Tab. 1: Drug content (μg) of indomethacin (IND) and itraconazole (ITR) on different substrates.

	PET (μg)	RS (μg)	RP (μg)
IND	177.9 \pm 68.5	234.0 \pm 2.4	194.8 \pm 9.1
ITR	230.9 \pm 34.8	46.1 \pm 3.6	341.9 \pm 36.3

*Average content (n=3) \pm standard deviation (μg).

PET – polyethylene terephthalate film; RS – Easybake[®] Rice sheet; RP – Blue Dragon[®] Rice Paper.

CONCLUSIONS

Printed solid dosage forms made from nanosuspensions were successfully produced by flexographic printing. The formulations contained printed solid particles without any observed agglomeration. In addition, the dissolution rate of the drug from the printed formulations increased compared to the pure API. The results indicate that the approach taken can be considered as a promising fabrication method for nanoparticulate systems.

REFERENCES

1. Liu P, Rong X, Laur J, van Veen B, Kiesvaara J et al. Nanosuspensions of poorly soluble drugs: Preparation and development by wet milling. *Int. J. Pharm.* 2011; 411: 215-222.
2. Van Eerdenbrugh B, Van den Mooter G, Augustijns P. Top-down production of drug nano-crystals: Nanosuspension stabilization, miniaturization and transformation into solid products. *Int. J. Pharm.* 2008; 364: 64-75.
3. Genina N, Fors D, Vakili H, Ihalainen P, Pohjala L et al. Tailoring controlled-release oral dosage forms by combining inkjet and flexographic printing techniques. *Eur. J. Pharm. Sci.* 2012; 47: 615-623.
4. Janßen EM, Schliephacke R, Breitenbach A, Breittkreutz J. Drug-printing by flexographic printing technology – A new manufacturing process for orodispersible films. *Int. J. Pharm.* 2013; 441: 818-825.
5. Rajada D, Genina N, Fors D, Wisaeus E, Peltonen J et al. A step toward development of printable dosage forms for poorly soluble drugs. *J. Pharm. Sci.* 2013; 102: 3694-3704.





AN *IN VITRO* INVESTIGATION OF THE CIPROFLOXACIN-FERROUS GLUCONATE INTERACTION (P59)

A. Stojković¹, V. Dobričić², J. Parojčić^{1*}, Z. Đurić¹, O.I. Corrigan³

¹ Department of Pharmaceutical Technology and Cosmetology, Faculty of Pharmacy, University of Belgrade, Vojvode Stepe 450, Belgrade, Serbia

² Department of Pharmaceutical Chemistry, Faculty of Pharmacy, University of Belgrade, Vojvode Stepe 450, Belgrade, Serbia

³ School of Pharmacy and Pharmaceutical Sciences, Trinity College, University of Dublin, Ireland

INTRODUCTION

Ciprofloxacin is characterized by pH dependent solubility and variable permeability along the gastrointestinal tract. Pharmacokinetic studies have shown reduced bioavailability of ciprofloxacin after simultaneous administration with iron containing preparations (1). Formation of a non-absorbable complex has been postulated as the interaction mechanism (1). In our previous study (2) a poorly soluble ciprofloxacin-iron complex was isolated from the reactive media used for ciprofloxacin hydrochloride solubility and tablet dissolution studies in the presence of ferrous sulfate. According to the Biopharmaceutics Classification System concept, drug dose, solubility and intestinal permeability are major determinants of oral drug bioavailability (3). The purpose of the study was to investigate the influence of ferrous gluconate on ciprofloxacin hydrochloride solubility, tablet dissolution and permeability in order to simulate the ciprofloxacin/ferrous gluconate interaction observed *in vivo*.

MATERIALS AND METHODS

Solubility

Ciprofloxacin hydrochloride solubility in water and reactive media containing ferrous gluconate was determined. Samples were continuously shaken on a laboratory shaker (Unimax 1010) for 6 h, centrifugated and filtrated, appropriately diluted and assayed UV spectrophotometri-

cally (Evolution 300) at 276 nm. pH values of the samples were monitored by pH meter (pH meter-HANNA 9321).

Dissolution studies

Dissolution studies of commercially available ciprofloxacin film tablets (Marocen 500 – Hemofarm STADA, Serbia) were performed in the mini-paddle apparatus (Erweka DT 700) at 50 rpm, using water without/with different amounts of ferrous gluconate added. Dissolution samples were withdrawn at regular time intervals and after filtration and appropriate dilution and assayed spectrophotometrically at 276 nm.

Permeability study – PAMPA test

Passive diffusion of ciprofloxacin hydrochloride without/with ferrous gluconate was determined using PAMPA test. Hydrophilic PVDF 96-well filtration plate was used as carrier of artificial membrane and receiving plate. The filter material of each well in the filtration (receiving) plate was coated with 5 µl egg lecithin solution in dodecane (1%, w/v). The receiving plate was placed on the donor plate, which was previously filled with 300 µl of donor solutions: (i) 0.15 mM ciprofloxacin-HCl solution; (ii) ciprofloxacin-HCl/ferrous gluconate mixture in the form of solution containing 25 mM of ciprofloxacin-HCl and 25 or 50 mM of ferrous gluconate, (iii) samples collected from ciprofloxacin tablet dissolution in the reactive media containing ferrous gluconate. Subsequently, 300 µl of water was added to each well of the receiving plate. The covered system was incubated for 2h at room temperature and concentrations of ciprofloxacin in the corresponding samples taken from the receiving plate were determined by HPLC (HPLC Dionex Ultimate 3000, Thermo Fisher Scientific, Germany).

Statistical analysis

Single factor ANOVA (SPSS Statistics 20, USA) was used to test statistical significance of the alteration in ciprofloxacin hydrochloride solubility and permeability in the presence of ferrous gluconate.

RESULTS AND DISCUSSION

Concentrations of ciprofloxacin dissolved in media containing increasing amounts of ferrous gluconate (final pH 3.22 - 4), as well as the apparent permeability coefficients (P_{app}) of ciprofloxacin hydrochloride in the presence of ferrous gluconate are shown in Fig. 1. The amount of ciprofloxacin hydrochloride dissolved was significantly reduced in the reactive media containing more than 40 mM ferrous gluconate ($p > 0.05$). In addition, permeability of ciprofloxacin hydrochloride was significantly reduced in reactive media containing ferrous gluconate ($p > 0.05$).

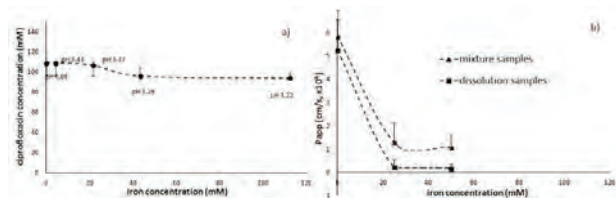


Fig. 1: Concentration of ciprofloxacin hydrochloride dissolved (a) and the relevant P_{app} coefficients (b) in reactive media containing different amounts of ferrous gluconate

Ciprofloxacin hydrochloride tablet dissolution in media with/without ferrous gluconate was rapid and almost complete (Fig 2). Freely soluble ferrous gluconate added to the dissolution media dissolved rapidly and ciprofloxacin tablet dissolution in the presence of ferrous gluconate was, generally, not affected, irrespective of the amount of the gluconate added.

Calculated P_{app} obtained in PAMPA and corresponding human P_{eff} values (estimated by conversion in the Simcyp™ simulator, Ltd, Sheffield, UK) for ciprofloxacin hydrochloride and ciprofloxacin-HCl mixtures with ferrous gluconate are shown in Table 1. It was reported that ciprofloxacin absolute bioavailability ranged between 60-80 % of the administered dose (4) and that it was reduced by 67 % when coadministered with ferrous gluconate (1). According to the results obtained reduction in ciprofloxacin permeability in the presence of ferrous gluconate predicted by PAMPA was in rank order with the data observed *in vivo*. Ciprofloxacin salts formed with organic acids have equal or, generally, higher solubility compared with the hydrochloride salt (5). According to the results obtained in the present study, it may be postulated that the excess gluconate contribute the formation of a highly soluble salt and prevented its complexation with iron. It was reported in the literature that high degree of ciprofloxacin ionization was observed in the presence of organic compounds, leading to proportionally lower permeability (5). The reduction of ciprofloxacin-HCl permeability in the presence of ferrous gluconate, observed in the present study could be attributed to the increased extent of ciprofloxacin ionization.

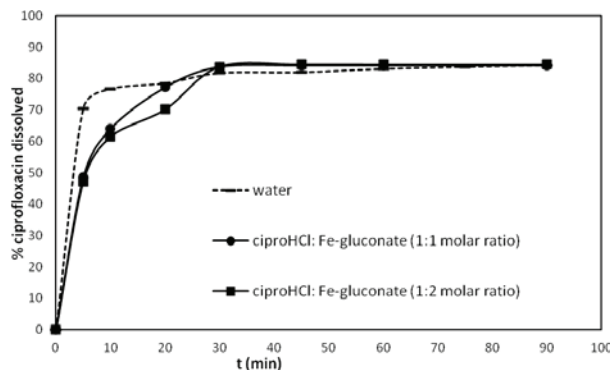


Fig. 2: Ciprofloxacin tablet dissolution in media without/with different amounts of ferrous gluconate added

Tab. 1: P_{app} values obtained in PAMPA and the relevant human P_{eff} values estimated by Simcyp™

Sample	P_{app} (cm/s, $\times 10^{-6}$)	P_{eff} (cm/s, $\times 10^{-4}$)	F_a^* (%)	pH
ciprofloxacinHCl (solution)	5.84±1.45	1.15	82	4.04
ciprofloxacinHCl (dissolution)	5.24±1.21	1.03	80	4.10
ciprofloxacinHCl:Fe-gluconate mixture (1:1)	1.30±0.94	0.27	33	3.88
ciprofloxacinHCl:Fe-gluconate mixture (1:2)	1.08±0.62	0.22	28	3.76
ciprofloxacinHCl:Fe-gluconate dissolution (1:1)	0.23±0.06	0.05	7.6	3.83
ciprofloxacinHCl:Fe-gluconate dissolution (1:2)	0.15±0.03	0.03	5	3.81

$$^*F_a = (1 - e^{-1.47P_{eff}}) \times 100 \quad [3]$$

CONCLUSIONS

The obtained results indicate that *in vitro* solubility and dissolution tests coupled with permeability test may be useful to simulate ciprofloxacin/ferrous gluconate interaction observed *in vivo*.

ACKNOWLEDGMENT

This work was supported by the Ministry of Education and Science, Republic of Serbia project TR34007

REFERENCES

1. Kara M et al. *Brit. J. Clin. Pharmacol.* 1991; 31: 257-261.
2. Parojčić J, et al. *J. Pharm. Sci.* 2011; 100: 5174-5184.
3. Amidon GL, et al. *Pharm Res.* 1995; 12: 413-20.
4. Drusano GL, et al. *Antimicrob Agents Chemother* 1986; 30: 444-446.
5. Florindo C, et al. *Int. J. Pharm.* 2014; in press





EFFECTS OF DRY GRANULATION METHOD AND CONTROLLING AGENT ON DRUG RELEASE KINETICS OF TABLETS (P60)

A. Penkina^{1,*}, T. Saarinen², O. Antikainen²,
A. Lust¹, P. Veski¹, K. Kogermann¹, J. Yliruusi²,
J. Heinämäki¹

¹ University of Tartu, Faculty of Medicine, Department of Pharmacy,
Nooruse 1, 50411 Tartu, Estonia

² University of Helsinki, Faculty of Pharmacy, Division of
Pharmaceutical Chemistry and Technology, P.O. Box 56 (Viikinkaari
5E), 00014 University of Helsinki, Finland

INTRODUCTION

Dry granulation is a widely used technique in the pharmaceutical industry for agglomeration of water and heat sensitive drugs and for improving the flowability and compressibility of powder mixtures. Dry granulation can be performed by conventional slugging or more established roller compaction technology (1). Past two or three decades, virtually no new methods for dry granulation have been introduced.

The design and synthesis of new bio-materials for pharmaceutical excipients have created much interest in the recent years. Lignin is a by-product of the pulping or bio-ethanol industry, and it is readily available and cheap, but still undervalued in the pharmaceutical industry (2,3). Recently, the powder and tablet compression properties of lignin were investigated and compared with the established direct compression excipients (4). With new compressible excipients and a rational-based materials combination, the performance of dry granulation and tablet compression could be improved.

The aim of this study was two-fold: (I) to investigate the effects of a novel aerodynamic dry granulation system (AGS) and conventional dry granulation (slugging) on the granule and tablet properties with a special attention on the drug release kinetics and (II) to study the effects

of hypromellose (HPMC) and lignin (Indulin AT) on the drug release of tablets compressed from the different dry granulated powder mixtures.

MATERIALS AND METHODS

Materials

Theophylline anhydrous (BASF Corp., USA) was used as a model drug. Two grades of hypromellose, HPMC (Methocel K100M and K4M, Colorcon Ltd., U.K.) and soft-wood lignin (Indulin AT) were used as release-controlling agents (Table 1). Lactose monohydrate (Pharmatose 80M, DFE Pharma, Germany) was used as a filler up to 89% (w/w). Magnesium stearate (Ph.Eur.) was used as a lubricant for tablet compression.

Tab. 1: Composition of final granules for tablet compression (in % w/w).

Batch	AGS	Theophylline	HPMC1	HPMC2	Lignin	Lactose	MgStear	SUM
1 no		10				89	1	100
2 no		10	10			79	1	100
3 no		10	30			59	1	100
4 no		10		10		79	1	100
5 no		10		30		59	1	100
6 no		10			10	79	1	100
7 no		10			30	59	1	100
8 yes		10				89	1	100
9 yes		10	10			79	1	100
10 yes		10	30			59	1	100
11 yes		10		10		79	1	100
12 yes		10		30		59	1	100
13 yes		10			10	79	1	100
14 yes		10			30	59	1	100

Methods

The powder mixtures were dry granulated using (I) a conventional compaction (slugging) method and (II) a novel AGS technique. Tablets (n = 100-120) were compressed in an instrumented Korsch EK-0 eccentric tableting machine (Erweka Apparatebau, Germany) equipped with 7-mm flat-faced punches. The target weight of tablets was 200 mg. The granules were characterized by means of scanning electron microscopy (SEM). The dimensions, weight variation, mechanical strength and in-vitro dissolution (USP basket method / 0.1 N HCl) of the tablets were investigated.

RESULTS AND DISCUSSION

The granules with more uniform size and shape distribution were obtained with the AGS than with the slugging (Fig. 1).

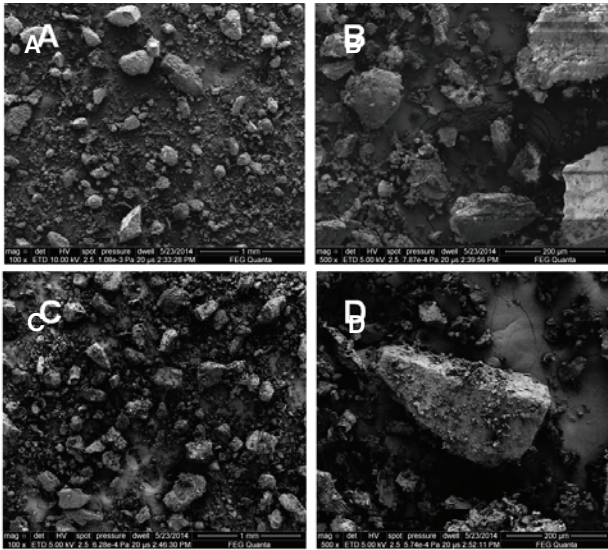


Fig. 1: SEM images of granules representing conventional slugging (A,B) and AGS (C,D) dry granulated lignin containing formulations (batches 7 and 14 in Tab. 1). Magnifications 100× (A,C) and 500× (B,D).

The dry granulation method and the release-controlling agent (HPMC, lignin) did not affect the mechanical strength of the tablets (Fig. 2). Interestingly, inclusion of lignin in the granule composition at a higher concentration (30% w/w) seems to slightly decrease the weight variation of the tablets (batches 7 and 14) suggesting improved flowing of the present granules.

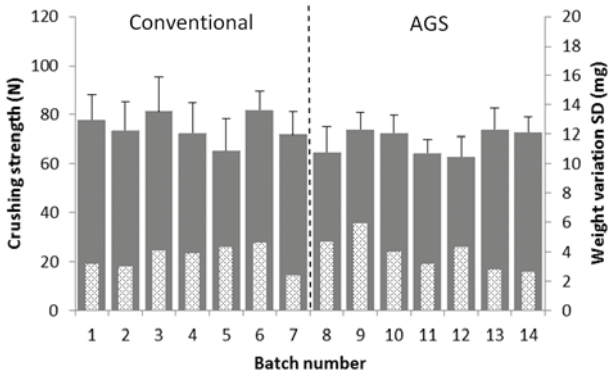


Fig. 2: Mechanical strength (dark columns) and weight variation (light columns) (standard deviation, SD) of the tablets prepared via conventional and aerodynamic (AGS) dry granulation (n = 20).

The dissolution of the tablets obtained via AGS dry granulation was faster compared to the tablets obtained via compaction (slugging) dry granulation (Fig. 3).

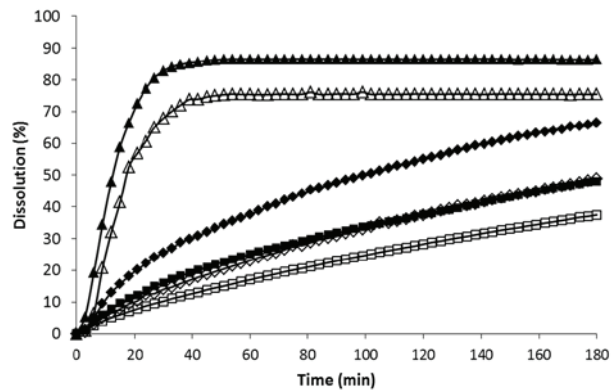


Fig. 3: Dissolution profiles of theophylline tablets (n = 3-5) prepared via conventional slugging (open markers) and aerodynamic AGS (filled markers) dry granulation. Key: HPMC K100M (□,■); HPMC K4M (◇,◆); Lignin (△,▲). The amount of release controlling agent is 30% (i.e. granule batches 3, 5, 7, 10, 12 and 14 in Tab. 1).

CONCLUSIONS

A novel aerodynamic granulation system (AGS) produces dry granules with good flowing and densification properties, and consequently, applicable in the tableting process. The dissolution behavior of tablets is dependent on both dry granulation method and release controlling agent used. Lignin incorporated in the granules does not affect the drug release kinetics.

Acknowledgements

This work is part of the targeted financing project no SF0180042s09 and ETF grant project no ETF7980. The research was also supported by the European Social Fund's Doctoral Studies and Internationalization Program DoRa.

REFERENCES

1. Kleinebudde P. Roll compaction/dry granulation: pharmaceutical applications. *Eur J Pharm Biopharm.* 2004; 58 (2): 317-326.
2. Doherty WOS, Mousavioun P, Fellows CM. Value-adding to cellulosic ethanol: Lignin polymers. *Ind Crops Prod.* 2011; 33: 259-276.
3. Hatakeyama H, Hatakeyama T. Lignin structure, properties, and applications. *Adv Polym Sci.* 2010; 232: 1-63.
4. Penkina A, Antikainen O, Hakola M, Vuorinen S, Repo T, Yliruusi J, Veski P, Kogermann K, Heinämäki J. Direct compression of cellulose and lignin isolated by a new catalytic treatment. *AAPS PharmSciTech* 2013; 14 (3): 1129-36.



EFFECT OF COMPOSITION ON THE RELEASE FROM MELT EXTRUDED LAMINAR SYSTEMS BY APPLICATION OF MIXTURE EXPERIMENTAL DESIGN ^(P61)

D.Hasa¹, M.Grassi², B.Perissutti^{1*}, S.Golob¹, I. Grabnar³, D.Voinovich¹

¹ Department of Chemical and Pharmaceutical Sciences, P.le Europa 1, I-34127, Trieste, Italy

² Department of Engineering and Architecture, Via A. Valerio 6/A, I-34127, Trieste, Italy

³ Chair of Biopharmaceutics and Pharmacokinetics, Faculty of Pharmacy, University of Ljubljana, Aškerčeva 7, SI-1000 Ljubljana, Slovenia

INTRODUCTION

Melt extrusion is a relatively recent pharmaceutical processing technique applicable to both immediate release and sustained release dosage forms. During the process, the mixture of thermoplastic binder, excipients and APIs are fed into the heated barrel, and extruded through the die attached at the end of the barrel. The physical shape of the final product depends on the geometrical design of the die, obtaining e.g. cylinders, pipes, laminates, helices or films. In particular, laminar extrudates show high versatility being suitable for oral, buccal or topical administration. This shape can be used both as a final dosage form and to fill hard gelatine capsules. In this context, Pinto and coworkers recently produced laminar extrudates at ambient temperature in the absence of solvents (1).

The aim of the present investigation is to produce laminar extrudates with a programmed *in vitro* release of theophylline (model drug) ranging from 35% after 1 h and 75% after 8 h (table 1), with the final aim of producing a retard formulation for oral administration. Thus, the drug release from such extrudates after 1 h (Y_1) and after 8 h (Y_2) was

evaluated as a function of their different composition (ternary mixture of theo, lac and wax).

MATERIALS AND METHODS

Materials

- Anhydrous theophylline (theo) Polichimica s.r.l. (Bologna, Italy),
- Monohydrate lactose Flowlac®100-Meggle (lac),
- Microcrystalline wax (Paracera P, wax) Paramelt (Heerhugowaard, NH).

Methods

Extrusion procedure and mixture experimental design

The extrudates were prepared using a lab scale ram extruder (Thalassia®, Trieste, Italy) (2), thermo-stated at 50°C. An experimental design for mixtures associated to a desirability function was used to project experimental trials using a reduced cubic model (3). From preliminary experiments, the constraints of 3 components in the mixtures were defined. Then, 50 g batches of each ternary mixture (previously mixed in a high shear mixer and equilibrated at 50°C for 1h), was extruded through a rectangular die (with a flat entry, 0.5 mm x 5 mm cross section). Once the samples have been cooled at ambient temperature, the laminar extrudates were sliced up by use of a hot cutter in unities of length (7.5 mm) suitable to have a drug content for dissolution studies in sink conditions. Absence of chemical degradation and physical interactions among components due to thermal treatment was verified by HPLC-MS analysis and XRPD (data not shown). XPS analysis was then used to detect the presence of the drug on the surface of the extrudates.

In vitro dissolution tests

In vitro dissolution tests (n=3; S.D. <5%) were performed using the USP rotating basket apparatus, a stirring rate of 100 rpm, at 37 ± 0.5°C, 900 ml of water plus 0.1% polysorbate 20.

In vivo Studies

A dose of 400 mg of theo was orally administered in hard gelatine capsule (size 00) containing the appropriate amount of extrudates to 4 healthy volunteers.

RESULTS AND DISCUSSION

Extrudates with the desired uniform laminar shape were produced, using a temperature (50°C) inferior to wax melting point of (~60°C) with all the 32 performed compositions.



In Table 1 the desired *in vitro* percent drug release after 1 h (Y_1) and 8 h (Y_2) is presented, while Fig. 1 and Fig.2 depict the desired *in vitro* profile and the optimal zones of desirability.

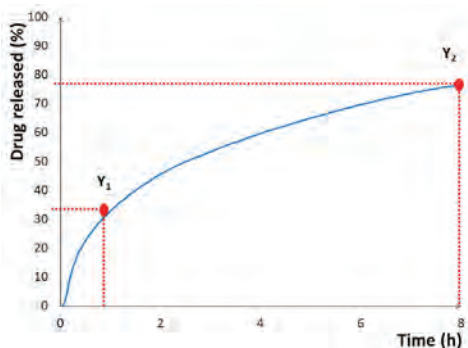


Fig. 1: Desired *in vitro* release of the model drug (theophylline)

Tab. 1: Optimal response range for both variables

Response	Comp. value (%) \pm S.D.	Desirability (%)
Y_1	33,15 \pm 1,74	62,96
Y_2	75,87 \pm 1,5	82,52
Global desirability		72,08

Then, the effect of each component of the mixtures on the experimental response was evaluated. As reported in Fig. 3, microcrystalline wax resulted to be the most influencing component (component 3).

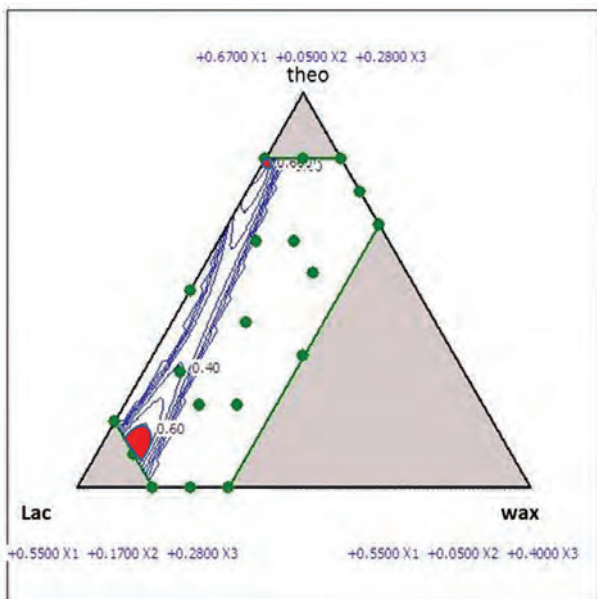


Fig. 2: Bidimensional image of the optimal space of desirability, highlighted in red. The green spots indicate the performed ternary mixtures.

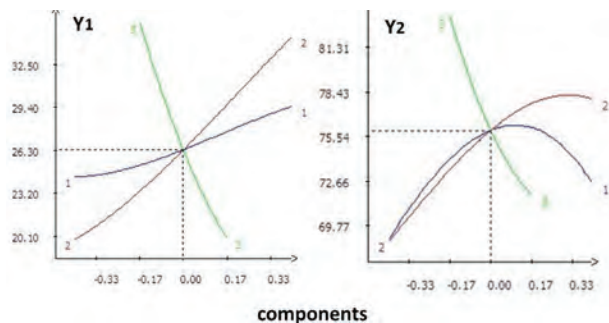


Fig. 3: Effects of the variation of the mixture components on both variables (where theo, lac and wax are component 1, 2 and 3, respectively).

The formulation (theo = 57%, lac = 14% wax = 29% w/w), selected based on the desirability zone, was subsequently used for *in vivo* studies. The obtained plasma profile after oral administration reveals the typical trend of an oral retard formulation.

CONCLUSIONS

The application of the experimental design for mixtures, associated to a desirability function, permitted to optimize the extruded system and to perform a quality control of both processing technique and final product.

REFERENCES

1. Oliveira, G., Wahl, M.A., Pinto, J.F. Characterization of laminar extrudates manufactured at room temperature in the absence of solvents for the delivery of drugs. *Int.J.Pharm.*2013;454:90-98.
2. Grassi M., Voinovich D., et al. Theoretical and experimental study on theophylline release from stearic acid cylindrical delivery systems. *J. Control. Rel.* 2003; 30: 275-289.
3. Voinovich, D., Campisi, B., e Phan-Tan-Luu, P., *Experimental Design for mixture studies, in Comprehensive Chemometrics: Chemical and Biochemical Data Analysis, vol. 1, Elsevier, Oxford, 2009, pp. 391-452.*





EVALUATION OF INDIVIDUAL DATA ON SMALL INTESTINAL TRANSIT TIME OF THE TABLETS (P62)

M. Pišlar*, H. Brelih, A. Mrhar, M. Bogataj

*The Chair of Biopharmaceutics and Pharmacokinetics,
Faculty of Pharmacy, University of Ljubljana,
Aškerčeva cesta 7, 1000 Ljubljana, Slovenia*

INTRODUCTION

Stomach, small intestine (SI), and colon are fundamental parts of a human gastrointestinal (GI) tract. They differ in anatomical structure and physiological conditions, which leads to different influences of each part on performance of a dosage form after oral administration and consequently on *in vivo* release and absorption kinetics of a drug.

Transit of a dosage form through each part of GI tract is a very important factor that affects *in vivo* drug release, since it determines time period, during which the dosage form is exposed to conditions in a particular part of GI tract.

Davis et al. [1] reported that transit through SI was not affected by size and type of dosage form, nor by feeding condition. However, in special feeding condition, such as tablet administration 45 min before breakfast, Fadda et al. [2] demonstrated that SI transit time is significantly shorter.

The aim of our research was to evaluate SI transit, ileo-caecal junction (ICJ) residence and colon arrival (CA) time of the individual tablets obtained from a systematic literature review, where attention was given to the influence of the meal intake.

METHODS

A systematic literature review of GI transit time of tablet was done in databases Medline, Web of Science, and Science Direct in July 2013. Individual data on CA times for non-disintegrating tablets that were administered in fasted state in humans were selected and evaluated.

Trend of the CA times in relation to the GE times was estimated by applying a local approximating regression to the measurements, denoted as loess [3]. The SI transit times were calculated as the time difference between GE and CA time.

RESULTS AND DISCUSSION

In total, 209 measurements of GI transit times were obtained from 19 articles, among which 133 measurements had the meal intake at 4 h post-dose. In these occasions, when feeding was at 4 h post-dose, 63 % of the tablets that were still in SI at time of the meal intake transit into the colon within 40 min after the meal intake.

CA and SI transit times were inspected in relation to the GE (Fig.1). At longer GE times longer CA times were observed in the range 0 – 120 min of GE time, which indicates that CA time correlates with the GE time. This is also seen by the increasing trend of loess curve (in Fig. 1 indicated by a dotted line). The loess curve is within the expected range (in Fig. 1 indicated by gray area), which is estimated by summation of observed GE time and most frequently reported SI transit time, i.e., 3 – 4 h [1, 4]. Nevertheless, at higher GE times (> 120 min) the loess curve does not increase anymore and becomes steady. Although the trend at higher GE times is estimated only upon 7 measurements, which might result from a random error, a possible explanation of the trend is that meal intake at 4 h post-dose accelerates the tablet transit through the SI, which results in shorter SI transit times, especially for tablets that are located in upper SI at the time of meal intake.

Additionally, residence time at the ICJ was measured and reported for 58 individual observations that had meal intake at 4 h post-dose. In 11 occasions (19 %) tablets moved rapidly from SI into the colon without stagnation at the ICJ. Tablets with residence time measurements at the ICJ that retained at the ICJ (47 occasions) on average stagnate for 65 min (range 10 – 266 min). 35 tablets arrived at the ICJ before the meal intake, whereas 23 tablets arrived at the ICJ after the meal intake. No statistical differences were observed between residence times at the ICJ for tablets that arrived at the ICJ before and after the meal intake.

There are 14 measurements where tablets were located at the ICJ at the time of meal ingestion. In 11 occasions (76%) of those measurements tablets exit the ICJ into the colon within 40 min after the food intake, which suggests that food intake triggers the tablet transit through the ICJ region. Correspondingly, it is reported that immediately after the food intake phasic and tonic activity of the ICJ is increased [5]. The other three tablets additionally stagnate at the ICJ more than 1 h after meal intake, which is a significant part of SI transit time.

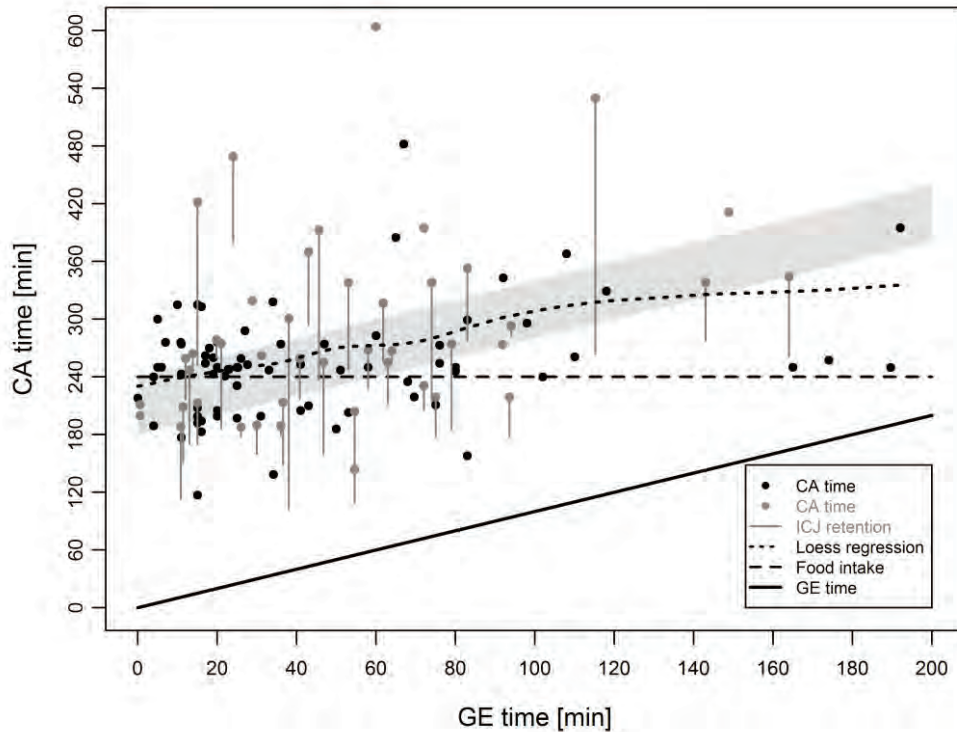


Fig. 1: Scatter plot of CA times versus GE times. Observations are divided into 2 groups; observations without measurement of the tablet residence time at the ICJ (black dots) and observations with measurement of the tablet residence time at the ICJ (gray dots). Gray vertical lines indicate duration of tablet retention at the ICJ. Meal intake at 4 h post-does is indicated by a horizontal dashed black line and GE time is also presented by an identity black line. Shaded gray area represents expected CA time, which is calculated from observed GE time plus most frequently reported SI transit times, i.e., 3 - 4 h. Local approximating regression (loess) is presented by dotted black line.

CONCLUSIONS

Several parameters that describe the tablet transit through SI and ICJ were presented indicating that time of the meal intake influences the tablet transit through the SI. However, additional research is needed in order to demonstrate the impact of the meal intake after the tablet administration on the tablet transit through the SI in more depth.

REFERENCES

1. S.S. Davis, J.G. Hardy, J.W. Fara, Transit of pharmaceutical dosage forms through the small intestine, *Gut*, 27 (1986) 886-892.
2. H.M. Fadda, E.L. McConnell, M.D. Short, A.W. Basit, Meal-induced acceleration of tablet transit through the human small intestine, *Pharm Res*, 26 (2009) 356-360.
3. W.S. Cleveland, S.J. Devlin, Locally Weighted Regression - an Approach to Regression-Analysis by Local Fitting, *J Am Stat Assoc*, 83 (1988) 596-610.
4. K.H. Yuen, The transit of dosage forms through the small intestine, *Int J Pharm*, 395 (2010) 9-16.
5. P.G. Dinning, P.A. Bampton, M.L. Kennedy, T. Kajimoto, D.Z. Lubowski, D.J. De Carle, I.J. Cook, Basal pressure patterns and reflexive motor responses in the human ileocolonic junction, *Am J Physiol-Gastr L*, 276 (1999) G331-G340.



INFLUENCE OF ADHESIVE AGENT ON *IN VITRO* DRUG RELEASE PROPERTIES OF ENTERIC-COATED PANTOPRAZOLE PELLETS (P63)

E. Vranić¹, O. Rahić¹, O. Planinšek², S. Srčić²

¹ Department of Pharmaceutical Technology, Faculty of Pharmacy, University of Sarajevo, Zmaja od Bosne 8, 71 000 Sarajevo, Bosnia and Herzegovina

² Department of Pharmaceutical Technology, Faculty of Pharmacy, University of Ljubljana, Aškerčeva 7, SI-1 000 Ljubljana, Slovenia

INTRODUCTION

Pantoprazole sodium sesquihydrate is a selective proton pump inhibitor (PPI) with prolonged effect (1). It belongs to BCS Class III of drugs (2). It decomposes at low pH values and shows a highly pH dependant solubility (1).

Considering the above mentioned, it is necessary to formulate a dosage form that will protect active substance during passage through stomach and to ensure its release in intestine, from where it will be absorbed into the systemic circulation.

Pellets, as dosage forms have been chosen, considering that they are ideal for coating and release control of active pharmaceutical substance.

In order to obtain desired pellets a solution/suspension layering method onto inert, sugar cores has been employed. In order to achieve good adhesion of pantoprazole, three different substances have been used as adhesive agents (talc, Opadry® II White and a combination of talc and povidone K25). The effect of adhesive agent on acid-resistance and drug release was then examined.

MATERIALS AND METHODS

Materials

Pantoprazole sodium sesquihydrate (Natco Pharma, India) was used as an active substance. Sodium hydrogen

phosphate (Synopharm GmbH & Co, Germany), sucrose spheres (Hans G. Werner GmbH Co, Germany), hydroxypropylmethyl- cellulose (Pharmacoat 606, Shin Etsu Chemical Co., Ltd, Japan) and ethylacrylate methylmethacrylate polymer (Eudragit® L30D55, Evonik Degussa, Germany) were used as buffering agent, inert cores, protective agent and enteric coating agent, respectively. Micronized talc (Luzenac Val Chizone SpA, Italy), Opadry® II White (Colorcon GmbH, Germany) and Povidone K25 (BASF ChemTrade GmbH, Germany) were used as adhesive agents.

Drug coating, protective and enteric coating

A solution/suspension of above mentioned substances was applied until desired weight gain was achieved. Coating was performed on fluid-bed HKC Labor 200 DJ (Hüttlin GmbH, Germany). Drug coating was applied onto inert cores. Protective coating was applied subsequently onto drug coated pellets, and enteric coating was applied at the end.

Acido-rezistance and drug release study

Acido-rezistance and drug release studies were performed by the rotating paddle method at a rotation speed of 100 rpm. Acid resistance was tested using 0.1 mol/l hydrochlorid acid (pH 1.2) as dissolution medium for 120 minutes. After 120 minutes dissolution medium was changed with phosphate buffer (pH 6.8) which denoted the start of drug release test and lasted for 45 minutes. acido-rezistance and drug release studies were performed using dissolution tester VanKel VK7025.

RESULTS AND DISCUSSION

Composition of three enteric-coated pantoprazole pellets is given in Table 1.

Tab. 1: Composition of three enteric-coated pantoprazole pellets.

Component	Function	F1	F2	F3
Pantoprazole sodium sesquihydrate	A c t i v e substance	9.6	9.6	9.6
Sucrose spheres	Core	57.3	57.3	57.3
Talc	Adhesive agent	23.2	-	27.3
Opadry® II White	Adhesive agent	-	22.6	-
Povidone K25	Adhesive agent	-	-	16.7
HPMC	Protective coat	100.0	100.0	100.0
Eudragit® L30D55	Enteric coat	95.5	95.5	95.5

Each component in Table 1 is represented as weight ratio in the corresponding coating (active, protective and enteric). Quantity of sucrose spheres and active substance



is given as weight ratio in total formulation. The results of *in vitro* acido-resistance and drug release tests are shown in Figure 1.

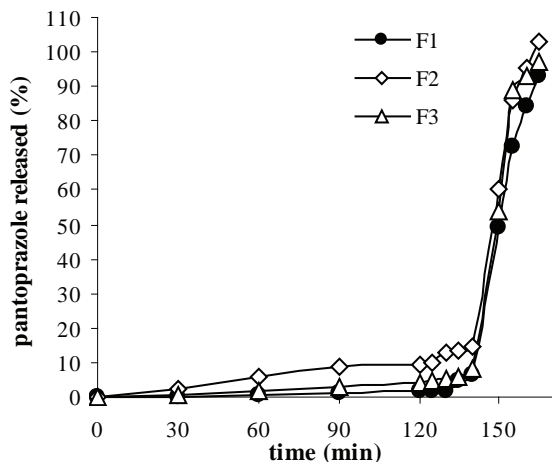


Fig. 1. Acido-resistance and drug release of three formulations of pantoprazole enteric-coated pellets.

As it can be seen from Figure 1, acid-resistance (9.5%) of Formulation 2 (F2) is at the upper acceptable limit (not more than 10% released in acidic media), while Formulations 1 and 3 (F1 and F3) have acceptable Acido-resistance properties (1.5% and 4.2%, respectively). Drug release from all formulations complies with the specification of not less than 75% (Q) pantoprazole released within 45 minutes. F1 and F2 have similar release profiles, while F2 has similar shape of release profile, but shifted to higher values.

There are indications in literature that coatings based on polyvinyl alcohol (such as Opadry® II White) can affect the start of release of an active from formulations (3), but no data that support the fact that these coatings can affect acid-resistance could be found.

F1 and F3 have proportionally low release of pantoprazole in acidic medium. It is assumed that this is due to the presence of talc, which reduces the release of active substances from the enteric-coated formulations (4). On the other hand, F3 shows a little higher release of an active compared to F1. This could be due to the presence of povidone, which is known to improve the release of active substances from the formulations (5).

CONCLUSIONS

According to performed tests and obtained results it can be concluded that the adhesive agent can affect acido-resistance of enteric-coated formulations. However, drug release from the formulations is affected very slightly by the presence of different adhesive agents.

REFERENCES

1. Cheer SM, Prakash A, Faulds H, Lamb HM. Pantoprazole. An update of its pharmacological properties and therapeutic use in the management of acid-related disorders. *Drugs*, 2003; 63: 101-132.
2. de Campos DR, Vieira NR, Bernasconi G, Barros FA, Meurer EC et al. Bioequivalence of two enteric coated formulations of pantoprazole in healthy volunteers under fasting and fed conditions. *Arzneimittelforschung*, 2007; 57: 309-314.
3. Ensslin S, Moll KP, Metz H. Modulation of pH-independent release from coated pellets: Effect of coating composition on solubilization processes and drug release. *Eur. J. Pharm. Biopharm.* 2009; 72: 111-118.
4. Nyamweya NN, Hoag SW. Influence of coloring agents on the properties of polymeric coating systems, in: McGinity JW, Felton LA (Eds) *Aqueous polymeric coatings for pharmaceutical dosage forms*, 3rd ed. Informa Healthcare, New York, 2008, pp. 171-199.
5. Foltmann H, Quadir A. Polyvinylpyrrolidone (PVP) – one of the most widely used excipients in pharmaceuticals: an overview. *Drug Delivery Technology*, 2008; 8: 22-27.





OPTIMIZATION OF SIMVASTATIN LOADING IN LONG CIRCULATING LIPOSOMES (P64)

A. Porfire¹, D. Muntean¹, M. Achim¹, L. Vlase¹, I. Tomuta^{1,*}

¹ University of Medicine and Pharmacy "Iuliu Hatieganu" Cluj-Napoca, Faculty of Pharmacy, Department of Pharmaceutical Technology and Biopharmaceutics, 41 V. Babes, 400012 Cluj-Napoca, Romania

INTRODUCTION

There are many drugs that are currently investigated or even used as liposomal formulations, due to the ability of these carriers to increase their circulation time and therapeutic index. Conventional liposomes have the major drawback that they are rapidly cleared by the reticular endothelial system and this can be overcome by using sterically stabilized liposomes. The sterical stabilization is achieved mainly by modifying the surface of the liposomes with hydrophilic polymers such as polyethylene glycol (PEG) (1,2). Long-circulating liposomes are useful tools for tumor imaging and therapy, due to their ability to passively accumulate in tumor tissues by extravasation through the leaky vasculature. However, their stability and tumor distribution are related to their composition and size.

The aim of this study was to establish the optimal formulation factors for the preparation of simvastatin-loaded long circulating liposomes (PEG-ylated liposomes), in order to get maximum efficiency of drug loading and to minimize their size.

MATERIALS AND METHODS

Materials

L- α -phosphatidylcholine (egg lecithin, 80%) was from Lipoid GmbH (Germany), cholesterol (>92.5%, GC) from Sigma-Aldrich (Germany) and simvastatin-SIM (99.89) was provided by Biocon Limited (India).

Experimental design

An experimental design with 3 factors and 3 levels was developed using Modde 10 software (Umetrics, Sweden). The studied variables (formulation factors) and their levels of variation are presented in Table 1

Tab 1: Independent variables and their level of variation

Formulation variables		Levels		
		-1	0	1
Phospholipids concentration	X ₁	10	40	70
Molar ratio phospholipids: cholesterol	X ₁	5	-	10
Concentration of SIM solution	X ₃	2	10	18

The liposomes were characterized in terms of simvastatin concentration, encapsulation efficiency, size and size distribution (polydispersity index), parameters that was used as responses. Table 2 presents the matrix of the performed experiments.

Tab 2: Matrix of experimental design

Exp. name	X ₁	X ₂	X ₃	Exp. name	X ₁	X ₂	X ₃
N1	10	5	2	N9	40	5	18
N2	40	5	2	N10	70	5	18
N3	70	5	2	N11	10	10	18
N4	10	10	2	N12	70	10	18
N5	70	10	2	N13	40	10	10
N6	10	5	10	N14	40	10	10
N7	40	10	10	N15	40	10	10
N8	10	5	18				

X₁-phospholipids concentration; X₂- molar ratio phospholipids: cholesterol; X₃- concentration of SIM solution

Preparation of liposomes

Liposomes were prepared using film hydration method and their size was reduced by high pressure extrusion through polycarbonate membranes using LiposoFast LF-50 equipment (Avestin Europe GmbH, Germany) (3).

Characterization of liposomes

SIM content and encapsulation efficiency were determined using a HPLC-UV validated method. Size and size distribution of liposomes (polydispersity index) were determined using Zetasizer Nano-ZS90 (Malvern, UK).



RESULTS AND DISCUSSION

The results obtained after fitting and the statistical parameters calculation, using data obtained from the experimental design are shown in Figure 1.

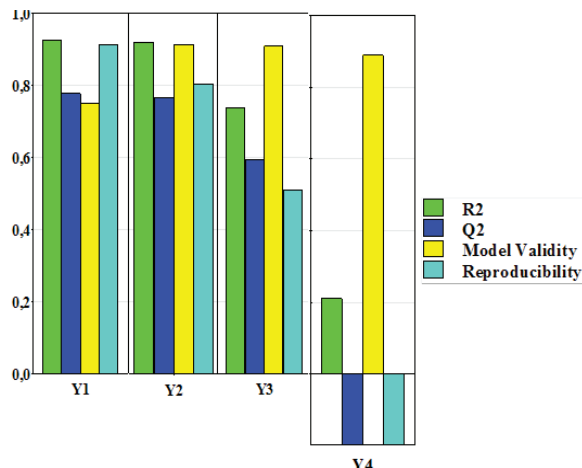


Fig. 1: Summary of fit for the experimental design

The results fit well for the responses Y_1 - Y_3 , while for Y_4 they did not fit at all. The influence of the formulation factors on responses are presented in Fig. 2-Fig. 5.

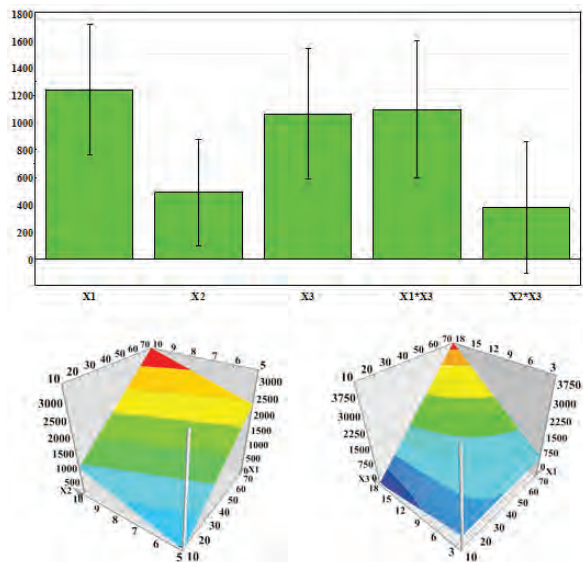


Fig. 2: The influence of the formulation factors on simvastatin concentration in liposomes (Y_1)

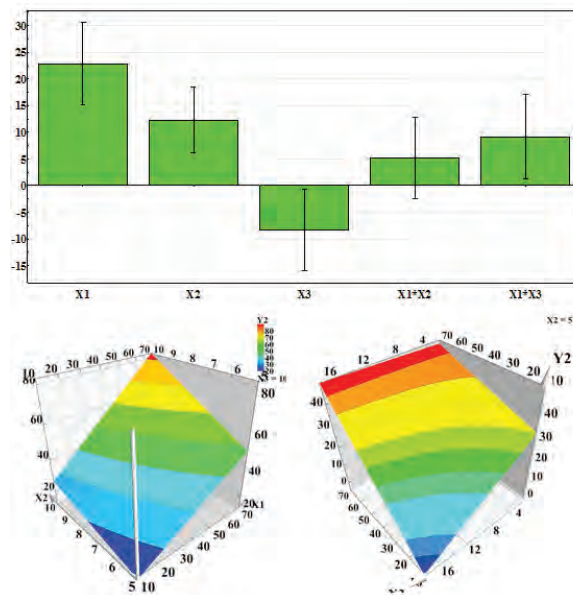


Fig. 3: The influence of the formulation factors on encapsulation efficiency (Y_2)

Concentration of SIM solution and the phospholipids' molar ratio have the most important influence on SIM concentration in liposomes and encapsulation efficiency. Both parameters increased when higher SIM concentrations and higher molar ratios were used in the preparation process.

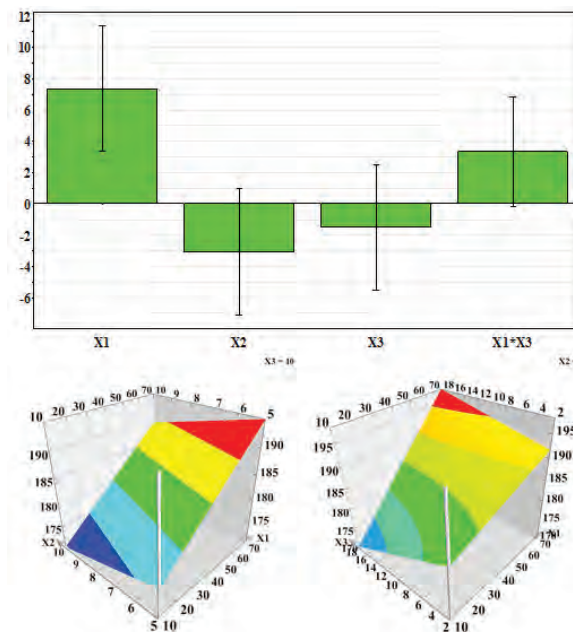


Fig. 4: The influence of the formulation factors on size of liposomes (Y_3)



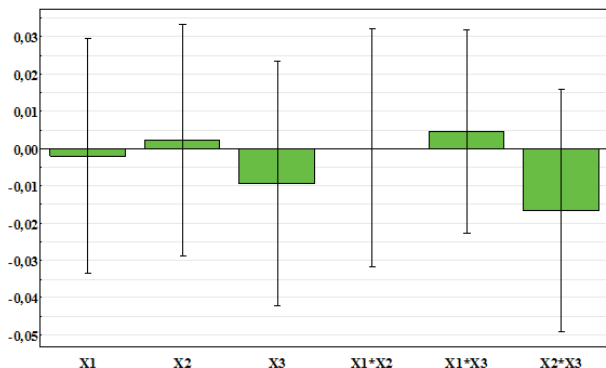


Fig. 5: The influence of the formulation factors on polydispersity index of liposomes (Y_4)

The optimal characteristics of liposomes (highest simvastatin concentration, encapsulation efficiency over 80% and liposomal size around 180 nm) were obtained using 70 mM phospholipids in a molar ratio of 10:1 to cholesterol and 18 mM initial simvastatin concentration.

CONCLUSIONS

In conclusion, optimization of formulation can be used for the design of long circulating liposomes for targeted antitumor therapy.

REFERENCES

1. Yang T, Choi MK, Cui FD, Kim JS, Chung SJ, Shim CK, Kim DD. Preparation and evaluation of paclitaxel-loaded PEGylated immunoliposome. *J. Control. Release.*, 2007; 120: 167-177.
2. Chang HI, Yeh MK. Clinical development of liposome-based drugs: formulation, characterization, and therapeutic efficacy. *Int J Nanomedicine.* 2012; 7: 49-60.
3. Porfire A, Tomuta I, Tefas L, Leucuta SE, Achim M. Simultaneous quantification of L-phosphatidylcholine and cholesterol in liposomes using near infrared spectrometry and chemometry. *J. Pharm. Biomed. Anal.* 2012; 63: 87-94.

FORMULATION OF IBUPROFEN-LOADED POLYCAPROLACTONE NANOFIBERS AND EVALUATION OF THE DRUG RELEASE

(P65)

T. Potrč^{1*}, P. Kocbek¹, J. Kristl¹, S. Baumgartner¹

¹ Faculty of Pharmacy, University of Ljubljana, 1000 Ljubljana, Aškerčeva 7, Slovenia

INTRODUCTION

Nanofibers represent one of the newest and extremely promising nanomaterials with wide application area. They have a particularly important role in biomedicine, where numerous studies have been performed in the field of tissue engineering, wound healing and drug delivery. Nanofibers can resemble the fibrillar elements of natural extracellular matrix, which results in faster tissue or organ regeneration. They enable also preparation of drug delivery system with desired release profile. The drug can be incorporated in the core of nanofibers or attached to their surface (1, 2).

The most common method for production of nanofibers with diameters ranging from few nanometers to few micrometers from polymer solutions or melts is electrospinning (3). Biodegradable and biocompatible polymers, such as polycaprolactone (PCL), are good candidates for nanofiber preparation for application in biomedicine (4). PCL is hydrophobic, semi-crystalline polymer with a high molecular weight. It is suitable for controlled drug delivery system preparation and exhibits good compatibility with many drugs (4, 5). The aim of our research was to prepare ibuprofen-loaded PCL nanofibers by electrospinning and to characterize the electrospun product.

MATERIALS AND METHODS

Materials

Polycaprolactone (PCL) Mw 70,000- 90,000 g/mol was purchased from Sigma-Aldrich, Germany. Sodium iodide (NaI) ($\geq 99.5\%$), chloroform, acetone ($\geq 99.5\%$), sodium



chloride ($\geq 99.5\%$), sodium hydroxide ($\geq 99.5\%$), potassium chloride ($\geq 99.5\%$), potassium dihydrogen phosphate ($\geq 99.5-100.5\%$) and di-sodium hydrogen phosphate ($\geq 99.0\%$) were all obtained from Merck, Germany.

Preparations of polymer solutions

PCL solutions (10%, w/w) were prepared by dissolving PCL in mixture of chloroform and acetone in weight ratio 75:25, respectively. The solutions were supplemented with 0.03% (w/w) NaI and stirred on a magnetic stirrer for 3-4 h at room temperature. Ibuprofen was then added (10 % or 15 %, w/w based on the dry weight of polymer) and the solutions were stirred for additional 1-2 h before electrospinning.

Electrospinning process

The solution was placed in a plastic syringe fitted with a metal needle (inner diameter 0.8 mm) and a high voltage of 15 kV was applied by a high voltage generator (model HVG-P60-R-EU, Linari Engineering s.r.l., Italy) to initiate the jet. The polymer solution feeding rate (1.63 ml/h in case of 10% and 1.98 ml/h in case of 15% ibuprofen solution) was controlled by the syringe pump (model R-99E, Razel Scientific, USA) and a grounded aluminium foil covered screen used as a collector was placed 15 cm from needle tip.

Characterization of electrospun product

The morphology of the electrospun drug-loaded PCL nanofibers was observed by scanning electron microscopy (Supra35 VP, Carl Zeiss, Oberkochen, Germany), using an accelerating voltage of 1 kV and a secondary detector.

Drug release study

A sample of nanofibers (~100 mg) was rolled on a glass carrier and placed in 250 ml of phosphate buffer with pH 7.4. The sample was stirred on a magnetic stirrer at room temperature and 1 ml aliquots were withdrawn at predetermined time points. The drug released was determined by HPLC analysis (Agilent 1100 Series, Hewlett Packard, Waldbron, Germany) using a Nucleosil C8 column (5 μm , 250 mm x 4 mm) at 35°C. The mobile phase was a mixture of acetonitrile and phosphate buffer (pH 7.5), 28.5:71.5 and the flow rate 1.2 ml/min. The drug was monitored by diode array detector at 225 nm.

RESULTS AND DISCUSSION

The electrospinning of PCL solution under optimal process parameters enabled preparation of beadless ibuprofen-loaded nanofibers (Fig. 1).

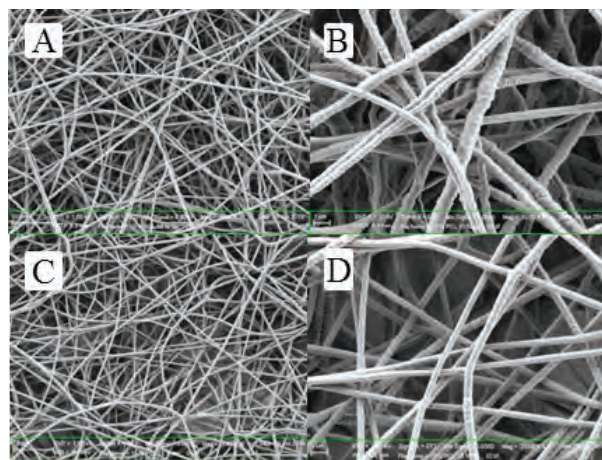


Fig. 1: SEM micrographs of electrospun PCL nanofibers loaded with 10% (A, B) and 15% (C, D) ibuprofen (based on the weight of dry polymer). The nanofibers were visualized at small (A, C) and high (B, D) magnification.

The surface of nanofibers loaded with 10% ibuprofen was rough and their average diameter was ~390 nm (Fig.1 A and B). Contrary, the nanofibers with 15% ibuprofen were mainly smooth and their average diameter was smaller (~280 nm). The surface morphology and the fiber thickness showed no influence on the drug release profile. The release of ibuprofen from both samples of nanofibers was surprisingly fast (Fig. 2), since 87.4% and 84.9% of drug was released in the first 4 h from PCL nanofibers with 10% and 15% ibuprofen, respectively.

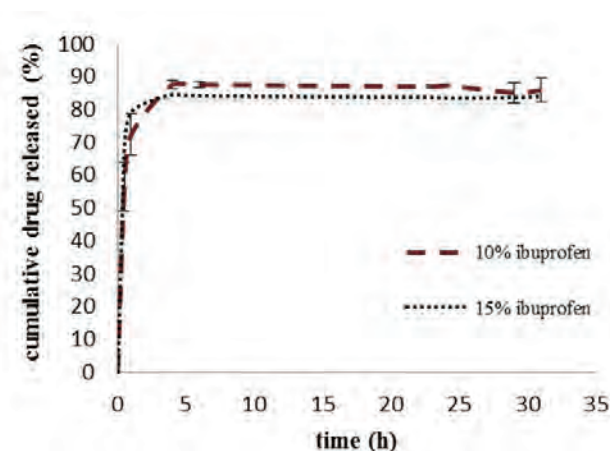


Fig. 2: In vitro release profiles of ibuprofen from PCL nanofibers.



CONCLUSION

The preparation of electrospun PCL nanofibers was shown to be an effective novel nanotechnological approach in formulation of fast release dosage forms with poorly soluble drugs.

REFERENCES

1. Huang Z.-M, Zhang Y.-Z, Kotaki M, Ramakrishna S: A review on polymer nanofibers by electrospinning and their applications in nanocomposites. *Composites Science and Technology* 2003; 63: 2223-2253.
2. Sill TJ, von Recum HA: Electrospinning: Applications in drug delivery and tissue engineering. *Biomaterials* 2008; 29: 1989-2006.
3. Bhardwaj N., Kundu C.S. Electrospinning: A fascinating fiber fabrication technique. *Biotechnology Advances* 2010; 28: 325-347.
4. Kenawy E.-R, Abdel-Hay F.I, El-Newehy M.H, Wnek G.I: Processing of polymer nanofibers through electrospinning as drug delivery systems. *Material Chemistry and Physics* 2009; 113: 296-302.
5. Dash T.K, Konkimalla V.B: Poly-ε-caprolactone based formulations for drug delivery and tissue engineering: A review. *Journal of Controlled Release* 2012; 158: 15-33.

THE IMPACT OF TERMINAL STERILIZATION BY AUTOCLAVING ON ACTIVE INGREDIENT RELEASE FROM NANOPARTICLES (IN PARENTERAL NANOSUSPENSION) (P66)

J. Praček^{1*}, M. Avanzo¹, Š Irman¹, T. Rozman Peterka¹, M. Oblak¹, K. Kristan¹, P. Kralj¹

¹ Sandoz Development Center Slovenia, Verovškova 57, SI-1526 Ljubljana, Slovenia, E-mail: jurij.pracek@sandoz.com

INTRODUCTION

The process of thermal sterilization employing saturated steam under pressure is carried out in a chamber called autoclave. It is probably the most widely employed sterilization process. The design or choice of a cycle for product depends on number of factors, including the heat lability of the material, knowledge of heat penetration into article and other factors (1). The product we have developed is a nanosuspension for intravenous administration. The nanoparticles of about 30 nm are engulfed by macrophages in the blood and the Active Pharmaceutical Ingredient (API) is then slowly released inside of the phagolysosomes. Autoclaving was chosen as final sterilization method of Finished Dosage Form (FDF).

MATERIALS AND METHODS

Nanosuspension

Nanoparticles with carbohydrate shell and active ingredient in the core were suspended in purified water. pH and osmolarity were adjusted to physiological conditions.

Sterilization process

We have studied the significance of two sterilization parameters, temperature and sterilization time, on FDF characteristics. During laboratory development the effect of





temperature was tested in the range of 110–134 °C and autoclaving time between 3 and 100 min. Final sterilization cycle was determined and confirmed on production scale equipment.

Nanoparticle stability and release study

API leaking from nanoparticles was determined by ultrafiltration of the FDF, using filter devices with MWCO of 30 kDa.

The stability of nanoparticles in human serum was followed up-to one week at 37°C. The reaction of the released API with a specific reagent was followed spectrophotometrically.

The API release from nanoparticles was determined at physiological pH (~4.9). The API release was followed spectrophotometrically, as described above.

Phagocytosis

Macrophages (cell line J774.2) were treated with nanoparticles for 48 hours. Then, the cells were washed and lysed. The amount of API, engulfed by macrophages, was determined spectrophotometrically.

RESULTS AND DISCUSSION

The stability of nanoparticles

The effect of autoclaving process on API leaking was determined by ultrafiltration. The results have shown that the API is not leaking from nanoparticles after autoclaving at all selected parameters. Undetectable levels of API were determined in a filtrate after ultrafiltration by using filters with 30 kDa MWCO.

Additionally, nanoparticles were incubated in human serum up-to one week. The results have shown that serum components have no influence on API leaking from nanoparticles, what is an excellent indicator for a safe product, since the API should not be released in the blood stream.

API release

After injection, the nanoparticles are engulfed by macrophages. The nanoparticles are trapped in a phagosome which then fuses with a lysosome to form a phagolysosome. Phagolysosome contains enzymes and toxic peroxides and equilibrates to a pH of 4.5–5.0 (2). There, the carbohydrate shell of nanoparticles is digested and the API is released.

We have studied the API release at pH ~4.9 for samples that underwent different autoclaving processes. We have discovered that the API release is the fastest in samples that were not sterilized by autoclaving. Prolonged sterilization time reduces the rate for API release, probably by further polymerization of carbohydrate shell.

Phagocytosis

Samples that underwent different autoclaving processes were tested for phagocytosis. Additionally, samples with different particle size were tested. We have discovered that only particle size influences the extent of phagocytosis, while autoclaving process does not.

Selected sterilization parameters

Different samples were produced by changing two process parameters of sterilization, temperature and time. Final sterilization cycle was defined after detailed FDF characterization. Results indicate strong influence of the terminal sterilization parameters on release of API from nanoparticles. The following parameters were selected: the sterilization temperature between 121 and 124 °C and the autoclaving time between 26 and 34 min.

CONCLUSIONS

Beside sterility assurance terminal sterilization has a major effect on characteristics of product Critical Quality Attributes (CQA), including release of API from nanoparticles. Setting the right process parameters for autoclaving leads us to a product essentially similar with respect to *in vitro* and *in vivo* behaviour with the reference product. Thus, a safe and effective parenteral nanosuspension, comparable to the reference product was developed.

REFERENCES

1. *The United States Pharmacopeia, <1211> STERILIZATION AND STERILITY ASSURANCE OF COMPENDIAL ARTICLES*
2. Russell DG, VanderVen BC, Glennie S, Mwandumba H, RS Heyderman. *The macrophage marches on its phagosome: dynamic assays of phagosome function. Nature reviews, Immunology 2009; 9: 594–600.*





MICROEMULSION HYDROGELS FOR PERCUTANEOUS DELIVERY OF IBUPROFEN: FORMULATION AND CHARACTERIZATION

(P67)

Lj. Djekic*, D. Djordjevic, M. Martinovic, M. Primorac

University of Belgrade-Faculty of Pharmacy, Department of Pharmaceutical technology and Cosmetology, Vojvode Stepe 450, 11221 Belgrade, Serbia

INTRODUCTION

The interest on evaluation of microemulsion hydrogels has grown in the last decade due to their unique gelation behaviour, coexistence of oil and aqueous phases, ease of preparation and a significant potential for improvement of effectiveness of topically applied drugs over the conventional creams, ointments, and hydrogels (1, 2). Current investigations are focused on development of biocompatible microemulsion systems comprising GRAS excipients, such as lecithin (3). Formulation of lecithin-based microemulsion hydrogels, their physico-chemical properties, morphology, internal mobility of constituents and drug release properties are poorly investigated (4, 5). The purpose of the current study was formulation of microemulsion hydrogels (MH) stabilised by lecithin and their evaluation as potential carriers for transdermal delivery of ibuprofen (5% w/w).

MATERIALS AND METHODS

The components of the formulated MHs were: lecithin, soy bean oil, poloxamer 407, and water, purified (Ph. Eur. 7.0 grade). MH samples were formulated at lecithin-to-poloxamer ratio 1:1 and water concentration in the range from 55.00 up to 60.62% w/w. Four samples (F1-F4) were prepared by admixing water solution of poloxamer to an oil solution of lecithin, until the mixture converts into the homogeneous gel, at room temperature. Drug-loaded MHs were prepared by dispersing of ibuprofen into

the carrier at the therapeutical concentration (5% w/w). Characterization of MHs was included: organoleptic examination (colour, odour, homogeneity, and spreadability), pH measurement (pH-meter HI 9321, Hanna Instruments Inc., USA), electrical conductivity determination (conductometer CDM 230, Radiometer, Denmark) (94 Hz frequency; at 20 ± 0.5 °C), determination of maximal apparent viscosity and flow behaviour (rotational rheometer Rheolab MC120 (Paar Physica, Germany) equipped with a cup and plate measuring device MK22, at 20 ± 0.1 °C). Evaluation of *in vitro* release from investigated PLMHs was performed at 32 °C in the rotating paddle apparatus (Erweka DT 70, Erweka, Germany) using Teflon enhancer cell with 4 cm² diffusion area (VanKel Technology Group, USA) covered with a cellulose membrane and dipped in 750 ml of the phosphate buffer pH 7.2, USP. The samples were analysed spectrophotometrically (Cary 50, Varian, Germany) at 220 nm.

RESULTS AND DISCUSSION

The prepared samples F1-F4 were homogenous yellow semisolids with mild lecithin odour, at room temperature (Figure 1).

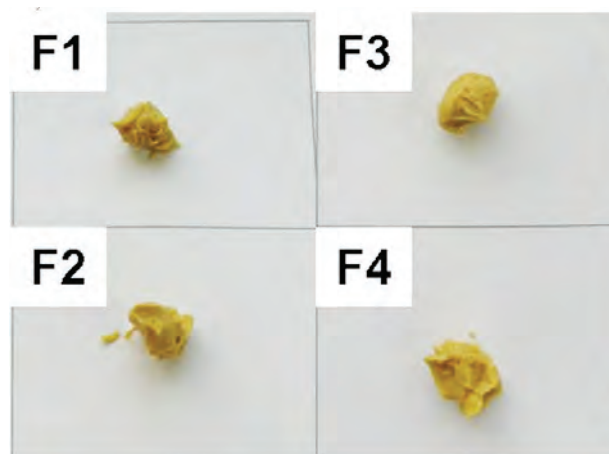


Fig. 1. Appearance of MHs F1-F4.

The pH value of the investigated MHs was ~5.3, which is acceptable for skin application. Electrical conductivity of the MHs ranged from 744 $\mu\text{S}/\text{cm}$ (F1), 983 $\mu\text{S}/\text{cm}$ (F2), 1089 $\mu\text{S}/\text{cm}$ (F3), up to 1147 $\mu\text{S}/\text{cm}$ (F4). The generally high conductivity values indicated water-continuous character of the investigated systems. Also, conductivity increases as the content of the water phase increase. The obtained shear rate ($\dot{\gamma}$) vs. shear stress (τ) described thixotropic pseudoplastic behaviour which is favourable for topical formulations. The apparent viscosity was: F1 662



Pas; F2 118 Pas ; F3 108 Pas; F4 57,1 Pas.

The proposed mechanism of the formation of MHs structure comprises the formation of mixed lecithin/poloxamer micelles with solubilized oil phase. The lecithin molecules enable the hydrophobic interactions with the oil phase, while the poloxamer 407 molecules interact with the water molecules *via* hydrogen bonds. As the relative content of the amphiphiles decreases, the hydrophobic interactions and hydrogen bonds were weakened and therefore the concentration of the unbound water was increased, that likely enhance the conductivity and decrease the viscosity of the investigated MHs.

The obtained release profiles (figure 1) described drug release controlled by the carrier. The cumulative amount of ibuprofen released after 6 h, was ~12.5%. In spite of the significantly different rheological behaviour of the investigated samples, the values of the release parameters were not affected by the relative content of the water phase. It was assumed that the diffusion of ibuprofen, a poorly water soluble drug substance, from the carrier is mainly limited by the drug partitioning between the oil and water phase of the MHs. Furthermore, the acceptor medium (phosphate buffer pH 7.2), enable a higher drug solubility as well as a driving gradient for drug release.

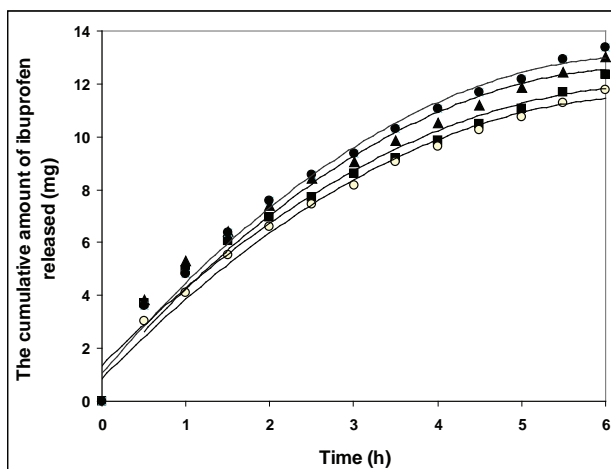


Fig. 1. *In vitro* ibuprofen release profile (F1○, F2■, F3● F4▲).

CONCLUSIONS

The analysis of the obtained results revealed that formation of the MHs was likely based on self-assembly of lecithin/copolymer mixed micelles with solubilised oil phase, into a gel network which was immersed in the surrounding water phase.

The *in vitro* drug release profile revealed drug release controlled by the carrier which implicated that formulated MHs are promising carriers for sustained release of ibuprofen.

ACKNOWLEDGEMENT

The authors would like to thank Ministry of Education and Science of Republic of Serbia for financial support within the projects III46010 and TR34007.

REFERENCES

1. Almeida H, Amaral MH, Lobão P, Lobo JMS. *Pluronic F-127 and Pluronic Lecithin Organogel (PLO): Main Features and their Applications in Topical and Transdermal Administration of Drugs.* *J Pharm Pharm Sci* 2012;15(4):592-605.
2. Murdan S. *Organogels in drug delivery.* *Exp Opin Drug Deliv* 2005;2:489-505.
3. Fanun M. *Biocompatible Microemulsions.* In: Fanun M. ed. *Colloids in Biotechnology.* CRC Press Taylor & Francis Group, Boca Raton, FL, USA, 2011; 417-436.
4. Djekic L, Primorac M, Filipic S, Agbaba D. *Investigation of surfactant/cosurfactant synergism impact on ibuprofen solubilization capacity and drug release characteristics of nonionic microemulsions.* *Int J Pharm* 2012;433(1-2):25-33.
5. Yang Y, Wang S, XuH, Sun C, Li X, Zheng J. *Properties of topically applied organogels: rheology and in vitro drug release.* *AJPS* 2008;3(4):175-183.





EVALUATING VARIOUS WET BINDERS TO GAIN LACTOSE BASED AGGLOMERATES APPLICABLE FOR ORALLY DISINTEGRATING TABLET FORMULATIONS (P68)

Th. Agnese¹, Th. Cech¹, B. Rabausch¹, M. Mistry²

¹ European Pharma Application Lab, BASF SE, Ludwigshafen, Germany

² Pharma Ingredients & Services, Sub-Sahara Africa, BASF West Africa Ltd., Ikoyi, Nigeria

INTRODUCTION

In regard to line extensions or improving administration convenience orally disintegrating tablets have become a popular dosage form over the last years (1). Nowadays, the formulator has some ready-to-use aids on hand, allowing quick and simple drug formulation (2).

However, not all drugs can be processed as direct compressible formulation, either because of their poor flow characteristics or due to their poor compressibility. As a result, granulation processes need to be applied to gain compressible blends.

The aim of this work was to investigate the performance of various wet binders onto the properties of the agglomerates, deriving from a high shear granulation process. Furthermore, the impact of the formulation on the disintegration characteristics was investigated.

MATERIALS AND METHODS

The following wet binders were used for the investigation: corn starch (Cargill), poly(vinyl pyrrolidone) (Kollidon[®] 25 and 90F, BASF), copovidone (Kollidon[®] VA64, BASF), poly(vinyl alcohol)-poly(ethylene glycol) graft copolymer

(Kollicoat[®] IR, BASF). As filling material lactose (Granu-Lac[®] 230, Meggle Pharma) was used.

For tableting 10.0% crospovidone (Kollidon[®] CL-SF, BASF) and 0.5% magnesium stearate (Bärlocher) were added to the agglomerates.

Wet granulation

The wet granulation processes were conducted in a high shear mixer (Diosna P 1/6) applying an impeller speed of 200 rpm and a chopper speed of 2,000 rpm. The binder (2.0% w/w final granules) was added as aqueous solution within 120 s, followed by a granulation time of 180 s.

The wetted agglomerates were passed through an oscillating sieving machine (w=1.6 mm, AR400, ERWEKA), dried on a tray (ambient conditions), and finally passed through a sieve (w=0.8 mm).

Tableting

The compression was done using a single punch press XP 1 (Korsch) equipped with flat faced, faceted punches with a diameter of 8.0 mm. Compression forces of 2 to 8 kN were applied at a tableting speed of 20 tablets per minute.

Analytical testing

The friability of the dried agglomerates was tested in an air jet sieve (Rheum) (3).

Disintegration time of the tablets (n=6) was tested (ERWEKA ZT 74) in demineralised water (37°C ± 1 K).

RESULTS AND DISCUSSION

Viscosity of the polymer solution is a crucial and important parameter when selecting a binder for high shear granulation processes. Solutions containing the synthetic polymers used in this investigation led to low or moderate viscosities whereas starch was prepared with hot water (80°C) resulting in a paste.

The binders used for this investigation could clearly be distinguished regarding their individual performance. Both particle size distribution and friability of the agglomerates revealed the lowest binding efficiency for Kollidon[®] VA64, followed by Kollidon[®] 25, Kollicoat[®] IR and Kollidon[®] 90F. The strongest and also largest agglomerates were gained with the binder corn starch (Fig. 1, Fig. 2).

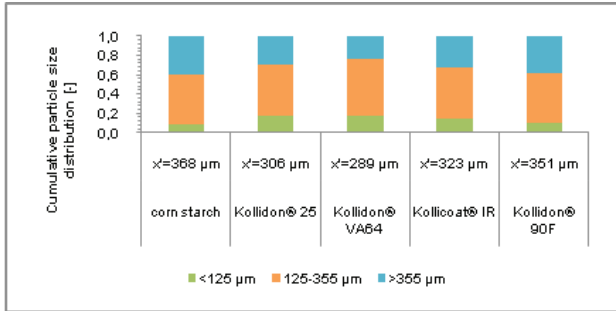


Fig. 1: Cumulative particle size distribution and mean particle size of agglomerates containing different binders.

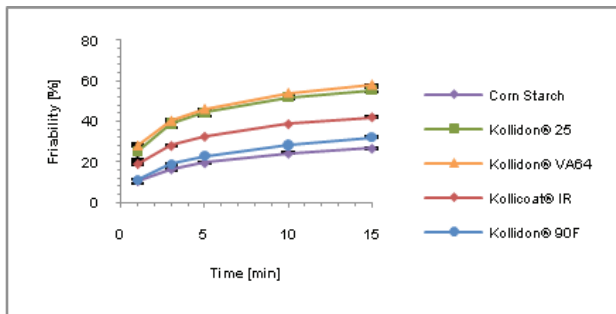


Fig. 2: Friability of agglomerates containing different binders as function of testing time.

Interestingly, the results of tablet's disintegration properties showed a varying picture (Fig. 3). When comparing tablets of the same tensile strength (0.9-1.0 N/mm²) formulations containing a synthetic polymer showed disintegration characteristics which could be correlated with the strength of the granules: stronger granules led to tablets of longer disintegration time. However, agglomerates containing corn starch resulted in tablets offering a disintegration time of merely about 30 seconds without any additional disintegrant added to the formulation (Fig. 3). As soon as a disintegrant was added (10% Kollidon® CL-SF), disintegration times of all tablets containing synthetic polymers were below 30 seconds as well (Fig. 4).

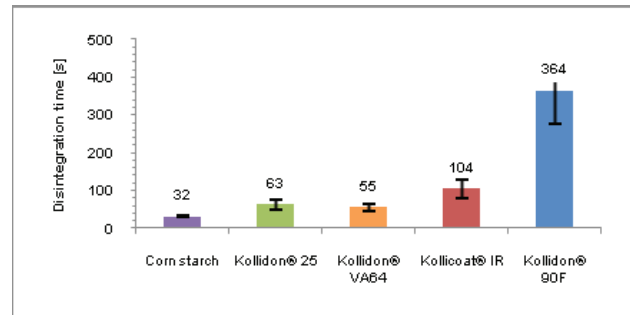


Fig. 3: Disintegration time of tablets, containing no disintegrant (mean value (n=6), ±SD).

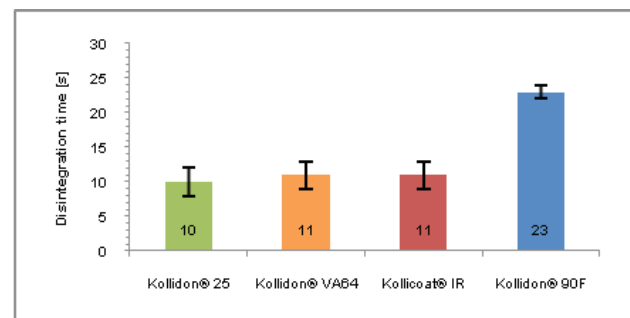


Fig. 4: Disintegration time of tablets, containing 10% of disintegrant (mean value (n=6), ±SD).

CONCLUSIONS

Even though starch paste offered distinct disadvantages in regard to its application, it offered some benefits regarding the resulting agglomerates. Firstly, strength of the formed agglomerates was high (low friability) allowing good blending and processing, and secondly, disintegration time of the tablets was low, even without disintegrant in the formulation.

Solutions of synthetic polymers were easier (and safer) to prepare (no heated water) and easier to process (low viscosities). But, tablet formulations required some disintegrant to allow quick disintegration.

REFERENCES

1. Bohnacker R, Streil F, Schweizer S, Müller I; Determination of the disintegration time of mouth melt tablets with texture analyser method; *Pharm. Ind.* 67 (3), 327-35 (2005).
2. Kruse S, Gebert S, Kolter K, et. al; Development of orally disintegrating tablets based on a new excipient, 2007 AAPS Annual Meeting and Exposition; November 11-15, 2007; San Diego (CA), USA
3. Agnese Th, Herting MG, et. al; An innovative method to determine the strength of granules; 2008 AAPS Annual Meeting and Exposition; November 16-20, 2008; Atlanta (GA), USA





SEROTONIN IN DIFFERENT COMPOUNDS: CRYSTALLOGRAPHIC AND COMPUTATIONAL INSIGHT (P69)

Denis A. Rychkov^{1,2,5*}, Elena V. Boldyreva^{1,2}, Viktor Yu. Kovalskii³, Steven Hunter⁴, Colin R. Pulham⁴, Carole A. Morrison⁴.

¹ Institute of Solid State Chemistry and Mechanochemistry, Kutateladze, 18, Novosibirsk, 630128, Russia,

² REC-008, Novosibirsk State University, Pirogova, 2, Novosibirsk, 630090, Russia.,

³ Borekov Institute of Catalysis, Siberian Branch of the Russian Academy of Sciences, pr. Lavrentieva 5, 630090 Novosibirsk, Russia

⁴ School of Chemistry and Centre for Science at Extreme Conditions, The University of Edinburgh, King's Buildings, West Mains Road, Edinburgh, EH9 3JJ, Scotland, UK.

⁵ Faculty of Pharmacy, University of Ljubljana, Aškerčeva 7, 1000 Ljubljana, Slovenia.

PURPOSE

Biologically active substances are in the focus of pharmaceutical and chemical research. Serotonin, one of the most common neurotransmitters, is widely studied in relation to its effect on humans from cellular to neurological levels. Although serotonin plays a key role in some biological processes, its chemistry and crystallography are not sufficiently understood (1, 2).

The aim of the present study was to crystallize serotonin adipate and creatinine sulfate monohydrate, determine their crystal structures, and analyze them in a comparison with other previously known serotonin crystal structures. The interrelation between the molecular conformation and crystalline environment was studied. This issue was addressed using crystallographic and computational chemistry (DFT-D, MD) approaches.

Special attention was paid to investigation of serotonin behaviour in aqua media, including minima and TS location. Different interactions in liquid and solid phases and their effect to serotonin conformation were compared for different crystal structures.

MATERIALS AND METHODS

Single molecule calculations in aqua media were performed using Gaussian 09, data was prepared, analyzed and described using GaussView 05 and Chemcraft 3.3. Potential energy surface (PES), minima search and transition states (TS) were calculated using B3LYP/6-31G(d,p) level of theory. To simulate aqua media the self-consistent reaction field (SCRF) method was employed with Tomasi's polarized continued model (PCM) defining the solvent cavities surrounding serotonin.

Solid state calculations at ambient pressure were performed using density functional theory with dispersion correction (DFT-D) coupled to the plane-wave pseudopotential methods, as implemented in CASTEP 5.5. version. The dispersion correction scheme of Tkachenko and Scheffler was used in all calculations. Treatment of electronic exchange and correlation was handled by the generalized gradient approximation (GGA) formalized by Perdew, Burke, and Ernzerhof (PBE). Use UPPER CASE Calibri 12 points bold for section headings.

X-Ray experiments were performed using Oxford Gemini Ultra R diffractometer, Mo K α radiation type. Structure was solved and refined using OLEX2, SHELXS97, SHELXL97 software. Crystals of serotonin adipate (PanaLife, 98%) and serotonin creatinine sulphate monohydrate (Sigma Aldrich, 99%) were crystallized for diffraction experiment using original technique (3) from water solution.

RESULTS AND DISCUSSION

The Potential energy surface (PES) with respect to ϕ_1 and ϕ_2 (Fig.1.) was calculated, constructed and examined.

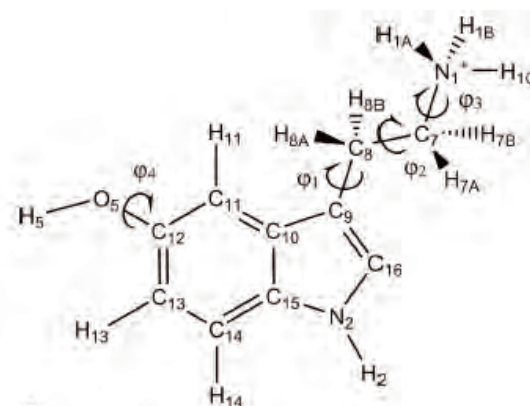


Fig.1. Definition of serotonin atom numbering and dihedral angles. The four torsion angles are defined as ϕ_1 (C10–C9–C8–C7), ϕ_2 (C9–C8–C7–N1), ϕ_3 (C8–C7–N1–HN1A) and ϕ_4 (C11–C12–O5–H5).



Minima were located and refined using fully relaxed scan procedure, no negative modes were observed in calculated vibration spectra for these structures. TS search was performed using QST3 method, using PES profile for initial guess of TS. Three independent and six in total minima were found for serotonin molecule in aqua media with fixed φ_4 angle. Energies of all minima and TS were calculated, showing high conversion probability of one minimum to another in liquid phase under ambient conditions.

Serotonin conformations in all known crystals (including one new and one refined structures) were compared and mapped to PES, showing that only two main conformations are found in the solid state. Computations have shown that serotonin conformations determined in X-Ray experiment are energetically very close to the minima calculated previously in aqua media. Differences in the conformations in crystalline state were studied, intermolecular interactions were highlighted and correlated to geometry differences in serotonin molecule. Conformational energies and energies of intermolecular interactions were calculated and compared.

CONCLUSIONS

One new structure (serotonin adipate) of serotonin was determined, one previously known structure was re-determined and refined (serotonin creatinine sulphate monohydrate - medical formulation). Serotonin conformations were compared, and two main conformations were distinguished that are realized in crystal structures. PES, minima and TS for serotonin were calculated. Energies in liquid and solid phases were calculated.

In this work serotonin conformation in solid state was shown to be energetically close to that in aqua media, supporting a theory of a limited number of conformations of bioactive molecules in the solid state.

CHALLENGES

Serotonin is unstable in the liquid phase what limits it direct investigation in aqua media by experimental techniques.

ACKNOWLEDGEMENT

The work was supported by the RFBR Grants №14-03-31866, 13-03-92704, Russian Ministry of Science and Education and RAS, Siberian Supercomputer Center SB RAS Integration Grant №130, Edinburgh Compute and Data Facility

REFERENCES

1. Mohammad-Zadeh, L. F., Moses, L. & Gwaltney-Brant, S. M. *Serotonin: a review*. 2008, *J. Vet. Pharmacol. Ther.* 31, 187–199.
2. Seo, D., Patrick, C. J. & Kennealy, P. J. ,2008. *Aggress. Violent Behav.* 13, 383–395.
3. Rychkov.D.A, Arkhipov S.G., Boldyreva E.V., *Simple and efficient modifications of well-known techniques for reliable growth of high-quality crystals of small bioorganic molecules* . Aug.2014, *J.Appl.Cryst.*, doi:10.1107/S1600576714011273





PREPARATION AND CHARACTERIZATION OF ELECTROSPUN SUBERIN AND CHLORAMPHENICOL LOADED NANOFIBERS (P70)

L. Rammo^{1,*}, U. Paaver¹, I. Laidmäe¹, K. Kirsimäe², N. Skalko-Basnet³, P. Veski¹, J. Heinämäki¹, K. Kogermann¹

¹ Department of Pharmacy, University of Tartu, Nooruse 1, 50411, Tartu, Estonia

² Department of Geology, University of Tartu, Ravila 14A, 50411, Tartu, Estonia

³ Department of Pharmacy, UiT The Arctic University of Norway, 9037, Tromsø, Norway

INTRODUCTION

Recently, nanofibrous nonwoven systems have gained much attention as drug delivery systems. One promising application of nanofibers is to use them as medicated wound dressings (1).

Suberin (SUB) is a natural polymer extracted from the outer birch bark. It is a surface wax-like material consisting of a polyaliphatic domain in association with a polyaromatic domain (2). Suberin can be hydrolyzed by base treatment and fractioned to suberin fatty acids (SUB FA) (3).

The aim of this work was to prepare and characterize novel nanofibers containing SUB FA and polyvinylpyrrolidone (PVP) as carrier polymers. Chloramphenicol (CAP) was used as a model antibiotic in the polymeric nanofibrous systems.

MATERIALS AND METHODS

Materials

PVP (Kollidon K90) was obtained from BASF Aktiengesellschaft, Germany. CAP was purchased from Sigma-Aldrich. SUB FA (Batch Pilot 1/14.01.2013) was obtained from VTT, Technical Research Centre of Finland, Espoo, Finland. Ethanol (96%) was used as a solvent.

Methods

Table 1 shows the nanofibrous systems. Electrospinning solutions were prepared by dissolving the solids in 5 ml of ethanol. Hence SUB:PVP solid nanofibers in weight ratio 1:4 and theoretical content of CAP 2.1% was prepared.

Tab. 1: Formulation composition of experimental nanofibers. The nanofibers were composed of (I) PVP, (II) SUB FA and PVP (1:4), (III) PVP and CAP (2.1%), (IV) SUB FA, PVP and CAP (2.1%). The compositions are given in mg.

NANOFIBERS				
	I	II	III	IV
PVP	240	192	240	192
SUB FA	0	48	0	48
CAP	0	0	5	5

The polymeric solutions were applied to electrospinning (ES) at controlled conditions. The voltage was set to 9 kV, distance between the needle and the collector 6 cm and the flow rate 1.5 ml/h. All nanofibers were collected onto an aluminium foil.

The nanofibers were characterized using scanning electron microscopy (SEM) and X-ray powder diffraction (XRPD).

The CAP content of nanofibers was determined by means of high-pressure liquid chromatography (HPLC). Average content deviation (%) from theoretical content was calculated using equation:

$$\frac{A - B}{A} \times 100\%$$

where A = theoretical CAP content in the nanofibers (2.1%) and B = measured average CAP content in nanofibers.

RESULTS AND DISCUSSION

ES produced nanofibrous mats with a uniform structure and white colour in appearance. Average fiber diameter ranged from 300 to 500 nm (Fig. 1). The absence of beads (= processing defects) suggested the optimal solvent and process parameter selection for the present nanofibrous system.

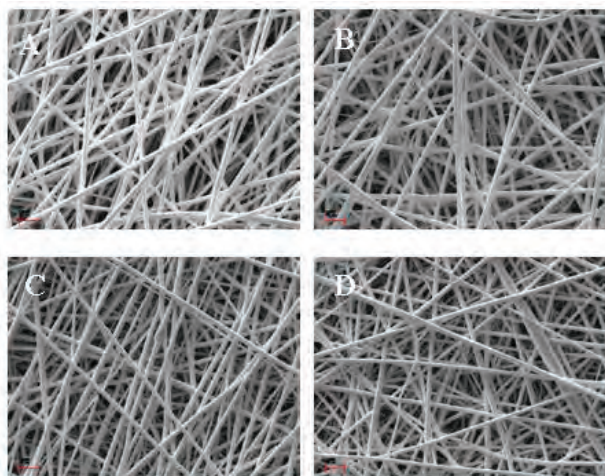


Fig. 1: Scanning electron micrographs (SEM) of nanofibers. Key: (A) I - PVP; (B) II - SUB FA:PVP; (C) III - PVP+CAP; (D) IV - SUB FA:PVP+CAP. Magnification 10,000x.

SUB FA and CAP powders were crystalline according to XRPD diffractograms (Fig. 2). Reflections that were present in (I) PVP, (II) SUB FA:PVP, (III) PVP+CAP and (IV) SUB FA:PVP +CAP diffraction patterns, were obviously originated from the collector plate made of aluminium foil, on which the nanofibers were ES. The incorporation of SUB FA and CAP into nanofibers resulted in an amorphous systems, since no reflections inherent to SUB FA or CAP were observed in the diffraction patterns.

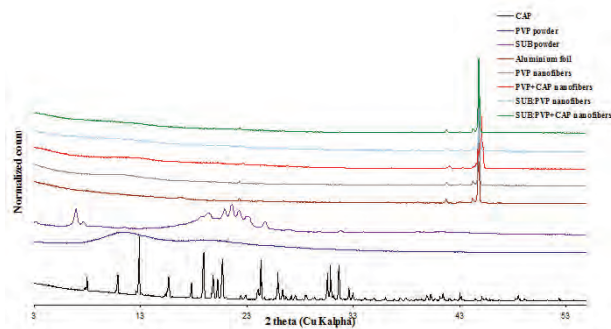


Fig. 2: X-ray powder diffraction (XRPD) patterns of starting materials and polymeric nanofibers.

The average content of CAP in the (III) PVP+CAP nanofibers was 1.9 and in the (IV) SUB FA:PVP+CAP nanofibers 1.8%. This suggests that the loss of CAP during ES process was 9.1 and 13.0%, respectively.

Tab. 2: CAP content of polymeric nanofibers determined by high pressure liquid chromatography (HPLC) and the deviation from theoretical content.

Formulation	Average CAP content in nanofibers (% \pm SD, n=3)	Average content deviation from theoretical content (%)
(III) PVP+CAP nanofibers	1.9 \pm 0.08	9.1
(IV) SUB FA: PVP+CAP nanofibers	1.8 \pm 0.07	13.0

CONCLUSIONS

The polymeric mixtures of SUB FA and PVP with the selected model antibiotic drug (CAP) can be successfully electrospun to produce homogeneous nanofibrous mats. CAP exists in amorphous form in the present nanofibers. The ES process slightly reduces the amount of CAP in the final nanofibers compared to the expected (theoretical) drug content value.

ACKNOWLEDGEMENTS

This study is part of the targeted financing project no SF0180042s09 and ETF grant project no 7980. The work is also supported by the European Social Fund's Doctoral Studies and Internationalization Programme DoRa and the Estonian Ministry of Education and Research. Jaan Aruväli is kindly acknowledged for XRPD measurements.

REFERENCES

1. Meinel AJ, Germershaus O, Luhmann T, Merkle HP, Meinel L, *Electrospun matrices for localized drug delivery: Current technologies and selected biomedical applications. Eur. J. Pharm. Biopharm.* 2012; 81: 1-13.
2. Franke R, Schreiber L, Suberin - a biopolyester forming apoplastic plant interfaces. *Curr. Opin. Plant Biol.* 2007; 10: 252-259.
3. Alakurtti S, *Synthesis of betulin derivatives against intra-cellular pathogens. Doctoral dissertation (articlebased), University of Helsinki,* 2013, pp. 99.





PREPARATION OF PELLETS WITH CONTROLLED RELEASE OF SUGAR FOR PREVENTION OF HYPOGLYCEMIA IN CHILDREN (P71)

D. Sabadková^{1,*}, A. Franc¹, J. Muselík¹,
D. Neumann²

¹ Department of Pharmaceutics, University of Veterinary and Pharmaceutical Sciences, Palackého tř. 1/3, 61242 Brno, Czech Republic

² University Hospital, Department of Paediatrics, Sokolská 581, 500 05 Hradec Králové, Czech Republic

INTRODUCTION

Hypoglycemia is an acute complication of diabetes mellitus therapy. The risk of severe hypoglycemia appears to be higher in children and adolescents than in adults. Furthermore, hypoglycemic episodes in children are profound and prolonged. The heightened risk in this age-group is at least partly attributable to the inability of children to recognize autonomic symptoms. In addition, prolonged exercise can make plasma glucose concentrations difficult to manage. The natural tendency of children and adolescents to eat reluctantly and irregularly exacerbates the danger (1).

Children and their parents who are extremely concerned about hypoglycemic events tend to keep blood glucose values above recommended targets in an effort to avoid a hypoglycemic episode. This leads to poorer glycemic control which may be significantly more detrimental to the individual's health than an episode of even moderately severe hypoglycemia (2).

The aim of this work is to develop a dosage form containing pellets with controlled release of glucose. Pellets can be mixed with food or dispersed in drink. The final formulation will release glucose after defined lag time which will ensure safe levels of blood sugar for a desired time interval.

MATERIALS AND METHODS

Materials

Glucose Anhydrous, Dr. Kulich Pharma, Czech Republic; Microcrystalline Cellulose (Avicel PH 101) FMC Biopolymer, Belgium; Microcrystalline Cellulose with Carboxymethylcellulose Sodium (Avicel RC 591) FMC Biopolymer, Belgium; Croscarmellose Sodium (Ac-Di-Sol) FMC Biopolymer, Belgium; Carboxymethyl Starch JRS Pharma, Germany; Polyethylene glycol (PEG 6000) Merck Schuchardt, Germany; Aqueous Ethylcellulose Dispersion (Surelease) Colorcon, USA.

Sample preparation

The powder components of various formulations (Table 1) were mixed in Tefal Kaleo blender at 400 rpm for 60 sec. The required amount of water was added to the powder in order to form a dough-like mixture. The wet mass was extruded through the 1 mm screen at 110 rpm using screw axial extruder. The extrudate was spheronized for 5 minutes at 1 000 rpm (Pharmex 35 T). Pellets were dried in a hot-air dryer (Horo 38 A) at 50 °C for 4 hours.

Tab. 1: Composition of samples

Composition	1G	2G	3G	4G
Glucose	80.0	75.0	75.0	80.0
Avicel PH 101	15.0	-	-	15.0
Avicel RC 591	-	25.0	-	-
Ac-Di-Sol	5.0	-	-	-
PEG 6000	-	-	25.0	-
CMS	-	-	-	5.0

Cores were coated in a fluid coater (Wurster MP 1) by a mixture of Surelease and purified water in ratio 1:1.5 in an amount to achieve the total content of dried coating film 25 % of the weight of pellets. Spray rate was 11 ml/min, nozzle diameter 1.0 mm, air pressure 1.2 bar, inlet temperature 65 °C and outlet temperature 50 °C. Coated pellets were cured in a hot-air dryer at 70 °C for 2 hours.

In vitro drug release studies

The dissolution of glucose pellets was monitored in a dissolution apparatus, paddle method (Sotax), under stirring at 100 rpm. The dissolution media consisted of 1000 ml of purified water at 37 °C ± 0.5 °C. Samples were withdrawn after 30, 60, 120, 240, 360 and 540 minutes and analysed using HPLC-ELSD method. The data represent the mean values of two separate experiments.



RESULTS AND DISCUSSION

The final multiparticulate formulation consists of an inert core in the form of pellets and of an ethylcellulose-based film coating which allows the controlled release of glucose during its passage through GI tract.

Figure 1 demonstrates that profiles of individual samples differ in dependence on the composition of cores. Samples 1G and 4G both released glucose after 120 min; however, glucose release was fastest of the sample 1G. This might be the result of rapid disintegration and dissolution caused by fast water wicking and swelling of cross-carmellose sodium due to its fibrous and cross-linked structure. Carboxymethyl starch contained in the sample 4G provides the ability of fast swelling, yet forms a gel structure which induces slower release of glucose comparing to the sample 1G. Sample 3G releases glucose after 240 min lag time caused presumably by the ability of polyethylene glycol 6000 to form a poorly soluble complex with the drug (3). The longest lag time was observed in the sample 2G as an effect of carboxymethylcellulose sodium which usually forms a gel structure preventing the drug release during the first dissolution phases. The sample 4G forms gel structure as well, however its content is five times lower than in the sample 2G, which is the reason of shorter lag time of the sample 4G.

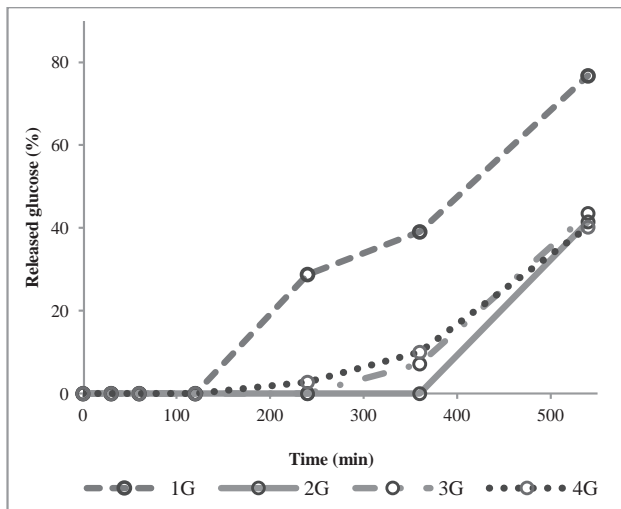


Fig. 1: Releasing of glucose from individual samples of pellets.

CONCLUSIONS

The glucose pellets with suitable dissolution profiles were produced. Coated pellets were evaluated by the dissolution method. Pellets with controlled release after 120, 240 and 360 minutes were successfully prepared. This lag time may lead to retention of the glucose release into the blood *in vivo*, which is advantageous for the diabetic population.

ACKNOWLEDGEMENT

This work was supported by IGA Ministry of Healthcare of Czech Republic NT14479/2013.

REFERENCES

1. Shalitin S, Moshe P: Hypoglycemia in Type 1 Diabetes, *Diabetes Care*. 2008; 31: 121-124.
2. Ryan Ch, Gurtunca N, Becker D: Hypoglycemia :A complication of diabetes therapy in children, *Sem. Paed. Neurol*. 2005; 12: 163-177.
3. Solvang S, Finholt P: Effect of tablet processing and formulation factors on dissolution rate of the active ingredient in human gastric juice, *J. Appl. Bacteriol*. 1970; 59: 49-54.





QUALITY BY DESIGN: A CASE STUDY FROM GENERIC INDUSTRY

(P72)

G. Sedmak^{1,*}, J. Beranek¹

¹ Zentiva, k.s., U kabelovny 130, 102 37 Praha 10, Czech Republic

INTRODUCTION

Product development in nearly every industry is a major, complex undertaking. Pharmaceutical industry is no exception, where product and process development can influence up to 50% of total R&D cost, and is a key determinant for all costs of goods sold from active pharmaceutical ingredient to final packaged product. Because of that, intelligent investment into product and process development and standardization of product development could lead to the considerable savings in the overall cost of product (1).

PHARMACEUTICAL QUALITY BY DESIGN

A high quality drug product can be defined as a product that is free of contamination and reproducibly delivers the therapeutic benefit promised in the label to the consumer (2).

In order to achieve required performance of a product, pharmaceutical development process should include these basic steps: define quality target product profile (QTPP), identify potential critical quality attributes (CQAs) of the drug product, determine the critical quality attributes of the drug substance and excipients, select an appropriate manufacturing process and define a control strategy (3,4). As a result, a systematic approach could facilitate continual improvement and innovation throughout the product lifecycle.

One of standard pharmaceutical manufacturing processes via dry granulation route usually consists of the following process steps: pre-dry granulation mixing and lubrication, dry granulation, granulate sieving, final mixing and lubrication, tableting and tablet coating. However, in a standard process like that we could need to assess a very high number of potentially critical process variables, as pointed out in (5). Therefore, it is important that during development, the best optimum between speed, efficiency and excellence is found.

MATERIALS AND METHODS

In this paper, we will provide a case study from generic pharmaceutical industry using previously described standard manufacturing process, where tablets are prepared via dry granulation technology, which is followed by tablet coating.

QTPP, CQAs of the drug product, CQAs of drug substance and excipients are provided. Manufacturing process is proposed and control strategy implemented. Formal risk assessment strategies are employed at all steps of development. A 7-factor, 2-level design of experiments study with 2 center points was performed to study influence of manufacturing process variables on CQAs of a drug product in the production process. For modeling data and design space optimization, software package Modde 9.0 was used.

RESULTS AND DISCUSSION

We have set up a robust design space for our process. We have decided for the following optimal settings:

Tab. 1: Proposed settings for a Design Space

Compactor gap size	2-4 mm
Compactor force	4-6
Compactor speed	middle
Sieve size	1 mm
Sieve speed	middle
Tableting dwell time	0.16-0.32 s
Tableting force	13.5-17.0 kN

These settings allow us to use a wide range of compactor gaps, forces, tableting speeds and tableting forces. By this design space, we have set up a very flexible working space both at compaction as well as tableting levels.

In order to validate our proposed design space, we used Monte Carlo simulation methods. By that, we have shown that the common pharmacopoeial criteria for the drug product Critical Quality Attributes can be met:

- Assay 95% - 105%
- AV < 15
- Dissolution in 30. minute > 80%

In addition, a good tablet hardness (100-200 N) and low friability (a way below 1%) can be obtained, indicating smooth coating and packaging processes.



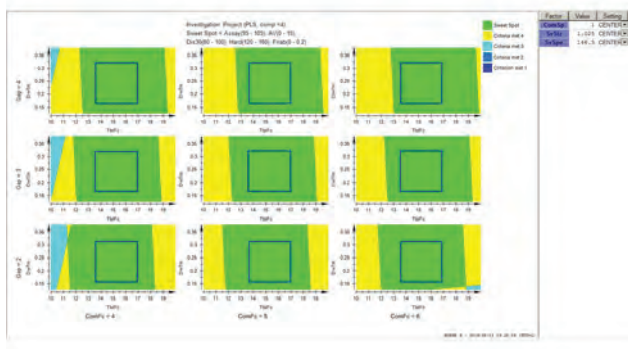


Fig. 1: Sweet spot plot. Green color indicates area where all criteria are met. Square inside green area indicates a proposed design space.

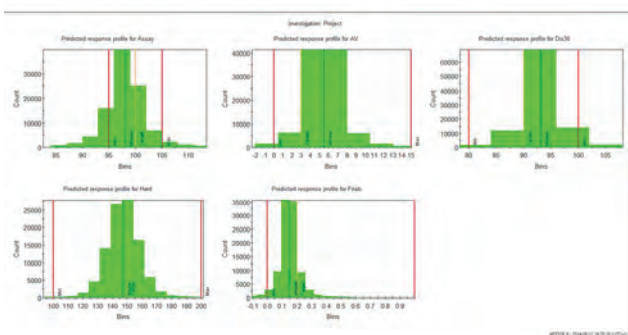


Fig. 2: Design Space validation using Monte Carlo simulation.

CONCLUSIONS

We have provided risk mitigation thru formal risk assessment approaches. We have also provided optimum design space, wherein we get a robust product. By this we expect a smooth transition between pilot to production size equipment as well between different production sites.

REFERENCES

1. T. Fuhr, M. Holcomb, P. Rutten. Why Quality-by-Design Should be on the Executive Team's Agenda: Developing New Strategies for New Times. In *Outpacing Change in Pharma Operations*, M. Losch, and U. Schrader, McKinsey & Co. December 2009, pp. 195–203
2. J. Woodcock. The concept of pharmaceutical quality. *Am. Pharm. Rev.* 2004; Nov/Dec: 1-3.
3. ICH Q8(R2), Annex to Note for guidance on pharmaceutical development, (EMA/CHMP/167068/2004). http://www.ema.europa.eu/docs/en_GB/document_library/Scientific_guideline/2009/09/WC500002872.pdf
4. FDA Applying ICH Q8(R2), Q9, and Q10 Principles to CMC Review. <http://www.fda.gov/downloads/AboutFDA/CentersOffices/CDER/ManualofPoliciesProcedures/UCM242665.pdf>
5. L. X. Yu. *Pharmaceutical Quality by Design: Product and Process Development, Understanding, and Control.* *Pharm. Res.* 2008; Vol. 25, No. 4: 781-791





AN *IN VITRO* AND *IN VIVO* PREFORMULATION STUDY OF TARGETED NANOSIZED DRUG DELIVERY SYSTEMS

(P73)

P. Sipos^{1*}, K. Dér¹, J. Maléth², A. Hunyadi³,
A. Zalatnai⁴, P. Hegyi², L. Puskás⁵, P. Szabó-Révész¹

¹ Dept. of Pharmaceutical Technology, University of Szeged,
H-6720, Szeged, Eötvös u. 6, Hungary

² First Dept. of Internal Medicine, Pancreatic Research Group,
University of Szeged, H-6720, Szeged, Korányi fasor 8-10, Hungary

³ Dept. of Pharmacognosy, University of Szeged, H-6720, Szeged,
Eötvös u. 6, Hungary

⁴ 1st Dept. of Pathology and Experimental Cancer Research,
Semmelweis University, H-1085, Budapest, Üllői út 26

⁵ Avidin Ltd., Szeged, Alsóikötő sor u., Hungary

INTRODUCTION

Associative colloids are bilayered vesicles which are able to encapsulate pharmaceuticals (hydrophilic/amphiphilic/lipophilic) and serve as potential drug carriers. These nanoparticles are formed from the self-assembly of non-ionic amphiphiles or biocompatible and biodegradable lipids and materials in aqueous media. Targeting can be achieved by labelling the bilayer with specific ligands of the cell transporters. The objective of the study was to prepare and characterize drug delivery systems with various formulation compositions having an average hydrodynamic size of 200 nm, made by different production methods.

The formulations were designed by varying the preparation methods and the concentration ratios of the components as independent variables. The average hydrodynamic size, zeta potential and drug content of the nanoparticles were evaluated. *In vivo* experiments included kinetic studies in mice.

MATERIALS AND METHODS

Components, chemicals and animals

Cholesterol and cholesterol derivatives, lecithin and phosphatidylcholine derivatives, biodegradable lipids,

PEG-based targeting materials, non-ionic surfactants, and other reagents were purchased from Sigma and Avanti Lipids. SCID mice were used for the *in vivo* measurements (National Institute of Oncology and Avidin Ltd.)

Methods

The structures of the nanoparticles and the structural changes due to the ingredients, the production methods and the targeting ligands were analysed by using thermoanalytical and spectroscopic methods. DSC was used to study the relationship between the changes in the independent variables and the thermal events of the nanovesicles (Mettler Toledo). DXR Raman and Antaris NIR spectroscopy devices were used to investigate and confirm the possible interactions between the components (Thermo Fisher).

A double-step protocol of liposome and niosome preparation was applied, using the BÜCHI evaporator (BÜCHI AG) and Emulsiflex high-pressure homogenizer devices.

RESULTS AND DISCUSSION

The presentation concentrates on the use of niosomes and liposomes as pharmaceutical carriers of the biologically active ingredient. The embedding of sensitive and biologically active substances is a challenging task and general phenomenon that increases bioavailability. The combination of pharmaceutical surfactants and biodegradable lipids was suitable for nanoparticle preparation. Various types of nanoparticles were considered, as were the mechanisms of their formation, factors influencing their stability and disintegration, their loading capacity towards sensitive pharmaceuticals, and their therapeutic potential.

Preformulation: The appropriate choice of the independent variables led to molecularly dispersed drug in the nanoparticles. Significant variations in the product structure, physicochemical parameters and drug liberation were demonstrated.

In vitro transport: After the fluorescent ink marker was loaded into the targeted liposomes, an *in vitro* transport study (Human adenocarcinoma cells) was performed. In parallel, chemical mapping of the active agent containing Capan-1 cells was carried out with a DXR Dispersive Raman spectrometer. Transport of the effective active agent through the cell wall was identified by these methods.

In vitro cytotoxicity: Real-time *in vitro* cytotoxicity measurements of the API-containing liposomes were performed in glioblastoma cells. The normalized cell index of the API-containing liposomes was one-fourth that of the native API solution.

In vivo survival: Structure-activity relationship studies



were performed by testing the synthesized API for anti-proliferative activity in lung adenocarcinoma cells, using viability assays and holographic microscopic imaging. Recording TNF α -induced NF- κ B inhibition and autophagy induction effects revealed a strong correlation with the cytotoxic potential of the API analogues. A significant inhibition of tumour growth was observed when the most potent API analogue was encapsulated into the liposomes at one-sixth of the maximally tolerated dose in the xenograft model. The novel spectrum of activity of the examined API warrants further preclinical investigations [1,2]. As concerns the survival of the SCID mice *in vivo*, 30% of the animals were living after 90 days, whereas the control mice had all died by the 40th day of the experiment.

In vivo study: An anti-tumourous active agent and an efflux-transport inhibitor agent were encapsulated into targeted and PEG-ylated liposomes and an *in vivo* study was performed on SCID mice having pancreatic tumorous cell xenografts. Minor necrosis of the tumorous cells was observed after 3 weeks and the mice were still alive, in contrast with the control animals.

CONCLUSIONS

The results indicate that the preformulation study of the nanoparticle preparation and the *in vitro* pre-examinations can lead to efficient *in vivo* biological studies. On use of the appropriate labelled nanoparticles containing different active agents, accumulation of the API was observed in the tumorous cells and organs as compared with other organs, in contrast with non-targeted nanoparticles.

ACKNOWLEDGEMENT

Supported by TÁMOP-4.2.2.A-11/1/KONV-2012-0035

REFERENCES

1. Gyuris M., Ózsvári B., Nagy IL., Marton A., Vellai T., Faragó V., Hackler L., Tóth K.G., Sipos P., Kanizsai I., Puskás G. L. *Novel Mannich-type Curcumin Analogs as Potent Anticancer Agents Inducing Autophagy*, *J. Med. Chem.*, accepted, 2014.
2. Ózsvári B., Gyuris M., Sipos P., Fábrián G., Molnár E., Marton A., Faragó N., Hackler L. Jr., Mihály L., Nagy L.I., Szénási T., Diron A., Kanizsai I., Puskás G.L. *Nanoformulated novel curcumin analogue as a potent multi-target agent against glioblastoma*. *Curr. Pharm. Design.* 2013, in press.

INFLUENCE OF THE POLYMER TYPE ON THE PERFORMANCES OF EXTENDED RELEASE HYDROPHILIC MATRIX TABLETS (P74)

E. Spaseska Aleksovska^{1,*}, S. Suljić¹, A. Aleksovski¹, E. Zahirović¹, A. Salkić, A. Butković, M. Jašić²

¹ ZADA Pharmaceuticals, Bistarac Donji bb, 75300 Lukavac, Bosnia and Herzegovina

² Faculty of Pharmacy, University of Tuzla, Univerzitetska 8, 75000 Tuzla, Bosna and Herzegovina

INTRODUCTION

Extended release drug formulations are promising patient-friendly modality for drug administration, since they overcome some of the disadvantages of conventional solid dosage forms (immediate release tablets and capsules) such as dose frequency, fluctuations of the drug concentration in the plasma and on the site of action, drug toxicity, costs etc (1).

Hydrophilic matrix tablets (containing hydrophilic and swellable polymers) are the most investigated type of extended release dosage forms. By contact with water the polymers form continuous porous hydrogel layer (on the surface) which enables water penetration inside the swelled layer and drug diffusion in the outer environment. When the outer gel layer fully hydrates it starts to erode and it is continuously replaced by new hydrated polymeric layer. By hydrogel erosion an amount of active compound is also released in the outer media (2).

Different types of hydrophilic polymers are used in terms of providing extended drug release. Polymer's molecular weight, viscosity and swelling capacity strongly influences drug release pattern and thus final product quality (2). HPMCs (high molecular weight) are well known hydrophilic polymers intended for extended release tablet preparation due to their inert nature, pH independency, suitable flowability and compressibility, and fast hydration and gel layer formation (3). High molecular weight poly-





ethylene oxide-s (PEO -Polyox®) are water soluble resins which are gaining huge attention recently as possible release retarding alternative to HPMC due to their pH independency, physic-chemical stability, compressibility, high hydration and swelling ability (4).

The aim of this work was to formulate hydrophilic matrix tablets for extended release of ascorbic acid, by using two types of polymers: HPMC (subtypes K4M, K15M and their mixture in ratio 1:1) and PEO (subtypes 1105, 301 and their mixture in ratio 1:1), and to note how do these polymers affect drug release and basic physic-chemical properties of the tablets.

MATERIALS AND METHODS

Materials

Materials used in the study are given in table 1.

Table 1 - Evaluated formulations (%)

	F1	F2	F3	F4	F5	F6	Producer
Ascorbic acid	55.5	55.5	55.5	55.5	55.5	55.5	ALAND Nutre- ceutics
PEO 1105	30	/	15	/	/	/	Colorcon
PEO 301	/	30	15	/	/	/	Colorcon
HPMC K4M	/	/	/	30	/	15	Colorcon
HPMC K15 M	/	/	/	/	30	15	Colorcon
Microcrystalline cel- lulose	10	10	10	10	10	10	JRS Pharma
Copovidone	3	3	3	3	3	3	BASF
Colloidal Si dioxide	0.5	0.5	0.5	0.5	0.5	0.5	Evonik
Mg stearate	1	1	1	1	1	1	Dr.Paul Loch- mann

Methods

All powder compounds (except magnesium stearate) were thoroughly blended for 5 minutes in PE bag. After adding the magnesium stearate, blends were mixed for additional 1 minute and subsequently investigated for bulk and tap density, Carr's index, Housner ratio and angle of repose.

Matrix tablets (650 mg; 12 mm; biconvex) were prepared by direct compression using FETTE 1200 rotary tablet press. Tablets were further evaluated regarding mass and content uniformity (PhEur 7), friability (PhEur 7) and hardness. Dissolution test was made in accordance with USP (paddle apparatus Varian VK7025), 75rpm speed, at temperature of 37°C, in phosphate buffer pH= 7.2 at time interval from 2,4,6,8, 10 and 12 hours. Drug amount was determined by using HPLC (Agilent technologies 1200 RRLC, VWD detector)

RESULTS AND DISCUSSION

Dissolution study (figure 1) pointed that PEO matrices showed faster drug release compared to the HPMC matrices, which is possible due to the general lower viscosity (table 2) and higher erodibility of PEO (seen during dissolution) compared to HPMC. When talking for only one type of polymer or their mixtures, results show that polymers having higher molecular weights and viscosities (HPMC K15M; PEO 301) provoke retardation in drug release compared to polymers having lower molecular weights and viscosities (HPMC K4M; PEO 1105).

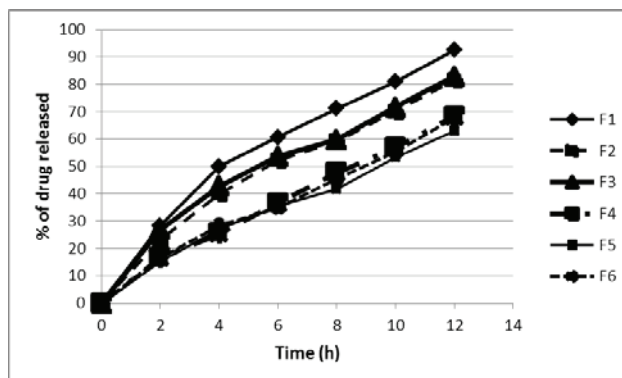


Fig. 1: Drug release from 6 different formulations.

Table 2 - Viscosity (mPas) of aqueous polymer solutions (5)

	1% solution	2% solution	5% solution
PEO 1105	/	/	8800-17600
PEO 301	1650-5500	/	/
HPMC K4M	/	3000-5600	/
HPMC K15M		11250-21000	

All powder formulations provided suitable flowability and die filling which led into formation of tablets with uniform mass and content. Additionally all six batches had sufficient hardness and 0% friability (table 3)

Table 3: Physical properties of powder mixtures and matrix tablets

	F1	F2	F3	F4	F5	F6
Carr's index (%)	21,59	13,27	19,17	24,36	27,12	26,33
Hausner ratio	1,27	1,15	1,24	1,32	1,37	1,36
Angle of repose	29,71	28,86	29,63	31,15	32,47	32,43
Average mass (mg)	649,58 ±2.35	652,52 ±1.87	653,09 ±3.41	647,95 ±1.97	648,41 ±4.15	650,30 ±2.74
Hardness (kP)	10,42	10,93	10,56	10,81	11,04	11,51
Friability (%)	0	0	0	0	0	0
Drug content (AV)	5.31	4.89	3.74	3.58	3.87	4.48



CONCLUSIONS

Polymer properties (molecular weight and viscosity) strongly influence drug release rate from hydrophilic matrix tablets. Already known HPMC-s are a gold standard when formulation extended release dosage forms, but however new polymers such as PEO-s are also interesting alternative regarding this issue.

REFERENCES

1. Aulton M. *Aulton's pharmaceutics - The design and manufacture of medicines, 3rd edition.* Elsevier, Edinburgh 2007
2. Wen X, Nokhodochi A, Rajabi SA. Oral extended release hydrophilic matrices: Formulation and design. In: Wen X and Park K: *Oral controlled release formulation design and drug delivery.* Wiley, New Jersey 2010
3. Rahman M, Roy S, Das CS, Jha MK, Ashan Q, Reza S. Formulation and evaluation of HPMC based matrix systems as oral sustained release drug delivery systems for ciprofloxacin HCl. *Int J Pharm Sci Rev Res* 2011; 6(2): 34-41 2011
4. Pinto JF, Wunder KF, Okoloekwe A. Evaluation of the potential usage of polyethylene oxide as tablet- and extrudate forming material. *AAPS PharmaSci* 2004; 6(2): 1-10
5. www.colorcon.com

MATHEMATICAL APPROACH TO COMPARE IN-VITRO PERFORMANCE OF TWO PANTOPRAZOLE ENTERIC-COATED DOSAGE FORMS (P75)

O. Rahić¹, E. Vranić¹, O. Planinšek², S. Srčić^{2,*}

¹ Department of Pharmaceutical Technology, Faculty of Pharmacy, University of Sarajevo, Zmaja od Bosne 8, 71000 Sarajevo, Bosnia and Herzegovina

² Department of Pharmaceutical Technology, Faculty of Pharmacy, University of Ljubljana, Aškerčeva 7, SI-1000 Ljubljana, Slovenia

INTRODUCTION

Pantoprazole sodium sesquihydrate, sodium 5-(difluoromethoxy)-2-[(RS)-[(3,4-dimethoxypyridine-2-yl)methyl] sulfinyl] benzimidazole-1-ide sesquihydrate is the active substance in antiulcerative drug products. It is known that pantoprazole degrades in acid media as a function of pH, but has acceptable stability under alkaline conditions (1). Consequently, registered pantoprazole drug products are in form of enteric-coated tablets. The formulation is designed in this manner in order to protect active substance from gastric conditions and release it in a more basic pH environment, so that the product provides targeted therapeutic action.

Film-coated tablets have one major disadvantage. Intra-individual and inter-individual differences in gastric emptying time after application of these tablets can lead to variation in absorption of active substance. In order to minimize this variability, multiparticulate dosage forms, such as pellets, can be used (2).

Since it is proved that pantoprazole enteric-coated tablets have desirable effect, it is important to prove that the pantoprazole enteric-coated pellets have equivalent therapeutic effect. The first step is to compare dissolution characteristics (profiles) of two formulations in question. The simplest method for dissolution profile comparison is a model independent mathematical approach using two factors, difference factor (f_1) and similarity factor (f_2) (3).





These factors were calculated using equations [1] and [2] (4).

$$f_1 = \frac{\sum_{i=1}^n |R_i - T_i|}{\sum_{i=1}^n R_i} \cdot 100 \quad [1]$$

$$f_2 = 50 \cdot \log \left\{ \left[1 + \left(\frac{1}{n} \right) \sum_{i=1}^n (R_i - T_i)^2 \right] \right\} \cdot 100 \quad [2]$$

MATERIALS AND METHODS

Materials

Pantoprazole pellets were prepared by solution/suspension layering technique. Pantoprazole film-coated tablets were purchased from the Public Pharmacy, Sarajevo, B&H. Both products had declared content of pantoprazole of 40 mg per dosage unit.

All reagents for the dissolution testing as well as for the quantification using UV-VIS spectrophotometric method were of analytical grade.

Methods

Dissolution testing

Dissolution testing was performed on VanKel VK7025 (Varian, USA). Samples were subjected to acid stage (2 hours in 0.1 mol/l hydrochloric acid; rotating basket method at 100 rpm), followed by an alkaline stage (45 minutes in phosphate buffer pH 6.8; rotating basket method at 100 rpm). Since the release of active substance is taking part in the intestine, dissolution profiles comparison was performed for the values obtained in phosphate buffer pH 6.8.

Samples were withdrawn from dissolution vessels after 5, 10, 15, 20, 30, 35, 40 and 45 minutes.

UV-VIS spectrophotometric method

UV-VIS spectrophotometric method was performed using UV-VIS Spectrophotometer UV-1601 (Shimadzu, Japan) at wavelength of 295 nm.

RESULTS AND DISCUSSION

Dissolution profiles of pantoprazole released from enteric-coated pellets and enteric-coated tablets are represented in Figure 1.

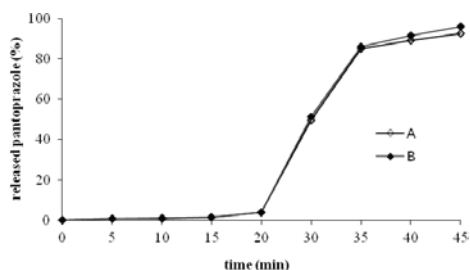


Fig. 1. Dissolution profile of pantoprazole released from: A-pantoprazole enteric-coated pellets, B-pantoprazole enteric-coated tablets.

Dissolution profile comparison was quantified by the calculation of difference factor (f_1) and similarity factor (f_2). Calculated values for f_1 and f_2 factors are given in Table 1.

Tab. 1: Values of f_1 and f_2 factors.

Parameter	Limits*	Results
f_1 factor (difference factor)	0%-15%	2.7%
f_2 factor (similarity factor)	50%-100%	88.6%

*According to Ref. (4)

Figure 1. indicates that both pantoprazole dosage forms release less than 10% pantoprazole in acidic media. When observing pantoprazole release obtained in buffer stage, it is visually notable that pantoprazole enteric-coated pellets (A) and pantoprazole enteric-coated tablets (B) have similar dissolution profiles. As it can be seen there is a slight difference for the last testing point (45 minutes). But when comparing percentage values obtained at this time point (92.72% for A, and 96.06% for B) it is obvious that the difference is not significant.

Table 1. presents the values of difference factor (f_1) and similarity factor (f_2). Since 2.7% and 88.6% are the values of difference factor and similarity factor respectively, it is obvious that compared dissolution profiles are similar. Having this in mind it is evident that the pantoprazole enteric-coated pellets and pantoprazole enteric coated tablets can be considered equivalent *in vitro*.

In order to determine whether those two dosage forms are also bioequivalent, it would be necessary to perform *in vivo* studies in human volunteers.

CONCLUSIONS

It can be concluded from these laboratory evaluations that under simulated *in vivo* physiological conditions pantoprazole enteric-coated pellets perform similarly as pantoprazole enteric-coated tablets.

REFERENCES

- Cheer SM, Prakash A, Faulds H, Lamb HM. Pantoprazole. An update of its pharmacological properties and therapeutic use in the management of acid-related disorders. *Drugs*, 2003; 63: 101-132.
- Gibaldi M. *Biopharmaceutics and clinical pharmacokinetics*, 4th ed. Lea & Febiger, Philadelphia, 1991, pp. 68-70.
- Costa P, Lobo JMS. Modeling and comparison of dissolution profiles. *Eur. J. Pharm. Sci.* 2001; 13: 123-133.
- Committee for medicinal products for human use (CHMP). Guideline on the investigation of bioequivalence. CPMP/EWP/QWP/1401/98 Rev. 1/Corr**



IN VITRO – IN VIVO – IN SILICO APPROACH IN IDENTIFYING BIOPERFORMANCE DISSOLUTION TEST: IBUPROFEN SR TABLETS (P76)

Sofija Stanković^{1*}, Sandra Grbić¹, Marija Bogataj²,
Jelena Parojčić¹

¹ Department of Pharmaceutical Technology and Cosmetology,
Faculty of Pharmacy, University of Belgrade, Vojvode Stepe 450,
11221 Belgrade, Serbia

² Department of Biopharmacy and Pharmacokinetics, Faculty of
Pharmacy, University of Ljubljana, Aškerčeva 7,
SI-1000 Ljubljana, Slovenia

INTRODUCTION

Dissolution testing is commonly used analytical tool to determine the rate and extent at which drug is released from dosage form. It plays many important roles in drug product development and particularly important feature is to be predictive of drug product bioavailability. However, quantitative prediction of *in vivo* performance directly from dissolution test results can be challenging since various physiological parameters can also play a role in drug bioavailability. That is why the integrated *in vitro* – *in vivo* – *in silico* approach, that couples results from *in vitro* dissolution tests with physiologically based pharmacokinetic (PBPK) models, to predict the *in vivo* drug performance, is getting more and more attention.

The purpose of this study was to: (1) develop a drug-specific absorption model for ibuprofen using PBPK modeling; (2) investigate the influence of different experimental conditions on ibuprofen dissolution from two commercially available sustained release (SR) formulations and (3) identify bioperformance dissolution test for ibuprofen SR tablets based on the *in vitro* - *in silico* - *in vivo* approach.

EXPERIMENTAL

In vitro study

Two commercially available bioequivalent ibuprofen SR tablet formulations were tested *in vitro* using various experimental conditions:

(I) first set of experiments was performed in a rotating paddle apparatus (Erweka DT 70, Germany) and rotational speed of 50 rpm, using 500 ml of phosphate buffer pH 7.2 and blank FaSSiF as dissolution media.

(II) second set of experiments was performed in BioDis apparatus (Varian Inc., USA), using 10 dpm and 20 dpm and media change pattern: 15 min blank FaSSGF, 3 h blank FaSSiF and 9h SCoF.

(III) third set of experiments was performed in the USP flow-through cell apparatus (Sotax CE7 Smart, Switzerland) using an open-loop configuration and 22.6 mm cells and flow rate 8 ml/min. Same media change pattern was used as with BioDis apparatus.

(IV) in the fourth set of experiments flow-through system with glass bead dissolution device, constructed in the laboratories of the Faculty of Pharmacy at the University of Ljubljana [1] with the experimental setup described by Klein et al [2] was employed i.e. 50 g of glass beads, stirring rate of 50 rpm, and the flow rate of 2 ml/min. Another setting of the experiment involved the use of 25 g of glass beads and 15 rpm rotation speed. Same media change pattern as with BioDis apparatus was used. After 15 min in blank FaSSGF appropriate amount of trisodium phosphate was added to achieve quick rise of the media pH to 6.5.

Details of the performed experiments are given in Table 1.

Table 1. *In vitro* experimental conditions employed

Exp	Apparatus	Media
I.1	paddle apparatus, 50 rpm	phosphate buffer pH 7.2
I.2	paddle apparatus, 50 rpm	blank FaSSiF
II.1	BioDis apparatus, 10 dpm	bFaSSGF/ bFaSSiF / SCoF
II.2	BioDis apparatus, 20 dpm	
III.1	flow trough cell, 8 ml/min	
IV.1	Glass beads device, 50 g glassbeads, 50 rpm	
IV.2	Glass beads device, 25 g glassbeads, 15 rpm	

In vivo data

Literature *in vivo* data reporting ibuprofen plasma concentration following administration of 600 mg ibuprofen IR tablets [3] and 800 mg ibuprofen SR tablets [4] were used for model evaluation.





In silico study

Simcyp Population-Based Simulator (version 13.1, Simcyp Ltd., Sheffield, UK) was used to simulate the time course of ibuprofen concentration in plasma. The required input parameters related to ibuprofen physico-chemical and pharmacokinetic properties were taken from literature and/or *in silico* estimated. Summary of the input parameters used is given in Table 2.

Table 2. Summary of the ibuprofen input parameters employed for *in silico* model development

Parameter	Value
Dose (mg)	600/800
Molecular weight	206.3
Log P _{ow}	4
Compound type	monoprotic acid
pKa	4.5 ^a
Fraction unbound in plasma	0.0128 ^b
Human jejunal permeability, P _{eff} (cm/s)	5.73 x 10 ⁻⁴ ^c
Volume of distribution at steady state V _{ss} (L/kg)	0.13 ^d
Renal clearance (L/h)	0.05 ^e

^a Ref [5]; ^b Ref [6]; ^c See text; ^dRef [7]; ^eRef [8];

Permeability in the small intestine was predicted based on the Caco-2 permeability values reported [9]. Enzyme kinetics mediated by CYP2C9 was taken into account, since it is the primary route of ibuprofen elimination. CL_{int} (0.6 L/h) for enzyme mediated clearance was predicted based on total oral clearance [7]. Model validation was performed based on the percent prediction error (%PE) between the simulated and *in vivo* observed values of the primary pharmacokinetic parameters after administration of 600 mg ibuprofen IR formulation. The same parameters were subsequently used for the SR formulation simulations, incorporating the dissolution profiles obtained under different experimental conditions. Bioperformance dissolution was identified by calculating percent prediction error (%PE) between the simulated and *in vivo* observed values of the primary pharmacokinetic parameters after administration of 800 mg ibuprofen SR formulation [4].

RESULTS AND DISCUSSION

The results of dissolution testing are presented in Fig 1. Although *in vivo* dissolution of the two formulations is expected to be similar, pronounced differences between the formulations were observed *in vitro* in the rotating paddle apparatus. However, when tested in the dynamic dissolution devices with the change of buffer media at specified time points, almost superimposable profiles were observed.

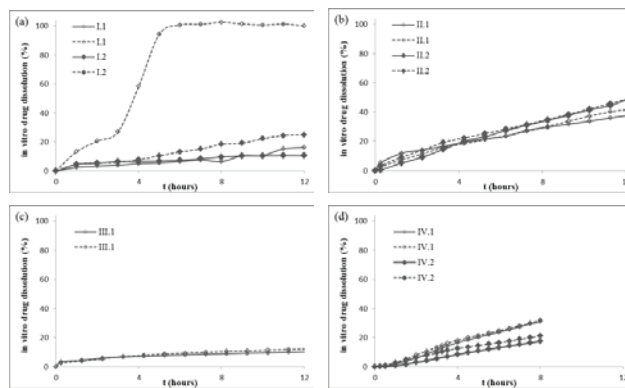


Figure 1. Dissolution profiles obtained in (a) paddle apparatus; (b) BioDis apparatus; (c) flow through cell apparatus; (d) glass bead device (product A – solid lines; product B – dotted lines)

Drug-specific absorption model for ibuprofen was developed using Simcyp Simulator. Relevant %PE values were 7.37 for C_{max} and 9.67 for AUC (compared to the literature data [3]).

The *in silico* model developed was used to investigate the influence of *in vitro* dissolution kinetics on drug disposition from ibuprofen SR products. Percent prediction errors (%PE) between the simulated and *in vivo* observed values of the primary pharmacokinetic parameters are presented in Table 3.

It can be noted that differences in the *in vitro* drug dissolution kinetics were well reflected on the primary pharmacokinetic parameters predicted. Based on the %PE values of the primary pharmacokinetic parameters, best relationship between the *in vitro* and *in vivo* data was obtained for drug dissolution profile observed in the glass bead dissolution device with the setup involving 50 g of glass beads and 50 rpm and BioDis apparatus at 20 dpm with the media change to account for the physiological pH gradient.



Table 3. Pharmacokinetic parameters and %PE values for product A

	C _{max pik1} (µg/ml)	% PE	C _{max pik2} (µg/ml)	%PE	AUC (µgh/ml)	%PE
I.1	6.85	51.79	na	-	71.3	73.47
I.2	4.83	66.00	na	-	43.9	88.66
II.1	12.20	14.14	na	-	189	29.68
II.2	14.30	0.63	14.70	2.90	274	1.93
III.1	na	-	4.88	67.76	69.8	74.03
IV.1	13.52	4.85	14.21	6.14	268.29	0.18
IV.2	na	-	11.08	26.81	201.17	25.15
observed <i>in vivo</i>	14.21		15.14		268.79	

CONCLUSION

According to the results obtained, glass bead dissolution device and BioDis apparatus with biorepresentative change in media pH might be considered as bioperformance dissolution in the case of the two ibuprofen SR products studied.

ACKNOWLEDGMENT

This work was done under the project TR 34007 funded by the Ministry of Education, Science and Technological Development, Republic of Serbia

REFERENCES

1. Bogataj M, Cof G, Mrhar A, PCT, WO 2010/014046 A1, 2010.
2. Klein S, Garbacz G, Pišlar M, et al. *J Control Release*, 166, 286-293 (2013).
3. Kallstrom E, Heikinheimo M, Quiding H. *J Int Med Res*. 16, 44-49 (1998).
4. Pargal A, Kelkar MG, Nayak PJ. *Biopharm Drug Dispos*. 17, 511-519 (1996).
5. Avdeef A, Box KJ, Comer JE, et al. *J Pharm Biomed Anal*. 20, 631-641 (1999).
6. Aarons L, Grennan DM, Siddiqui M. *Eur J Clin Pharmacol*, 26, 815-818 (1983).
7. Geisslinger G, Dietzel K, Bezler H, et al. *Int J Clin Pharmacol Ther Toxicol* 27, 324-8 (1989).
8. Davies N. *Clin Pharmacokinet*. 34, 101-54 (1998).
9. Yee S. *Pharm Res* 14, 763-766 (1997).

THE EFFECT OF CHITOSAN GELS WITH MICROEMULSION ON THE RELEASE OF METRONIDAZOLE (P77)

L. Starýchová^{1,*}, M. Čuchorová¹, M. Špaglová¹, M. Čierna¹, K. Bartoníková¹, M. Vitková¹, K. Gardavská¹, J. Turská¹

¹ Faculty of Pharmacy, Department of Galenic Pharmacy, Comenius University in Bratislava, Odbojárův 10, 83232 Bratislava, Slovakia

INTRODUCTION

Metronidazole (MTZ) is an antimicrobial drug that is used topically to treat bacterial vaginosis and various forms of acne, including acne rosacea. The aqueous solubility of metronidazole in water at room temperature is only about 0.87%. However, for many topical applications, a concentration of 1.0% or higher is desired.

The lack of solubility of such drugs, and the inability to obtain sufficiently high concentrations of drugs in solution in pharmaceutically acceptable carriers, is a serious problem in the formulation of topical therapeutic products for the treatment of medical conditions affecting the skin or mucosa (1).

Microemulsions are isotropic, thermo-dynamically stable solutions in which substantial amounts of two immiscible liquids (i.e., water and oil) are brought into a single phase by means of an appropriate surfactant or surfactant mixture (2).

The objective of this work was to study the effect of various types of chitosan gels and their mixtures with O/W microemulsion on the release of antimicrobial drug – metronidazole – through dialysis membrane *in vitro*. Microemulsion has been used as potential drug delivery vehicle to improve the solubility of metronidazole.

MATERIALS AND METHODS

Materials

Metronidazole (MTZ) was from Merck KGaA (Darmstadt, Germany). Chitosan (MMW, Brookfield viscosity 200 000 cps), dialysis membranes were purchased from Spectrum Laboratories, Inc. (Netherlands).





Methods

Preparation of gels

The various types of chitosan gels were prepared at 1-2.5% concentrations of chitosan in dilute acid solutions (type A – in lactic; type B – glycolic; type C- mandelic acid). MTZ was incorporated into the formulations at 1% concentration.

Preparation of microemulsion chitosan gel samples

The appropriate amounts of metronidazole, microemulsion and chitosan gel were weighed in the ratio 0.5: 1: 4. Metronidazole was added in a concentration of 1%.

In vitro release of drug

The release of metronidazole from different chitosan gels and their mixtures with microemulsion was determined by using Franz diffusion cells with cellulose dialysis membrane (M.W.C.O. 12000–14000). The artificial membrane was mounted between the receptor and donor compartments. The donor compartment was charged with 1.2 g of samples. The receptor compartment was filled with volume of Phosphate Buffered Saline (PBS, pH 7.4) which was maintained at 37 ± 0.5 °C. The system was maintained throughout the experiment at 37°C. Samples 5 ml were withdrawn at intervals of 15, 30, 45, 60, 90, 120, 180, and 360 min, the volume of each sample was replaced by the same volume of fresh buffer to maintain constant volume, samples were analyzed for indomethacin content spectrophotometrically at $\lambda_{\max} = 320$ nm (UV spectrophotometer Philips, PV 9652 UV/VIS, Great Britain).

RESULTS AND DISCUSSION

The physical and chemical properties of formulated dosage form were modified in order to become stable and suitable for application. Prepared dispersions of drug in the topical formulations with O/W microemulsion were appropriate in terms of solubilization and rheological properties. Figure 1 shows the comparison of released amounts of metronidazole from all types of gels of various concentrations and their mixtures with microemulsion after 6 hrs.

As evident from the figure, released amounts of metronidazole decrease with increasing concentrations of chitosan.

Microemulsion had positive effect on the liberation of drug from chitosan gels containing lactic and mandelic acid. The highest amount of metronidazole was released from the mixture of O/W microemulsion with 1.5% gel of chitosan containing lactic acid, which was up to 48.06% of the total amount of metronidazole. The amount of the

released drug from this mixture with ME was about 6.25% higher comparing to pure gel. In the case of samples containing glycolic acid the amounts of released drug were higher from the pure chitosan gels.

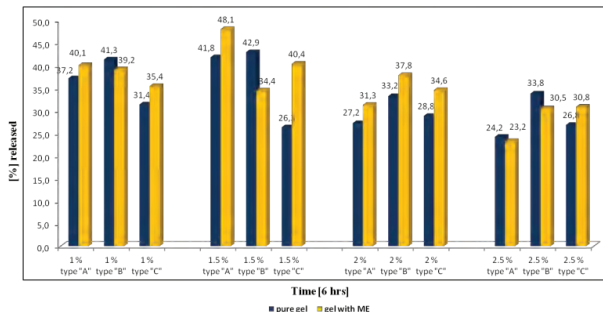


Fig. 1: The released amounts of MTZ from various types of chitosan gels and their mixtures with ME after 6 hrs.

CONCLUSIONS

It can be concluded that higher amounts of the drug were released from the chitosan gels with lower content of chitosan. Microemulsion had positive effect on the liberation of drug from chitosan gels containing lactic and mandelic acid. In the case of samples containing glycolic acid amounts of released drug from the pure chitosan gels were higher. The highest amount of metronidazole was released from the mixture of O/W microemulsion with 1.5% gel of chitosan containing lactic acid.

ACKNOWLEDGEMENT

This work was supported by a grant from FAF UK/55/2014, UK/356/2014, UK/432/2014.

REFERENCES

1. Yang M, Chen H, *Methods and Compositions for Increasing Solubility of Azole Drug Compounds that are Poorly Soluble in Water*, U.S. Patent 8658678, February 25, 2014.
2. Žabka M, Škoviera F, *Microemulsions as vehicles for transdermal permeation of drugs*, Acta Facult Pharm Univ Comenianae 2003, 50, 147-55.



THE USE OF TOPICAL CORTICOSTEROIDS AMONG PATIENTS IN THE REPUBLIC OF MACEDONIA (P78)

V. Sulevski¹, M. Simonoska-Crcarevska², A. Starova³, R. S. Raicki², K. Mladenovska², Z. Sterjev², S. Dimchevska², M. Gigovski¹, M. Glavas-Dodov^{2,*}

¹ BELUPO Representative Office-Skopje, 3-ta Makedonska Udarna Brigada 68, 1000 Skopje, Macedonia
² Faculty of Pharmacy, Majka Tereza 47, 1000 Skopje, Macedonia
³ University Clinic of Dermatology, Majka Tereza 17, 1000 Skopje, Macedonia

INTRODUCTION

For more than six decades, topical corticosteroids (TC) have formed the mainstay of treatment for many dermatological conditions. Since the synthesis of hydrocortisone in 1951, an increasing number of formulations as topical dosage forms have been placed on the market, with attention being focused on the development of more powerful drug molecules with improved bioavailability and reduced side-effect risks (1).

When used appropriately, according to advices given from health care professional (doctor and pharmacist), TC treatment can be a highly safe method for controlling the symptoms/disease and restoring patients quality of life.

In everyday practice, it is not uncommon for patients to express irrational fear and/or anxiety about using TC, and this may lead to poor medication adherence and lack of successful clinical outcomes. "Corticosteroid phobia" among patient population may be accentuated by personal experience, divergent advise from pharmacists and doctors, divergent advise from friends and family, information found on the internet etc. Also, patients have a misconception about TC, relating them with anabolic steroids or oral steroids (2).

Therefore, the aim of the present study was to obtain information of the frequency of TC use among patients in the Republic of Macedonia and to determine the reasons (if any) for not adhering to TC treatment recommendations.

MATERIALS AND METHODS

The anonymous questionnaire specifically designed for the current study addressed the following topics: demographics, TC treatment used in the last year and the source and prevalence of corticosteroid phobia among the patients. The qualitative data were collected between October 2013 and March 2014 from patients who attended a doctor appointment or community pharmacy in different regions of the Republic of Macedonia.

150 validated surveys were distributed and 113 were returned (75.34% response rate) and were included in the analysis. An attached cover letter served as informed consent for the questionnaire.

Data were tabulated using Microsoft Excel® (Microsoft Corp. Redmond, WA, USA) and were evaluated using multivariate statistical analysis software (SIMCA 13, Unmetrics AB, Sweden). Values of p less that .05 were considered significant.

RESULTS AND DISCUSSION

Among survey responders, 36.6% were men and 63.4% were women. Mean ± standard deviation (SD) age of the respondents was 42.2 ± 8.1 years. 15.2% of the patients were with low, 49.1% were with medium and 35.7% were with high socioeconomic status (income per capita per month; 100, 200 and more that 200 euro, respectively). 1.8% of the survey responders were without any education, 14.2% were with elementary education, 33.6% were with secondary education and 50.4% were with university degree diploma. 91.1% of the responders were not health-care professionals, vs. 8.9%, as doctors, pharmacists, technicians, nurses, etc.

Fig. 1 presents the scatter plot (map) of X observations (demographic characteristics of the sample - sex, age, socioeconomic status, educational background), displaying that the X observations are well suited with respect to each other without presence of outliers and other patterns in the data.

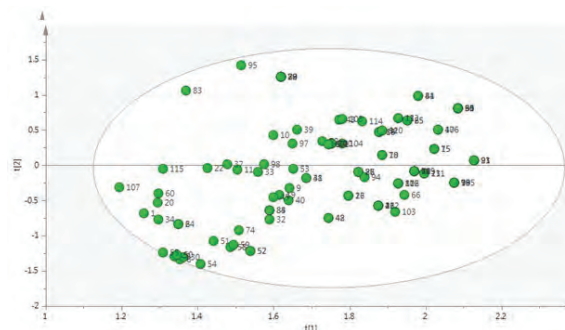


Fig. 1: The window of X space for performed analysis.





On average, 68.2% of the subjects or close family members used TC in the past year, mainly for treatment of contact dermatitis. Participants were asked how long they used their most recent TC. Duration of treatment was not defined in 19.5% of the subjects and 5.3% were unsure. The majority of responders (48.7%) used TC less than two times, vs. 25.5% who applied TC more than four times in the past year.

Overall, 58.4% of the patients believed that TC treatment is safe and they used TC without a fear, especially 1) low socioeconomic status group patients and those with 2) elementary education (Fig. 2 - negative values). Responders from 3) medium socioeconomic status group, 4) group with secondary education and 5) university degree, as well as 6) non-health care professionals (Fig. 2 - positive values) were significantly concerned about the TC usage ($p < .05$) as a result of previous dissatisfaction with the treatment efficacy or fear of potential side effects (3). Interestingly, 62.1% of the patients, although not knowing the side effects of TC or not having any experience, were still afraid of using them.

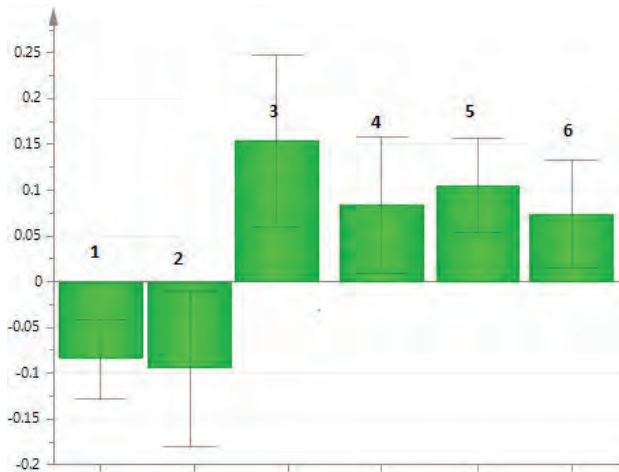


Fig. 2: Corticophobia among patients participating in the study ($n = 113$).

CONCLUSIONS

Corticophobia is present among patients in the Republic of Macedonia and is linked to various factors. Understanding the difficulties faced by patients and their potential fears about TC will provide a framework of strategies to increase patient confidence in and adherence to treatment with TC. Further studies will be focused on community pharmacists with the aim to investigate their role in managing corticophobia and improving patient compliance.

REFERENCES

1. Charman C, Williams H, *The use of corticosteroids and corticosteroid phobia in atopic dermatitis. Clinics in Dermatology* 2003; 21: 193-200.
2. Moret L, Anthoine E, Aubert-Wastiaux H, Le Rhun A, Leux C et al. TOPICOP©: A New Scale Evaluating Topical Corticosteroid Phobia among Atopic Dermatitis Outpatients and Their Parents. *PLoS ONE* 2013; 8(10): e76493.
3. Brown K.K, Rehmus W.E, Kimball A.B, *Determining the relative importance of patient motivations for nonadhering to topical corticosteroid therapy in psoriasis. J. Am. Acad. Dermatol.* 2006; 55: 607-613.



EVALUATION OF COMPRESSIBILITY OF PHARMACEUTICAL FILLERS USING STRESS RELAXATION TEST AND FORCE-DISPLACEMENT RECORD (P79)

P. Svačinová^{1*}, M. Řehula¹, P. Ondřejček¹, M. Rabišková¹

¹ Department of Pharmaceutical Technology, Charles University in Prague, Faculty Of Pharmacy, Heyrovského 1203, 500 05 Hradec Králové, Czech Republic

INTRODUCTION

The principle of tablet compression process is the transformation of undeformed particles of compressed material to elastically and plastically deformed particles due to the action of compression force. Therefore it is necessary to evaluate the compression process from terms of the energy balance and physicochemical properties of the compressed material. This evaluation used the force-displacement record and the stress relaxation test. The force-displacement record evaluates the phase of compression and relaxation. Parameters E_1 , E_2 and E_3 characterize the energy of precompression, the energy accumulated during the tablet compression cycle and the energy released from the tablet after the compression (1). Besides these parameters, we used the factor of plasticity FP and factor of elasticity FE. Using these factors we can deduce the ability of deformation of different materials depending on the compression pressure (2). The stress relaxation method evaluated the interphase between tablet compression and its relaxation. The two-exponential equation was previously used for a description of stress relaxation test. Laylin used this equation in his work that studied the viscoelastic properties of proteins (3). Later the three-exponential equation was developed. This equation is able to give us a more accurate description of the compression process (4).

In this experiment, we newly performed a determination of energy for tablets compressed without any delay and with the delay of 180 second. We compared the energy parameters of the force-displacement record and stress relaxation test in the terms of impact of the structure of all tested fillers.

MATERIALS AND METHODS

Microcrystalline cellulose (Avicel PH 200, FMC Europe N.V, Belgium), lactose (Lactochem Fine Crystals, DFE Pharma, Germany) and dibasic calcium phosphate dihydrate (Emcompress, JRS Group, United Kingdom) were used as model pharmaceutical fillers for direct compression. All materials complied with the European Pharmacopoeia and were used without any adjustment.

The compression force for stress relaxation test and force-displacement record was 10 kN.

The three-parametric equation was used to calculate the parameters of stress relaxation test.

RESULTS AND DISCUSSION

Energy values E_1 and E_2 obtained from the force-displacement record without delay were lower than the energies obtained from force-displacement record with the delay of 180 second. On the other hand, for energy E_3 the situation was the opposite. The amount of energy released after compression was reduced and the structure of tablets was firmed up. The delay also increased the plasticity factor. The results showed that the factor of plasticity decreased in the order of microcrystalline cellulose, lactose, dibasic calcium phosphate dihydrate. Plasticity factor obtained from stress relaxation test also decreased in the order of microcrystalline cellulose, lactose, dibasic calcium phosphate dihydrate. The comparison of plasticity factor of force-displacement record with a delay and stress relaxation test showed the linear relationship. Linear relationship was found among elasticity parameters and plasticity parameters in stress relaxation test.

CONCLUSIONS

The force-displacement record and stress relaxation test are based on different principles. Using three different model fillers we obtained results, which indicate, that both methods are comparable.





REFERENCES

1. Vachon MG, Chulia D, *The use of energy indices in estimating powder compaction functionality of mixtures in pharmaceutical tableting*. *Int. J. Pharm.* 1999; 177: 183-200.
2. Antikainen O, Yliruusi J, *Determining the compression behaviour of pharmaceutical powders from the force-distance compression profile*. *Int. J. Pharm.* 2003; 252: 253-261.
3. Laylin KJ, *Adsorbed layers of protein II. Film hysteresis and stress relaxation*. *Colloid Interface Sci.* 1968; 28: 260-265.
4. Řehula M, Adámek R, Špaček V, *Stress relaxation study of fillers for directly compressed tablets*. *Powder Technol.* 2012; 217: 510-515.

INFLUENCE OF BUFFER AND PRESERVATIVE CHOICE ON THE STABILITY OF AQUEOUS LECITHIN DISPERSIONS (WLD) INTENDED FOR PARENTERAL ADMINISTRATION (P80)

M. Płaczek¹, K. Kościńska¹, M. Sznitowska^{1*}

¹ Department of Pharmaceutical Technology, Medical University of Gdansk, Hallera 107, 80-416 Gdansk, Poland

INTRODUCTION

WLD is a newly-developing, biocompatible drug delivery system intended for solubilization and safe parenteral administration of drugs with low water solubility (1). Unique properties of the system result from the presence of lecithin, which is used as pharmaceutical excipient in different parenteral formulations for years (2). However, because of the natural origin of the main constituent, the formulation may be physicochemically and microbiologically unstable. For this reason, during R&D studies, it is necessary to test stabilizers, e.g. buffers and preservatives, as components of the system. So, the aim of the study was to determine the influence of these excipients on the stability of WLD.

MATERIALS AND METHODS

Materials

Egg yolk lecithin (Lipoid E 80) was purchased from Lipoid (Ludwigshafen, Germany) and glycerol, Na₂HPO₄, NaH₂PO₄, KH₂PO₄, NaHCO₃, Na₂CO₃, NaCl, citric acid, NaOH, and HCl were purchased from POCh (Gliwice, Poland). Succinic acid was manufactured by Loba (Fischamend, Austria), phenol by Fluka (Steinheim, Germany), Tris by Baker (Deventer, Holland), benzyl alcohol by Merck (Ho-





henbrunn, Germany), thiomersal and methyl- and propylparaben by Caelo (Hilden, Germany).

Preparation of WLD

Egg lecithin (5%) and glycerol (2.4%) were stirred for 1 h at temp. 60°C in aqueous buffer solutions: BB, CB, PB, PLB, PBS, PCB, PCLB, CbB and Tris (see table 1).

Tab. 1: Type and properties of buffers used for WLD production.

Buffer type	Symbol	pH	Osmotic pressure [mosmol/kg]
Succinate	BB	4.6	180
Citrate	CB	5.0	230
Phosphate	PB	5.4	140
	PLB	7.0	70
	PBS	7.4	280
Phosphate-Citrate	PCB	5.5	320
	PCLB	5.5	160
Carbonate	CbB	10.0	120
Tris	Tris	10.0	150

Additionally to PCB buffer different preservatives were added: phenol (PH), thiomersal (TH), benzyl alcohol (BA) and parabens – methyl and propyl (MP).

The dispersions were homogenized for 2 min with Ultra-Turrax (IKA, Staufen, Germany) and then using high-pressure homogenizer (APV 2000; APV, Gatwick, UK) - 8 cycles at 500 bar. Dispersions were filtered (0.45 µm cellulose acetate filter; Sartorius, Göttingen, Germany), dispensed into glass vials in a nitrogen atmosphere and sterilized by autoclaving (121°C, 15 min).

WLD analysis

WLD observations

The color, clarity and sedimentation were determined visually and light transmittance (%T) at 540 nm with Jasco V 530 spectrophotometer (Jasco, Tokyo, Japan) was also measured.

Microscopic observations were performed using optical microscope Nikon Eclipse 50i (Nikon, Tokyo, Japan).

Lecithin particles characterization

The mean hydrodynamic diameter (Z-average) of lecithin particles and polydispersity index (Pdl) were determined in WLD by photon correlation spectroscopy (PCS), using a Zetasizer Nano-ZS (Malvern, Malvern, UK).

RESULTS AND DISCUSSION

Just after preparation all WLD formulations were light-cream coloured, homogenous and their pH was in accordance with the pH of the buffers (see Tab. 1 and Tab. 2). Microscopic and PCS analyses revealed in all WLDs the presence of phospholipid vesicles, which size was in the range about 100-200 nm (Z-av., Tab. 2). Most uniform were particles in WLDs with phosphate or phosphate-citrate buffers (Pdl<0.300), while the most polydisperse were formulations with CbB and Tris buffer (Pdl>0.440).

Tab. 2: Characterization of WLD formulations.

Buffer type	pH	Z-average [d, nm]	Pdl	Stability (1 month)
BB	4.7	125	0.297	sedimentation
CB	5.1	140	0.402	sedimentation
PB	5.5	209	0.262	sedimentation
PLB	6.7	144	0.331	sedimentation
PBS	6.9	180	0.316	sedimentation
PCB	5.6	199	0.280	stable
PCLB	5.6	162	0.283	sedimentation
CbB	8.8	170	0.443	clods
Tris	9.1	139	0.467	clods

During storage sedimentation or clods formation in all formulations except PCB were observed (Tab. 2) and for this reason for further studies (compatibility with preservatives) only PCB-WLD was chosen.

Tab. 3: Influence of preservatives on WLD-PCB properties.

Preservative	pH	Z-av [d, nm]	Pdl	Stability (1 week)
PH (0.5%)	5.6	238	0.221	clods
TH (0.1%)	5.6	220	0.285	clods
MP (0.2%)	5.4	156	0.276	clods
BA (2.0%)	5.5	155	0.320	clods

Our studies indicated, that although in the day of production preservatives had no adverse influence on the WLD properties (Tab. 3), during first week of storage physical incompatibility was visible. In all dispersions clods were found, which size averaged several hundred microns. After shaking or pressing through the injection needle, the larger clods disintegrated to smaller ones. Microscopic analysis indicated, that these particles are formed by lecithin vesicles (up to 20 µm), which clustered together during storage. Presence of such a sediment is undesirable in parenteral preparation, but acceptable for some routes of drug administration.





CONCLUSIONS

Phosphate-citrate buffer can be used as aqueous dispersing medium for egg lecithin in WLD production. The obtained formulation is physically stable submicron dispersion, which can be considered as parenteral carrier of drugs. However, because of possible incompatibilities between WLD and other excipient, further stability studies are needed.

ACKNOWLEDGMENTS

This study was supported by National Sciences Center (Cracow, Poland) – grant number N N405 668440.

REFERENCES

1. Sznitowska M, Klunder M, Płaczek M, Paclitaxel solubility in aqueous dispersions and mixed micellar solutions of lecithin. *Chem. Pharm. Bull.* 2008; 56: 70-74.
2. Fowler K, Lecithin, in: Rowe RC, Sheskey PJ, Owen SC, *Handbook of Pharmaceutical Excipients*. Pharmaceutical Press, London, 2006, pp. 409-411.

COMPARISON OF LOCAL PELLET VELOCITY IN WURSTER AND SWIRL ENHANCED WURSTER COATER (P81)

R. Šibanc^{1*}, R. Dreu¹

¹ Department of Pharmaceutical technology, Faculty of Pharmacy, University of Ljubljana, Aškerčeva 7, 1000 Ljubljana, Slovenia

INTRODUCTION

Pellets belong to multiple unit particulate systems (MUPS) - dosage forms, which offer several advantages over single unit dosage forms. Pellets are normally coated in fluidized bed with the purpose of adhering the active ingredient and/or the coating for modified release or protection of the drug.

Wurster coater belongs to a group of bottom spray fluid bed devices and can be also seen as a spouted bed with an insert - Wurster draft tube (1).

A very important parameter of coated pellets is their coating thickness variability, which is a result of pellet circulation time variability and amount of coating gained during each pass of the coating zone (2). Both of these are affected by the velocity of the particle in and above the coating zone.

For determination of high velocity of small particles an expensive camera with very high frame rate and a strong light source is required. In our case a low cost photographic system employing dual exposure technique was employed for determination of local pellet velocity at the draft tube exit.

MATERIALS AND METHODS

Methods

A lightning setup with dual flash speedlight (YN-460 ii, Yongnou, China) was used. One was gelled with red colour filter (#026 Bright Red, Lee filters) and other with green colour filter (#736 Twickenham Green, Lee filters). Six megapixel colour digital camera (Exilim EX-F1, Casio, Japan) equipped with macro lens (DCR-250, Raynox, Japan) was used to obtain the images of pellets. The





same white pellet would appear on a picture as a red and a green one, i.e. at different position on the image due to its movement and due to the delay in firing of the coloured flashes (Figure 1). The camera and the flashes were connected to a custom built microcontroller circuit (dsPIC30F2010, Microchip, USA) in order to control the delay between the firing of flashes with microsecond resolution. Measurements were performed from the edge of the draft tube towards the center of the draft tube with aid of a macro rail (454 Positioning Slide Plate, Manfrotto, Italy). A custom in-house OpenCV based image postprocessing program was used for analysis of particle velocity. Pellet axial and tangential velocity were determined from image as the difference in vertical (image y direction) and horizontal displacement (image x direction) during the time between both flash pulses.

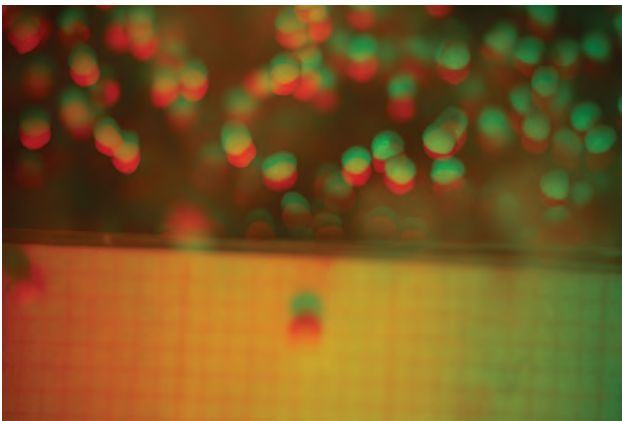


Fig. 1: Sample image of dual exposed pellets

Wurster chamber (GPCG1, Glatt GmbH, Germany) and its swirl modification (3) were employed at three fluidizing air flow rates, three draft tube gaps with three different sieved size fractions of pellets (Cellets, Harke Pharma).

RESULTS AND DISCUSSION

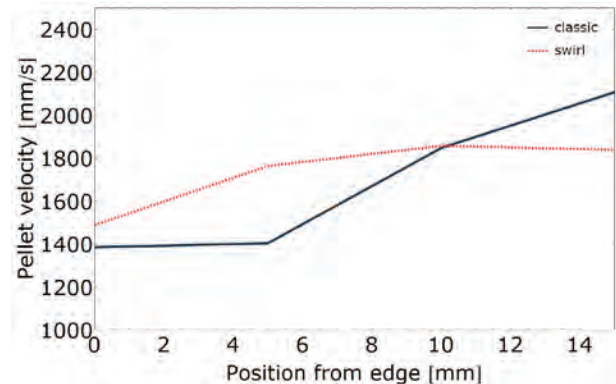


Fig. 2: Pellet velocity profile for both chambers at 20 mm gap, airflow of 156 m³/h and particle size 1120 – 1250 μm

Classical Wurster chamber

The minimum value of average axial velocity measured at the edge of the draft tube at any process setting was 761 mm/s, the median 1211 mm/s and maximum 2638 mm/s. For classical Wurster chamber it was observed that increase in fluidizing air flow rate increases local pellet velocity. This effect was most pronounced at smallest tested gap (10 mm).

There is no significant difference in pellet velocity at 20 and 25 mm gap, whereas pellet velocity is higher at 10 mm gap.

Smaller pellets were achieving higher velocities, but only at the smallest gap.

An increase in particle velocity was observed when moving from the edge of the draft tube towards the centre.

Swirl enhanced Wurster chamber

Swirl chamber shows less dependence on process and particle parameters than Wurster chamber. The minimum value of average axial velocity measured at the edge of the draft tube at any process setting was 1168 mm/s, the median 1576 mm/s and maximum 2042 mm/s.

Higher fluidizing air flow rate results in higher particle velocity.

Pellet velocities at 10 mm gap are higher or equal to 20 mm gap.

Highest particle velocity was observed for middle particle size (900 – 1000 μm) at 20 mm gap, whereas at 10 mm gap no size dependence was observed.

Angle

Analysis of pellet direction after exiting the draft tube in terms of inclination angle from vertical line was also per-



formed. Determination of angle was based on ratio of tangential and axial velocity of the pellet. On average there was no observable trend for classical Wurster chamber, however for swirl Wurster chamber the pellets had significant angle after exiting the draft tube. The angles were in the range from about 8 to 20 degrees. Lower angle values were normally observed at higher air flow rates and higher angle values at lower air flow rates.

CONCLUSIONS

A low cost dual exposure imaging system was constructed and was successfully used in comparison of particle velocity in classical Wurster chamber and its modification - Swirl Wurster chamber. Significant differences were elucidated by particle velocity measurements, which can explain the performance of both chambers when coating pellets with particle size distribution (4).

REFERENCES

1. Abdul S, Chandewar AV, Jaiswal SB. A flexible technology for modified-release drugs: Multiple-unit pellet system (MUPS). *J Controlled Release*. 2010 Oct 1;147(1):2–16.
2. Cheng XX, Turton R. The prediction of variability occurring in fluidized bed coating equipment. I. The measurement of particle circulation rates in a bottom-spray fluidized bed coater. *Pharm Dev Technol*. 2000;5(3):311–22.
3. Perpar M, SI, Savic S, SI, Gregorka M, SI, et al. Process device for coating particles. U.S. Patent 8689725, 2014.
4. Luštrik M, Dreu R, Šibanc R, Srčić S. Comparative study of the uniformity of coating thickness of pellets coated with a conventional Wurster chamber and a swirl generator-equipped Wurster chamber. *Pharm Dev Technol*. 2010 Nov 15;1–9.

PERMEATION ENHANCEMENT OF INDOMETHACIN BY TRANSCUTOL® AND MICROEMULSION SYSTEM THROUGH RAT SKIN AND A SEMIPERMEABLE MEMBRANE (P82)

M. Špaglová^{1,*}, L. Starýchová¹, M. Čuchorová¹, K. Bartoníková¹, M. Čierna¹, M. Vitková¹, K. Gardavská¹

¹ Department of Galenic Pharmacy, Faculty of Pharmacy, Comenius University, Odbojárov 10, 832 32 Bratislava, Slovakia

INTRODUCTION

The skin has evolved to prevent excessive water loss from the internal organs and to limit the ability of xenobiotics and hazardous substances to enter the body. Notwithstanding this barrier function, a number of strategies have been developed by scientists to deliver drugs to and through the skin (1). Chemical permeation enhancers (CPE) are of the highest interest of this study. CPEs may act by one or more of three main mechanisms. They either disrupt the highly ordered structure of lipids in stratum corneum or interact with intercellular protein or improve partition of the drug, coenhancer or solvent into stratum corneum (2). Numerous compounds have been evaluated for penetration enhancing activity, including sulphoxides, azones, pyrrolidones, alcohols and alkanols, glycols, surfactants (common in dosage forms) and terpenes (3).

The aim of this study is to consider the enhancing activity of Transcutol® (TR) and prepared microemulsion (ME) as multicomponent enhancer system in terms of liberation of indomethacin (IND) from carbopol gel through rat skin and semipermeable membrane.





MATERIALS AND METHODS

The preparation of microemulsion consisted of homogenisation of water, oil and Tween 80 followed by titration with different cosurfactants. The drug release studies were performed on Franz diffusion cells. Franz diffusion method is a representative diffusion cell approach which utilizes either animal or human skin membranes obtained either from split skin, full-epidermis skin or from artificial skin models. In our study rat skin and dialysis membrane SpectraPor® were compared as barriers. The membranes were clamped into a two-chamber system. While the substances topically applied were put into the donor chamber, the bottom chamber was filled with a receptor fluid (phosphate buffer saline, pH 7.0) which was heated to 32°C by thermostat. From this receptor fluid, samples were taken at different time intervals and the concentration of the topically applied IND which diffused through the skin or membrane was spectrophotometrically analyzed.

RESULTS AND DISCUSSION

The release of IND dissolved in different permeation enhancers and subsequently formulated in carbopol gels at 6 hrs compared to control is shown in Figures 1 and 2. When the membrane was used as a barrier, the formulation containing ME (20%; w/w) showed the released amount of drug to $307.81 \pm 25.86 \mu\text{g}/\text{cm}^2$, and the formulation containing TR (20%; w/w) to $337.79 \pm 36.88 \mu\text{g}/\text{cm}^2$ in 6 hrs.

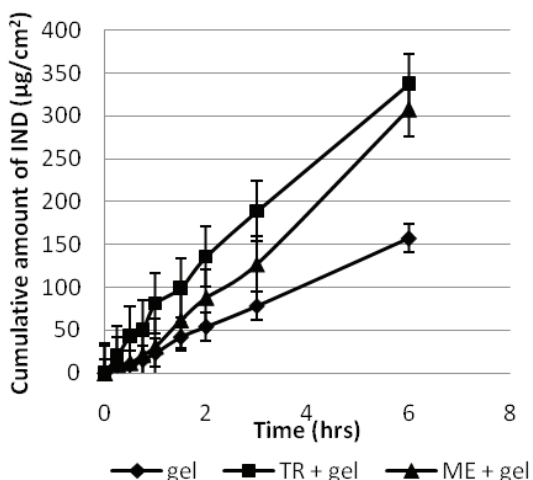


Fig. 1: The permeation profiles of IND through SpectraPor®

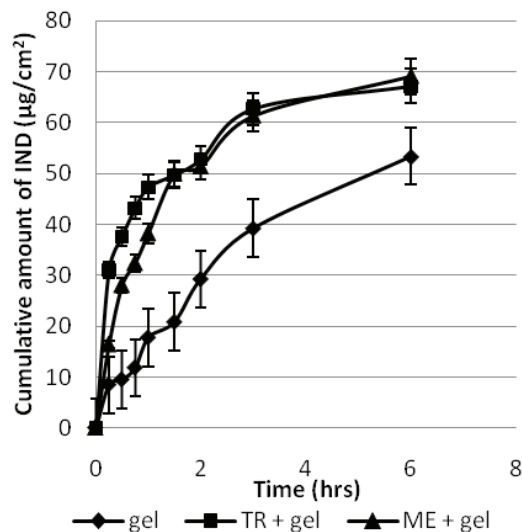


Fig. 2: The permeation profiles of IND through rat skin

On the other hand, using rat skin maximum cumulative amount permeated was seen with formulation containing ME ($69.10 \pm 1.38 \mu\text{g}/\text{cm}^2$), followed by formulation containing TR ($67.15 \pm 4.34 \mu\text{g}/\text{cm}^2$). The difference between the permeation curves with ME and TR is statistically significant ($P=0.038$).

CONCLUSION

In transdermal delivery, due to excellent barrier function of skin, the choice of an efficient chemical permeation enhancer is important. In the present study, both TR and prepared ME act as enhancers for release of IND. The increase of drug released through semipermeable membrane to 96% (ME) and 115% (TR) was observed compared to the control formulation. In permeation method through rat skin, TR seems to be more successful enhancer during first 2 hrs, however the permeation curves behave very similar and the amount of drug released is approximately the same after 6 hrs.

ACKNOWLEDGEMENT

This study was supported by grants from Comenius University and Faculty of Pharmacy UK/432/2014, UK/356/2014, FaF/55/2014.

REFERENCES

1. Lane ME. Skin Penetration Enhancers. *Int. J. Pharm.* 2013; 447: 12-21.
2. Prasanthi D, Lakshmi PK. Effect of Chemical Enhancers in Transdermal Permeation of Alfuzosin Hydrochloride. *ISRN Pharm.* 2012; 1-14.
3. Williams AC, Barry BW. Penetration enhancers. *Adv. Drug Deliv. Rev.* 2004; 56: 603-618.





DETERMINATION OF REMIFENTANIL IN DRIED PLASMA SPOTS BY LIQUID CHROMATOGRAPHY TANDEM MASS SPECTROMETRY (P83)

J. Trontelj

¹ Faculty of Pharmacy, University of Ljubljana, Aškerčeva 7, 1000 Ljubljana, Slovenia

INTRODUCTION

Remifentanil is a newer synthetic opioid-class analgesic with ultra short duration of action. It is given only intravenously and is very quickly cleaved by plasma esterases resulting in biological half-life of only 3-10 min (1). It is being used as an analgesic for pain management during anaesthesia and in intensive care units because of its rapid initiation and subsequent termination of action. It is also being used "off-label" as pain management during labour. The patient controlled analgesia (PCA) is used, where the parturient can increase the rate of i.v. infusion of remifentanil just before each birth pang. However, until now, the safety and efficacy of such labour pain management through remifentanil PCA has not been fully demonstrated yet (1). Remifentanil target plasma concentration is 3 - 8, and up to 15 µg/L (1), however the concentrations as low as 1 - 3 µg/L can already cause respiratory depression and bradycardia, which can be especially dangerous for the newborn (2).

Dried plasma spots and dried blood spots are novel sampling techniques particularly convenient for paediatric and animal studies because they are less invasive and require 50-100 times lower sample volumes than traditional plasma methods.

The aim of our study was to develop a rapid and sensitive method for determination of remifentanil in dried plasma spots to support efficacy and safety trials of remifentanil during labour.

MATERIALS AND METHODS

Materials

Remifentanil and remifentanil-¹³C₆ as internal standard (IS) has been purchased from Toronto research, Canada. Blank human blood plasma was obtained from University Clinical centre, Ljubljana, Slovenia.

Preparation of calibration and quality control (QC) samples

Plasma calibrators were prepared by spiking standard solutions (50 µL) into 930 µL of blank plasma, which was stabilized by addition of 20 µL of 50% citric acid solution to inhibit plasma esterases. The calibration range spanned from 0.15 to 40 µg/L. Quality control samples were prepared the same way as calibration samples, but from a separate weighing, resulting in the following concentrations: 1,5; 15 and 30 µg/L. Using a repeater pipette, 20 µL samples in triplicates were applied to Whatman 903 DBS cards.

Sample preparation

After two hour drying time at room temperature, the whole DPS was cut out and extracted with 500 µL of mixture water: methanol 1:1 with added 1% formic acid and 50 µL of internal standard solution (50 µg/L). Afterwards, five different solid phase extraction sorbents were tested for recovery, matrix effect and repeatability: Ostro® 96 (Waters), HybridSPE® (Supelco), Strata-X (Phenomenex), BondElut Plexa® (Varian-Agilent) and Oasis® MCX (Waters). The highest recovery, nearly 100 % was achieved with Strata-X with the following extraction procedure: conditioning: 1 mL of methanol, and 1 mL water, loading of diluted sample with 1.5 mL of water, washing with 1 mL water, 1 mL 10% methanol and 0.5 mL of 20% methanol in water, drying for 10 min at maximum vacuum, elution with 1 mL methanol. The samples were then dried under a gentle stream of nitrogen and reconstituted in 50 µL of 10 % acetonitrile in 0.1% solution of formic acid.

Liquid chromatography-tandem mass spectrometry (LC-MS/MS)

The reconstituted samples were subjected to analysis by LC-MS/MS comprised of Agilent 1290 coupled to Agilent 6460 triple quadrupole mass spectrometer. 6 µL were injected onto a 50 x 2.1 mm Kinetex C₁₈ column (2.6 µm particles) at 50°C and eluted with mobile phase A (0.1% formic acid in water) and B (acetonitrile) at 0.65 mL/min using the following linear gradient (time, %B): (0,10); (0.5,20); (1,30); (1.25,50); (1.7,50). Total run time was 2.7 min. For MS detection, ESI interface in positive mode was used. The following (MRM) mass transitions were moni-



tored (parent→daughter m/z ; collision energy): remifentanil: 377.2→317.2; 8 eV, IS: 383.4→113.0; 25 eV (figure 1).

RESULTS AND DISCUSSION

The method has been successfully developed and validated according to the FDA guidelines on bioanalytical method validation. Assay accuracy, precision and recovery are presented in table 1 and calibration curve on figure 2. Relative matrix effect was determined to be insignificant as the variability in slopes of regression lines obtained from 5 different donors, was only 3,5 % RSD (3).

Tab. 1: Accuracy, precision and recovery (rec.) data determined on QC samples

	intraday precision [%RSD]	interday precision [%RSD]	bias [%]	rec. [%]
QC1	1,95	4,20	-3,6	83
QC2	3,05	2,31	1,9	-
QC3	1,04	1,45	5,5	81

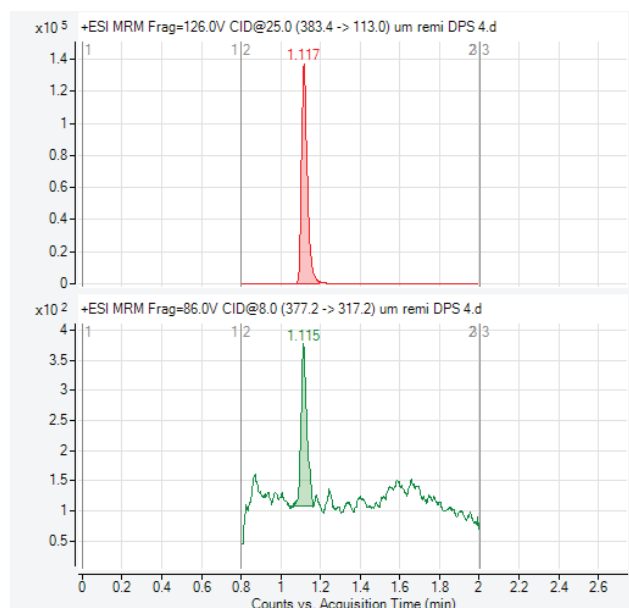


Fig. 1: MRM chromatogram of a LLOQ sample (top trace represents IS, bottom remifentanil).

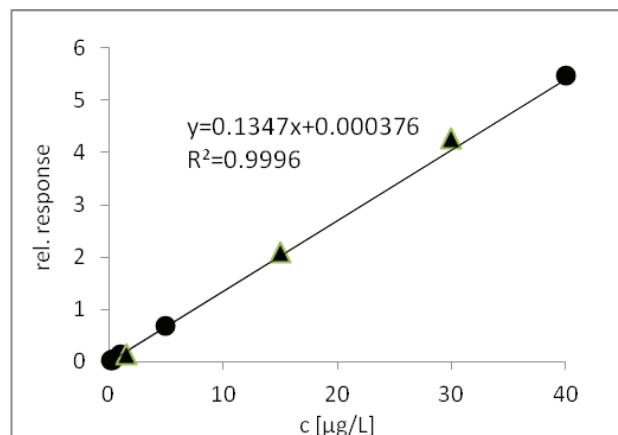


Fig. 2: Calibration curve for remifentanil in human dried plasma spots; circles represent calibrators, triangles represent QCs; weight: $1/c^2$.

CONCLUSIONS

The presented method has good accuracy, precision and sensitivity to reliably quantify remifentanil in only 20 μ L of plasma at subtherapeutic concentrations. This achievement will enable non invasive remifentanil level monitoring, for example from the umbilical cord blood, for safety and efficacy trials of labour pain management by remifentanil PCA.

REFERENCES

1. Summary of product characteristics (SmPC) Ultiva, GSK (14/4/2014).
2. Hsu Y., Cortinez L., Robertson K. et al.: Dexmedetomidine Pharmacodynamics: Part I: Crossover comparison of the respiratory effects of dexmedetomidine and remifentanil in healthy volunteers. *Anesthesiology* 2004; 101: 1066-76.
3. Matuszewski BM. Standard line slopes as a measure of a relative matrix effect in quantitative HPLC-MS bioanalysis. *J Chromatogr B Analyt Technol Biomed Life Sci.* 2006; 18;830(2):293-300.





DEVELOPMENT OF A NOVEL ALGINATE MICROPARTICLE PREPARATION METHOD FOR PROTEIN DELIVERY (P84)

E. Vranić^{1*}, D. Grizić², A. Lamprecht^{2,3}

¹ Department of Pharmaceutical Technology, Faculty of Pharmacy, University of Sarajevo, Zmaja od Bosne 8, 71 000 Sarajevo, Bosnia and Herzegovina

² Laboratory of Pharmaceutical Technology and Biopharmaceutics, Institute of Pharmacy, University of Bonn, Gerhard-Domagk-Str. 3, 53121 Bonn, Germany

³ Laboratory of Pharmaceutical Engineering, University of Franche-Comté, Place Saint Jacques, 25030 Besançon, France

INTRODUCTION

Alginate is a naturally occurring biopolymer, used as a versatile excipient in pharmaceutical technology. It can easily be gelled with multivalent cations (1) under gentle conditions. Therefore, it is applicable for the entrapment of sensitive materials (2) like proteins (BSA). BSA is a globular protein with an isoelectric point of about 5 (3). It is often being used as a model protein substance. Alginate microparticles can be prepared using ionotropic gelation combined with dropping, emulsification, atomization etc. (4). In this study we present a novel preparation method of alginate microparticles containing BSA using a modified solvent-extraction method.

MATERIALS AND METHODS

Materials

BSA was purchased from Roth (Karlsruhe, Germany). Sodium alginate, anhydrous glycerol and acetone were purchased from Sigma-Aldrich (Steinheim, Germany). All other chemicals were of analytical grade.

Methods

Phase miscibility study

This step was done in order to evaluate and to find the optimal volume fractions of all three components (acetone, glycerol and 1%-sodium alginate solution), for the preparation of microparticles. Briefly, specified volumes

of glycerol and sodium alginate were mixed. Acetone was added gently. This two-layered system was then mixed together, using a magnetic stirrer at 1000 rpm at 25°C for 1 minute.

Microparticle preparation

The microparticles were prepared using a novel emulsification/ionotropical gelation/ solvent diffusion approach. At first, sodium alginate (1.5%) was mixed with anhydrous glycerol and BSA (1-5% BSA in 0.9% NaCl). Thereafter acetone was added. After mixing at 1000 rpm on a magnetic stirrer, 150 µl of calcium chloride (10%) was added. The microparticles were filtrated, and washed with deionized water. Two formulations (containing 25% and 60% of BSA) were prepared.

Microparticle morphology

The surface morphology of both formulations was analyzed after ethanol-mediated dehydration and sputter coating with gold, using a Scanning electron microscope (Hitachi S-2460N, Tokyo, Japan) at 15kV.

In-vitro release study

The drug release was evaluated using an Erlenmeyer flask containing 100 mL of PBS (pH 7.4), held constantly at 37°C ± 0.5°C and stirred at 150 rpm using a magnetic stirrer. All aliquots were withdrawn at specific time intervals, centrifuged and the protein content was evaluated using a micro BCA assay.

RESULTS AND DISCUSSION

Phase miscibility study

Firstly, since no surfactant is being used, a pseudoemulsion is formed. The inner phase of this pseudoemulsion consists of sodium alginate, dissolved BSA, and glycerol. The outer phase consists of acetone. Figure 1. shows that after mixing, either a pseudoemulsion (green area) or a solution with precipitate (blue area) is formed.

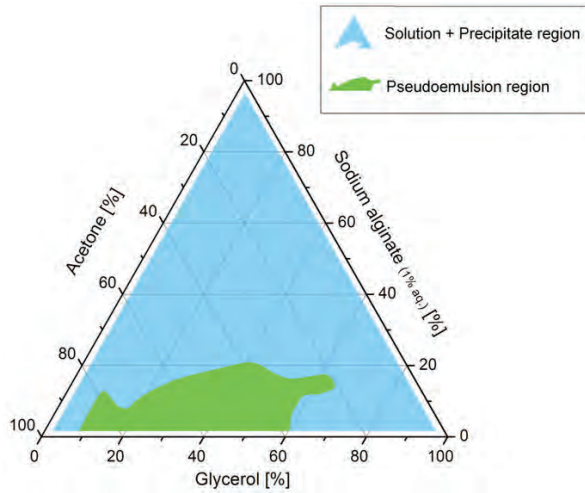


Fig. 1: Ternary phase miscibility diagram Acetone/Glycerol/Sodium alginate

The green region is suitable to use for further microparticle preparation steps.

Microparticle morphology

Figure 2. depicts the microparticle surface morphology, which is mainly porous and rough in both sample formulations, due to the fast extraction of the solvent, described also by Lamprecht et al.(5).

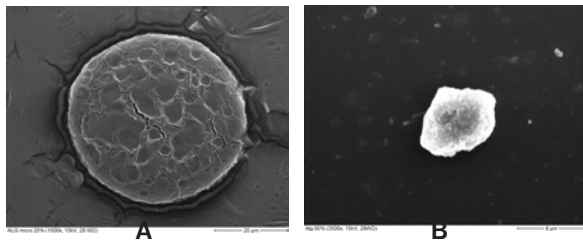


Fig. 2: Morphology of alginate microparticles; A - 25% BSA, B - 60% BSA

Also, additional analysis showed the following characteristics:

Tab.1: Characteristics of alginate microparticles prepared by the solvent-diffusion method

BSA content	25%	60%
Size and size distribution (µm)	301.3 ± 13.6	282.0 ± 4.3
Encapsulation efficiency (%)	24.80 ± 7.9	68.72 ± 5.7

In-vitro release study

Figure 3. shows the release of BSA from alginate microspheres, prepared with low and high amounts of BSA. The protein is released completely after 2 hours. This fast release is happening because the matrix of both formulations is filled with aqueous glycerol solution, which has a high tendency of diffusing into the dissolution medium. The slower release in high BSA content microspheres can be attributed to the electrostatic interaction between BSA and calcium alginate, which was evaluated by Neiser et al. (3).

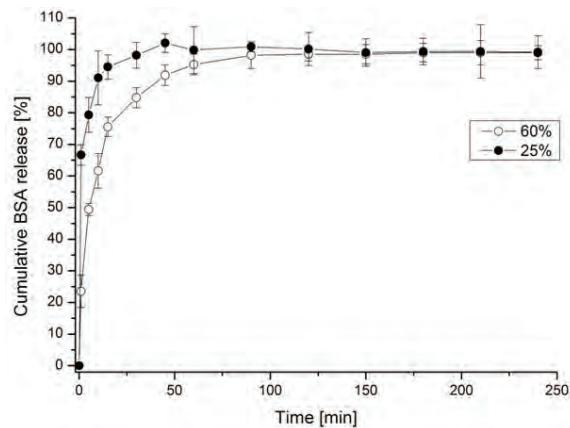


Fig. 3: Bovine serum albumin release from 25% and 60% alginate microparticles (n=3)

CONCLUSIONS

Alginate microparticles containing a model protein substance (BSA) were successfully formulated. Using data from the ternary miscibility diagram, we managed to overcome the problem of polymer/protein precipitation. Using glycerol as a protectant for alginate and BSA against the dehydration influence of acetone, we obtained microparticles using low (25%) and high (60%) amounts of BSA with satisfactory morphology and protein release.

REFERENCES

- Alnaief M., Alzaitoun M.A., Garcia-Gonzales C.A., Smirnova I. Preparation of biodegradable nanoporous microspherical aerogel based on alginate. *Carbohydr. Polym.* 2011; 84: 1011-1018.
- Paques J.P., Van der Linden E., Van Rijn C.J., Sagis L.M.C. Preparation methods of alginate nanoparticles. *Adv. Colloid Interface Sci.* 2014; in press
- Neiser S., Draget K.I., Smidsrod O. Interactions in bovine serum albumin-calcium alginate gel systems. *Food Hydrocolloids.* 1999; 13: 445-458.
- Gombotz W., Wee F.S. Protein release from alginate matrices. *Adv. Drug Deliv. Rev.* 1998; 31: 267-285.
- Lamprecht A., Yamamoto H., Takeuchi H., Kawashima Y. Microsphere design for the colonic delivery of 5-fluorouracil. *J. Control. Release* 2003; 90: 313-322.





PREPARATION OF INKJET-PRINTED FORMULATIONS WITH IMPROVED DISSOLUTION RATE OF INDOMETHACIN ^(P85)

H. Wickström^{1*}, R. Kolakovic¹, A. Määttänen², K. Gunnelius², P. Ihalainen², J. Peltonen², N. Genina¹, K. Löbmann³, T. Rades³, N. Sandler¹

¹ Pharmaceutical Sciences Laboratory, Åbo Akademi University, Artillerigatan 6A, FI-20520 Åbo, Finland

² Laboratory of Physical Chemistry, Åbo Akademi University, Porthansgatan 3-5, FI-20500 Åbo, Finland

³ Department of Pharmacy, University of Copenhagen, Universitetsparken 2, DK-2100 Copenhagen, Denmark

INTRODUCTION

Efficient drug delivery is needed for an active pharmaceutical ingredient (API) to have an effect in the human body. However, an increasing part of the new API candidates experience poor aqueous solubility. This is a major challenge that possibly could be tackled by implementation of technologies in combination with formulation development. The suitability of producing solid dosage forms using printing technology has recently been studied. It has been reported that printing could be a fast and flexible way of producing pharmaceuticals to meet the growing need to produce tailored and personalized medicine (1,2).

There are some methods already known which can be carried out in order to improve the solubility of poorly water soluble drugs. A temporary increase in the dissolution rate can be achieved by converting the crystalline drug to the thermodynamically unstable amorphous counterpart (3). Stabilization of the amorphous form with small molecular weight additives such as amino acids has recently been achieved (4).

The main objective of this work was to use piezoelectric inkjet technology to create drug delivery systems using indomethacin (IMC) containing ink solvent systems. Furthermore, the aim was to formulate inks with and without small molecular weight additives in order to investigate

the potential of the different printed systems as drug delivery systems and their effect on the dissolution rate. The effect of the different amounts of printed layers was also studied.

MATERIALS AND METHODS

Four IMC containing solvent systems as “inks” were studied. Two, Indo_50 and Indo_200, consisted of only IMC with the concentrations 50mg/ml and 200mg/ml, respectively. The amino acid L-arginine and the polymer polyvinylpyrrolidone (PVP) were dissolved into the two other IMC containing 50mg/ml systems in a 1:1 and 1:1000 molar ratio, respectively. Indo_Arg and Indo_PVP were the names of the inks. The drug delivery systems were prepared by printing 1x1cm² squares of the formulated inks using a piezoelectric inkjet printer (PixDro LP 50) onto a paper substrate applying 1, 3, 6 and 9 layers to gain different samples.

The content uniformity and the dissolution rates of the printed drug delivery systems were studied. Spectroscopic methods were applied to identify the solid state of the drug. Scanning electron microscopy (SEM) imaging was also done to get further understanding of the systems studied.

RESULTS AND DISCUSSION

Uniform yellow colored samples with low relative standard deviation percentages (RSD%) were generated using the piezoelectric inkjet technology. The RSD% for all 50 mg/ml and 200mg/ml inks were below 3% and 6.5%, respectively.

Improved dissolution rates were seen for all four ink formulations compared to the crystalline reference. The drug delivery systems made from the three 50mg/ml concentration inks showed similar dissolution profiles and were completely dissolved within 15-20 minutes. However, some differences could be seen in the dissolution profile between the different layers for the high concentration ink Indo_200 (Fig 1).

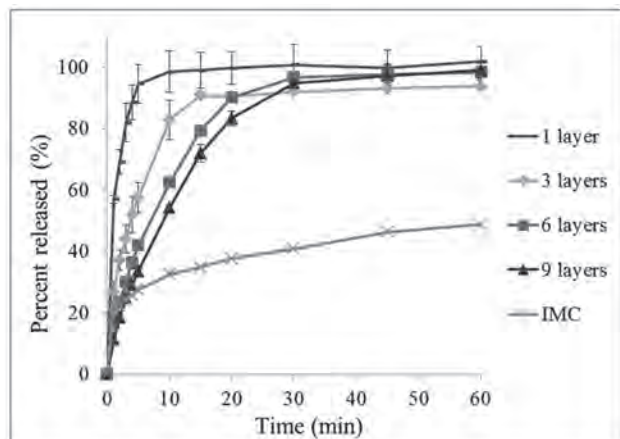


Fig. 1: Release profiles of the one and multi-layer samples of Indo_200 (200mg/ml) compared to the content uniformity values. Crystalline IMC served as a reference.

The main contributing factor for the improved dissolution rate for all four formulations remained unclear. One reason could be the even and spatially accurately separated distribution of the drug substance alone. Another reason could be conversion of the crystalline API to the amorphous counterpart and the interactions between the components of the printed systems. The API was identified by spectroscopic methods but the accurate determination of solid state form was not possible due to strong interference with the spectra of the substrate.

The samples were yellow after printing, after 6 months of storage in the dark and after evaporation of the solvents in vacuum oven (Fig 2). The yellow color could indicate that IMC was either present in a dissolved form or an amorphous form (5).

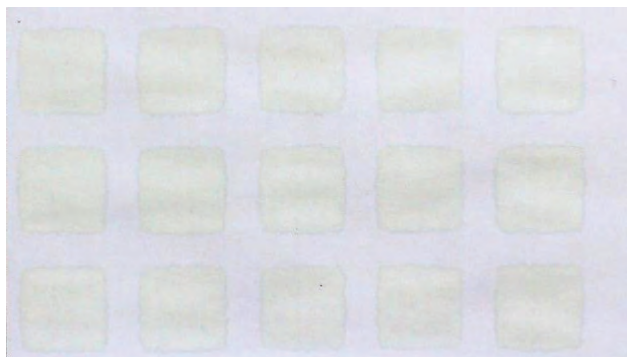


Fig. 2: A picture of the 1x1cm² printed samples containing IMC. The picture was taken the same day as the samples were printed.

CONCLUSIONS

Formulations containing the poorly water soluble drug IMC were successfully prepared and distributed on a paper substrate using piezoelectric inkjet technology. Accurately dosed samples were generated as a result of the optimal droplet formation and increased dissolution rates were obtained for all formulations compared to the reference. The approach taken is promising in formulation of poorly water soluble APIs, but further studies are still needed. Detection of the solid state of the drug as well as the interactions of the different components in the printed systems will be focused on in the future.

REFERENCES

1. Sandler N, Määttänen A, Ihalainen P, et al. Inkjet printing of drug substances and use of porous substrates-towards individualized dosing. *J.Pharm. Sci.* 2011; 100:8: 3386-3395.
2. Voura C, Gruber MM, Schroedl N, et al. Printable medicines: A microdosing device for producing personalized medicines. *Pharm. Tech. Europe.* 2011;23(32-36).
3. Perrie Y and Rades T, *Pharmaceutics-Drug delivery and targeting, II*, Pharmaceutical Press, London, UK, 2012
4. Löbmann K, Grohganz H, Laitinen R, Strachan C, Rades T. Amino acids as co-amorphous stabilizers for poorly water soluble drugs - part 1: Preparation, stability and dissolution enhancement. *Eur. J. Pharm. and Biopharm.*2012; 85:3: 873-881.
5. Wu T, Sun T, Li N et al., Inhibiting Surface Crystallization of Amorphous Indomethacin by Nanocoating. *Langmuir*, 2007; 23: 9: 5148-5153.





THE EFFECT OF LIPID CARRIERS ON CYCLOSPORIN A PERMEATION THROUGH THE ISOLATED CORNEA AND DETERMINATION OF OCULAR IRRITATION (P86)

E. Wolska^{1*}, J. Chorążewicz², D. Michna¹, M. Sznitowska¹

¹ Department of Pharmaceutical Technology, Medical University of Gdańsk, Hallera 107, 80-416 Gdańsk, Poland

² Department of Ophthalmology, Medical University of Gdańsk, Smoluchowskiego 17, 80-214 Gdańsk, Poland

INTRODUCTION

Cyclosporin A (Cs) is used as an immunosuppressive agent in the treatment of severe inflammatory and immunorelated ocular diseases (1).

Many carriers have been examined for ophthalmic delivery of Cs (2, 3). In our studies prolonged released solid lipid microparticles (SLM) have been proposed. Besides self emulsifying oil (SEO) was tested in comparison with oily solution.

SLM are lipid biodegradable microspheres with the size of one to several micrometers and can be administered as eye drops in the form of an aqueous suspension. Such formulation can help to avoid blurred vision occurring after administration of oily solutions and to reduce the frequency of application.

SEO contains surfactants in the composition, what facilitates mixing with the lacrimal fluid and is more comfortable for the patient than oily solutions.

MATERIALS AND METHODS

Cs-loaded SLM formulations were prepared using a hot emulsification method (4). The homogenization process was performed at 80°C using a high-shear mixer Ultra-

Turrax (T25 Janke-Kunkel, IKA Labortechnik, Germany). After cooling the pH was adjusted to 8.0 and the formulations were sterilized in an autoclave.

SEO was obtained by dissolving Cs in a mixture of oil and surfactant at 80°C.

The emulsions were prepared employing a hot-stage high-pressure homogenization (High Pressure Homogenizer APV-2000, APV Gaulin, Netherlands). Cs was dissolved in the emulsions followed by thermal sterilization by autoclaving.

The compositions of all tested formulations with Cs are illustrated in Tab. 1. The formulations contained 0.5% or 2% (w/w) of Cs (LC Laboratories, Boston USA).

Tab. 1: Composition (w/w) of tested formulations with Cs.

Formulation	SLM	Emulsion	SEO	Oil
Cyclosporin	0.5/2.0	0.5	0.5/2.0	2.0
Compritol	20.0		-	
Tween 80	3.0	3.0	5.0	-
Glycerol	1.8	2.3		-
Castor oil	-	20.0		to 100.0
Water		to 100.0		

Ex vivo permeation/penetration studies were performed using isolated pig corneas, which were placed between the donor and acceptor chambers in diffusion cells. The formulations (1 ml) were added to the donor chamber, and Krebs buffer was used as acceptor fluid. Samples of the acceptor fluid were taken after 5 h and 24 h. At the end of the experiment each cornea was extracted with methanol. Cs concentrations in the acceptor fluid and in the extract from cornea were determined by a validated HPLC method.

In vivo tolerance of SLM, o/w emulsion or castor oil solution was tested in the rabbit eye. The preparations were applied topically as eye drops, twice a day (20 µl) for 7 days. Ocular tolerance was evaluated with the modified Draize test.

RESULTS AND DISCUSSION

Penetration of Cs into the excised cornea from SLM and SEO was significantly higher ($p < 0.05$) than from the oily solution (Fig. 1.). Very good penetration of Cs from SLM can be explained by the high concentration of Cs on the SLM surface, what was shown in our previous studies (4).

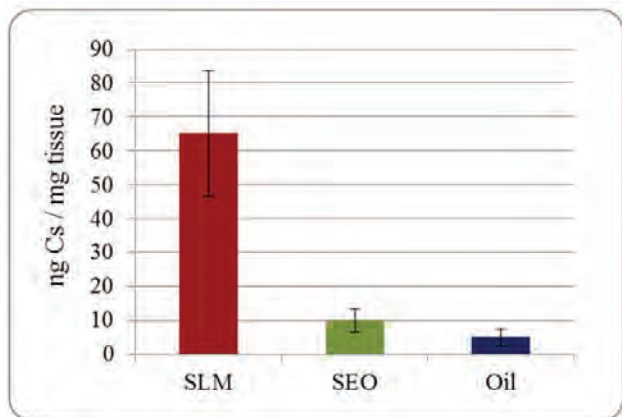


Fig. 1: Cs concentration in the excised pig cornea after ex vivo experiment (all tested formulations contained 2% of Cs).

The results of ex vivo experiments of Cs permeating across cornea are summarized in Tab. 2. Despite the high accumulation of Cs in the cornea, in the acceptor fluid there were no statistically significant differences ($p < 0.05$) among the tested Cs-loaded formulations. The study evaluating the emulsion with Cs is currently in progress.

Tab. 2: The amount of Cs permeating to the acceptor medium across pig cornea ($\mu\text{g}/\text{cm}^2$) after 5 h and 24 h.

Formulation	Time	
	5 h	24 h
SLM	0.40	0.99
SEO	0.52	0.67
Oil	0.67	1.06

Cs-SLM formulations administered to rabbit eyes were well tolerated. The modified Draize test did not reveal redness of the conjunctiva, neither opacity of the cornea nor any pathological discharge in the rabbit's eye. Although administration of the oily solution caused hyperemia and/or swelling of the conjunctiva, however the formulation was classified as non-irritating.

CONCLUSIONS

Cs-SLM suspension is a stable system suitable for ocular delivery of Cs resulting in high drug accumulation in the cornea.

The drug penetration to the ocular tissue from SEO or oily solution was much lower, but some enhancement of the absorption in the presence of surfactant was demonstrated.

On the basis of the *in vivo* results conducted in rabbits good tolerance to Cs-loaded SLM in the human eye may be expected (5).

ACKNOWLEDGEMENT

Research financially supported by the Ministry of Science and Higher Education in Poland (MN - 01-0085/08/), "Corneal permeation/penetration studies of selected active substances used in ophthalmology depending on the lipid carriers."

REFERENCES

- Gokce EH, Sandri G, Egrilmez S, Bonferoni MS, Guneri T et al. Cyclosporine A-loaded solid lipid nanoparticles: ocular tolerance and in vivo drug release in rabbit eyes. *Curr. Eye Res.* 2009, 34: 996-1003.
- He Y, Liu Y, Wang J, Zhang X, Lu W et al. Cs-loaded microspheres for treatment of uveitis: in vitro characterization and in vivo pharmacokinetic study. *Invest. Ophthalm. Vis. Sci.* 2006, 47: 3983-3988.
- Lallemand F, Felt-Baeyens O, Besseghir K, Behar-Cohen F, Gurny R. Cyclosporine A delivery to the eye: a pharmaceutical challenge. *Eur. J. Pharm. Biopharm.* 2003, 56: 307-318.
- Wolska E, Sznitowska M. Technology of stable, prolonged-release eye-drops containing Cyclosporine A, distributed between lipid matrix and surface of the solid lipid microspheres (SLM). *Int. J. Pharm.* 2013, 441: 449-457.
- Hutak CM, Jacaruso RB. Evaluation of primary ocular irritation: alternatives to the Draize test. *Ocular Therapeutics and Drug Delivery.* Lancaster, PA: Technomic Publishing, 1996, 489-525.





COATING OF DRUG LOADED MESOPOROUS SILICA NANOPARTICLES WITH BIOADHESIVE POLYMERS (P87)

K. Yoncheva^{1,*}, B. Tzankov¹, M. Popova², A. Szegedi³, N. Lambov¹

¹ Department of Pharmaceutical Technology and Biopharmaceutics, Faculty of Pharmacy, 2 Dunav Str., 1000 Sofia, Bulgaria

² Institute of Organic Chemistry with Centre of Phytochemistry, Bulgarian Academy of Sciences, 103 Akad. G. Bonchev Str., 1113 Sofia, Bulgaria

³ Research Centre for Natural Sciences, Institute of Materials and Environmental Chemistry, Hungarian Academy of Sciences, Magyar tudósok körútja 2, 1117 Budapest, Hungary

INTRODUCTION

Mesoporous silica nanoparticles are promising drug delivery carriers due to the variety of pore size, high drug loading and opportunity for surface modification. The latter is one of the main approaches intended for reduction of the initial burst release that is frequently observed in these systems (1-2). In addition, the surface modification with bioadhesive polymers could improve the interactions between nanoparticles and absorptive cells in gastrointestinal tract.

In the present study, surface modification of the mesoporous nanoparticles was performed in order to provide low initial release and longer budesonide residence in gastrointestinal tract.

MATERIALS AND METHODS

Methods

MCM-41 was prepared according to the procedure of Huh et al. (3). The sol-gel procedure is carried out at 353 K and the relative molar composition of the reaction mixture was: 1 TEOS: 0.12 C₁₆TMABr: 0.31 NaOH: 1190 H₂O. The formed gel was aged at 353 K for 2 h, then washed with distilled water until neutral pH, and dried at ambient. Template removal was carried out in air at 823 K with 1 K/min rate for 5 h.

The loading of model drug (budesonide) was achieved

by incubation of drug and mesoporous carrier MCM-41 in ethanol under continuous magnetic stirring at 310 K. After 24 hours, the mixture was centrifuged at 15,000 rpm, rinsed with purified water, separated by a second centrifugation, and dried at room temperature under vacuum. Drug loading of mesoporous silica particles was determined by thermogravimetry with a heating rate of 5 K/min in nitrogen flow (Setaram TG92).

For the coating procedure, drug loaded particles were incubated in an aqueous phase containing chitosan (0.1 % wt/wt). Double coated particles were prepared by further incubation of dried chitosan coated particles in aqueous phase containing sodium alginate (0.1 % wt/wt). The incubation was performed under stirring (700 rpm) for 2h. After that, the dispersions were centrifuged at 15,000 rpm for 15 min., rinsed with distilled water, separated by a second centrifugation, and finely dried at room temperature. Determination of nanoparticle size, polydispersity index and zeta potential was performed in distilled water using a Zetasizer (Malvern Instruments, UK).

For *in vitro* release studies, 10 mg of the drug loaded nanoparticles were incubated in 200 ml acid or phosphate buffer under stirring (100 rpm). The concentration of the released budesonide in the samples was determined by spectrophotometry at a wavelength of 250 nm (Hewlett Packard 8452A).

RESULTS AND DISCUSSION

The aim of the study was to modify the surface of the mesoporous silica nanoparticles with bioadhesive polymers in order to reduce the burst release and to enhance the interaction between nanoparticles and gastrointestinal mucosa. First, the mesoporous structure and drug loading into pores was proved by nitrogen physisorption. Then, the drug loaded particles were post coated only with chitosan or double coated with chitosan and alginate. As shown in Fig. 1, the coating increased the size of the mesoporous silica nanoparticles.

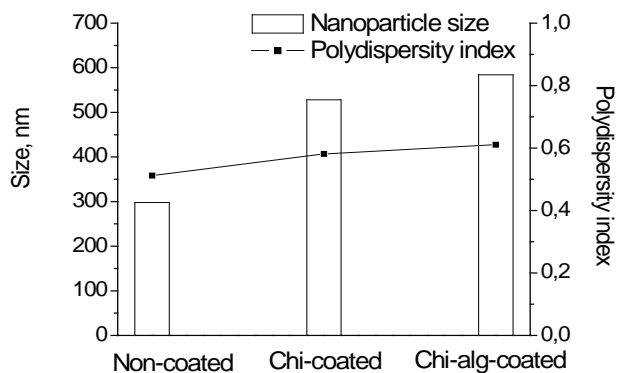


Fig. 1. Influence of the coating on the size of budesonide loaded mesoporous silica nanoparticles.

The different zeta-potential values for coated and non-coated particles were considered as indication for the achievement of coating layer on particle surface (Fig. 2).

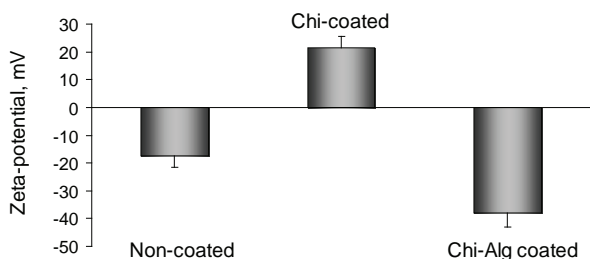


Fig. 2. Influence of the coating on the zeta-potential of budesonide loaded mesoporous silica nanoparticles.

As shown, chitosan-coated particles were positively charged, whereas chitosan-alginate coated nanoparticles possessed higher negative charge than non-coated. The *in vitro* release studies demonstrated lower burst effect in the case of coated particles compared to the non-coated (Fig. 3 and 4). As shown, this reduction was more pronounced for the release from chitosan-coated.

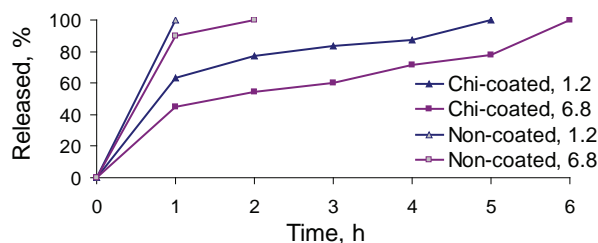


Fig. 3. *In vitro* release profiles of budesonide from chitosan-coated mesoporous silica nanoparticles.

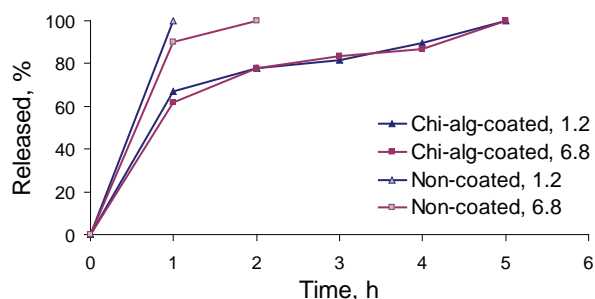


Fig. 4. *In vitro* release profiles of budesonide from chitosan-alginate coated mesoporous silica nanoparticles.

CONCLUSIONS

The coating of mesoporous silica nanoparticles with the selected polymers led to the opportunity to obtain desirable surface charge. In addition, the coating reduced the burst drug release, which is one of the problems of these nanoparticulate systems. Further investigations should be performed in order to evaluate the parameters and mechanism of coating with the selected polymers.

REFERENCES

1. Yoncheva K, Popova M, Szegedi A, Mihaly J, Tzankov B, Lambov N, Konstantinov S, Tzankova V, Pessina F, Valoti M, Functionalized mesoporous silica nanoparticles for oral delivery of budesonide. *J. Solid State Chem.* 2014; 211: 154-161.
2. Bhattacharyya S, Wang H, Ducheyne P, Polymer-coated mesoporous silica nanoparticles for the controlled release of macromolecules. *Acta Biomaterialia* 2012; 8: 3429-3435.
3. Huh S, Wiench JW, Yoo J-Ch, M. Pruski M, Lin VS-Y, Organic functionalization and morphology control of mesoporous silicas via a co-condensation synthesis method. *Chem. Mater.* 2003; 15: 4247-4256.





DEVELOPMENT OF A VALIDATED UPLC METHOD FOR DETERMINATION OF SOLUBILITY AND CHEMICAL STABILITY OF RESVERATROL FOR DESIGN OF NANOSIZED DELIVERY SYSTEMS

(P88)

Š. Zupančič¹, Z. Lavrič¹, J. Kristl¹

¹ University of Ljubljana, Faculty of Pharmacy, Aškerčeva 7, 1000 Ljubljana, Slovenia

INTRODUCTION

Resveratrol (3,5,4'-trihydroxystilbene, RSV), a naturally occurring polyphenol, has been shown to exhibit a wide range of therapeutic and preventive abilities, such as anti-inflammatory, cardioprotective, antitumoral and antioxidant. However, *in vivo* application of RSV is severely limited due to low bioavailability, which is a consequence of its poor aqueous solubility, limited stability and high metabolism rate (1). Trans isomer of RSV is photosensitive and it rapidly isomerizes to therapeutically less active cis form when exposed to ultraviolet light (2). A number of recent studies have aimed at designing novel RSV carriers to increase its bioavailability (3,4), but many of these studies lack analytical specificity for quantification of RSV. Especially, the most frequently used spectroscopic methods can provide false higher concentration due to absorbance also of cis-RSV and other degradation products at trans-RSV detection wave-length around 306 nm. In this context, authors provide different perspective on the determination of *in vitro* RSV solubility at different pH conditions simulating those found in intestinal tract, blood or skin, and this has a significant influence on results obtained in drug release studies (5). The aim of this

study is the development and validation of a new ultra-performance liquid chromatography (UPLC) method, able to separate and quantitate trans-RSV in a complex mixture with its degradation products and other impurities. Solubility and stability of RSV will be evaluated at pH 6.8 and 7.4, and at different storage conditions.

MATERIALS AND METHODS

Materials

RSV was obtained from LGC Standards GmbH, D, orthophosphoric acid 85%, KH_2PO_4 , and NaOH (for analysis) from Merck KGaA, D, and acetonitrile and MeOH (HPLC grade) from J.T.Baker, NL.

Development and validation of the UPLC method for RSV

Trans-RSV concentration and degradation products were determined by chromatographic system Acquity UPLC (Waters, USA). UV-VIS photodiode array module (PDA) equipped with high sensitivity flow cell was used for detection. Column used was Acquity UPLC HSS C18 SB 1.8 μm 2.1 x 100 mm (Waters, USA). Mobile phase was prepared by mixing 20 (V/V)% of acetonitrile with 30 mM phosphate buffer (PBS) with pH 2.8. The flow rate was 0.6 mL/min and run time 4.5 min. Purity of RSV peak was checked by examining UV-VIS spectra recorded by PDA detector. The UPLC method was validated in terms of specificity, linearity, accuracy, precision, detection limit, and quantitation limit according to the ICH guidelines (6).

Determination of RSV solubility

An excess of RSV was added to 100 ml of PBS with pH 6.8 and 7.4. The suspension was then continuously stirred at 25°C. At different time points samples were collected, filtered and then the trans-RSV concentration was determined by UPLC.

Determination of RSV chemical stability

The concentrations of trans-RSV in PBS with pH 6.8 and 7.4 at different time points were determined by UPLC. Also trans-RSV stability in PBS with pH 7.4 were evaluated at two light conditions and three different temperatures: exposed to light at 25°C and protected from light at -22°C, 4°C, and 25°C.

RESULTS AND DISCUSSION

The UPLC method dramatically increases resolution, sensitivity, and speed of analysis compared to HPLC due to advantage of using sub-2 μm particles and mobile phases at high linear velocities, and instrumentation that





operates at higher pressures (7). The UPLC method was developed and validated according to the guidelines of ICH (6) and was shown to be fast, simple, and reliable. The specificity of the method is shown in chromatogram (Fig. 1), where trans- and cis-RSV peaks are nicely separated from other degradation products.

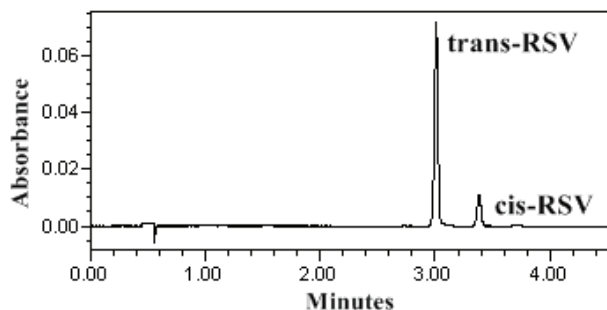


Fig. 1: Chromatogram of trans-RSV (UPLC at 306 nm)

Concentration of trans-RSV reached its maximum value after 4 hours at pH 7.4 (26.27 $\mu\text{g/ml}$) and then it dropped to $19.7 \pm 0.7 \mu\text{g/ml}$ due to degradation (Fig. 2). Solubility of trans-RSV at pH 6.8 was determined to be $32.8 \pm 1.4 \mu\text{g/ml}$.

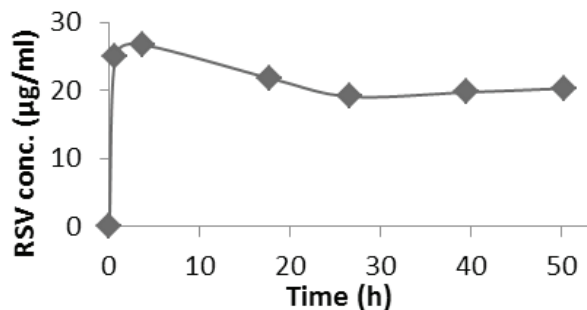


Fig. 2: The saturated solubility of RSV at pH 7.4

Stability of trans-RSV was tested protected from light in PBS at pH 6.8 and 7.4 since those pH values are most often used for controlled release studies (Fig. 3). After 40 hours the concentration of trans-RSV dropped for 4.9 % at pH 6.8 and for 78.4 % at pH 7.4. Stability of RSV at pH 7.4 is much increased during storage at 4°C , whereas at -22°C the solution remains stable for over 28 days. Cis-RSV was observed in samples exposed to light.

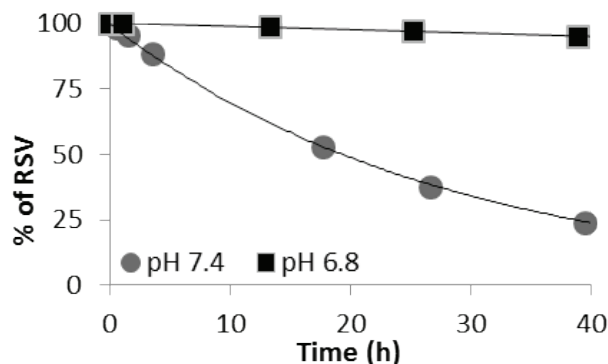


Fig. 3: Stability of RSV in solutions with pH 6.8 and 7.4 in dark

CONCLUSIONS

UPLC is proposed as a rapid method, for selective quantification of trans-RSV in heterogeneous mixture of RSV with its isomers and degradation products. Results show that solubility and stability of RSV are pH, temperature and light dependant. This insight improves the selection of the right parameters during formulation design step that could result in effective new delivery systems with trans-RSV.

REFERENCES

1. Amri A, Chaumeil JC, Sfar S, Charrueau C. Administration of resveratrol: What formulation solutions to bioavailability limitations? *J Control Release*. 2012;158(2):182–93.
2. Silva CG, Monteiro J, Marques RRN, Silva AMT, Martinez C, Canle M, et al. Photochemical and photocatalytic degradation of trans-resveratrol. *Photochem Photobiol Sci*. 2013;12(4):638–44.
3. Caddeo C, Teskac K, Sinico C, Kristl J. Effect of resveratrol incorporated in liposomes on proliferation and UV-B protection of cells. *Int J Pharm*. 2008;363(1-2):183–91.
4. Teskac K, Kristl J. The evidence for solid lipid nanoparticles mediated cell uptake of resveratrol. *Int J Pharm*. 2010;390(1):61–9.
5. Das S, Lin H-S, Ho PC, Ng K-Y. The impact of aqueous solubility and dose on the pharmacokinetic profiles of resveratrol. *Pharm Res*. 2008;25(11):2593–600.
6. Validation of analytical procedures: text and methodology Q2(R1). *International Conference on Harmonization (ICH) 2005*: 6-10.
7. Swartz ME. *UPLC TM: An Introduction and Review*. *J Liq Chromatogr Relat Technol*. Taylor & Francis; 2005;28(7-8):1253–63.





INVESTIGATION OF POLYCAPROLACTONE NANOFIBERS WITH RESVERATROL

(P89)

Š. Zupančič¹*, Z. Lavrič¹, P. Kocbek¹, J. Kristl¹

¹ University of Ljubljana, Faculty of Pharmacy, Aškerčeva 7, 1000 Ljubljana, Slovenia

INTRODUCTION

Nanofibers are fibers with a diameter in nanometer range and a theoretically unlimited length. Their high surface area to volume ratio and resemblance to extracellular matrix provide them as a promising strategy for tissue regeneration and drug delivery. They can be produced using different techniques. Among them the electrospinning is widely used, since it is a simple, one-step method, although, influenced by many different parameters (1). The most appropriate materials for preparation of nanofibers used as drug delivery systems are biodegradable and biocompatible polymers, such as polycaprolactone (PCL) (2, 3).

Resveratrol (RSV), highly photosensitive poorly soluble compound, has several beneficial effects including antioxidant, anti-inflammatory, cardioprotective, and anti-tumor activities, however, it lacks *in vivo* efficacy due to unfavourable pharmacokinetic properties (3). Therefore, the development of a delivery system to improve its therapeutic and prophylactic potential is still a technological challenge.

The aim of this research was preparation of electrospun RSV loaded PCL nanofibers and their characterisation.

MATERIALS AND METHODS

Materials

RSV was obtained from LGC Standards (Germany), PCL (Mr 70.000-90.000 g/mol) from Sigma Aldrich (Germany). NaI, chloroform, and acetone were purchased from Merck KGaA (Germany).

Preparation of RSV loaded nanofibers

PCL was dissolved in mixture of chloroform and acetone in 1:3 mass ratio, then 0.03% (w/w) NaI was added, resulting in 10% (w/w) conductive polymer solution. Differ-

ent quantities of RSV (1, 5, 10, and 20%, w/w based on the mass of dry polymer) were added to the solution. The polymer solution was placed in a 20 ml plastic syringe fitted with a metallic needle with an inner diameter of 0.8 mm. The electrospinning was conducted at 15 kV (model HVG-P50-R-EU, Linari Engineering s.r.l., Italy), needle-to-planar collector distance 15 cm, and solution flow rate 1.3- 2.5 ml/h (model R-99E, Razel Scientific, USA).

Characterisation of nanofibers

The morphology of dry nanofibers was determined using scanning electron microscope (SEM, Carl Zeiss, Germany). Interactions of RSV with PCL in nanofibers was studied by Nicolet Nexus FTIR (Thermo Electron Corporation, USA). Thermal analysis was carried out using a DSC (Mettler Toledo DSC 1, Switzerland). Samples were analyzed using heating rate of 10°C/min in the temperature range 25 to 300°C.

The release of RSV from nanofibers was investigated in phosphate buffered saline, pH 6.8. The electrospun RSV loaded nanofibers (50 mg) were put in 700 ml of medium and stirred on a magnetic stirrer at 150 rpm and 37.0±0.5°C. The samples (2 ml) were withdrawn, filtered immediately through 0.2 µm filters (Minisart RC 4, Sartorius Stedim Biotech GmbH, Germany) and analysed using UPLC system (Waters, USA).

RESULTS AND DISCUSSION

The optimization of electrospinning parameters enabled preparation of PCL nanofibers with average diameter ~500 nm (Fig. 1A). RSV was successfully incorporated in nanofibers, when its mass fraction in nanofibers was lower than 10%, whereas some crystals were observed on the surface of nanofibers with 10 and 20% RSV. The diameter of nanofibers increased with increasing amount of RSV loaded i.e. from 480±140 nm (plain PCL nanofibers) to 730±55 nm (nanofibers loaded with 20% RSV) (Fig. 1).

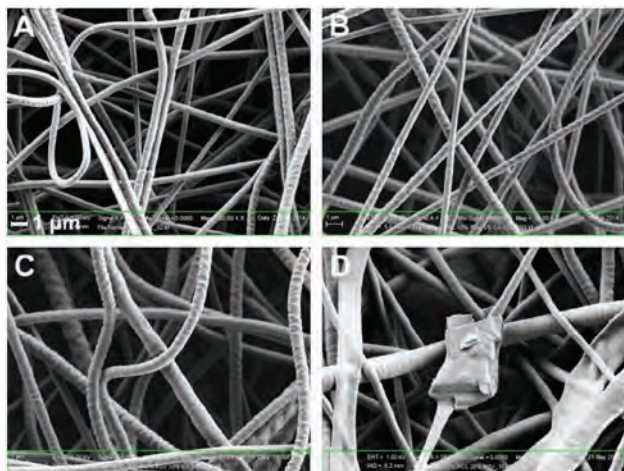


Fig. 1: SEM images of PCL nanofibers with (A) 0%, (B) 5%, (C) 10%, and (D) 20% of RSV.

In order to investigate the crystalline structure of RSV in nanofibers DSC measurements were performed (Fig. 2). DSC curves of nanofibers with 1 and 5% RSV did not show endothermic peak at 269.8°C characteristic for pure RSV, indicating its amorphous state or presence of the drug dissolved in melted polymer ($T_{m, PCL} = 60.7^{\circ}\text{C}$). The large surface area of the jet formed during electrospinning allows fast and efficient solvent evaporation that limits the time available for crystallization of RSV to occur and thus favours the formation of the amorphous RSV. DSC curves of nanofibers with 10 and 20% RSV showed small endothermic peak at 148.1 and 161.0°C, respectively.

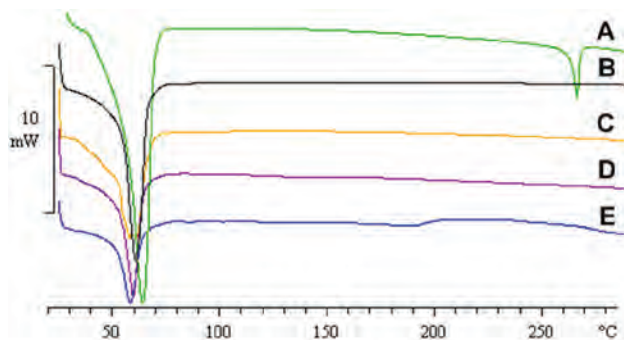


Fig. 2: DSC curves of (A) physical mixture of RSV and PCL, PCL nanofibers with (B) 0%, (C) 5%, (D) 10%, and (E) 20% of RSV.

The FTIR spectra did not reveal any interactions of RSV and PCL in nanofibers.

Although PCL is usually used for preparation of prolong drug release dosage forms, the formulated nanofibers released ~80% of RSV in the first 3 h. The rate of RSV release correlated with the amount of the drug loaded. The difference observed between samples is most probably related to the distribution of RSV in nanofibers, where more RSV was on the surface of nanofibers with 20% RSV compared to those with 5% RSV.

CONCLUSIONS

PCL nanofibers loaded with RSV were successfully formulated. When the drug loading was smaller than 10%, RSV was in amorphous state or RSV dissolved in melted polymer during the DSC analysis. Nanofibers with higher amount of RSV were thicker with visible crystals on the surface. Although hydrophobic polymer was used for preparation of nanofibers, RSV was rapidly released. The results of this study support design of nanofibers as a carrier for local or systemic RSV delivery.

REFERENCES

1. Rosic R, et al. Nanofibers and their biomedical use. *Acta Pharm*, 2013; 63(3): 295-304.
2. Khadka DB, et al. Protein- and peptide-based electrospun nanofibers in medical biomaterials. *Nanomedicine*. 2012; 8(8): 1242-62.
3. Wang X, et al. Biomimetic electrospun nanofibrous structures for tissue engineering. *Mater Today*. 2013; 16(6): 229-41.
4. Neves a R, et.al. Resveratrol in medicinal chemistry: a critical review of its pharmacokinetics, drug-delivery, and membrane interactions. *Curr Med Chem*. 2012; 19(11): 1663-81.



INDEX OF AUTHORS





- Abrami M 61
 Abramović Z 117
 Achim M 194
 Agnese Th 202
 Ahlin Grabnar P 69
 Alakurtti S 56
 Aleksovski A 24, 213
 Alhaique F 19
 Amaral MH 105
 Ambrus R 48, 71, 75
 Amelian A 73
 Antikainen O 186
 Avanzo M 198
 Bartoníková K 88, 219, 228,
 Bartos Cs 48, 75
 Basa A 73
 Baumgartner B 45, 77, 145, 196
 Bekčić K 63
 Bělohlav Z 149
 Benda L 109
 Beranek J 210
 Beránek J 34
 Bernkop Schnürch A 28, 50
 Bogataj M 6, 190, 217
 Bogdan C 123
 Böhm J 111
 Boldyrev V 32
 Boldyreva EV 32, 204
 Bonengel S 28
 Bozkır A 93
 Brandl M 79
 Brelih H 190
 Brniak W 22
 Bugarski B 89
 Bukovec P 101
 Butković A 213
 Čaklec I 160
 Čalija B 129, 131
 Cavallaro G 26
 Cech Th 80, 202
 Cegnar M 82
 Cekić N 119, 121
 Čerpnjak K 86
 Cetina-Čižmek B 39, 113, 137, 160, 162
 Chorążewicz J 236
 Cielecka-Piontek J 180
 Čierna M 88, 219, 228
 Conceição J 105
 Connell Y 91
 Corrigan OI 185
 Coviello T 19
 Čuchorová M 219
 Čuchorová M 228
 Čuchorová M 88
 Čujić N 89
 Cvan Trobec K 59
 Cvetković N 168
 Cvijić S 84, 168
 Cybula W 147
 D'Arcy DMn 91
 D'Arrigo G 19
 Danhof M 12
 Daniels R 119
 Dapas B 26
 Değim İsmail Tuncer 17
 Đekić Lj 84
 Demetzos C 54
 Denčić I 131
 Dér K 212
 Devrim B 93
 Di Meo C 19
 Dimchevska S 95, 221
 Dinte E 123
 Djekic Lj 200
 Djordjevic D 200
 Djurdjic B 95
 Djuris J 139
 Dobričić V 129, 184
 Đorđević S 119
 Dovnik I 97
 Dreu R 24, 99, 226
 Dular A 101
 Dumicic A 34, 149
 Dünnhaupt S 50
 Đurić Z 63,151,166,184
 Đuriš J 166
 Dürriegl M 162
 Duvnjak Romić M 39, 113
 Egart M 103
 Engesland A 41
 Estanqueiro M 105
 Ewing A 34
 Farra R 26, 56
 Fattal E 8
 Filipović-Grčić J 39, 41, 107, 113, 137, 160,162, 176
 Flaten GE 41
 Franc A 208
 Franceschinis E 109
 Furlanetto S 135
 Gancheva V 95
 Gardavská K 219
 Gardavská K 228
 Gardavská K 88
 Gašperlin M 86, 121



- Genina N 182
Genina N 234
Georgiev G 95
German T 111
Geskovski N 95
Giammona G 26
Gigovski M 221
Glavas-Dodov M 221
Goepferich A 5
Golob S 188
Goracinova K 95
Gošciańska J 180
Grabnar I 188
Grabnar I 59, 69
Grassi G 26, 56
Grassi M 26, 56,188
Grbić S 217
Grießinger J 50
Grizic D 232
Gunnelius K 234
Hæggström E 178
Hafner A 113, 160
Lovrić J 160
Hafner A 176, 39
Halenius A 56
Hasa D 61, 188
Hauptstein S 28
Healy AM 172
Hebestreit P 80
Hegy P 212
Heinämäki J 56, 186, 178, 206
Hinna A 79
Hirvonen J 52
Homar M 35, 115
Horvat M 30
Horváth T 48, 75
Hudovornik G 43
Hunter S 204
Hunyadi A 212
Hupfeld S 79
Hurler J 107
Ibric S 63, 89, 139, 151,154, 166
Ihalainen P 234
Ilić I 97,99,103
Ilić M 117
Irman Š 198
Isailović T 119, 121
Iurian S 123
Jablan J 125
Jachowicz R 22
Jaklič M 127
Janičijević J 129,131,133
Janković B 30, 45, 99, 103
Jašić M 213
Jazbinšek V 156
Jelčić Ž 162
Jug M 125,135
Juretić M 39,137,160,176
Jurić M 143
Jurković P 30
Kaljevic O 139
Kartal-Hodzic A 52
Kassamakov I 178
Kazarian SG 34
Kelemen A 65
Kerč J 82, 115
Kerec Kos M 59
Kirsimäe K 206
Klančar A 141
Klančar U 37, 117
Kleinebudde P 63, 158, 166
Kluk A 147
Kocbek P 45, 143,196, 242
Kocjan D 35
Kogermann K 56, 178,186, 206
Kolakovic R 182,234
Korać R 133
Korasa K 43
Kosalec I 135
Košcińska K 224
Košir D 145
Kotłowska H 147
Koutsoulas C 54
Kovalskii VY 204
Krajišnik D 129,133
Krajnc U 127
Kralj P 198
Kralj S 143
Krejzová E 149
Kristan K 198
Kristl J 45, 82, 77, 196, 240, 242
Kristó K 65
Krstić M 151
Krstić M 154
Krtalić I 137
Kujundžić N 125
Kuntsche J 79
Kuznetsova SA 32
Laaksonen T 52, 182
Lah N 103
Laidmäe I 178, 206
Lainscak M 59
Lambov N 238



- Lamprecht A 232
 Langguth P 84
 Lavrič Z 156, 240,242
 Lazzari A 158
 Lebar A 117
 Legen I 37, 58
 Lehr CM 13
 Leucuța SE 123
 Lewandowska K 180
 Liang H 52
 Licciardi M 26
 Liu P 52
 Löbmann K 234
 Lovrić J 39, 137,176
 Lusina Kregar M 162
 Lust A 186
 Lužnik J 156
 Määttänen A 182, 234
 Madanecka A 147
 Mäder K 80
 Makraduli L 164
 Maléth J 212
 Malyar YuN 32
 Marković B 119, 131
 Markovska R 164
 Markum B 37
 Martinovic M 200
 Mašlak E 22
 Matricardi P 19
 Medarević Đ 63,166
 Medarevic Dj 139,168
 Mennini N 135
 Michna D 236
 Mikac U 77
 Mikhailenko MA 32
 Miklavžin A 82
 Milić J 129,131,133
 Mistry M 202
 Mizera M 180
 Mladenovska K 221
 Moldovan M 123
 Momčilović M 168
 Montanari E 19
 Morrison CA 204
 Mrhar A 190
 Muntean D 194
 Mura P 135
 Muselík J 208
 Musial W 170
 Nardin I 50
 Neumann D 208
 Norris BA 172
 Oblak M 198
 Ondrejček P 174, 223
 Opara J 58
 Orbančić A 176
 Orlandini S 135
 Owcarz K 147
 Paaver U 56, 178, 206
 Paavo M 56
 Paczkowska M 180
 Palac Z 41, 107
 Palo M 182
 Păltinean R 123
 Pantelić I 119
 Parojčić J 84, 151,168,184, 217
 Pein M 158
 Pelipenko J 45
 Peltonen J 182, 234
 Peltonen L 52
 Penkina A 186
 Pepić I 39, 137, 160,176
 Perera G 28
 Perissutti B 61,109,188
 Petek B 115
 Petelin P 115
 Peternel L 35
 Petrov P 95
 Petrusevska M 35
 Pietrzak R 180
 Piotrowska H 180
 Pippa N 54
 Pirnat J 156
 Pirttimaa M 56
 Pišlar M 190
 Pitkänen P 56
 Płaczek M 224
 Planinšek O 97, 111,192, 215
 Pljevljakušić D 89
 Pluta J 170
 Pomazi A 71
 Popova M 238
 Porfire A 194
 Potrč T 196
 Praček J 198
 Primorac M 200
 Pulham CR 204
 Punčochová K 34
 Puskás L 212
 Quodbach J 158
 Rabausch B 202
 Rabišková M 174,223
 Rades T 234
 Radivojša M 69, 84





- Rafailović D 84
Rahić O 192, 215
Raicki RS 221
Rammo L 206
Ražić S 154
Realdon N 109
Regdon jr. G 65
Řehula M 174, 223
Rošić R 45
Roškar R 141
Rožman A 162
Rozman Peterka T 198
Rychkov DA 204
Saarinen T 186
Sabadková D 208
Salkić A 213
Sandler N 182,234
Santomaso AC 109
Santos HA 178
Santos-Martinez MJ 91
Sardo C 26
Savić S 119,121
Šavikin K 89
Scialabba C 26
Sedmak G 210
Šegvić-Klarić M 113
Seliger J 156
Sepe A 77
Serrano DR 172
Shakhtshneider TP 32
Šibanc R 226
Šibanc R 99
Sieber D 158
Simonoska-Crcarevska M 221
Sipos P 212
Škalko-Basnet N 41, 107, 206
Sousa Lobo JM 105
Sovány T 65
Špaglová M 88, 219, 228
Spaseska Aleksovska E 213
Spasojević Dj 154
Srčić S 99, 103,156,192, 215
Stanić Ljubin T 30
Stanković N 131
Stanković S 151, 217
Starova A 221
Starýchová L 88, 219, 228
Stasiak P 149
Štěpánek F 34
Sterjev Z 221
Stojković A 184
Stoniš J 174
Suleiman E 54
Sulevski V 221
Suljić S 213
Svačinová P 174,223
Szabó-Révész P 48, 71, 75, 212
Szegedi A 238
Szekalska M 73
Sznitowska M 147, 224,236
Szymanowska-Powałowska D 180
Tislér Zs 65
Todosijević M 121
Tomužã I 123,194
Tonon F 26
Trifković K 89
Trontelj J 59, 141, 230
Trontelj Z 156
Trotter A 109
Tucker GT 10
Turská J 219
Tzankov B 238
Vanić Ž 41, 107
Vasiljević D 154
Veski P 56, 178,186, 206
Viitala T 52
Vitková M 219,228
Vitková M 88
Vlase L 194
Voinovich D 56,109,188
Volmajer Valh J 170
Vovk T 59
Vranić E 192, 215, 232
Vrečer F 43, 86,101,111,145
Wagner A 54
Wickström H 234
Wilczewska AZ 73
Windorf M 80
Winnicka K 73
Wolska E 236
Yliruusi J 56,178, 186
Ylitalo T 178
Yoncheva K 238
Zabka M 54
Žagar E 82
Žagar V 156
Zahirović E 213
Zajacová I 88
Zalatnai A 212
Zamai AS 32
Zimmer A 15
Zupančič Š 45, 240, 242
Zvonar A 86

SPONSORS AND ADVERTISERS



Krka, d. d., Novo mesto, Slovenia is one of the leading generic drug manufacturing pharmaceutical companies in the world, maintaining its advantage in over 70 countries. The company is strengthening its position globally by investing into development, maintaining steady growth of sales and achieving positive results on existing markets as well as entering new markets. It develops generic medicines with added value which are based on its own, innovative synthesis procedures, its own, innovative pharmaceutical forms and technologies, and extensive studies, which ensure quality, safety and efficacy.



Lek is a part of Sandoz, a global generics leader. We save and improve lives by developing, producing and distributing high-quality, affordable pharmaceuticals. Thanks to our global network, Sandoz medicines are now available to 90% of people worldwide. In addition to the direct cost savings to patients, we contribute to the stability of healthcare systems worldwide and free up resources for new and innovative medicines. We make far more than just traditional off-patent medicines. We stand out from the crowd thanks to our ability to develop and produce a wide range of differentiated products, ranging from complex delivery systems for standard generics through to modern biopharmaceutical medicines (biosimilars).



HARKE Pharma GmbH

You innovate - we enable

HARKE Pharma is a technological driven distribution company based in Mülheim, an der Ruhr, Germany active in the field of pharmaceutical technology. Core competencies span from coatings, SR-Matrices, tableting aids, pellet systems to granulation binders, to be realized by cellulose derivatives, PVA, PEO or various blends. Meet us in the exhibition to discuss latest application techniques in classical dosage forms or to gain value in novel dosage forms.



Are you looking for?

commitment
flexibility
speed
know-how
support
care
quality
productivity
expertise
dedication
solutions
reproducibility
simplicity
optimization



Enjoy all inclusive
treatment with



sales@biaseparations.com
tel: +386 59 699 500
www.biaseparations.com

Leaders in Monolith
Chromatography



SkinPharma

**Made in Galenic laboratory
of Lekarna Ljubljana.**



Available in Lekarna Ljubljana units
and in the online pharmacy
at www.lekarna24ur.com.



Taking care of your health.

*Helping make your special moments even richer
and happier is at the very core of our mission
as a pharmaceutical company.*

*The path we are taking is paved with scientific knowledge,
high technology, and products
that offer you a healthy life.*

*And our future is as a leading
pharmaceutical generics producer.*



www.krka.si

Living a healthy life.



I'm going to be a scientist.

"Mummy took us to visit her office. She works at Lek, where they make medicines for sick children and adults. We met nice people at her office who showed us interesting experiments.

I've never seen anything like it. A lot of times I wonder what I'm going to be when I grow up. Maybe an athlete or a musician. But I would most like to do what my Mum does. I'm going to be a scientist."



a Sandoz company

Lek Pharmaceuticals d.d., Verovškova 57, SI-1526 Ljubljana, Slovenia • www.lek.si